UNCLASSIFIED

AD NUMBER
AD379234
CLASSIFICATION CHANGES
TO: unclassified
FROM: confidential
LIMITATION CHANGES
TO: Approved for public release, distribution unlimited
FROM: Distribution authorized to U.S. Gov't. agencies and their contractors; Administrative/Operational Use; JUN 1965. Other requests shall be referred to Director of Supersonic Transport Development, Federal Aviation Agency, Washington, DC 20553.
AUTHORITY
FAA ltr, 10 Oct 1972; FAA ltr, 10 Oct 1972

THIS PAGE IS UNCLASSIFIED

Best
Available
Copy

Best Available Copy

AD-379 234

Best Available Copy

NOTICES

When Government drawings, specifications, or other data are used for any purpose other than in connection with a definitely related Government procurement operation, the United States Government thereby incurs no responsibility nor any obligation whatsoever; and the fact that the Government may have formulated, furnished, or in any way supplied the said drawings, specifications, or other data, is not to be regarded by implication or otherwise as in any manner licensing the holder or any other person or corporation, or conveying any rights or permission to manufacture, use, or sell any patented invention that may in any way be related thereto.

Copies have been placed in the DDC collection. U.S. Government agencies may obtain copies from DDC. Other qualified DDC users may request, by submission of a DDC Form 1, through:

Director of Supersonic Transport Development
Federal Aviation Agency
Washington, D.C. 20553

Defense Documentation Center release to the Clearinghouse for Federal, Scientific, and Technical Information (CFSTI) and foreign announcement and dissemination are not authorized. The distribution of this report is limited because it contains technology identifiable with items excluded from export by the Department of State (U.S. Export Control Act of 1949 as amended).

CONFIDENTIAL

Report No. PWA-2600
Date: 30 June 1965

Volume 4

SUPERSONIC TRANSPORT AIRCRAFT ENGINE

PHASE II-B DEVELOPMENT PROGRAM

FINAL REPORT (U)

Prepared Under Contract FA-SS-65-18

Period Covered 1 January through 30 June 1965



PWA-E. H. Document Control
Eng. Sub-Control Station

JUN 25 1965

Number C63-5-C27L-B

This document contains information affecting the national defense of the United States within the meaning of the Espionage Laws, Title 18 U.S.C. Sections 793 and 794. Its transmission or the revelation of its contents in any manner to an unauthorized person is prohibited by law.

Reproduction, distribution and use of this document are limited as specified in the contract under which it was prepared. Use for other than U. S. Governmental purposes is subject to prior approval of United Aircraft Corporation.

Approved by C. W. Bristol Jr.

C. W. Bristol, Jr.
Project Engineer

Pratt & Whitney Aircraft DIVISION OF UNITED AIRCRAFT CORPORATION

EAST HARTFORD • CONNECTICUT

FAA SECURITY CONTROL
NO. [illegible]-79

COPY NO. _____

DOWNGRADED AT 3 YEAR INTERVALS.
DECLASSIFIED AFTER 12 YEARS
DOD DIR 5200.10

CONFIDENTIAL

ITEM 3

COMPRESSOR DEVELOPMENT



ITEM 3 - COMPRESSOR DEVELOPMENT

OBJECTIVE

The objective of the Phase II-B program for this item of the contract was the continued development testing of the compressor directed toward the verification of compressor performance. The goals of this program included the design and development testing of a two-stage fan which is aerodynamically similar to that of the STF219 engine and the further improvement of the performance of the five-stage compressor which was tested during the Phase II-A contract period. Also, tests were scheduled to investigate the aeroelastic behavior of fan blades in a series of controlled single-stage tests using the TS4 rotor blade configuration as the basic test rig.

A. INTRODUCTION

During Phase II-B of the SST program, a completely new two-stage fan rig was designed and fabricated. This is an entirely new fan, not an adaptation of existing aerodynamic hardware, and its aerodynamic design is the same as the SST engine. Single-stage fan rig tests were conducted in an existing test rig, using modifications of the TS4 blade, to investigate the flutter phenomena in shrouded rotor blades. Work on the multi-stage compressor involved essentially an extension and continuation of the last configuration tested during the Phase II-A program.

B. DEVELOPMENT PROGRAM

1. TWO-STAGE FAN RIG

The aerodynamic design of the two-stage fan rig is identical, except for size, to the fan required for the STF219 engine. The rig will be used to evaluate the aerodynamic performance and some of the mechanical problems associated with the SST engine.

DOWNGRADED AT 3 YEAR INTERVALS
DECLASSIFIED AFTER 12 YEARS
DOD DIR 5200.10

THIS DOCUMENT CONTAINS INFORMATION AFFECTING THE NATIONAL DEFENSE OF THE UNITED STATES WITHIN THE MEANING OF THE ESPIONAGE LAWS, TITLE 18 U.S.C. SECTIONS 793 AND 794. THE TRANSMISSION OR THE REVELATION OF ITS CONTENTS IN ANY MANNER TO AN UNAUTHORIZED PERSON IS PROHIBITED BY LAW.

The general design criteria used in the design of this two-stage fan are:

Corrected Airflow, $W\sqrt{\theta}/\delta$, lb/sec	250
Flow per Unit Area, W/A, lb/sec-ft^2	40
Overall Pressure Ratio	2.63
Tip Speed, U_t, ft/sec	1550
Hub-to-Tip Ratio	0.40

A more detailed list of the design parameters is shown in Figure 3.1. Since this fan rig will be used to evaluate engine problems, it is necessarily an almost exact model of the full-scale engine fan. During the design procedures, particular attention was paid to all details, and the same design criteria were applied as would have been done for any actual engine design. Short chord blades were used to achieve light weight. This necessitated the use of two part-span shrouds in each blade row to reduce flutter problems. A detailed discussion of the fan design is given in the Design Section (Section 2) of this report.

The aerodynamic design of this fan took into account the test results of a number of transonic fan rigs which were previously designed and tested at Pratt & Whitney Aircraft. The test results were used in correlating various design parameters such as airfoil aerodynamic loadings and losses, blade inlet Mach numbers, incidence angles, loss of airfoil turning, etc. Based on the results of previous rig testing, the fan root pressure ratio at design conditions was limited to 2.5:1 to retain reasonable efficiency levels. The fan was designed for a bypass ratio of 1.3:1 at the design point with a flow splitter in close proximity to the trailing edge of the second-stage blade. No inlet guide vane assembly was planned for this fan design. The design of the two-stage fan rig is illustrated by Figure 3-2.

At the end of June, rig parts had been received and were being assembled and instrumented prior to test. This delay in the test program was caused by fabrication bottlenecks encountered early in the rig procurement period. Testing will be conducted during early July.

DOWNGRADED AT 3 YEAR INTERVALS
DECLASSIFIED AFTER 12 YEARS
DOD DIR 5200.10

PAGES NOT FILMED ARE BLANK.

2. AEROELASTICITY INVESTIGATIONS

During Phase II-B, it was planned to use a single-stage fan rig for the investigation of aeroelasticity phenomena and flutter problems. Two single-stage fan designs, based on the TS4 blade, were tested during the current phase. In addition, rotating tests were conducted on small-scale rubber models to substantiate theories of fan blade flutter.

During Phase II-A, a single-stage fan rig was used to study various possibilities for stress reduction in the fan blades. One of the fan configurations which was tested at that time incorporated mid-span shroud segments that were welded together at alternate blade gaps, as shown in Figure 3-3, to reduce the possibility of a disk-blade-shroud coupled vibration mode. After a preliminary survey of blade stresses at part speed and operation for about one hour at design speed, a change was observed in the stress pattern, and the rig was shut down for inspection. Cracks were found in two of the welded shrouds. However, the blades showed no tendency toward flutter.

Based on the results of this preliminary test, it was decided to evaluate a more carefully constructed fan stage utilizing the so-called paired-welded shroud configuration. During Phase II-B, work was begun on modification of the single-stage fan rotor incorporating TS4 blades having a root thickness-to-chord ratio of seven percent and paired-welded shrouds.

In order to provide a baseline for comparison, another single-stage fan rotor was assembled incorporating TS4 blades having a conventional shroud configuration and a root thickness-to-chord ratio of nine percent. When this rotor was tested, a premature failure occurred in the region of the blade shroud. Cause of the failure was determined to be a manufacturing error and unrelated to flutter. The limited test results before failure, however, showed no specific tendency of the nine-percent root thickness blades to flutter.

In further support of the aeroelasticity investigations, small-scale rubber models of a typical shrouded compressor rotor were built and evaluated in rotating vibratory tests. It was found that the disk and shroud modes are characterized by modes along diametral lines. Figure 3-4 shows this type of vibration in a rubber model operating in severe resonance. These tests were conducted to gain a more complete understanding of this complex vibration.

DOWNGRADED AT 3 YEAR INTERVALS
DECLASSIFIED AFTER 12 YEARS
DOD DIR 5200.10

THIS DOCUMENT CONTAINS INFORMATION AFFECTING THE NATIONAL DEFENSE OF THE UNITED STATES WITHIN THE MEANING OF THE ESPIONAGE LAWS, TITLE 18, U.S.C., SECTIONS 793 AND 794. THE TRANSMISSION OR THE REVELATION OF ITS CONTENTS IN ANY MANNER TO AN UNAUTHORIZED PERSON IS PROHIBITED BY LAW.

The results of the tests on rubber models and associated mathematical analysis have strengthened the theory that the flutter condition is the result of an interaction between the aerodynamic system (aerodynamic forces on the blade) and the elastic system (inertial and elastic forces in the disk, blade and shroud). Under flutter conditions, the interaction between the air and the structure is such that the air supplies oscillatory energy to the blade during each cycle of motion of the elastic system. Consequently, a small air disturbance quickly produces a blade vibration of large amplitude.

In order to amelioriate this situation, it was necessary to modify the elastic system in such a way as to alter the fundamental mode shape and reduce the torsional amplitude in relation to the bending amplitude at the blade tip. This was accomplished by cutting back alternate shroud contact surfaces to preclude contact during operation and welding the remaining shroud contact surfaces together. In this way, the shroud continuity was destroyed, thus preventing the "snaking motion" which induces the coupled flutter through the shroud, while the welds provide sufficient torsional stiffness to prevent torsional flutter.

Figure 3-5 shows the reduced "snaking motion" of a rubber model incorporating this segmented shroud. A close-up of a full-scale rotor incorporating the segmented or paired-welded shroud concept is shown in Figure 3-6.

Substantiation of the flutter-free potential of the paired-welded shroud concept was provided by the test of a full-scale rotor. This fan stage utilized TS4 blades having a root thickness-to-chord ratio of seven percent and a paired-welded shroud. This rotor was operated for approximately 5 hours at speeds up to the design value with no indication of coupled flutter in the blades and with stresses less than ± 5,000 psi at the leading edge of the blade root over the entire operating range. The original blade configuration for this stage encountered coupled flutter just above the design point at 100% speed with stresses in excess of ±15,000 psi at the root leading edge.

3. MULTISTAGE COMPRESSOR

Development testing of the five-stage variable-geometry compressor during Phase II-B of the contract was a continuation and extension of the work that was done during Phase II-A. Three configurations of the five-stage rig were built and tested during Phase II-A. Build three, the last configuration tested during Phase II-A, achieved an airflow capacity that was 99.7 percent of the desired flow and a design-point surge margin of 5.8 percent.

Build four of the five-stage rig, initiated at the beginning of Phase II-B, incorporated modifications that were directed toward an increase in work level and efficiency, while continuing the high solidity configuration. Compared to build three, the trailing edges of the first-stage rotor blades were overcambered ten degrees at the root and five degrees at the tip, and the trailing edges of the fifth-stage rotor blades were overcambered seven degrees across the full span.

Testing of build four was terminated after 29 hours of operation when a rapid increase in linear vibration and stress level was observed during a slow acceleration to 105 percent of design speed. Subsequent disassembly and inspection revealed a failure of the rear seal retaining ring resulting in minor damage to the fifth-stage blades.

Analysis of the test data verified that build four successfully demonstrated an increase in high-speed surge pressure ratio. Figure 3-7 compares the performance of build four with that of build three from the previous Phase II-A. At the design speed of 7580 rpm, the surge pressure ratio for build four was 4.62:1 compared to 4.52:1 for build three. The design point efficiency for build four decreased from that of build three, but at least two percent of this reduction is attributed to the additional instrumentation in the flow path of the build four configuration. The test was terminated before the variable-stator-vane schedule had been optimized; as a result, the ultimate performance potential of build four was not fully evaluated.

Internal instrumentation in build four of the compressor rig included leading edge total temperature and total pressure probes on all stators at seven radial locations, and outer-wall static pressure taps at the leading and trailing edges of all stators. Test data from this instrumentation were recorded at all performance points.

[redacted]

Analysis of the interstage data showed that the work level of both the first and fifth stages was increased as planned. The effect of overcambering the first-stage rotor blades was greater than expected resulting in a stalled incidence in the first-stage stator and second stage rotor. This condition, in turn, caused increased choking and reduced efficiency in the third and fourth stages. The fifth stage responded as expected to the changes that were made; the test data showed increases in both work level and efficiency. Spanwise data disclosed a local choking condition at the root of the first-stage rotor resulting in a pressure-rise defect at the root which carried through all stages.

In order to alleviate the deficiencies of build four, the following modifications were made.

- The trailing edges of the inlet guide vanes were uncambered ten degrees at the root to zero degrees at the tip to relieve the first-stage rotor root choking.
- The trailing edges of the first-stage rotor blades were uncambered five degrees at the root, three and one-half degrees at the mean radius, and two degrees at the tip to correct the first-stage stator stalling incidence.
- The leading edges of the second-stage rotor blades were overcambered zero degrees at the root, three degrees at the radius of the first-stage rotor shroud, and zero degrees at the tip to match the spanwise incidence profile.
- The leading edges of blades in stages three, four, and five were overcambered to eliminate choking in the second-, third-, and fourth-stage stators.

After reassembly, the compressor incorporating the modifications described above was designated as build five.

Testing of build five showed that its performance was slightly superior to build four as shown in Figure 3-8. The airflow at 95 percent of design speed was increased by 3 percent and the efficiency increased approximately 1 percent. At 100 percent of design speed the performance was unchanged Test time on this build amounted to approximately 15 hours.

DOWNGRADED AT 3 YEAR INTERVALS
DECLASSIFIED AFTER 12 YEARS
DOD DIR 5200.10

An analysis of the interstage data revealed that the second stage was operating in the stalled condition and hence at the low efficiency level. This could be corrected with a stagger change of the first stage stator. This change could result in a further increase in performance.

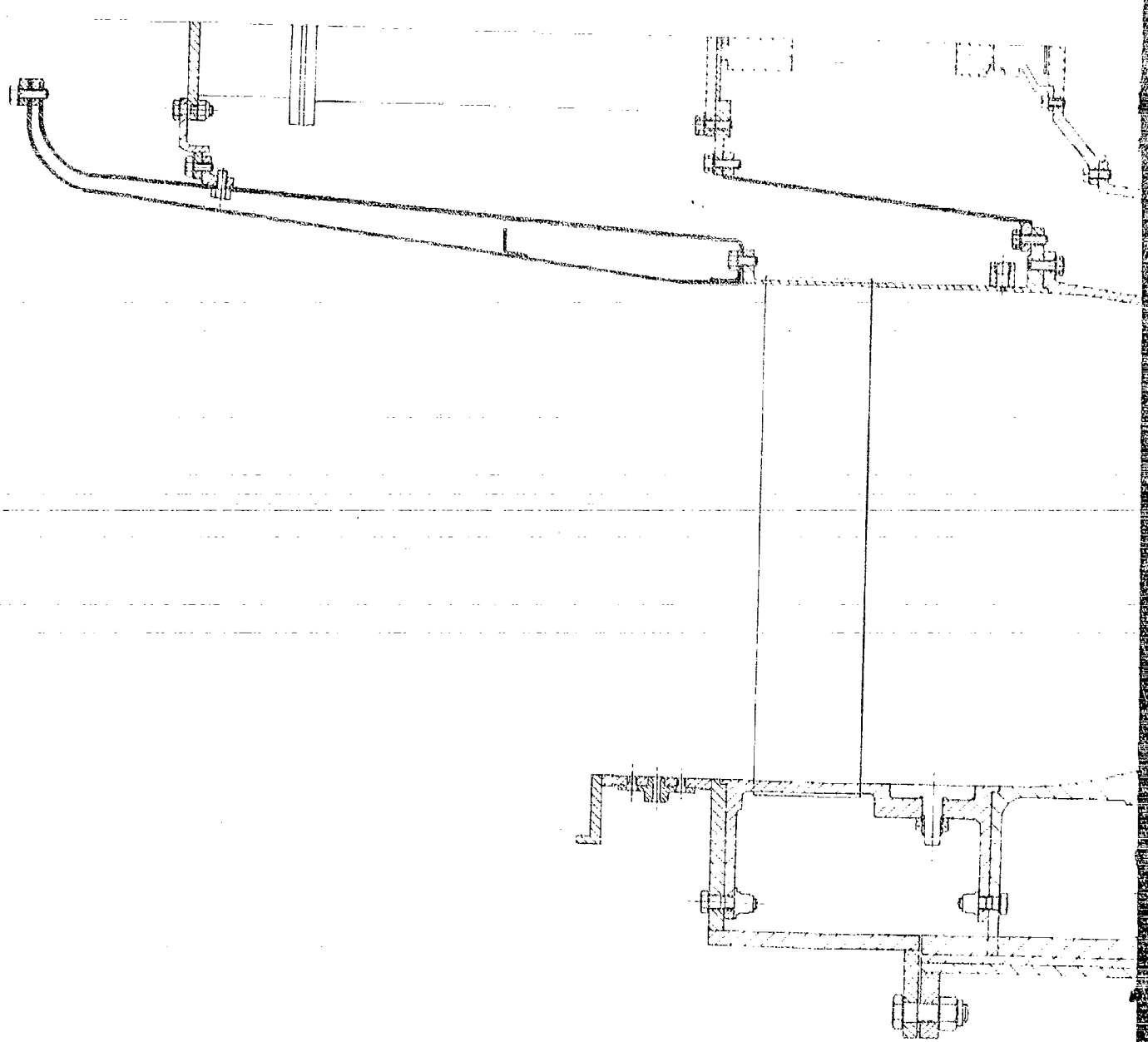
In summary, an improvement in efficiency and airflow was accomplished relative to the previous builds of this compressor. This completes the planned test program of this five-stage compressor rig.

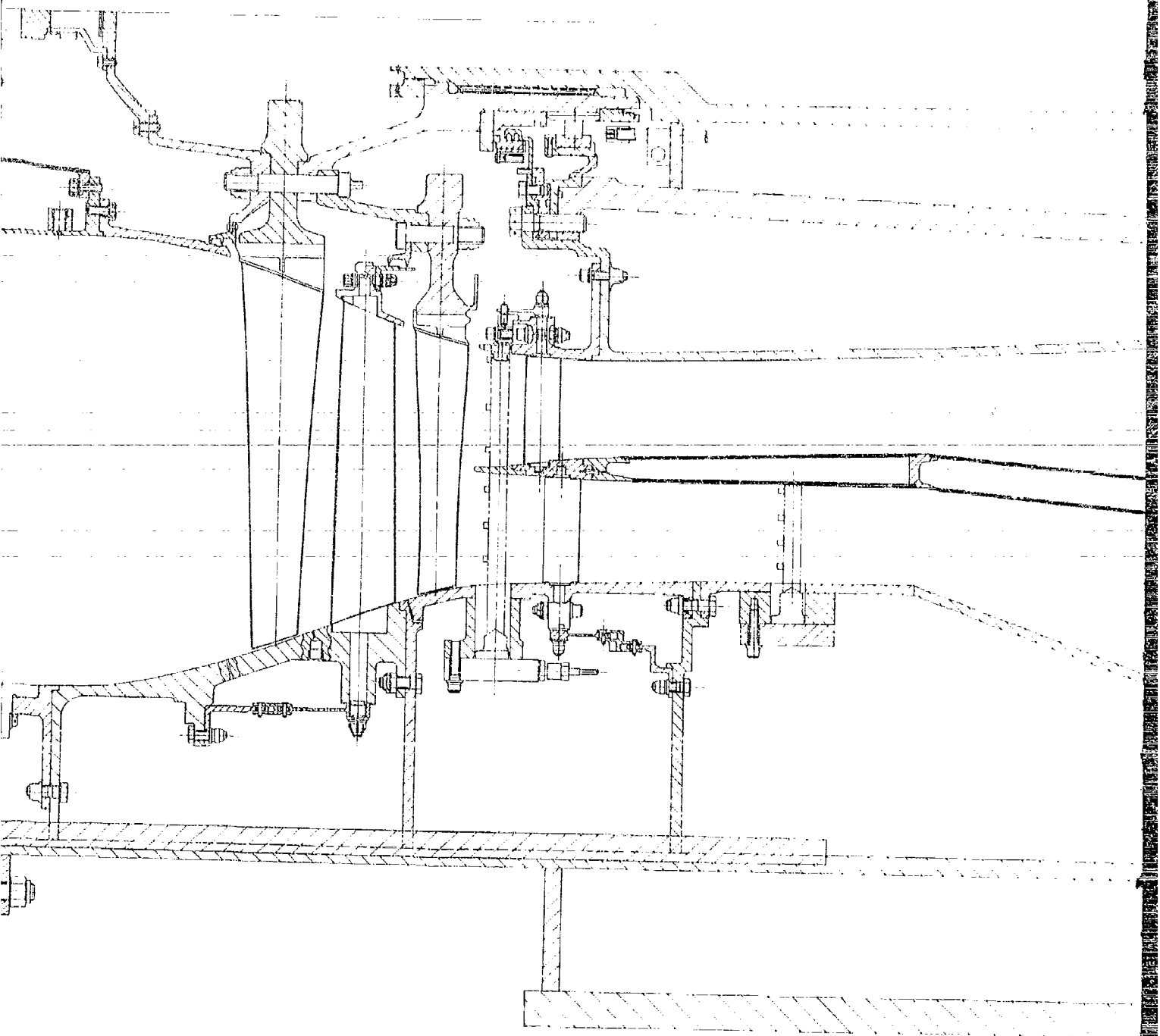
DOWNGRADED AT 3 YEAR INTERVALS
DECLASSIFIED AFTER 12 YEARS
DOD DIR 5200.10

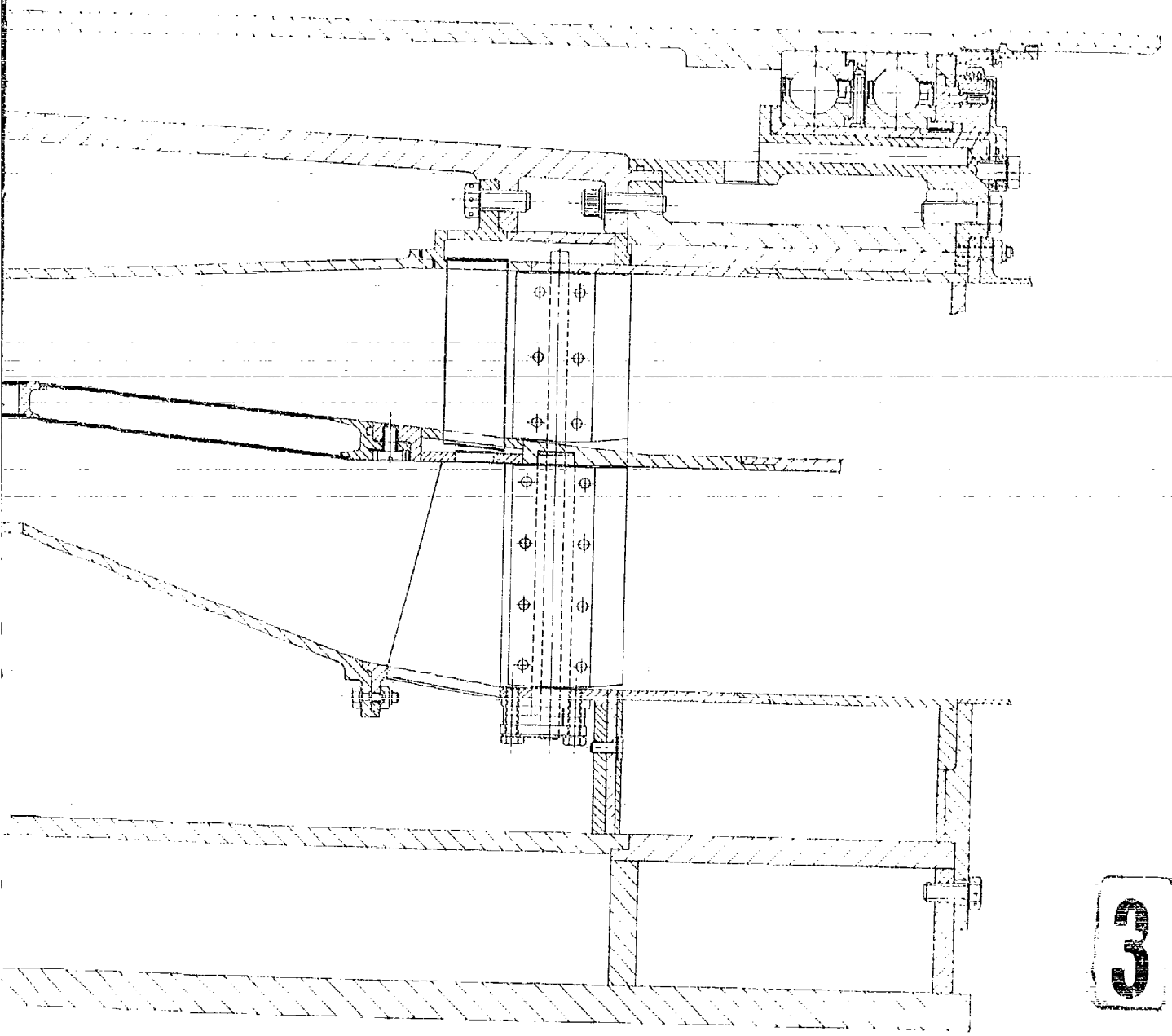
TWO-STAGE FAN DESIGN SPECIFICATIONS

FIRST-STAGE ROTOR	Root Section	Tip Section
Pressure Ratio	1.600	1.720
Blade Loading, ΔP/Q	0.732	0.434
Inlet Relative Mach No.	0.774	1.560
Gap-Chord Ratio	0.460	0.882
Thickness-Chord Ratio	0.086	0.030
Tip Speed, ft/sec	1550	-
FIRST-STAGE STATOR		
Vane Loading, ΔP/Q	0.458	-0.013
Inlet Mach No.	0.784	0.634
Gap-Chord Ratio	0.525	0.893
Thickness-Chord Ratio	0.060	0.086
SECOND-STAGE ROTOR		
Pressure Ratio	1.720	1.710
Blade Loading, ΔP/Q	0.675	0.552
Inlet Relative Mach No.	0.883	1.400
Gap-Chord Ratio	0.475	0.705
Thickness-Chord Ratio	0.086	0.0315
SECOND-STAGE STATOR		
Vane Loading, ΔP/Q	0.492	0.373
Inlet Mach No.	0.852	0.690
Gap-Chord Ratio	0.500	0.653
Thickness-Chord Ratio	0.050	0.070
FAN EXIT GUIDE VANE		
Vane Loading, ΔP/Q	0.591	0.330
Inlet Mach No.	0.614	0.330
Gap-Chord Ratio	0.502	0.617
Thickness-Chord Ratio	0.070	0.070
OVERALL PERFORMANCE	Engine Section	Fan Duct Section
Pressure Ratio	2.50	2.71
Design Efficiency, %	86.4	80.0

Figure 3-1







3

DESIGN LAYOUT OF TWO-STAGE FAN RIG

Figure 3-2

DOWNGRADED AT 3 YEAR INTERVALS
DECLASSIFIED AFTER 12 YEARS
DOD DIR 5200.10



DETAIL OF SINGLE-STAGE FAN ROTOR ASSEMBLY WITH WELDED MID-SPAN SHROUDS (PHASE II-A)

Figure 3-3

DOWNGRADED AT 3 YEAR INTERVALS
DECLASSIFIED AFTER 12 YEARS
DOD DIR 5200.10

THIS DOCUMENT CONTAINS INFORMATION AFFECTING THE NATIONAL DEFENSE OF THE UNITED STATES WITHIN THE MEANING OF THE ESPIONAGE LAWS, TITLE 18, U.S.C., SECTIONS 793 AND 794. ITS TRANSMISSION OR THE REVELATION OF ITS CONTENTS IN ANY MANNER TO AN UNAUTHORIZED PERSON IS PROHIBITED BY LAW.



RUBBER MODEL OF TYPICAL SHROUDED COMPRESSOR ROTOR OPERATING IN SEVERE RESONANCE

Figure 3-4



TEST OF RUBBER MODEL OF COMPRESSOR ROTOR INCORPORATING SEGMENTED SHROUD

Figure 3-5

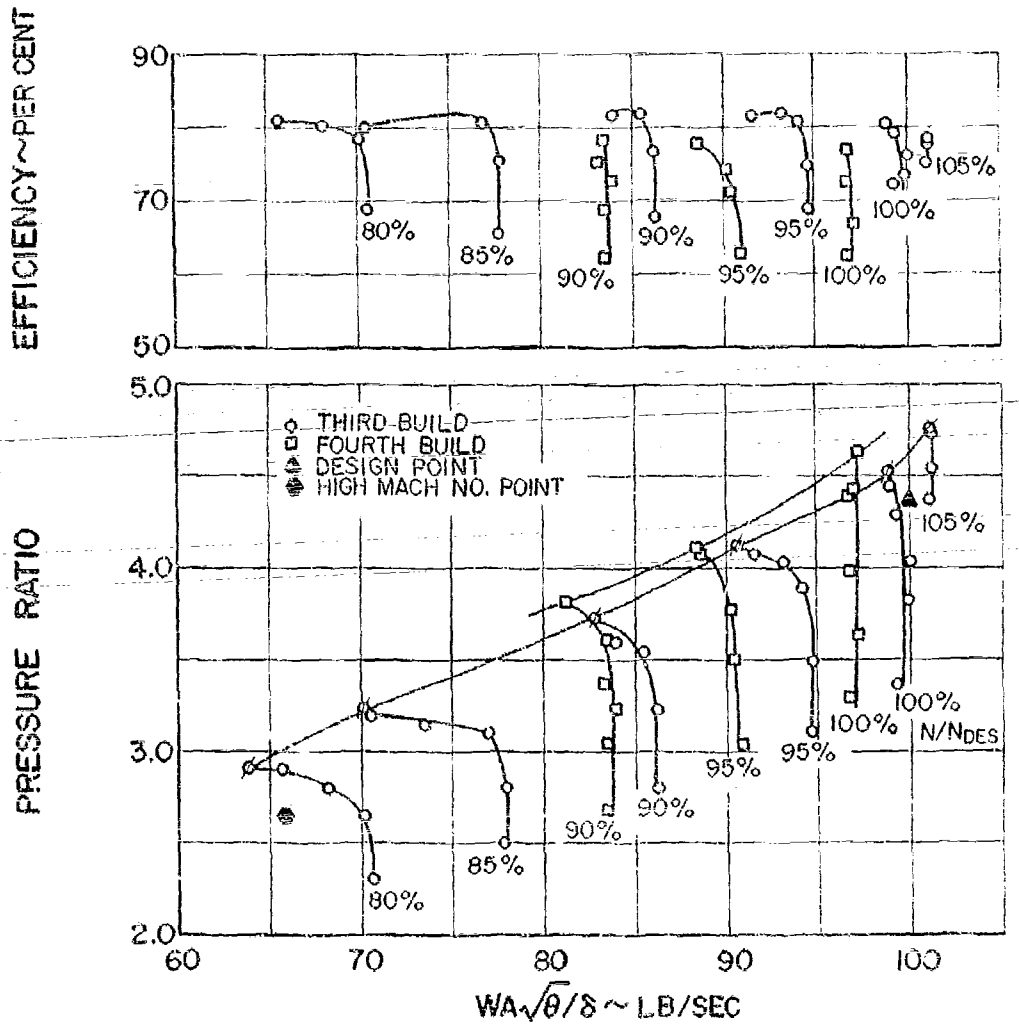
DOWNGRADED AT 3 YEAR INTERVALS
DECLASSIFIED AFTER 12 YEARS
DOD DIR 5200.10



DETAIL OF SINGLE-STAGE FAN ROTOR ASSEMBLY WITH PAIRED-WELDED MID-SPAN SHROUDS (PHASE II-B)

Figure 3-6

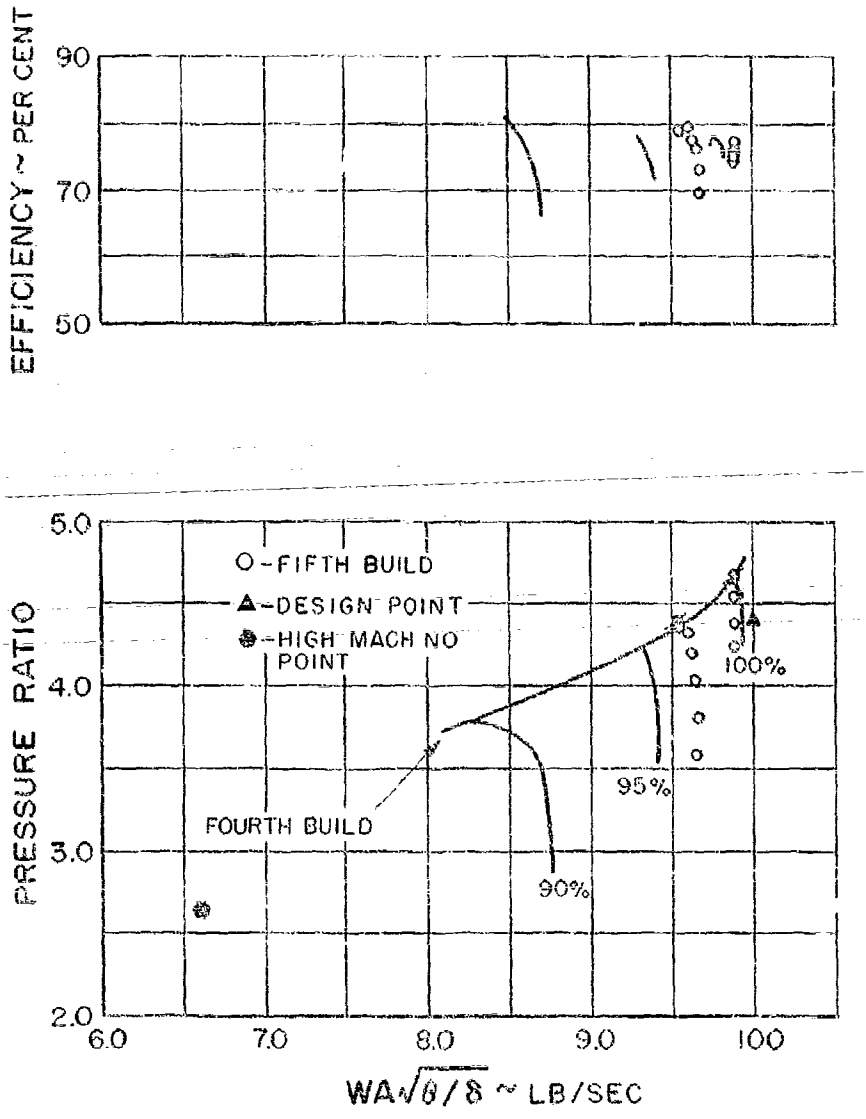
DOWNGRADED AT 3 YEAR INTERVALS
DECLASSIFIED AFTER 12 YEARS
DOD DIR 5200.10



PERFORMANCE COMPARISON OF THIRD AND FOURTH BUILDS OF THE MULTISTAGE COMPRESSOR

Figure 3-7

DOWNGRADED AT 3 YEAR INTERVALS
DECLASSIFIED AFTER 12 YEARS
DOD DIR 5200.10



PERFORMANCE COMPARISON OF FOURTH AND FIFTH BUILDS OF THE MULTISTAGE COMPRESSORS

Figure 3-8

DOWNGRADED AT 3 YEAR INTERVALS
DECLASSIFIED AFTER 12 YEARS
DOD DIR 5200.10

THIS DOCUMENT CONTAINS INFORMATION AFFECTING THE NATIONAL DEFENSE OF THE UNITED STATES WITHIN THE MEANING OF THE ESPIONAGE LAWS, TITLE 18, U.S.C., SECTIONS 793 AND 794. THE TRANSMISSION OR THE REVELATION OF ITS CONTENTS IN ANY MANNER TO AN UNAUTHORIZED PERSON IS PROHIBITED BY LAW.

ITEM 4

PRIMARY COMBUSTION

ITEM 4 - PRIMARY COMBUSTION

OBJECTIVE

This item of the contract required that Pratt & Whitney Aircraft conduct testing of engine combustor and combustor components directed toward verification of design characteristics.

The specific goals of the combustor are:

1. A heat release rate of about 5×10^6 Btu/hr/ft^3/atm.

2. A maximum pressure drop of 6% at sea level static conditions

3. A burner efficiency of 98.5%

4. Combustor exit temperature profiles with a temperature distribution parameter ΔT max/ΔT Avg not exceeding 1.11, and exit temperature profiles consistent with turbine cooling requirements.

A. INTRODUCTION

In order to achieve the low engine weight desired for economic supersonic flight, not only must the primary burner section be smaller, and thus lighter than the burner section in present production engines, but also it must provide good temperature profiles for the turbine and be satisfactory in other respects as well. Prior to receipt of the contract, Pratt & Whitney Aircraft conceived a combination diffuser and burner which was unusually short and also held promise of low pressure loss. In this concept, air is ducted from the diffuser to each hole in the burner and it is turned into the burner by an efficient elbow or by turning vanes. Since the air is only diffused to the burner hole velocity, instead of to a much lower velocity, much of the required diffuser length is eliminated, and some of the diffuser loss is also avoided. This concept, referred to as ram induction because the velocity head of the air carries it into the burner, appeared to provide an excellent solution to the problem of shortening the burner section while maintaining or improving all other characteristics. Consequently, the

DOWNGRADED AT 3 YEAR INTERVALS
DECLASSIFIED AFTER 12 YEARS
DOD DIR 5200.10

primary burner effort under this contract has been directed towards investigating and developing this concept for application to the SST engine. Tests were also conducted on numerous other burner configurations to investigate combustor characteristics. These tests were conducted using a two-dimensional segmented annular burner rig and a full-annular burner rig. The testing conducted under this contract has led to the conclusions presented in the following paragraphs.

As with the tests during Phase II-A, those changes which had to do with front-end fuel-air amount, mixing location, etc., had the greatest effect on burner performance. Their overall effect has been to reinforce the knowledge that the annular burner is "front-end" sensitive and that this is the area where the emphasis of any subsequent work should be directed.

The ignition capabilities of the present liquid-injection burner are very good and should not present problems in subsequent engine testing. In addition, the operating range of the annular burner is so wide as to present no problems in any sea level engine tests that might be considered at the present time.

No great changes in ΔTVR were obtained from the full-annular rig even even with extreme changes in the radial inlet pressure profile. This is, or course, dependent on the hole pattern so that this insensitivity will have to be demonstrated for any burners developed in the future.

Changes in burner length have not shown corresponding changes in burner performance or temperature distribution. This may be due to the non-optimized hole pattern used in the "long" configuration.

A low overall pressure loss of 6.3 percent at .288 WA $\sqrt{T}$/APt at the diffuser inlet has been achieved without sacrificing other burner performance characteristics.

The follow-on statistical program produced two principal conclusions: (1) increasing the front-end airflow (above those limits attained in Phase II A) decreases ΔTVR and (2) the first row O.D. holes should be in line with the fuel nozzle.

The hot-cone burner has continued to show promise. Removal of the fuel-air reduction lip decreased ΔTVR substantially.

DOWNGRADED AT 3 YEAR INTERVALS
DECLASSIFIED AFTER 12 YEARS
DOD DIR 5200.10

The partial-annular configuration has demonstrated that producing a discrete primary combustion zone around each nozzle, this burner attains a very low ΔTVR.

As stated previously, the goals appear reasonable. Comparison of the attained performance with the goals shows that the burner ΔTVR goal has not yet been attained. It was expected that this would require extensive work and, with the gains made thus far, appears certain to be realized.

B. DESCRIPTION OF BURNER SECTION

The burner section has remained essentially the same as it was during Phase II A. Physically, the main burner section encompasses the area from the compressor exit to the turbine inlet and includes the diffusing section and burner liner. Figure 4-1 is a sketch of the burner section. The combustion chamber (burner) and diffuser overlap axially with the front end of the burner forming the inner walls of the diffusing passages. This provides a minimum overall length for the burner section.

The diffuser section is split into three airflow passages, the outer and inner annuli which diffuse the main airflow into the shroud passages, and the center section which provides air to the swirlers. Once diffusion is accomplished in the inner and outer annuli, the air flows from the respective shrouds into the liner with an axial airflow distribution determined by the hole pattern.

C. DESCRIPTION OF RIGS

1. TWO-DIMENSIONAL ANNULAR SEGMENTAL RIG

One of the principal rigs used for annular burner evaluation was the two-dimensional burner rig. This is the same rig used during Phase IIA and, as the name implies, is two-dimensional as opposed to the annular segment design of previous segmental burner rigs. Figure 4-2 indicates how the removable top and bottom covers allow for easy access to the burner liner. In addition to being able to space the rig covers inward or outward for varying shroud areas, the diffuser walls are removable. The extreme flexibility of this rig allowed the screening of many new and different annular burner configurations with a minimum of effort.

DOWNGRADED AT 3 YEAR INTERVALS
DECLASSIFIED AFTER 12 YEARS
DOD DIR 5200.10
THIS DOCUMENT CONTAINS INFORMATION AFFECTING THE NATIONAL DEFENSE OF THE UNITED STATES WITHIN THE MEANING OF THE ESPIONAGE LAWS, TITLE 18, U.S.C., SECTIONS 793 AND 794. ITS TRANSMISSION OR THE REVELATION OF ITS CONTENTS IN ANY MANNER TO AN UNAUTHORIZED PERSON IS PROHIBITED BY LAW.

A sketch of the test setup may be seen in Figure 4-3. A heat exchanger presents hot unvitiated air to the burner section and inlet pressure and temperature instrumentation is used to determine the Mach number of the approach air. A temperature-pressure rake at the rectangular burner exit is used to determine burner exit conditions.

2. LARGE-SCALE FULL-ANNULAR BURNER RIG

The large-scale full-annular burner rig incorporates appropriate engine hardware. Figures 4-4, 4-5, and 4-6 show the rig in various stages of assembly. Removable spacer sections allow for burners of various lengths to be tested. This is the same rig that was used in Phase II A.

Figure 4-7 is a schematic of the rig. The rotating temperature pressure rake makes for easy determination of burner exit conditions. Instrumentation is similar to that of the two-dimensional segmental rig, and determination of pressure loss, burner efficiency, and burner ΔTVR are made in the same manner.

3. RAM INDUCTION PRIMARY BURNER RIGS

Two combustion test rigs have been used in this investigation.

The first test rig is a straightened 72° segment of an annular burner. The burner segment is approximately 24 inches wide, and uses a length of approximately 29 inches to perform the diffusion and burning accomplished in approximately 52 inches with conventional diffuser and burner can designs. Figure 4-8 shows a typical burner liner for this rig.

The second test rig is a burner development rig for the STF219 engine. It is a curved, 120° sector and incorporates engine flow geometry from compressor discharge to turbine inlet. The rig design is based on the 600 lb/second size engine des .

The two rigs are similar as regards stand installation, instrumentation and method of test. A description of associated hardware for the 72° straight sector rig is presented herein as representative of the two rigs. The 72° straight sector test rig, shown in Figure 4-9 consists of the following components: air inlet section, venturi, heater burner, transition section, instrumentation section, and main

DOWNGRADED AT 3 YEAR INTERVALS
DECLASSIFIED AFTER 12 YEARS
DOD DIR 5200.10

burner support section. The rig air is supplied by bleeding air from the compressor of a turbojet slave engine.

D. TEST DESCRIPTION AND RESULTS

1. TWO-DIMENSIONAL ANNULAR SEGMENTAL BURNER RIG TESTING

a. Statistical Test Program Follow-on

During Phase II A, in an attempt to optimize the burner as quickly as possible and at the same time to determine some firm design information, a statistically-designed program was run. The basic parameters investigated were:

pressure loss
hole area distribution
number of holes per row in each of 5 rows
axial location of each of 5 rows.

The results of this program were reported in the Phase II A final report. In order to build upon this initial knowledte and further optimize the burner, a study was made of the effects of combustion hole stagger relative to the fuel nozzles. The effects of hole area distribution and number of holes per row were also studied. A total of 215 hours of testing were conducted on this rig during Phase II B.

Results of this program led to these conclusions.

1. The first row O. D. holes showed a significant preference to be lined up with the fuel nozzles.

2. The data indicated that the lowest value of ΔTVR has the first row of holes in line with the fuel nozzles and the second row of holes out of line.

3. There was no significant difference between six and nine holes in the first row.

b. Lighting Tests

Initial lighting tests on JP-4R and JP-5 fuel were done on the 2-D annular burner rig. The burner used in the 2-D rig was the same as that

DOWNGRADED AT 3 YEAR INTERVALS
DECLASSIFIED AFTER 12 YEARS
DOD DIR 5200.10

used in the full-annular tests. It also had 3 O.D. ribs and 1/2 blocked co-rotating swirlers. However, the cooling was less than that used in the full-annular burner. The fuel nozzles and igniter were the same type as would be used in the engine and in the full-annular rig. The igniter was immersed .34 inches.

Starting tests on the 2-D burner rig were conducted in much the same manner as those on the full-annular rig. The same type of instrumentation was used on the 2-D rig to record "fuel on" to full light times.

Test conditions were as follows:

Inlet Air Temperature:	ambient and 100-150°F
Inlet Total Pressure:	17 psia
Burner Inlet M_n:	.14, .20, .29

Figure 4-10 shows the minimum fuel-air ratio required to light this burner. As with the full-annular rig results, lighting times have been included. Because of the unrealistically long time required for the 2-D fuel manifold to fill, a 20-second light line has been drawn on Figure 4-10 in addition to the 10 second light line. The 20 second line compares quite favorably to the 10 second light line for the full-annular rig. In addition to JP-5 fuel, tests were also run with JP-4. The results of the JP-4 tests are also shown on Figure 4-10

c. Partial Annular Burner

A schematic of this burner may be seen in Figure 4-11 and photographs are presented in Figure 4-12. The major feature of this configuration is the extreme depth of the swirl cups which allows for good mixing and flame stabilization in the primary combustion zone. Air is introduced much closer to the center of the burner at fuel nozzle tangencies than with the standard liquid injection annular configuration. At the 667°F inlet (a realistic SST point) the ΔTVR at 1440° ΔT was 1.25.

d. Hot-cone Burner

Another version of the 2-D SST burner incorporates a hot-cone feature in the front-end to pre-mix and partially vaporize the fuel prior to injection into the combustion chamber. Figure 4-13 shows a cross-section of this burner. About 10 percent of the engine airflow is admitted to the hot-cone section through holes in the blunt leading edge

DOWNGRADED AT 3 YEAR INTERVALS
DECLASSIFIED AFTER 12 YEARS
DOD DIR 5200.10

of the burner, as shown by (1) of Figure 4-13. Half of this air is admitted through swirlers (2) to the vaporizing passages along with the fuel. The rich mixture (F/A~ 0.4) in this passage allows mixing and vaporization of the fuel but prevents combustion upstream of the cone because the mixture is too rich to burn. This partially vaporized fuel-air mixture is then injected into the combustion region downstream of the cone through holes (3). The remainder of the air taken in through the blunt leading edge section is injected into the recirculation zone through additional holes (4). Ignition is provided in the recirculation region and additional combustion and dilution air is injected through holes in the liner walls to provide the desired temperature pattern and to provide liner cooling. This additional air represents the bulk of the engine airflow which flows through the inner and outer diffusing passages into the liner shroud areas.

This burner was discussed in some detail in the SST Phase II A final report. Recent tests have been made with the fuel/air redirection lip removed entirely. This has produced a fairly good reduction in Δ TVR from the previous configurations run. Evidently, with the fuel-air redirection lip removed, the slot-feed air was allowed to also mix with the fuel before introduction into the burner front-end. The addition of this air apparently produced better initial combustion conditions at the burner front-end. The extreme number of variables present in the hot-cone burner have made this a slow item to develop.

2. LARGE-SCALE FULL-ANNULAR BURNER RIG TESTING

a. Inlet Profile Effect

A test series was run on the full-annular burner rig for the purpose of evaluating the effect of inlet pressure profile on annular burner performance. Results of the tests indicate that the subject burner is fairly insensitive to inlet profile and, in fact, produces a lower Δ TVR with an I.D. peaked profile. A total of 131 hours of testing were conducted on this rig during Phase II B.

Figure 4-14 shows the location of various trips and Figure 4-15 shows the inlet pressure profile attained for each run.

Figure 4-16 shows the effect of inlet profile on the minimum and average segmental Δ TVR's. With the clean inlet as a baseline, it appears that the upstream I.D. trip hurt the Δ TVR slightly while the I.D. downstream and O.D. upstream trips both seemed to lower the Δ TVR - especially at the 800 to 1100°F Δ T points.

DOWNGRADED AT 3 YEAR INTERVALS
DECLASSIFIED AFTER 12 YEARS
DOD DIR 5200.10

There are many possible reasons for the improvement of Δ TVR with a profile change. One basic reason may be the flow spreading effect of a ramp type trip. This may tend to distribute the airflow more evenly around the burner and offset any detrimental effects of an uneven I. D. to O. D. split. Another possibility is that with increased airflow to one side or the other, the burner pressure loss has actually been increased sufficiently to produce a better Δ TVR.

(1) Burner Exit Temperature Profile

It was assumed that the change in burner inlet pressure profile would drastically affect the burner exit temperature profile. Figure 4-17 is a curve of the selected runs - each with a different inlet profile showing the effect on exit temperature. Obviously, the effect of temperature rise on profile is as great as the effect of inlet profile. In order to obtain a better analysis of the data, Figure 4-18 was prepared. This curve shows the change in local Δ T with average Δ T. Surprisingly, the I. D. downstream trip caused a heating of the profile tip. It would seem logical that the increased O. D. flow would cool rather than heat the tip. On closer observation, it appears that the midspan was cooled, indicating better penetration of the air which would tend to heat the extremes of the profile. The I. D. was heated by the I. D. trip, as expected.

The O. D. trip which increased airflow to the I. D. (or root) caused a heating of the tip, a cooling of the midspan and very little reaction at the root of the exit profile. The resultant profile, except for the cold root was more in line with the desired profile than any of the other runs.

(2) Burner Pressure Loss

The airflow distortions have produced an apparent increase in burner pressure loss, thereby decreasing Δ TVR through the resultant increase in penetration and mixing.

It should be noted that the above is an overall pressure loss obtained using the average diffuser inlet total pressure. Because there was almost certainly separated flow with some of the trips, there is some question as to the true inlet total pressure.

DOWNGRADED AT 3 YEAR INTERVALS
DECLASSIFIED AFTER 12 YEARS
DOD DIR 5200.10

(3) Conclusions

The following conclusions may be drawn from the results obtained during the inlet pressure profile studies.

Δ TVR was not adversely affected by a profile change.

Burner exit temperature profile was favorably altered with the I. D. peaked profile.

The burner exit isothermal plot was not affected by the changing inlet pressure profile.

b. Operating Range

A test program was conducted in order to determine the operating range (lean blowout and rich blowout) of the basic burner.

(1) Description of Hardware

The burner used in the full-annular rig had half blocked swirlers (co-rotating), 3 O. D. ribs, and all keyhole slots welded on the I. D. The hole-pattern was the same as developed in the 2-D rig.

Dual orifice fuel nozzles were used. The igniters (2) were Champion AA635-A (20 joule) and were immersed about .84 inches into the burner (see Figure 4-19).

(2) Test Description and Results

Operating range tests were run on the full-annular rig in order to determine the lean and rich limits of the burner. For this test, various inlet air temperatures and liner Mach numbers were set, the burner lit, and the fuel flow increased until a rich blowout condition occurred. For the lean blowout points, the fuel flow was decreased until the flame went out.

These points are also plotted on Figure 4-20. It should be noted that no rich or lean blowout points were encountered. The rich limits recorded were stand limits. At that point the stand exit stack became too hot and precluded further testing. At no time was there any indication of roughness or instability and it appears certain that the rich blowout limit was by no means even approached.

DOWNGRADED AT 3 YEAR INTERVALS
DECLASSIFIED AFTER 12 YEARS
DOD DIR 5200.10
THIS DOCUMENT CONTAINS INFORMATION AFFECTING THE NATIONAL DEFENSE OF THE UNITED STATES WITHIN THE MEANING OF THE ESPIONAGE LAWS, TITLE 18, U.S.C., SECTIONS 793 AND 794. THE TRANSMISSION OR THE REVELATION OF ITS CONTENTS IN ANY MANNER TO AN UNAUTHORIZED PERSON IS PROHIBITED BY LAW.

The low limits reported were also due to stand limits because the flowmeters at the test stand do not go to a zero flow condition. Their physical limit set the lean limit. At all minimum recorded fuel flows, the burner was only partially lit. That is, perhaps only 1 or 2 fuel nozzle segments were burning. There was no flame visible, yet, when the fuel flow was increased only slightly, the flame propagated through the entire burner. This was not a "glow plug" reaction - not ignition due to hot walls or a hot plug, but due to a flame already present in the burner. Note that the extinction of the flame on even half of the fuel nozzles is not considered as a true low blowout point. As long as the burner is able to repropagate (without igniter aid) with fuel flow increase, the low blowout point has not been reached.

c. Lighting Tests

A test series was run on the full-annular burner rig to determine the lighting capability JP-5 fuel. Hardware was the same as described above.

Instrumentation was set up to record elapsed time between "fuel on" to full light. This method gives a slightly pessimistic indication since there is some finite fuel manifold fill-up time required, especially at the low flow-low pressure conditions that were run. Thermocouples in the air stream at the burner exit gave an indication of burner ignition and propagation.

Figure 4-21 shows the minimum fuel-air ratio required to light the basic burner. Lighting times are noted next to the data point. The full light line has been drawn through the 10-second light points and is intended only as a guide. The no-light points indicated were aborted after 12 seconds - an extremely short time. It appears that the minimum lighting line may be extended to a much lower level without too great an increase of lighting time. It should be noted that this is lighting time, fuel on to full light. Propagation time, the time from first light to full light was virtually instantaneous at all lighting points, on the order of 0.1 to 0.2 seconds, indicating no crossover problem whatsoever.

3. RAM INDUCTION PRIMARY BURNER RIG

The test results for this program are categorized by burner model number, and include a description of each burner.

DOWNGRADED AT 3 YEAR INTERVALS
DECLASSIFIED AFTER 12 YEARS
DOD DIR 5200.10

b. Model 2

(1) Description of Burner

Five modifications of the Model 2 primary burner have been tested. This configuration simulates a straightened 72 degree arc of an annular primary burner and incorporates eight fuel nozzles. The burner segment is approximately 24-inches wide and 28-inches long. The burner forms an integral part of the diffuser with its nose lying within 1.4 inches of the compressor exit. The diffusing and burning are accomplished in approximately 29 inches as compared with about 56 inches for the conventional diffuser and burner designs.

The Model 2-1 is shown in Figure 4-22. The secondary scoops are cut back to 2 inches from the burner centerline. Turning vanes are incorporated in these scoops. The airflow distribution is as follows for all of the Model 2 liners.

Model	2-1	2-2, 2-3	2-4, 2-6	2-5	2-7
Nozzle swirlers	8%	8%	10%	10%	10%
Primary cooling slots	4%	4%	4%	4%	4%
Primary scoops					
Short	7.3%	7.3%	7.3%	6.3%	6.3%
Medium	7.3%	7.3%	7.3%	6.3%	6.3%
Long	7.3%	7.3%	7.3%	6.3%	6.3%
Secondary cooling slot	12%	8%	8%	12%	12%
Dilution scoops	42%	42%	42%	39%	39%
Rear cooling slot	8%	12%	12%	10%	12%
Bypass cooling slot	4%	4%	2%	6%	4%

The Model 2-2 has the rear scoops cut back to 3 inches from the centerline and the turning vane has been removed. This was done in order to reduce the penetration of the dilution air, and to reduce the pressure loss. High temperatures were noticed on the Model 2-1 transition ducts behind the secondary scoops. Therefore, the transition cooling strip was doubled, and the gaps between the secondary scoops were closed by welding a piece of sheet metal behind the scoops.

Turning vane type secondary scoops have replaced the rear scoops in the Model 2-3. A lower pressure loss was the objective of this modification. The airflow distribution is the same as in the Model 2-2.

DOWNGRADED AT 3 YEAR INTERVALS
DECLASSIFIED AFTER 12 YEARS
DOD DIR 5200.10

THIS DOCUMENT CONTAINS INFORMATION AFFECTING THE NATIONAL DEFENSE OF THE UNITED STATES WITHIN THE MEANING OF THE ESPIONAGE LAWS, TITLE 18, U.S.C., SECTIONS 793 AND 794. THE TRANSMISSION OR THE REVELATION OF ITS CONTENTS IN ANY MANNER TO AN UNAUTHORIZED PERSON IS PROHIBITED BY LAW.

The Model 2-4 burner is the result of adding a round nose dome assembly with slots across the nose to the Model 2-2 in order to make the burner can less sensitive to the inlet provile.

The round nose dome assembly with slots was put on the Model 2-3 resulting in the Model 2-5. The primary zone has been made narrower by eliminating the dome wiggle strip in order to increase the cooling gaps under the primary scoops and outside the transistion duct.

The rear most primary air scoops of the Model 2-4 were cut back to a length about one-half way between the short and middle primary scoops to make the Model 2-6. The airflow distribution is the same as the Model 2-4.

The Model 2-7 incorporates a transition duct cooling modification to the Model 2-5. A second transition cooling gap was installed by decreasing the present gap, and by decreasing the transition bypass flow gap.

The eight fuel nozzles were standard JT-11 "Vado" nozzles for the testing of Models 2-1, 2-2 and part of 2-3. Delavan fixed area nozzles were used for the remainder of the testing.

(2) Method of Test

A variety of types of tests have been used in the investigation and development of the ram induction primary burner. These have included:

Cold airflow tests of individual scoops of different designs to determine pressure loss and discharge airflow pattern.

Cold airflow testing of the complete diffuser-burner combination. These were used to determine whether the cold pressure loss and general airflow characteristics were in agreement with predictions, and for locating the source of aerodynamic difficulties.

Combustion tests were conducted in which the complete burner-diffuser combination was operated essentially as it would be operated in an engine so that the overall characteristics of the system could be measured and recorded. With the burner exhausting to the atmosphere, the inlet air pressure was increased until the desired diffuser inlet Mach number was obtained. Burner fuel was then turned on, and the burner was ignited. The fuel-air

DOWNGRADED AT 3 YEAR INTERVALS
DECLASSIFIED AFTER 12 YEARS
DOD DIR 5200.10

THIS DOCUMENT CONTAINS INFORMATION AFFECTING THE NATIONAL DEFENSE OF THE UNITED STATES WITHIN THE MEANING OF THE ESPIONAGE LAWS, TITLE 18, U.S.C., SECTIONS 793 AND 794. THE TRANSMISSION OR THE REVELATION OF ITS CONTENTS IN ANY MANNER TO AN UNAUTHORIZED PERSON IS PROHIBITED BY LAW.

ratio was increased to the desired value, and the rig inlet pressure was readjusted, if necessary, to maintain the desired inlet Mach number. At this condition, the exit cross section was traversed to determine the temperature pattern, and various pressures were measured.

Configuration changes were made and additional tests were run as necessary to improve the burner characteristics, and in particular, the temperature profile.

(3) Test Results

The testing of the Models 2-1 and 2-2 showed a poor outlet temperature profile which was traced to a poor inlet profile. The inlet profile was corrected during the testing of the Model 2-3.

Two curves were plotted for most test points - a temperature profile and a burner outlet temperature distribution. The burner outlet temperature distribution gives the temperature at 3/4-inch horizontal increments across the 24-inch width of the outlet, and at 1/2-inch vertical increments up the 4-inch height. Only the center 9 inches of the outlet has been used for determination of Δ TVR and temperature profile to eliminate side wall effects. Isotherms are drawn on the temperature distribution sheets. The temperature profile is obtained by averaging the temperature values in each row across the outlet.

Combustion efficiency is based on the complete exit traverse.

The Model 2-5 burner was tested over its entire operating range of inlet Mach numbers and temperatures, and gave excellent performance. The burner gave an extremely good exit temperature pattern during the heated inlet tests corresponding to cruise conditions. The Δ TVR for this run was 1.07. Δ TVR at sea level take off conditions was approximately 1.15.

Three tests were completed on the Model 2-7 burner. Figure 4-23 and 4-24 show the temperature pattern and radial temperature profile for a test made at simulated SLTO burner inlet conditions. The burner yielded a Δ TVR value of 1.10 at a burner temperature rise of 1867°F. This temperature rise is more than 200°F above that required in the SST engine. Figures 4-25 and 4-26 show the results of a test made at simulated cruise burner inlet conditions. Again, the burner exhibited excellent outlet temperature pattern control with a ΔTVR value of 1.10. The third test was made with an inlet Mach number of .45, and an inlet

temperature of 509°F. The results of this test are presented in Figures 4-27 and 4-28. Such conditions simulate SLTO conditions in an engine with considerably higher compressor discharge Mach number. The burner yielded a Δ TVR of 1.08. The outlet temperature was limited to 1954°F by fuel nozzle capacity. The burner appears to perform equally well at the higher value of inlet Mach number, but must suffer the higher burner pressure loss which increases approximately with the square of the inlet Mach number.

The low value of Δ TVR which was obtained during this series of tests is worthy of note. The value of 1.10 is close to the lowest, or ideal, Δ TVR which can be obtained when the exit radial temperature profile is intentionally cooled below the average temperature at the I. D. and O. D. for turbine vane, and shroud considerations.

Later testing was directed at determining the effects of compressor discharge velocity profile distortion on the outlet temperature profile of the burner. It appears that the burner is very insensitive to variations in inlet velocity profile. This is desirable because the inlet velocity profiles vary with the operating conditions of an engine. Two of the compressor discharge profiles investigated are shown in Figure 4-29. The warped profile shown in Figure 4-29 has the flow concentration farther to one side than either the sea level takeoff or high Mach number cruise profiles of a high Mach number engine, which are shown in Figure 4-29 for comparison. Figure 4-30 shows the outlet temperature profiles obtained when testing with the two inlet profiles of Figure 4-29. The two temperature profiles are essentially identical, indicating insensitivity to the inlet flow profile.

c. Model 3

The Model 3 primary ram induction burner is a parallel development effort rather than an evolution from the Model 2 design. The objectives of this design are the same as the Model 2, and are to be attained in a reduced burner length.

(1) Description of Burner

Two configurations of the Model 3 primary burner have been tested. The Model 3-1 has a length of only 21.4 inches as compared with a length of 28.1 inches for the Model 2 burner. Both the primary and secondary scoops are of the turning vane type. The Model 3-1, shown in Figure 4-31.

DOWNGRADED AT 3 YEAR INTERVALS
DECLASSIFIED AFTER 12 YEARS
DOD DIR 5200.10

Model	3-1	3-2
Nozzle Swirlers	12%	12%
Primary cooling slot	4%	4%
Primary scoops		
Short	11%	11%
Long	11%	11%
Secondary cooling slot	10%	8%
Dilution scoops		
Short	20%	20%
Long	20%	20%
Rear cooling slot	6%	8%
Bypass cooling slot	6%	6%

The Model 3-2 is a lengthened version of the 3-1. The cooling gaps are also changed so that the gap under the primary scoop is decreased and the gap under the secondary scoops is increased to an equal dimension. The airflow distribution of the Model 3-2, shown in Figure 4-32.

(2) Method of Test

The method of test for the Model 3 is the same as for the Model 2.

(3) Results

The Model 3-1 was tested at only one point (low Mach number, low fuel-air ratio). The test showed a severely center peaked outlet temperature profile, indicating that the penetration of the dilution air was insufficient for the short length of the burner.

Testing of the burner Model 3-2 showed little change in the outlet temperature profile, the profile still being center peaked.

No effort was made to improve the performance of the short Model 3-1, and it has not been concluded that the length of 21 inches is unfeasible for this type of burner. It is felt that relocation of the dilution scoops or a change in scoop geometry will be required to improve air penetration within the Model 3 burner, thereby flattening the temperature profile.

d. Discussion of Results

The testing discussed in the previous section demonstrates the feasibility of ram induction main burner design in attaining acceptable

DOWNGRADED AT 3 YEAR INTERVALS
DECLASSIFIED AFTER 12 YEARS
DOD Dir 5200.10

burner performance in substantially reduced length as compared to conventional Pratt & Whitney Aircraft burners.

Pressure drops ranging from 4 to 10% were obtained at inlet Mach numbers ranging from 0.30 to 0.40. Such pressure losses being obtained with relatively high scoop entrance velocity gives evidence of the effectiveness of the ram induction scoops in utilizing velocity head to drive the air into the burner. The small amount of diffusion required with this system can be incorporated into the burner shroud and allows a very short combined diffuser and burner length.

In addition, the attainment of combustion intensities on the order of 6×10^6 BTU/hr/ft^3/atm have been no problem. This is attributed to the strong turning of the air into the burner by the scoops and the resultant excellent mixing. Operation at high combustion intensity also contributes to the burner's short length.

The operating range of the burner has been excellent. The design has been operated from .0005 to .030 fuel-air ratios.

Combustion efficiencies ranging from 98 to 100 percent have been obtained. The attainment of consistently high combustion efficiency has not been a major objective of the program. The primary objective has been to obtain good outlet temperature profile control in the short length of the burner system. Temperature profile control is the usual problem of high intensity or extremely short burner systems but excellent results have been obtained from this program.

Durability under extended running with high inlet temperature has not been investigated. However, no trouble with scoop burning has been experienced.

e. Model 4

The model 4, curved 120° segment, primary ram induction burner was specifically designed to duplicate the geometry and compressor discharge conditions of the 600 lb/sec STF 219 engine. The rig is shown mounted on the test stand in Figure 4-33.

The objective of this program is to integrate the burner principles of the model 2-7 into a realistic engine configuration. This model includes engine type struts with auxiliary bleed air being taken off through the struts.

DOWNGRADED AT 3 YEAR INTERVALS
DECLASSIFIED AFTER 12 YEARS
DOD DIR 5200.10

(1) Description of Burner (see Figure 4-34 and 4-35)

The burner section tested is a 120° segment of a full annular burner with a mean burner radius of 16.029 inches. The segment being tested is based on an engine with 32 struts and 32 fuel nozzles mounted with the struts. The diffuser is built as an integral part of the rig while the burner section is separate and easily removable. The diffuser is divided into three separate sections; two of these supply air to the inner and outer burner liners while an intermediate diffuser supplies swirler air. The intermediate diffuser is sized to accept more flow than that required by the swirlers. This excess air is reaccelerated around the burner and rejoins the air from the outer diffusers.

(2) Test Results

The model 4 burner has been tested for 24.5 hours at inlet Mach numbers of 0.32 to 0.38. The initial tests consisted of determining the burner cold pressure loss and burner performance at fuel/air ratios of 0.01 and 0.02 with no auxiliary bleed air being removed from the diffuser section. The data obtained is tabulated below

inlet Mach No.	.32	.32
inlet temp.	335°F	344°F
F/A ratio	.011	.022
exit temp. (avg)	1098°F	1765°F
Δ TVR	1.48	1.45
Δ P/P	12.4%	12.0%

A test was conducted with the design bleed airflow (16.6%) and a fuel/air ratio of .021. A significantly lower burner pressure loss (7.7%) was measured. The data is tabulated below

inlet Mach No.	.33
bleed airflow	16.6%
inlet temp.	321°F
F/A ratio	.021
exit temp. (avg)	1750°F
Δ TVR	1.45
Δ P/P	7.7%

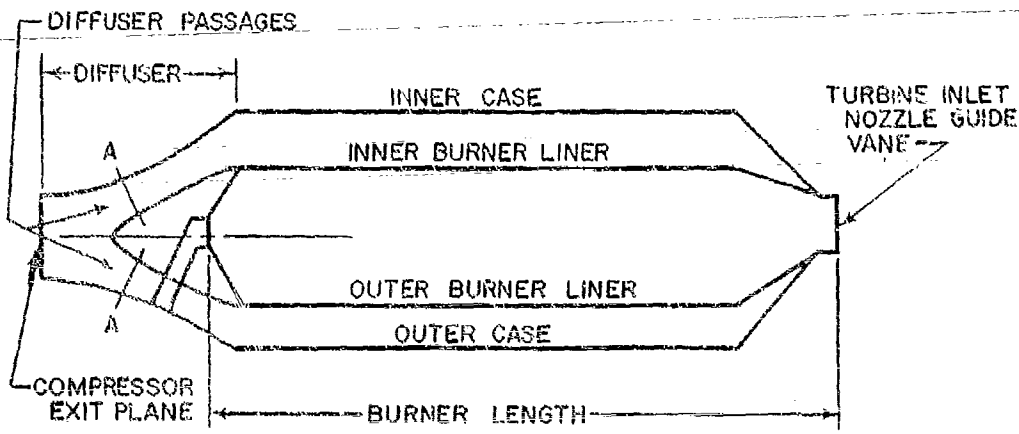
DOWNGRADED AT 3 YEAR INTERVALS
DECLASSIFIED AFTER 12 YEARS
DOD DIR 5200.10

(3) Conclusions

Since this 120° segment rig has just started testing, it is too early to make any firm conclusions. It is encouraging, however, to have an exit temperature profile variation (Δ TVR) as low as 1.45 so early in the test program.

DOWNGRADED AT 3 YEAR INTERVALS
NOT AUTOMATICALLY DECLASSIFIED AFTER 12 YEARS
DOD DIR 5200.10

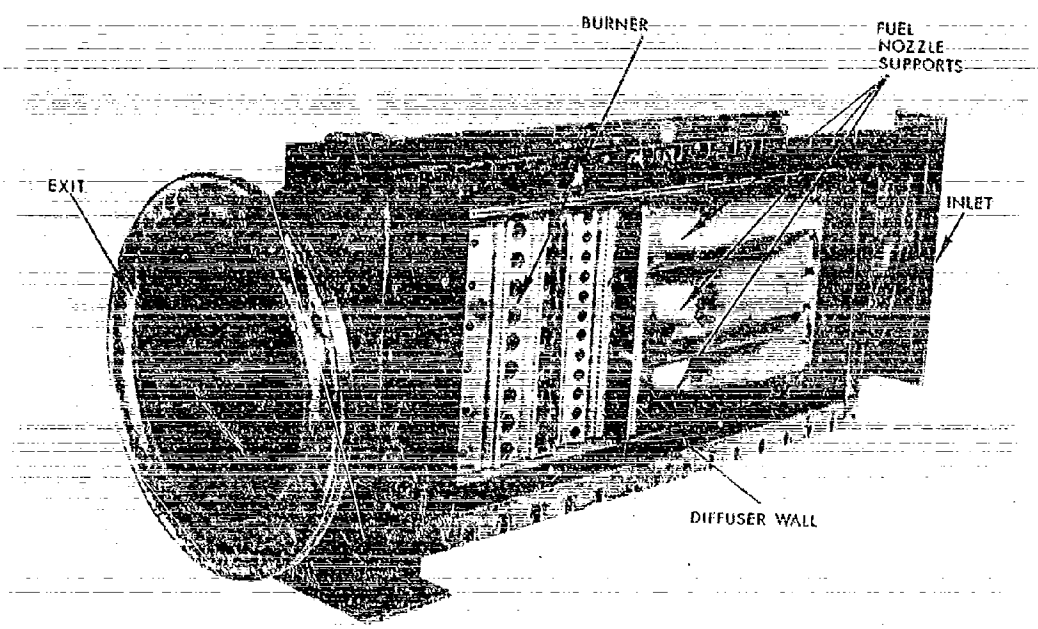
ENGINE &



SKETCH OF ANNULAR BURNER CONFIGURATION

Figure 4-1

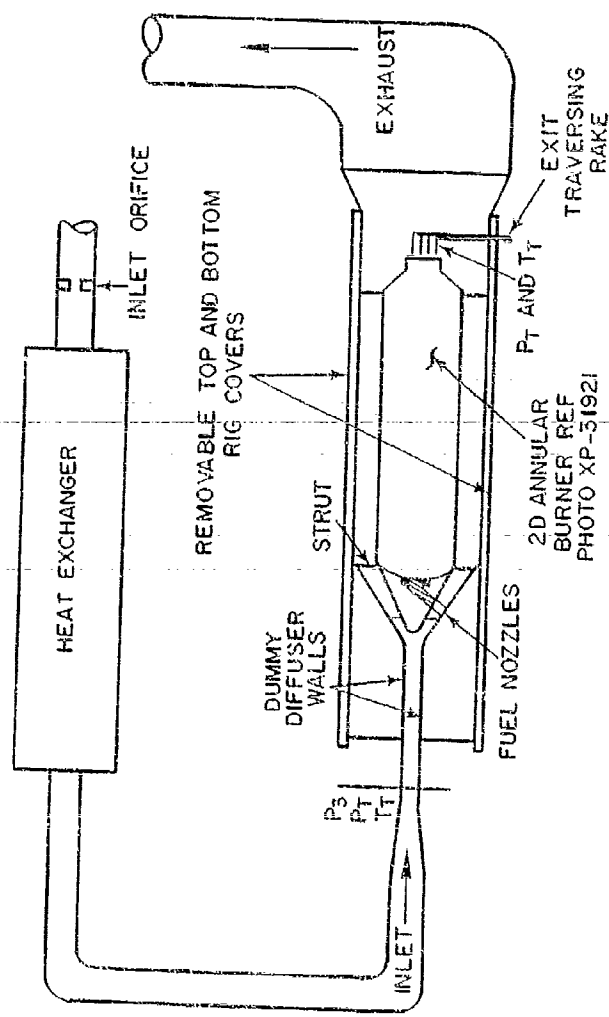
DOWNGRADED AT 3 YEAR INTERVALS
DECLASSIFIED AFTER 12 YEARS
DOD DIR 5200.10



TWO-DIMENSIONAL ANNULAR SEGMENTAL BURNER RIG ASSEMBLY

Figure 4-2

DOWNGRADED AT 3 YEAR INTERVALS
DECLASSIFIED AFTER 12 YEARS
DOD DIR 5200.10



SST TWO-DIMENSIONAL ANNULAR BURNER RIG

Figure 4-3

DOWNGRADED AT 3 YEAR INTERVALS
DECLASSIFIED AFTER 12 YEARS
DOD DIR 5200.10



LARGE-SCALE FULL-ANNULAR BURNER RIG MOUNTED IN TEST STAND

Figure 4-4



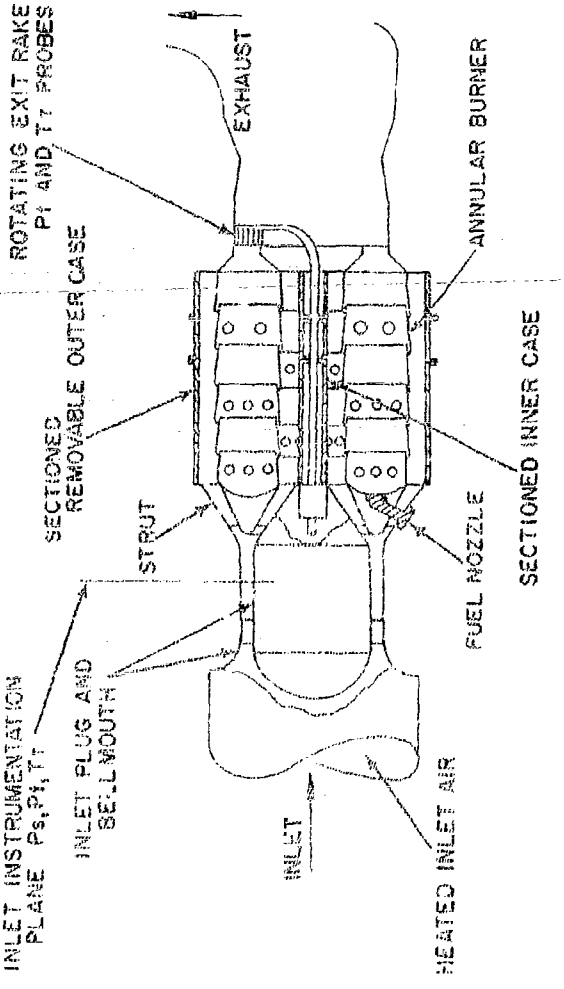
LARGE-SCALE FULL-ANNULAR BURNER RIG WITH EXIT DUCT REMOVED

Figure 4-5



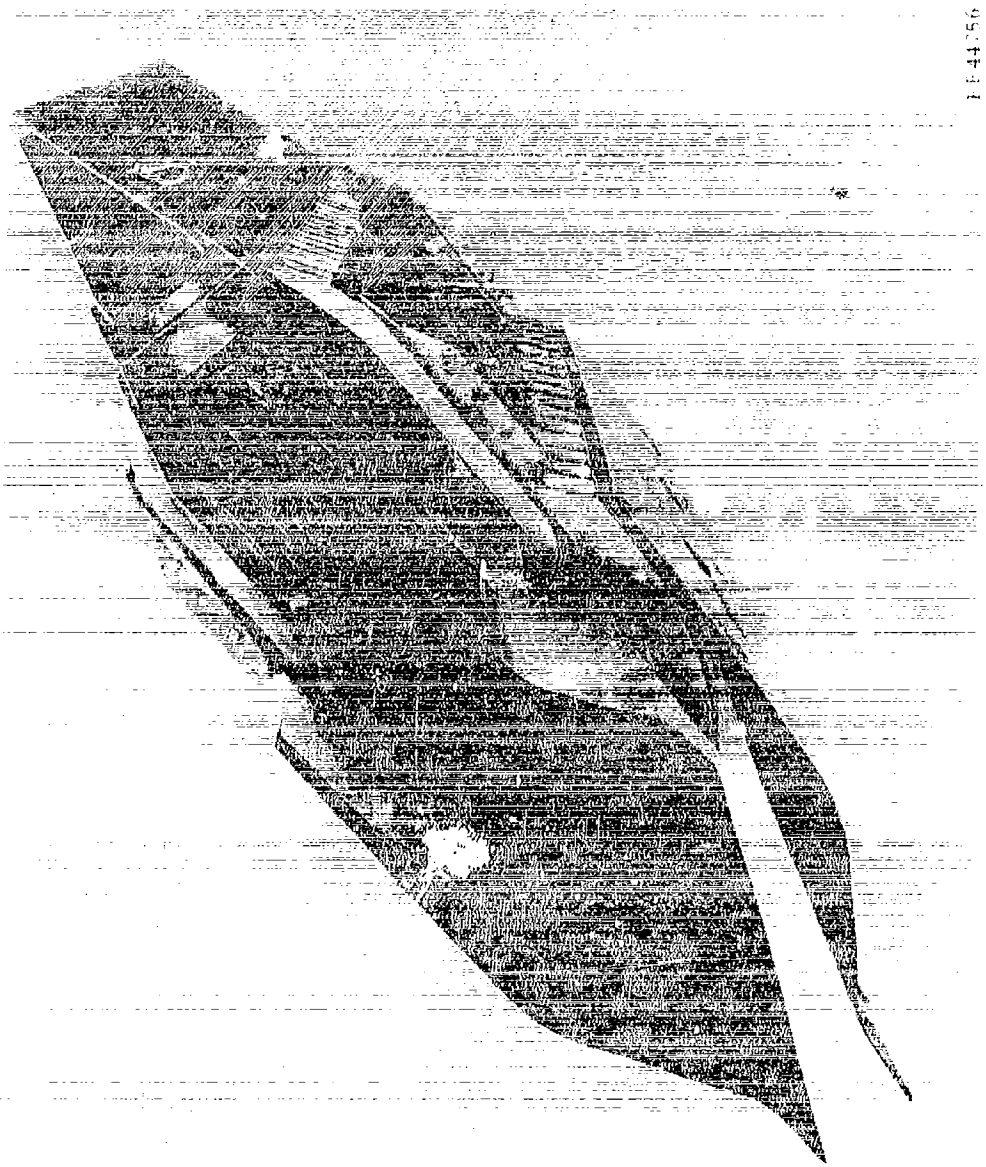
LARGE-SCALE FULL-ANNULAR BURNER RIG

Figure 4-6



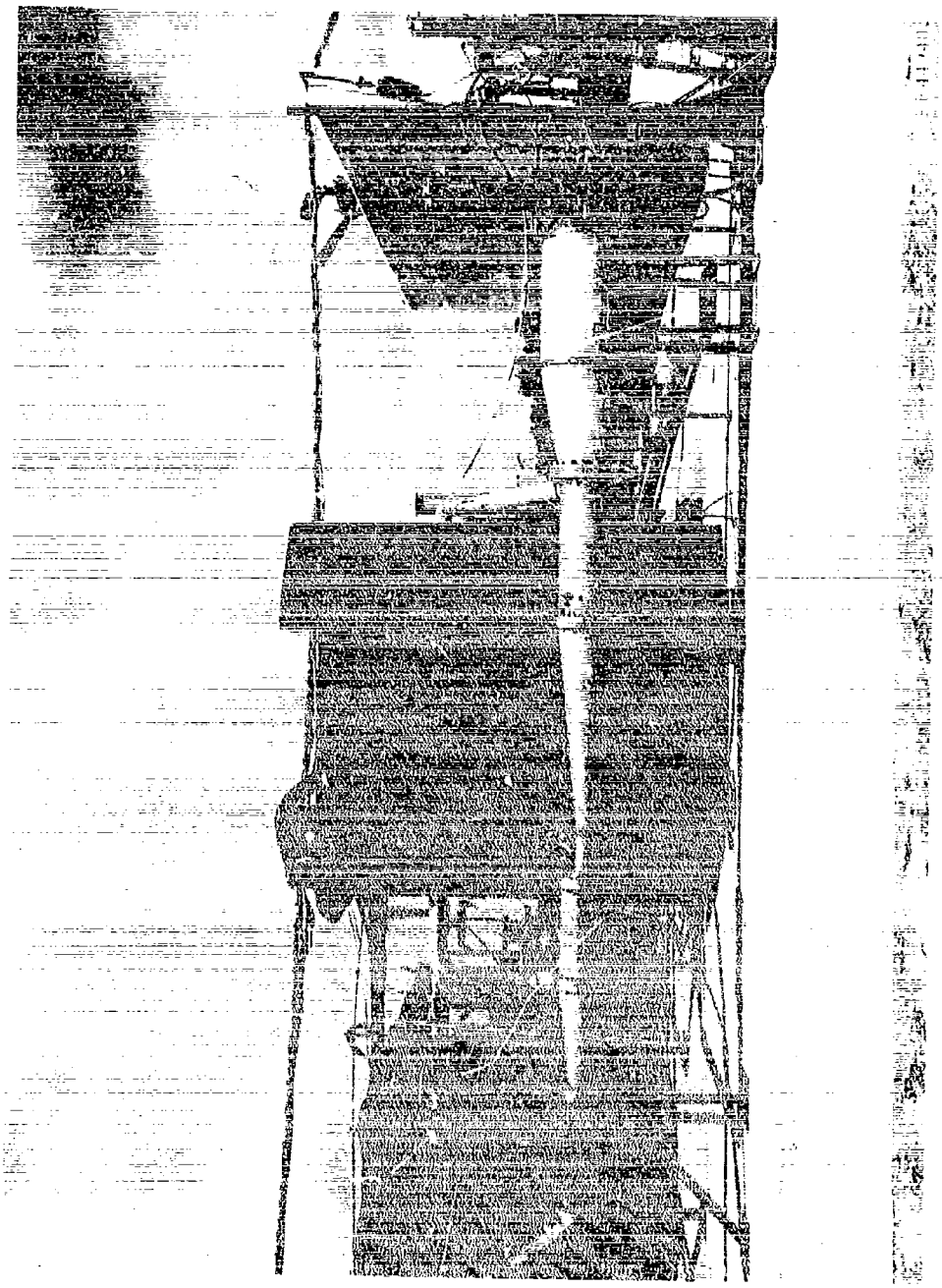
SCHEMATIC OF LARGE-SCALE FULL-ANNULAR BURNER RIG

Figure 4-7



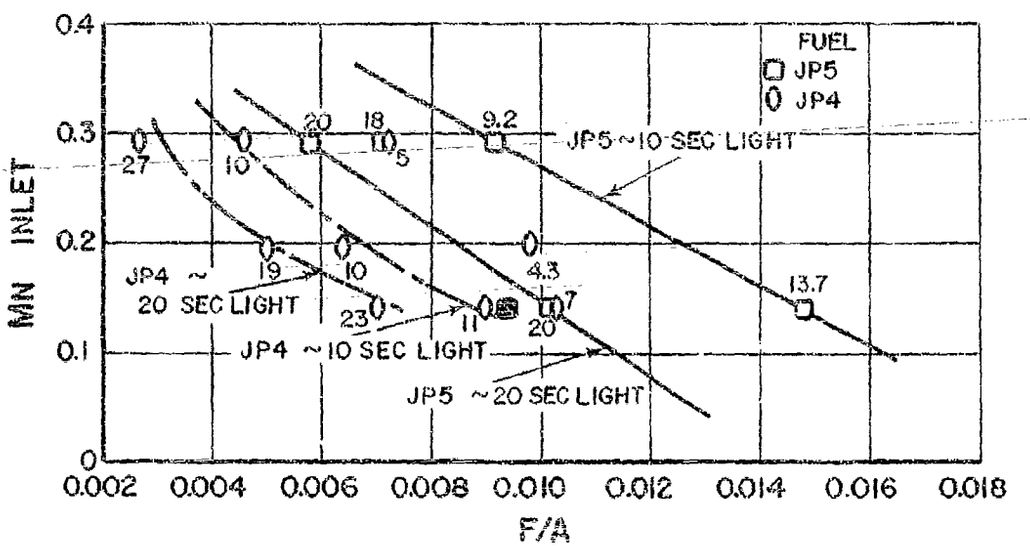
TYPICAL BURNER FOR RAM INDUCTION 72° STRAIGHT SECTOR BURNER RIG

Figure 4-8



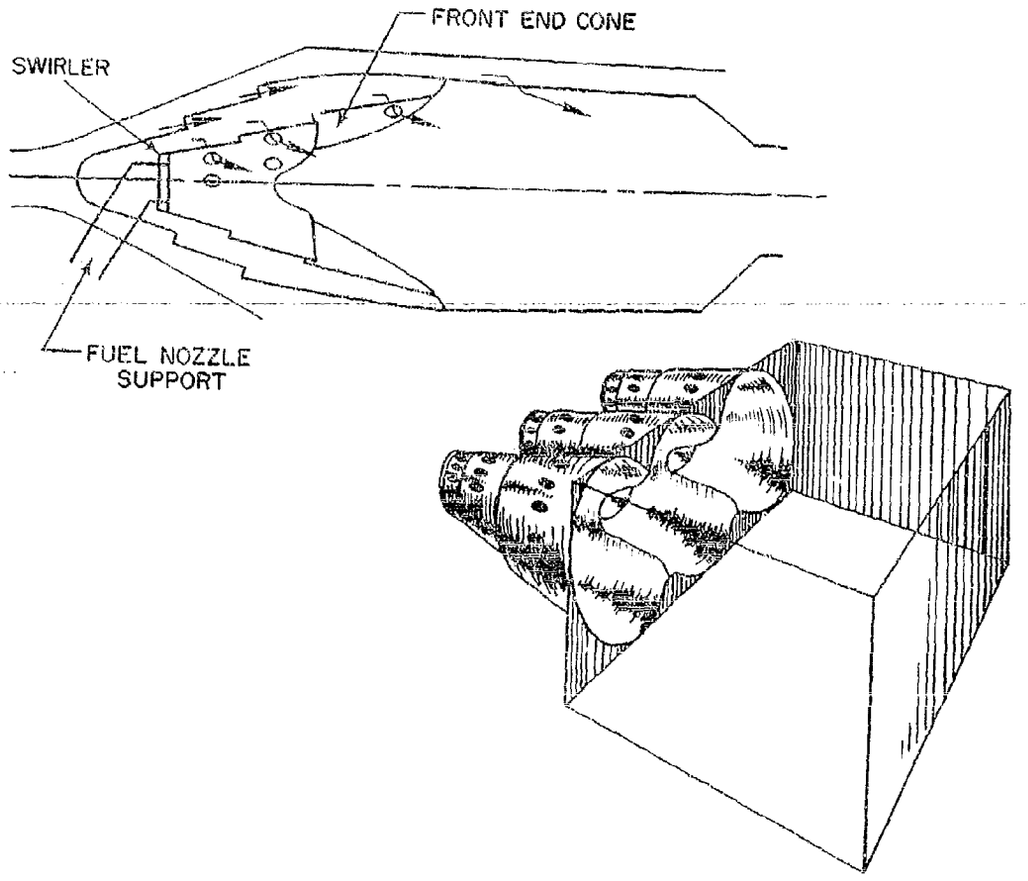
72-DEGREE STRAIGHT SECTOR TEST RIG MOUNTED IN TEST STAND

Figure 4-9



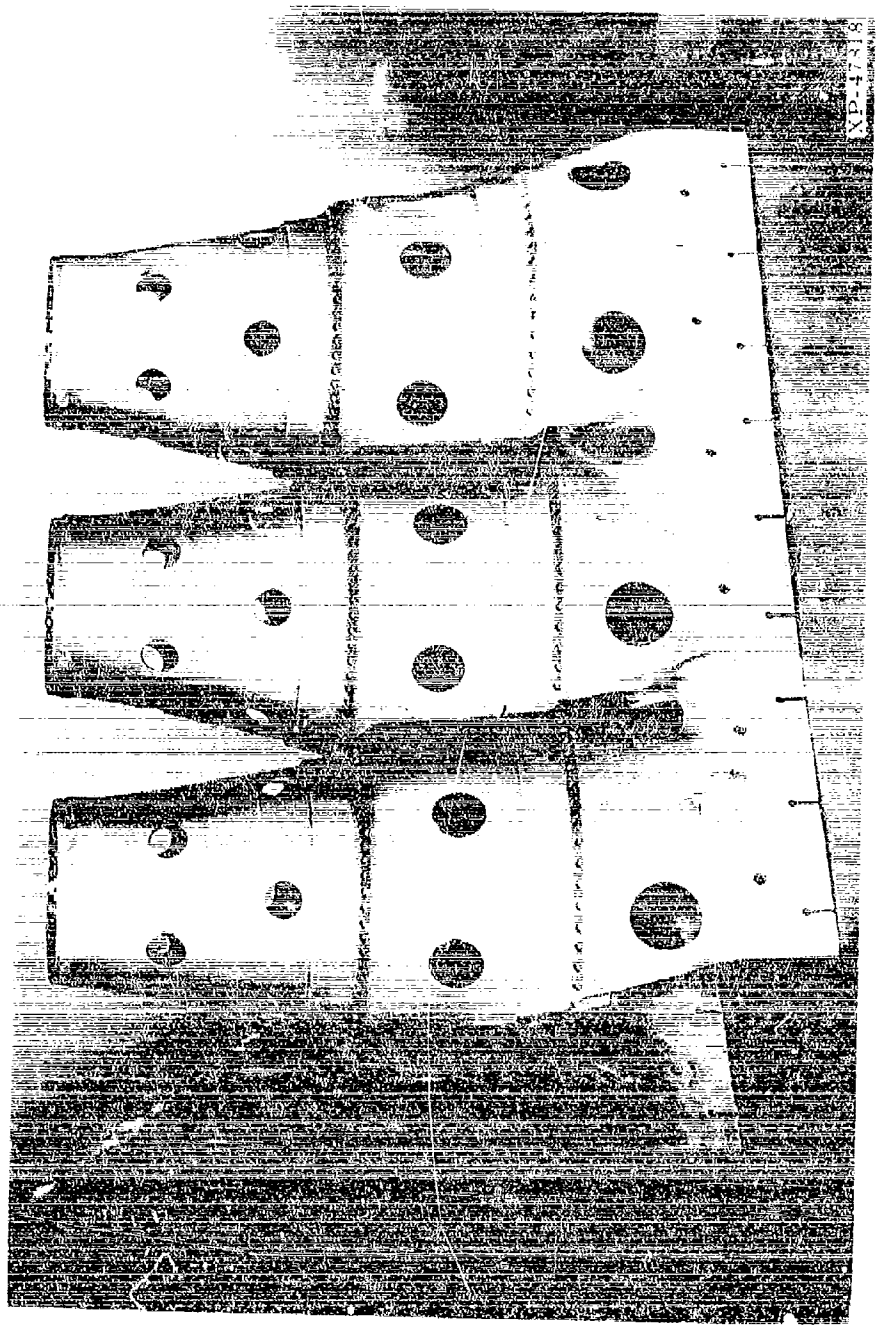
MINIMUM LIGHTING CURVE FOR THE 2-D BURNER

Figure 4-10



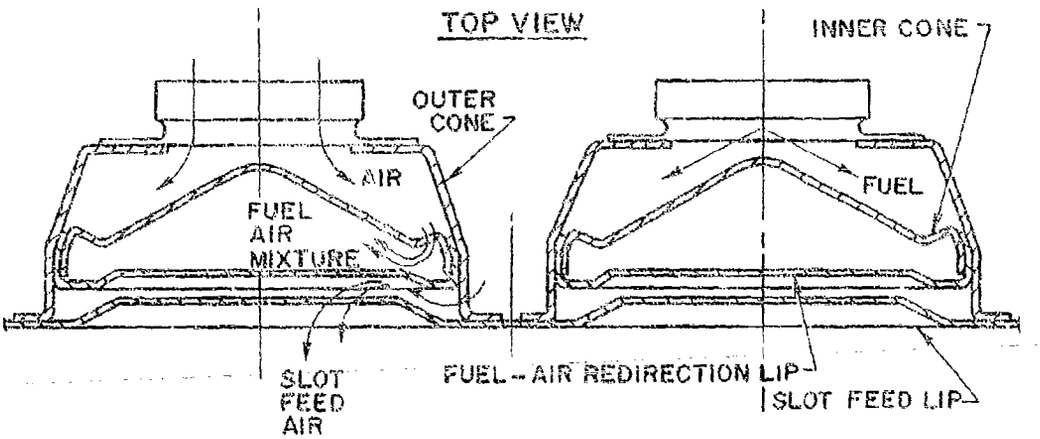
PARTIAL ANNULAR BURNER SCHEMATIC

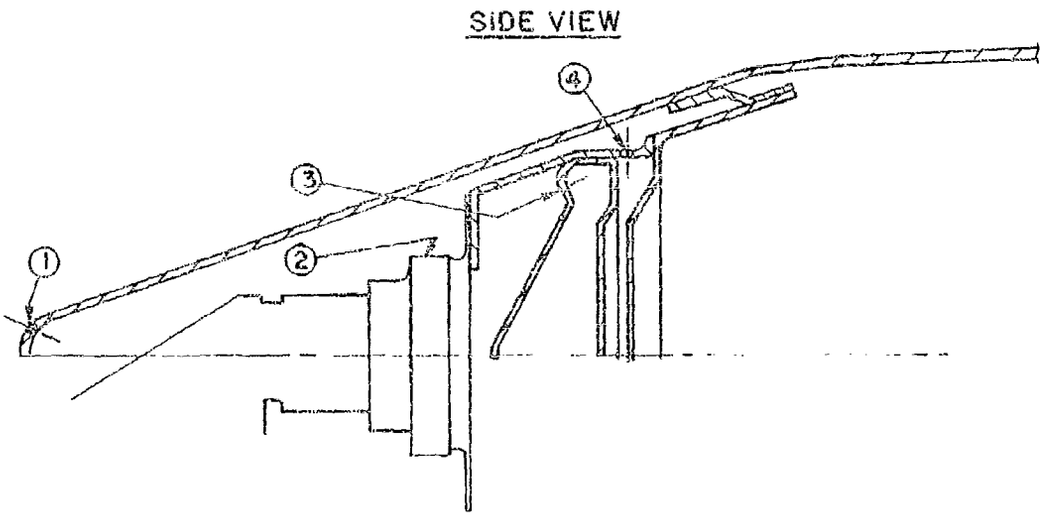
Figure 4-11



PARTIAL ANNULAR BURNER

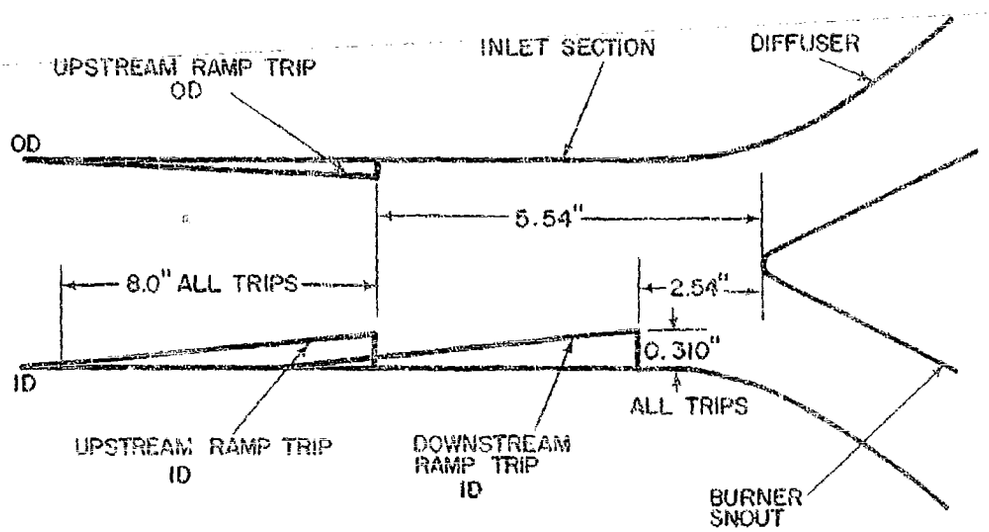
Figure 4-12





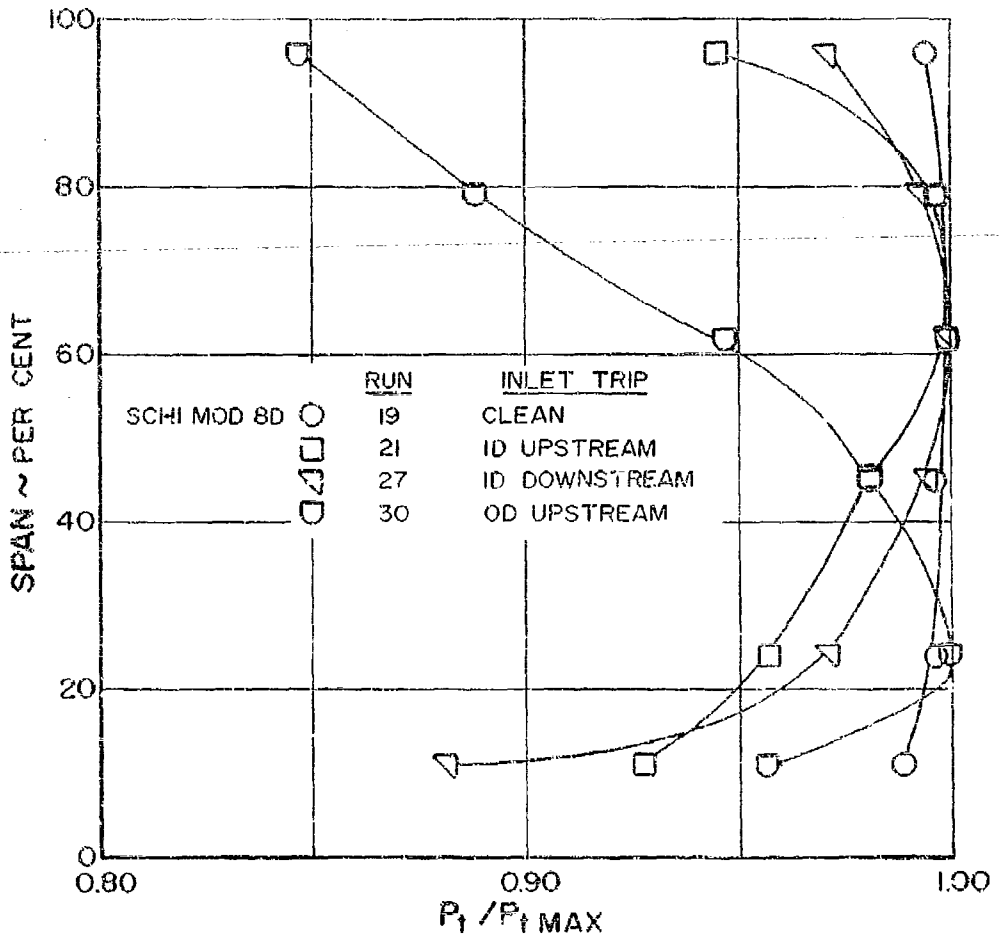
CROSS-SECTION OF HOT-CONE BURNER

Figure 4-13



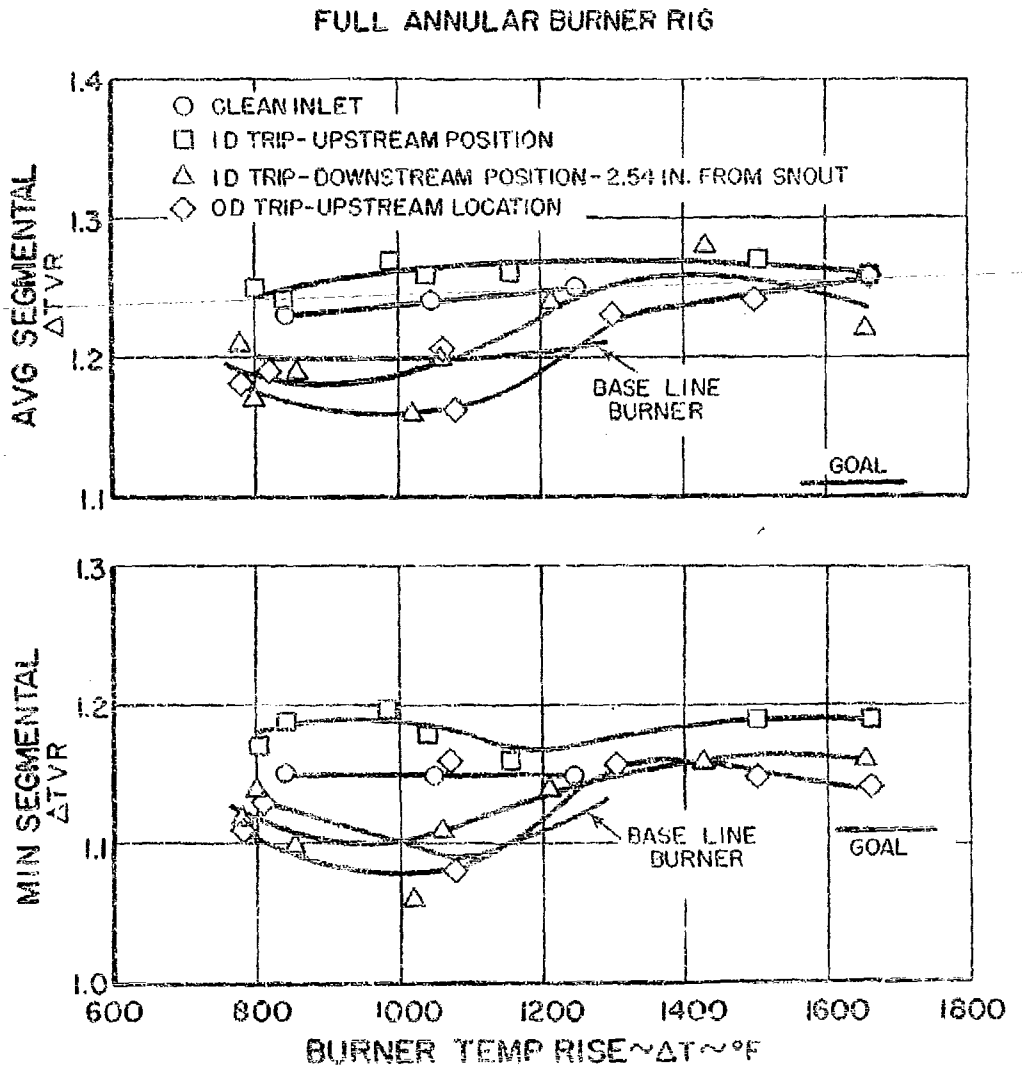
LOCATION OF INLET TRIPS ON FULL-ANNULAR BURNER RIG

Figure 4-14



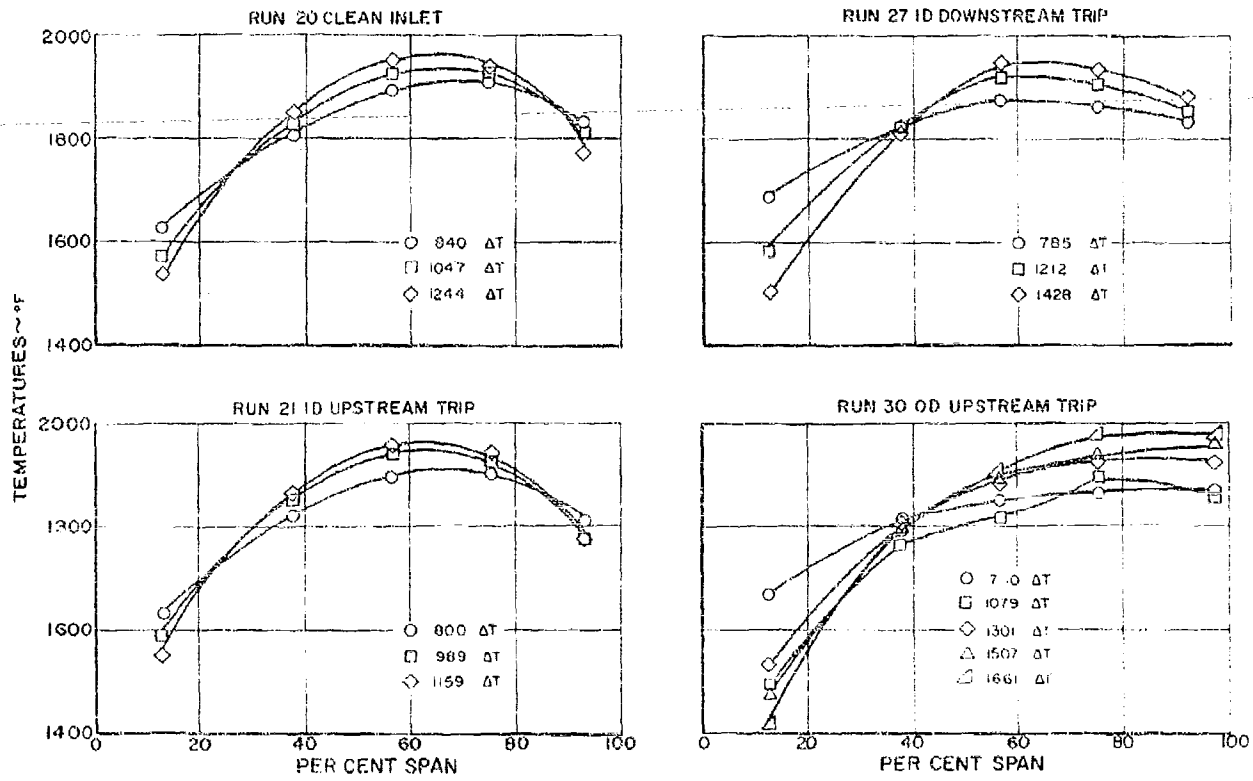
DIFFUSER INLET PRESSURE PROFILE ON FULL-ANNULAR BURNER RIG

Figure 4-15



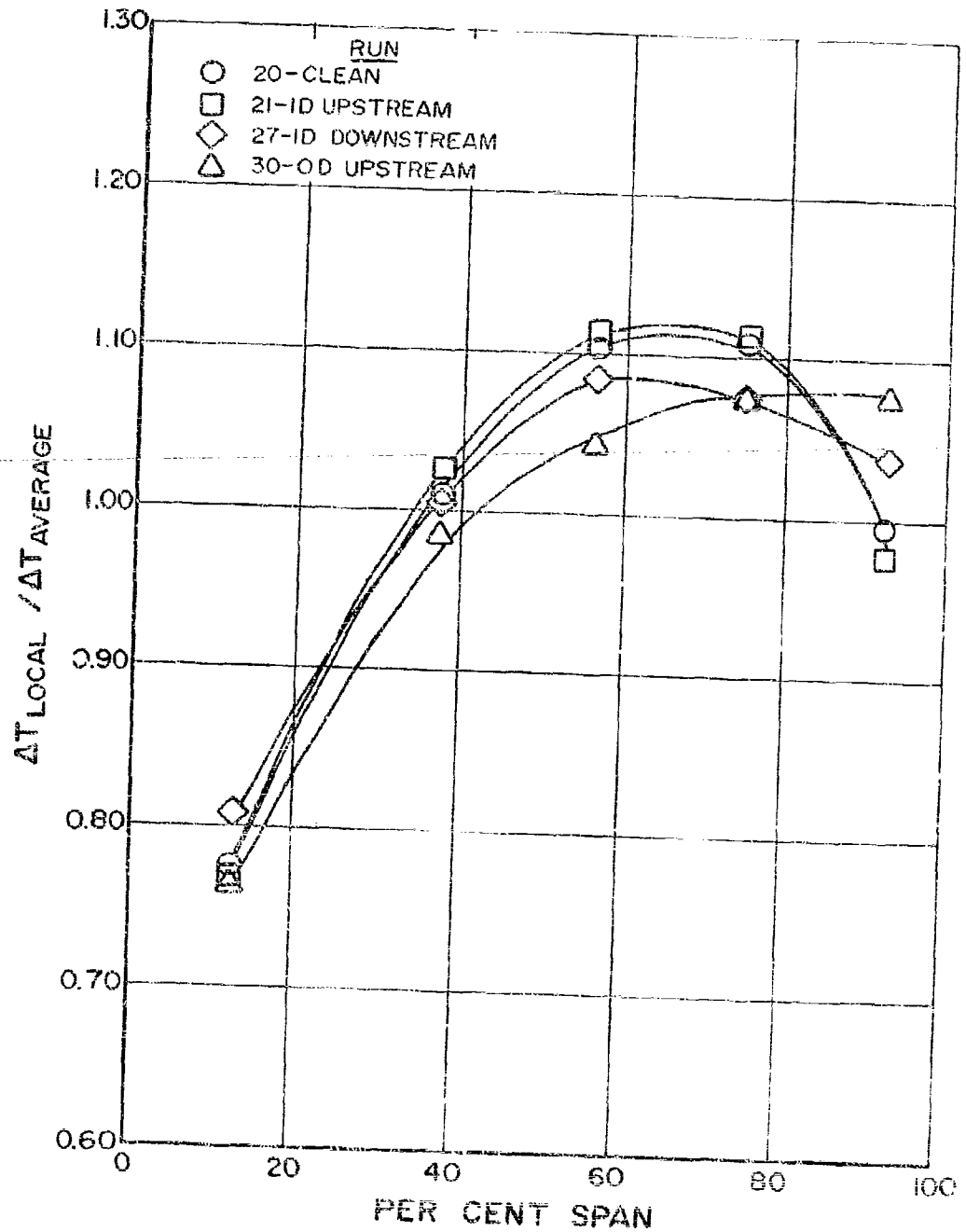
EFFECT OF INLET PROFILE ON Δ TVR

Figure 4-16



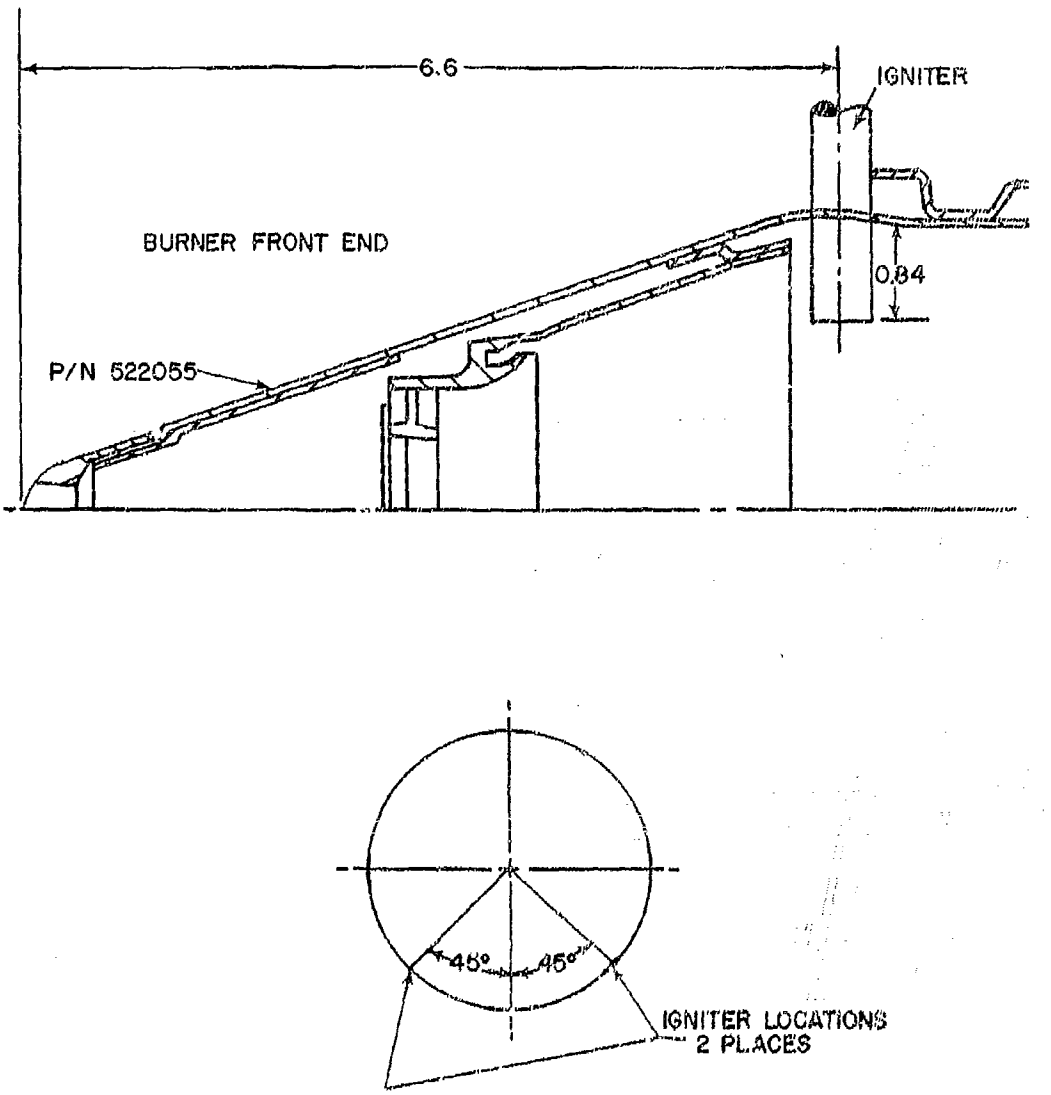
VARIATION OF BURNER EXIT TEMPERATURE PROFILE WITH TEMPERATURE PROFILE WITH TEMPERATURE RISE

Figure 4-17



EFFECT OF INLET PRESSURE PROFILE ON BURNER EXIT TEMPERATURE PROFILE

Figure 4-18

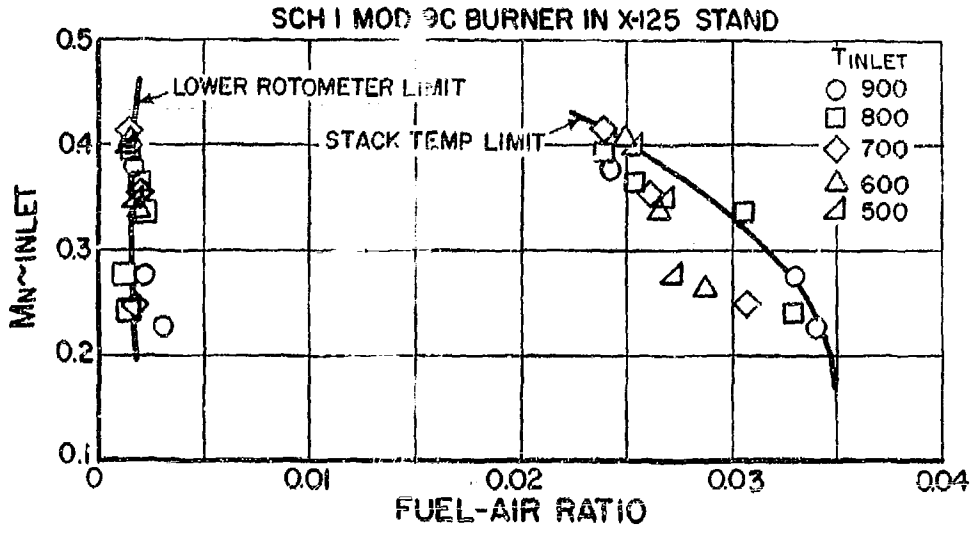


FULL-ANNULAR BURNER RIG IGNITER LOCATION

Figure 4-19

DOWNGRADED AT 3 YEAR INTERVALS
DECLASSIFIED AFTER 12 YEARS
DOD DIR 5200.10

THIS DOCUMENT CONTAINS INFORMATION AFFECTING THE NATIONAL DEFENSE OF THE UNITED STATES WITHIN THE MEANING OF THE ESPIONAGE LAWS, TITLE 18, U.S.C., SECTIONS 793 AND 794. THE TRANSMISSION OR THE REVELATION OF ITS CONTENTS IN ANY MANNER TO AN UNAUTHORIZED PERSON IS PROHIBITED BY LAW.

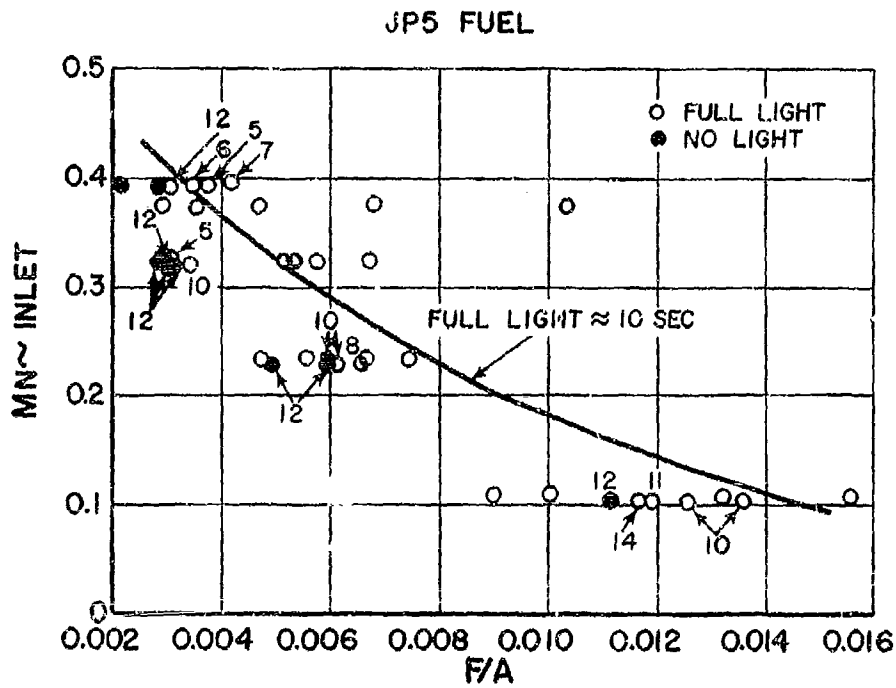


RICH AND LEAN OPERATING LIMITS

Figure 4-20

DOWNGRADED AT 3 YEAR INTERVALS
DECLASSIFIED AFTER 12 YEARS
DOD DIR 5200.10

THIS DOCUMENT CONTAINS INFORMATION AFFECTING THE NATIONAL DEFENSE OF THE UNITED STATES WITHIN THE MEANING OF THE ESPIONAGE LAWS, TITLE 18, U.S.C., SECTIONS 793 AND 794. ITS TRANSMISSION OR THE REVELATION OF ITS CONTENTS IN ANY MANNER TO AN UNAUTHORIZED PERSON IS PROHIBITED BY LAW.

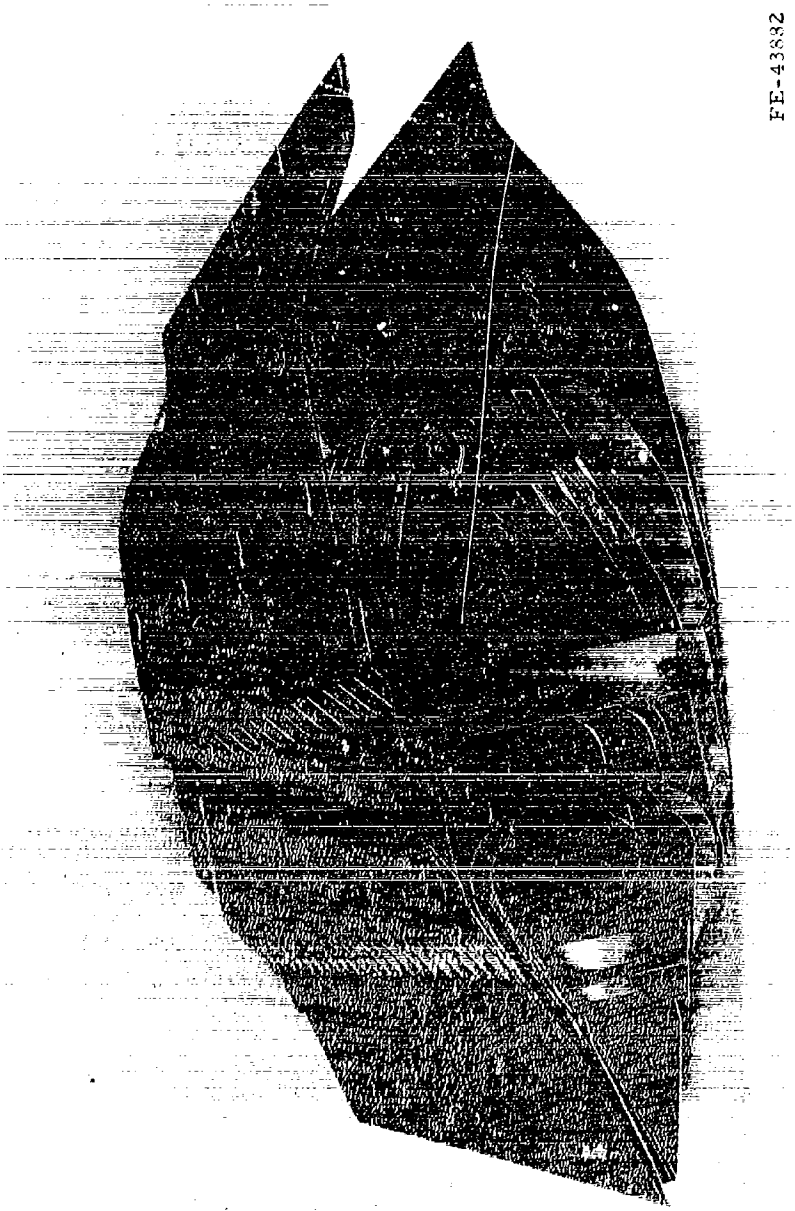


MINIMUM LIGHTING CURVE - JP-5 FUEL

Figure 4-21

DOWNGRADED AT 3 YEAR INTERVALS
DECLASSIFIED AFTER 12 YEARS
DOD DIR 5200.10

THIS DOCUMENT CONTAINS INFORMATION AFFECTING THE NATIONAL DEFENSE OF THE UNITED STATES WITHIN THE MEANING OF THE ESPIONAGE LAWS, TITLE 18, U.S.C., SECTIONS 793 AND 794. ITS TRANSMISSION OR THE REVELATION OF ITS CONTENTS IN ANY MANNER TO AN UNAUTHORIZED PERSON IS PROHIBITED BY LAW.

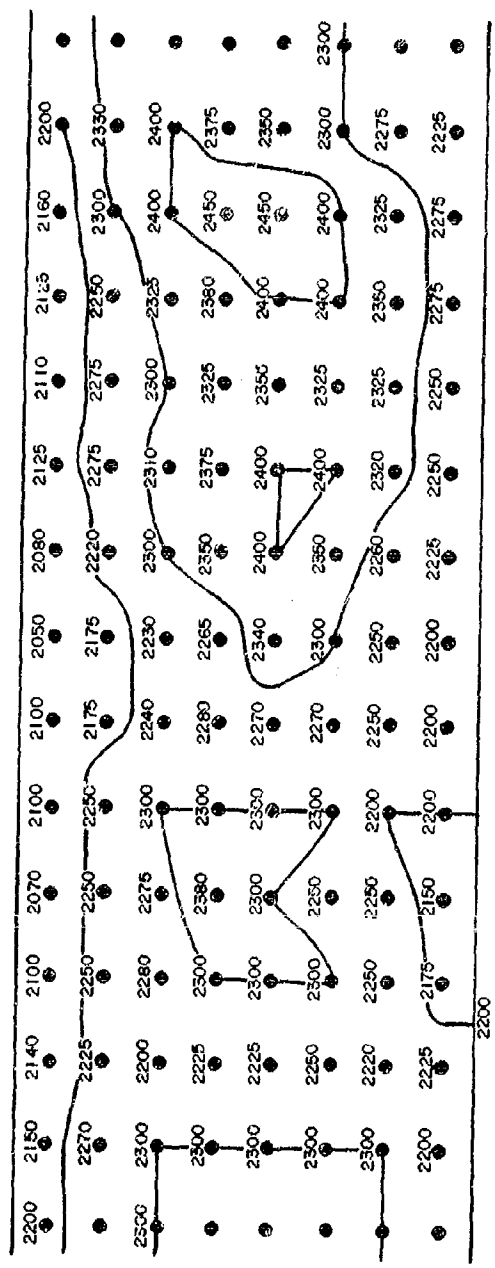


FE-43882

MODEL 2-1 RAM INDUCTION BURNER

Figure 4-22

DOWNGRADED AT 3 YEAR INTERVALS
DECLASSIFIED AFTER 12 YEARS
DOD DIR 5200.10

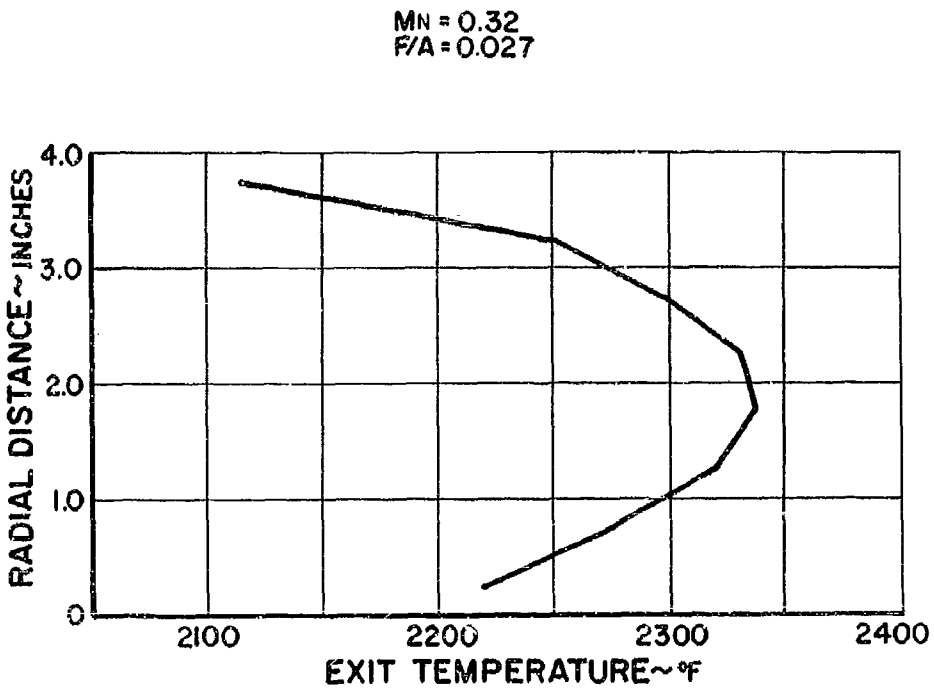


BURNER OUTLET TEMPERATURE DISTRIBUTION OF THE MODEL 2-7 RPM INDUCTION BURNER

Figure 4-23

DOWNGRADED AT 3 YEAR INTERVALS
DECLASSIFIED AFTER 12 YEARS
DOD DIR 5200.10

THIS DOCUMENT CONTAINS INFORMATION AFFECTING THE NATIONAL DEFENSE OF THE UNITED STATES WITHIN THE MEANING OF THE ESPIONAGE LAWS, TITLE 18, U.S.C., SECTIONS 793 AND 794. THE TRANSMISSION OR THE REVELATION OF ITS CONTENTS IN ANY MANNER TO AN UNAUTHORIZED PERSON IS PROHIBITED BY LAW.

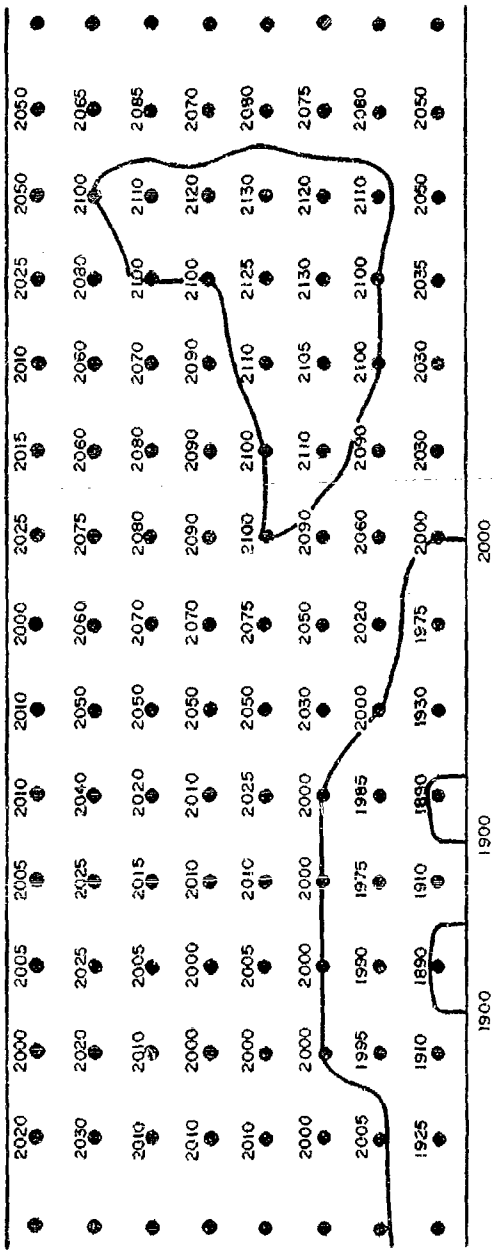


TEMPERATURE PROFILE OF THE MODEL 2-7 RAM INDUCTION BURNER

Figure 4-24

DOWNGRADED AT 3 YEAR INTERVALS
DECLASSIFIED AFTER 12 YEARS
DOD DIR 5200.10

THIS DOCUMENT CONTAINS INFORMATION AFFECTING THE NATIONAL DEFENSE OF THE UNITED STATES WITHIN THE MEANING OF THE ESPIONAGE LAWS, TITLE 18, U.S.C., SECTIONS 793 AND 794. ITS TRANSMISSION OR THE REVELATION OF ITS CONTENTS IN ANY MANNER TO AN UNAUTHORIZED PERSON IS PROHIBITED BY LAW.

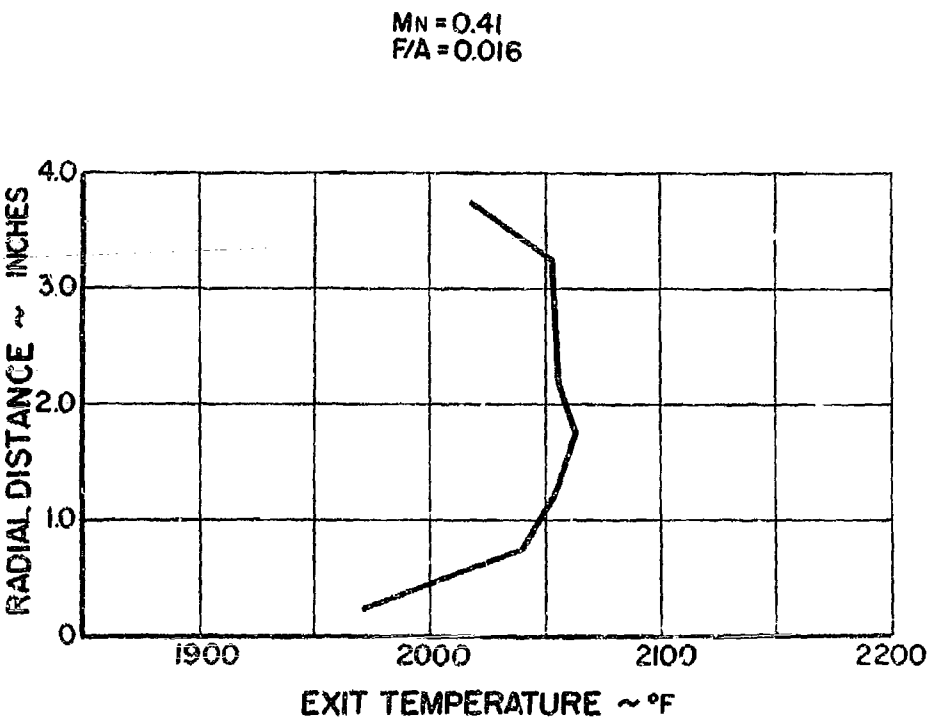


BURNER OUTLET TEMPERATURE DISTRIBUTION OF THE MODEL 2-7 RAM INDUCTION BURNER

Figure 4-25

DOWNGRADED AT 3 YEAR INTERVALS
DECLASSIFIED AFTER 12 YEARS
DOD DIR 5200.10

THIS DOCUMENT CONTAINS INFORMATION AFFECTING THE NATIONAL DEFENSE OF THE UNITED STATES WITHIN THE MEANING OF THE ESPIONAGE LAWS, TITLE 18, U.S.C., SECTIONS 793 AND 794. THE TRANSMISSION OR THE REVELATION OF ITS CONTENTS IN ANY MANNER TO AN UNAUTHORIZED PERSON IS PROHIBITED BY LAW.

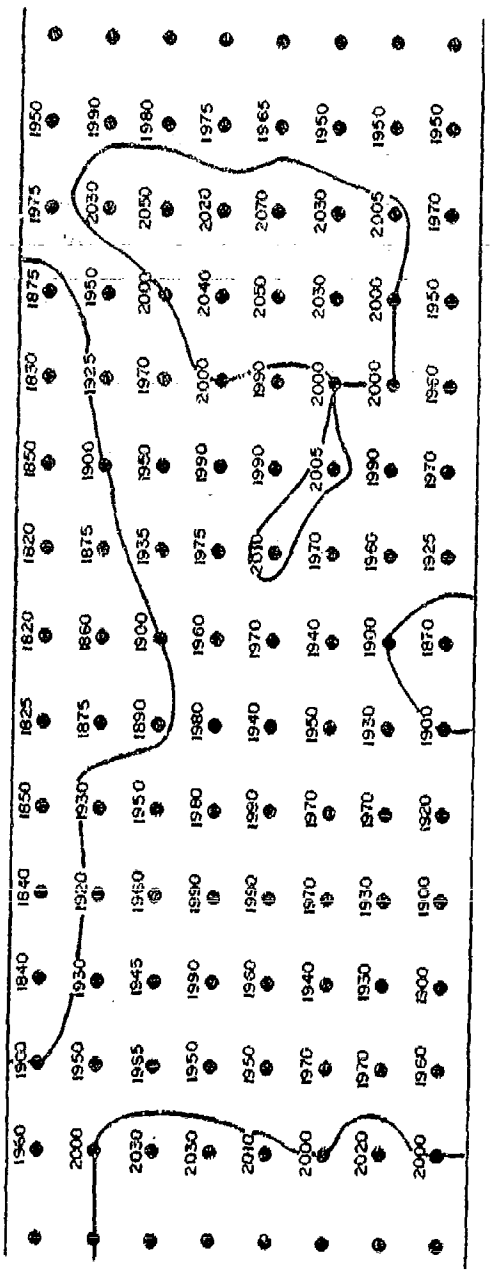


TEMPERATURE PROFILE OF THE MODEL 2-7 RAM INDUCTION BURNER

Figure 4-26

DOWNGRADED AT 3 YEAR INTERVALS
DECLASSIFIED AFTER 12 YEARS
DOD DIR 5200.10

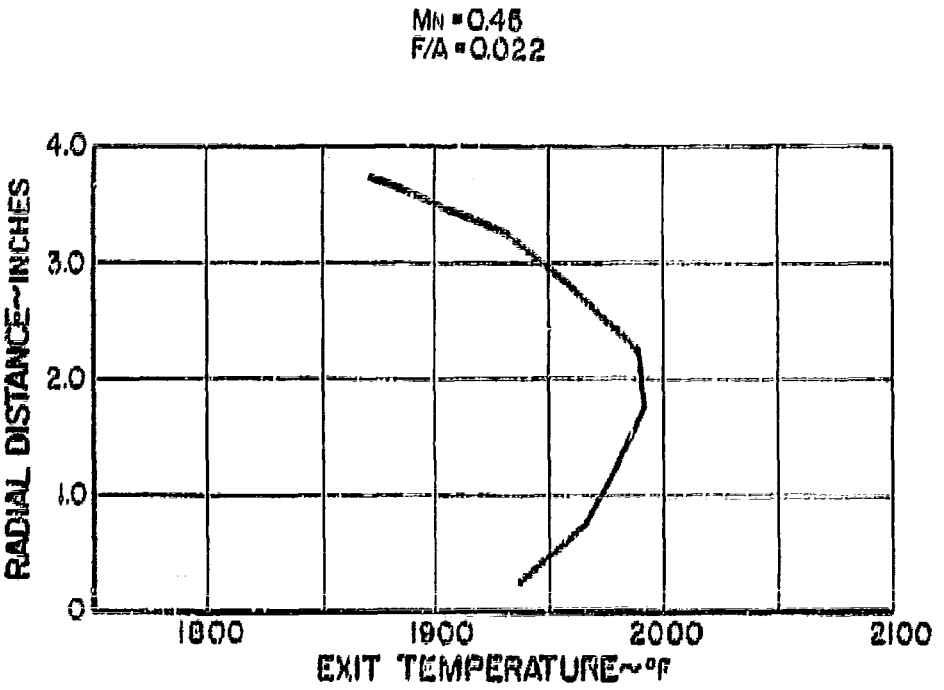
THIS DOCUMENT CONTAINS INFORMATION AFFECTING THE NATIONAL DEFENSE OF THE UNITED STATES WITHIN THE MEANING OF THE ESPIONAGE LAWS, TITLE 18 U. S. C. SECTIONS 793 AND 794. THE TRANSMISSION OR THE REVELATION OF ITS CONTENTS IN ANY MANNER TO AN UNAUTHORIZED PERSON IS PROHIBITED BY LAW.



BURNER OUTLET TEMPERATURE DISTRIBUTION OF THE MODEL 2-7 RAM INDUCTION BURNER

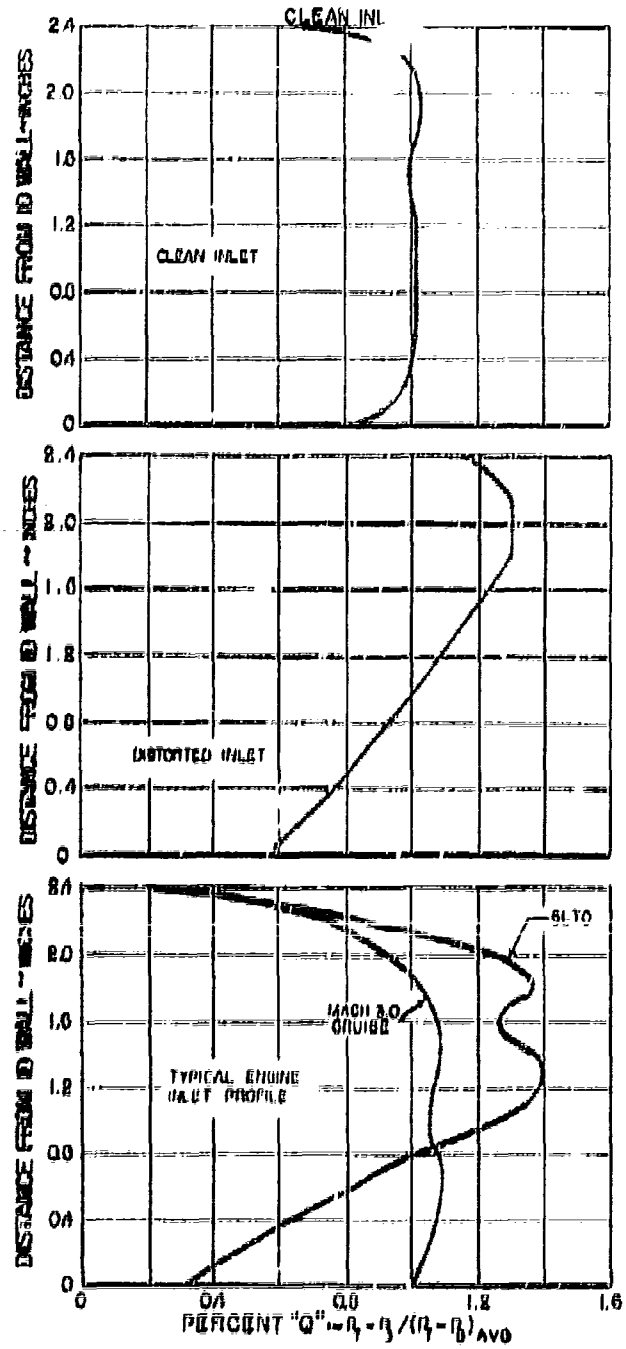
Figure 4-27

DOWNGRADED AT 3 YEAR INTERVALS
DECLASSIFIED AFTER 12 YEARS
DOD DIR 5200.10



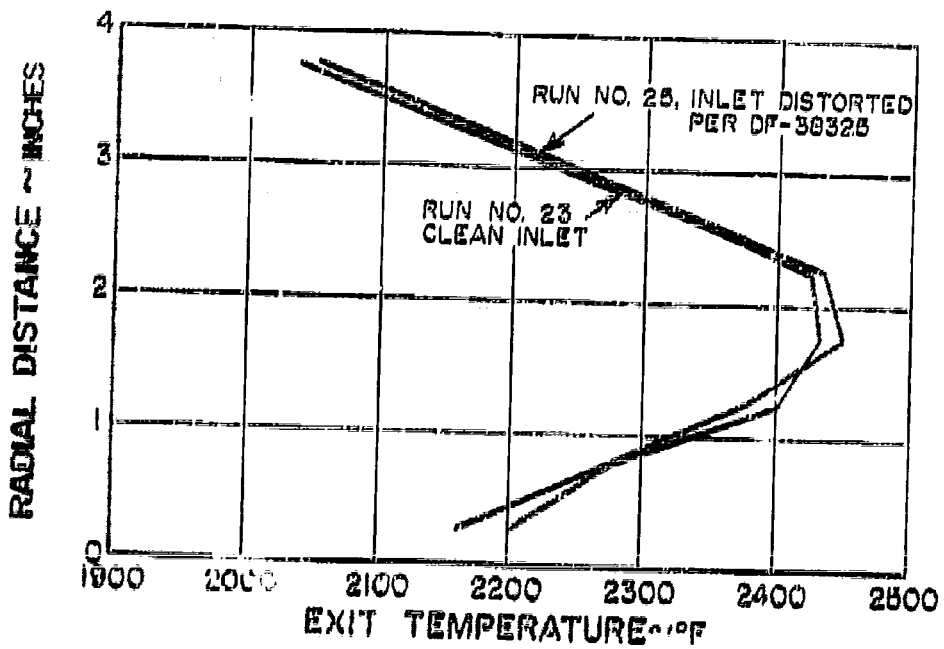
TEMPERATURE PROFILE OF THE MODEL 2-7 RAM INDUCTION BURNER

Figure 4-28



PERCENT OF AVERAGE VELOCITY HEAD AT BURNER DIFFUSER INLET VERSUS DISTANCE FROM I.D. WALL

Figure 4-29



EFFECT OF INLET VELOCITY PROFILE ON OUTLET TEMPERATURE PROFILE OF MODEL 2-7 BURNER

Figure 4-30



MODEL 3-1 RAM INDUCTION BURNER

Figure 4-31



MODEL 3-2 RAM INDUCTION BURNER

Figure 4-32



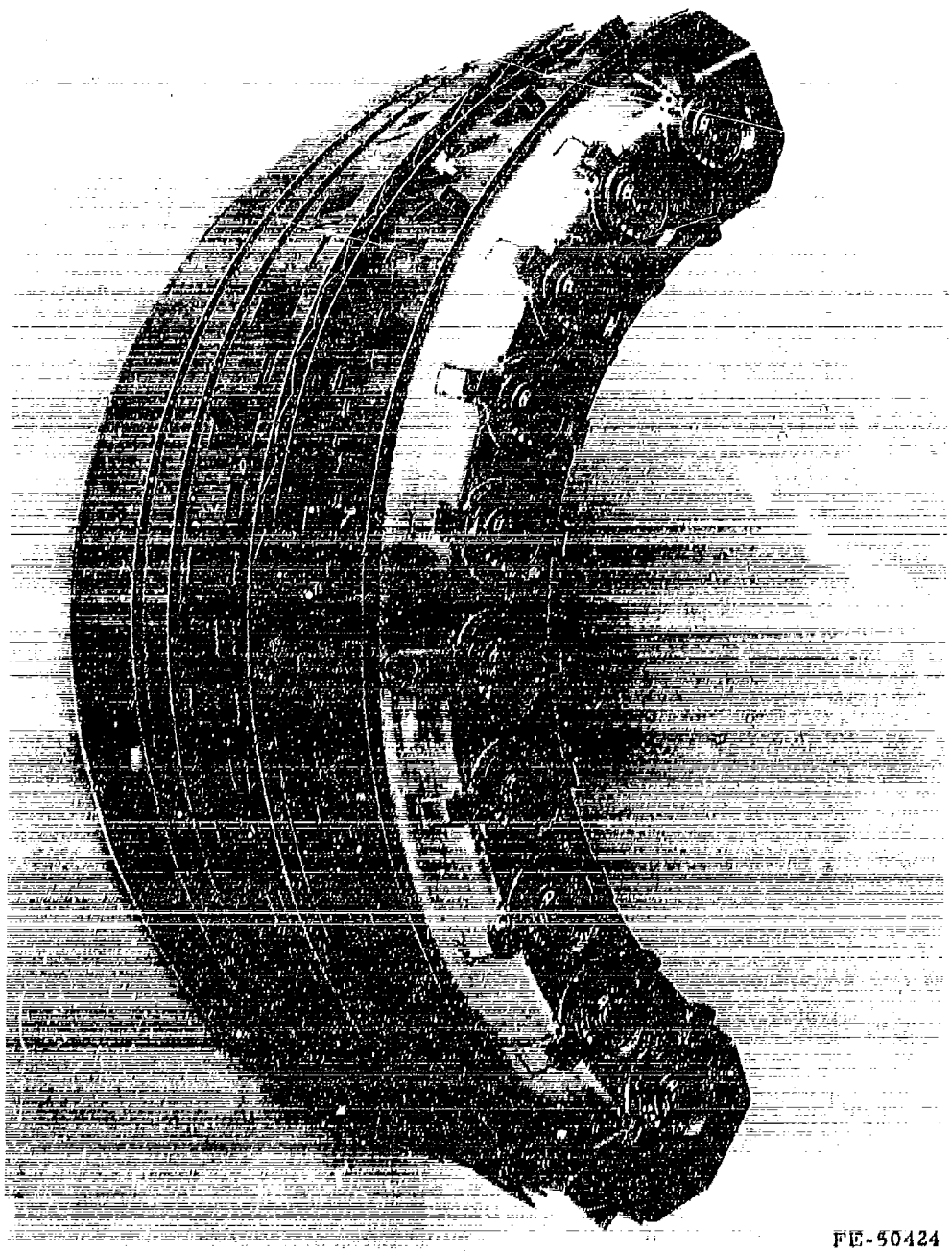
TEST STAND FOR MODEL 4 120-DEGREE SEGMENT RAM INDUCTION BURNER

Figure 4-33



MODEL 4 120-DEGREE SEGMENT RAM INDUCTION BURNER

Figure 4-34



FE-50424

MODEL 4 120-DEGREE SEGMENT RAM INDUCTION BURNER

Figure 4-35

DOWNGRADED AT 3 YEAR INTERVALS
DECLASSIFIED AFTER 12 YEARS
DOD DIR 5200.10

THIS DOCUMENT CONTAINS INFORMATION AFFECTING THE NATIONAL DEFENSE OF THE UNITED STATES WITHIN THE MEANING OF THE ESPIONAGE LAWS, TITLE 18, U.S.C., SECTIONS 793 AND 794. THE TRANSMISSION OR THE REVELATION OF ITS CONTENTS IN ANY MANNER TO AN UNAUTHORIZED PERSON IS PROHIBITED BY LAW.

ITEM 5

TURBINE DEVELOPMENT

ITEM 5 - TURBINE DEVELOPMENT

OBJECTIVE

To conduct development testing of turbine components directed toward verifying the turbine design and determining the effectiveness of turbine blade and nozzle cooling. The specific goals of this program were to further advance the technology available for turbine design by conducting steady state and cyclic tests of turbine components employing advanced cooling techniques and to further substantiate the effect of turbine cooling on turbine performance parameters.

A. INTRODUCTION

In support of the turbine design effort, laboratory, rig and engine tests were continued to evaluate the capability of new blade and vane configurations. This work included testing of advanced film cooled turbine components as well as additional investigations of convectively cooled blade and vane designs Hardware was primarily of JT4 size to expedite testing. When possible, existing parts were modified to permit the early evaluation of the various vane and blade schemes under consideration.

The turbine development program was divided into six principal areas of effort which are briefly defined below:

1. INVESTIGATION OF THE HEAT TRANSFER CHARACTERISTICS OF AIR COOLED VANES

An extensive experimental program was conducted to study the heat transfer characteristics of various turbine vane cooling schemes with emphasis placed on film cooled designs. This work was divided into two major areas of effort: (a) an investigation of the basic factors governing the cooling effectiveness of film cooled blades and (b) the testing of full-scale air cooled vane configurations in a heat transfer cascade rig. The first investigation was aimed at increasing fundamental knowledge of film cooling phenomena and correlating this

DOWNGRADED AT 3 YEAR INTERVALS
DECLASSIFIED AFTER 12 YEARS
DOD DIR 5200.10

THIS DOCUMENT CONTAINS INFORMATION AFFECTING THE NATIONAL DEFENSE OF THE UNITED STATES WITHIN THE MEANING OF THE ESPIONAGE LAWS, TITLE 18, U.S.C., SECTIONS 793 AND 794. ITS TRANSMISSION OR THE REVELATION OF ITS CONTENTS IN ANY MANNER TO AN UNAUTHORIZED PERSON IS PROHIBITED BY LAW.

information, where possible, with published data. In the second program, tests were conducted to determine the heat transfer characteristics of full-scale turbine engine vane designs which were being considered for incorporation in the SST engine.

2. INVESTIGATION OF NEW FABRICATION TECHNIQUES

As part of the development effort on air-cooled turbine vanes, a program was undertaken to develop a "wafer vane" design. A wafer vane is an assembly composed of a large number of stamped segments bonded together to produce an airfoil shape. This method of construction has two advantages - it permits the rapid fabrication of test components avoiding the long lead times necessary for cast parts and permits the use of elaborate cooling passage configurations which cannot be incorporated in ordinary cast vanes.

3. THERMAL FATIGUE TESTING OF AIR COOLED VANES IN A HOT CHOKED CASCADE RIG

To permit investigating the durability of air-cooled vanes under thermal fatigue conditions, a choked cascade rig which had been built under the Phase IIA contract was made operational during this period.

4. EVALUATION OF AIR COOLED TURBINE BLADES AND VANES IN A FULL-SCALE TURBINE DEVELOPMENT ENGINE

Since the final evaluation of turbine vane and blade designs must depend on their performance in an engine, the development testing of full-scale blades and vanes was undertaken in a turbine development engine at conditions simulating operation in a supersonic transport engine. The test programs included steady-state endurance tests to evaluate cooling and creep characteristics and cyclic endurance tests to evaluate the thermal fatigue properties of these parts.

5. PERFORMANCE TESTING OF FILM COOLED VANES AND BLADES

Performance tests were conducted on various film-cooled blade and vane designs in order to obtain quantitative information on how the air used for film cooling effected the aerodynamic performance of the turbine. The effect of different cooling flow rates and hole configurations was investigated. The blade configurations were run in a single stage rotating rig; the vanes were tested in a cascade rig.

DOWNGRADED AT 3 YEAR INTERVALS
DECLASSIFIED AFTER 12 YEARS
DOD DIR 5200.10

THIS DOCUMENT CONTAINS INFORMATION AFFECTING THE NATIONAL DEFENSE OF THE UNITED STATES WITHIN THE MEANING OF THE ESPIONAGE LAWS, TITLE 18, U.S.C., SECTIONS 793 AND 794. ITS TRANSMISSION OR THE REVELATION OF ITS CONTENTS IN ANY MANNER TO AN UNAUTHORIZED PERSON IS PROHIBITED BY LAW.

6. LABORATORY TESTING OF ADVANCED VANE AND BLADE MATERIALS

In support of the design effort on air-cooled turbine blades and vanes, a series of laboratory tests was conducted to determine the effect of drilling holes in specimens of advanced high temperature alloys on their fatigue and stress rupture characteristics. Other laboratory investigations conducted during this period on advanced high temperature alloys included long time creep tests, cyclic stress rupture tests and creep rupture tests.

A discussion of the work completed in each of these areas is presented in the sections which follow.

B. BASIC INVESTIGATION OF THE EFFECTIVENESS OF FILM COOLING

1. INTRODUCTION

Numerous investigators have experimentally studied film cooling and have determined the effect of important variables such as slot configuration and coolant flow on cooling effectiveness. Configurations similar to those being considered for current engine blade and vane designs have been included in these studies but have generally been tested with low main stream velocities, temperatures and low pressure differentials between the primary and secondary air streams. These tests were also generally conducted with much larger geometries than those which will be used for vane and blade cooling in the SST engine.

The current program to investigate basic film cooling performance parameters was performed to verify and extend existing correlations to engine operating conditions. The overall goals of this program were:

a. To determine if currently available design information on film cooling is valid throughout the anticipated range of engine temperature, pressure and flow conditions to be encountered in the supersonic transport engine.

b. To evaluate the effect of cooling slot geometries on cooling effectiveness,

c. To apply the data and correlations obtained from these studies to film-cooled turbine vanes and blades.

d. To determine the optimum mass flow ratios for specific film-cooled geometries.

DOWNGRADED AT 3 YEAR INTERVALS
DECLASSIFIED AFTER 12 YEARS
DOD DIR 5200.10

THIS DOCUMENT CONTAINS INFORMATION AFFECTING THE NATIONAL DEFENSE OF THE UNITED STATES WITHIN THE MEANING OF THE ESPIONAGE LAWS, TITLE 18 U.S.C. SECTIONS 793 AND 794. ITS TRANSMISSION OR THE REVELATION OF ITS CONTENTS IN ANY MANNER TO AN UNAUTHORIZED PERSON IS PROHIBITED BY LAW.

2. DESCRIPTION OF TEST RIG

The test rig used in the basic investigation of film-cooling performance is shown in Figure 5-1. Schematic diagrams of the overall rig and a detailed schematic of the test section are shown in Figure 5-2. The major components of the basic flow rig consisted of the following:

a. A bellmouth for measuring primary flow i.e. simulated engine airflow,

b. A plenum section to stabilize the primary flow,

c. A burner section,

d. A mixing plenum to provide a uniform temperature profile,

e. The test section,

f. An exhaust duct,

g. A secondary air supply (i.e. simulated cooling airflow) with its associated meters and burner to regulate pressure, temperature and airflow.

The test section was a six-foot long rectangular duct with an internal cross-sectional area of three square inches (2 inches x 1.5 inches). The test plate which contained the film cooling configuration being evaluated was installed four feet from the entrance of the test section. Immediately upstream and downstream of the test section were temperature and pressure probes for measuring primary gas stream conditions. The rig was designed to operate at main stream temperatures up to 1800°F and pressures up to 200 psi with compatible cooling air temperatures and pressures.

3. DESCRIPTION OF PARTS TESTED

The specimens tested in the film cooling flow rig were made up in the form of rectangular plates and were mounted in holders of the type shown in Figure 5-3. The specimen installed in the holder shown in the above figure incorporated a double row of film cooling slots. The location of the thermocouples used to measure upstream and downstream metal temperatures may also be seen in this figure. A total of five test plates, incorporating three different cooling slot configurations were tested. The plate configurations are listed below; schematic diagrams of each are shown in Figure 5-4.

DOWNGRADED AT 3 YEAR INTERVALS
DECLASSIFIED AFTER 12 YEARS
DOD DIR 5200.10

THIS DOCUMENT CONTAINS INFORMATION AFFECTING THE NATIONAL DEFENSE OF THE UNITED STATES WITHIN THE MEANING OF THE ESPIONAGE LAWS, TITLE 18, U.S.C., SECTIONS 793 AND 794. ITS TRANSMISSION OR THE REVELATION OF ITS CONTENTS IN ANY MANNER TO AN UNAUTHORIZED PERSON IS PROHIBITED BY LAW.

Test Plate	Description	Plate Material	Results
1	Single row, 30°, 0.016 slot	Wood	Adiabatic wall temperatures obtained
2	Single row, 30°, 0.016 slot	Hastelloy	Plate failed
3	Single row, 30°, 0.016 slot	Hastelloy	Metal temperature distribution obtained
4	Double row, 30°, 0.015 slot	Hastelloy	Metal temperature distribution obtained
5	Single row, 30°, 0.006 slot	Hastelloy	Metal temperature distribution obtained

4. TEST PROCEDURE

After the installation of the desired test specimen in the rig, a steady primary flow condition was established using the controls available to regulate the primary burner pressure, flow rate and exit temperature. Except for the first run using the wooden plate, tests were conducted at five primary gas stream conditions which included several pressure levels in the range between 50 and 200 psia and temperatures between 1400°F and 1600°F. Five coolant to primary gas stream ratios were set, providing a total of twenty-five test points. The testing conducted to date has been performed in the absence of a pressure gradient across the plate (which would result from changes in flow velocity due to the curvature of the blading). This was done to simplify analysis and allow direct comparisons with existing published film cooling data.

A non-dimensional form is generally employed when presenting film cooling data. The data is correlated as a temperature effectiveness parameter versus a term which includes the mass velocity ratio of the coolant slot and the distance downstream from the slot. These terms are: $\frac{T_p - T_F}{T_p - T_c}$ and X/MS, respectively

DOWNGRADED AT 3 YEAR INTERVALS
DECLASSIFIED AFTER 12 YEARS
DOD DIR 5200.10

where

T_p = Adiabatic wall temperature without a film, °F

T_F = Effective film temperature, or adiabatic wall temperature with film, °F

T_c = Coolant temperature, °F

X = Distance downstream from the slot, inches

S = Characteristic width of slot, inches

M = Mass velocity ratio of coolant to primary streams

5. TEST PROGRAM AND RESULTS

After the initial shakedown of the rig, an instrumented wooden plate with a single 30°, 0.016" slot (Test Sample #1) was installed and tested in the rig. The wooden plate provided a means for obtaining a direct measurement of adiabatic wall temperatures since conduction through the wood was small enough to be considered negligible. In addition, since these tests were run at comparatively low temperatures, the effect of radiation was not significant. Figure 5-5 presents a comparison of the tests results with data based on available published results. At the 200°F primary and 70°F coolant stream conditions shown in this curve, the measured effective film temperature was about 12 to 13 degrees higher than that derived from existing published data. This difference was considered to be within the limits of experimental accuracy.

Following the low temperature tests, it was necessary to determine if the available published data were equally valid at the high temperature levels and high primary-to-coolant gas stream ratios anticipated in the SST engine. Figure 5-6 shows the results of one such test and compares the test results obtained for a plate having a single 30° 0.016 inch slot with predictions based on published data. The comparison for the first inch downstream of the slot is good indicating that measuring techniques used were satisfactory. However, the spread between extrapolations based on published data and test results tends to deviate excessively beyond this point indicating the need for an experimental rather than a purely analytical approach to this problem.

In order to obtain accurate wall temperature measurements, it was necessary to compensate for radiation and conduction effects in this

rig. The procedures necessary to correct the data for each point were much too involved and time consuming to be performed manually. Therefore a computer data reduction program was written to take resulting film cooled metal plate temperatures and convert the results directly into the non-dimensional parameters previously presented with corrections for radiation and conduction effects included.

A sample of the uncorrected metal temperature data obtained from the rig is shown in Figure 5-7. The same information corrected for conduction and radiation effects and replotted to indicate cooling effectiveness is shown in Figure 5-8. The results with the other two configurations, a double row, 30°, 0.015" slot (Specimen 4) and a single row, 30° 0.006" slot (Specimen 5) are shown in Figures 5-9 and 5-10 respectively.

All pertinent data obtained in this rig was turned over to the design department to assist them in the design of film cooled vanes and blades. It is planned to continue this program and evaluate other film cooling and transpiration cooling schemes.

C. INVESTIGATION OF THE HEAT TRANSFER CHARACTERISTICS OF AIR COOLED VANES IN A HIGH PRESSURE CASCADE RIG

A test program was conducted in a high pressure three-vane choked cascade rig to determine the cooling characteristics of the various air-cooled turbine vane designs being considered for incorporation in the SST engine. The rig used simulated all aspects of the turbine vane environment and incorporated provisions for measuring vane metal temperatures and main gas stream and cooling air pressures, temperatures and air flows. The basic simplicity of this rig enabled the evaluation of proposed air-cooled vane designs over a wide range of conditions in a rapid and economical manner.

DESCRIPTION OF RIG

An overall view of the high pressure cascade rig is shown in Figure 5-11 and a schematic of the rig is shown in Figure 5-12. Essentially, the rig consisted of a series of ducts for measuring, pre-heating, mixing and directing air flow through a three-vane cascade. The center vane in the cascade was the test vane, the vanes on either side were "slave" vanes which were used to simulate an engine environment for the test vane.

[illegible]

Three separate air systems were incorporated in the rig. These were used to supply (a) main stream air (b) cooling air for the test vanes (c) cooling air for the "slave" vanes. The main stream air was heated directly by a gas turbine type JP fuel burning combustion chamber located upstream of the test section. The cooling air for the test vane was supplied through a second system (shown in Figure 5-12) which incorporated flow control valves, flow measuring orifices and an alcohol heater-burner upstream of the test vane. The cooling air which was not discharged into the gas stream through the test vane air foil surface slots or holes passed through the airfoil and was collected at the opposite end of the vane. It was piped through a cooler, a flow measuring orifice and a back pressure valve before being exhausted to atmosphere. The slave vanes were convectively cooled by radial cooling holes. The slave vane airflow was regulated to maintain surface temperatures in the vanes to match those of the test vanes. This arrangement minimized radiation losses and resulted in a close simulation of actual engine conditions.

The vanes were installed in the test section so as to provide gap chord ratios at the root and tip which duplicated engine dimensions. An instrumentation section containing sight ports and probe bosses was located immediately upstream of the test section. The sight ports were used for infrared pyrometer temperature measuring devices and the probe bosses were used for the installation of instrumentation to measure mainstream pressures and temperatures. A water-jacketed pilot-type pressure probe and a water jacketed aspirated pressure probe were used to monitor test conditions. These probes could be traversed across the gas stream during testing. The mixing, transition, test and exhaust-diffuser sections were water jacketed.

All vanes used in these tests, excluding the "slave vanes", were instrumented with chromel alumel thermocouples to measure metal surface temperatures at the mid span of the airfoil on both the concave and convex surfaces. The thermocouple leads were insulated from the gas stream with a high temperature ceramic insulation material and were capable of measuring metal temperatures up to 1900°F for prolonged periods and 2000°F for short periods. A small longitudinal groove was machined in the airfoil to contain each thermocouple wire. Lead wire and shielding diameters were kept small to minimize configuration changes in the test vane. The thermocouple wires were routed to an exit tube which extended through the top plenum of the test section. The test vane cooling air was introduced through a tube which was welded to the bottom shroud of the vane and protruded through the bottom plenum section of the rig. Cooling air temperatures were measured at the entrance to this tube.

DOWNGRADED AT 3 YEAR INTERVALS
NOT AUTOMATICALLY DECLASSIFIED
DOD DIR 5200.10

TEST PROGRAM

A total of nine different cooling schemes for air cooled vanes were evaluated during this contract period. For convenience in evaluating the results, all test vanes utilized the same airfoil envelope. These configurations are listed below:

Cooling Schemes	Shown In
Pressure Distribution*	Figures 5-13 and 5-14
Shower Head	Figures 5-15 and 5-16
TD Nickel	Figures 5-17 and 5-18
Wafer #1	Figures 5-19 and 5-20
Pedestal Trailing Edge	Figures 5-21 and 5-22
Wafer #2	Figures 5-23 and 5-24
Pierced Sheet	Figures 5-25 and 5-26
Wafer #3	Figure 5-27
Wafer #4	Figure 5-28

* Used to determine airfoil profiles only.

Before running any of the cooling air schemes listed above, tests were conducted to determine typical pressure profiles on the test vane surfaces. Two special vanes with pressure taps at mid-span on both the convex and concave surfaces were used in this test. These vanes had the same airfoil envelope as the cooling scheme test vanes. Two test vanes were used to obtain a sufficient number of chordwise locations.

The vanes were tested at the following main gas stream and cooling air conditions:

Main Stream Pressure - psia	Main Stream Temperature °F	Cooling Air Temperature °F
30	2300	1200
45	2300	650
175	2300	650

Data was recorded at three cooling airflow levels for each mainstream pressure levels, one at the test vane design cooling air flow level, one slightly above and the other slightly below this level.

DOWNGRADING AT 3 YEAR INTERVALS
DECLASSIFIED AFTER 12 YEARS
DOD DIR 5200.10

TEST RESULTS

The data obtained from the initial tests to determine pressure profiles around the vanes is shown in Figure 5-29. This information was used for computing the heat transfer coefficients along the test vane airfoils.

Vane metal temperatures measured during the testing of the film cooled vane designs was plotted on curves showing metal temperature versus percent chord position for each of the three coolant flow levels used at each test condition. The test results for the showerhead vanes, the pedestal trailing edge vanes and the Wafer #1 and #2 vanes are shown in Figure 5-30 through 5-33. The tests on number 3 and 4 wafer vanes were run in a similar but larger heat transfer cascade rig. The test results are shown in Figures 5-34 thru 5-37. Analysis of the data from tests of the No. 3 vane demonstrated excellent chordwise cooling except for the trailing edge which was not cooled sufficiently. Analysis of the data from the tests of the No. 4 vane demonstrated an excellent coolant capability. Testing of the T. D. nickel vanes and the pierced sheet vanes was still in progress at the close of this report period. Information obtained in this program will be used to assist in the SST engine design. Running time on the choked cascade rig during this report period totalled 58.9 hours.

D. DEVELOPMENT OF A CHOKED CASCADE THERMAL SHOCK RIG FOR THE THERMAL FATIGUE TESTING OF FULL-SCALE TURBINE VANES

During the Phase IIA contract period, a choked cascade thermal shock rig for the thermal fatigue testing of full-size turbine vanes was constructed and initial shakedown tests were completed. During the Phase IIB period, additional shakedown tests were performed and modifications were made to the rig in order to improve test section inlet temperature distribution patterns. A satisfactory temperature profile was obtained. The rig is now ready for accelerated endurance testing.

1. DESCRIPTION OF TEST RIG

The choked cascade rig, which is shown in Figure 5-38 and Figure 5-39 consists of a translating water-cooled vane holder mounted in a test chamber to which air is supplied from a common source through a centrally located hot gas duct and two cold air side ducts. In operation the

DOWNGRADED AT 3 YEAR INTERVALS
DECLASSIFIED AFTER 12 YEARS
DOD DIR 5200.10

vane holder which has a capacity for testing twenty vanes simultaneously, can be translated to a position in which ten vanes are exposed to the hot gas stream and ten to the cold gas stream. After a predetermined exposure period, the holder is moved rapidly in the reverse direction, exposing the ten heated vanes to the cold air stream and positioning the ten cold vanes in the hot gas stream. This alternate exposure to hot gas and cold air constitutes one thermal shock cycle. A stand heater burner was installed in the cooling air ducts to permit varying the cold air supply over a temperature range from 200°F to 1000°F. A radiation shield was mounted in the test chamber downstream of the vane cascade to reduce radiation heat losses from the vane trailing edges thereby simulating the engine installation which would have a turbine disc located aft of the vanes.

2. TEST PROGRAM

Testing was initiated to determine if the burner exit profile simulated engine operating conditions. Vane inlet gas temperature profile calibrations were run at approximately 1700°F, 2000°F and 2300°F inlet temperature. The gas temperature gradient across the transition duct (located upstream of the vane cascade) was measured using five water-cooled traversing probes. The results obtained were inconclusive because a post-test inspection revealed a collapsed main combustion chamber exit duct.

Following this test, a cermet transition duct was installed, the rig was reassembled and a two-point calibration at approximately 1900°F and 2000°F was performed to recheck the test section inlet gas temperature profile. An analysis of the results revealed the profiles to be unacceptable since a temperature gradient of approximately 600°F existed at the 1900°F point. A post-test inspection of the rig showed that all components were in good condition.

In an attempt to improve the inlet profile, the main combustion chamber hole pattern was modified to increase the center tube combustion hole area. The LT-1 ceramic transition duct was removed and a water cooled transition duct was installed. After reassembly of the rig, testing was resumed and data was recorded at average test section inlet temperatures ranging from 1800°F to 2300°F. An analysis of the data revealed an improved vane inlet gas temperature profile with a reduction in the maximum temperature gradient to 450°F at the three lower points.

DOWNGRADED AT 3 YEAR INTERVALS
DECLASSIFIED AFTER 12 YEARS
DOD DIR 5200.10

The rig was reassembled and another test was run. An analysis of the results indicated no significant improvements in the vane inlet gas temperature profile.

The rig was modified in an attempt to improve the inlet gas temperature profile by plugging eighteen holes around the #1 and #6 fuel nozzle swirlers. An analysis of the data obtained showed no significant improvements in inlet temperature profile.

The main combustion chamber was reoperated to increase the secondary combustion air flow area by plugging 43 holes on the circumference of the burner head. A five point program was conducted at test vane temperature levels of approximately 1600°F, 1900°F, 2000°F and 2100°F. Results indicated no improvement over previous runs with a reduction in the maximum temperature gradient to 430°F.

Subsequently, a five point program was run using combustion chambers with a more symmetrical hole patterns. An analysis of the results indicated a gas temperature gradient of 330°F at the 2000°F vane inlet temperature condition.

The main combustion chamber was reoperated to reduce the maximum temperature gradient by plugging three of the secondary combustion air holes to increase the gas temperature on the "cold" left side. The results of tests with this burner revealed a temperature profile with a maximum temperature gradient of 340°F.

The main combustion chamber was reoperated to increase the gas stream temperature in the lower right hand corner of the cascade. Tests conducted after this change indicated that this reoperation produced an acceptable burner profile with a maximum temperature variation of 295°F at the 2000°F inlet temperature condition. Following completion of these tests, the side air ducts were balanced by adjusting the butterfly valves and the rig was deemed to be ready to start thermal fatigue programs on advanced air-cooled vanes. The total running time on this rig is 174.4 hours.

E. EVALUATION OF FULL-SCALE AIR-COOLED BLADES AND VANES IN THE TURBINE DEVELOPMENT ENGINE

The purpose of this program was to continue the engine testing of full-scale air-cooled turbine blades and vanes at turbine inlet temperatures of 2300°F and above. During the Phase II B contract in addition to the cyclic testing a total of 200 hours of endurance testing was accomplished in the turbine development engine.

DOWNGRADED AT 3 YEAR INTERVALS
DECLASSIFIED AFTER 12 YEARS
DOD DIR 5200.10

1. DESCRIPTION OF TURBINE DEVELOPMENT ENGINE

The turbine development engine used in this program was basically a JT4 engine with the low compressor and low turbine sections removed.

The basic hardware consisted of a bellmouth inlet, a seven-stage compressor, complete diffuser and burner sections and a single stage turbine. The exhaust area was designed to produce optimum conditions required by the compressor for starting and continuous operation. The vehicle was equipped with instrumentation in the turbine section allowing for strain gage and thermocouple measurements through a slip ring assembly attached to the turbine shaft. In addition, the normal instrumentation requirements for measuring airflow, pressures and temperatures throughout the vehicle were incorporated.

In order to permit running at elevated turbine inlet temperatures at conditions simulating supersonic transport operation, this engine was installed in a test stand incorporating provisions for heating the inlet air. Figure 5-40 shows a view of the heated inlet hardware which was provided for this test; Figure 5-41 shows a schematic diagram of the test installation. The turbine blade and vane cooling air was supplied by a JT12 engine with the cooling air bled off from the compressor discharge as shown in Figure 5-42. The JT12 engine was used in order to permit varying cooling airflow and pressure differentials independent of engine conditions. The vane and blade cooling air system incorporated a heater burner in the supply line to allow pre-heating the air to any desired temperature. An overall view of the engine installation including the vane and blade cooling air supply system is shown in Figure 5-43. The turbine inlet temperature was measured with eight Platinum-Platinum Rhodium water cooled, aspirated, gas temperature probes which were traversed periodically across the gas stream approximately 3" upstream of the first nozzle vanes. These probes were located circumferentially around the engine, one behind each burner can, to sense an "average" burner can exit temperature.

2. DESCRIPTION OF BLADES AND VANES TESTED IN THE TURBINE DEVELOPMENT ENGINE

During this contract period both film-cooled and convectively-cooled turbine blades were tested in the turbine development engine. All of the film-cooled blades were to a "shower-head" design. The "shower-head" blades incorporate provisions for film cooling the leading edge with air discharged through a series of holes in the blade leading edge. In addition, some of the blades had holes drilled near the trailing edge

DOWNGRADED AT 3 YEAR INTERVALS
DECLASSIFIED AFTER 12 YEARS
DOD DIR 5200.10

THIS DOCUMENT CONTAINS INFORMATION AFFECTING THE NATIONAL DEFENSE OF THE UNITED STATES WITHIN THE MEANING OF THE ESPIONAGE LAWS, TITLE 18, U.S.C., SECTIONS 793 AND 794. ITS TRANSMISSION OR THE REVELATION OF ITS CONTENTS IN ANY MANNER TO AN UNAUTHORIZED PERSON IS PROHIBITED BY LAW.

on both the suction and pressure surfaces to provide trailing edge cooling. The shower head type blade configurations tested during this period are listed below:

Leading Edge Cooling Scheme	Shown In
Three rows of .013" dia. holes at 90° to L.E.	Figure 5-44
Three rows of .013" dia. holes at 30° to L.E.	Figure 5-45
Three rows of .008" dia. holes at 90° to L.E.	Figure 5-46
Five rows of .008" dia. holes at 90° to L.E.	Figure 5-47
Five rows of .008" dia. holes at 30° to L.E.	Figure 5-48
One row of .030" dia. holes at 30° to L.E.	Figure 5-49
Three rows of .030" dia. holes at 30° to L.E.	Figure 5-50

The convectively cooled blades and vanes tested in this phase of the program are listed below:

Blade Design	Material
.020" Sawtooth	PWA-659
.030" Sawtooth	PWA-655, 663
Eleven Hole	PWA-658, 659, 663
Ribbed Core	PWA-658, 659, 663

Sample blades of each of these types cut away to show the cooling passages are presented in Figure 5-51. All of the test blades were coated with either JC14L (Jo Coat) or $TaAl_3$ (Chromally).

The vane designs evaluated in the turbine development engine during Phase II B included the following configurations:

Vane Design	Material
Slotted trailing edge	PWA-657, AMS 5382
Pedestal Cor. Trailing Edge	PWA-657, AMS 5382

The test vanes were coated with either Jo Coat or Chromalloy coatings.

3. TEST PROCEDURE

Two types of endurance tests were conducted during this program - steady state endurance tests and cyclic endurance tests. In a steady state endurance test, the engine was brought up to the desired test conditions and run at these conditions for the scheduled duration of

DOWNGRADED AT 3 YEAR INTERVALS
DECLASSIFIED AFTER 12 YEARS
DOD DIR 5200.10

THIS DOCUMENT CONTAINS INFORMATION AFFECTING THE NATIONAL DEFENSE OF THE UNITED STATES WITHIN THE MEANING OF THE ESPIONAGE LAWS, TITLE 18 U.S.C. SECTIONS 793 AND 794. THE TRANSMISSION OR THE REVELATION OF ITS CONTENTS IN ANY MANNER TO AN UNAUTHORIZED PERSON IS PROHIBITED BY LAW.

the test except for shutdowns required for inspections and maintainence. The inspections were performed at twenty-five hour intervals and included visual inspections and growth measurements of the vanes and blades.

The cyclic endurance test schedule was designed with a view to exposing the blades and vanes to a severe thermal fatigue environment. In the cyclic endurance tests, the engine was accelerated in 3 seconds to the maximum turbine inlet temperature desired and operated at these conditions for a predetermined time interval. At the end of this period, the engine was decelerated in 5 seconds to the minimum turbine inlet temperature level established for the program. Thereafter the engine was cycled back and forth between these two temperature levels. The JT12 auxiliary blade and vane cooling air supply engine and the heated inlet facility were operational during the entire test. The heated inlet was cycled in unison to produce the desired temperature level. The JT12 engine was not cycled but was maintained at one cooling air temp. and pressure level throughout the test.

Cycling was controlled electronically in order to insure a repeatable cycle. The engine was controlled by a system of timers, solenoids and valves that coordinated the engine and heated inlet fuel flows to obtain the required idle turbine inlet temperature.

4 TEST PROGRAM AND RESULTS

For the initial run the turbine development engine was assembled with the following film cooled blades:

Configuration			Quantity
5 Row	.008/30°	Showerhead	2
5 Row	.008/90°	Showerhead	3
3 Row	.008/90°	Showerhead	5
3 Row	.013/30°	Showerhead	2
3 Row	.013/90°	Showerhead	3
1 Row	.030/30°	Showerhead	4
			19

The remaining blades were convectively cooled.

These blades had previously accumulated five hundred cycles of a cyclic endurance consisting of two minutes at a turbine inlet temperature of 2350°F followed by two minutes at 1500°F. This program was continued to 1987 cycles under this contract. Eight visual inspections

DOWNGRADED AT 3 YEAR INTERVALS
DECLASSIFIED AFTER 12 YEARS
DOD DIR 5200.10
THIS DOCUMENT CONTAINS INFORMATION AFFECTING THE NATIONAL DEFENSE OF THE UNITED STATES WITHIN THE MEANING OF THE ESPIONAGE LAWS, TITLE 18, U.S.C. SECTIONS 793 AND 794. ITS TRANSMISSION OR THE REVELATION OF ITS CONTENTS IN ANY MANNER TO AN UNAUTHORIZED PERSON IS PROHIBITED BY LAW.

of the blades were made during this course of this test. Two of the film cooled blades were removed after two hundred cycles because of foreign object damage. The remaining seventeen film cooled blades completed the entire test and were in excellent condition at the end of the program, as were the convectively cooled blades which made up the balance of the rotor.

The turbine vane assembly used in this test consisted of 24 pedestal core trailing edge, 41 slotted trailing edge, and 15 cutback pedestal core trailing edge vanes. The latter vanes had been cut back to increase nozzle area. After 1430 cycles of testing, 40 of these vanes were removed because of burning and cracking in the leading edges. They were replaced by new parts of the same configuration.

Upon completion of the cyclic endurance test noted above, the engine was disassembled and special instrumented turbine vanes containing shielded leading edge, metal, and cooling air thermocouples were installed. Typical vanes containing this instrumentation are shown in Figures 5-52 and 5-53. The engine was reassembled and calibrations were performed to check the turbine inlet temperature readings determined from this data with the results obtained with the eight platinum rhodium gas temperatures traversing probes installed in the turbine inlet. An analysis of the data indicated good agreement between the temperatures measured by these two instrumentation systems.

The engine was disassembled, with all the instrumentation noted above still installed, the engine was reassembled with a turbine disc incorporating blades with metal temp measuring thermocouples. These blades are listed below. Tests were conducted to record transient gas and metal temperatures during a cyclic endurance test.

Design		Type of Air Cooling	Quantity
One row	.030/30° Showerhead	Film	5
Three row	.008/90° Showerhead	Film	5
Three row	.013/90° Showerhead	Film	5
Three row	.013/30° Showerhead	Film	5
.020	Sawtooth	Convective	2
.030	Sawtooth	Convective	2

DOWNGRADED AT 3 YEAR INTERVALS
DECLASSIFIED AFTER 12 YEARS
DOD DIR 5200.10

THIS DOCUMENT CONTAINS INFORMATION AFFECTING THE NATIONAL DEFENSE OF THE UNITED STATES WITHIN THE MEANING OF THE ESPIONAGE LAWS, TITLE 18 U.S.C. SECTIONS 793 AND 794. THE TRANSMISSION OR THE REVELATION OF ITS CONTENTS IN ANY MANNER TO AN UNAUTHORIZED PERSON IS PROHIBITED BY LAW.

As before, the balance of the blades were uninstrumented convectively cooled parts. Temperature readings from the above thermocouples plus six on the front and rear side plates, the blade cooling air temperature, the vane cooling air temperature, turbine discharge temperature and compressor discharge temperature were recorded on an IBM tape which was later reduced and plotted for analysis. Representative gas and blade metal temperatures measured during a typical endurance cycle are shown in Figures 5-54 and 5-55. The actual metal temperatures agreed with predicted values. This agreement is shown in Figures 2A-186, 2A-187, 2A-188 and 2A-189.

After the tests noted above were completed the instrumented vanes were removed and replaced with previously tested parts. The instrumented disc was replaced with one containing the following convectively cooled blades:

Quantity	Configuration	Material	Coating
40	Ribbed Core	PWA 663	JC14L (Jo Coat)
11	Ribbed Core	PWA 663	$TaAl_3$ (Chromally)
16	Ribbed Core	PWA 659	JC14L (Jo Coat)
29	Ribbed Core	PWA 658	JC14L (Jo Coat)

A 200 hour steady state endurance test was conducted at simulated SST cruise conditions with a turbine inlet temperature of 2300°F and with 1200°F cooling air supplied to the blades. The parts were removed at 25 hour intervals for visual inspections and growth measurements. Values of blade growth versus elapsed time measured during this test are shown in Figure 5-56. The data is in good agreement with the predicted values. In order to avoid the possibility of a premature failure, blades indicating high growth rates were removed at the twenty-five hour inspections and replaced with new parts. First indications of blade fatigue were noted at 150 hours when stress rupture cracks were observed on the concave surface of a PWA 663 blade at approximately one third of the blade span as shown in Figure 5-57. During the 175 hour inspection another blade, was found cracked in the same manner. Seven minutes before the end of the 200 hour endurance test, a PWA 663 blade failed at approximately one-third span damaging six other blades. All of the blades run in this test were

DOWNGRADED AT 3 YEAR INTERVALS
DECLASSIFIED AFTER 12 YEARS
DOD DIR 5200.10

visually inspected for cracks and then X-rayed for further indications of cracking. The results of this inspection revealed the following:

	PWA 658	PWA 659	PWA 663	
			Jo Coat	Chromally
Visual Crack Indications	2	1	3	11
X-Ray Indications	17	6	12	12
No Indications	2	9	4	5
Impact Damage	8	0	2	9

At the close of this report period, the running time accumulated on the turbine development engine was:

	During Phase II B
Total Engine Time	344
Running Time Between 2200°-2300°F	9
Running Time Between 2300°-2400°F	229
Total Time Above 1900°F	320
Total Number of Endurance Cycles	657

F. PERFORMANCE TESTING OF FILM COOLED VANES

Performance tests on film-cooled vanes were run in a cascade rig to investigate how the airflow discharged through the vane cooling holes affected overall vane aerodynamic performance. The effect of cooling flow rate and discharge hole location were investigated in this program.

1. DESCRIPTION OF TEST RIG

The vane cascade test rig is shown in Figure 5-58. In this photograph a transparent vane pack is shown installed in the rig to illustrate the orientation of the vanes with respect to the main air supply which enters from the right. Figure 5-59 shows a closeup view of a vane pack with cooling air plenum chamber, thermocouples and pressure taps. The rig instrumentation included cascade inlet total temperature and pressure probes, inlet static pressure taps, an exit total pressure traverse probe, exit static taps and orifice instrumentation sufficient to calculate mainstream and cooling air weight flow. A schematic diagram of the rig showing instrumentation locations is presented in Figure 5-60.

DOWNGRADED AT 3 YEAR INTERVALS
DECLASSIFIED AFTER 12 YEARS
DOD DIR 5200.10

2. DESCRIPTION OF PARTS TESTED

JT4-size first-stage turbine vanes with six cooling hole configurations were tested in this program. The airfoil section diagram in Figure 5-61 shows the dimensions of the holes in the basic vane. Five different permutations were generated from this basic vane by plugging the appropriate holes. The sixth configuration was obtained by plugging all the holes and adding holes to the leading edge which were left open. The six configurations are summarized below:

Holes open in the pressure surface, suction surface upstream of the gaging point, and suction surface downstream of the gaging point (i.e. see Figures 5-62 and 5-63).

Holes open in the pressure surface and in the suction surface upstream of the gaging point only.

Holes open only in the suction surface upstream of the gaging point.

Holes open in the pressure surface only.

Holes open in the leading edge only (Figure 5-64).

All holes plugged; no cooling

One set of six blades constituted a vane cascade test pack. All holes on the pressure and suction surfaces were rectangular slots; the holes on the leading edges were all round. The centerlines of all pressure and suction surface holes are at a 30-degree angle to the airfoil surface. The leading edge holes are inclined at a 45-degree angle to the vane leading edge.

3. METHOD OF TEST

In the test program, the six vane packs were tested over a range of cascade inlet pressures and cooling airflows. With each of the six vane packs the cascade inlet pressure was varied over a range which, as found from the recorded data, yielded cascade exit Mach numbers from 0.5 to approximately 1.1. At each cascade inlet pressure on the five vane packs with cooling air holes open, several runs were made at various cooling-to-mainstream pressure ratios, including zero (no cooling air). On each run a traverse was made at the cascade exit. During this traverse the pressure drop across the cascade was automatically recorded. From this data the profile loss coefficient ($1-\Phi^2$)

was computed for each run. The cooling air weight flow (W_c) and the mainstream air weight flow (W_v) were computed from orifice data and the cascade exit Mach number (Mn) was also calculated, as noted above. For each vane pack the profile loss coefficient and the percent cooling air ($100\ W_c/W_v$) were both plotted against exit Mach number, for different ratios of cooling total pressure to mainstream total pressure.

From this a correlation of turbine efficiency with percent cooling air was derived. This same correlation was also obtained for turbine blades. The results are shown in section G.

G. PERFORMANCE TESTING OF FILM COOLED BLADES

Performance tests were conducted on film cooled blades with the objective of obtaining quantitative information on how the air discharged through the film cooling holes affected turbine aerodynamic performance. This series of tests were conducted in a single-stage rotating turbine rig and were performed at the Andrew Willgoos Turbine Laboratory.

1. DESCRIPTION OF TEST RIG

The test rig was essentially a single-stage turbine utilizing parts from a JT12 engine which had been modified for cold flow turbine testing. A schematic diagram of the overall test installation is shown in Figure 5-65. The turbine was supplied with high pressure air at approximately 200°F from the laboratory air supply. The blade cooling air was supplied from the same source but was metered and controlled separately. The flowpath of the main and cooling airflow through the turbine section is shown in the diagram in Figure 5-66. The location of the instrumentation is shown in Figure 5-67. An overall view of the test installation is shown in Figure 5-68. Turbine shaft power was absorbed by two eddy current dynamometers connected in tandem and located upstream of the rig.

2. DESCRIPTION OF PARTS TESTED

Three sets of film-cooled blades were used in the performance tests under the Phase II B contract. An airfoil section of one blade is shown in Figure 5-69. This set was modified in stages, by plugging the ap-

DOWNGRADED AT 3 YEAR INTERVALS
DECLASSIFIED AFTER 12 YEARS
DOD DIR 5200.10

propriate holes with silver solder, to produce the four cooling hole configurations listed below:

- Holes near the trailing edge in the suction surface plus leading edge slots only (Figure 5-70).
- Holes near the trailing edge on the suction surface only (Figure 5-71).
- Holes near the trailing edge on the pressure surface only (Figure 5-72).
- Leading edge slots only (Figure 5-73).

The holes which were plugged with silver solder appear white in the Figures listed above.

A second set of blades with an entirely different cooling hole arrangement was used to make up the fifth configuration tested during this period. These blades had suction and pressure surface cooling slots near the leading and trailing edges. This configuration, shown in the blade section diagram in Figure 5-74 and Figure 5-75.

Both sets of blades noted above were made by welding closed the blade tip slots in two sets of pedestal-core JT12 convectively cooled turbine blades and machining the various holes and slots through the airfoil into the existing internal cavity using the electrical discharge machining process. The centerlines of all holes (including slots) in the pressure (concave) and suction (convex) surfaces were in planes perpendicular to the turbine radius. However, because of the twist of the blades and the method of machining, the centerline-to-airfoil-tangent angle for holes near the trailing edge varied from approximately 15 degrees near the root to 45 degrees near the tip on the suction surface, and 45 degrees near the root to 15 degrees near the tip on the pressure surface. A somewhat greater variation existed for the leading edge pressure surface and suction surface slots.

The third set of blades had no cooling holes and was used in tests to determine seal leakage and the performance losses due to leakage air.

3. TEST PROGRAM

With each blade configuration, the turbine was operated at expansion ratios of 1.78:1 (design pressure ratio) and 1.55:1. These pressure

DOWNGRADED AT 3 YEAR INTERVALS
DECLASSIFIED AFTER 12 YEARS
DOD DIR 5200.10

ratios were set by adjusting the inlet throttling valve in the main air flow duct. Operation was at the design rim velocity ratio of 0.43, which was maintained by varying the load of the dynamometers. Secondary airflow (cooling plus leakage) was varied from zero to six percent of the main airflow by means of a valve in the secondary line.

In order to determine leakage flow rates, tests were run with solid blades installed. Using this data, secondary flow rates were plotted as a function of the static pressure drop across the labyrinth seal. The results of this leakage flow calibration were then used to determine the portions of the secondary flow which could be attributed to leakage and to blade cooling.

4. TEST RESULTS

The performance loss due to leakage flow only is plotted in Figure 5-76 as a function of the leakage weight flow and the loss due to cooling flow only is plotted in Figure 5-77 as a function of cooling weight flow with hole configuration as the parameter. Since the change in turbine performance due to both cooling and leakage flow was independent of the turbine expansion ratio, the referenced curves do not distinguish between the data taken at the two ratios which were used. From the curve in Figure 5-76 it can be seen that the greater the leakage flow, the more rapidly the efficiency losses due to leakage increased. By comparing solid blade test flow data with cooled blade data, as indicated above, the cooling flow can be separated from the leakage flow.

The loss in efficiency was a nearly linear function of cooling airflow rate, as seen in Figure 5-77. The lowest losses occurred with the configuration having holes near the trailing edge on the pressure surface only. Highest losses resulted from the configuration having slots on both surfaces near both the leading and trailing edges and the configuration having leading edge slots only. Lower losses resulted from the use of holes near the trailing edge on the suction surface only.

Figure 5-78 shows the ratio of cooling air chamber static pressure to turbine inlet total pressure required to produce cooling airflow rates up to two percent for each cooling hole configuration. For smaller hole areas it was necessary to have a pressure ratio as high as 2.0:1 for a one percent flow. This relationship shows the advantage of using larger cooling hole areas which will result in a smaller required pressure ratio for the cooling flow and hence lower leakage flow.

DOWNGRADED AT 3 YEAR INTERVALS
DECLASSIFIED AFTER 12 YEARS
DOD DIR 5200.10

H. LABORATORY TESTING OF ADVANCED VANE AND BLADE MATERIALS

The laboratory program to test advanced vane and blade materials which was started under Phase II-A was continued and expanded under Phase II-B. The goals of this program have been the evaluation of candidate materials and manufacturing processes and the production of design data for application to the SST turbine design. To this end, numerous laboratory programs were conducted to investigate the characteristics of various high temperature materials at conditions simulating operation in an SST powerplant. These programs included long term creep tests, cyclic stress rupture tests, low cycle fatigue tests, and creep rupture tests. The work completed on each of these items is summarized briefly below:

1. CYCLIC STRESS RUPTURE TESTS

The purpose of this program was to investigate the notch sensitivity of several superalloys when subjected to the combined effects of stress rupture and fatigue. This type of testing produces time-strain failures which are similar to those which may be experienced during engine operation. The relative notch effect produced by three drilling processes was examined to provide design data applicable to film-cooled blades and vanes.

The tests were conducted in the creep machine which is shown in Figure 5-79. This machine was capable of providing automatic cycling of the tensile load while maintaining the test temperatures by means of a wire wound electrical furnace. For these tests, the creep machine was programed to produce a cycle consisting of thirty minutes at full load and two minutes at no load.

The specimens used for these tests were machined from cast test bars of the various materials being investigated. Before machining, these bars were examined for grain size and porosity to insure that the material met or exceeded the minimum specifications of the PWA acceptance test. The test specimens were 1.690 inches long and .230 inches in diameter. Figure 5-80 shows a cross section of one of these specimens. The specimen size was selected to provide good correlations with blade and vane leading edge size.

Four specimens were prepared for each of the candidate drilling processes along with four smooth specimens of each alloy. Five holes .030 in. in diameter were drilled in these specimens. The specimens

DOWNGRADED AT 3 YEAR INTERVALS
DECLASSIFIED AFTER 12 YEARS
DOD DIR 5200.10

were then given the same coating cycle that blades of similar materials would receive in production.

PWA663 alloy was chosen for the cyclic stress rupture tests during the Phase II-B contract. Sufficient stress rupture data has been accumulated for this material under previous programs to establish expected trends in the time and temperature range of interest. During Phase II-A similar testing had been conducted on PWA659 and PWA657 alloys; data from these tests was compared with results on PWA663 alloy which was obtained during this period.

Two methods of drilling the PWA663 specimens were investigated during this period. These were (a) electro-chemical mechanical drilling and (b) ordinary mechanical drilling. The results of these tests and similar tests on PWA659 and PWA657 are shown in Figure 5-92. As shown in this figure, the mechanically drilled specimens showed a slight increase in life in the low cycle range. This phenomenon has been observed in previous stress rupture tests of similar super alloys. In the region, however, where the number of cycles becomes appreciable this increase in strength became very small. With the electro-chemical drilled specimens, endurance life was reduced by a factor of almost ten. A similar loss in life was observed for the EDM (electro discharge machined) specimens of PWA659 and PWA657 tested previously as shown in Figure 5-81.

The cyclic stress rupture tests conducted to date have indicated the following:

- The cyclic stress rupture strength of the three superalloys tested was reduced by drilling with the ECM and EDM processes.
- The cyclic stress rupture strength of these materials did not seem to be greatly affected by mechanical drilling.

2. LOW CYCLE FATIGUE TESTING

Pratt & Whitney Aircraft has developed an analytical technique for predicting the thermal cyclic life of turbine blades and vanes. The accuracy of this technique, which is described in the design section of this report, is predicted on the availability of reliable data on the low cycle fatigue properties of the materials in question. One method of obtaining accurate data is to conduct LCF tests on specimens which simulate the section of the airfoil for which the fatigue life is being predicted. This type of testing results in the generation of design data for configurations as well as materials and is particularly applicable to film cooled airfoils containing holes or slots.

DOWNGRADED AT 3 YEAR INTERVALS
DECLASSIFIED AFTER 12 YEARS
DOD DIR 5200.10

This document contains information affecting the national defense of the United States within the meaning of the espionage laws, Title 18, USC Sections 793 and 794. The transmission or the revelation of its contents in any manner to an unauthorized person is prohibited by law.

The goal of the program conducted during this report period was to evaluate the effect of various methods of drilling holes on the low cycle fatigue properties of various blade and vane materials. The tests were conducted on a hydraulically operated push-pull testing machine. The specimen loading levels was selected to produce pre-selected maximum stresses at a rate of 24 cycles per minute. Metal temperatures were maintained at 1400°F throughout the tests with wire heating coils. A typical test specimen is illustrated in Figure 5-82. As shown in this figure, the minimum diameter through the test section was .25 inches. Through this section, three .030 inch holes were drilled in each of four specimens using the drilling methods being evaluated. Following machining and drilling operations, each specimen was given the same protective coating that the material would receive in a production component.

During Phase II-A effort some low cycle fatigue data had been obtained on PWA657 and PWA659 alloys. In Phase II-B the program was expanded to include PWA658 and PWA663, both nickel base alloys. Additional tests were also run on PWA659 to evaluate the effect of drilling methods which had not been considered during Phase II-A. The drilling methods evaluated were mechanical drilling, electro-chemical machining and electrical discharge machining. Smooth bars were also run to establish a basis for comparison.

The results of these tests are shown in curve form in Figure 5-83 and in tabular form in Figure 5-84. The method of presenting the data shown in Figure 5-83 permits an accurate comparison of specimen lives at various stress levels. This is particularily important in the comparing cyclic stress life because examination of the raw data for various stress levels cannot show the expected life-stress relationship.

The trends noted in these tests were as follows:

- In the 1000 to 10,000 cycle range, PWA658 alloy exhibits a reduction in strength when drilled.
- In the 1000 to 10,000 cycle range all methods of drilling produced about the same reduction in the strength of IN 100.
- In the 10,000 to 50,000 cycle range PWA659 showed a lower reduction in life due to drilling than PWA658 in the 1000 - 10,000 cycle range.

DOWNGRADED AT 3 YEAR INTERVALS
DECLASSIFIED AFTER 12 YEARS
DOD DIR 5200.10

THIS DOCUMENT CONTAINS INFORMATION AFFECTING THE NATIONAL DEFENSE OF THE UNITED STATES WITHIN THE MEANING OF THE ESPIONAGE LAWS, TITLE 18 U.S.C. SECTIONS 793 AND 794. THE TRANSMISSION OR THE REVELATION OF ITS CONTENTS IN ANY MANNER TO AN UNAUTHORIZED PERSON IS PROHIBITED BY LAW.

3. TESTING TO DETERMINE THE LONG TERM CREEP PROPERTIES OF PWA 657 COBALT BASE ALLOY

Tests were conducted to determine the long term creep properties of PWA 657 cobalt base alloy over a temperature range from 1400°F to 1800°F. All specimens were tested in the as-cast condition. Stress levels for this program were selected to produce an elongation of one percent after approximately 1000 hours of testing. The results are tabulated in Figure 5-85. As shown in this table, specimens tested at 1500°F and 1600°F reached the desired one percent elongation earlier than anticipated while specimens tested to 1400, 1700 and 1800°F reached the desired elongation at approximately the time predicted. The predicted stress levels were based on limited short time creep test results from other test programs.

After completing the creep tests, the specimens were subjected to tensile tests to determine how exposure to high temperature creep conditions affected room temperature tensile properties. In general, the results (Fig. 5-85) showed a decrease in tensile properties including ultimate strength, 0.2% yield strength and .020% yield strength with increased exposure temperature. All specimens exhibited very low tensile ductility with less than one percent elongation and reduction in area. The specimen exposed at 1500°F showed the highest ultimate strength of all specimens tested; however, this specimen was exposed to test conditions for the shortest time.

4. CREEP RUPTURE TEST OF PWA 658 NICKEL BASE ALLOY

Creep rupture tests were conducted on specimens of PWA 658 nickel base alloy to complement previous test programs conducted to determine the elevated temperature creep stability of turbine blade materials. The tests were run at temperatures of 1500, 1600, and 1700°F with stress levels selected to produce failures in 500 to 1000 hours. All specimens were coated with PWA-47L (Jo Coat) and were aged at 1600°F for twelve hours prior to test. Duplicate specimens were run at each set of test conditions. To save time, if one of the specimens in a pair attained an endurance life of 1000 hours, testing was discontinued on the other specimen as soon as the one percent creep point was reached. In all, eighteen specimens were tested. The test results are tabulated in Figure 5-86. The creep and rupture data showed very little scatter and the results were in generally good agreement with data obtained in previous test programs as indicated in Figures 5-87 and 5-88.

DOWNGRADED AT 3 YEAR INTERVALS
DECLASSIFIED AFTER 12 YEARS
DOD DIR 5200.10

THIS DOCUMENT CONTAINS INFORMATION AFFECTING THE NATIONAL DEFENSE OF THE UNITED STATES WITHIN THE MEANING OF THE ESPIONAGE LAWS, TITLE 18 U.S.C. SECTIONS 793 AND 794. THE TRANSMISSION OR THE REVELATION OF ITS CONTENTS IN ANY MANNER TO AN UNAUTHORIZED PERSON IS PROHIBITED BY LAW.

5. COMBINED STRESS RUPTURE FATIGUE TESTS ON TURBINE BLADE MATERIALS

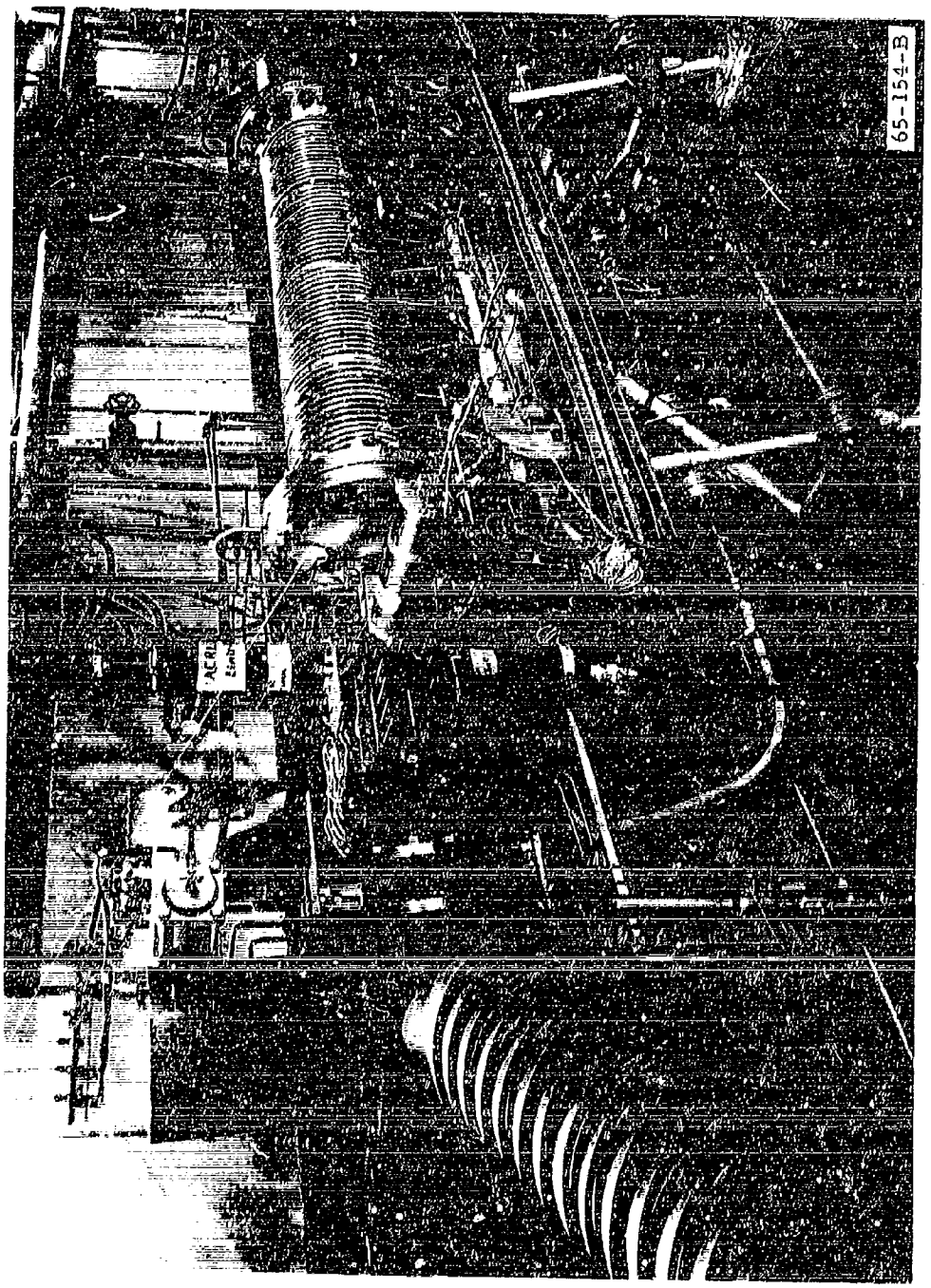
Tests were conducted to determine the stress rupture life of nickel-base turbine blade materials under combined steady state and cyclic stresses at temperatures consistent with the anticipated operating temperatures of the SST engine. A test rig was used which superimposed a reverse bending stress and a steady state stress simultaneously on a specimen maintained at elevated temperature levels. In this program smooth specimens of PWA-659 and PWA-663 materials which had been Chromally coated and aged before the test were tested at 1700°F. The test results are tabulated in Figure 5-89. Figure 5-90 shows the test results for PWA-663 plotted on a Goodman diagram.

6. STRAIN CYCLE FATIGUE TESTS

Strain cycle fatigue tests were conducted on specimens of PWA-663, PWA-659 and PWA-657 alloys using a test rig which was essentially a hydraulically operated device for the axial loading of hollow cylindrical specimens between the desired total strain limits. The strain rate used was six cycles per minute. Testing was conducted at 1300°F, 1700°F and 2000°F and stress levels selected to produce failures in 10 to 1000 test cycles. The results of these tests are tabulated in Figure 5-91.

DOWNGRADED AT 3 YEAR INTERVALS
DECLASSIFIED AFTER 12 YEARS
DOD DIR 5200.10

THIS DOCUMENT CONTAINS INFORMATION AFFECTING THE NATIONAL DEFENSE OF THE UNITED STATES WITHIN THE MEANING OF THE ESPIONAGE LAWS, TITLE 18, U.S.C., SECTIONS 793 AND 794. ITS TRANSMISSION OR THE REVELATION OF ITS CONTENTS IN ANY MANNER TO AN UNAUTHORIZED PERSON IS PROHIBITED BY LAW.

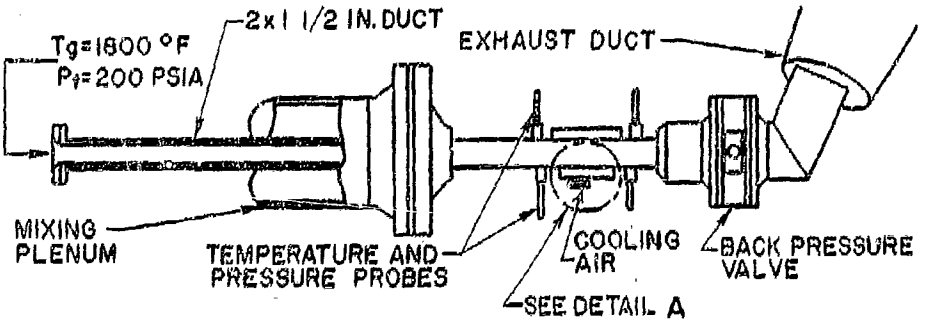


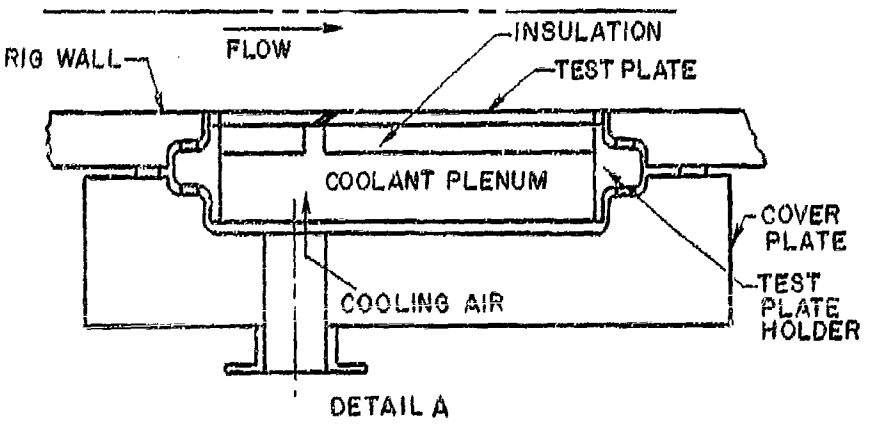
OVERALL VIEW OF BASIC FLOW RIG TEST INSTALLATION

Figure 5-1

DOWNGRADED AT 3 YEAR INTERVALS
DECLASSIFIED AFTER 12 YEARS
DOD DIR 5200.10

THIS DOCUMENT CONTAINS INFORMATION AFFECTING THE NATIONAL DEFENSE OF THE UNITED STATES WITHIN THE MEANING OF THE ESPIONAGE LAWS, TITLE 18, U.S.C., SECTIONS 793 AND 794. ITS TRANSMISSION OR THE REVELATION OF ITS CONTENTS IN ANY MANNER TO AN UNAUTHORIZED PERSON IS PROHIBITED BY LAW.



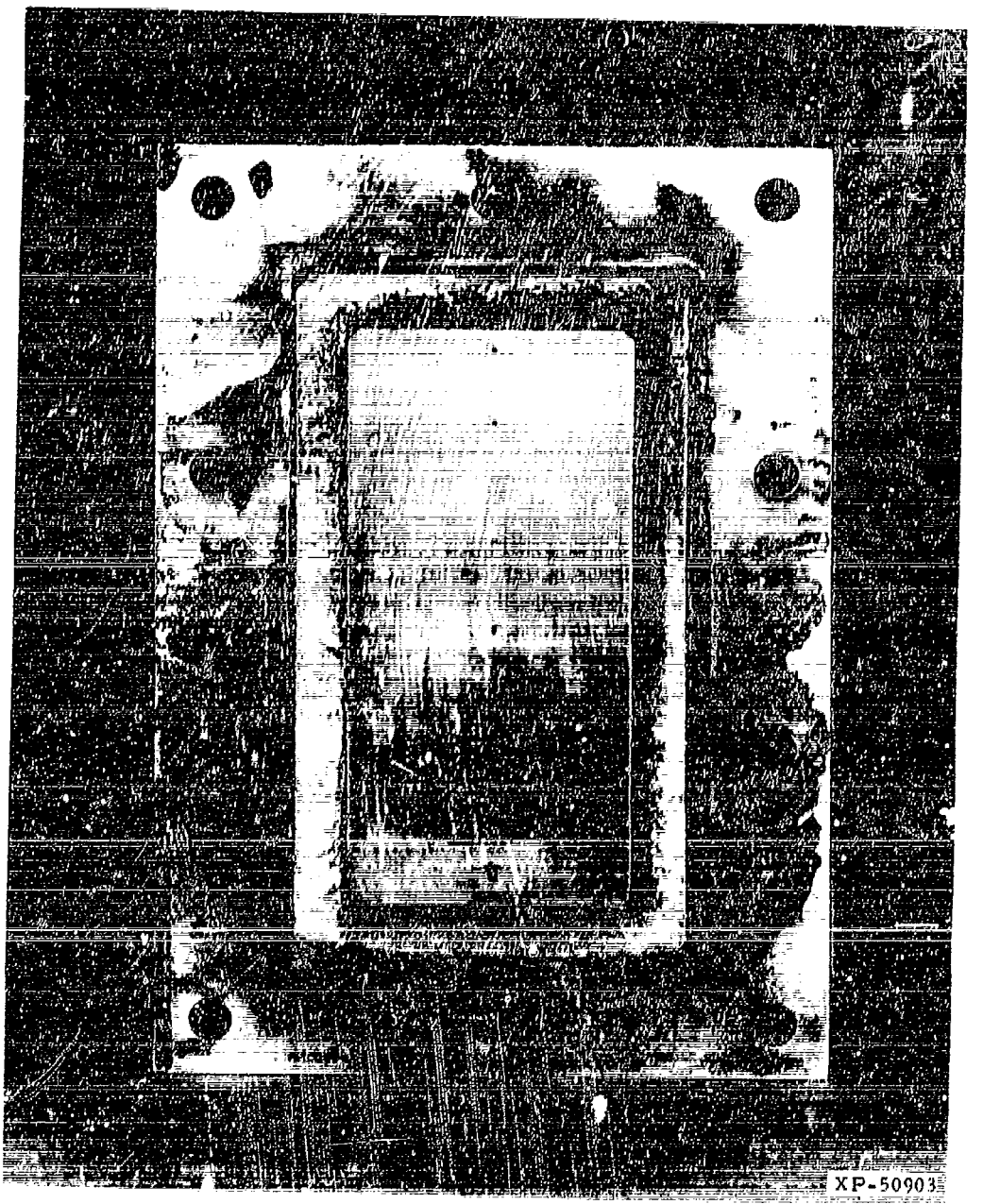


SCHEMATIC DIAGRAM OF BASIC FLOW RIG

Figure 5-2

DOWNGRADED AT 3 YEAR INTERVALS
DECLASSIFIED AFTER 12 YEARS
DOD DIR 5200.10

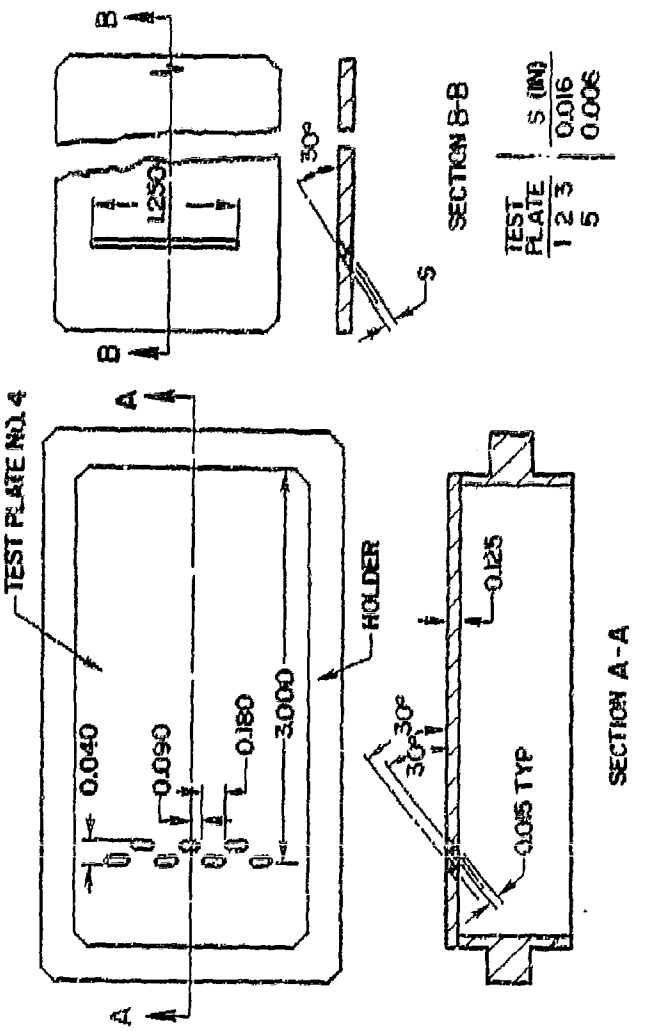
THIS DOCUMENT CONTAINS INFORMATION AFFECTING THE NATIONAL DEFENSE OF THE UNITED STATES WITHIN THE MEANING OF THE ESPIONAGE LAWS, TITLE 18, U.S.C., SECTIONS 793 AND 794. THE TRANSMISSION OR THE REVELATION OF ITS CONTENTS IN ANY MANNER TO AN UNAUTHORIZED PERSON IS PROHIBITED BY LAW.



BASIC FLOW RIG - TEST PLATE HOLDER AND TEST PLATE

Figure 5-3

DOWNGRADED AT 3 YEAR INTERVALS
DECLASSIFIED AFTER 12 YEARS
DOD DIR 5200.10

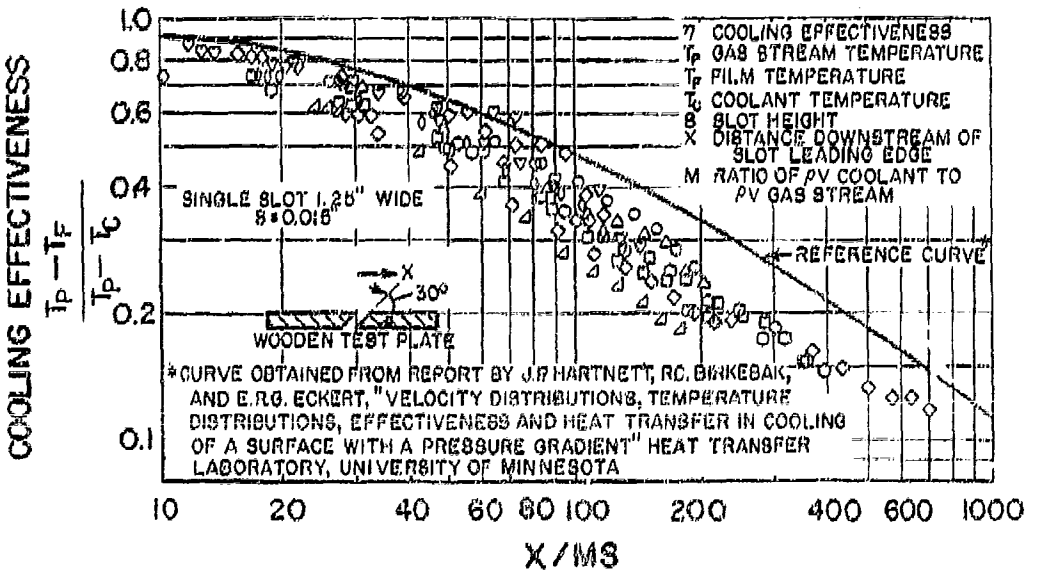


FILM COOLED PLATES TESTED IN BASIC FLOW RIG

Figure 5-4

DOWNGRADED AT 3 YEAR INTERVALS
DECLASSIFIED AFTER 12 YEARS
DOD DIR 5200.10

THIS DOCUMENT CONTAINS INFORMATION AFFECTING THE NATIONAL DEFENSE OF THE UNITED STATES WITHIN THE MEANING OF THE ESPIONAGE LAWS, TITLE 18, U.S.C., SECTIONS 793 AND 794. THE TRANSMISSION OR THE REVELATION OF ITS CONTENTS IN ANY MANNER TO AN UNAUTHORIZED PERSON IS PROHIBITED BY LAW.

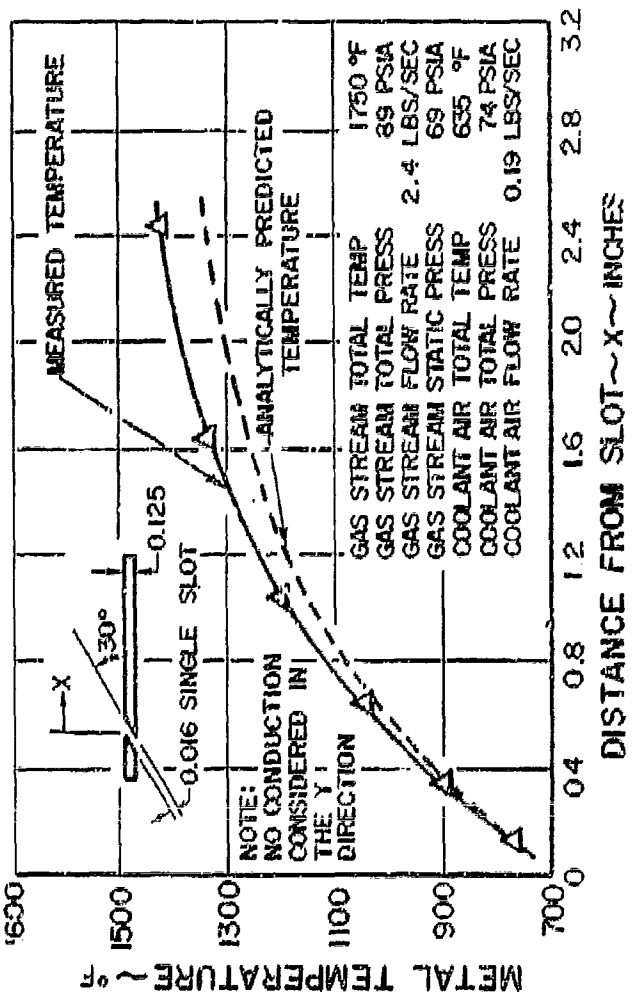


COOLING EFFECTIVENESS TEST RESULTS OBTAINED IN BASIC FLOW RIG USING WOODEN PLATE - LOW TEMP.

Figure 5-5

DOWNGRADED AT 3 YEAR INTERVALS
DECLASSIFIED AFTER 12 YEARS
DOD DIR 5200.10

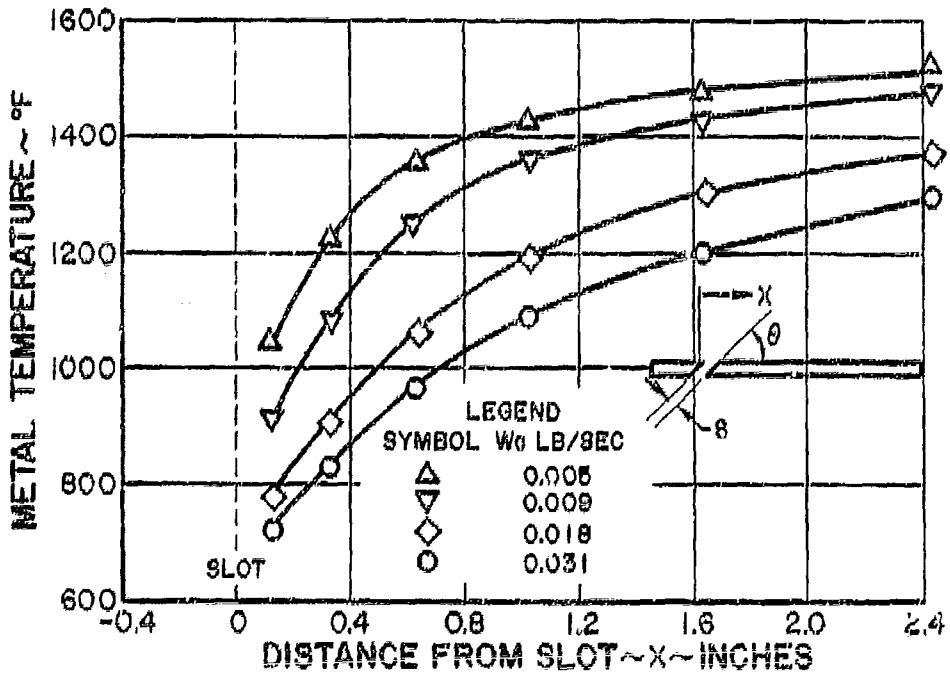
THIS DOCUMENT CONTAINS INFORMATION AFFECTING THE NATIONAL DEFENSE OF THE UNITED STATES WITHIN THE MEANING OF THE ESPIONAGE LAWS, TITLE 18, U.S.C., SECTIONS 793 AND 794. ITS TRANSMISSION OR THE REVELATION OF ITS CONTENTS IN ANY MANNER TO AN UNAUTHORIZED PERSON IS PROHIBITED BY LAW.



COMPARISON OF MEASURED TEMPERATURE DISTRIBUTION WITH ANALYTICALLY PREDICTED DATA - HIGH TEMP.

Figure 5-6

DOWNGRADED AT 3 YEAR INTERVALS
DECLASSIFIED AFTER 12 YEARS
DOD DIR 5200.10

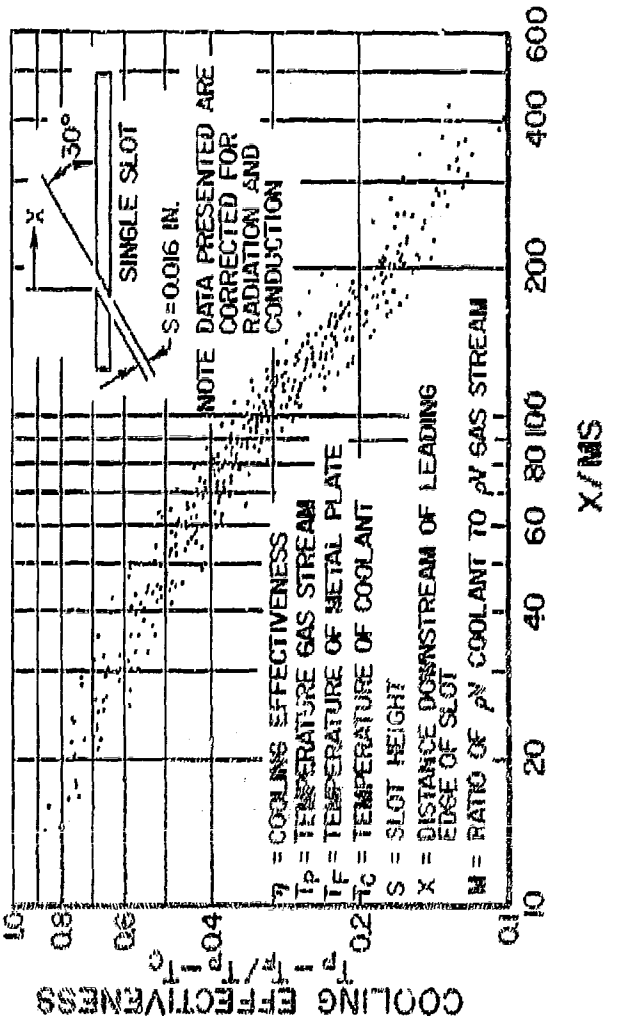


METAL TEMPERATURES MEASURED IN TYPICAL TEST WITH FILM COOLED PLATE - UNCORRECTED FOR RADIATION EFFECTS

Figure 5-7

DOWNGRADED AT 3 YEAR INTERVALS
DECLASSIFIED AFTER 12 YEARS
DOD DIR 5200.10

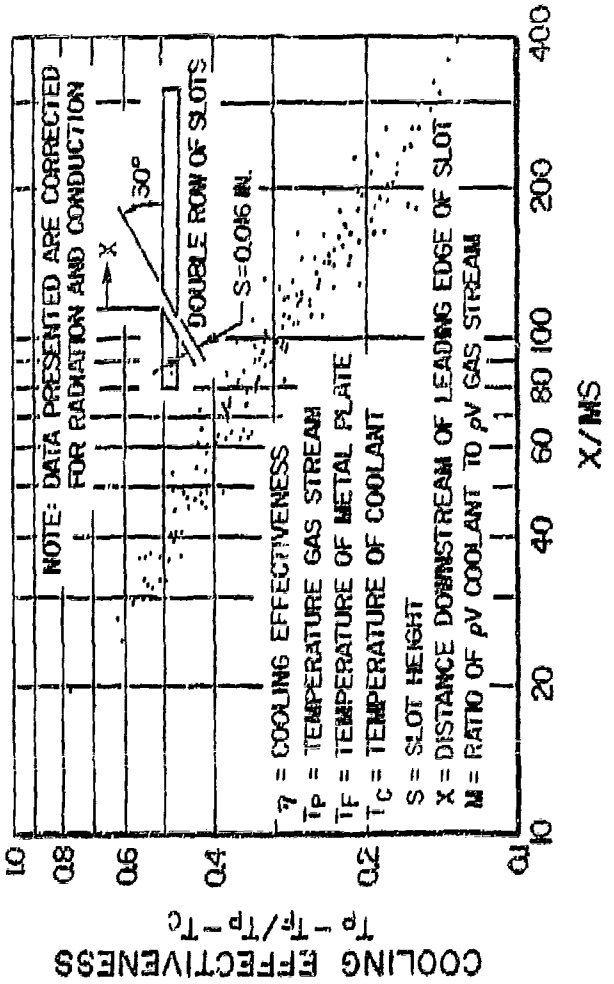
THIS DOCUMENT CONTAINS INFORMATION AFFECTING THE NATIONAL DEFENSE OF THE UNITED STATES WITHIN THE MEANING OF THE ESPIONAGE LAWS, TITLE 18, U.S.C., SECTIONS 793 AND 794. THE TRANSMISSION OR THE REVELATION OF ITS CONTENTS IN ANY MANNER TO AN UNAUTHORIZED PERSON IS PROHIBITED BY LAW.



COOLING EFFECTIVENESS DATA FOR PLATE #3

Figure 5-8

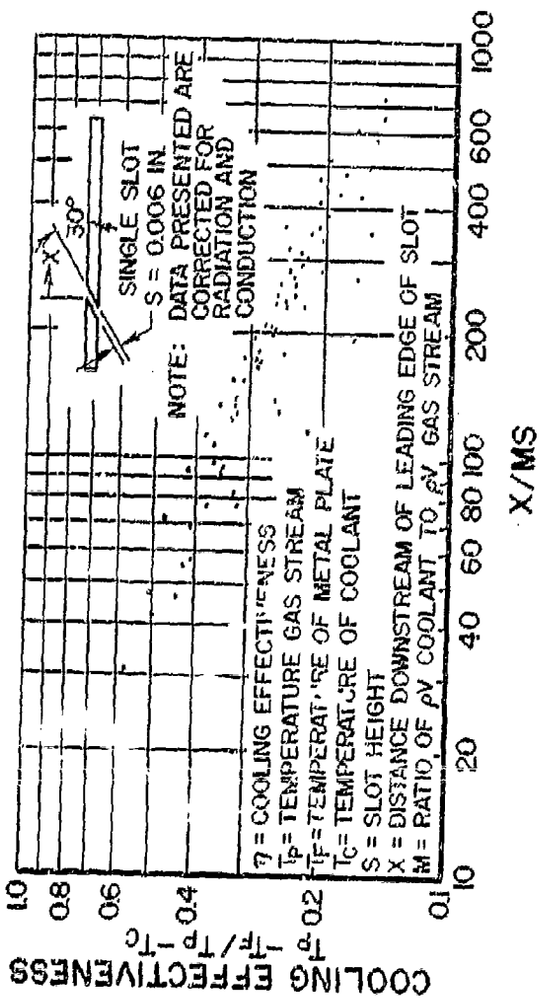
DOWNGRADED AT 3 YEAR INTERVALS
DECLASSIFIED AFTER 12 YEARS
DOD DIR 5200.10



COOLING EFFECTIVENESS DATA FOR PLATE #4

Figure 5-9

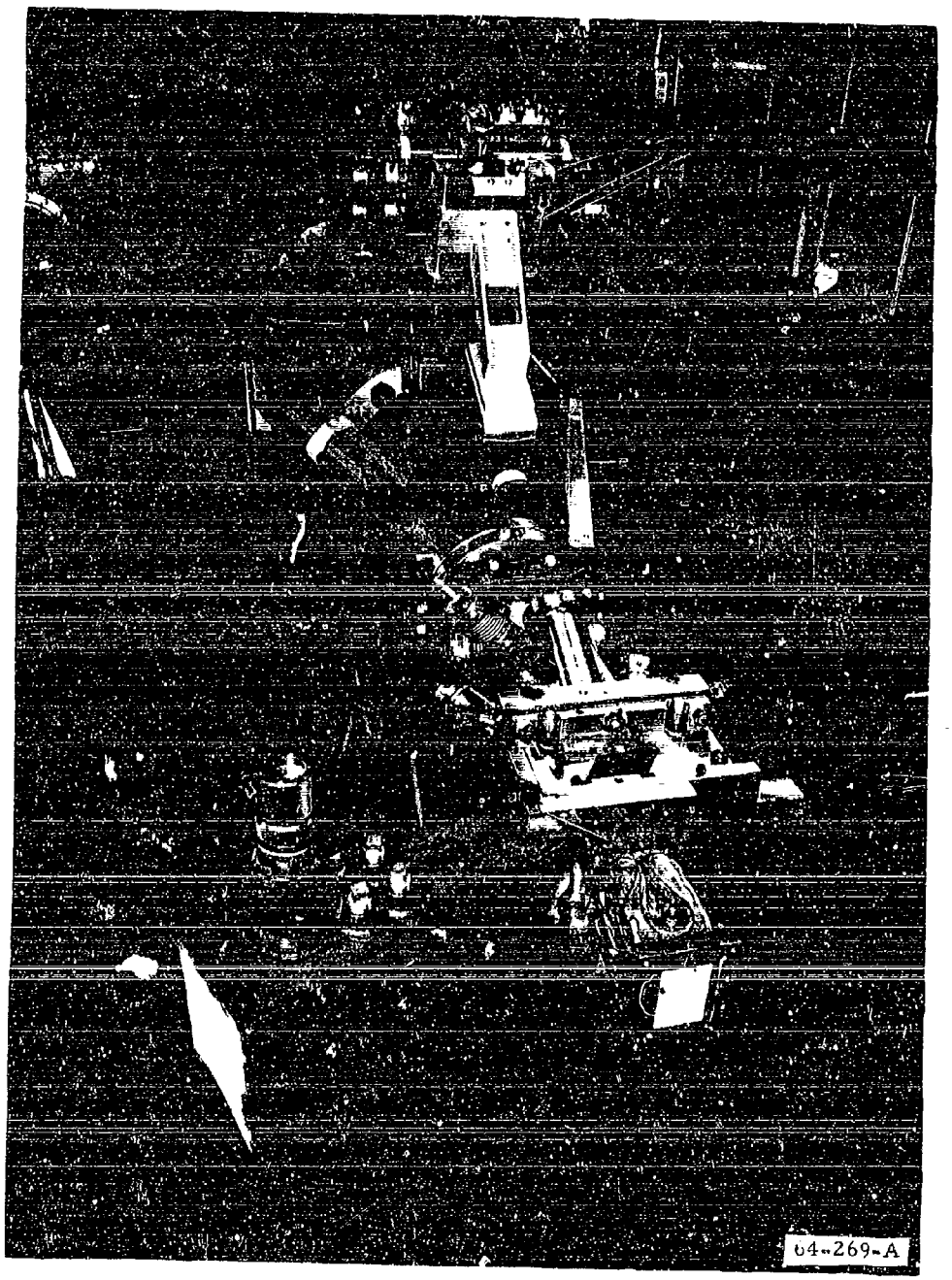
DOWNGRADED AT 3 YEAR INTERVALS
DECLASSIFIED AFTER 12 YEARS
DOD DIR 5200.10



COOLING EFFECTIVENESS DATA FOR PLATE #5

Figure 5-10

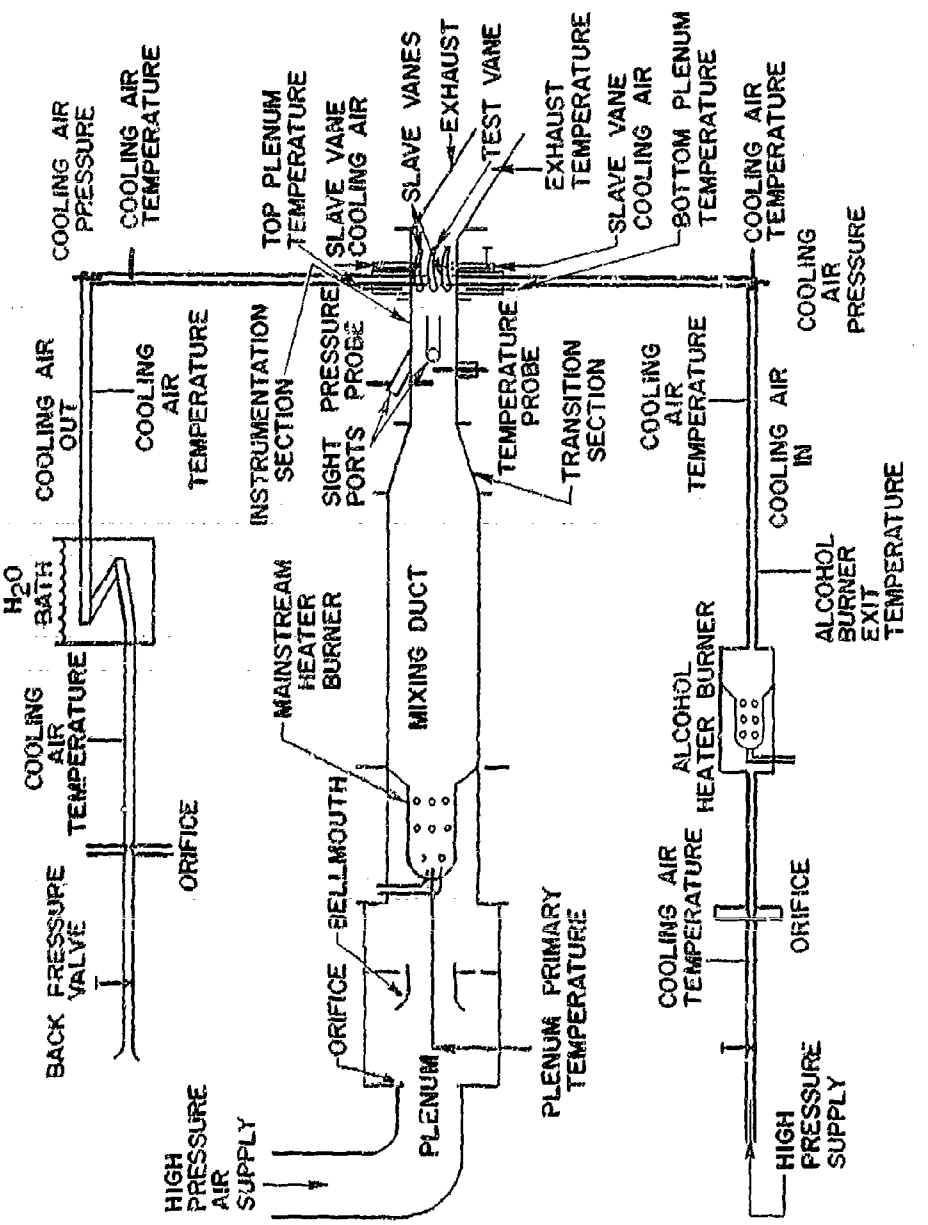
DOWNGRADED AT 3 YEAR INTERVALS
DECLASSIFIED AFTER 12 YEARS
DOD DIR 5200.10



OVERALL VIEW OF HIGH PRESSURE CASCADE RIG TEST INSTALLATION

Figure 5-11

DOWNGRADED AT 3 YEAR INTERVALS
DECLASSIFIED after 12 YEARS
DOD DIR 5200.10

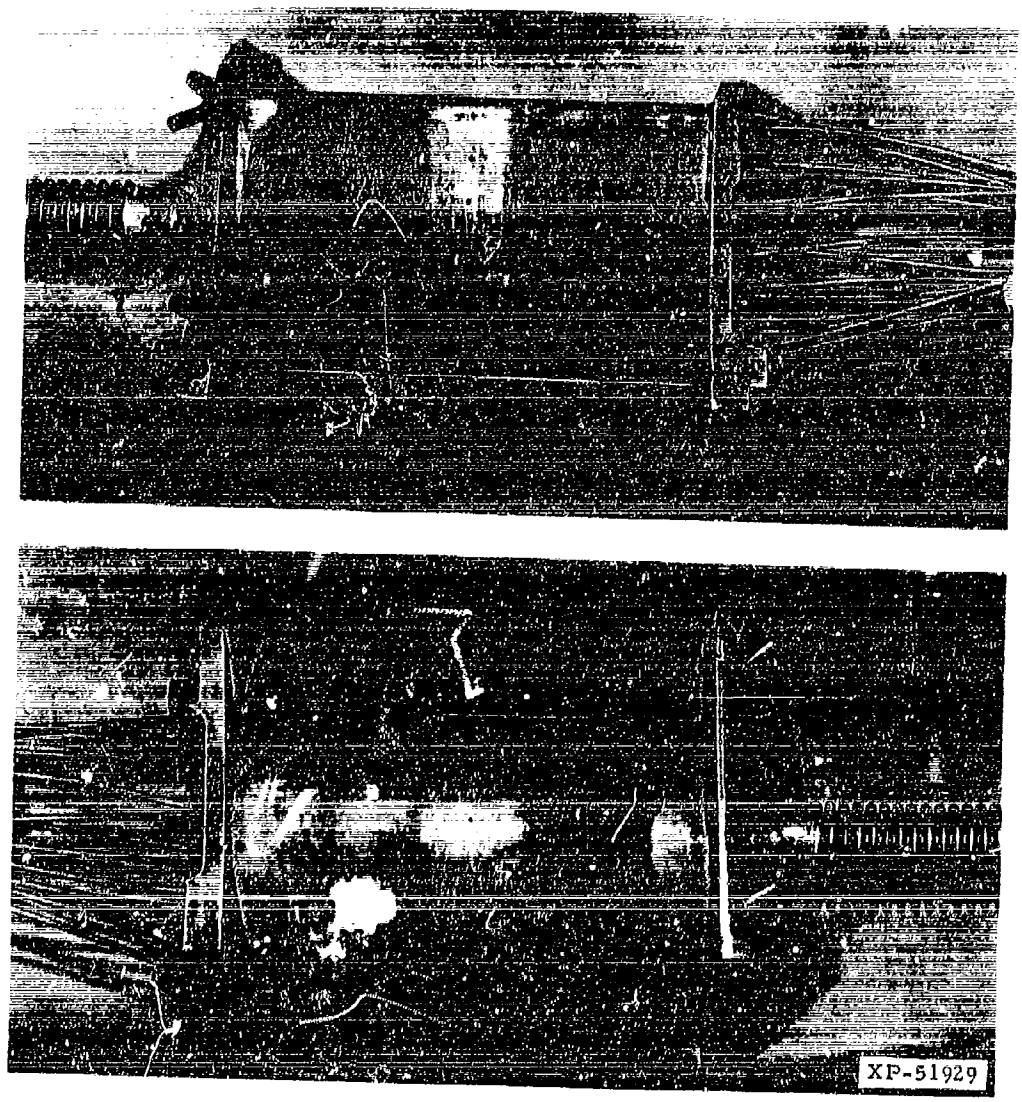


SCHEMATIC DIAGRAM OF HEAT TRANSFER CASCADE RIG

Figure 5-12

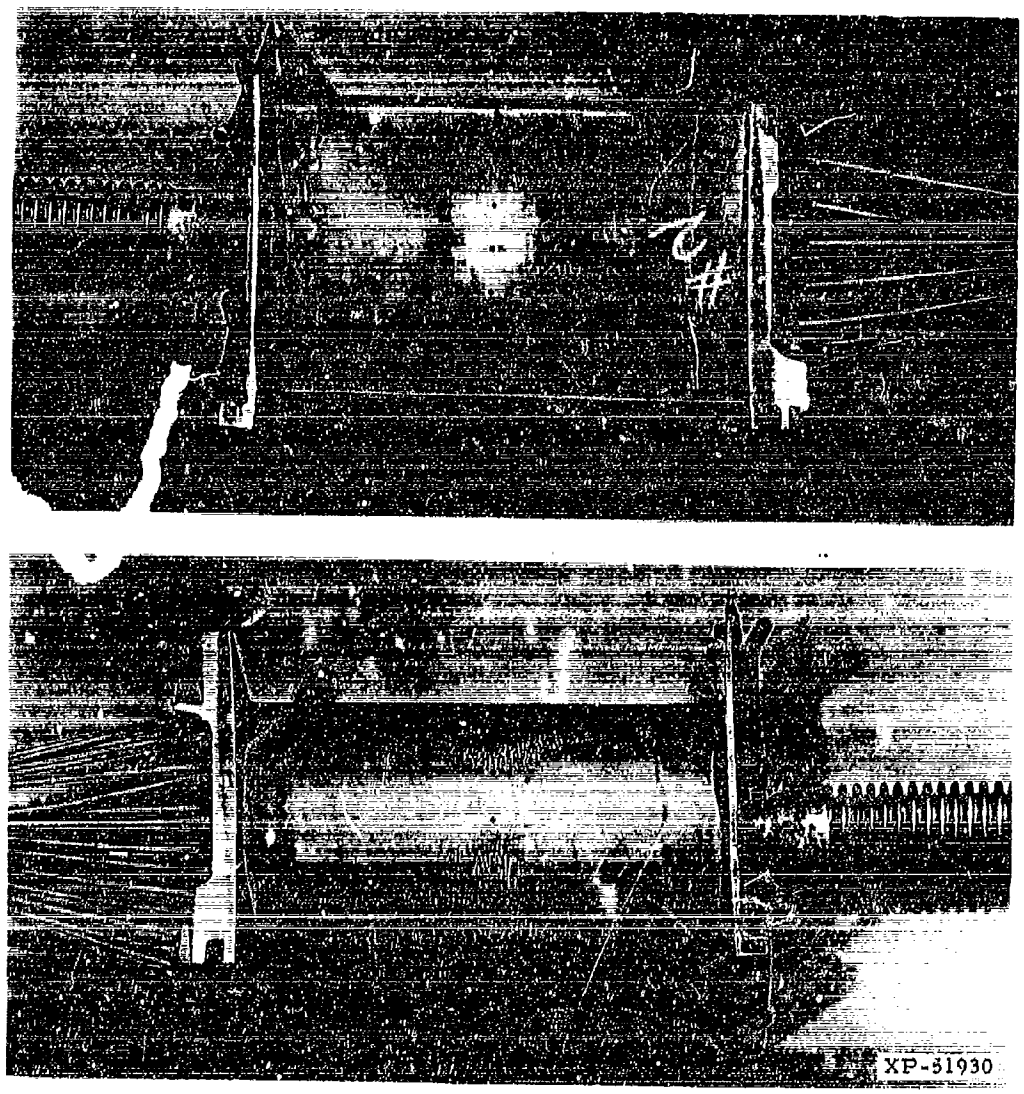
DOWNGRADED AT 3 YEAR INTERVALS
DECLASSIFIED AFTER 12 YEARS
DOD DIR 5200.10

THIS DOCUMENT CONTAINS INFORMATION AFFECTING THE NATIONAL DEFENSE OF THE UNITED STATES WITHIN THE MEANING OF THE ESPIONAGE LAWS, TITLE 18, U.S.C., SECTIONS 793 AND 794. THE TRANSMISSION OR THE REVELATION OF ITS CONTENTS IN ANY MANNER TO AN UNAUTHORIZED PERSON IS PROHIBITED BY LAW.



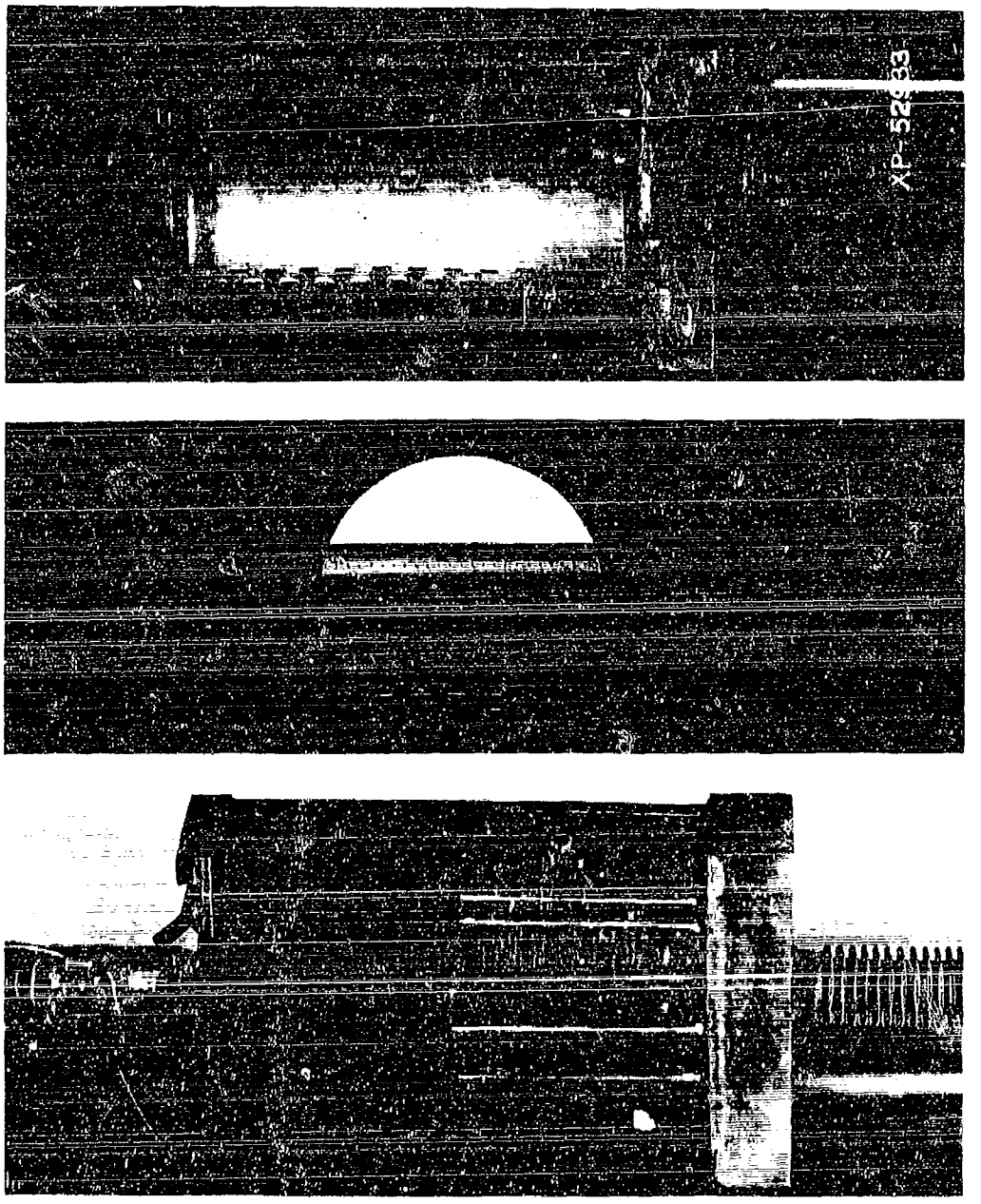
INSTR MENTED PRESSURE DISTRIBUTION VANE #1 USED FOR MEASURING AIRFOIL PRESSURE PROFILES IN HIGH PRESSURE CASCADE RIG

Figure 5-13



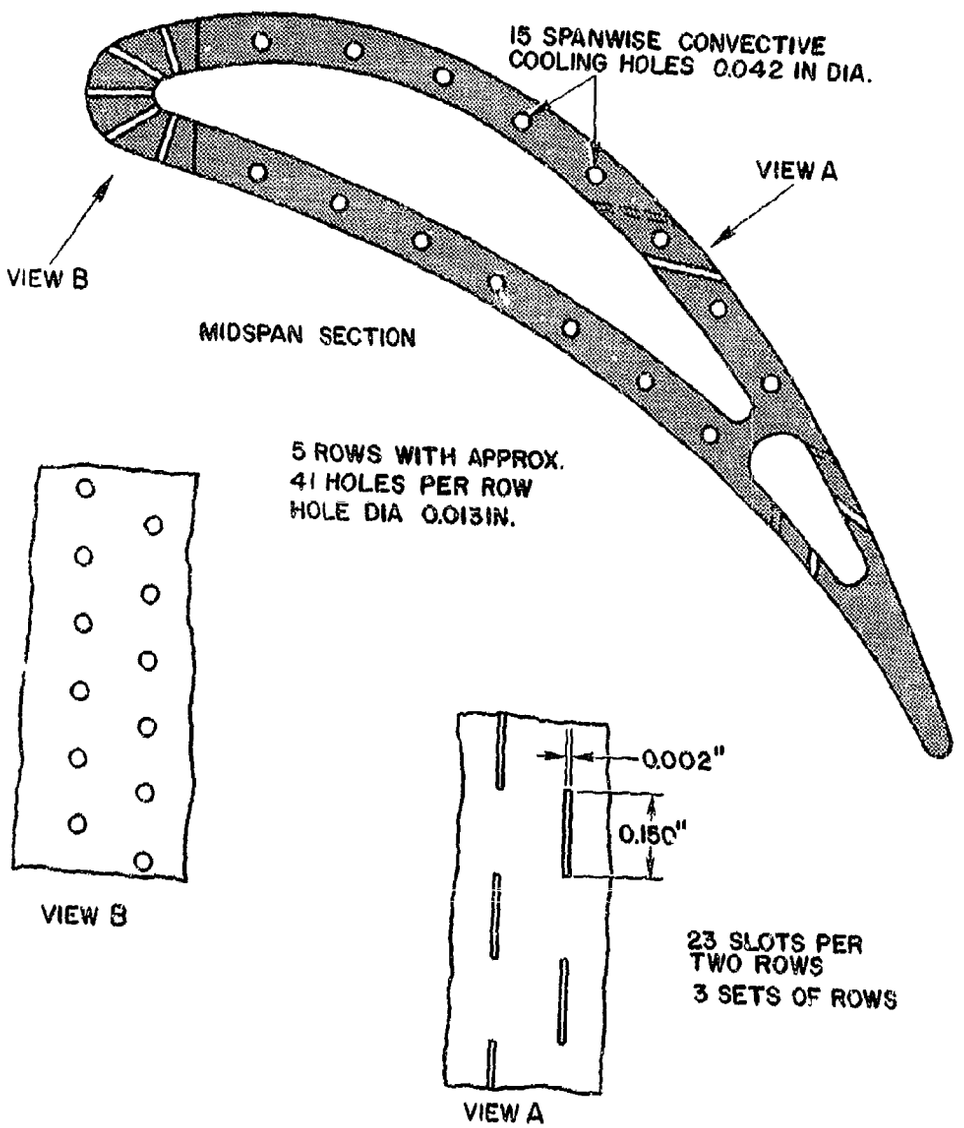
PRESSURE DISTRIBUTION VANE #2 USED FOR MEASURING AIRFOIL PROFILES IN HIGH PRESSURE CASCADE RIG

Figure 5-14



INSTRUMENTED SHOWERHEAD VANE AFTER TESTING IN HIGH PRESSURE CASCADE RIG AT 30, 45, 175 PSIA, AND 2300° F MAIN GAS STREAM CONDITIONS

Figure 5-15

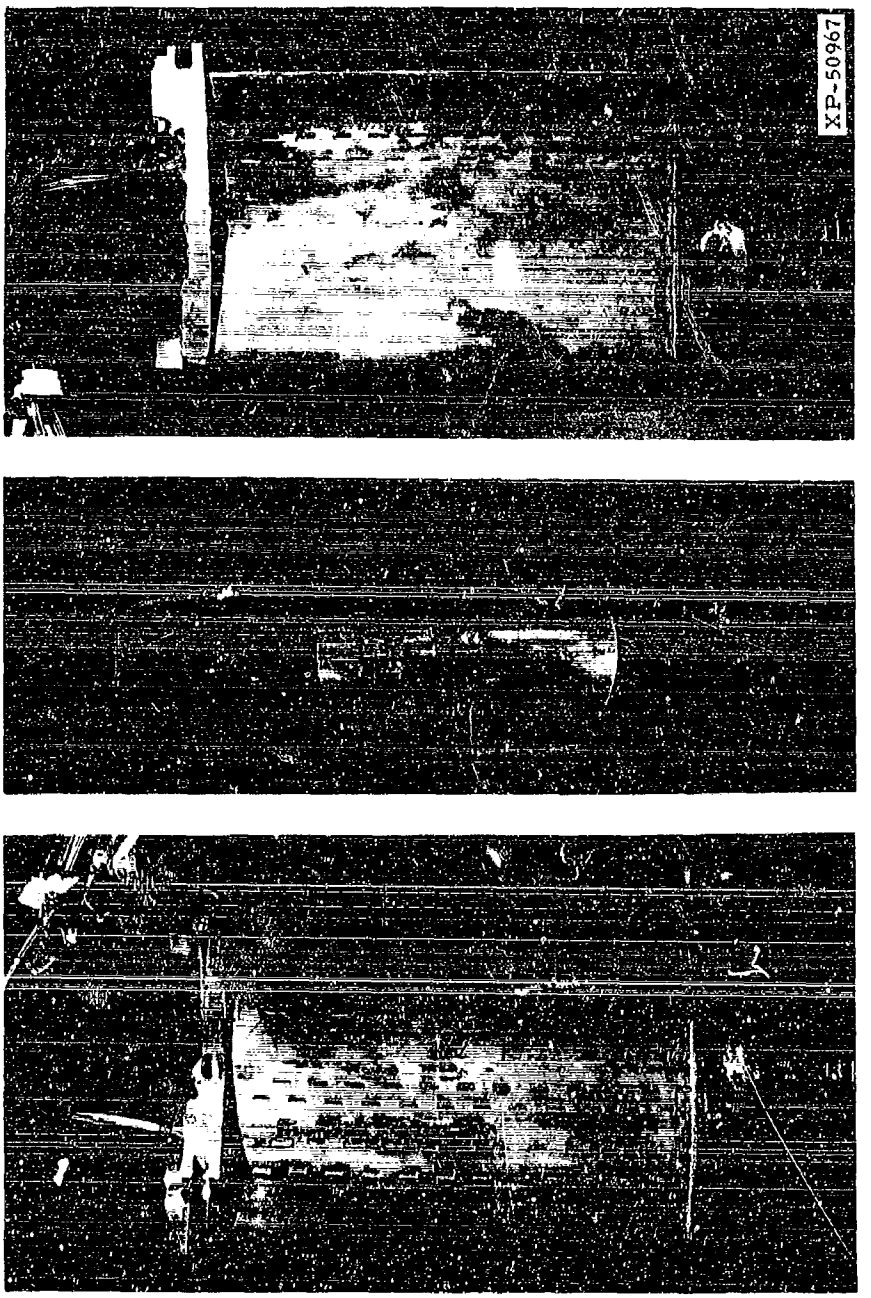


SCHEMATIC OF SHOWERHEAD VANE

Figure 5-16

DOWNGRADED AT 3 YEAR INTERVALS
DECLASSIFIED AFTER 12 YEARS
DOD DIR 5200.10

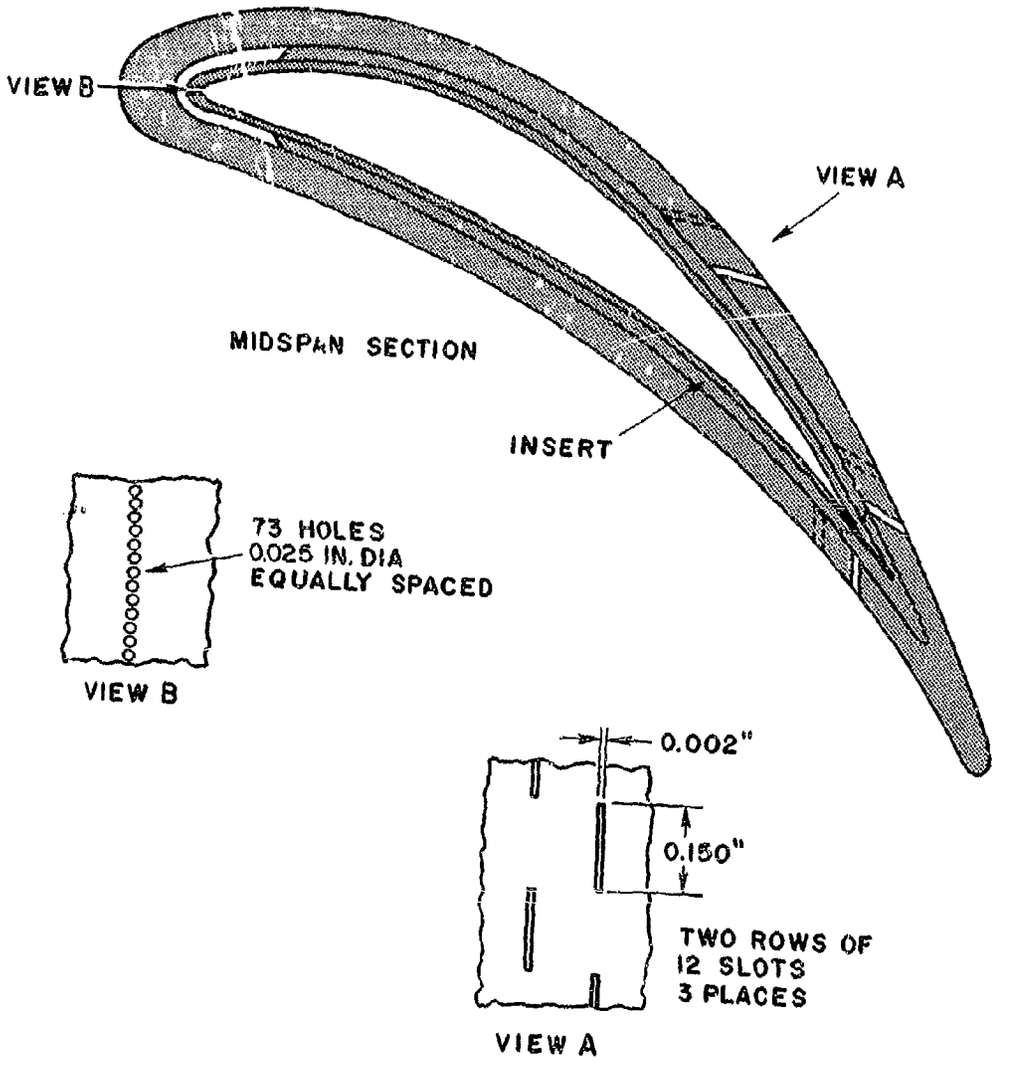
THIS DOCUMENT CONTAINS INFORMATION AFFECTING THE NATIONAL DEFENSE OF THE UNITED STATES WITHIN THE MEANING OF THE ESPIONAGE LAWS, TITLE 18, U.S.C., SECTIONS 793 AND 794. ITS TRANSMISSION OR THE REVELATION OF ITS CONTENTS IN ANY MANNER TO AN UNAUTHORIZED PERSON IS PROHIBITED BY LAW.



INSTRUMENTED TD NICKEL VANE TESTED IN HIGH PRESSURE CASCADE RIG

Figure 5-17

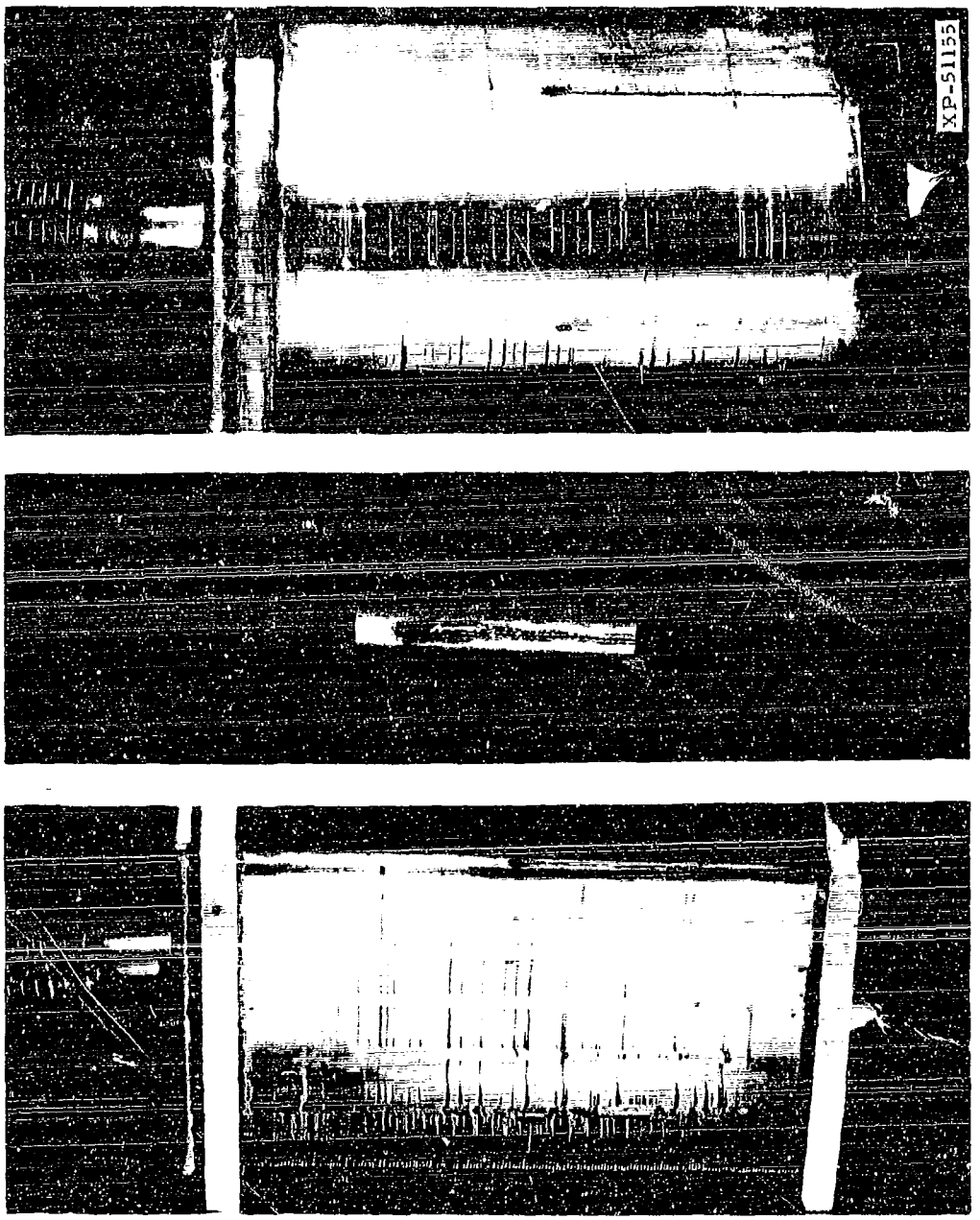
DOWNGRADED AT 3 YEAR INTERVALS
DECLASSIFIED AFTER 12 YEARS
DOD DIR 5200.10



SCHEMATIC OF TD NICKEL VANE TESTED IN HIGH PRESSURE CASCADE RIG

Figure 5-18

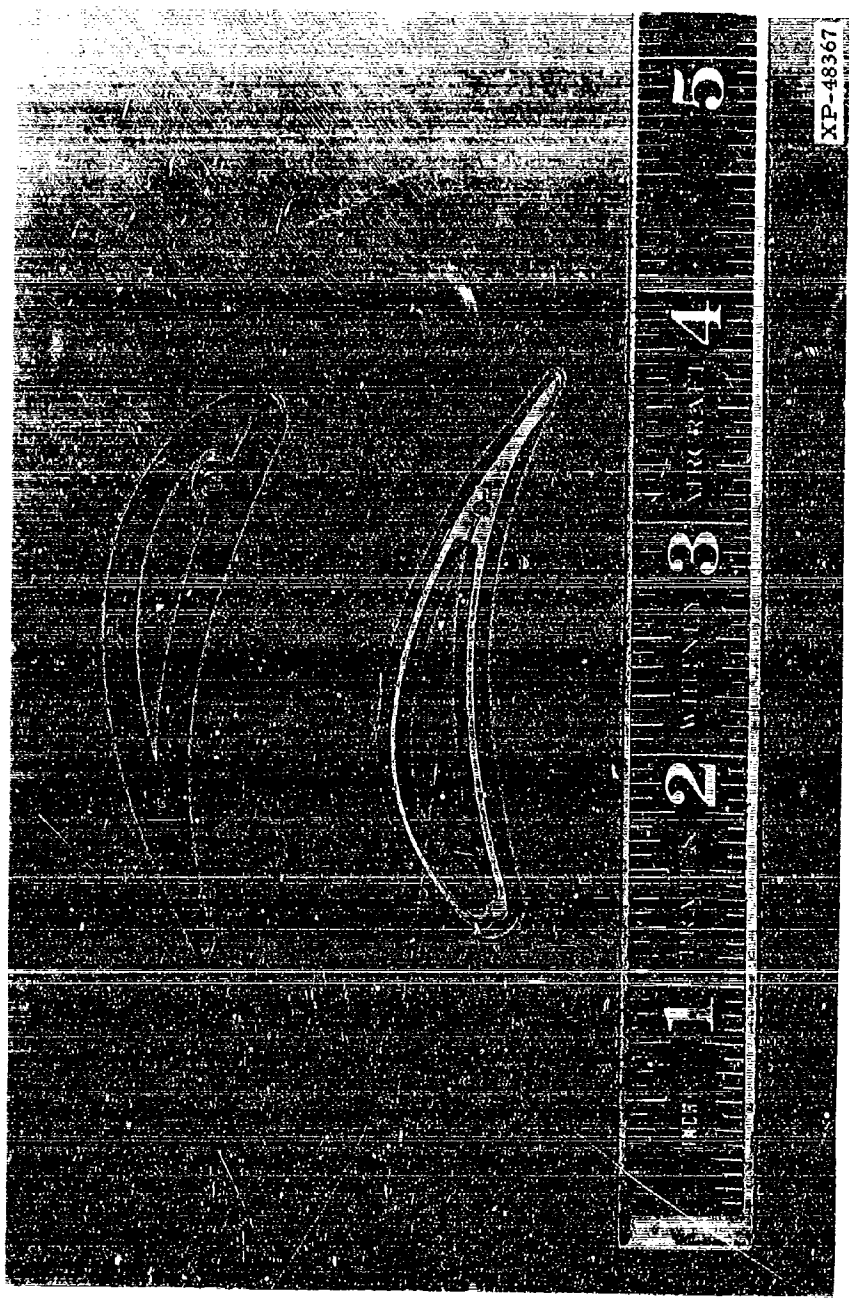
DOWNGRADED AT 3 YEAR INTERVALS
DECLASSIFIED AFTER 12 YEARS
DOD DIR 5200.10



INSTRUMENTED WAFER #1 VANE TESTED IN HIGH PRESSURE CASCADE RIG

Figure 5-19

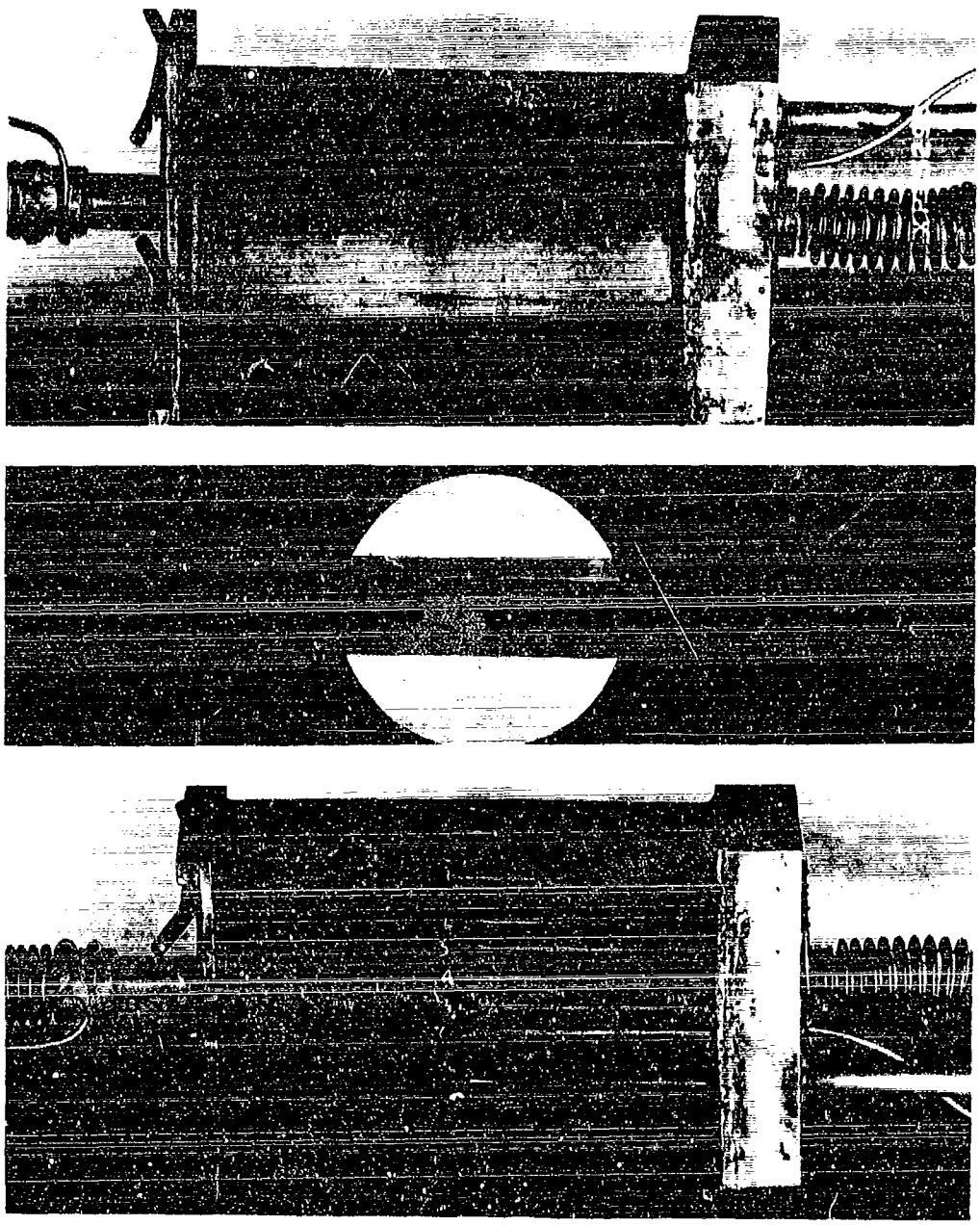
DOWNGRADED AT 3 YEAR INTERVALS
DECLASSIFIED AFTER 12 YEARS
DOD DIR 5200.10



FRONT AND REAR VIEWS OF SEGMENTS USED IN ASSEMBLY OF WAFER #1

Figure 5-20

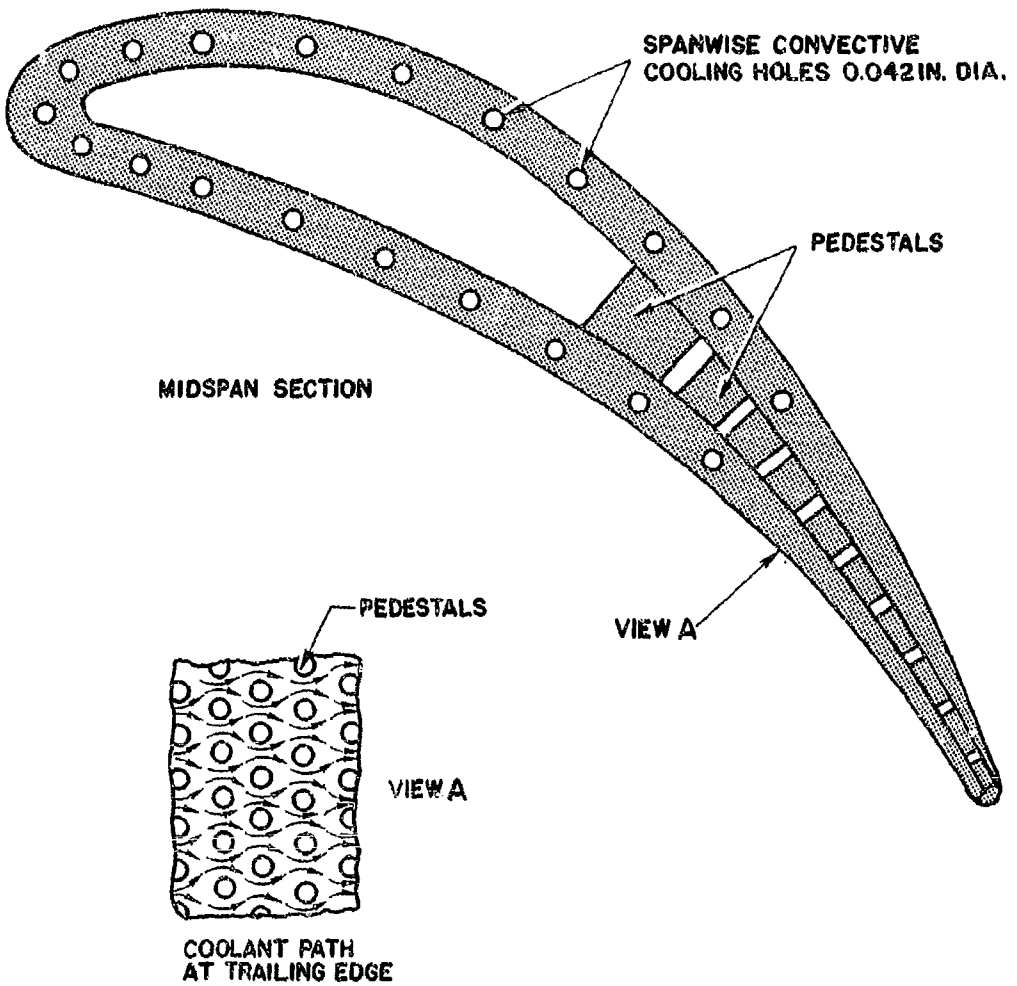
DOWNGRADED AT 3 YEAR INTERVALS
DECLASSIFIED AFTER 12 YEARS
DOD DIR 5200.10



INSTRUMENTED PEDESTAL TRAILING EDGE VANE TESTED IN HIGH PRESSURE CASCADE RIG AT 30, 45, 175 PSIA, 2300° F GASTREAM CONDITIONS

Figure 5-21

DOWNGRADED AT 3 YEAR INTERVALS
DECLASSIFIED AFTER 12 YEARS
DOD DIR 5200.10

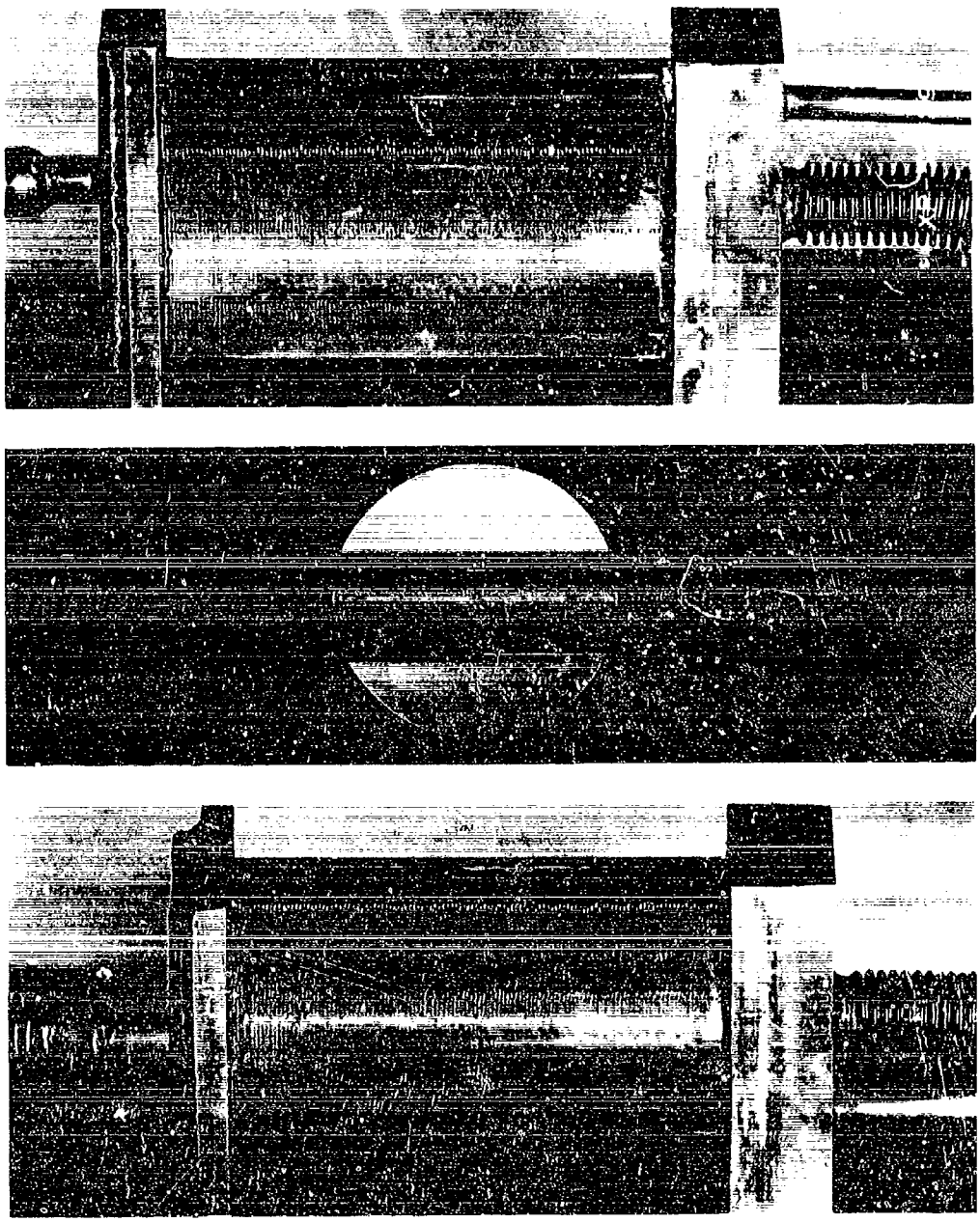


SCHEMATIC OF PEDESTAL TRAILING EDGE VANE

Figure 5-22

DOWNGRADED AT 3 YEAR INTERVALS
DECLASSIFIED AFTER 12 YEARS
DOD DIR 5200.10

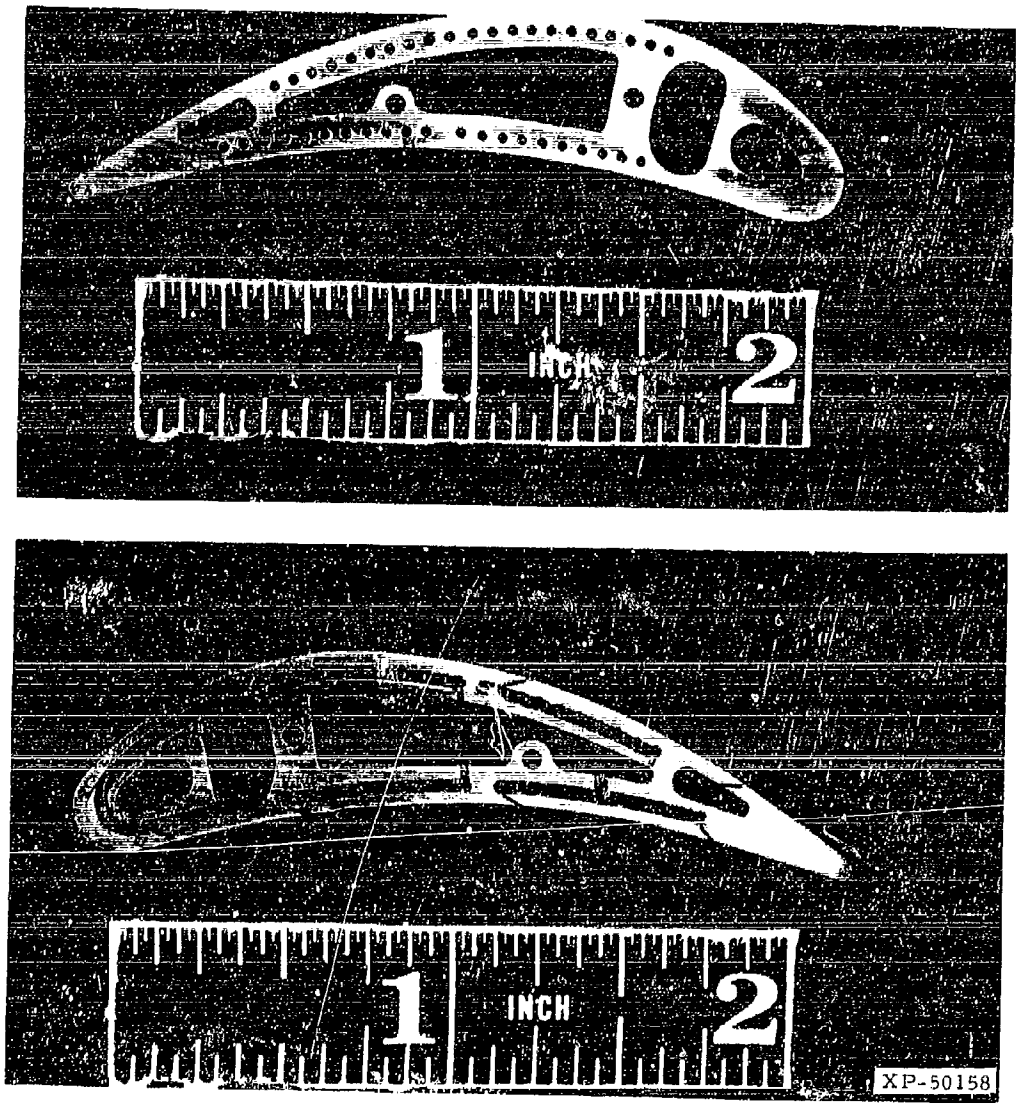
THIS DOCUMENT CONTAINS INFORMATION AFFECTING THE NATIONAL DEFENSE OF THE UNITED STATES WITHIN THE MEANING OF THE ESPIONAGE LAWS, TITLE 18 U.S.C. SECTIONS 793 AND 794. ITS TRANSMISSION OR THE REVELATION OF ITS CONTENTS IN ANY MANNER TO AN UNAUTHORIZED PERSON IS PROHIBITED BY LAW.



WAFER #2 VANE TESTED IN HIGH PRESSURE CASCADE RIG AT 45 PSIA, 2300°F GASTREAM CONDITIONS

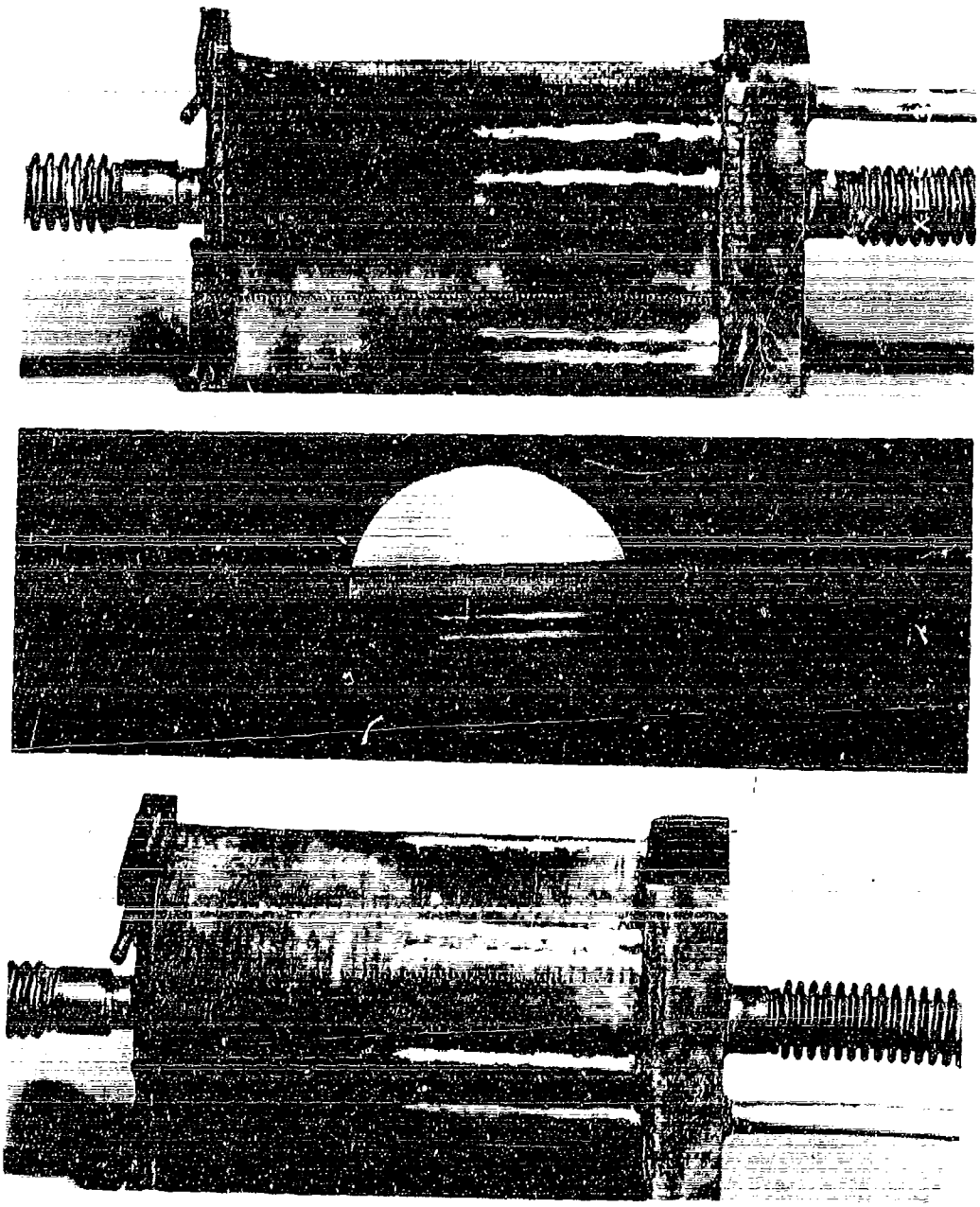
Figure 5-23

DOWNGRADED AT 3 YEAR INTERVALS
DECLASSIFIED AFTER 12 YEARS
DOD DIR 5200.10



FRONT AND REAR VIEWS OF SEGMENTS USED IN WAFER VANE #2

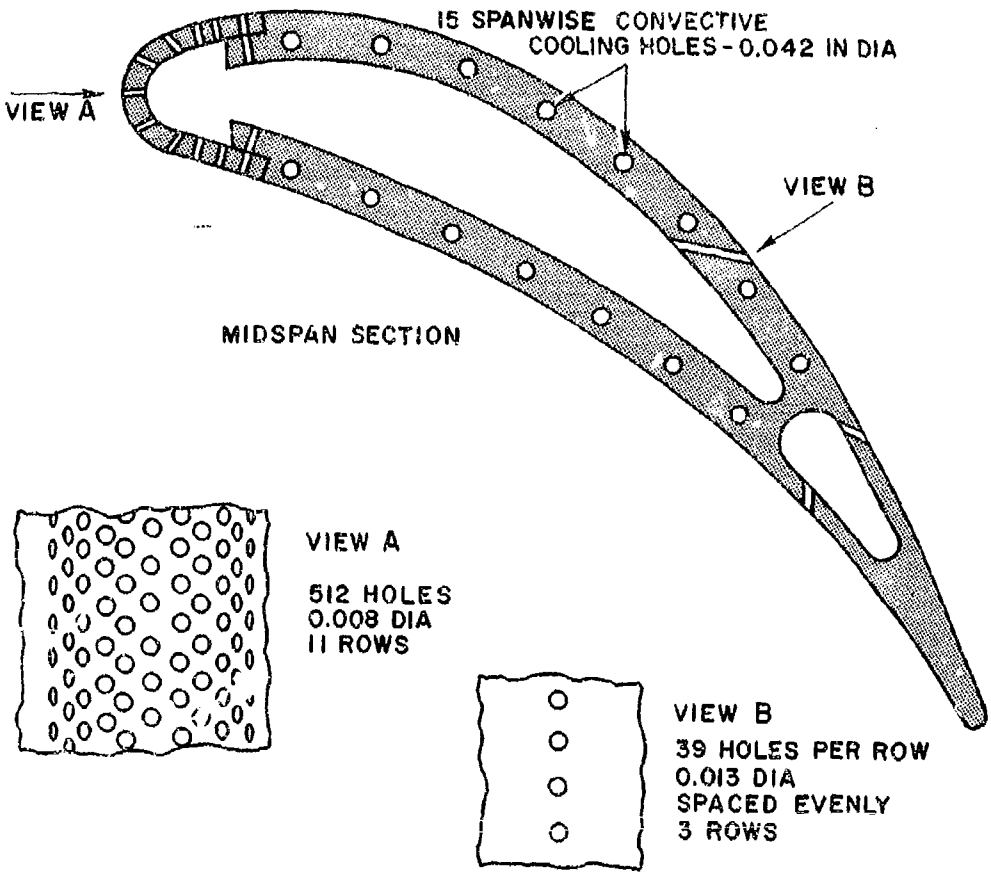
Figure 5-24



PIERCED SHEET LEADING EDGE VANE TESTED IN HIGH PRESSURE CASCADE RIG AT 30, 45 PSIA, 2300° F GASTREAM CONDITIONS

Figure 5-25

DOWNGRADED AT 3 YEAR INTERVALS
DECLASSIFIED AFTER 12 YEARS
DOD DIR 5200.10

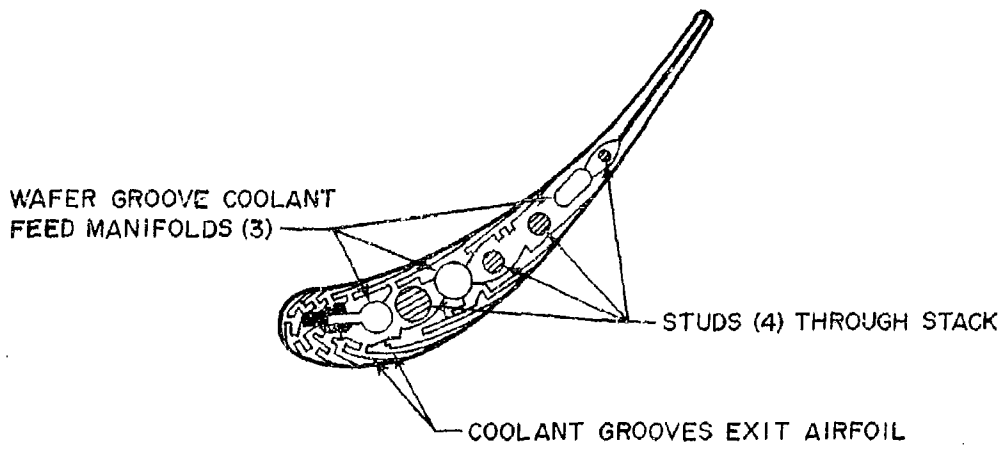


SCHEMATIC OF PIERCED SHEET VANE TESTED IN HIGH PRESSURES CASCADE RIG

Figure 5-26

DOWNGRADED AT 3 YEAR INTERVALS
DECLASSIFIED AFTER 12 YEARS
DOD DIR 5.200.10

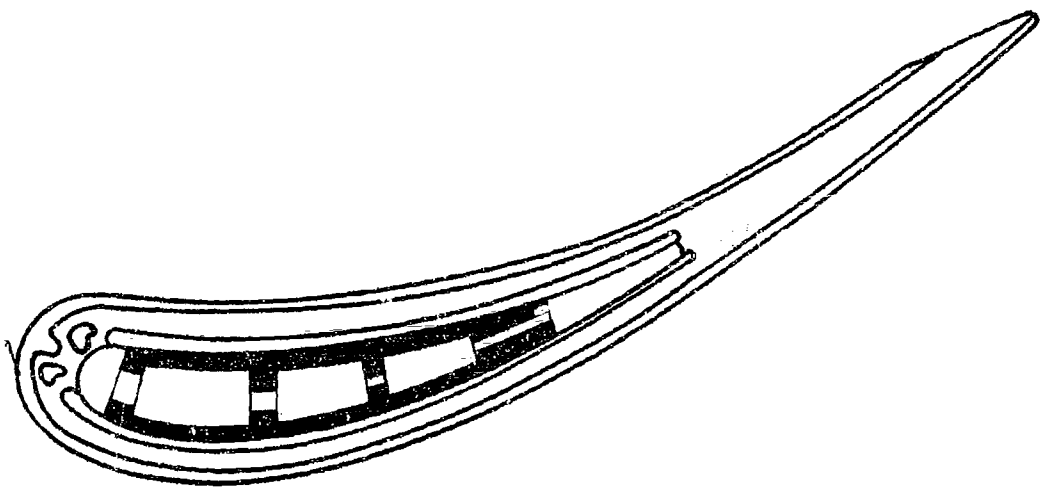
THIS DOCUMENT CONTAINS INFORMATION AFFECTING THE NATIONAL DEFENSE OF THE UNITED STATES WITHIN THE MEANING OF THE ESPIONAGE LAWS, TITLE 18, U.S.C., SECTIONS 793 AND 794. THE TRANSMISSION OR THE REVELATION OF ITS CONTENTS IN ANY MANNER TO AN UNAUTHORIZED PERSON IS PROHIBITED BY LAW.



SEGMENTS USED IN ASSEMBLY OF WAFER VANE #3

Figure 5-27

DOWNGRADED AT 3 YEAR INTERVALS
DECLASSIFIED AFTER 12 YEARS
DOD DIR 5200.10

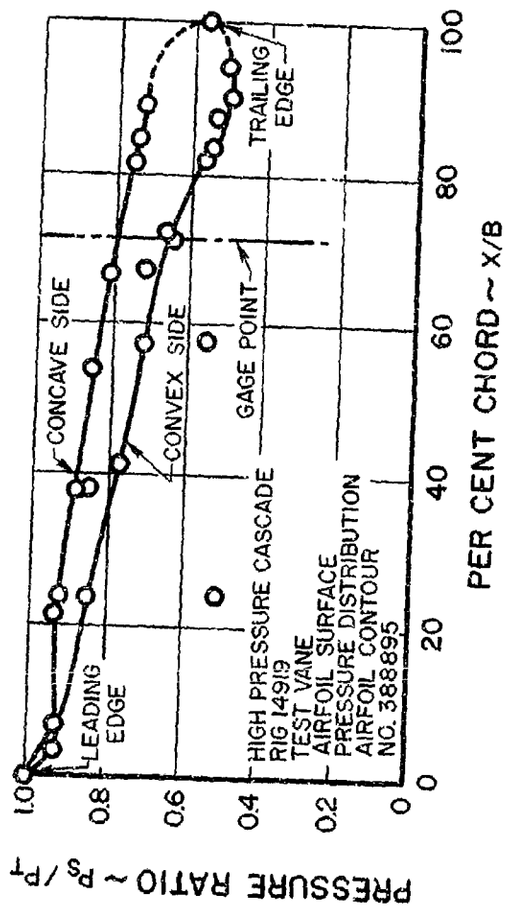


SEGMENTS USED IN ASSEMBLY OF WAFER VANE #4

Figure 5-28

DOWNGRADED AT 3 YEAR INTERVALS
DECLASSIFIED AFTER 12 YEARS
DOD DIR 5200.10

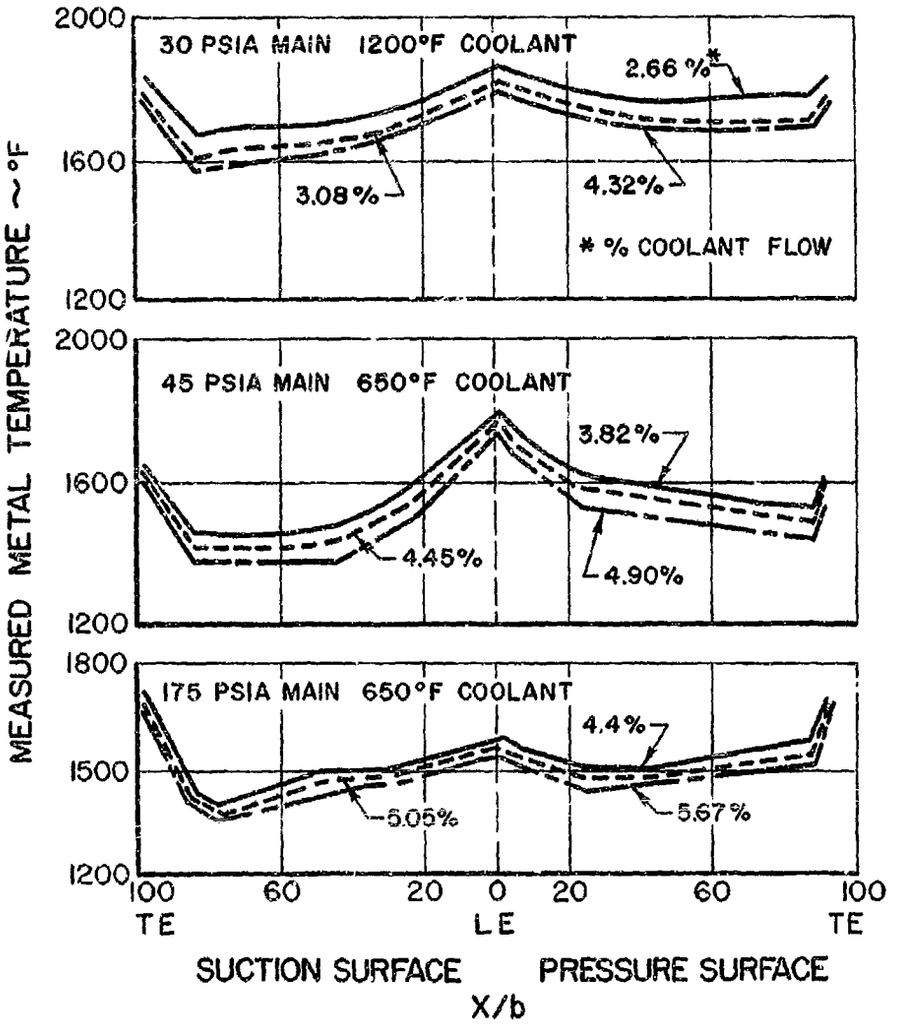
THIS DOCUMENT CONTAINS INFORMATION AFFECTING THE NATIONAL DEFENSE OF THE UNITED STATES WITHIN THE MEANING OF THE ESPIONAGE LAWS, TITLE 18, U.S.C., SECTIONS 793 AND 794. ITS TRANSMISSION OR THE REVELATION OF ITS CONTENTS IN ANY MANNER TO AN UNAUTHORIZED PERSON IS PROHIBITED BY LAW.



PRESSURE PROFILE DATA DERIVED FROM TESTS

Figure 5-29

DOWNGRADED AT 3 YEAR INTERVALS
DECLASSIFIED AFTER 12 YEARS
DOD DIR 5200.10

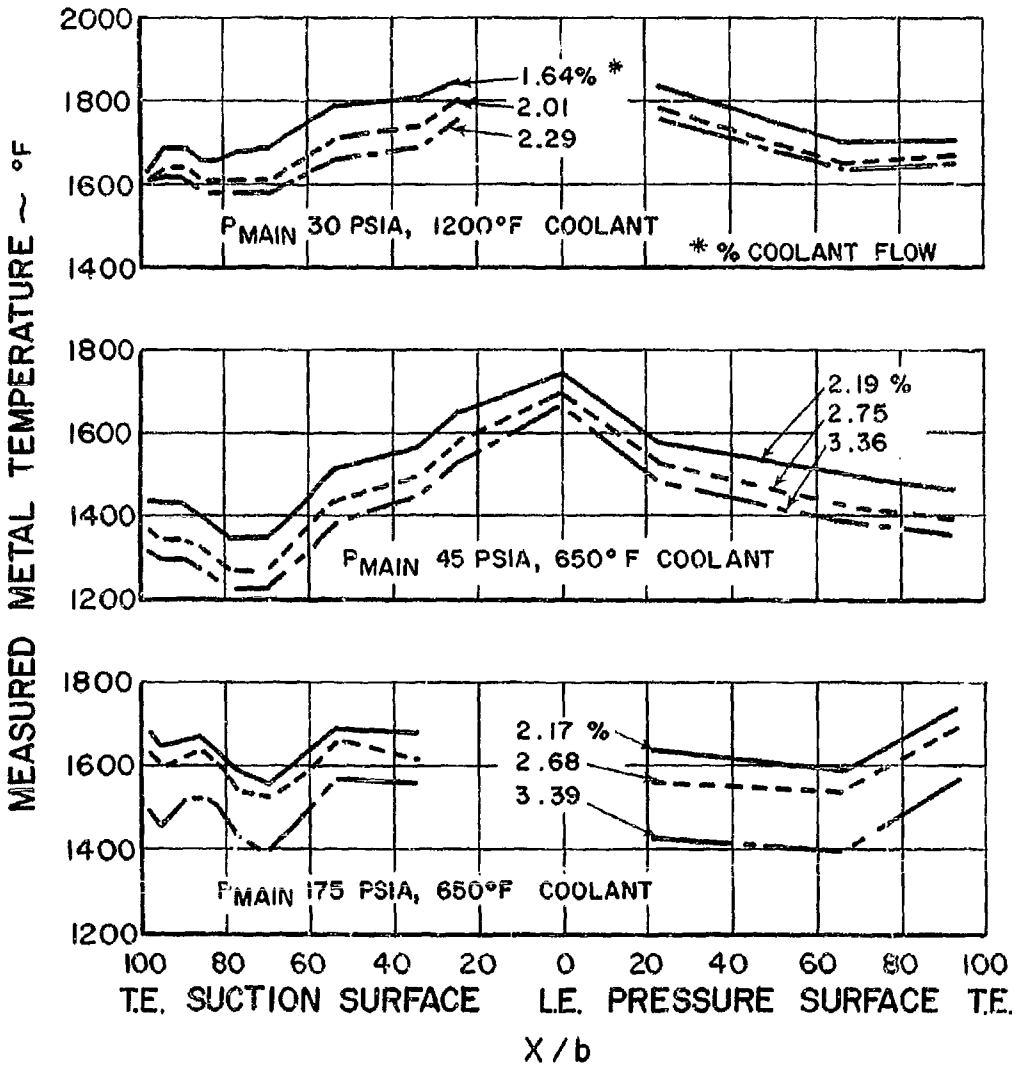


METAL TEMPERATURES MEASURED ON SHOWERHEAD VANE IN HIGH PRESSURE CASCADE RIG. MAIN GASTREAM TEMP 2300°F

Figure 5-30

DOWNGRADED AT 3 YEAR INTERVALS
DECLASSIFIED AFTER 12 YEARS
DOD DIR 5200.10

THIS DOCUMENT CONTAINS INFORMATION AFFECTING THE NATIONAL DEFENSE OF THE UNITED STATES WITHIN THE MEANING OF THE ESPIONAGE LAWS, TITLE 18, U.S.C. SECTIONS 793 AND 794. ITS TRANSMISSION OR THE REVELATION OF ITS CONTENTS IN ANY MANNER TO AN UNAUTHORIZED PERSON IS PROHIBITED BY LAW.

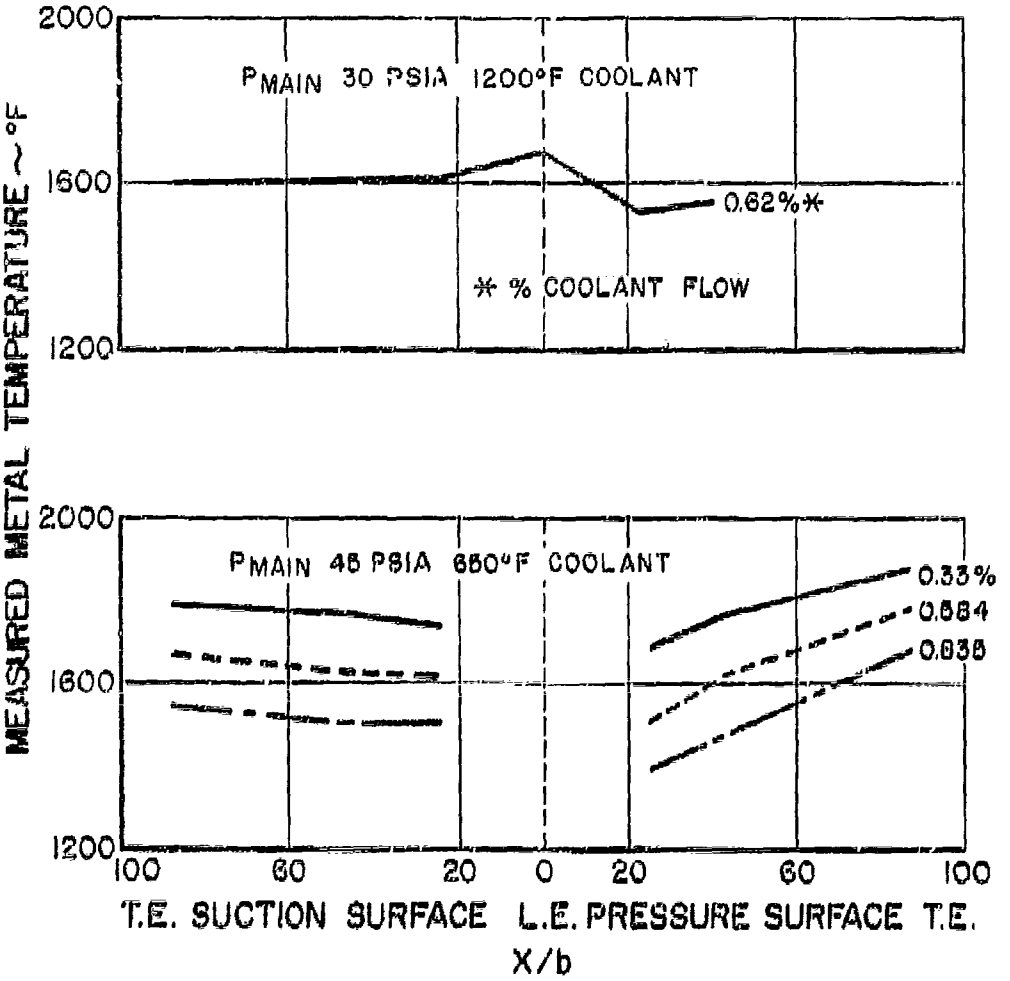


METAL TEMPERATURES MEASURED ON PEDESTAL TRAILING EDGE VANE IN HIGH PRESSURE CASCADE RIG. MAIN STREAM TEMP. 2300°F - ALL CASES

Figure 5-31

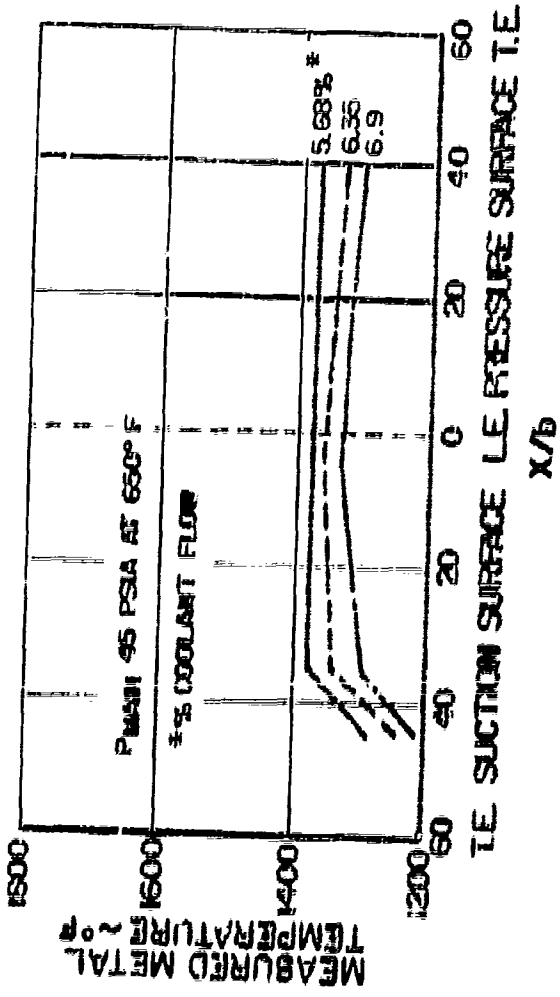
DOWNGRADED AT 3 YEAR INTERVALS
DECLASSIFIED AFTER 12 YEARS
DOD DIR 5200.10

THIS DOCUMENT CONTAINS INFORMATION AFFECTING THE NATIONAL DEFENSE OF THE UNITED STATES WITHIN THE MEANING OF THE ESPIONAGE LAWS, TITLE 18 U.S.C. SECTIONS 793 AND 794. ITS TRANSMISSION OR THE REVELATION OF ITS CONTENTS IN ANY MANNER TO AN UNAUTHORIZED PERSON IS PROHIBITED BY LAW.



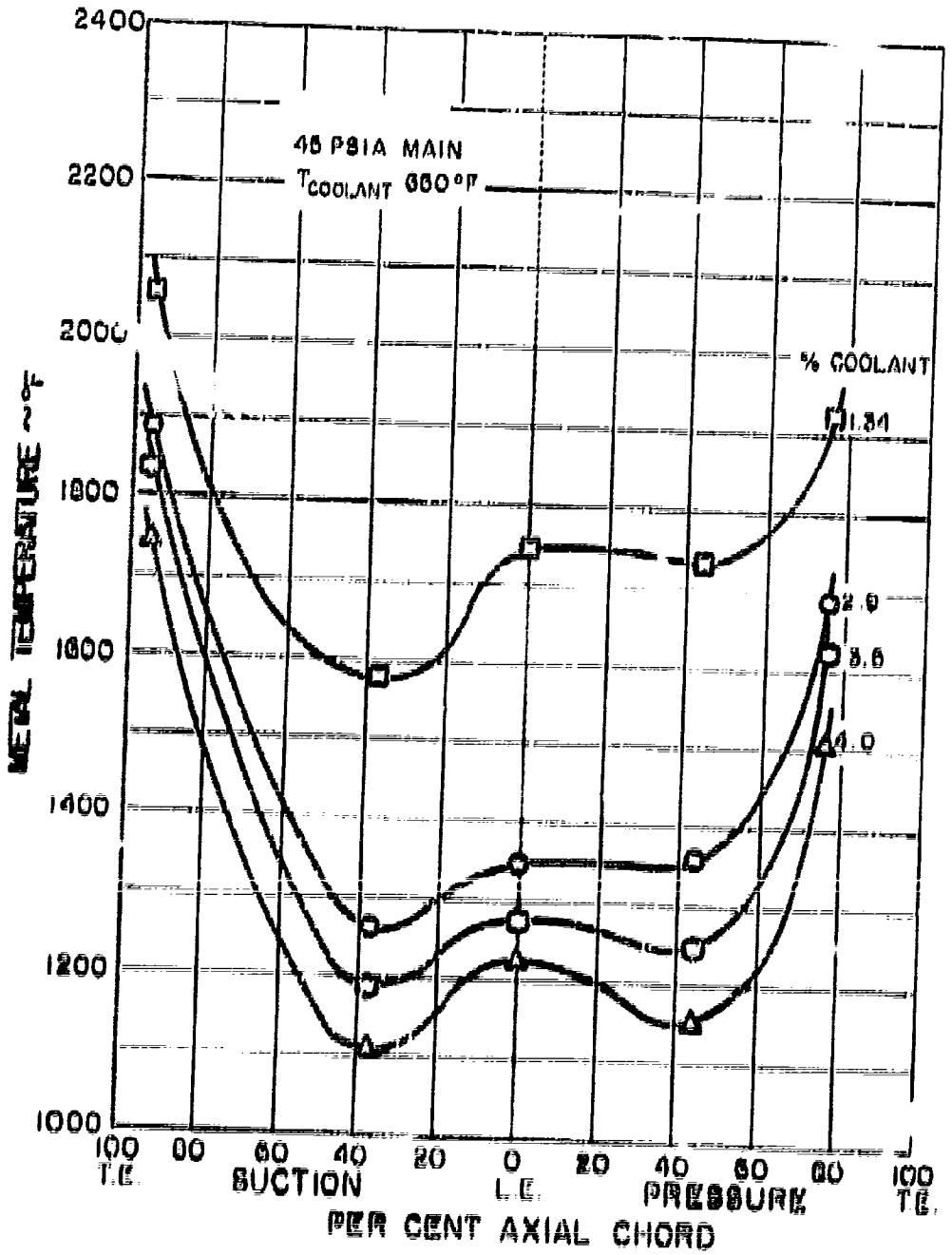
METAL TEMPERATURES MEASURED ON WAFER #1 VANE IN HIGH PRESSURE CASCADE RIG. MAIN STREAM TEMP. 2300° F - ALL CASES

Figure 5-32



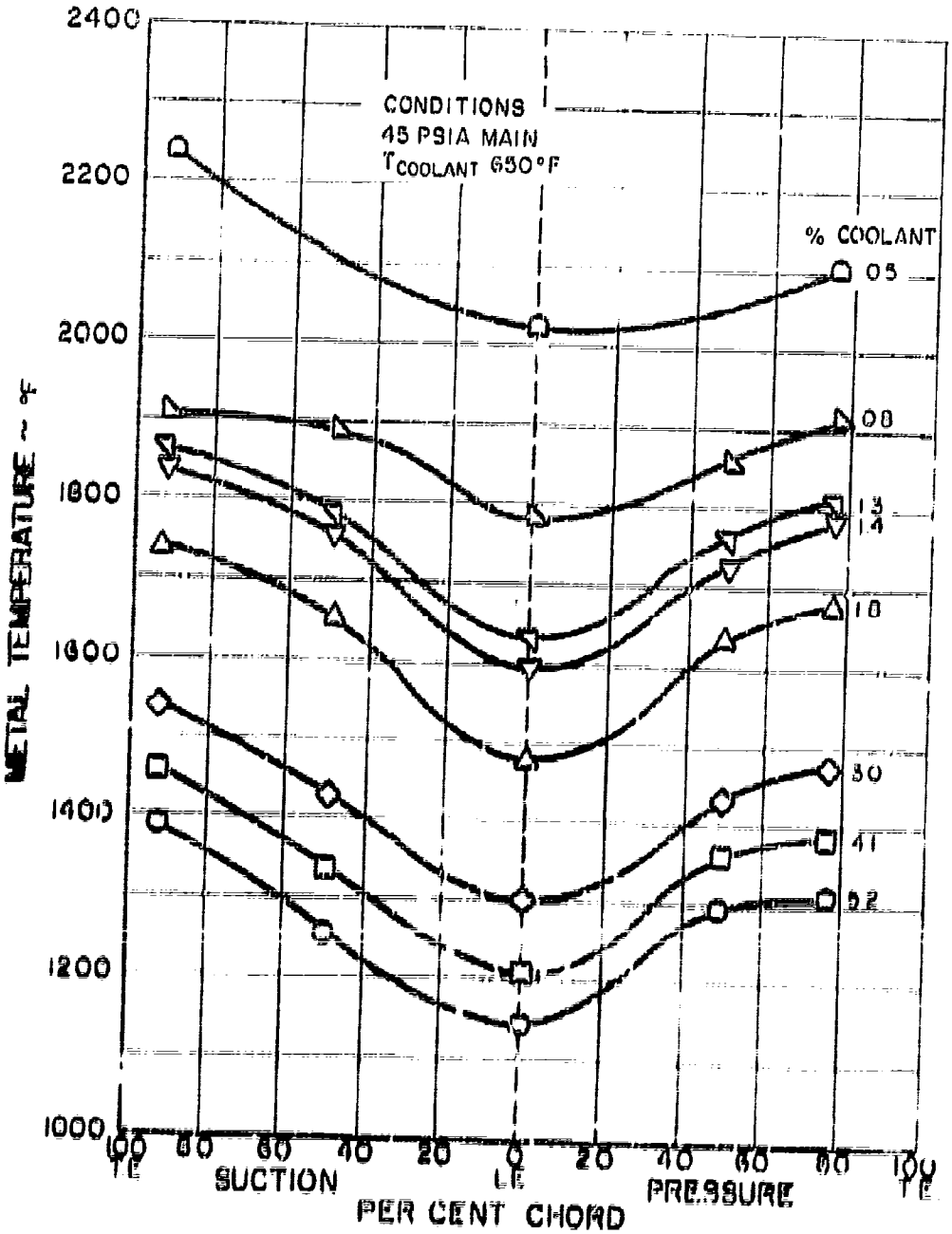
METAL TEMPERATURES MEASURED ON WAVER #2 VANE IN HIGH PRESSURE CASCADE RIG. MAINSTREAM TEMP. 2300°F - ALL CASES

Figure 5-11



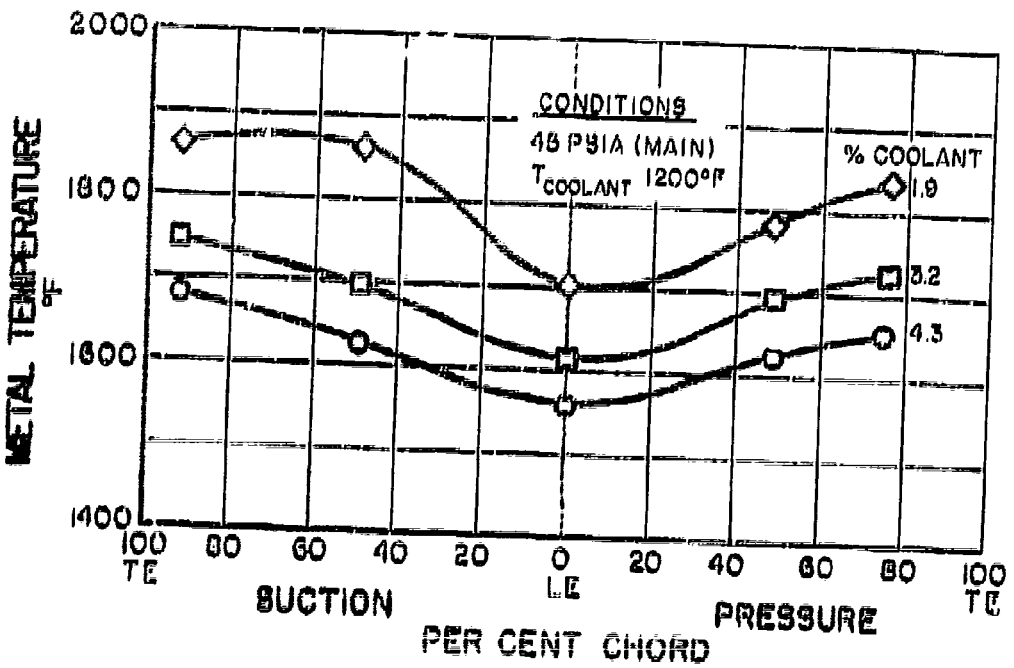
METAL TEMPERATURES MEASURED ON WATER VANE #3 MAINSTREAM TEMP. 2300°F

Figure 5-34



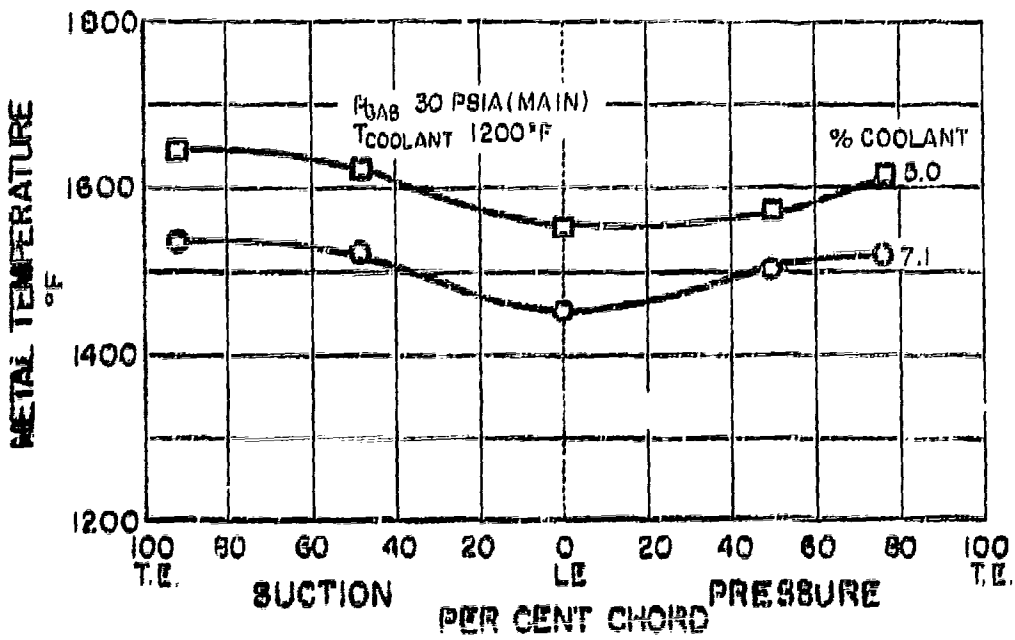
METAL TEMPERATURES MEASURED ON WAFER #4. MAINSTREAM TEMP. 2360° F

Figure 5-15



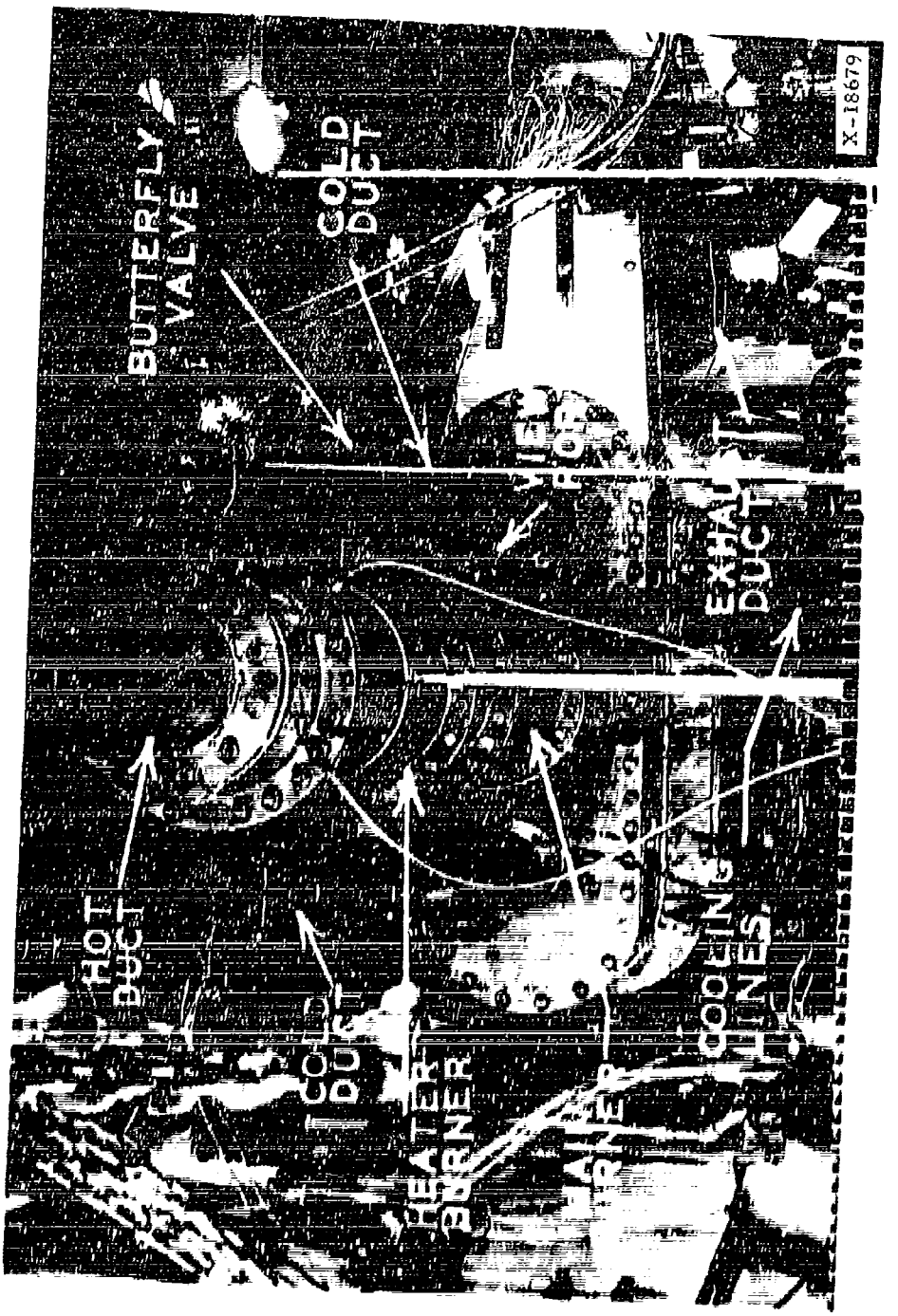
METAL TEMPERATURES MEASURED ON WAFER #4. MAINSTREAM TEMP. 2300°F

Figure 5-36



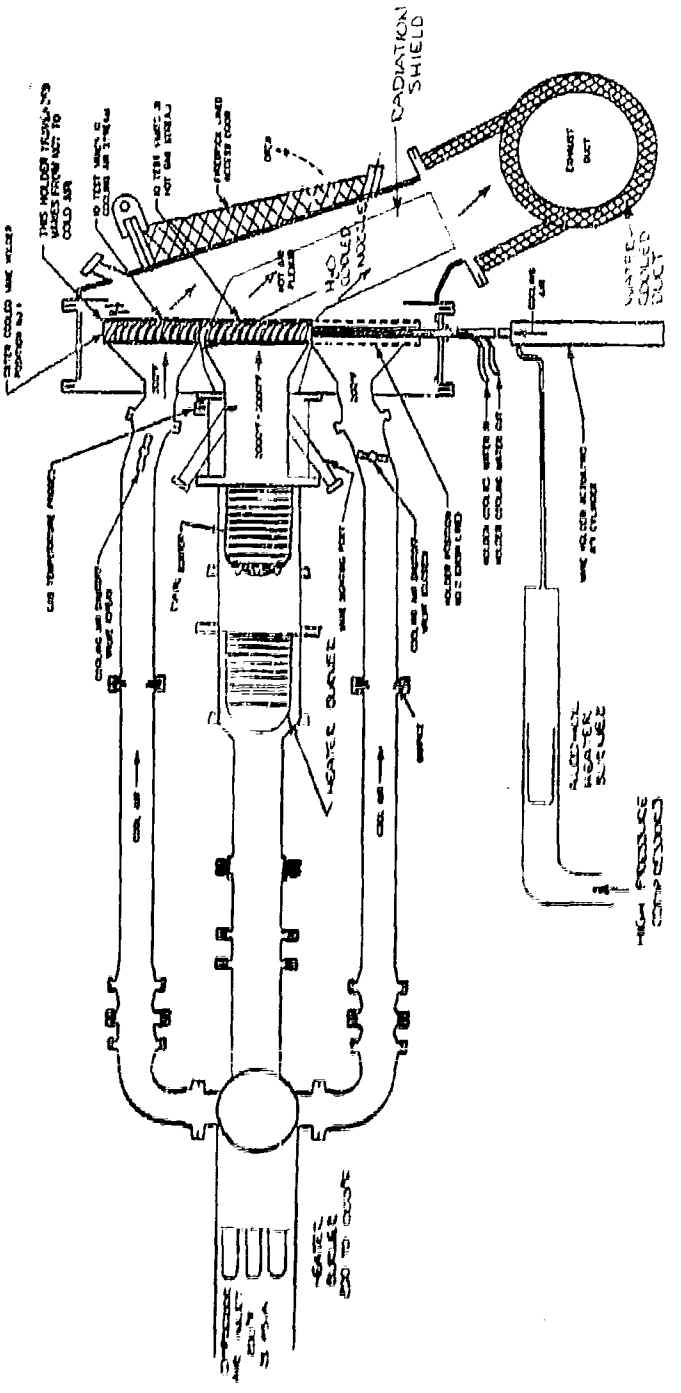
METAL TEMPERATURES MEASURED ON WAFER #4, MAINSTREAM TEMP. 2300°F

Figure 5-37



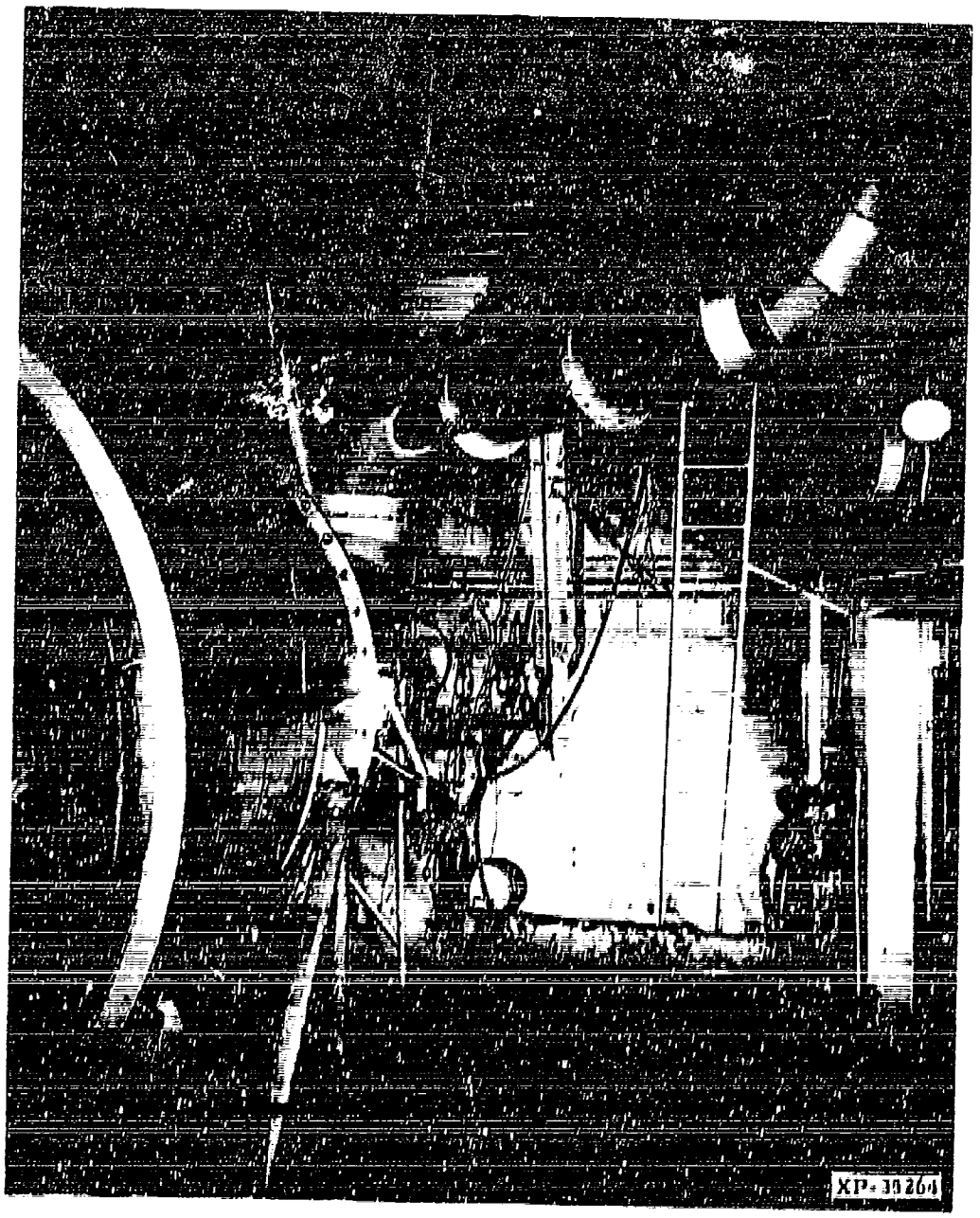
FRONT VIEW OF CHOKED CASCADE - THERMAL SHOCK RIG

Figure 5-18



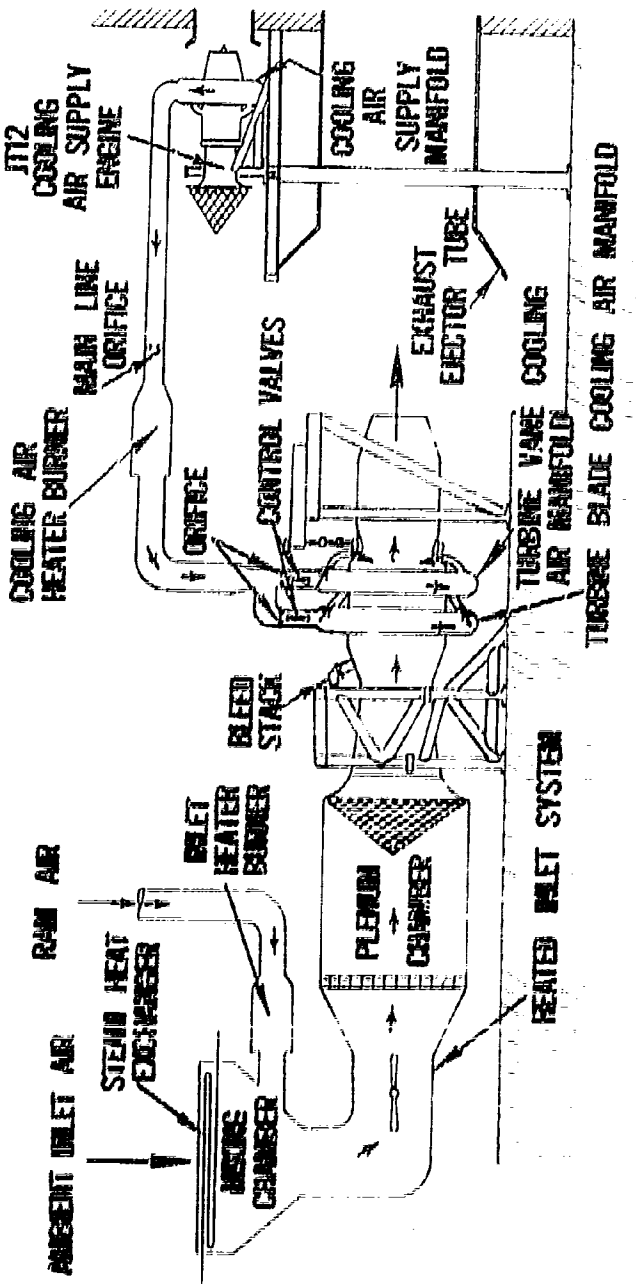
SCHEMATIC DIAGRAM OF CHOKED CASCADE THERMAL SHOCK RIG

Figure 6. 9



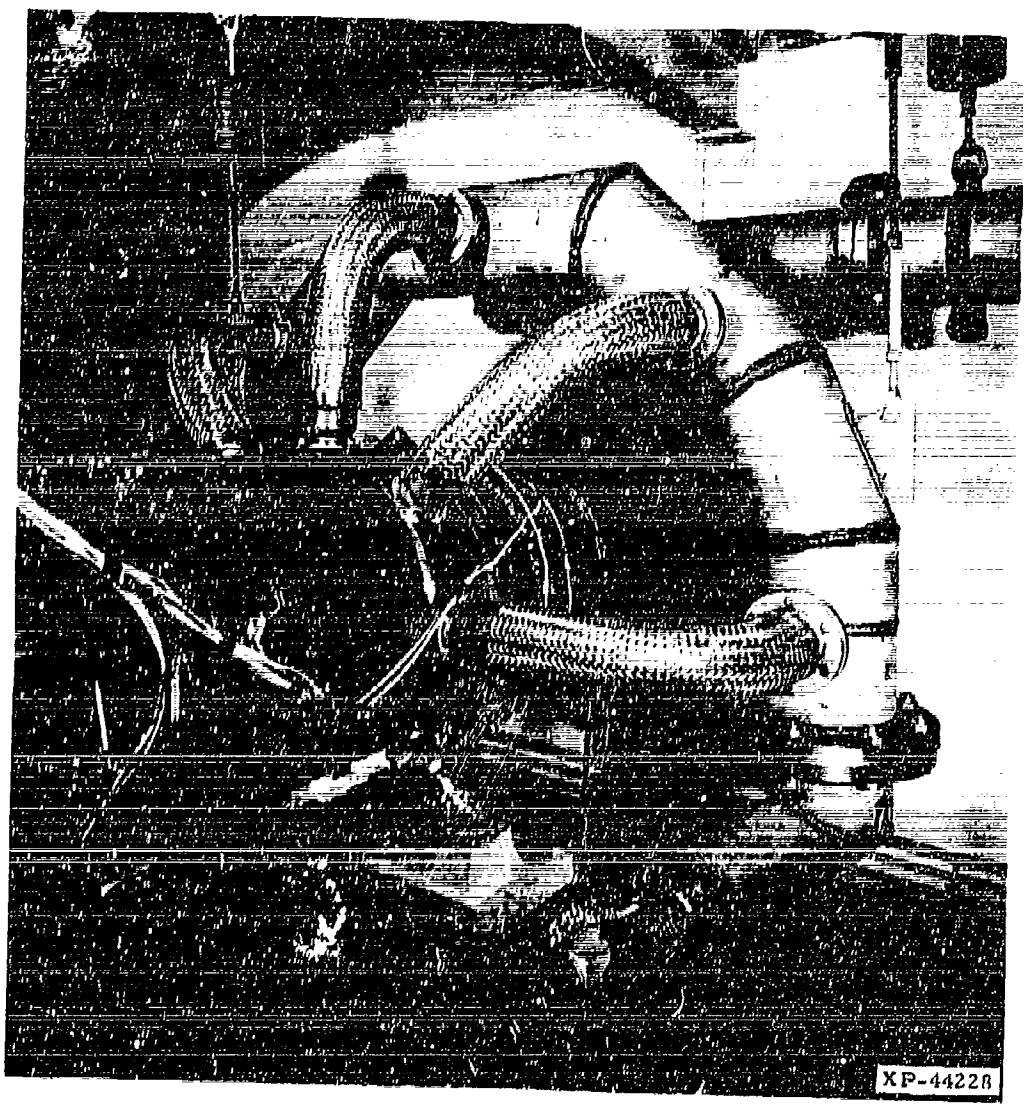
SIDE VIEW OF TEST INSTALLATION FOR HIGH TEMP. TURBINE DEVELOPMENT ENGINE SHOWING HEATED INLET

Figure 5-40



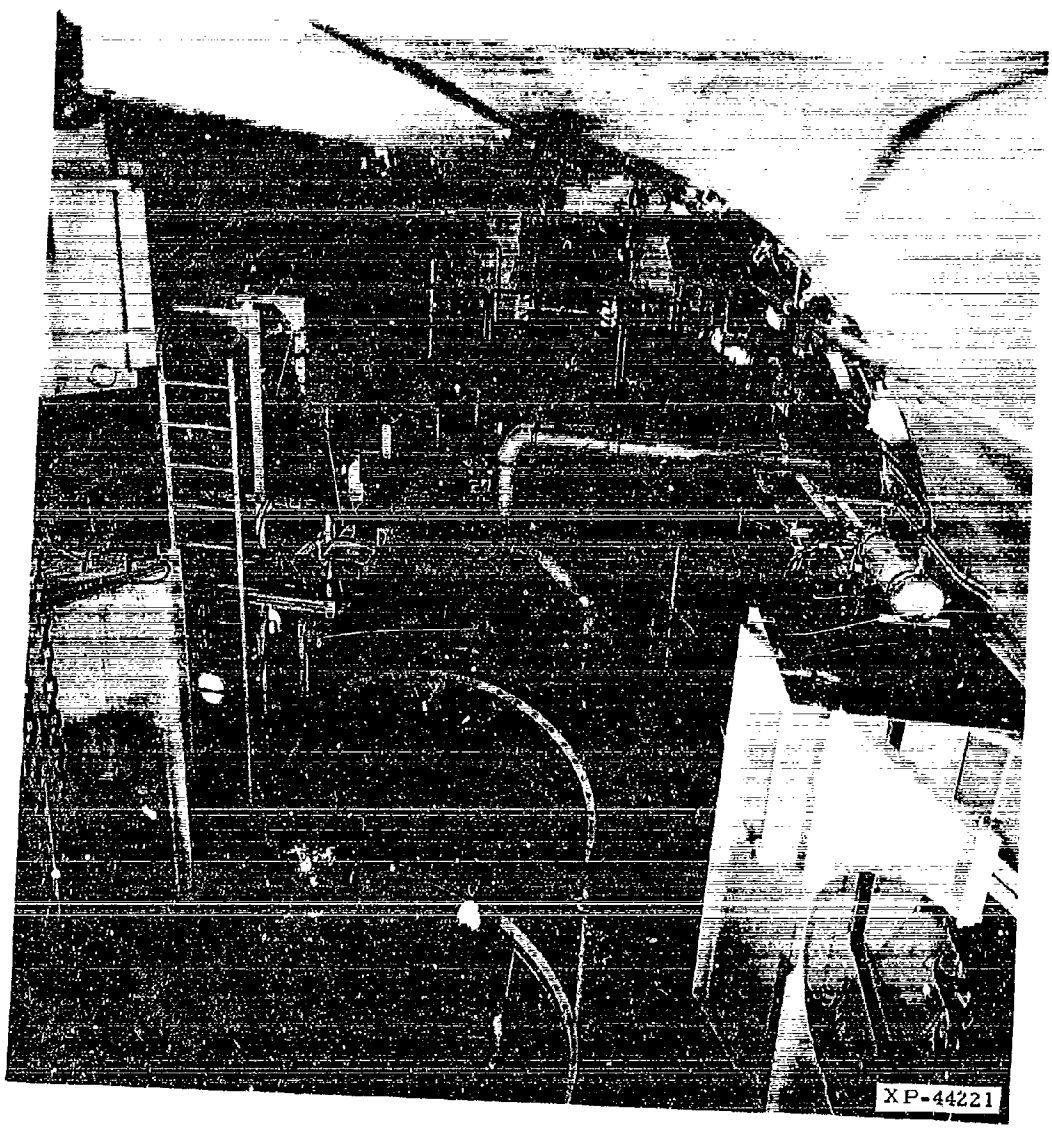
SCHEMATIC DIAGRAM OF HIGH TEMP. TURBINE DEVELOPMENT ENGINE INSTALLATION

Figure 5-41



JT12 ENGINE USED TO SUPPLY BLADE AND VANE COOLING AIR TO HIGH TEMP TURBINE DEVELOPMENT TEST ENGINE

Figure 5-42

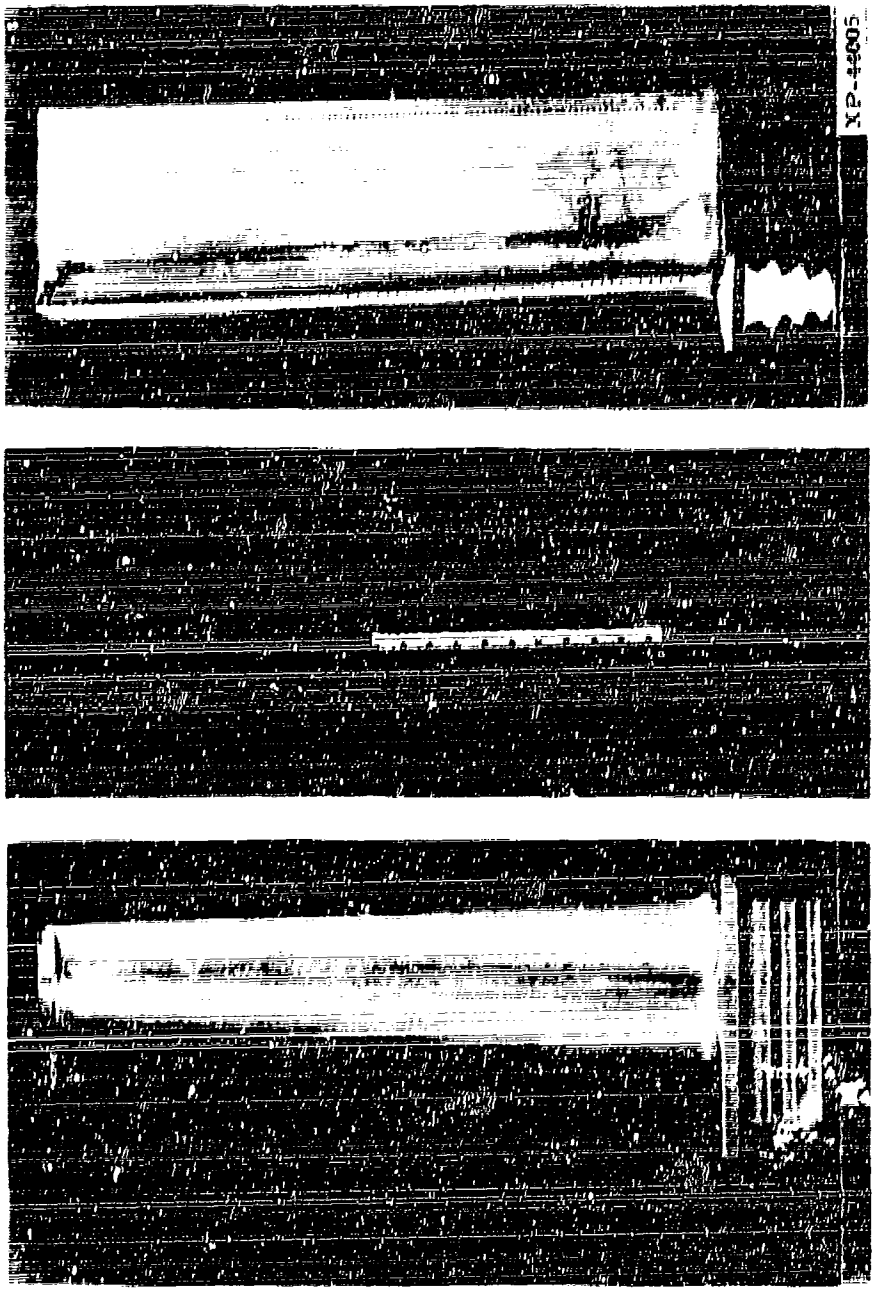


OVERALL VIEW OF HIGH TEMP. TURBINE DEVELOPMENT ENGINE TEST INSTALLATION

Figure 5-43

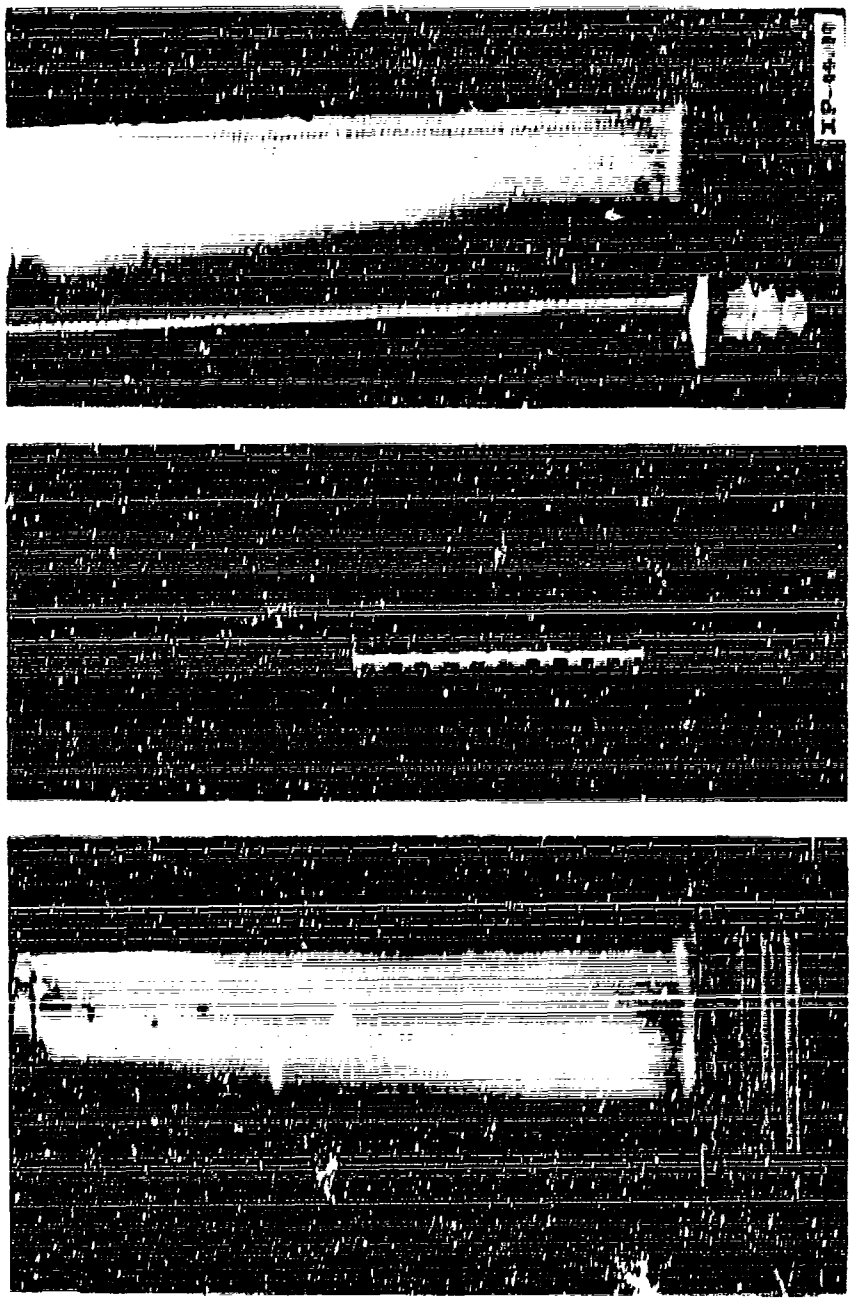
DOWNGRADED AT 3 YEAR INTERVALS
DECLASSIFIED AFTER 12 YEARS
DOD DIR 5200.10

THIS DOCUMENT CONTAINS INFORMATION AFFECTING THE NATIONAL DEFENSE OF THE UNITED STATES WITHIN THE MEANING OF THE ESPIONAGE LAWS, TITLE 18, U.S.C., SECTIONS 793 AND 794. ITS TRANSMISSION OR THE REVELATION OF ITS CONTENTS IN ANY MANNER TO AN UNAUTHORIZED PERSON IS PROHIBITED BY LAW.



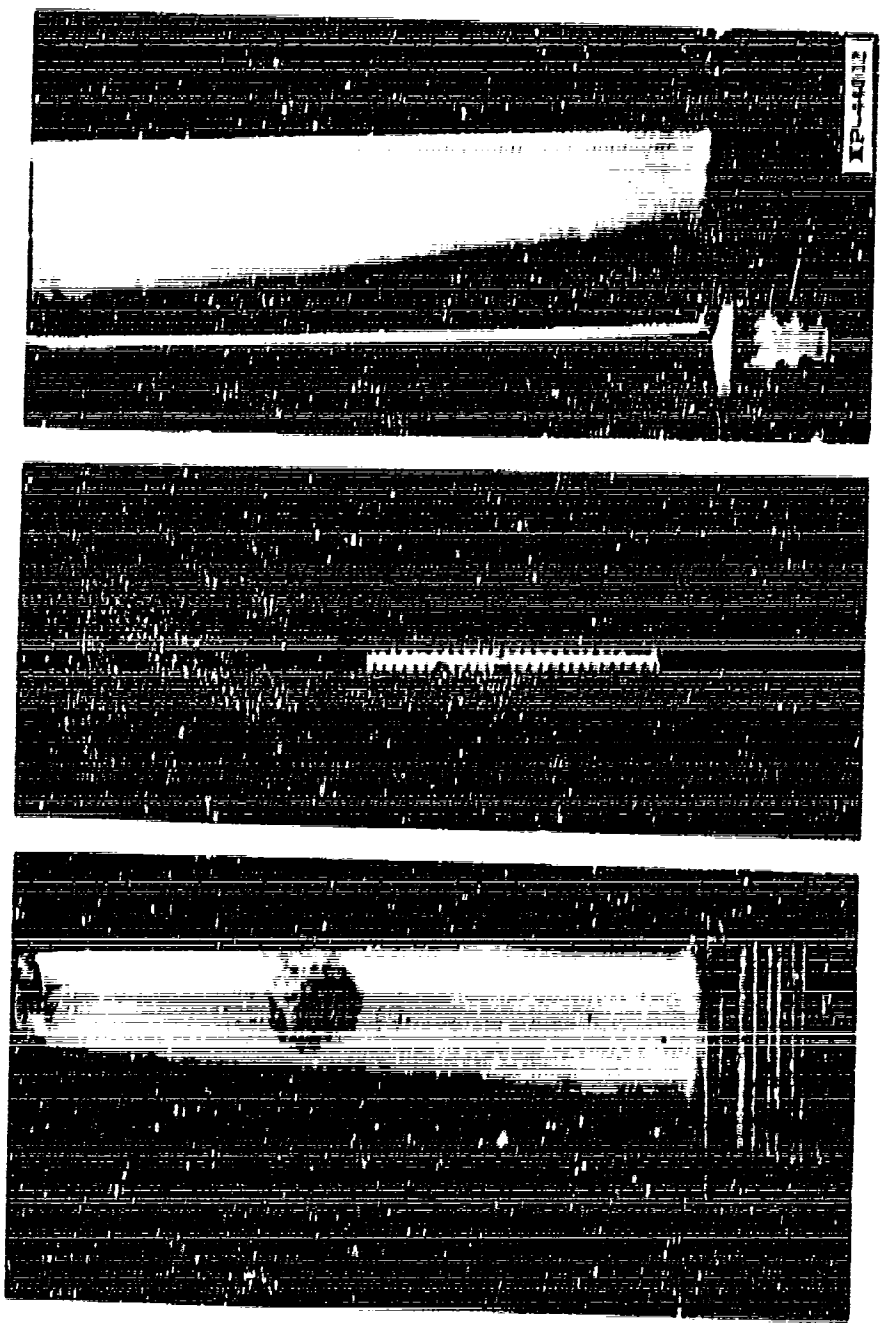
FILM COOLED TURBINE BLADE WITH THREE ROWS OF .013" DIAMETER HOLES AT 90° TO L. E.

Figure 5-44



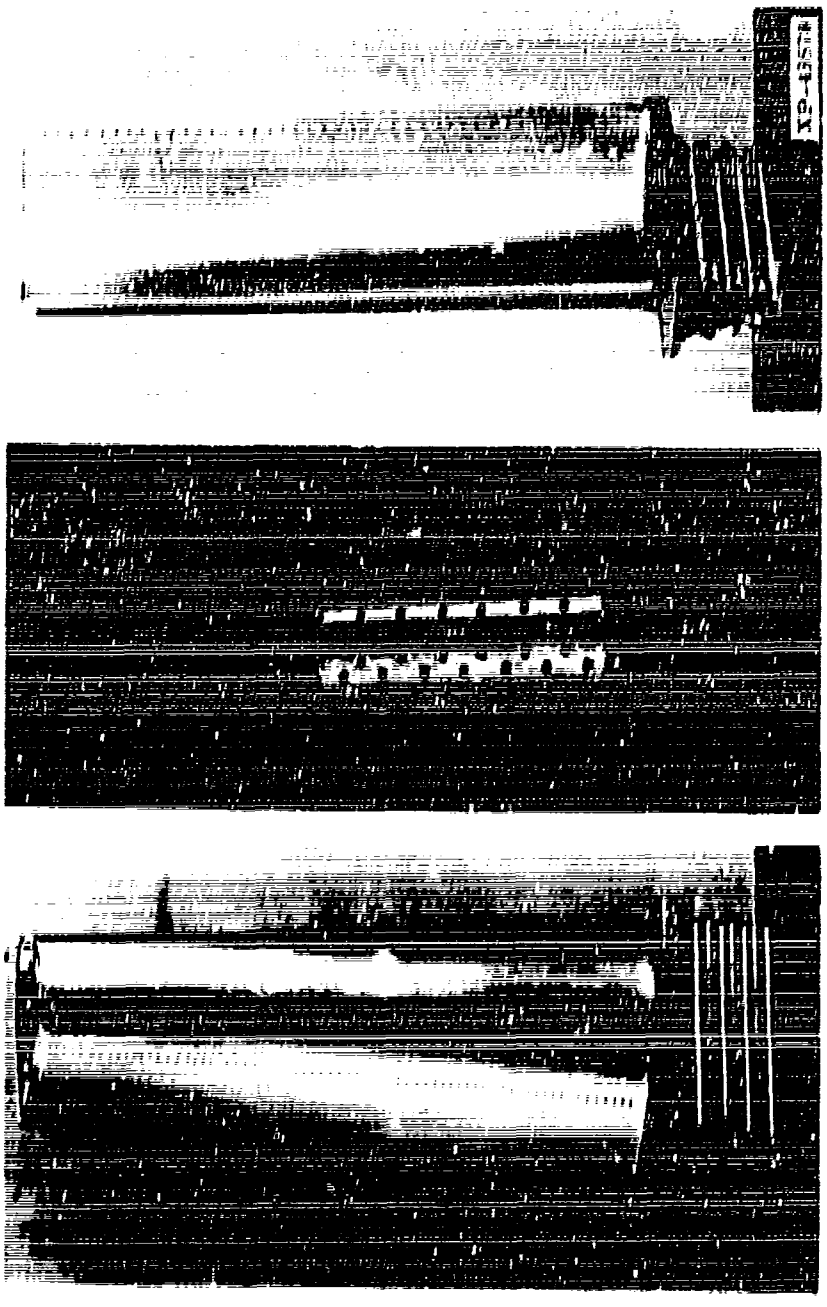
FILM COOLED TURBINE BLADE WITH THREE ROWS OF .013" DIAMETER HOLES AT 30° TO L. E.

Figure 5-45



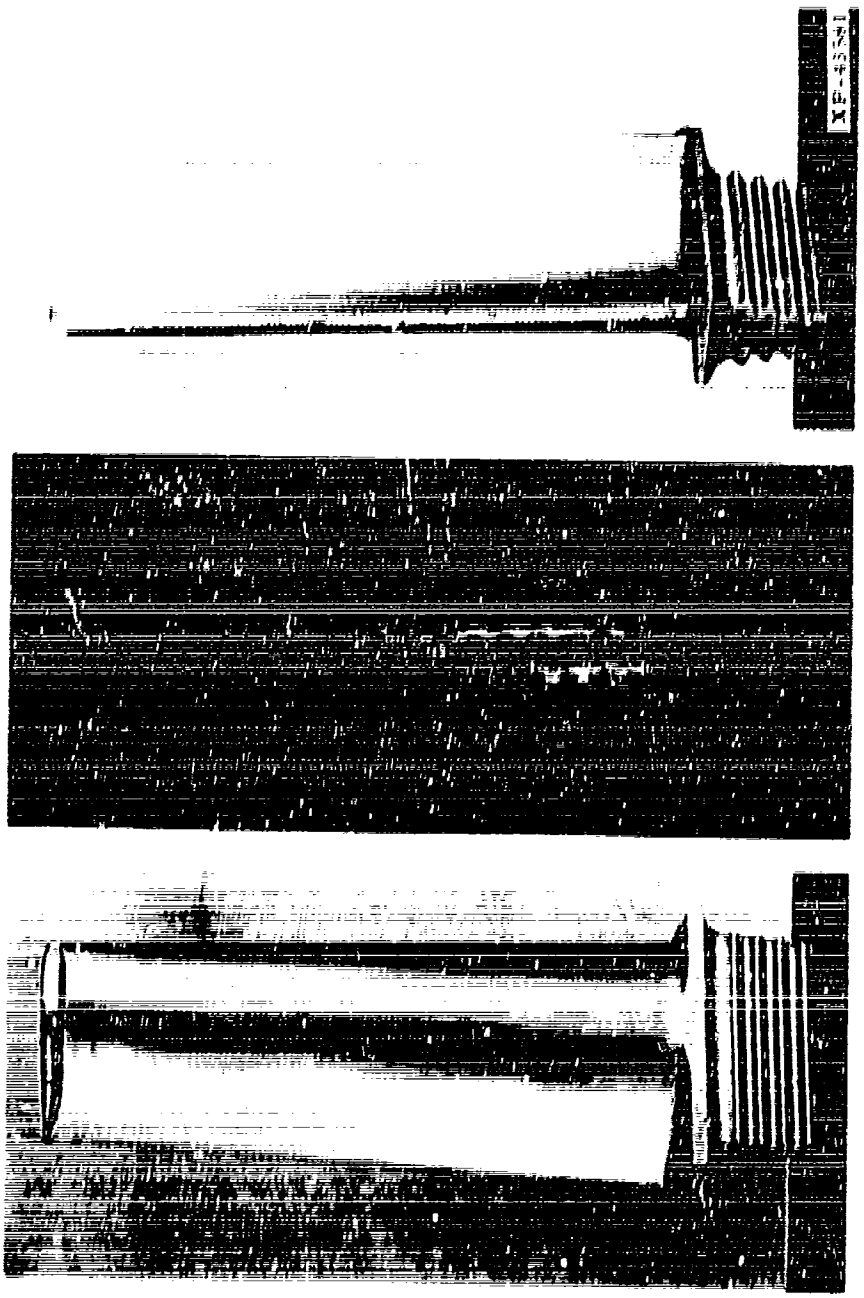
FILM COOLED TURBINE BLADE WITH THREE ROWS OF .008 DIAMETER HOLE AT 90° TO L. E.

Figure 5-40



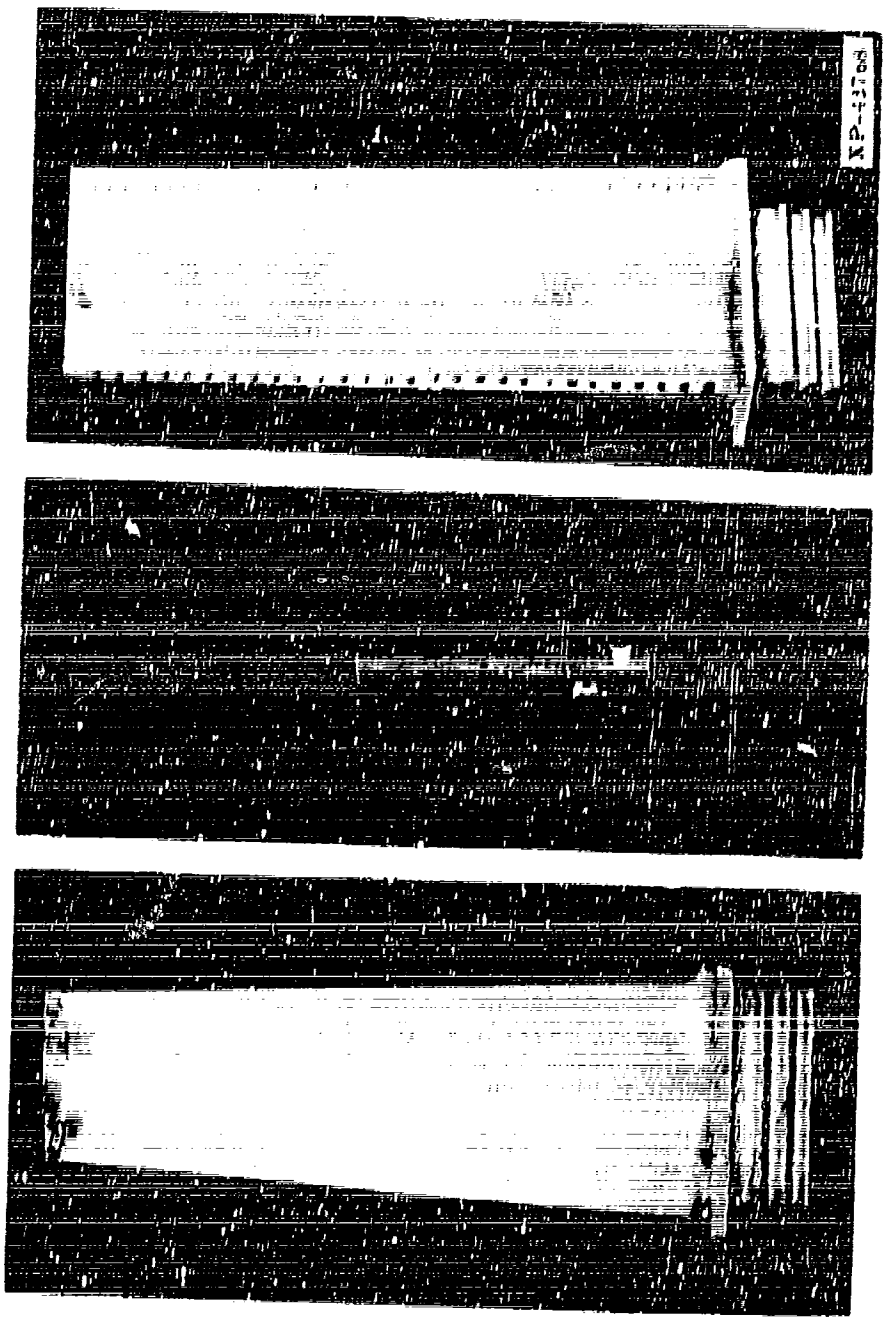
FILM COOLED TURBINE BLADE WITH FIVE ROWS OF .008 DIAMETER HOLES AT 90° TO [illegible]

Figure 5-47



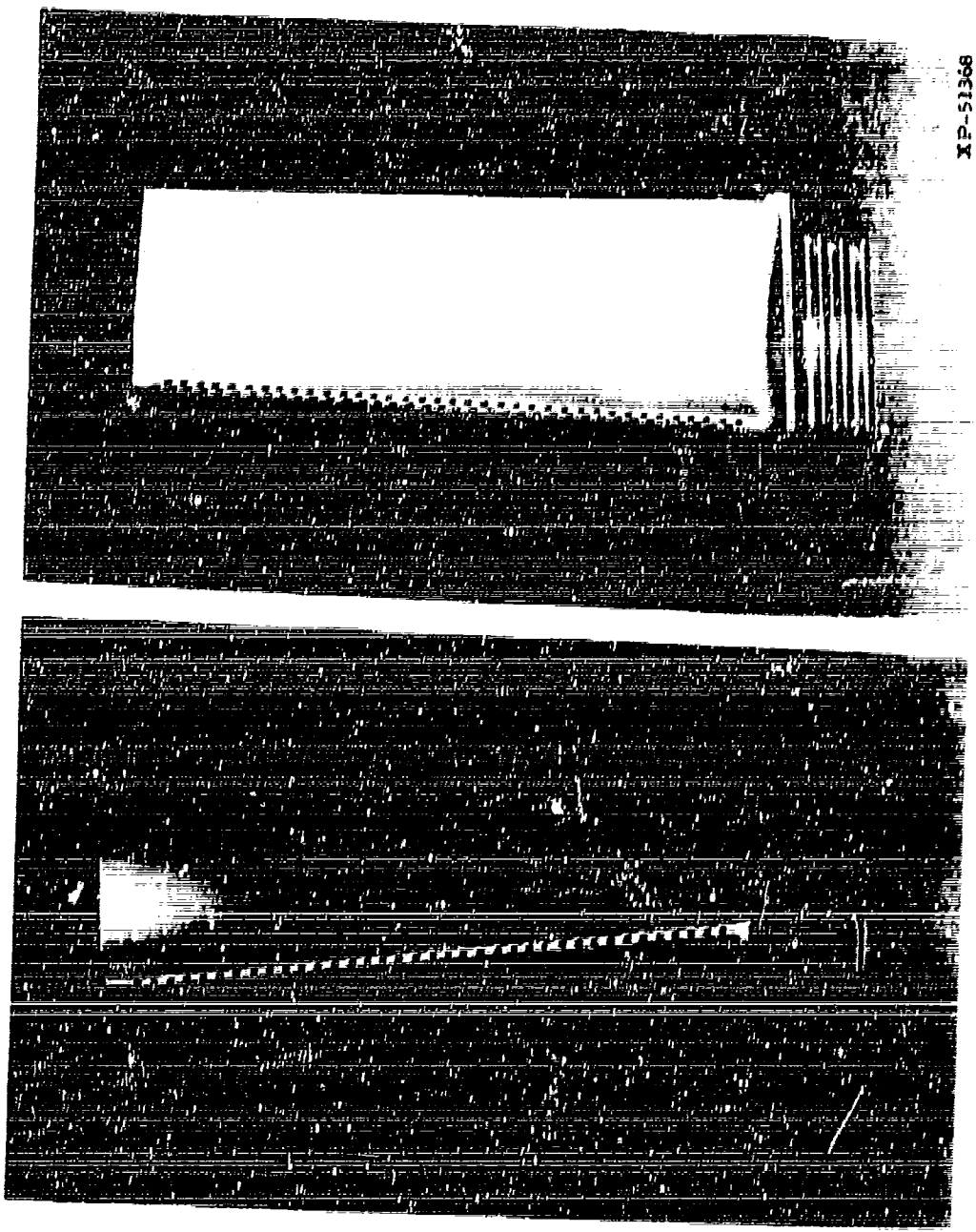
FILM COOLED TURBINE BLADE WITH FIVE ROWS OF .008 DIAMETER HOLES AT 30° TO L. E.

Figure 5-48



FILM COOLED TURBINE BLADE WITH SINGLE ROW OF .030 DIAMETER HOLES AT 30° TO L. E.

Figure 5-49



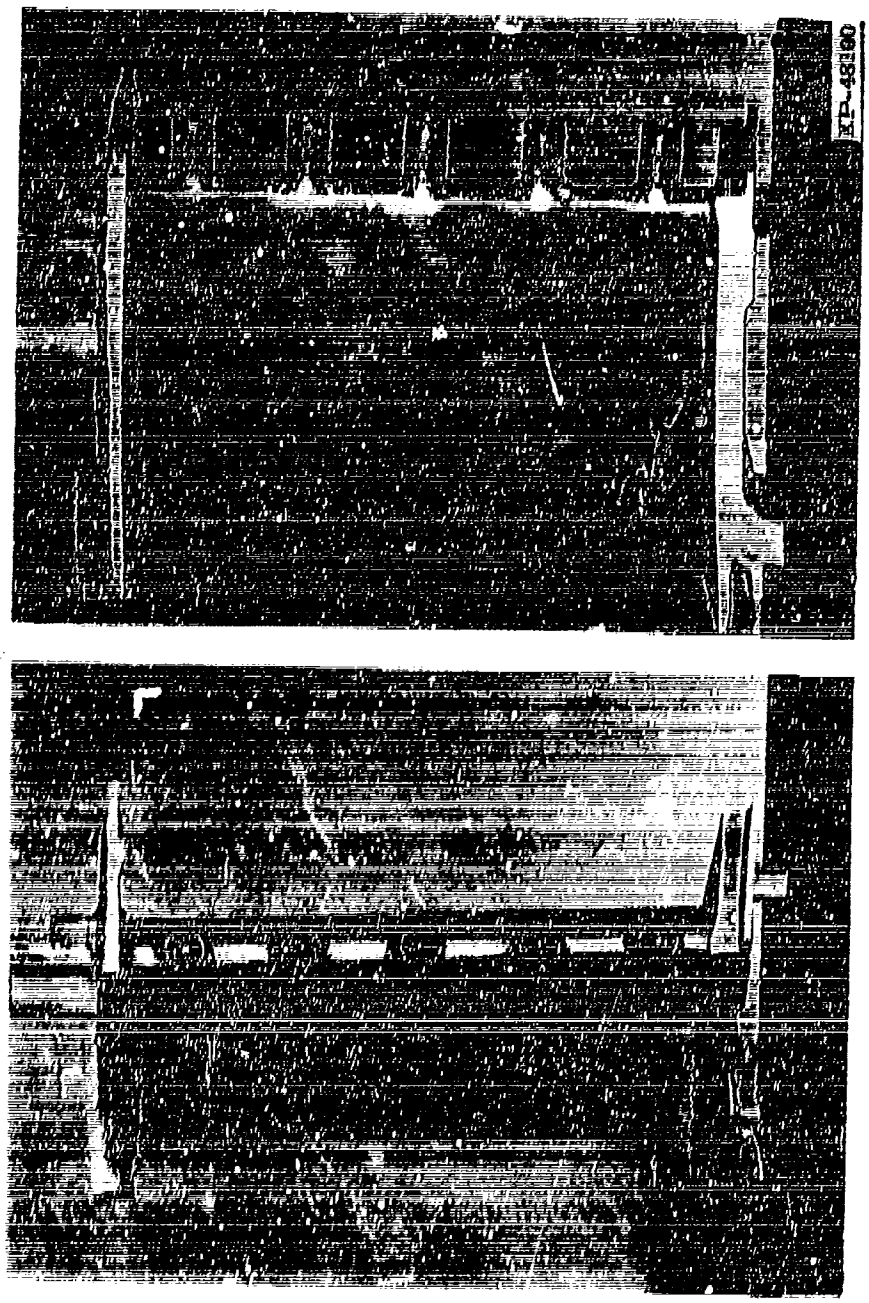
FILM COOLED TURBINE BLADE WITH THREE ROWS OF .030 DIAMETER HOLE AT 30° TO L. E.

Figure 5-50



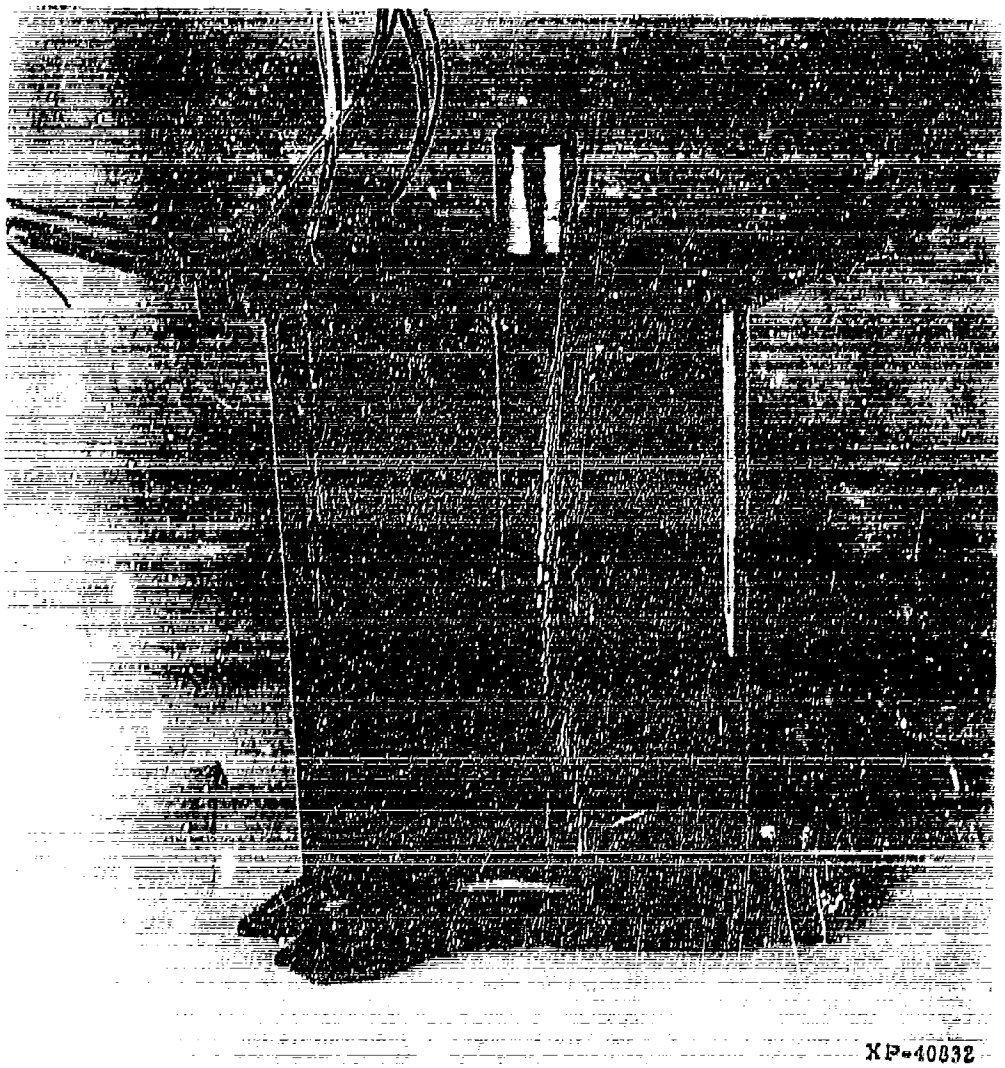
CUTAWAY SECTIONS OF CONVECTIVELY-COOLED BLADES SHOWING CONFIGURATION OF COOLING PASSAGES SHOWING LEFT TO RIGHT .020 SAWTOOTH BLADES, .030" SAWTOOTH BLADE, RIBBED CORE BLADE, AND ELEVEN HOLE BLADE.

Figure 5-51



INSTRUMENTED TURBINE VANE WITH SHIELDED THERMOCOUPLES INSTALLED ON LEADING EDGE

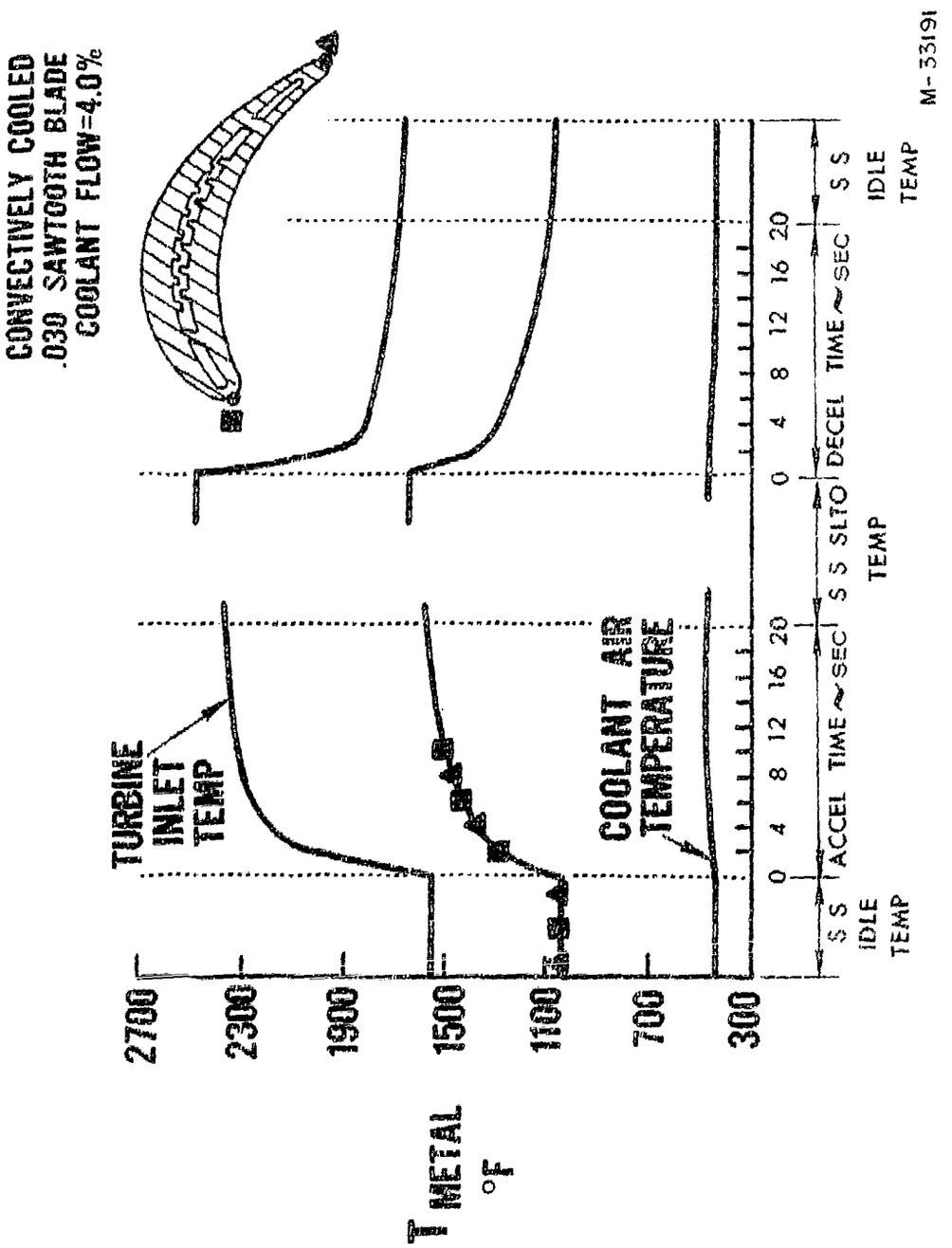
Figure 5-32



XP-40832

INSTRUMENTED TURBINE VANE WITH MID CHORD LEADING AND TRAILING EDGE THERMOCOUPLES FOR MEASURING METAL TEMP.

Figure 5-53

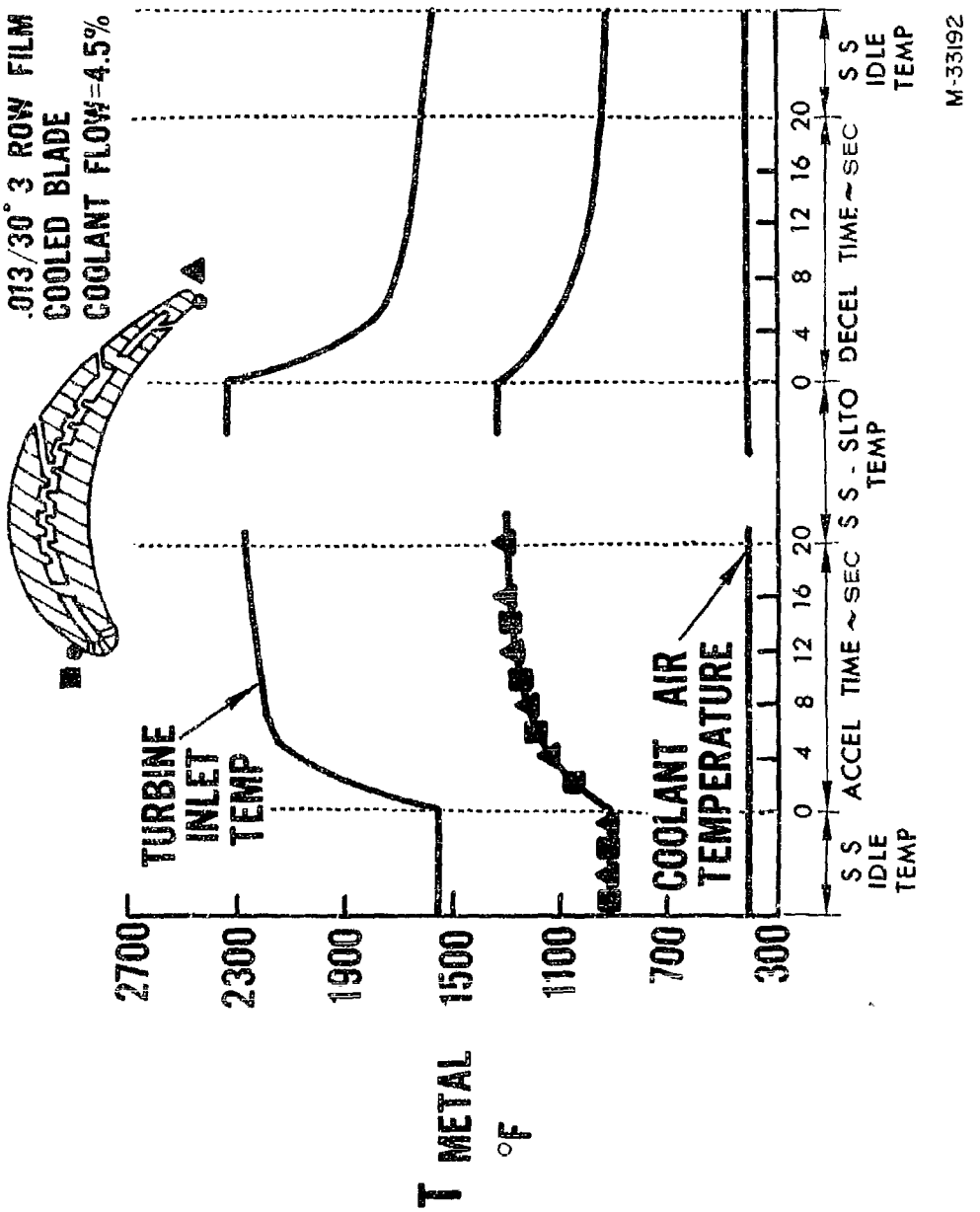


TYPICAL TEMPERATURE READINGS RECORDED ON CONVECTIVELY COOLED SAWTOOTH BLADE DURING CYCLIC ENDURANCE TEST

Figure 5-54

DOWNGRADED AT 3 YEAR INTERVALS
DECLASSIFIED AFTER 12 YEARS
DOD DIR 5200.10

THIS DOCUMENT CONTAINS INFORMATION AFFECTING THE NATIONAL DEFENSE OF THE UNITED STATES WITHIN THE MEANING OF THE ESPIONAGE LAWS, TITLE 18, U.S.C., SECTIONS 793 AND 794. THE TRANSMISSION OR REVELATION OF ITS CONTENTS IN ANY MANNER TO AN UNAUTHORIZED PERSON IS PROHIBITED BY LAW.

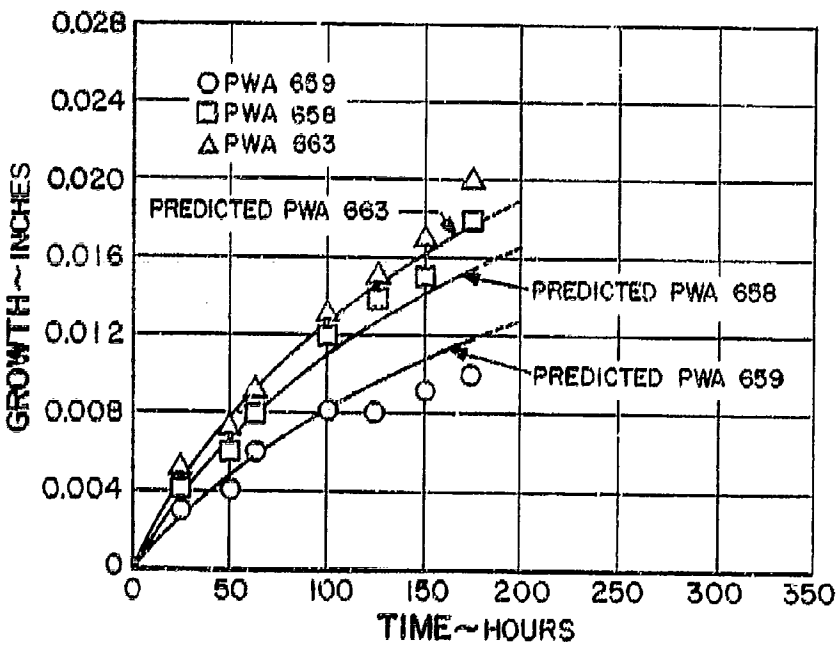


TYPICAL TEMPERATURE READINGS RECORDED ON FILM COOLED BLADE DURING CYCLIC ENDURANCE TEST

Figure 5-55

DOWNGRADED AT 3 YEAR INTERVALS
DECLASSIFIED AFTER 12 YEARS
DOD DIR 5200.10

THIS DOCUMENT CONTAINS INFORMATION AFFECTING THE NATIONAL DEFENSE OF THE UNITED STATES WITHIN THE MEANING OF THE ESPIONAGE LAWS, TITLE 18, U.S.C., SECTIONS 793 AND 794. ITS TRANSMISSION OR THE REVELATION OF ITS CONTENTS IN ANY MANNER TO AN UNAUTHORIZED PERSON IS PROHIBITED BY LAW.

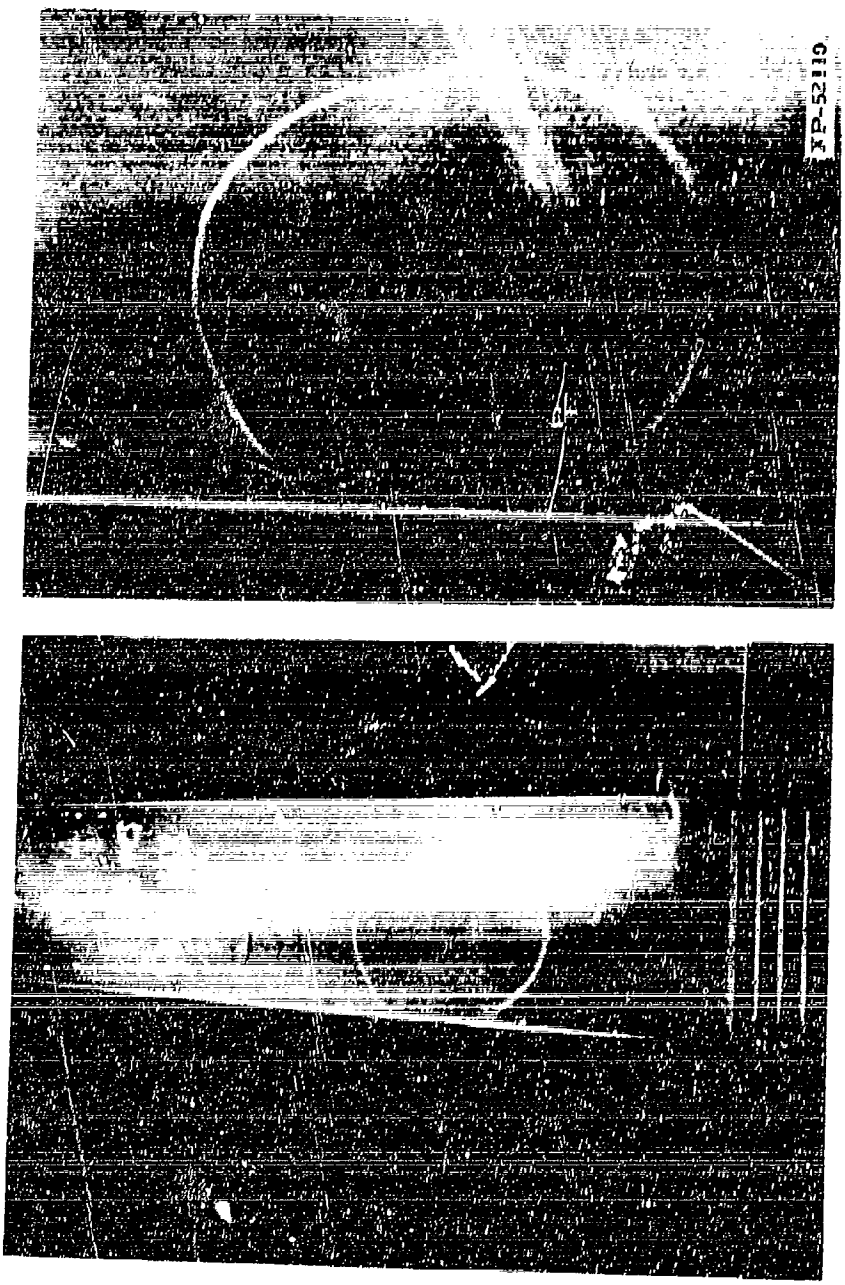


BLADE GROWTH MEASUREMENT RECORDED DURING 200 HOUR STEADY STATE ENDURANCE TEST AT 2300°F TURBINE INLET TEMPERATURE AND 1200°F COOLING AIR TEMPERATURE

Figure 5-56

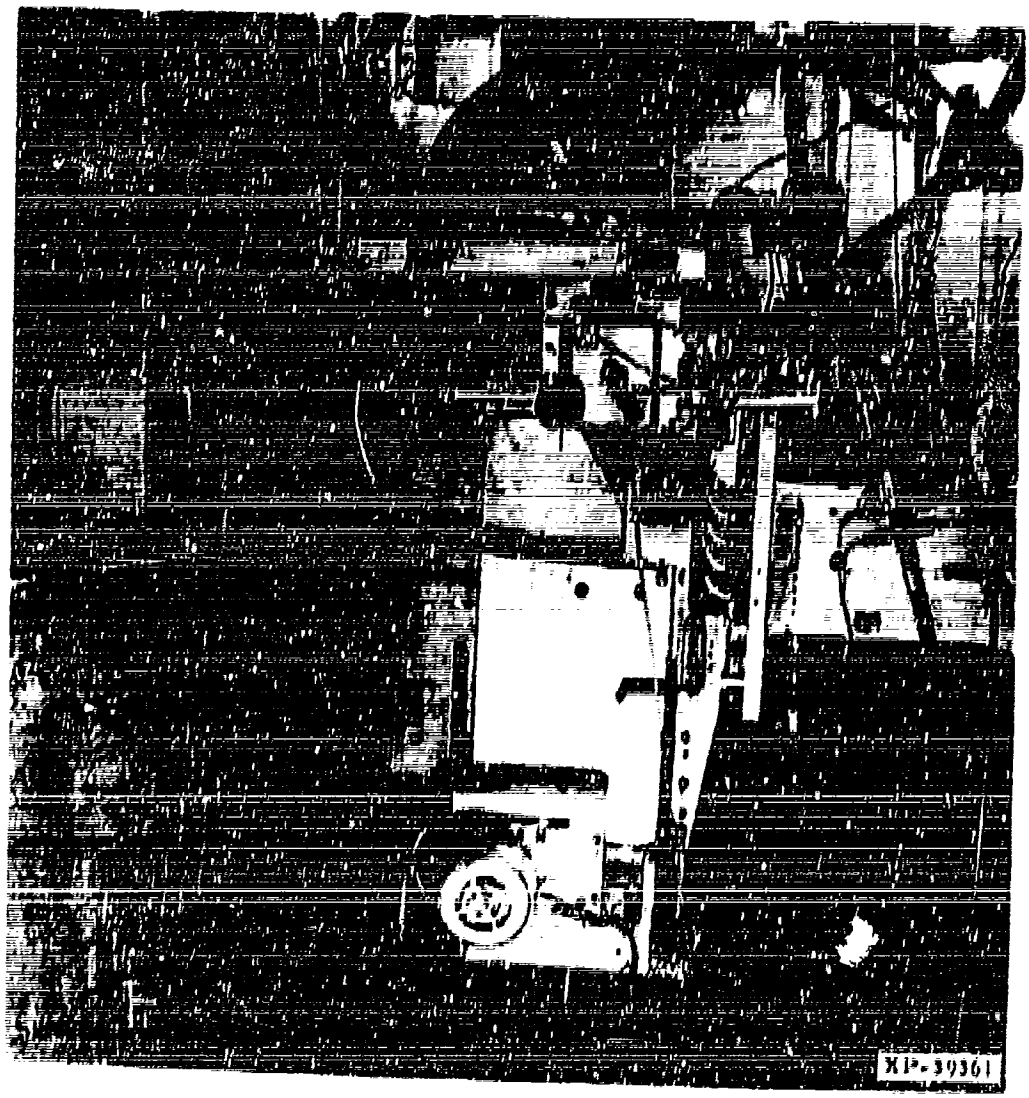
DOWNGRADED AT 3 YEAR INTERVALS
DECLASSIFIED AFTER 12 YEARS
DOD DIR 5200.10

THIS DOCUMENT CONTAINS INFORMATION AFFECTING THE NATIONAL DEFENSE OF THE UNITED STATES WITHIN THE MEANING OF THE ESPIONAGE LAWS, TITLE 18, U.S.C., SECTIONS 793 AND 794. ITS TRANSMISSION OR THE REVELATION OF ITS CONTENTS IN ANY MANNER TO AN UNAUTHORIZED PERSON IS PROHIBITED BY LAW.



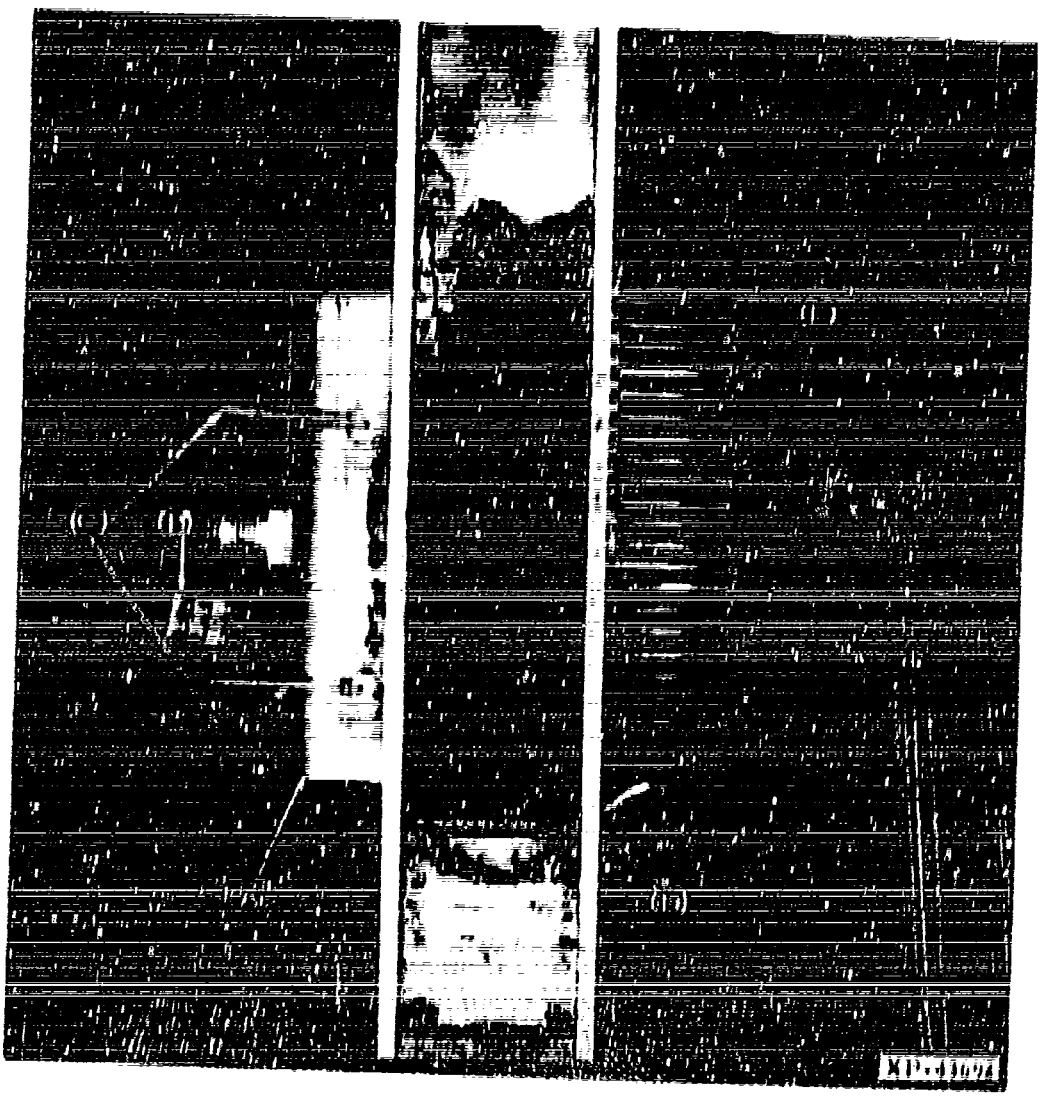
PWA 663 RIBBED CORE BLADE WITH STRESS RUPTURE CRACKS FOLLOWING 150 HOURS OF STEADY STATE ENDURANCE TESTING AT 2300°F T.I.T.

Figure 5-57



CASCADE RIG USED FOR VANE PERFORMANCE TESTING

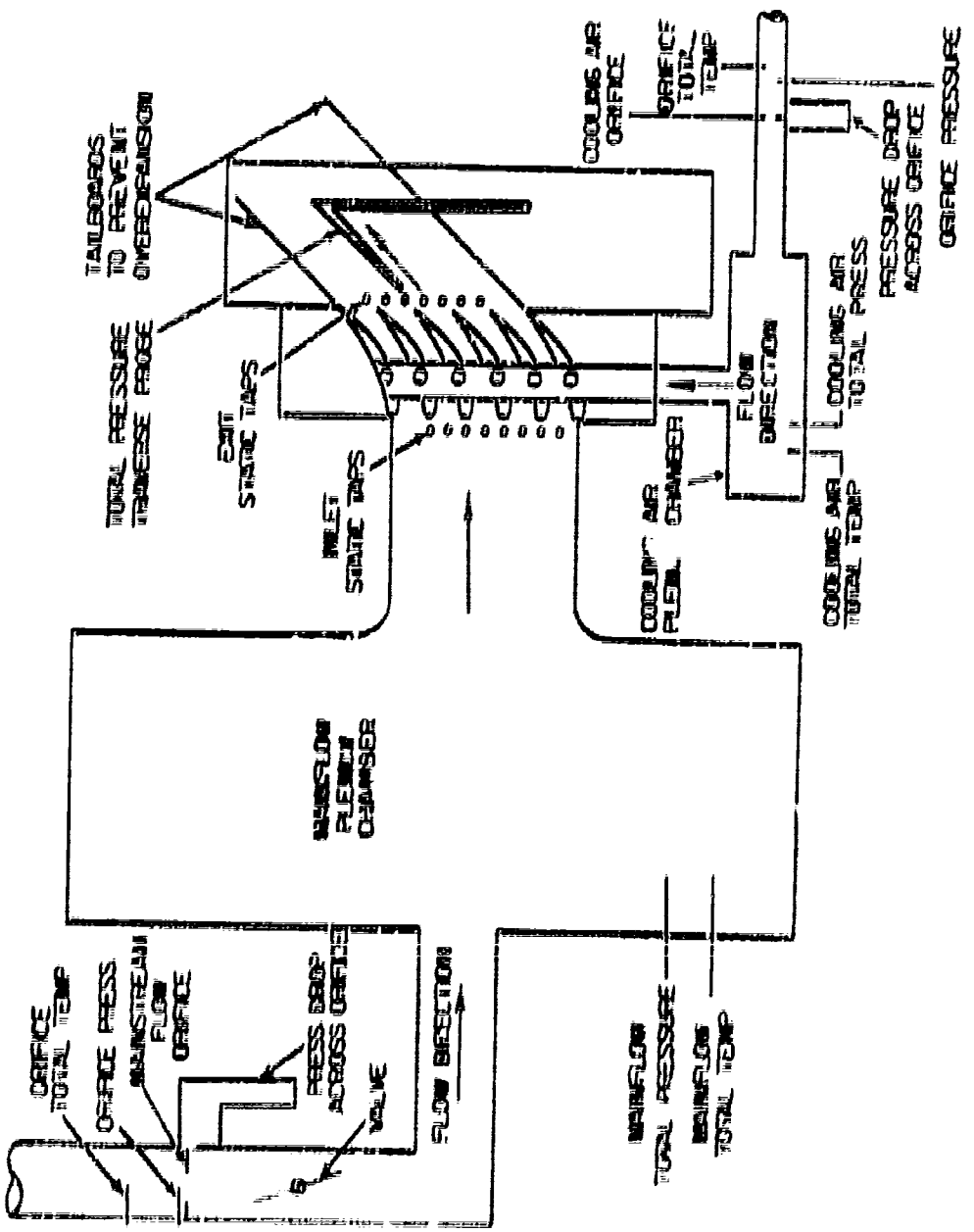
Figure 5-58



CLOSE UP VIEW OF VANE CASCADE TEST SECTION

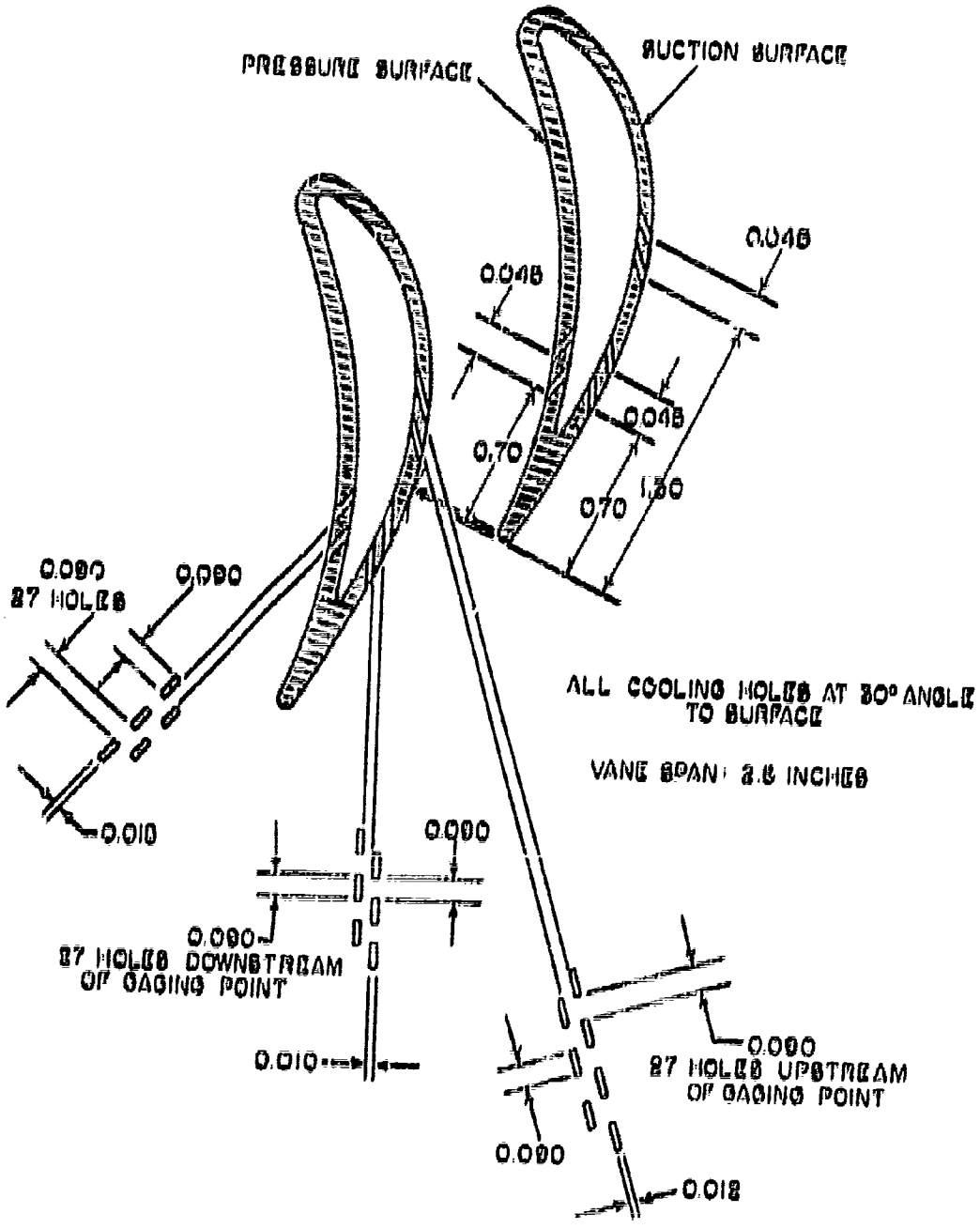
A. Plenum Chamber Cool Air
B. Cooling Air Plenum Chamber T/C
C. Cooling Air Plenum Chamber Press. Taps
D. Cooling Air Holes Leading Edge
E. Wall Static Press Taps

Figure 5-59



SCHEMATIC DIAGRAM OF FILM COOLED VANE PERFORMANCE CASCADE RIG

Figure 5-60



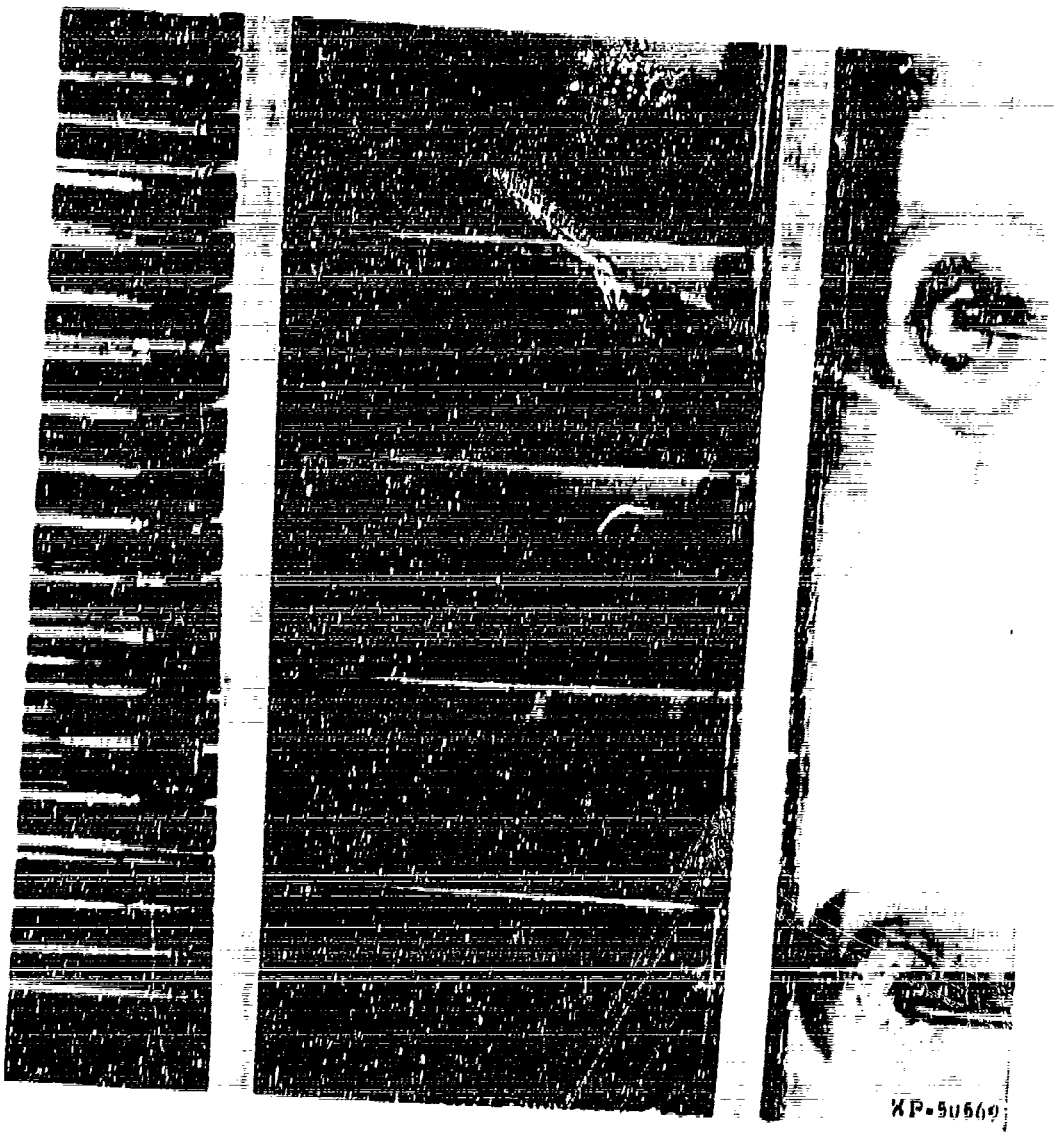
BASIC VANE USED FOR EVALUATING PERFORMANCE OF FILM COOLED VANES

Figure 5-61



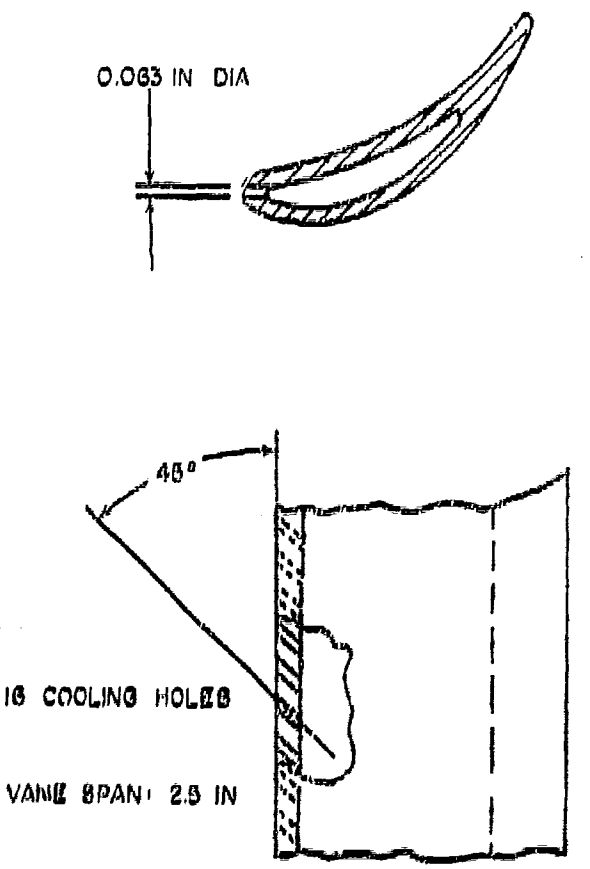
FRONT VIEW OF VANE PACK SHOWING PRESSURE SURFACE COOLING AIR SLOTS

Figure 5-62



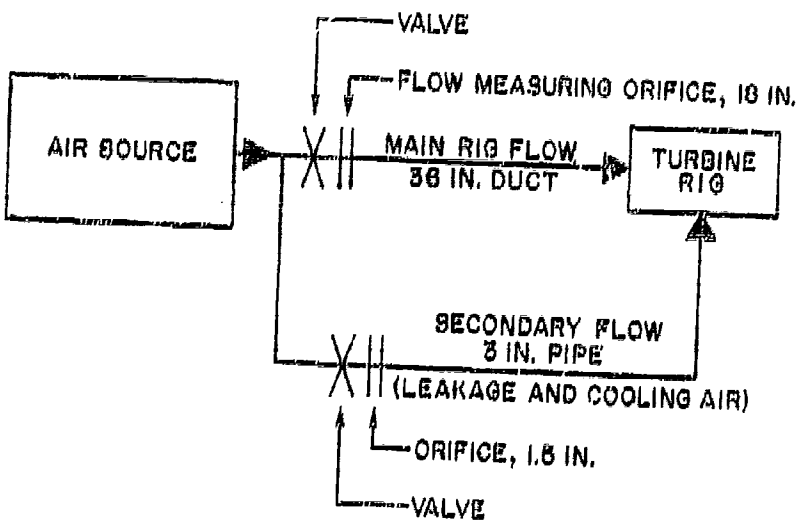
REAR VIEW OF VANE PACK SHOWING PRESSURE SURFACE COOLING AIR SLOTS

Figure 5-63



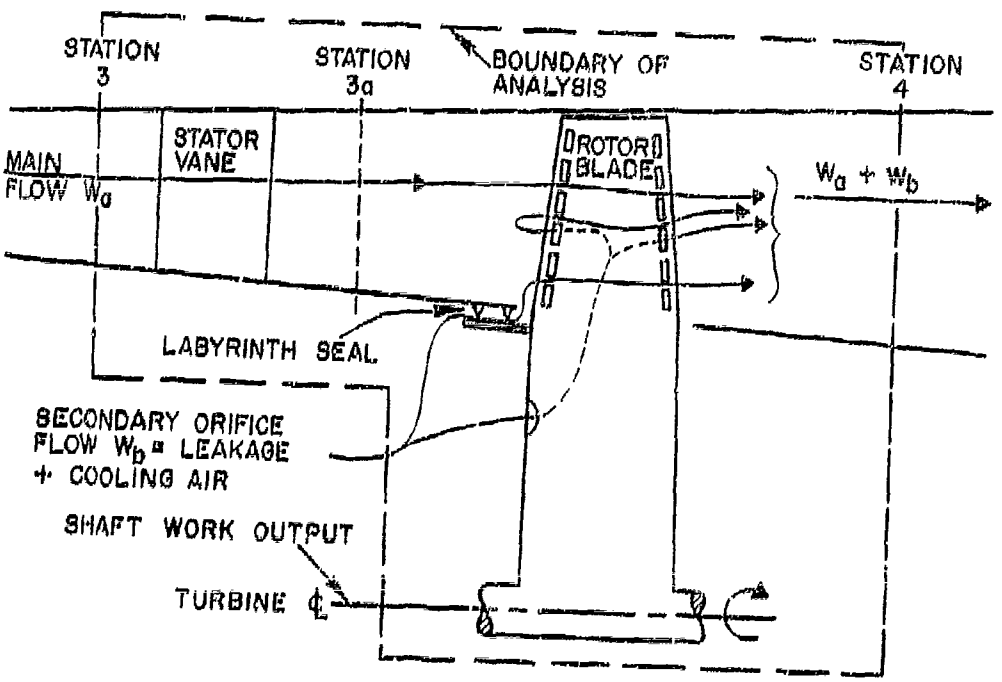
CROSS-SECTION OF VANES WITH LEADING EDGE HOLES ONLY OPEN USED IN VANE PERFORMANCE TESTS

Figure 5-64



SCHEMATIC OF FILM COOLED TURBINE BLADE PERFORMANCE RIG INSTALLATION

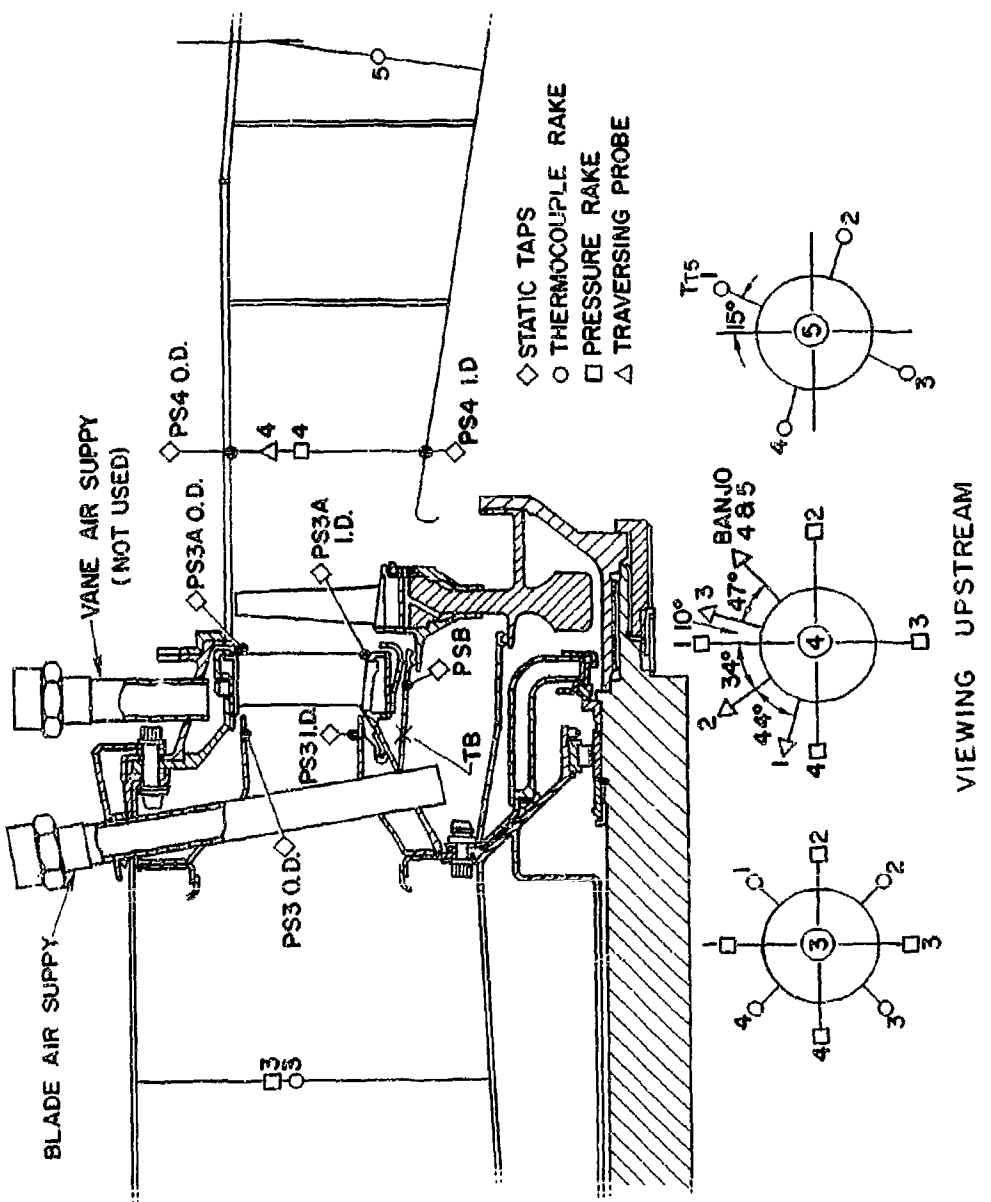
Figure 5-65



SCHEMATIC OF TURBINE PERFORMANCE RIG TEST SECTION SHOWING PATH OF MAIN GASTREAM, COOLING AND LEAKAGE AIR

Figure 5-66

DOWNGRADED AT 3 YEAR INTERVALS
DECLASSIFIED AFTER 12 YEARS
DOD DIR 5200.10

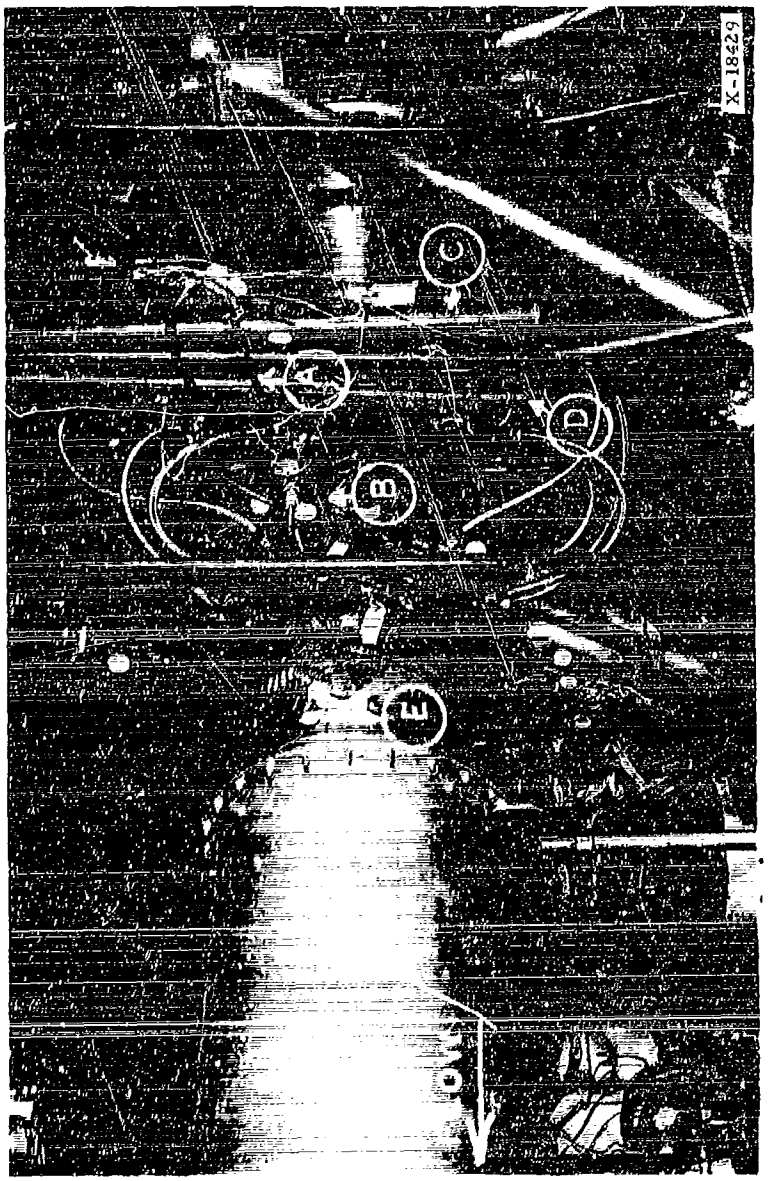


SCHEMATIC OF TURBINE PERFORMANCE RIG INSTRUMENTATION

Figure 5-67

DOWNGRADED AT 3 YEAR INTERVALS
DECLASSIFIED AFTER 12 YEARS
DOD DIR 5200.10

THIS DOCUMENT CONTAINS INFORMATION AFFECTING THE NATIONAL DEFENSE OF THE UNITED STATES WITHIN THE MEANING OF THE ESPIONAGE LAWS, TITLE 18, U.S.C., SECTIONS 793 AND 794. THE TRANSMISSION OR THE REVELATION OF ITS CONTENTS IN ANY MANNER TO AN UNAUTHORIZED PERSON IS PROHIBITED BY LAW.

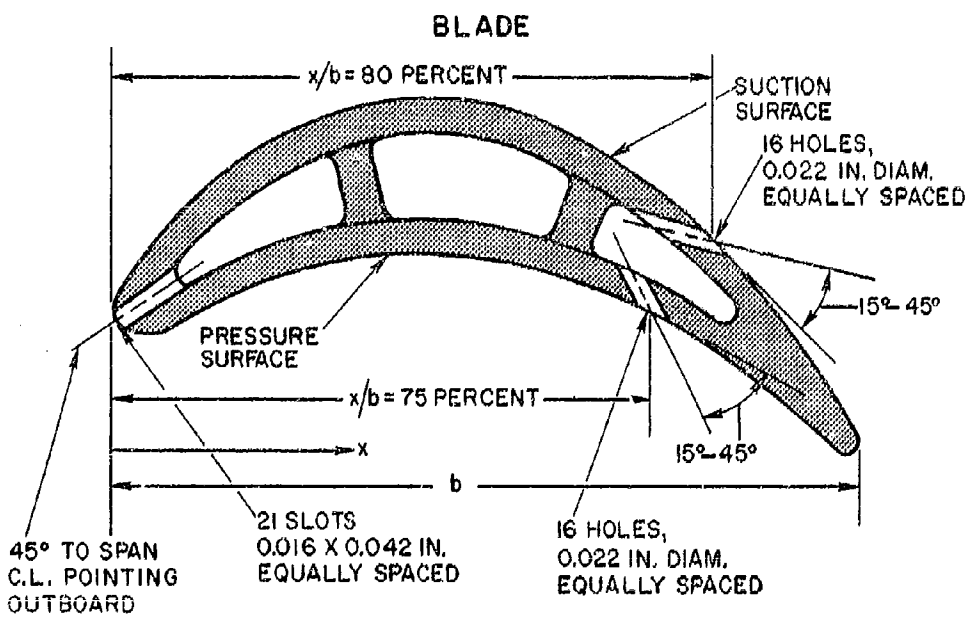


OVERALL VIEW OF TURBINE BLADE PERFORMANCE RIG

A. TRAVERSE PROBE
B. ACTUATING CAN
C. BLADE COOLING-AIR MANIFOLD
D. VANE COOLING AIR-MANIFOLD
E. EXHAUST CASE

Figure 5-68

DOWNGRADED AT 3 YEAR INTERVALS
DECLASSIFIED AFTER 12 YEARS
DOD DIR 5200.10

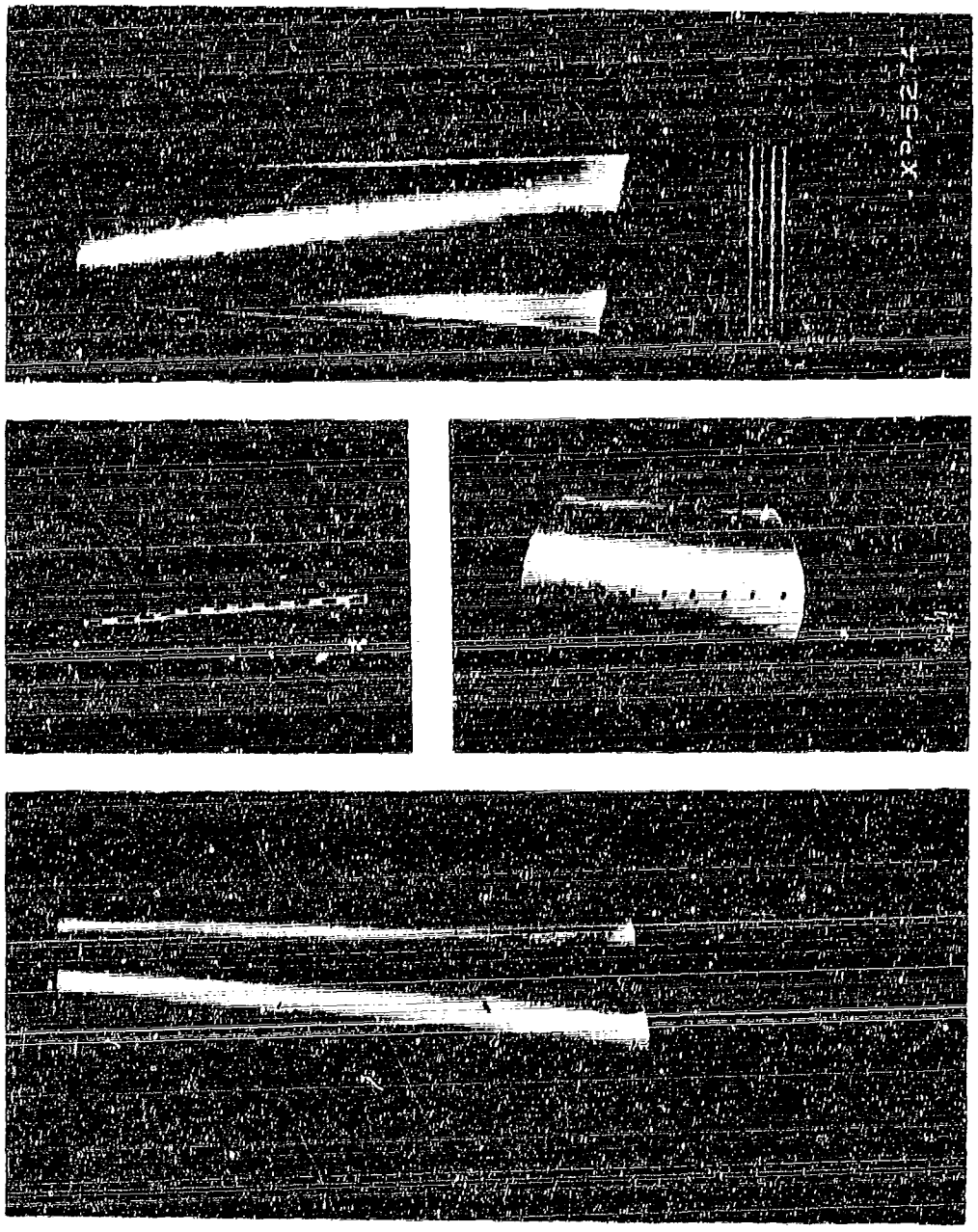


CROSS-SECTION OF INITIAL BLADES TESTED DURING PHASE II-B PERFORMANCE TESTS

Figure 5-69

DOWNGRADED AT 3 YEAR INTERVALS
DECLASSIFIED AFTER 12 YEARS
DOD DIR 5200.10

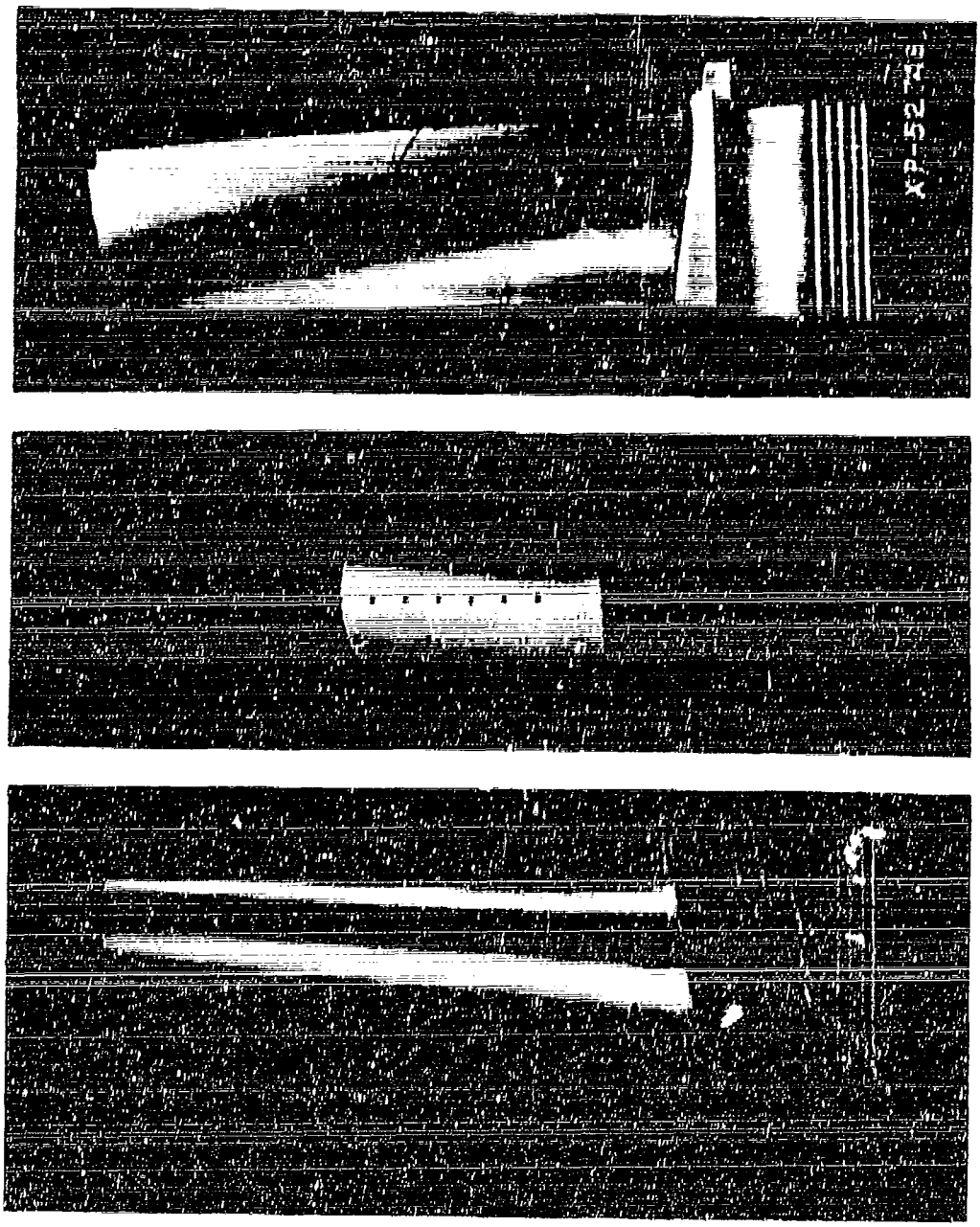
THIS DOCUMENT CONTAINS INFORMATION AFFECTING THE NATIONAL DEFENSE OF THE UNITED STATES WITHIN THE MEANING OF THE ESPIONAGE LAWS, TITLE 18, U.S.C., SECTIONS 793 AND 794. ITS TRANSMISSION OR THE REVELATION OF ITS CONTENTS IN ANY MANNER TO AN UNAUTHORIZED PERSON IS PROHIBITED BY LAW.



TYPICAL BLADE WITH LEADING EDGE SLOTS AND HOLES NEAR TRAILING EDGE ON SUCTION SURFACE TESTED IN PERFORMANCE RIG. HOLES ON PRESSURE SURFACE NEAR T. E. ARE PLUGGED.

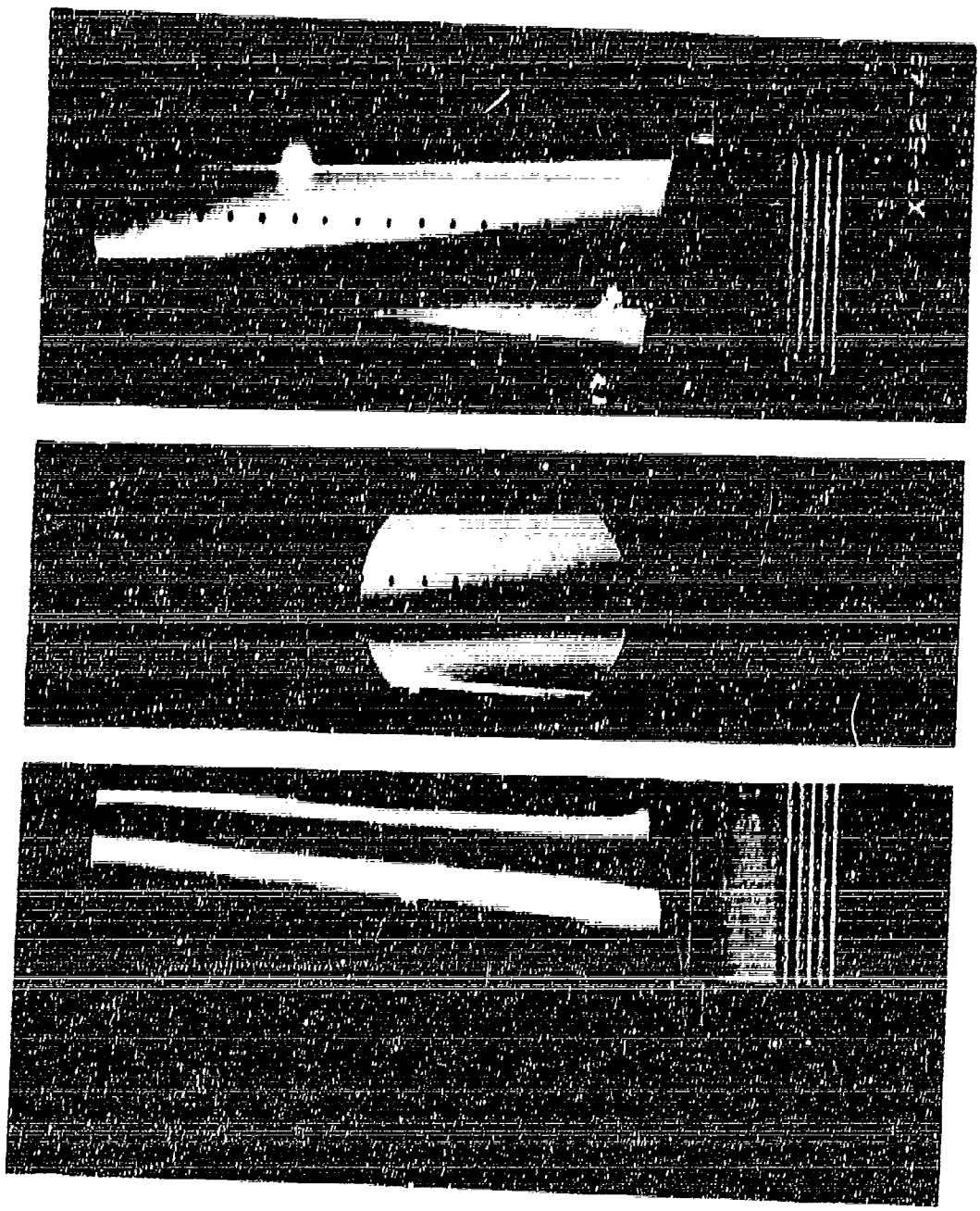
Figure 5-70

DOWNGRADED AT 3 YEAR INTERVALS
DECLASSIFIED AFTER 12 YEARS
DOD DIR 5200.10



TYPICAL BLADE WITH HOLES NEAR TRAILING EDGE ON SUCTION SURFACE TESTED IN PERFORMANCE RIG. HOLES ON PRESSURE SURFACE NEAR T. E. ARE PLUGGED.

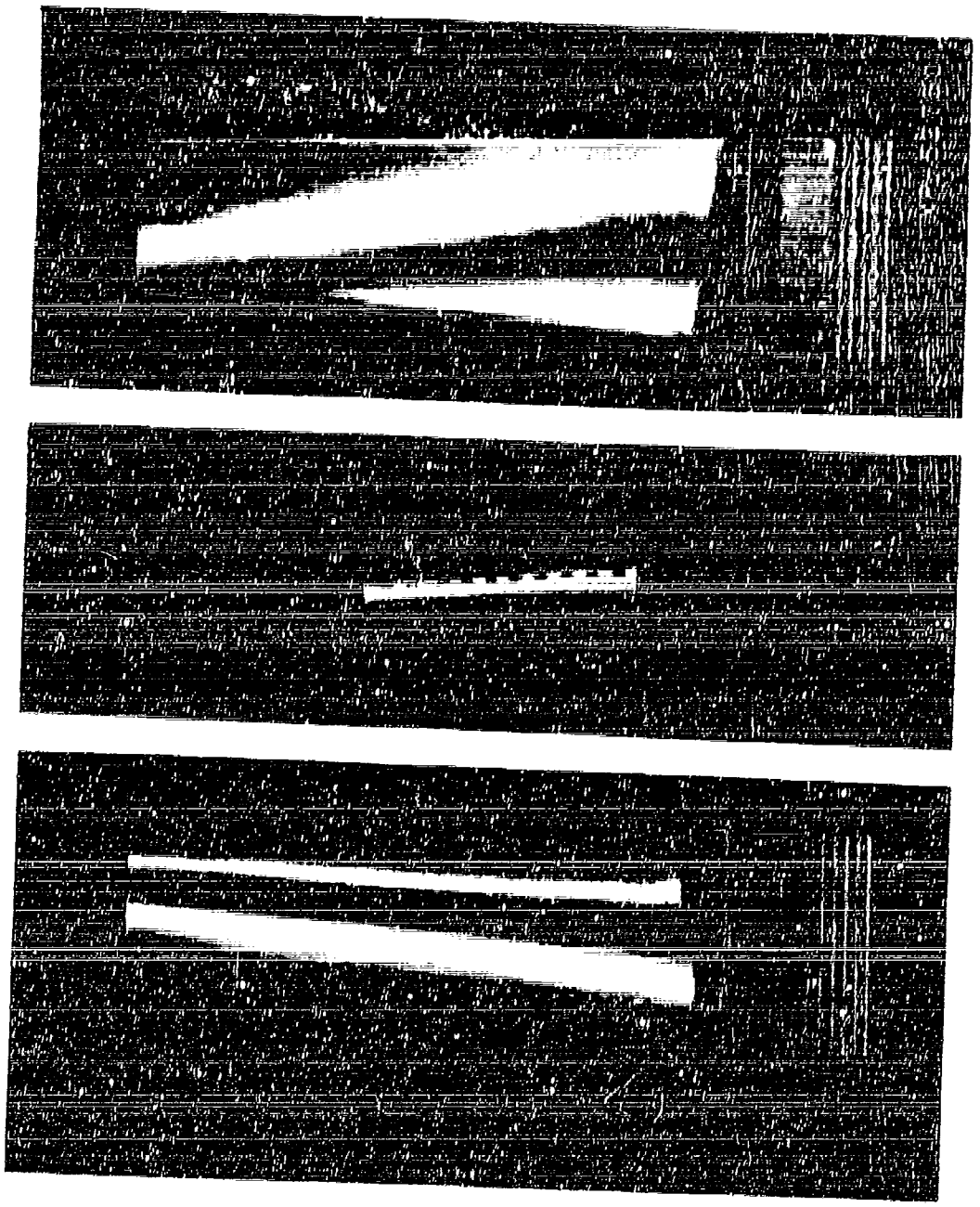
Figure 5-71



TYPICAL BLADE WITH HOLES NEAR TRAILING EDGE ON PRESSURE SURFACE TESTED IN PERFORMANCE RIG. HOLES ON SUCTION SURFACE NEAR T. E. ARE PLUGGED.

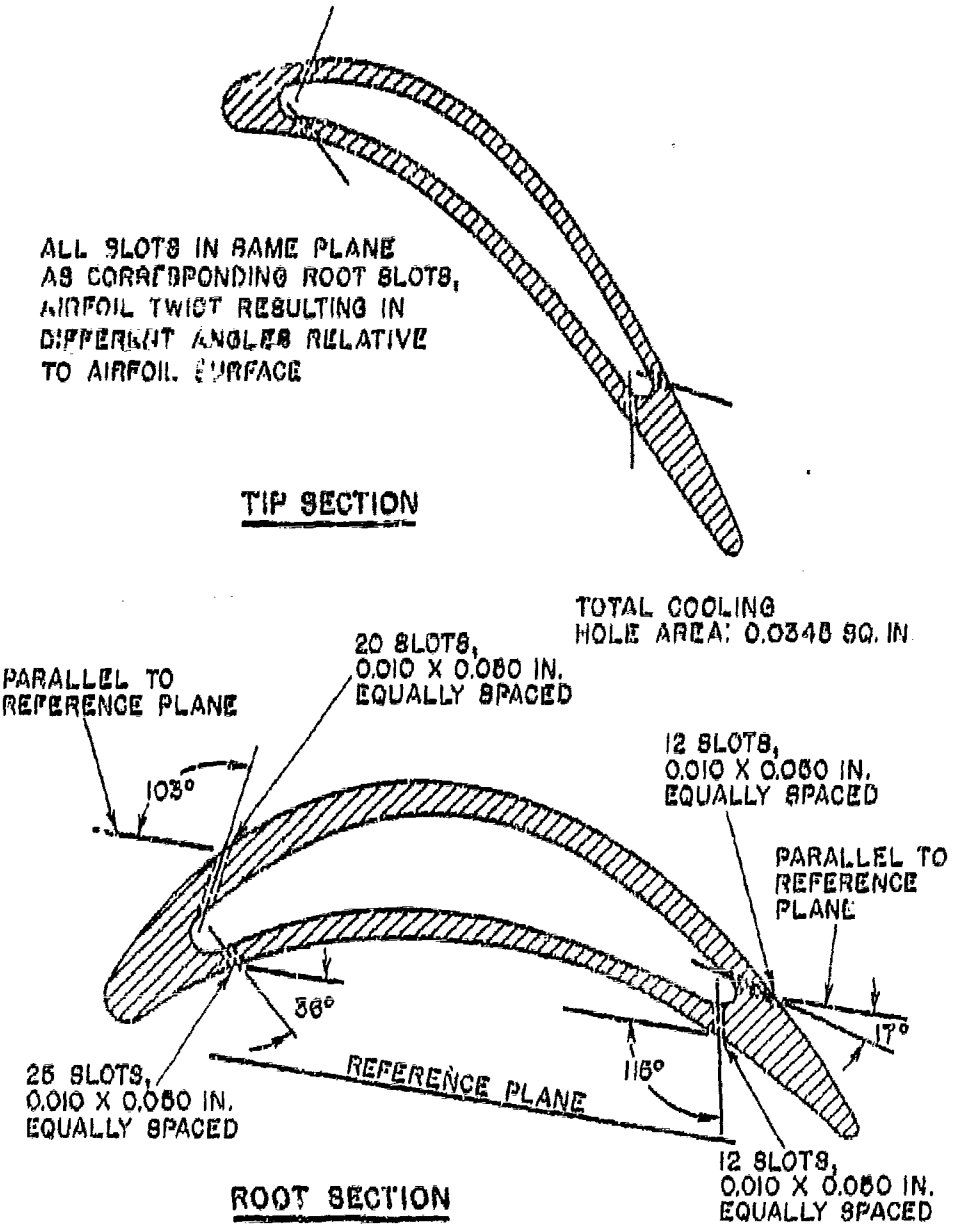
Figure 5-72

DOWNGRADED AT 3 YEAR INTERVALS
DECLASSIFIED AFTER 12 YEARS
DOD DIR 5200.10



TYPICAL BLADE WITH LEADING EDGE SLOTS ONLY OPEN TESTED IN PERFORMANCE RIG. HOLES ON BOTH SIDES NEAR T. E. ARE PLUGGED.

Figure 5-73

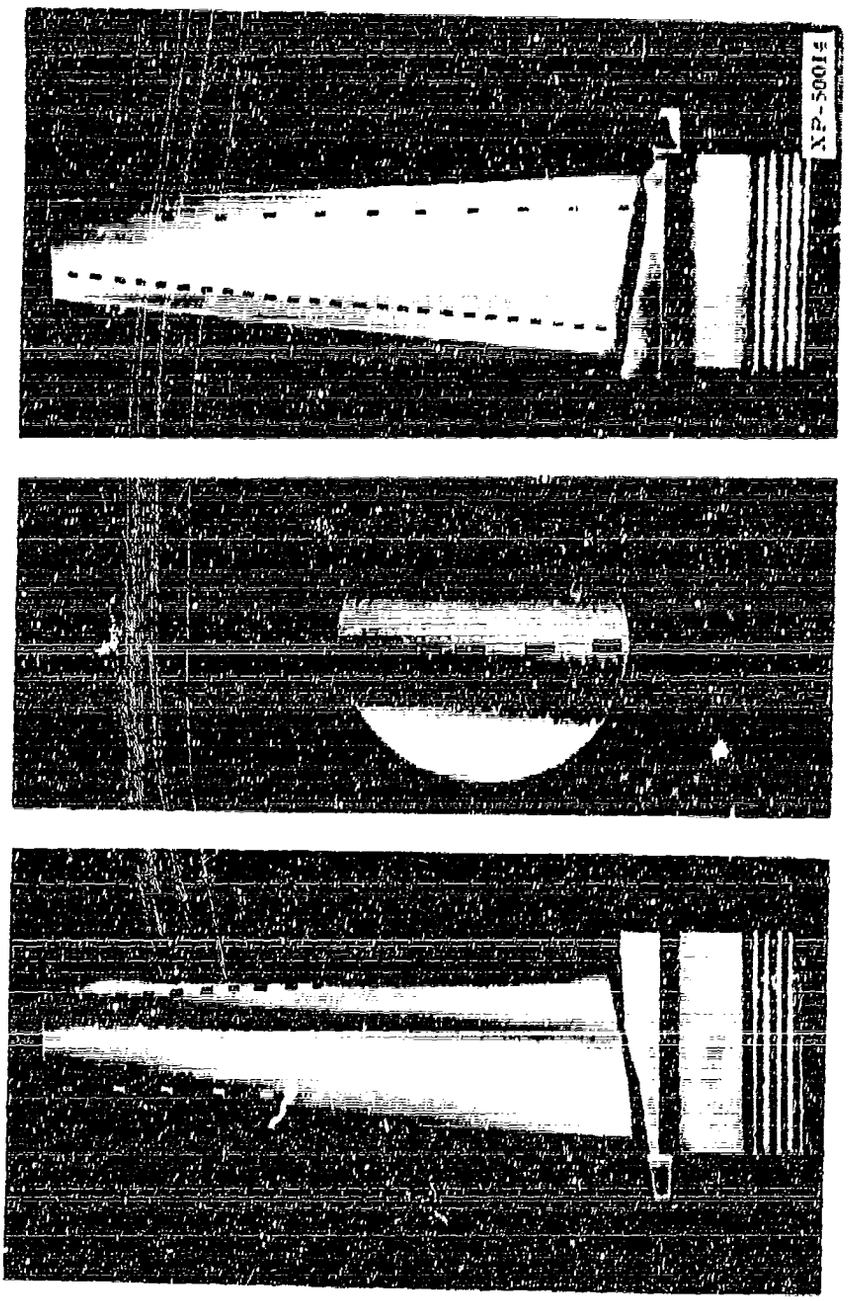


CROSS-SECTION OF BLADE WITH SUCTION AND PRESSURE SURFACE SLOTS AT LEADING AND TRAILING EDGE

Figure 5-74

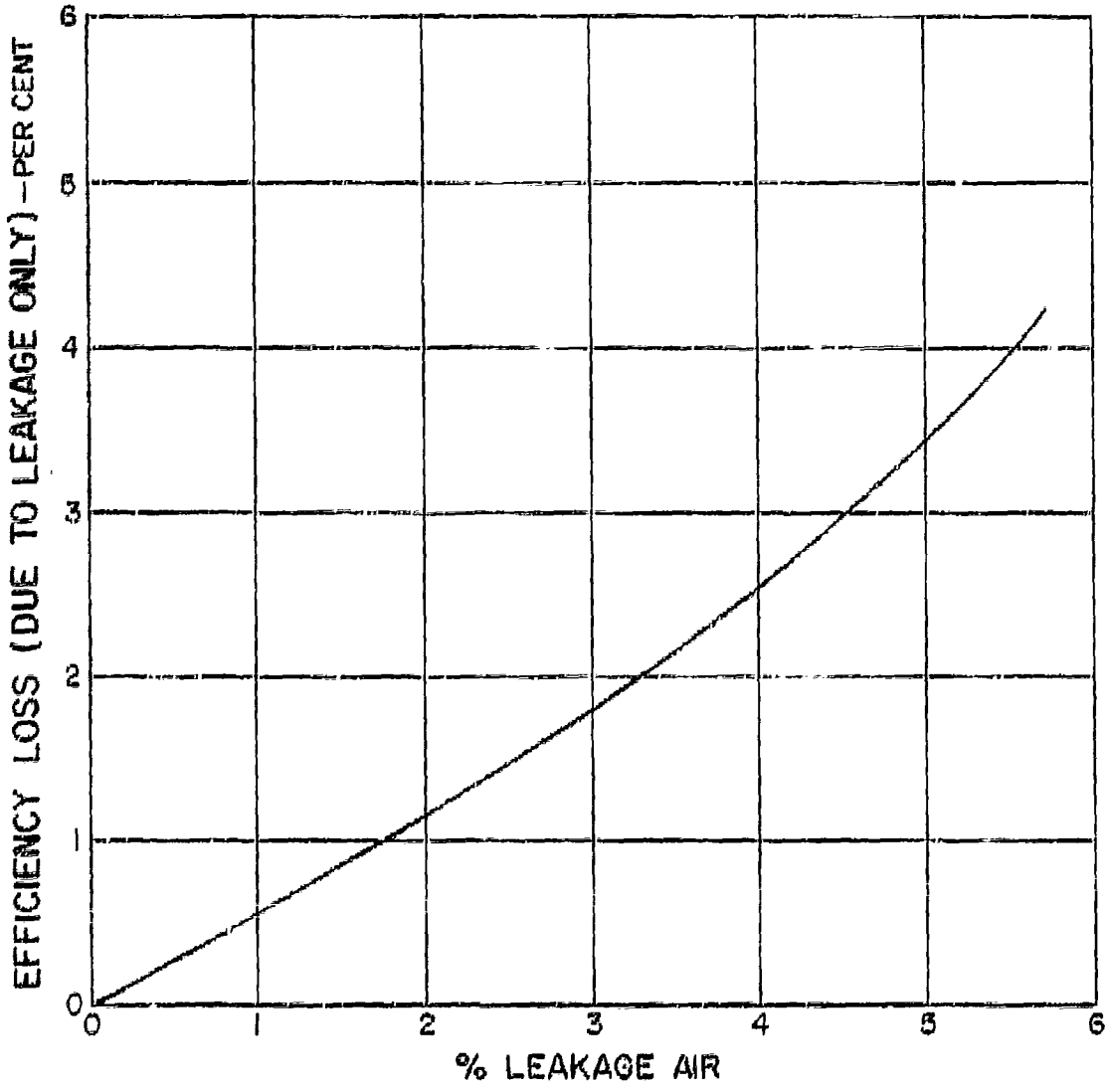
DOWNGRADED AT 3 YEAR INTERVALS
DECLASSIFIED AFTER 12 YEARS
DOD DIR 5200.10

THIS DOCUMENT CONTAINS INFORMATION AFFECTING THE NATIONAL DEFENSE OF THE UNITED STATES WITHIN THE MEANING OF THE ESPIONAGE LAWS, TITLE 18, U.S.C., SECTIONS 793 AND 794. THE TRANSMISSION OR THE REVELATION OF ITS CONTENTS IN ANY MANNER TO AN UNAUTHORIZED PERSON IS PROHIBITED BY LAW.



TYPICAL BLADE WITH SUCTION AND PRESSURE SURFACE SLOTS AT LEADING AND TRAILING EDGES

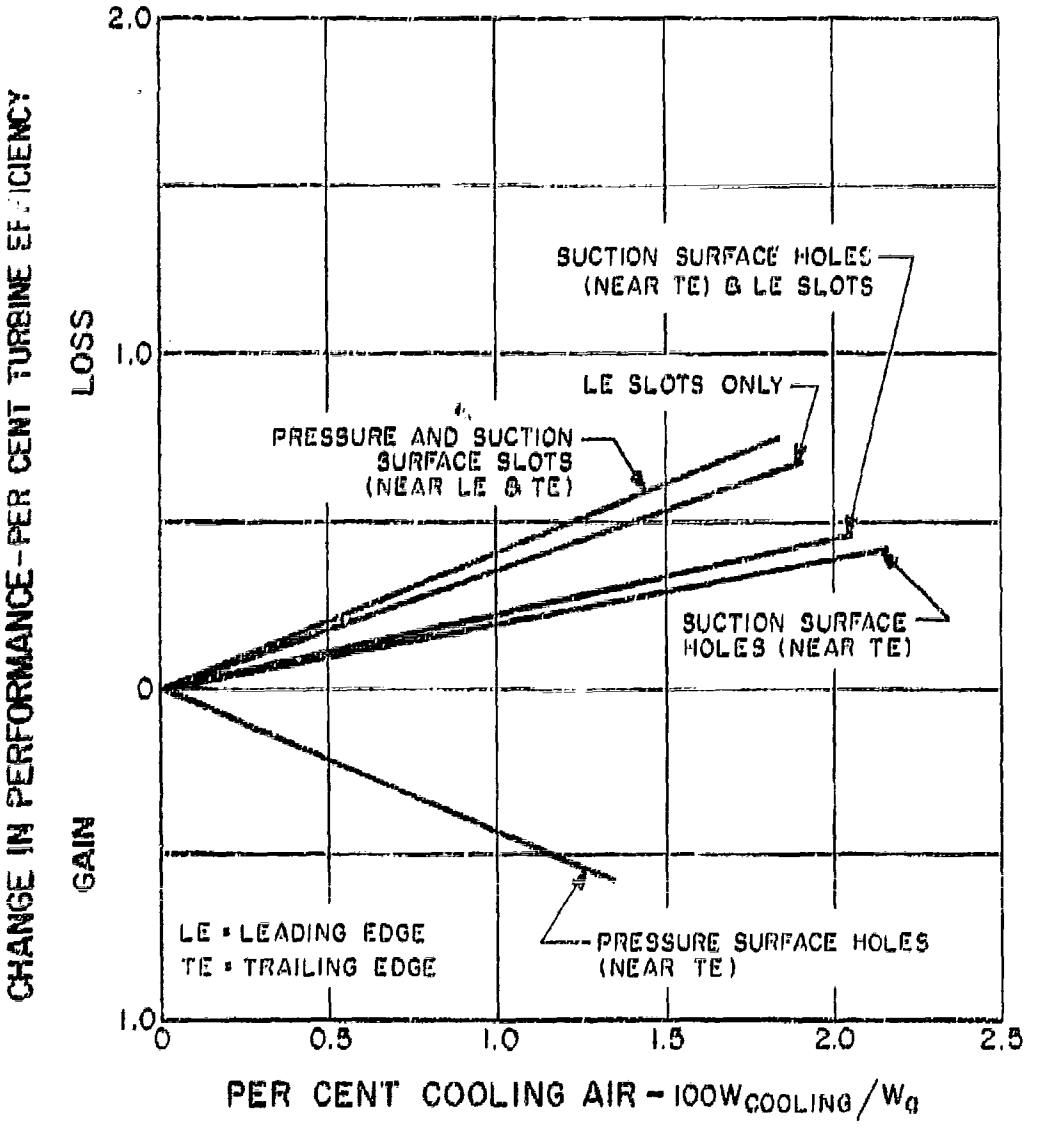
Figure 5-75



CHANGE IN TURBINE EFFICIENCY DUE TO LEAKAGE ONLY

Figure 5-76

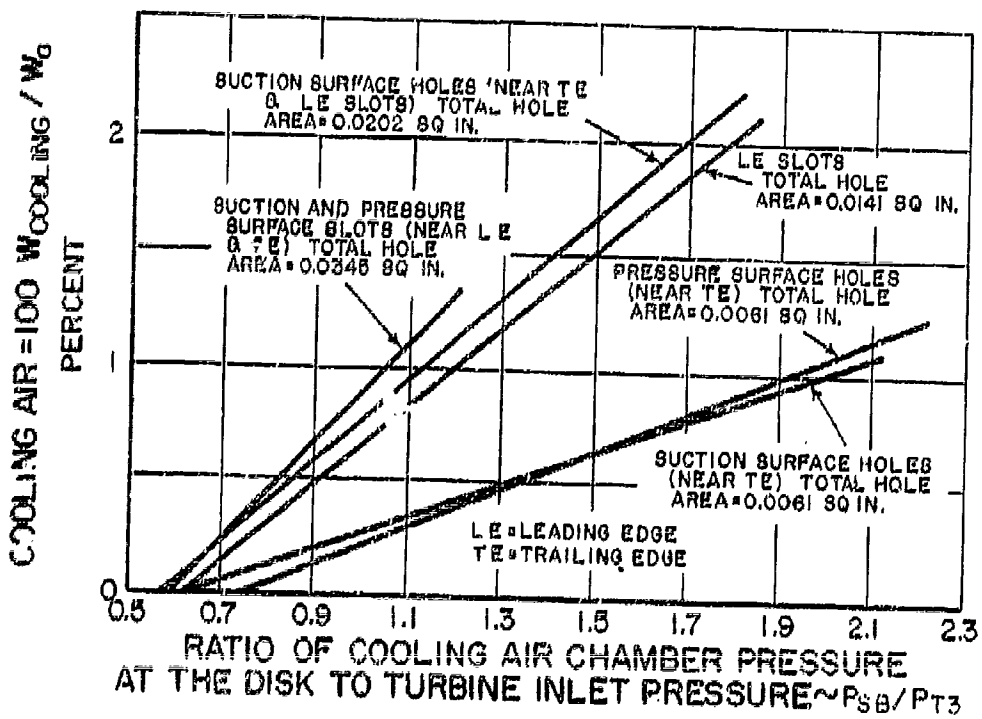
DOWNGRADED AT 3 YEAR INTERVALS
DECLASSIFIED AFTER 12 YEARS
DOD DIR 5200.10



CHANGE IN TURBINE EFFICIENCY WITH VARIOUS BLADE COOLING SCHEMES AS A FUNCTION OF COOLING FLOW

Figure 5-77

DOWNGRADED AT 3 YEAR INTERVALS
DECLASSIFIED AFTER 12 YEARS
DOD DIR 5200.10

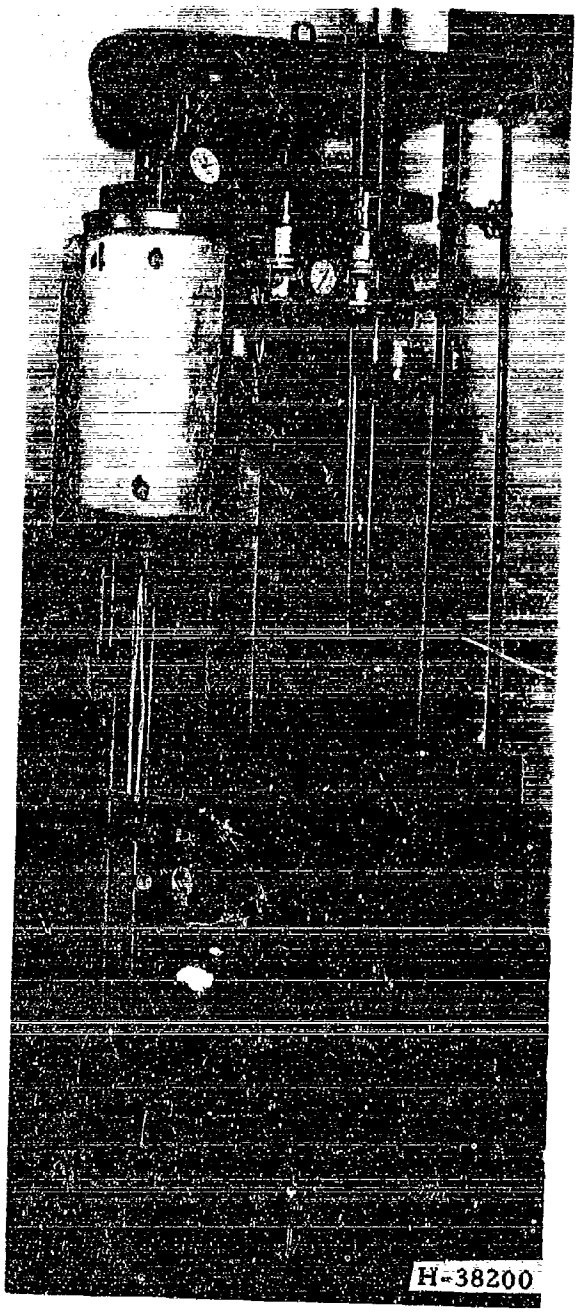


EFFECT OF COOLING HOLE AREA ON COOLING AIR FLOW AND PRESSURE

Figure 5-78

DOWNGRADED AT 3 YEAR INTERVALS
DECLASSIFIED AFTER 12 YEARS
DOD DIR 5200.10

THIS DOCUMENT CONTAINS INFORMATION AFFECTING THE NATIONAL DEFENSE OF THE UNITED STATES WITHIN THE MEANING OF THE ESPIONAGE LAWS, TITLE 18, U. S. C., SECTIONS 793 AND 794. THE TRANSMISSION OR THE REVELATION OF ITS CONTENTS IN ANY MANNER TO AN UNAUTHORIZED PERSON IS PROHIBITED BY LAW.

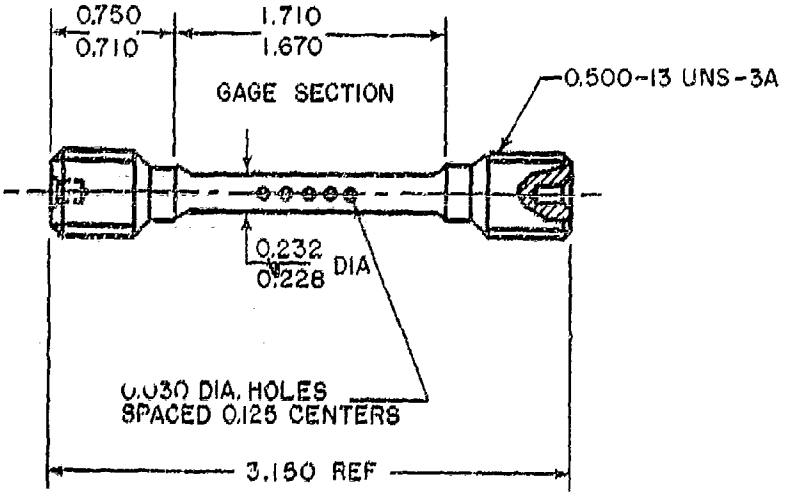


CREEP MACHINE USED FOR CYCLIC STRESS RUPTURE TESTS

Figure 5-79

DOWNGRADED AT 3 YEAR INTERVALS
DECLASSIFIED AFTER 12 YEARS
DOD DIR 5200.10

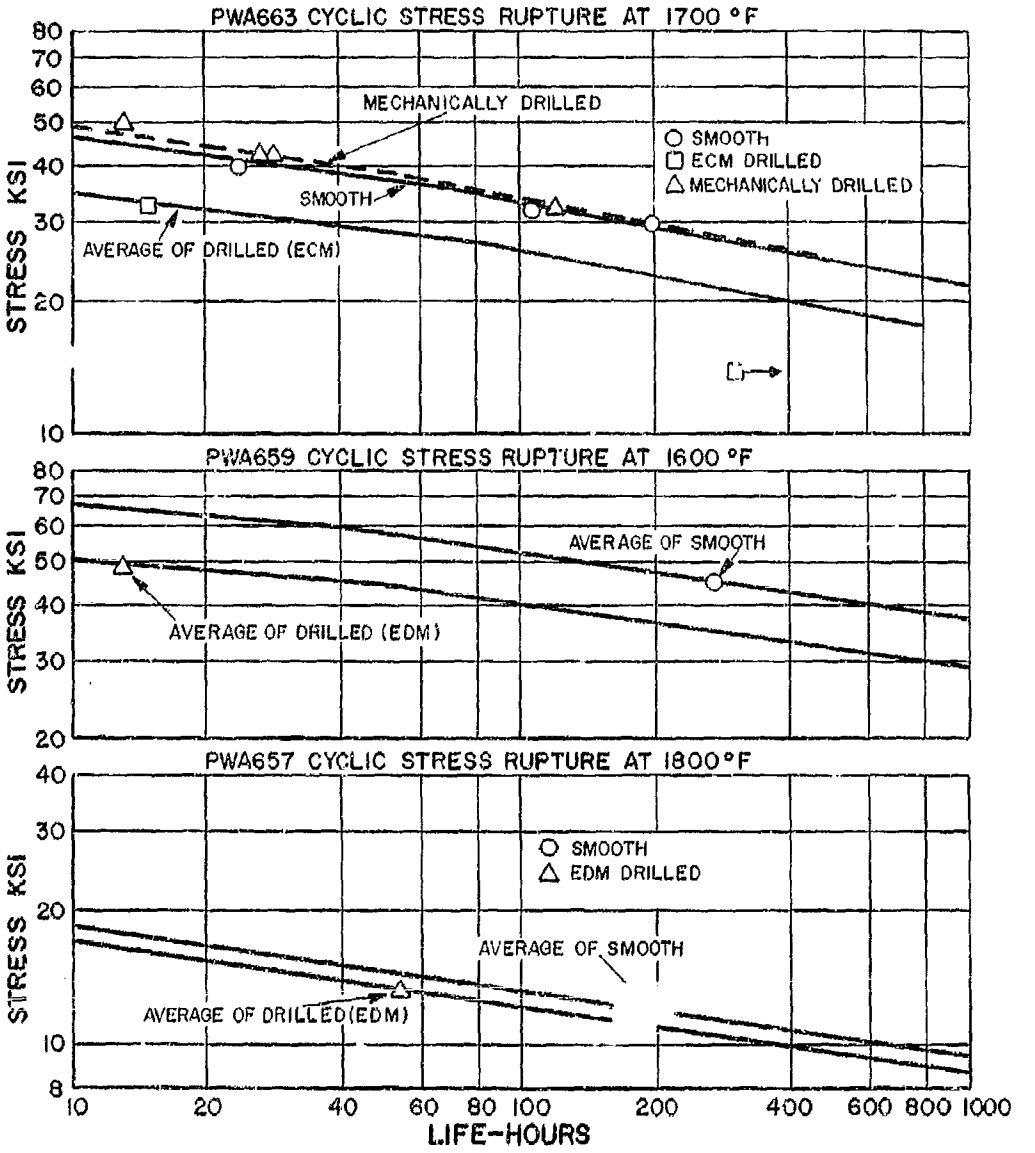
THIS DOCUMENT CONTAINS INFORMATION AFFECTING THE NATIONAL DEFENSE OF THE UNITED STATES WITHIN THE MEANING OF THE ESPIONAGE LAWS, TITLE 18, U.S.C., SECTIONS 793 AND 794. ITS TRANSMISSION OR THE REVELATION OF ITS CONTENTS IN ANY MANNER TO AN UNAUTHORIZED PERSON IS PROHIBITED BY LAW.



CYCLIC STRESS RUPTURE SPECIMEN

Figure 5-80

DOWNGRADED AT 3 YEAR INTERVALS
DECLASSIFIED AFTER 12 YEARS
DOD DIR 5200.10

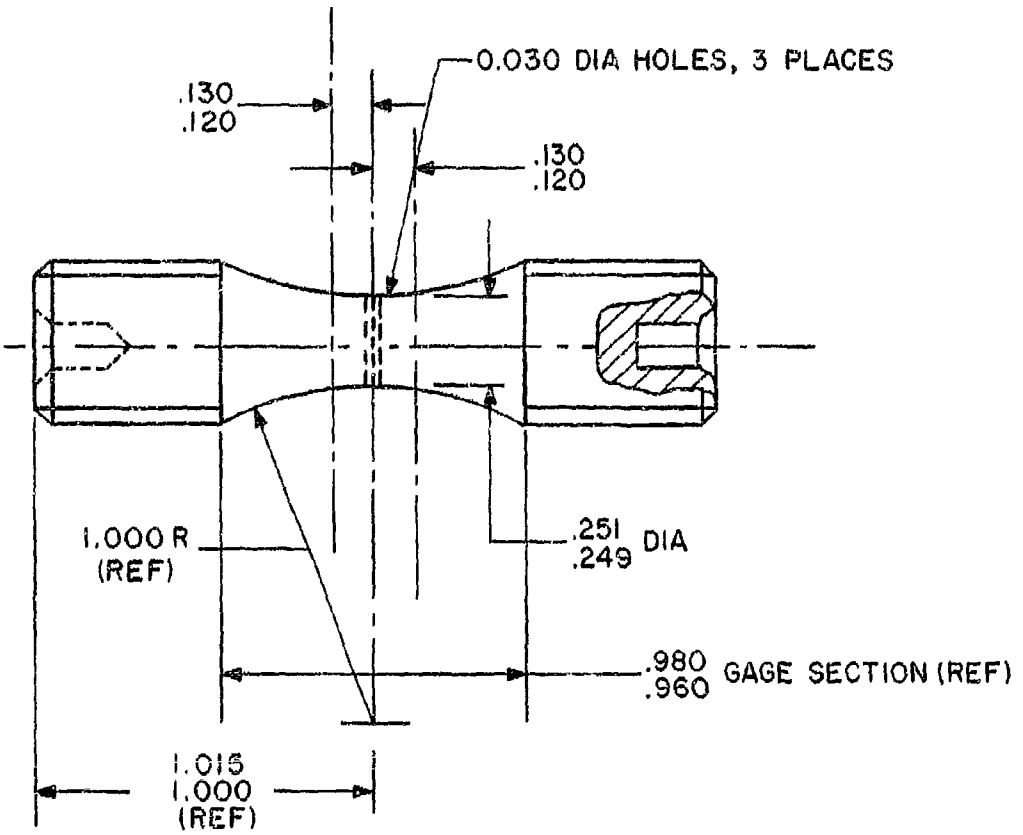


CYCLIC STRESS RUPTURE DATA ON PWA 663, PWA 659, AND PWA 657 ALLOYS

Figure 5-81

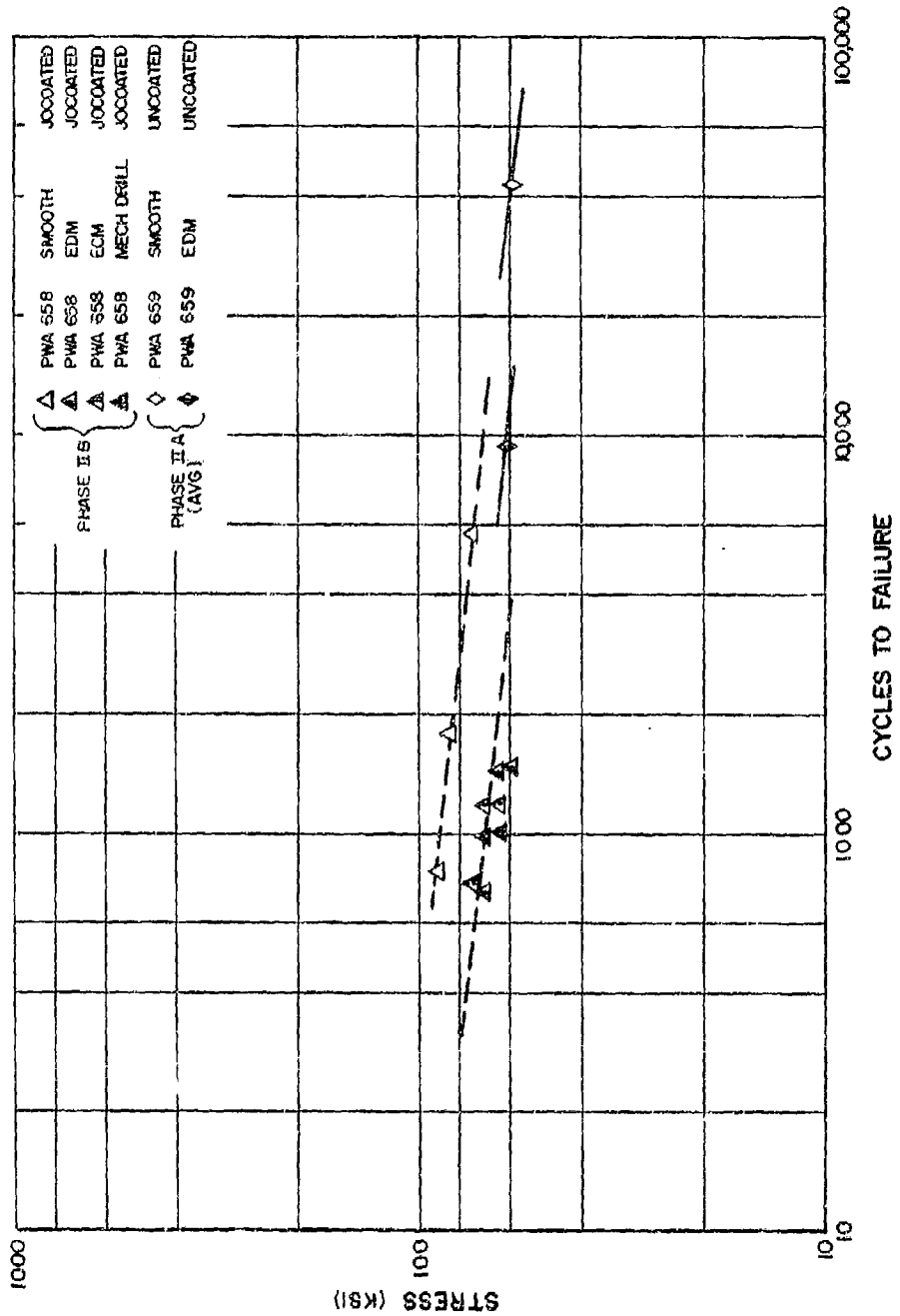
DOWNGRADED AT 3 YEAR INTERVALS
DECLASSIFIED AFTER 12 YEARS
DOD DIR 5200.10

THIS DOCUMENT CONTAINS INFORMATION AFFECTING THE NATIONAL DEFENSE OF THE UNITED STATES WITHIN THE MEANING OF THE ESPIONAGE LAWS, TITLE 18, U.S.C., SECTIONS 793 AND 794. THE TRANSMISSION OR THE REVELATION OF ITS CONTENTS IN ANY MANNER TO AN UNAUTHORIZED PERSON IS PROHIBITED BY LAW.



LOW CYCLE FATIGUE SPECIMEN

Figure 5-82



COMPARISON OF LCF STRENGTH OF SMOOTH AND NOTCHED CAST NICKEL BASE ALLOYS AT 1400°F

Figure 5-83

DOWNGRADED AT 3 YEAR INTERVALS
DECLASSIFIED AFTER 12 YEARS
DOD DIR 5200.10

THIS DOCUMENT CONTAINS INFORMATION AFFECTING THE NATIONAL DEFENSE OF THE UNITED STATES WITHIN THE MEANING OF THE ESPIONAGE LAWS, TITLE 18, U.S.C., SECTIONS 793 AND 794. THE TRANSMISSION OR THE REVELATION OF ITS CONTENTS IN ANY MANNER TO AN UNAUTHORIZED PERSON IS PROHIBITED BY LAW.

Material and Specimen	Stress (psi)	Cycles to Failure	
PWA 659 (Uncoated)[1]			
Smooth	59,000	54,803	
Smooth	59,000	22,069	
Notched	59,000	51,149	
Notched	61,000	9,510	EDM Holes
Notched	61,000	16,787	
Notched	61,000	7,916	
Notched	61,000	3,746	
PWA 658 (1 WA47 Coated)[2]			
Smooth	75,000	5,703	
Smooth	85,000	1,790	
Smooth	90,000	801	
Notched	60,000	1,485	ECM Holes
Notched	65,000	1,466	ECM Holes
Notched	70,000	727	ECM Holes
Notched	65,000	1,195	EDM Holes
Notched	70,000	1,197	EDM Holes
Notched	75,000	748	EDM Holes
Notched	65,000	1,012	Mech. Drilled Holes
Notched	70,000	992	Mech. Drilled Holes

NOTES:

(1) Fully Heatreated Condition (2000°F (4)AC + 1600°F (50) AC)

(2) Fully Heatreated Condition (2000°F (4)AC + 1600°F (12) AC)

LOW CYCLE FATIGUE TEST DATA

Figure 5-84

DOWNGRADED AT 3 YEAR INTERVALS
DECLASSIFIED AFTER 12 YEARS
DOD DIR 5200.10

THIS DOCUMENT CONTAINS INFORMATION AFFECTING THE NATIONAL DEFENSE OF THE UNITED STATES WITHIN THE MEANING OF THE ESPIONAGE LAWS, TITLE 18, U.S.C., SECTIONS 793 AND 794. THE TRANSMISSION OR THE REVELATION OF ITS CONTENTS IN ANY MANNER TO AN UNAUTHORIZED PERSON IS PROHIBITED BY LAW.

Creep Exposure			Room Temperature Tensile Properties				
Temp. °F	Stress ksi	Time To 1% Creep* Hours	UTS ksi	0.2% YS ksi	0.02% YS ksi	Elong. %	RA %
1400	30	1128.0	110.5	**	85.0	<1	<1
1500	22	215.0	116.0	106.0	64.25	<1	<1
1500	17	374.0	100.0	94.5	57.75	<1	<1
1700	10.5	1177.0	89.0	81.3	45.75	<1	<1
1800	7	970.0	85.5	**	54.6	<1	<1

* All tests discontinued after 1.0% strain
** Specimen Broke Before 0.2% Yield

CREEP AND ROOM TEMPERATURE TENSILE PROPERTIES FOR AS-CAST PWA 657 ALLOY

Figure 5-85

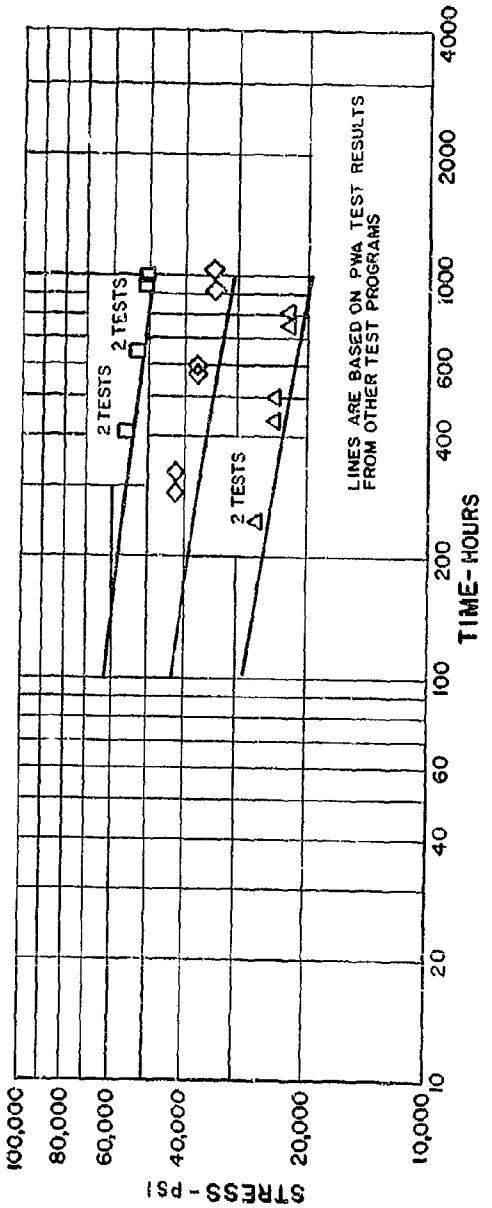
DOWN GRADED AT 3 YEAR INTERVALS
DECLASSIFIED AFTER 12 YEARS
DOD DIR 5200.10

Test Temp. °F	Stress ksi	Time To 1% Creep Hours	Life Hours	Elong. %	RA %
1500	56	411	976.0	5.9	14.6
1500	56	411	895.1	4.9	12.4
1500	53	645	Discontinued	-	-
1500	53	645	1522.4	6.7	16.8
1500	50	990	1979.2		
1500	50	946	Discontinued	-	-
1600	41	323	799.6	7.5	12.3
1600	41	288	795.7	9.1	14.6
1600	37	568	1370.7	7.8	10.9
1600	37	594	Discontinued	-	-
1600	34	1025	1955.5		
1600	34	915	Discontinued	-	-
1700	27	248	541.6	8.0	11.2
1700	27	240	582.1	11.8	18.9
1700	24	500	1024.5	8.5	12.8
1700	24	434	966.2	12.1	17.6
1700	22	751	Discontinued	-	-
1700	22	815	1488.0	8.4	17.4

CREEP RUPTURE PROPERTIES OF CAST PWA 658 NICKEL BASE ALLOY - PWA 47 COATED AND AGED AT 1600 °F

Figure 5-86

DOWNGRADED AT 3 YEAR INTERVALS
DECLASSIFIED AFTER 12 YEARS
DOD DIR 5200.10

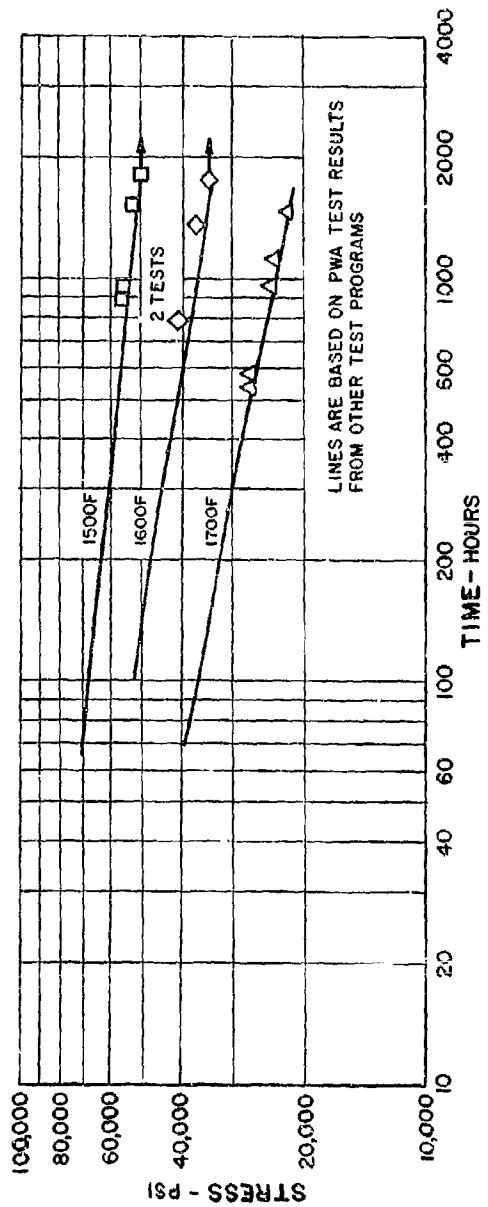


STRESS VERSUS TIME TO PRODUCE ONE PERCENT CREEP FOR PWA 658 JO COATED AND AGED AT 1600°F(12)

Figure 5-87

DOWNGRADED AT 3 YEAR INTERVALS
DECLASSIFIED AFTER 12 YEARS
DOD DIR 5200.10

THIS DOCUMENT CONTAINS INFORMATION AFFECTING THE NATIONAL DEFENSE OF THE UNITED STATES WITHIN THE MEANING OF THE ESPIONAGE LAWS, TITLE 18, U.S.C., SECTIONS 793 AND 794. THE TRANSMISSION OR THE REVELATION OF ITS CONTENTS IN ANY MANNER TO AN UNAUTHORIZED PERSON IS PROHIBITED BY LAW.



STRESS VERSUS RUPTURE LIFE FOR PWA 658 JO COATED AND AGED AT 1600°F(12)

Figure 5-88

DOWNGRADED AT 3 YEAR INTERVALS
DECLASSIFIED AFTER 12 YEARS
DOD DIR 5200.10

THIS DOCUMENT CONTAINS INFORMATION AFFECTING THE NATIONAL DEFENSE OF THE UNITED STATES WITHIN THE MEANING OF THE ESPIONAGE LAWS, TITLE 18, U.S.C., SECTIONS 793 AND 794. THE TRANSMISSION OR THE REVELATION OF ITS CONTENTS IN ANY MANNER TO AN UNAUTHORIZED PERSON IS PROHIBITED BY LAW.

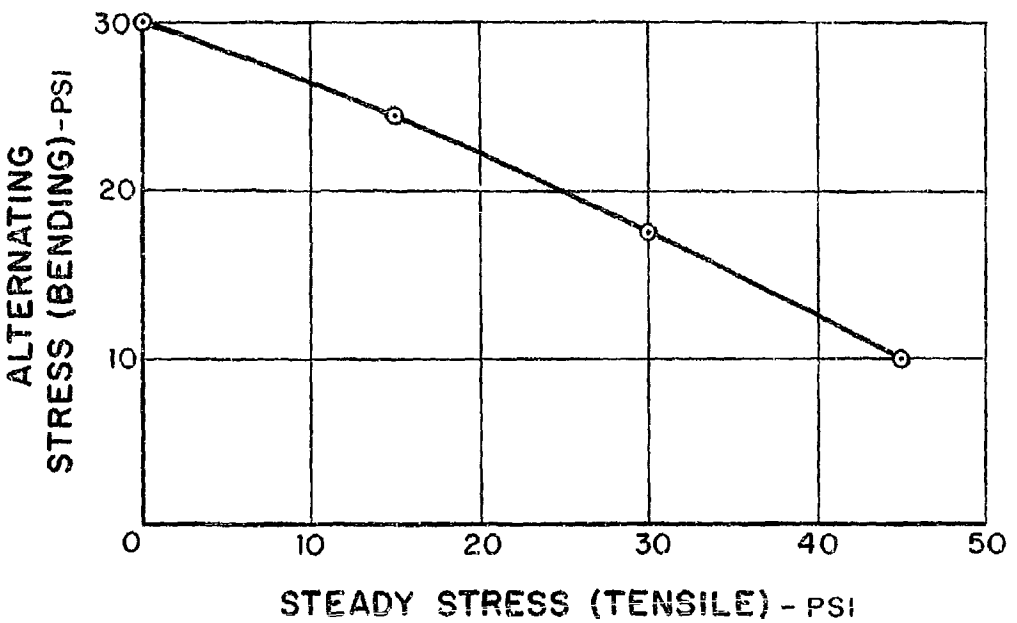
Alloy	Condition	Steady Stress Preload	Bending Fatigue Strength (10^7 Cycles)
PWA 663	Jo Coat+1650F(10)	45 ksi	±10 ksi
PWA 663	Jo Coat+1650F(10)	30 ksi	±17.5 ksi
PWA 663	Jo Coat+1650F(10)	15 ksi	±24.5 ksi
PWA 663	Jo Coat+1650F(10)	0 ksi	±30 ksi
PWA 659	Jo Coat+1600F(50)	30 ksi	±20 ksi

COMBINED STRESS-FATIGUE PROPERTIES OF PWA 659 AND PWA 663 ALLOYS AT 1700°F

Figure 5-89

DOWNGRADED AT 3 YEAR INTERVALS
DECLASSIFIED AFTER 12 YEARS
DOD DIR 5200.10

THIS DOCUMENT CONTAINS INFORMATION AFFECTING THE NATIONAL DEFENSE OF THE UNITED STATES WITHIN THE MEANING OF THE ESPIONAGE LAWS, TITLE 18, U.S.C., SECTIONS 793 AND 794. THE TRANSMISSION OR THE REVELATION OF ITS CONTENTS IN ANY MANNER TO AN UNAUTHORIZED PERSON IS PROHIBITED BY LAW.



MODIFIED GOODMAN DIAGRAM FOR SMOOTH PWA 663 ALLOY TESTED AT 1700°F

Figure 5-90

DOWNGRADED AT 3 YEAR INTERVALS
DECLASSIFIED AFTER 12 YEARS
DOD DIR 5200.10

THIS DOCUMENT CONTAINS INFORMATION AFFECTING THE NATIONAL DEFENSE OF THE UNITED STATES WITHIN THE MEANING OF THE ESPIONAGE LAWS, TITLE 18, U.S.C., SECTIONS 793 AND 794. ITS TRANSMISSION OR THE REVELATION OF ITS CONTENTS IN ANY MANNER TO AN UNAUTHORIZED PERSON IS PROHIBITED BY LAW.

Alloy	Total Strain (%)	Grain Size	Temp. (°F)	Cycles To Failure
PWA 663	1.49	1/8" - 1/4"	1300	7
	1.30			12
	0.75			107
	0.67			123
	0.60			1114
	0.56			848
	0.55			475
	0.54			3296
	0.51			3139
	2.30	1/32 - 1/16		1
	1.20			6
	0.92			25
	0.83			167
	0.74			272
	0.61			442
	0.60			1035
	0.58			1289
PWA 659	2.28	1/8" Nominal		1.5
	2.34			2.5
	1.54			6
	1.19			42
	1.06			110
	0.90			340
	0.83			1593
	0.51			1256
PWA 657	0.32	1/8" Nominal	1300	9
	0.36			11
	0.20			2735
PWA 657	0.19	1/8" Nominal	1300	3590
PWA 663	2.06	1/8" - 1/4"	1700	8
	1.67			17
	1.40			28
	0.94			63
	0.93			108
	0.84			121
	0.55			2334
	0.54			629
	0.54			1008

STRAIN CYCLE DATA ON PWA 657, PWA 659 AND PWA 663 MATERIALS

Figure 5-91

DOWNGRADED AT 3 YEAR INTERVALS
DECLASSIFIED AFTER 12 YEARS
DOD DIR 5.200.10

THIS DOCUMENT CONTAINS INFORMATION AFFECTING THE NATIONAL DEFENSE OF THE UNITED STATES WITHIN THE MEANING OF THE ESPIONAGE LAWS, TITLE 18, U.S.C., SECTIONS 793 AND 794. ITS TRANSMISSION OR THE REVELATION OF ITS CONTENTS IN ANY MANNER TO AN UNAUTHORIZED PERSON IS PROHIBITED BY LAW.

Alloy	Total Strain (%)	Grain Size	Temp. (°F)	Cycles To Failure
	2.06	1/32 - 1/16		6
	1.68			20
	0.80			110
	0.67			1880
	0.65			281
	0.61			442
	0.56			807
	0.55			940
PWA 659	2.75	1/8" Nominal		6
	1.98			13
	1.20			75
	0.84			282
	0.66			592
	0.55			1205
PWA 663	2.76	1/8" - 1/4"	2000	12
	2.50			24
	1.91			33
	1.29			166
	0.66			550
	0.62			533
	0.62			360
	0.49			872
	2.90	1/32" - 1/16"		14
	2.11			29
	1.48			81
	1.42			101
	0.79			400
	0.61			409
	0.60			203
	0.46			1252

STRAIN CYCLE DATA ON PWA 657, PWA 659 AND PWA 663 MATERIALS

Figure 5-91 (Cont.)

DOWNGRADED AT 3 YR INTERVALS
DECLASSIFIED AFTER 12 YEARS
DOD DIR 5200.10

ITEM 6

AUGMENTORS

ITEM 6 - AUGMENTORS

OBJECTIVE

The contractor has conducted experimental testing of the augmentor components directed toward verification of augmentor performance and durability. The goal of this program was to develop an augmentation system having a high combustion efficiency at SST cruise and acceleration conditions.

A. AERODYNAMIC FLAMEHOLDER TESTS IN SMALL-SCALE DUCT HEATER RIGS

1. INTRODUCTION AND SUMMARY

Testing was conducted in a small-scale duct heater rig during Phase IIB to continue evaluation of the fan duct burner components. Since the original high performance goals have been demonstrated, emphasis during this phase has been placed on determining the optimum combination of various variables, testing alternative hardware arrangements to achieve better durability, and providing support to the full-scale rig program. A total of 635 hours of testing were conducted.

The best performance obtained to date was obtained during Phase IIA and is shown in Figure 6-1. The data shown was obtained at simulated SST flight conditions using an external-fuel cross-jet flameholder system. The performance shown meets the performance goals for the STF219 engine. The combustion stability of the system is shown in Figure 6-2 and the cold pressure losses are shown in Figure 6-3. Although the rig losses are relatively high, the rig and flameholder losses (excluding diffuser losses) were only 2 percent with the maximum bleed flow (4 percent) at Mach 0.15 and were 1 percent without bleed flow.

The test program during Phase IIB was conducted in a 12-inch by 16-inch simulated altitude rig and in a 6.5-inch by 8-inch sea-level rig. Combustion testing employed the burner system shown in Figures 6-4 and 6-5.

Testing during Phase IIB demonstrated the ignition capabilities of the system and provided data for evaluating various primary fuel system

DOWNGRADED AT 3 YEAR INTERVALS
DECLASSIFIED AFTER 12 YEARS
DOD DIR 5200.10

THIS DOCUMENT CONTAINS INFORMATION AFFECTING THE NATIONAL DEFENSE OF THE UNITED STATES WITHIN THE MEANING OF THE ESPIONAGE LAWS, TITLE 18 U. S. C. SECTIONS 793 AND 794. ITS TRANSMISSION OR THE REVELATION OF ITS CONTENTS IN ANY MANNER TO AN UNAUTHORIZED PERSON IS PROHIBITED BY LAW.

parameters, secondary fuel system spray patterns, the effects of combustion chamber length bleed flow and flameholder trailing edge geometry on efficiency, and a porous cooling liner. Ignition was demonstrated at fuel-to-air ratios well below 0.008, which is specified in the engine specification, using a 20-joule spark ignition system. A 4-joule system also gave good results. Evaluation of the primary fuel system indicated that best results are achieved using a sprayring located upstream of the flameholder. This places the sprayring in the cool fan air and avoids fuel clogging and durability problems. Several methods for duplexing the primary fuel system appear to be satisfactory. The performance of the secondary fuel system was found to be quite sensitive to the spray pattern. In general, best results were obtained by using many small sources located to spray fuel into areas not covered by the primary system. Evaluation of the effects of chamber length and bleed flow on efficiency revealed that, within the range studied, increasing the chamber length by one inch increases the combustion efficiency by 0.85 percent and that increasing the bleed flow by one percent increases the efficiency by 7 percent.

2. DETAILED PROGRAM DESCRIPTION

a. Ignition Demonstrations

Ignition tests were conducted with a 20-joule spark source, a 4-joule spark source, and a 24-volt glow plug. The test results for the 20-joule spark system are shown in Table 6-1 and Figure 6-6. Figure 6-6 also shows the results for the 4-joule system. As shown, the 20-joule system provided ignition at fuel-to-air ratios well below 0.008, the ratio presently planned for duct heater lighting. The 4-joule system required approximately double the ratio required for the 20-joule system. Reliable ignition could not be obtained with the glow plug system.

b. Primary Fuel System

The primary fuel system was studied to determine the feasibility of using sprayrings upstream of the flameholders, the feasibility of using a duplex fuel supply system, and the effect of locating the sprayring off of the flameholder centerline.

DOWNGRADED AT 3 YEAR INTERVALS
DECLASSIFIED AFTER 12 YEARS
DOD DIR 5200.10

TABLE 6-1

Ignition Characteristics of 20-Joule Spark Ignition System

Flight Mach Number	Altitude (feet)	Inlet Temperature (°F)	Minimum Fuel - Air Ratio for Ignition
0	0	280	0.003
0.9	36,089	218	0.006
2.0	55,000	455	0.002
3.0	65,000	812	0.001

Previous testing was conducted with the sprayring downstream of the flameholder and injecting fuel upstream. However, temperature measurements have shown that the temperature at the trailing edge of the flameholder is approximately 3000°F. These temperatures could cause durability problems and might also cause coking and cracking of the fuel. Consequently, it is desirable to move the sprayring upstream of the flameholder where the maximum temperature is only 700°F, providing the efficiency penalty is not excessive. Tests were conducted, therefore, with the sprayring moved upstream, and the results are shown in Figure 6-7. The efficiency level is unchanged and is somewhat less sensitive to mixture than with the sprayring downstream of the flameholder. The optimum efficiency is obtained with a richer mixture but with geometry changes, a shift of the optimum point to a leaner mixture can be made. It therefore appears advantageous to locate the spray ring upstream of the flameholder in the SST engine.

Because of the large range of airflows and fuel-to-air ratios required for the SST engine, it will be necessary to use at least a three-stage fuel system if present pump technology is to be used. This will require the primary system to have two stages. Testing was conducted to determine if any performance penalty would result from the use of a

DOWNGRADED AT 3 YEAR INTERVALS
DECLASSIFIED AFTER 12 YEARS
DOD DIR 5200.10

THIS DOCUMENT CONTAINS INFORMATION AFFECTING THE NATIONAL DEFENSE OF THE UNITED STATES WITHIN THE MEANING OF THE ESPIONAGE LAWS, TITLE 18, U.S.C., SECTIONS 793 AND 794. THE TRANSMISSION OR THE REVELATION OF ITS CONTENTS IN ANY MANNER TO AN UNAUTHORIZED PERSON IS PROHIBITED BY LAW.

duplex primary system, and the results indicated that no penalty was incurred. It is expected that a two-stage secondary system would also function without a performance penalty.

A series of tests was conducted to determine the effect of off-setting the primary fuel system from the jet flameholder. The results of these tests are shown in Figure 6-8. It was found that no performance penalty results from the degree of misalignment anticipated as a consequence of differential thermal expansion. In fact, it appears that an actual improvement results from slightly off-setting the sprayring from the flameholder centerline, although misalignment by more than about 3/8 inch causes instable combustion and significantly narrows the combustion limits.

c. Secondary Fuel System - Flow Patterns

During acceleration, efficient combustion is required with high fuel-to-air ratios. Good performance has been obtained for fuel-to-air ratios up to 0.06, but the secondary system should provide operation with ratios up to 0.08, and consequently a number of secondary spray bar patterns were tested (see Figure 6-9). For all these tests, the gap between the splash plate and the fuel nozzle was 1/2 inch in order to eliminate the effect of fuel penetration. The primary fuel-to-air ratio was set at 0.019 on the basis of previous testing which has indicated that the primary mixture should be slightly leaner than that which provides optimum primary efficiency if the over-all efficiency is to be optimum. The actual mixture used is dependent upon the location and fuel distribution pattern of the secondary fuel system.

Placing the secondary system in line with the primary system resulted in performance and range of operation similar to that obtained with only the primary system operating, as expected.

The results of injecting the secondary fuel into areas not covered by the primary system are shown in Figure 6-10. As shown, subtle changes in the spray pattern can cause very large changes in the performance. Figure 6-11 shows the performance obtained with the addition of secondary fuel in the region of primary fuel injection as well as providing uniform fuel coverage over the entire crossjet flameholder. As shown, the performance is improved by this method, although care must be taken not to add too much fuel to the primary region.

DOWNGRADED AT 3 YEAR INTERVALS
DECLASSIFIED AFTER 12 YEARS
DOD DIR 5200.10

The effect of mixing length is shown in Figure 6-12. For all lengths tested, the performance was about the same, but the operating range was greater for the test with shorter mixing lengths.

Fuel atomization is a function of the width of the splash plate gap used, and, therefore, three gap widths were tested. The results are shown in Figure 6-13. Increasing the gap width from 1/4 inch to 3/4 inch caused a slight performance improvement. However, with a 3/4-inch width, some of the fuel missed the splash plate, resulting in a greater spread of fuel than desired and one which might cause engine burn-out. Consequently, a one-half-inch gap width is recommended.

d. Effect of Combustion Chamber Length

A series of tests was performed to determine the effect of combustion chamber length on combustion performance. All tests were performed using primary fuel injection only. The results of these tests are shown in Figure 6-14. For the test conditions used, it was found that the efficiency decreased by 0.85 percentage point for each inch of combustion chamber length reduction. However, this relationship is dependent on the over-all efficiency level, which for these tests was intentionally lowered to make the effect more pronounced. The relationship is also dependent on the inlet temperature and the duct Mach number.

e. Effect of Bleed Flow Rate

The bleed flow required for the jet flameholder imposes a performance penalty on the turbofan engine cycle, and, therefore, it is desirable to reduce the bleed flow as much as possible without incurring an excessive flameholder efficiency loss. Two approaches were tested. For the first, the pressure ratio was reduced, and, for the second, the hole area was reduced without changing the pressure ratio. As shown in Figures 6-15 and 6-16, a one-percent reduction in bleed flow caused a maximum efficiency loss of approximately 7 percent.

Alternate approaches which combine the use of non-aerodynamic and aerodynamic flameholders were attempted. Generally using a combination of aerodynamic and non-aerodynamic flameholders results in higher cold pressure losses but lower bleed flow. A single-bar jet flameholder perpendicular to a conventional vee-gutter was tested (see Figure 6-17). The results were encouraging. As shown in Figure 6-18,

DOWNGRADED AT 3 YEAR INTERVALS
DECLASSIFIED AFTER 12 YEARS
DOD DIR 5200.10

THIS DOCUMENT CONTAINS INFORMATION AFFECTING THE NATIONAL DEFENSE OF THE UNITED STATES WITHIN THE MEANING OF THE ESPIONAGE LAWS, TITLE 18, U.S.C., SECTIONS 793 AND 794. ITS TRANSMISSION OR THE REVELATION OF ITS CONTENTS IN ANY MANNER TO AN UNAUTHORIZED PERSON IS PROHIBITED BY LAW.

the performance was 7 percent better than the base line with operation with the same bleed flow. However, the system had 1/3 higher cold pressure losses.

f. Testing of Porous Cooling Liner

A porous cooling liner was constructed from 0, 120, and 230 SCFM N-155 stock and instrumented for testing. The liner construction is shown in Figure 6-19, and the fuel system and jet flameholder used for testing the liner are shown in Figure 6-20. Some testing was conducted but sufficient data was not obtained to permit a cooling correlation to be made.

g. Effect of Flameholder Trailing Edge Geometry

Water table tests were conducted to determine the flow around the jet flameholder. The tests were conducted in the water table shown on Figure 6-21, and the results are shown in Figure 6-22. These results indicated a high-velocity reverse flow directly behind the flameholder, and, therefore, a series of tests was conducted to determine the effect of this flow on the flameholder performance. The tests were conducted with flameholders with scooped trailing edges to favor the high velocity flow and with flameholders with extended trailing edges to reduce the reverse flow. The results obtained are shown in Figure 6-23 together with those for a conventional flameholder. As shown, changing the trailing edge had little effect on the combustion limits and efficiency.

B. RAM INDUCTION BURNER TESTS IN SMALL-SCALE DUCT HEATER RIGS

1. INTRODUCTION

As an alternative to the jet flameholder system, a low pressure loss can-type burner which used ram induction for air admission was studied. During Phase IIA, several models of the burner were built and tested. The last of the series (Model E) provided excellent performance at simu-

DOWNGRADED AT 3 YEAR INTERVALS
DECLASSIFIED AFTER 12 YEARS
DOD DIR 5200.10

THIS DOCUMENT CONTAINS INFORMATION AFFECTING THE NATIONAL DEFENSE OF THE UNITED STATES WITHIN THE MEANING OF THE ESPIONAGE LAWS, TITLE 18, U.S.C., SECTIONS 793 AND 794. ITS TRANSMISSION OR THE REVELATION OF ITS CONTENTS IN ANY MANNER TO AN UNAUTHORIZED PERSON IS PROHIBITED BY LAW.

iated sea-level take-off and cruise conditions, but the blow-out characteristics at the low pressures and temperatures associated with transonic flight were poor. During Phase IIB, efforts were made to improve the blow-out characteristics.

2. PHASE IIB PROGRAM SUMMARY

Initially, efforts to improve the blow-out characteristics of the ram-induction burner were concentrated on the Model E burner (see Figure 6-24). Several modifications were made and a substantial improvement in the rich operating range at Mach 0.12 was achieved as shown in Figure 6-25. However, the operating capability deteriorated rapidly with increasing Mach number as shown in Figure 6-26. In addition, the modifications caused a pronounced reduction in combustion efficiency at high pressure conditions. Whereas the original Model E burner demonstrated combustion efficiencies between 95 and 99 percent with high inlet pressures, the modified Model E burner demonstrated an efficiency of only 85 percent at these conditions.

Consequently, analytical studies of the various burners developed during the program were conducted. These studies indicated that the Model D burner would have the best blow-out characteristics of the burners developed because of its larger radial height, its lower flow velocity, and its provision for gradual air admission along the length of the burner. The use of gradual air admission in the Model D burner eliminates the larger step changes in fuel-to-air ratio produced in the Model E burner. The Model D burner is shown in Figure 6-27.

Testing confirmed that the Model D burner did have considerably better blow-out characteristics than the Model E burner (see Figure 6-28). To extend the blow-out limits, a secondary zone of fuel injection was added by installing splash plate injectors in front of the second row of primary scoops. The improvement achieved is shown in Figure 6-28. With three zones, combustion was achieved with fuel-to-air ratios of 0.06, and it is believed that combustion with higher ratios can be achieved through optimization of the fuel-to-air ratios used in zones 1 and 2.

The Model D burner was superseded by the Model E burner in order to achieve a higher cruise efficiency, and, even at the low pressures associated with transonic flight, the peak efficiency of the Model E burner is higher than that of the Model D burner. Consequently, the airflow through the Model E burner was increased from 4.3 percent to 8 percent by replacing the original swirlers with toroidal swirlers. The result was an efficiency improvement of about 12 percent as shown in Figure

6-29. In addition, the blow-out limits were increased both for zone 1 and for combined zone 1 and zone 2 operation. The improvement was the result of the better mixing provided by the toroidal-type swirler, permitting the use of a higher fuel-to-air ratio in zone 1.

Two additional modifications were considered. The first of these would be the replacement of the zone 2 spray bar arrangement with a 1-inch diameter, 3-inch long tube attached to a conventional swirler and extending downstream into the burner. This arrangement injects fuel into the center of the burner and provides some vaporization of the fuel as it passes down the tube. The second modification would completely revise the secondary scoop section to incorporate external scoops with zone 3 spray bars. This arrangement would raise the fuel-to-air ratio at which the peak efficiency occurs.

C. FULL SCALE DUCT HEATER RIG

1. INTRODUCTION

The small-scale, two-dimensional rig program must be supplemented by full-scale, three-dimensional testing in a realistic test environment. This testing could be conducted on an actual engine, but it may be more easily and economically conducted on a full-scale test rig. The use of a rig provides accurate performance data earlier in the program and benefits the design systems studies and cycle studies.

2. TEST RESULTS

During the report period, a fiery cross jet flameholder was tested (see Figure 6-30). Fuel was injected upstream from primary sprayrings located two inches downstream of the flameholder. The injection hole patterns for both the jet flameholder air and the primary fuel were based on two-dimensional test results. The pattern used provided holes grouped in patches to ensure good stability with low fuel-to-air ratios. The groups of holes in the primary sprayrings were aligned with the groups in the flameholder. The flameholder tested had eight radial members circumferentially separated by about 22 inches.

A total of 102 hours of testing was conducted. In general, the results indicated steady progress is being made toward the duct heater goals. At a simulated cruise condition, an efficiency of 91 percent has been demonstrated.

Performance

Performance testing was conducted with primary fuel alone and with both primary and secondary fuel. Pressure losses were measured and the combustion stability over a range of fuel-to-air ratios was observed. The effect of bleed flow rate and bleed temperature were also determined.

(1) Testing with Primary Fuel Only

The key to the development of a high performance duct heater system utilizing a jet flameholder is stable, efficient operation of the jet flameholder with only primary fuel injection. Consequently, initial testing was conducted without secondary fuel injection.

Promising results were obtained with an inlet temperature of 600°F, an inlet total pressure of 36 in HgA, 5.5 percent bleed flow, and a jet flameholder pressure ratio of 2.0. At these conditions, the efficiency was 91 percent. The complete results are shown in Figure 6-31. As shown, the efficiency obtained with an inlet temperature of 600°F is comparable to that obtained during the previous test program with annular ring jet flame-holders, indicating that the performance at altitude cruise conditions is satisfactory.

(2) Testing with Secondary Fuel Injection

Small-scale rig testing has indicated that small changes to the secondary fuel injection system can cause large changes in performance. However, all testing during this period with secondary fuel injection used a basic secondary fuel pattern produced by four sprayrings located approximately 8 inches upstream of the jet flameholder. Fuel injection was normal to the stream flow and no splash plates were used so that the hole pattern could be changed more easily.

The efficiency levels obtained are shown in Figure 6-32. Although these results indicate that the efficiency attained with primary fuel injection can also be attained with primary and secondary fuel injection, a satisfactory secondary injection pattern has not yet been tested in the full-scale rig. It should be noted, however, that the results of small-scale testing could not be fully utilized during this report period because of the lead time required to procure full-scale rig hardware.

The test results indicate that the primary fuel-to-air ratio should be kept relatively lean because the secondary fuel enriches the primary zone, and, as secondary fuel is added, the efficiency decreases until the secondary flow reaches a flammable level. Without secondary fuel injection, the primary fuel-to-air ratio should be kept at a maximum.

(3) Pressure Loss

The cold pressure losses of the rig were measured to determine if additional losses were introduced by the modifications made to the sprayring and the jet flameholder to increase durability. The results (see Figure 6-33) indicate that no significant changes resulted.

(4) Stability

The combustion stability was monitored throughout the test program. No instability was observed for any inlet temperature or pressure with fuel-to-air ratios between 0.007 and 0.05.

(5) Effect of Bleed Flow

The effect of bleed flow on the duct heater efficiency was evaluated by varying the bleed flow from 1.0 to 9 percent of the duct flow. The flow was varied by varying the injection area while maintaining a constant pressure ratio of 2.0. The results, shown in Figure 6-34, indicate that increasing the bleed flow improves the performance, but not to the extent found during small-scale rig testing.

(6) Effect of Bleed Flow Temperature

Tests were conducted with bleed flow at temperatures of 600°F and 1200°F to determine if the temperature affected the performance. The performance was unaffected by the bleed temperature. These results are in agreement with previous results.

(7) Comparison With Small-Scale Rig Results

Although exact comparisons cannot be made between the results of small scale and full-scale rig testing because of differing test conditions, it is apparent from Figure 6-35 that a reasonable correlation has been obtained. Considering that the program is still in the early stages, considerable promise for improvement to the full scale rig or the tests of small-scale testing is indicated.

3. DESCRIPTION OF RIG AND TEST STAND

a. Rig

The full-scale duct heater rig was designed to simulate an annular duct heater combustion system typical of that used in a turbofan engine for the supersonic transport. It is approximately the same size and has the same geometry and airflow capacity as the actual duct heater combustion system, and all ducting upstream of the exit nozzle is air cooled so that actual engine conditions are simulated. Water cooling is used downstream of the exit nozzle to facilitate testing at the high exit temperature (3100°F) required. The rig is 18 feet long and has a maximum diameter of 70 inches. The rig is shown in Figure 6-36.

Although provisions were made for testing with inlet diffusers which accurately simulate actual engine diffusers, initial testing was conducted with a long diffuser with a small wall angle to provide as uniform a flow profile as possible. Uniform flow is required during early testing so that combustor problems can be isolated and corrected. A preliminary design of a full-scale offset diffuser has been made on the basis of the most recent information. This diffuser was not built and tested, however, because the fabrication lead time exceeded the length of Phase IIB. The rig has a fixed mount point at the upstream end of the diffuser, and the support struts also feed and drain the water-cooled sections of the inner body. Tubes through which the inner-body instrumentation lines are led are also located in this region. At the downstream end of the diffuser are bosses for inlet temperature and pressure rakes (see Figure 6-37). The primary and secondary fuel systems are housed in a short section which is accessible so that the fuel system components being tested can be changed readily. Extra bosses in this section permit the installation of up to 4 secondary sprayrings and up to 16 jet flameholder elements. Hydrogen-oxygen ignition torches are also provided in this area. The cooling liner is extended downstream with fuel baffles to a point upstream of the secondary fuel sprayrings to prevent combustion adjacent to the inner and outer duct walls and to pick up fuel-free cooling air. The fuel injection system is shown in Figures 6-38 and 6-39.

Combustion occurs in an annular combustion chamber which has a total length of 75 inches from the jet flameholder to the exit nozzle throat. Porous cooling liners shield both the inner and outer walls and provide transpiration cooling. Extensive instrumentation is used to measure and record the cooling air flow rate and the temperatures and pressures of the rig structure.

Fixed-area exit nozzles are used to provide simulation of various settings of a variable-area exit nozzle. Typical acceleration and cruise conditions are simulated with nozzles that have areas of 20.4 and

6.36 square feet, respectively. As in the actual powerplant, all convergence occurs in the outer duct wall with the variation in area resulting from varying the convergence angle. A diverging section extends downstream from the nozzle throat to the rear support section. The nozzles used for performance testing are water cooled over the converging section, but alternate air-cooled nozzles are also available. The diverging section is water cooled in all cases. Sixteen bosses for the installation of water-cooled exit total pressure rakes are installed at the exit nozzle throat. The design of a variable-area exit nozzle has been completed.

The rig connects to the test stand exhaust ducting through a water-cooled rear support with a slip joint to permit thermal expansion.

Extensive instrumentation is installed to provide a maximum amount of information on each run including combustion performance (exit temperature and efficiency), pressure loss, cooling, and structural durability.

b. Test Stand

The rig was tested in X-207 stand at the Pratt & Whitney Aircraft Andrew Willgoos Laboratory. This stand has the capacity for high air flow at a range of pressure levels which provide simulation for most SST flight conditions.

All testing performed during the early portions of Phase IIB were conducted at ambient inlet conditions (a temperature of about 130°F) which are more stringent than the SST duct heater inlet temperature requirements. Later, however, the stand was connected to the heat exchanger units available at the Willgoos Laboratory. These exchangers are capable of heating the test stand air to 700°F without vitiation. Final testing, therefore, was conducted with the inlet air heated to temperatures up to 600°F.

A separate high-pressure air line provides secondary air to the jet flameholders at pressure ratios between 1.5 and 3.0 in sufficient quantities to simulate compressor bleed at 600°F or turbine bleed at temperatures from 1200 to 1400°F.

Three fuel systems provide fuel for the duct heater primary and secondary systems and for the burner which heats the jet flameholder air. The system supplying the primary duct heater burner provides flow rates from 2,000 to 67,000 pph, while the system for the secondary burner provides flow rates from 2,900 to 70,000 pph. The flameholder air heater is supplied with fuel at rates up to 900 pph.

4. PROCEDURE

For a typical performance run, the desired operating conditions are established, the duct heater is ignited, and the desired jet flameholder air flow and fuel flow are set. The rig is then permitted to run for a sufficient time for conditions to stabilize, after which the data is taken. The next operating point is established by changing the fuel flow, thereby changing the fuel-to-air ratio. Usually data at 6 to 8 performance points is obtained during a run.

A large quantity of data is taken at each point so that the performance and cooling can be accurately determined. Mainstream and jet flameholder air flow are calculated from measured pressure, pressure drop, and temperature across standard orifices. Fuel flows for the three systems are measured by turbine meters and read on electronic counters. Pressures are measured with standard manometers. Included are exit total pressure, diffuser total pressure immediately upstream of the flameholder section, several combustion chamber pressures, and pressures in the coolant air passages. Four pressure rakes, each with eleven equally spaced pickups, are used at the rig exit to provide data for calculating the exit temperature. Twelve pickups are used at the diffuser exit to provide data for calculating pressure losses.

Temperatures are measured with chromel-alumel thermocouples. Temperatures are measured at the duct inlet and on the inner and outer liners and walls. The temperatures of the fuel and of the fuel-air mixture supplied to the flameholder are also measured.

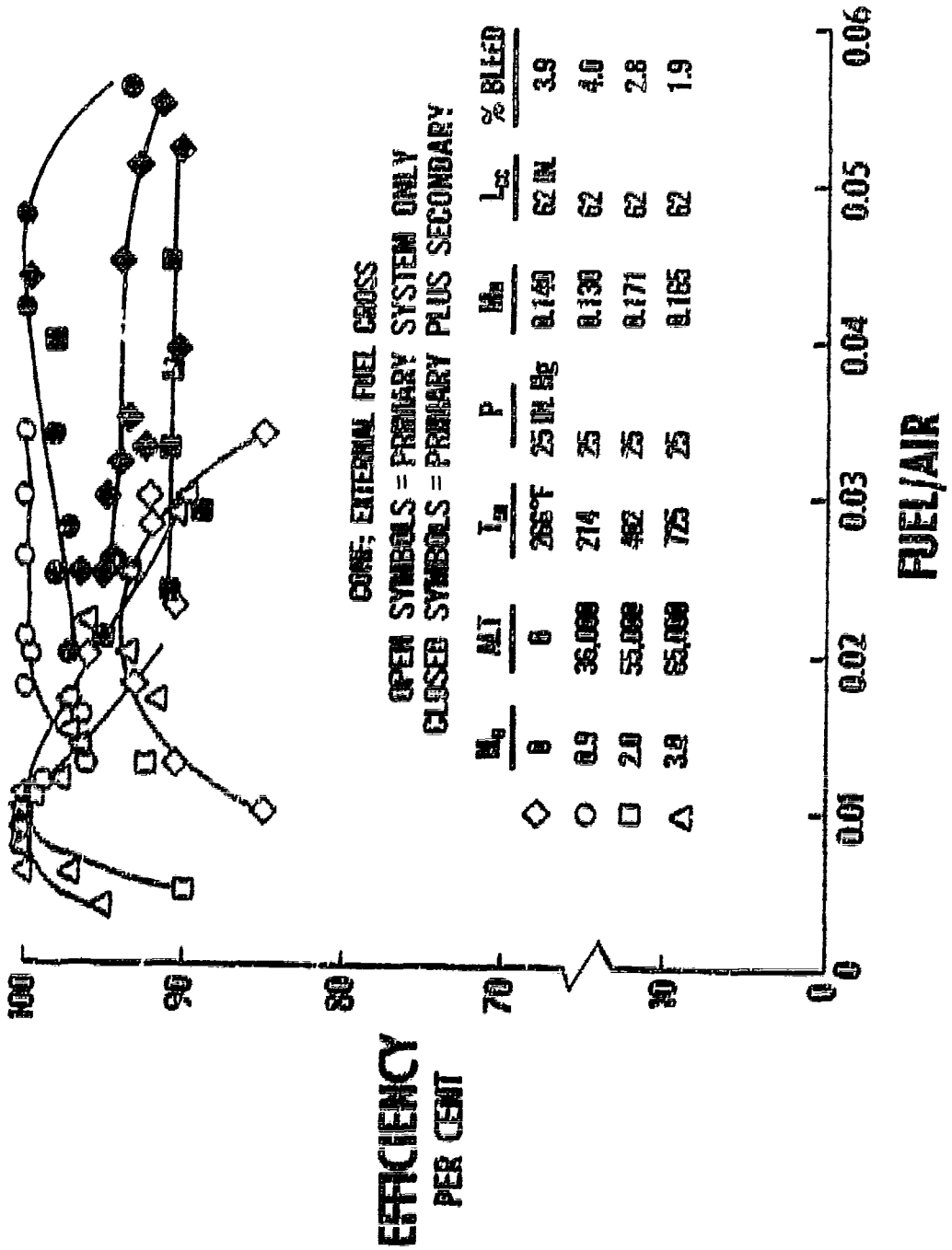
Since a choked, fixed-area, exit nozzle is used, the inlet Mach number will decrease as the exit temperature is increased. For preliminary testing, however, the inability to maintain a specific Mach number is not a serious disadvantage, and a variable-area nozzle has been designed for use during future testing.

5. CONCLUSIONS AND RECOMMENDATIONS

Testing during Phase IIB has confirmed the necessity of full-scale rig testing to verify small-scale rig results before engine testing is begun. The program to date has verified the feasibility of duct heater augmentation.

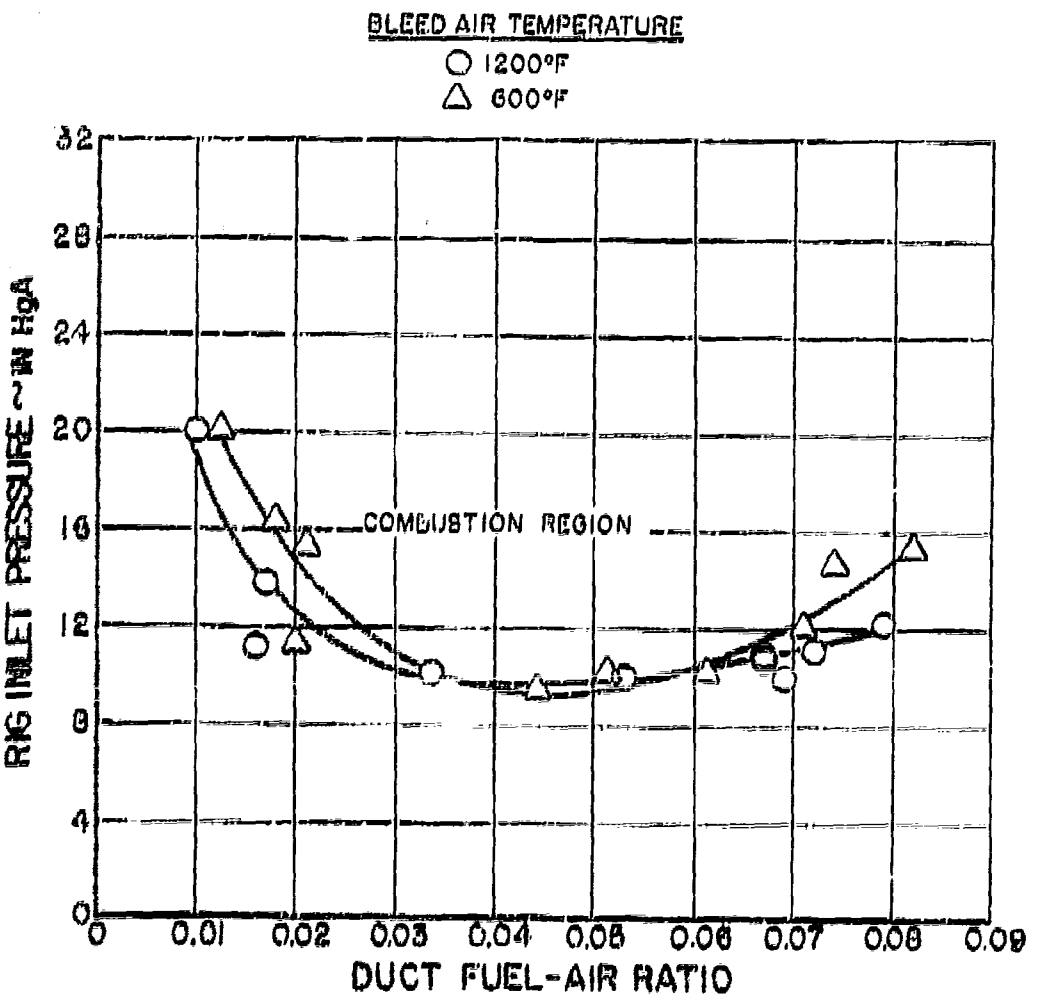
Considerable additional full-scale rig testing is recommended. Several promising configurations tested in the small-scale rig which provided

either better performance or greater simplicity should be tested, and development testing is required to determine a fully compatible primary and secondary fuel system. In addition, the effects of an off-set diffuser need to be determined and an air-cooled, variable-area exit nozzle should be tested. It is recommended further that the full-scale rig be updated to the latest engine design and used to supplement the testing of a duct heater augmentor on a prototype engine.



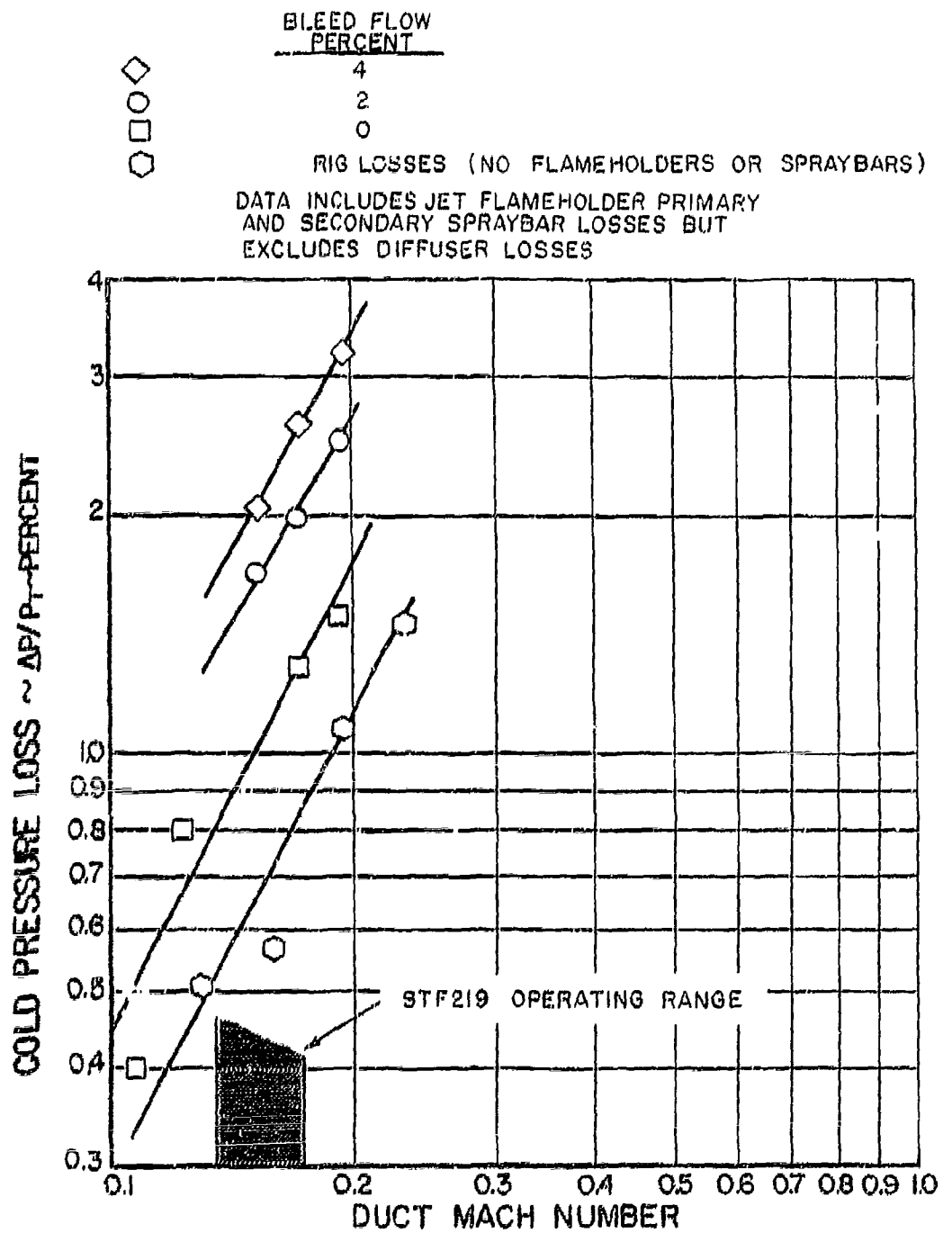
EFFICIENCY OF SMALL SCALE DUCT HEATER RIG

Figure (-)



STABILITY LIMITS OF CROSS JET FLAMEHOLDER

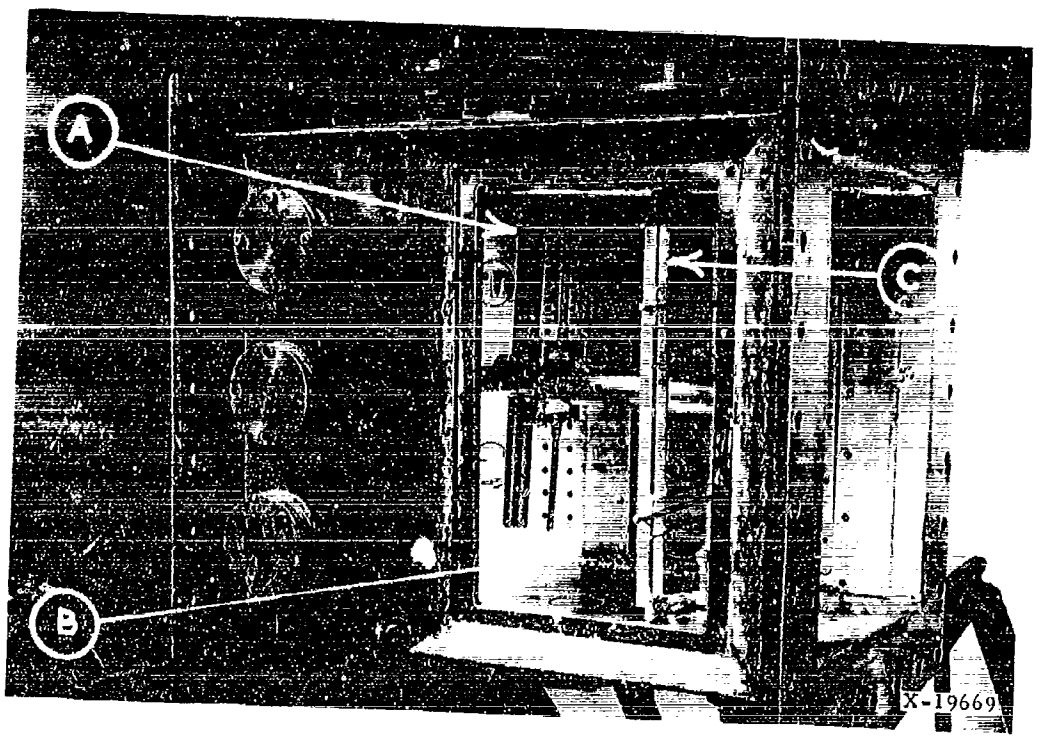
Figure 6.2



COLD FLOW PRESSURE LOSSES OF JET FLAMEHOLDER SYSTEM

Figure 6-3

DOWNGRADED AT 3 YEAR INTERVALS
DECLASSIFIED AFTER 12 YEARS
DOD DIR 5200.10



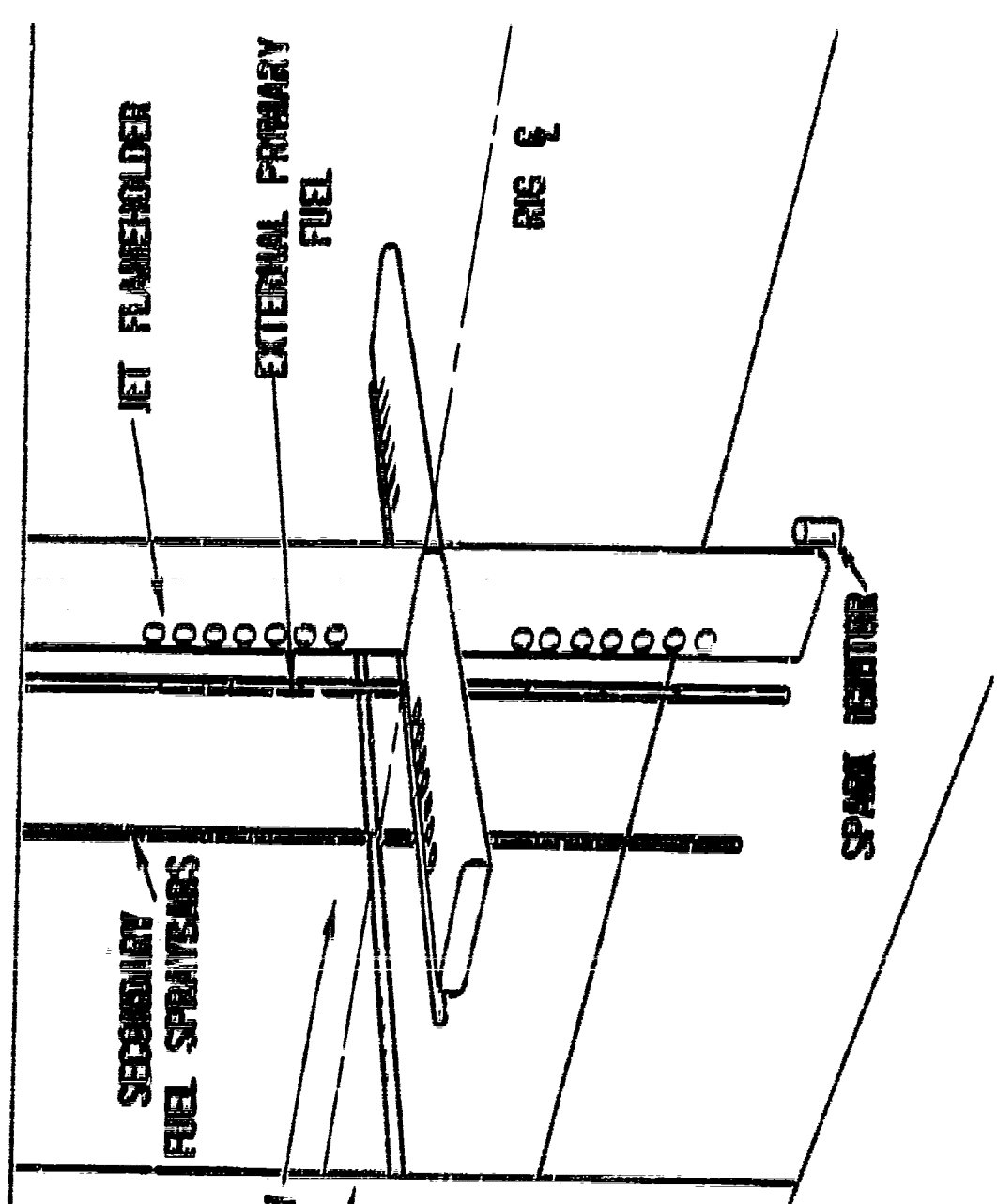
JET FLAMEHOLDER WITH PRIMARY AND SECONDARY SPRAYBARS INSTALLED IN TEST RIG

A. Jet Flameholder B. Primary Spraybar
C. Secondary Spraybar

Figure 6-4

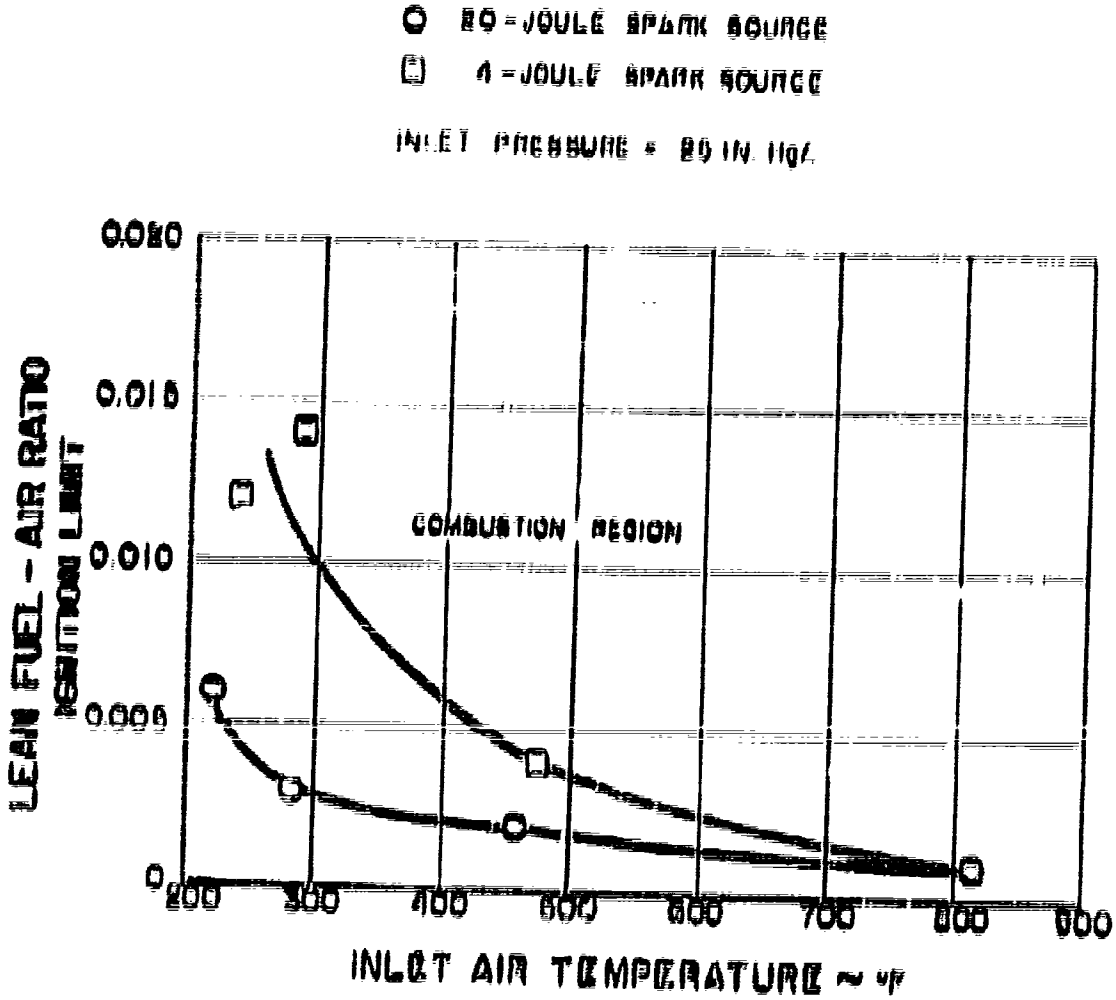
DOWNGRADED AT 3 YEAR INTERVALS
DECLASSIFIED AFTER 12 YEARS
DOD DIR 5200.10

THIS DOCUMENT CONTAINS INFORMATION AFFECTING THE NATIONAL DEFENSE OF THE UNITED STATES WITHIN THE MEANING OF THE ESPIONAGE LAWS, TITLE 18, U.S.C. SECTIONS 793 AND 794. THE EXPORTATION OR THE REVELATION OF ITS CONTENTS IN ANY MANNER TO AN UNAUTHORIZED PERSON IS PROHIBITED BY LAW.



SCHEMATIC DIAGRAM OF CROSS JET FLAMEHOLDER INSTALLED IN 12-INCH BY 16-INCH TEST RIG

Figure 6.5



IGNITION CHARACTERISTICS OF 20-JOULE AND 4-JOULE SPARK IGNITION SYSTEMS

Figure [illegible]

○ UPSTREAM PRIMARY FUEL INJECTING DOWNSTREAM

□ DOWNSTREAM PRIMARY FUEL INJECTING UPSTREAM

SOLID SYMBOLS REFER TO BLOWOUT DATA POINTS

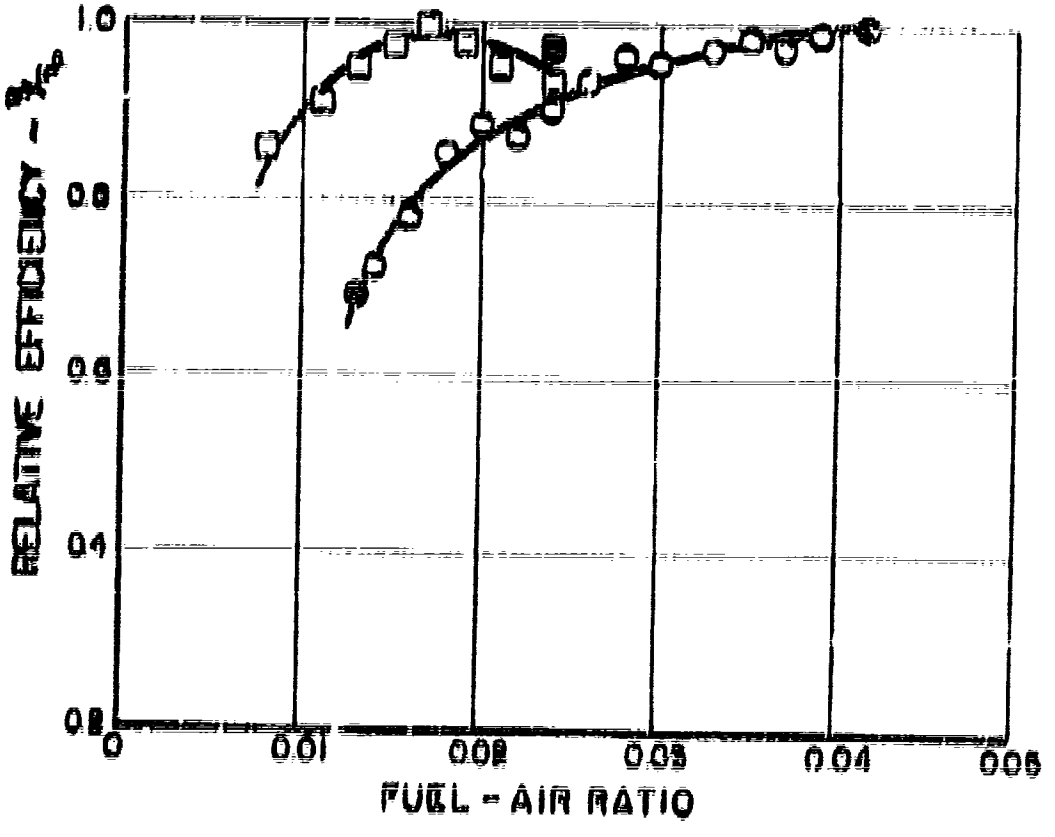
T_T INLET = 266°F

P_T INLET = 25 IN. HgA

PRESSURE RATIO = 2.0

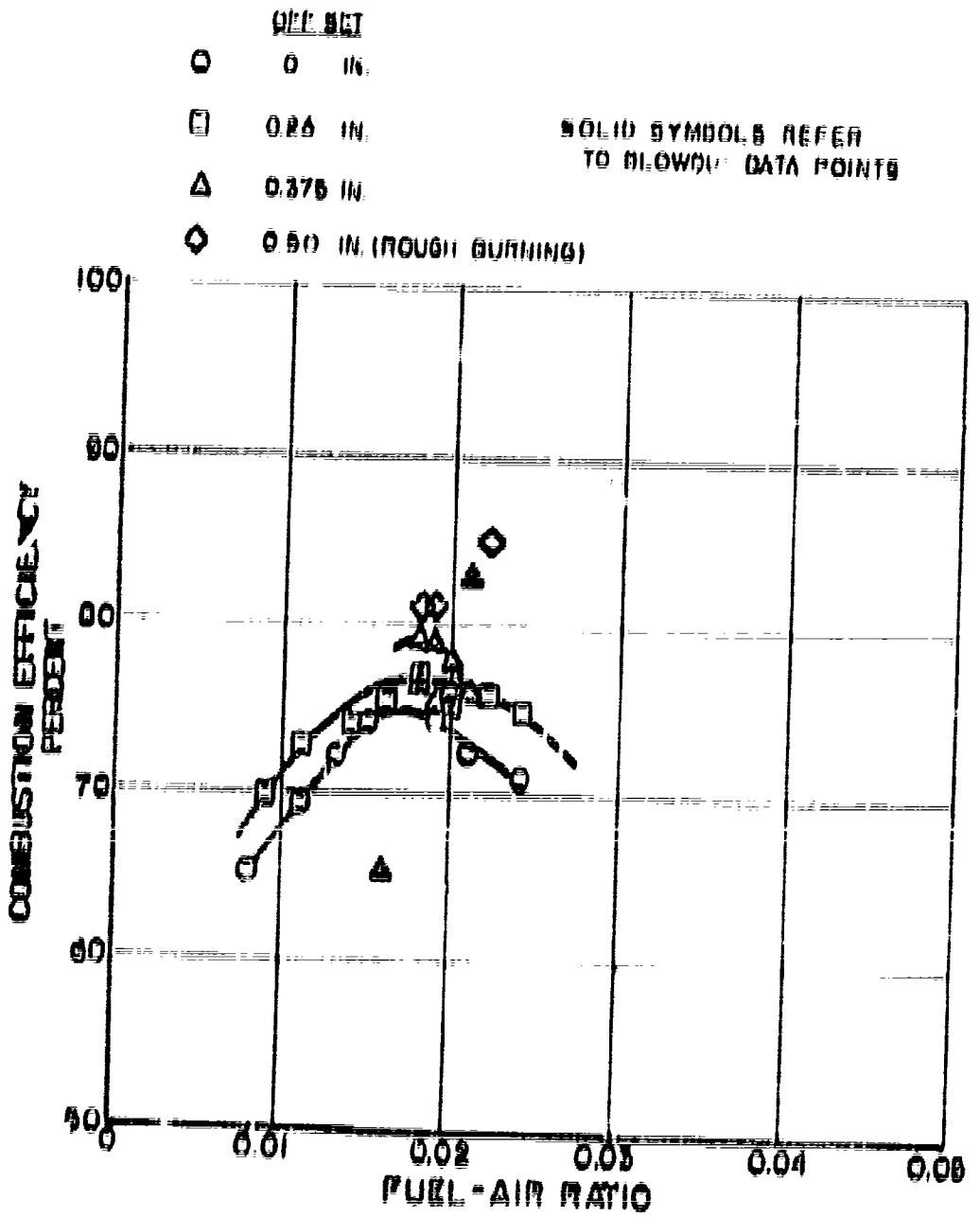
BLEED = 4%

MACH NO. = 0.15



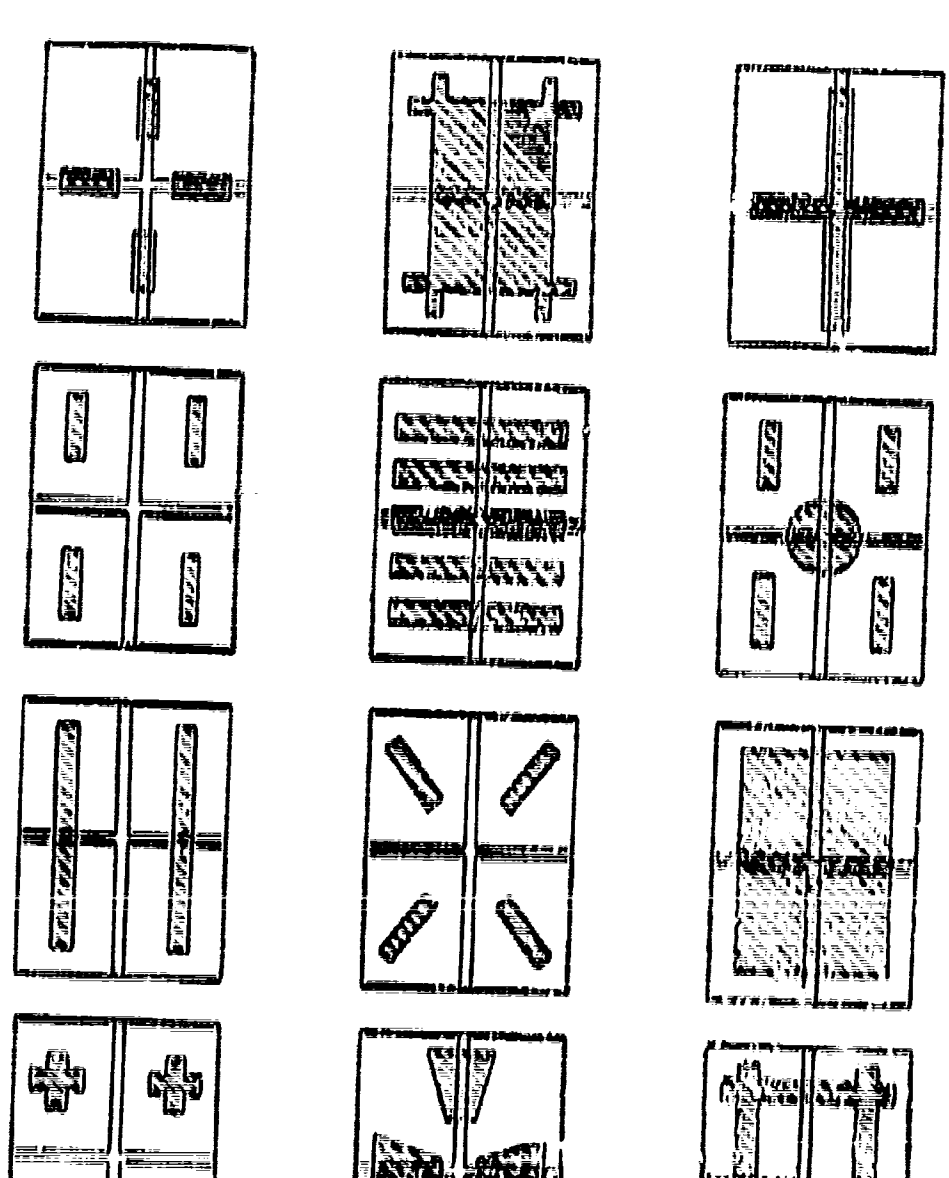
EFFECT OF LOCATION OF PRIMARY SPRAYRING ON COMBUSTION EFFICIENCY

Figure C-7



EFFECT OF PRIMARY SPRAYRING MISALIGNMENT

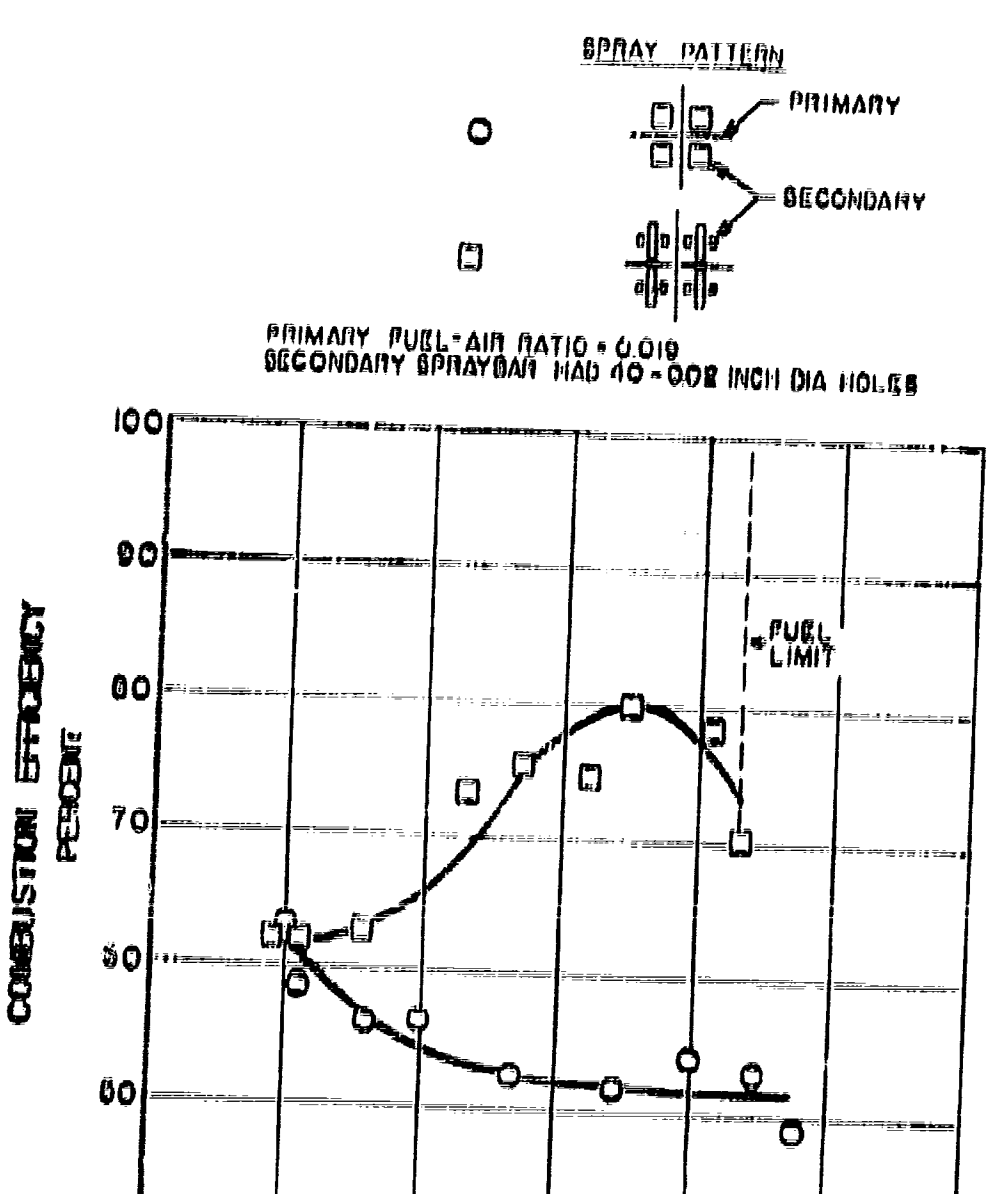
Figure 6-8



SECONDARY FUEL INJECTION PATTERNS

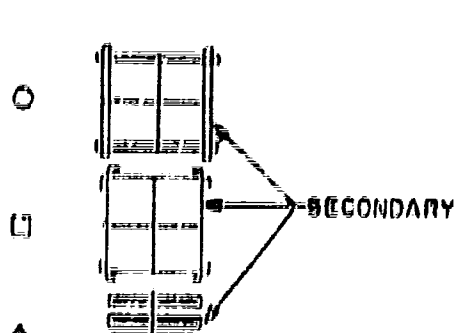
Primary Injection Shown by Cross; Secondary Injection Area is Cross Hatched

Figure 4-9

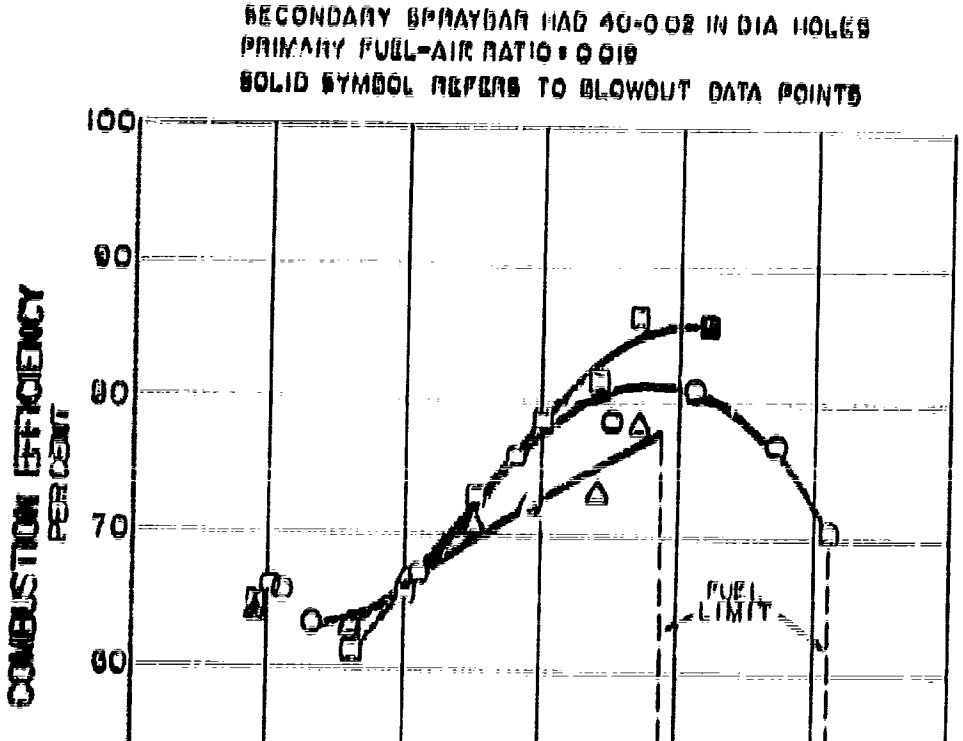


COMBUSTION EFFICIENCY OBTAINED WITH SEVERAL SECONDARY FUEL SPRAY PATTERNS

Figure 6.10

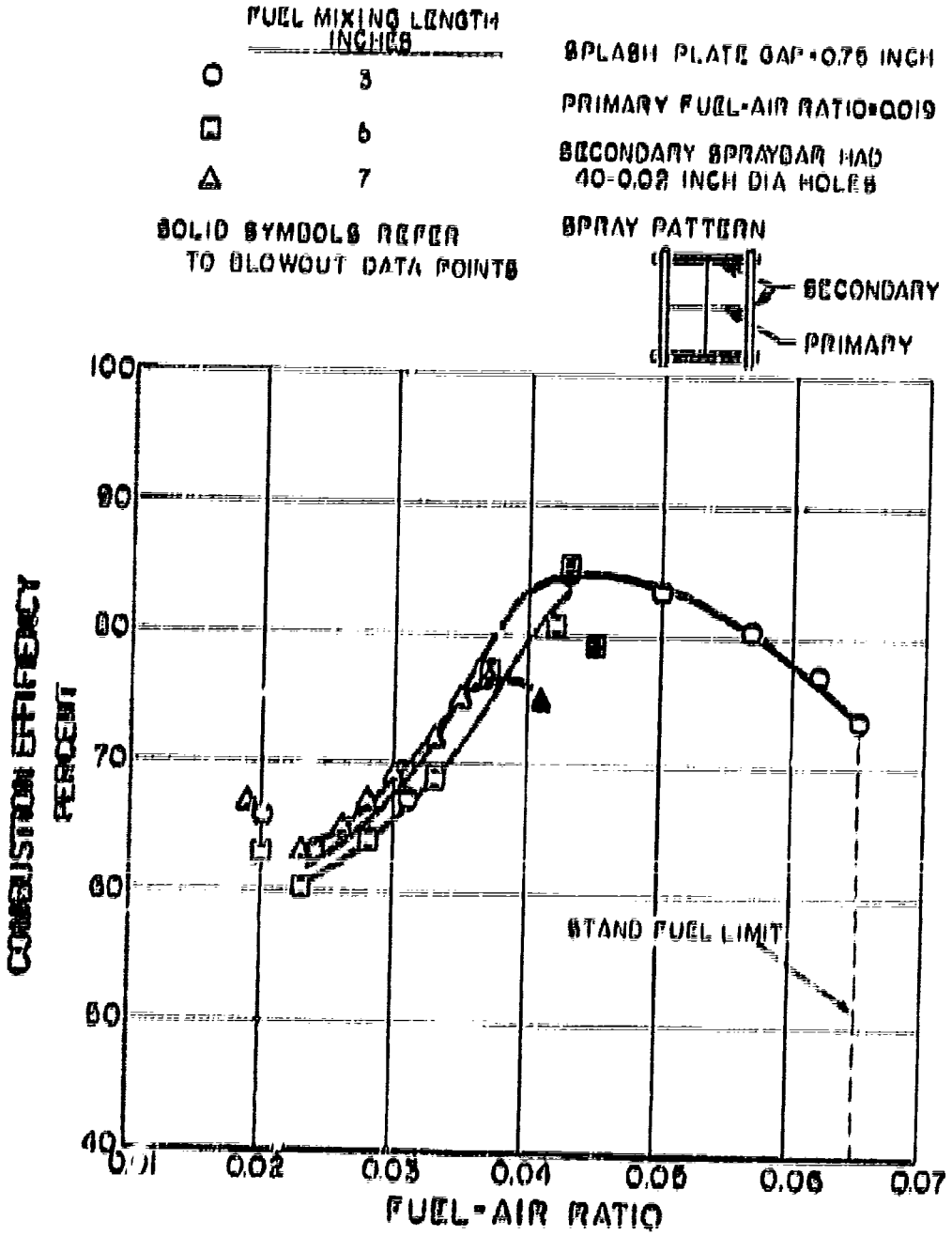


SECONDARY SPRAYBAR HAD 40-0.02 IN DIA HOLES
PRIMARY FUEL-AIR RATIO = 0.010
SOLID SYMBOL REFERS TO BLOWOUT DATA POINTS



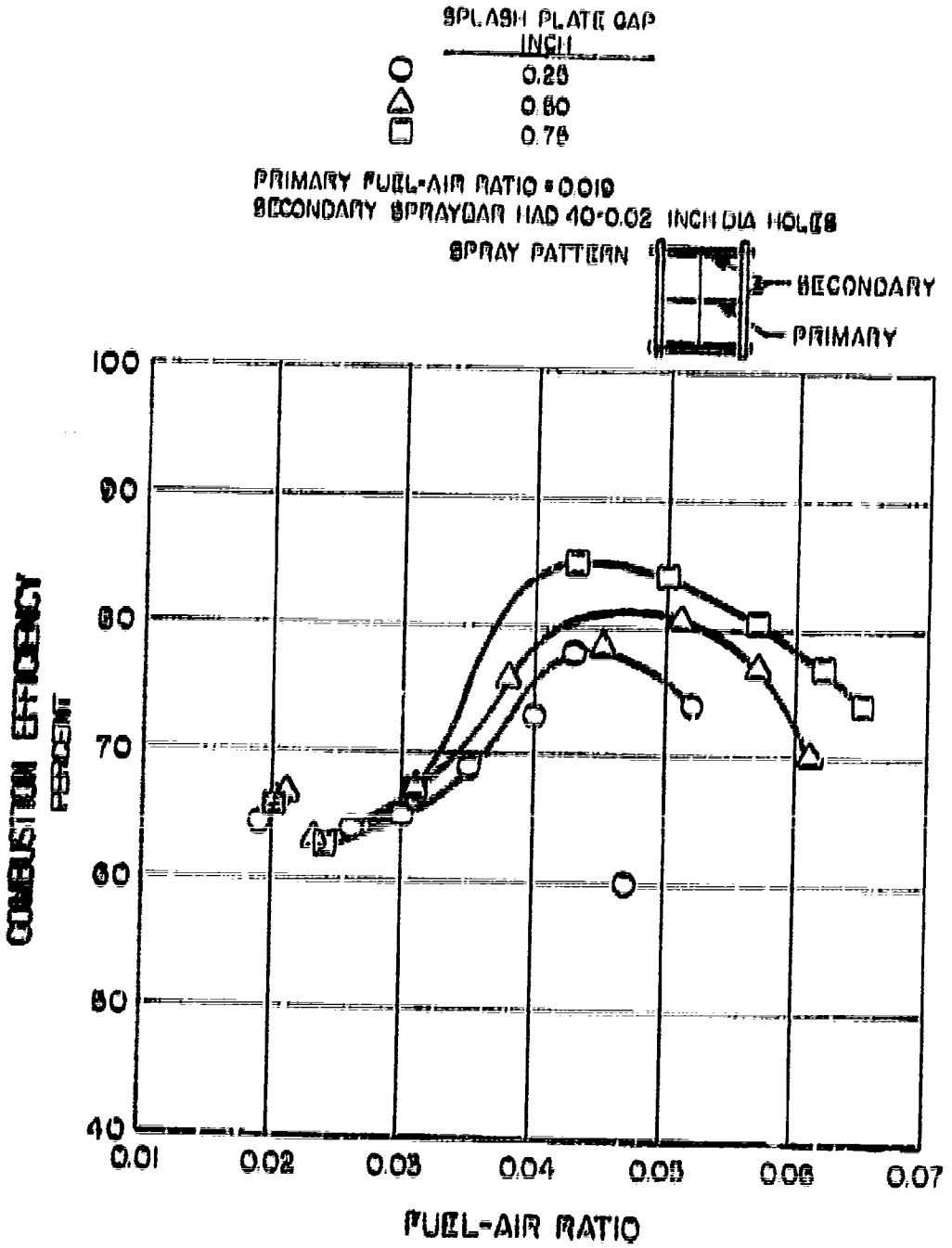
COMBUSTION EFFICIENCY OBTAINED WITH THE ADDITION OF SECONDARY FUEL IN REGION OF PRIMARY SYSTEM AND UNIFORM FLAMEHOLDER COVERAGE

Figure 7-11



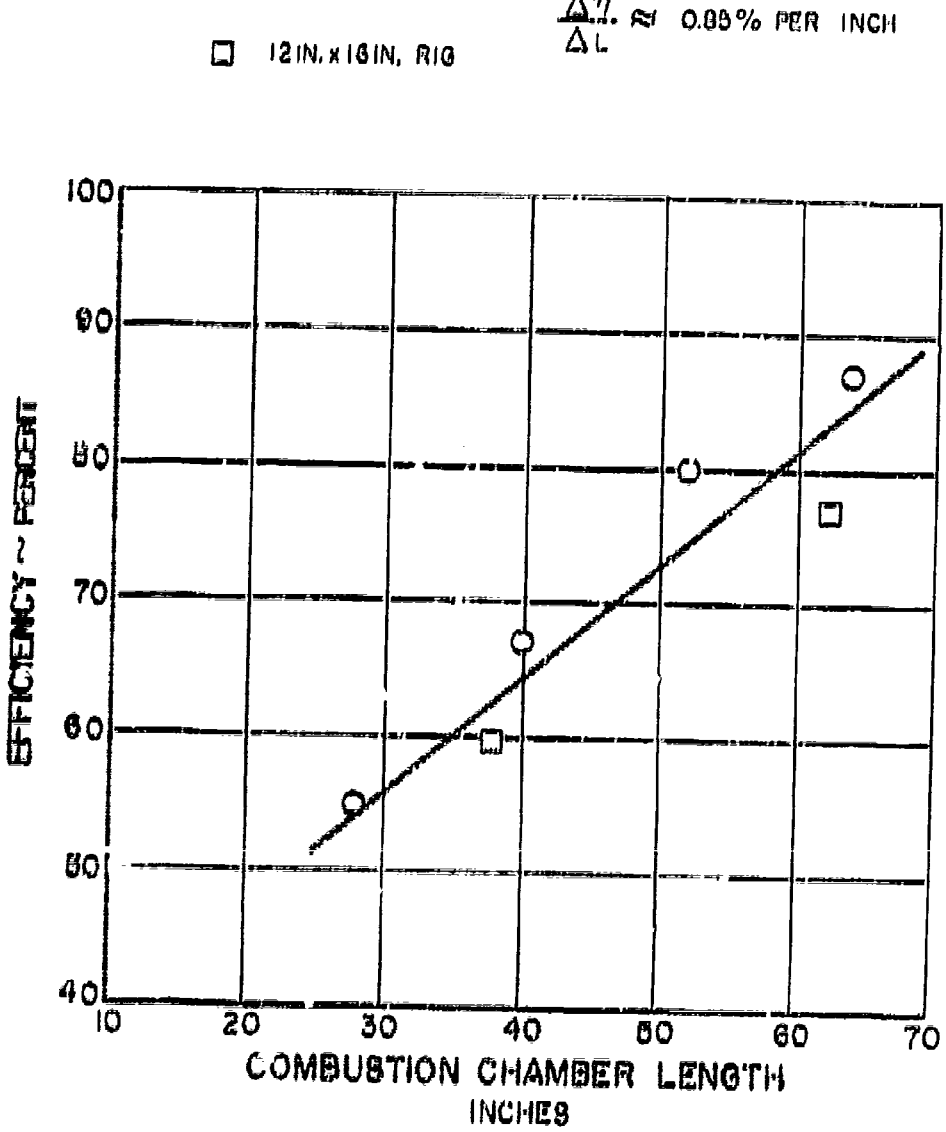
EFFECT OF FUEL MIXING LENGTH ON COMBUSTION EFFICIENCY

Figure 6-12



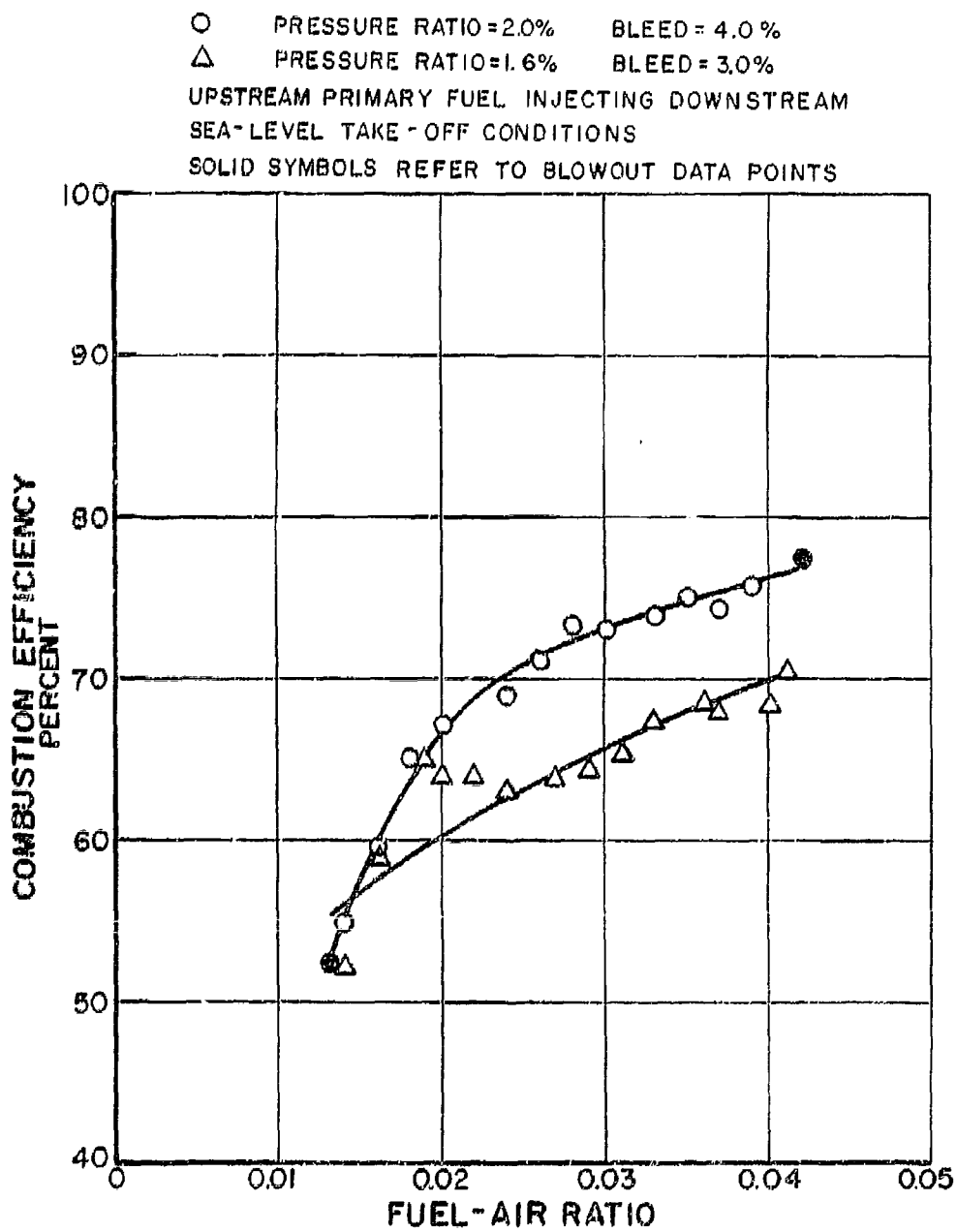
EFFECT OF SPLASH PLATE GAP WIDTH
ON COMBUSTION EFFICIENCY

Figure 6-11



EFFECT OF COMBUSTION CHAMBER LENGTH
ON COMBUSTION EFFICIENCY

Figure 6-14

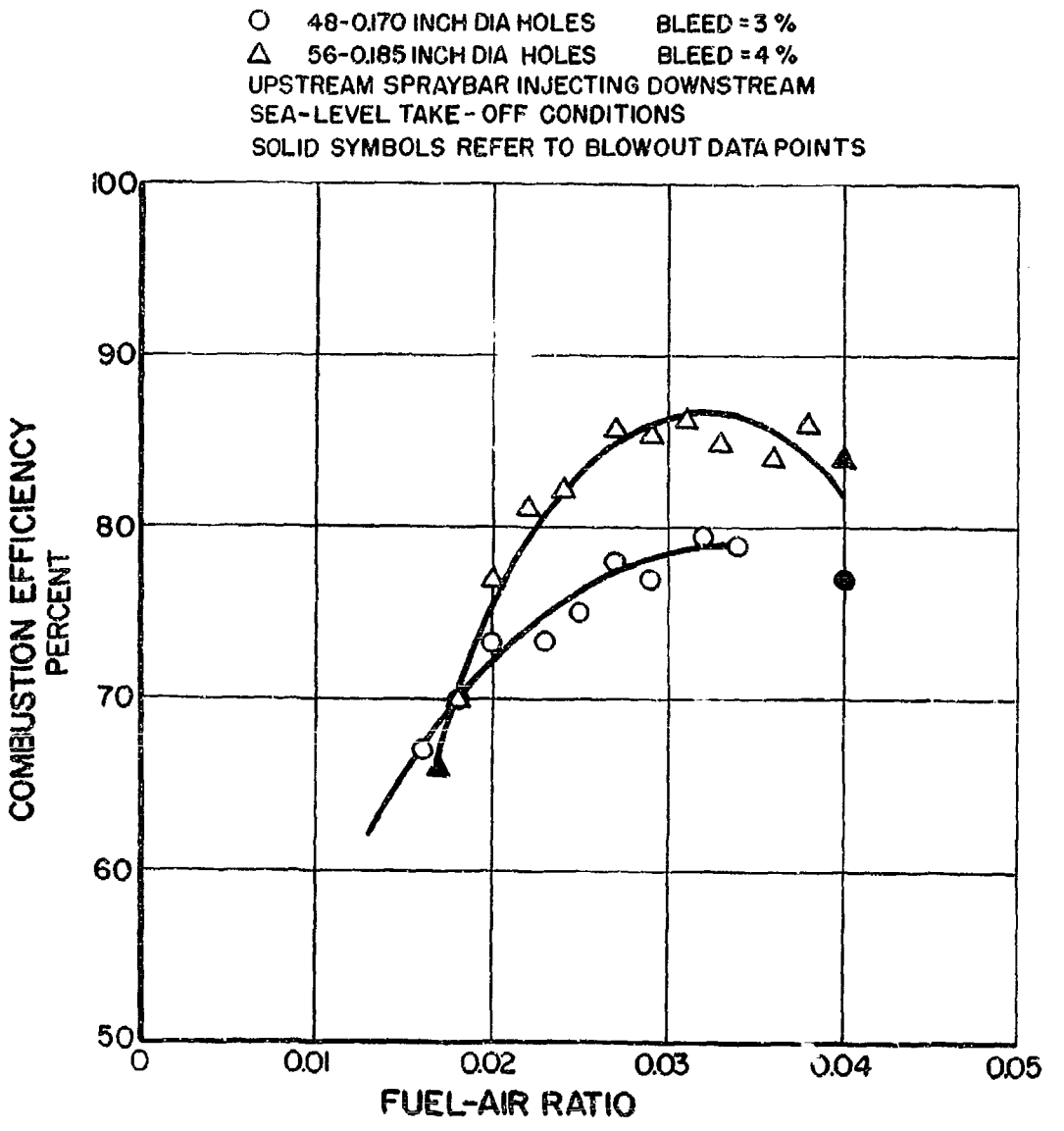


EFFECT OF BLEED FLOW VARIED BY
CHANGING THE PRESSURE RATIO ON COMBUSTION EFFICIENCY

Figure 6-15

DOWNGRADED AT 3 YEAR INTERVALS
UNCLASSIFIED AFTER 12 YEARS
DOD DIR 5200.10

THIS DOCUMENT CONTAINS INFORMATION AFFECTING THE NATIONAL DEFENSE OF THE UNITED STATES WITHIN THE MEANING OF THE ESPIONAGE LAWS, TITLE 18, U.S.C., SECTIONS 793 AND 794. ITS TRANSMISSION OR THE REVELATION OF ITS CONTENTS IN ANY MANNER TO AN UNAUTHORIZED PERSON IS PROHIBITED BY LAW.

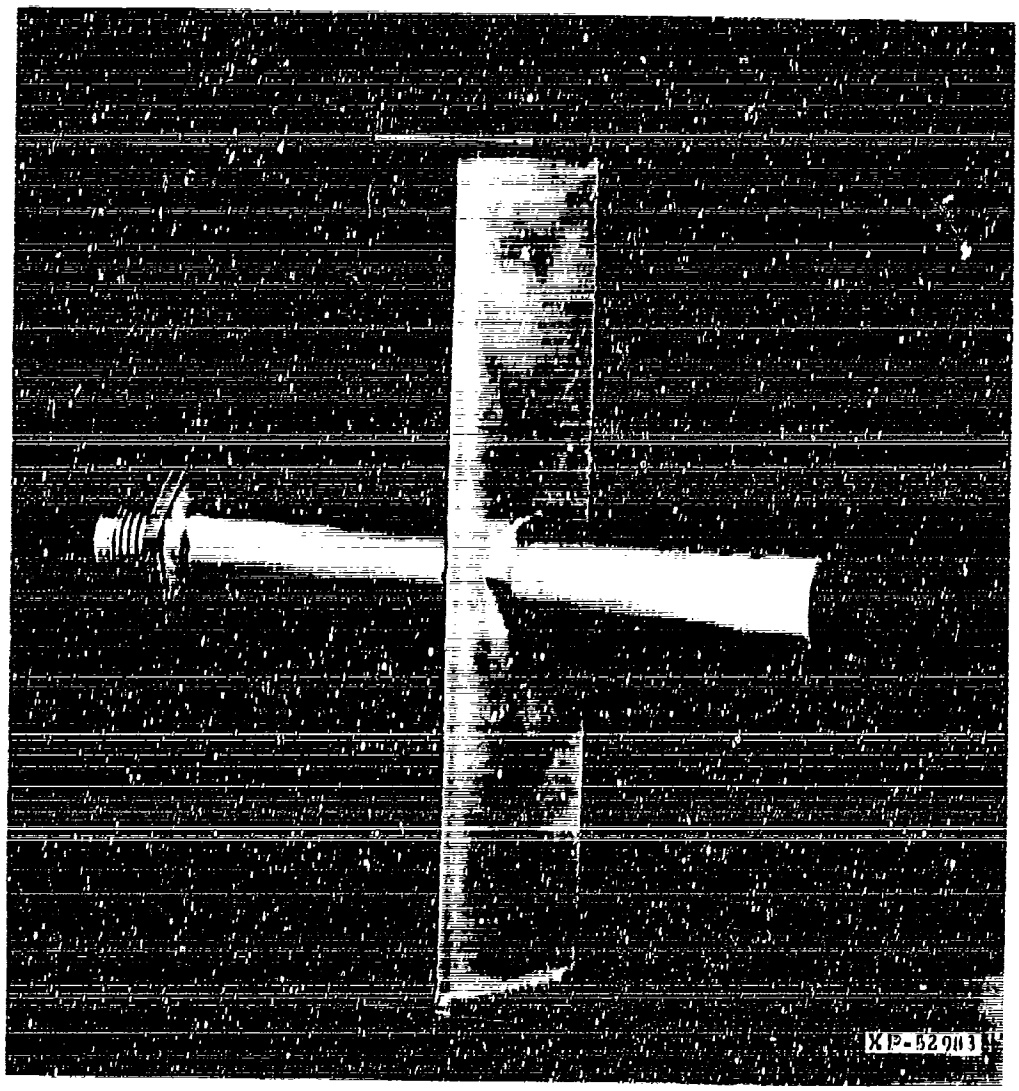


EFFECT OF BLEED FLOW VARIED BY
CHANGING HOLE SIZE ON COMBUSTION EFFICIENCY

Figure 6-16

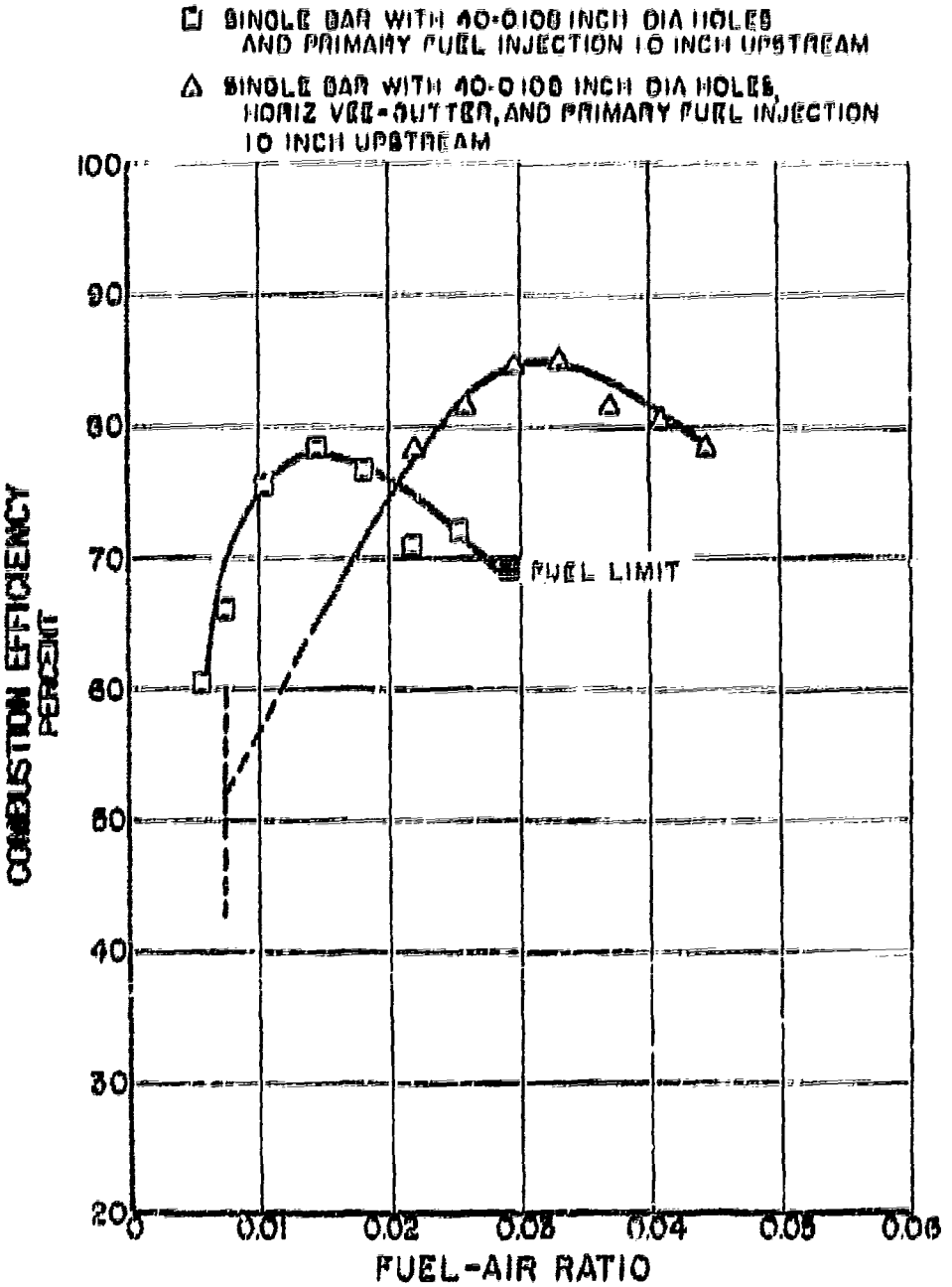
DOWNGRADED AT 3 YEAR INTERVALS
DECLASSIFIED AFTER 12 YEARS
DOD DIR 5200.10

THIS DOCUMENT CONTAINS INFORMATION AFFECTING THE NATIONAL DEFENSE OF THE UNITED STATES WITHIN THE MEANING OF THE ESPIONAGE LAWS, TITLE 18, U.S.C., SECTIONS 793 AND 794. ITS TRANSMISSION OR THE REVELATION OF ITS CONTENTS IN ANY MANNER TO AN UNAUTHORIZED PERSON IS PROHIBITED BY LAW.



SINGLE-BAR JET FLAMEHOLDER
PERPENDICULAR TO CONVENTIONAL VEE GUTTER

Figure C-17



PERFORMANCE OF SINGLE-BAR JET FLAMEHOLDER WITH AND WITHOUT PERPENDICULAR VEE GUTTER

Figure 6-18



POROUS COOLING LINER CONSTRUCTED OF 0, 120, AND 240 SCFM N-155 MATERIAL AND INSTALLED IN 12-INCH BY 16-INCH RIG

Figure C-19



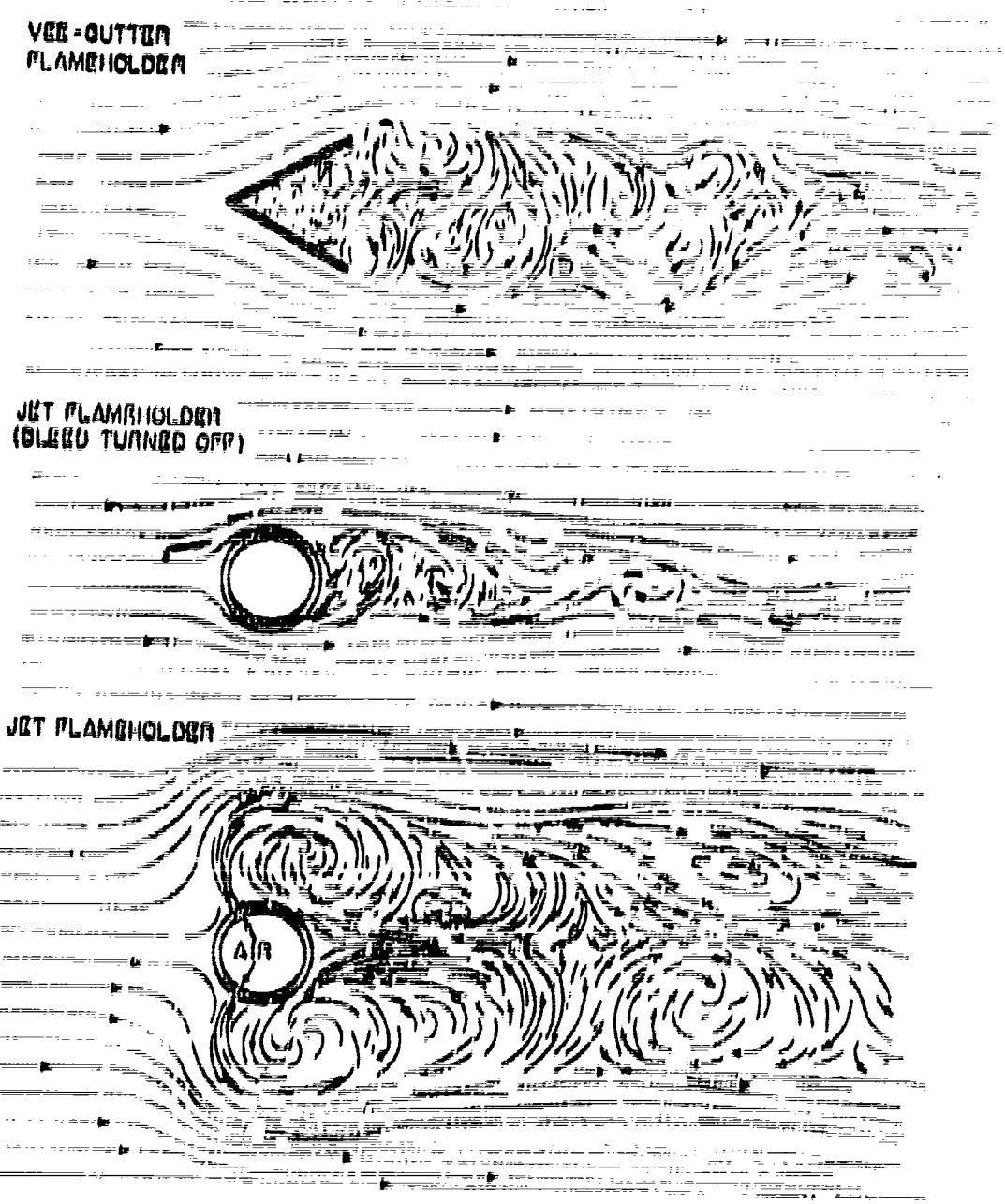
COMBUSTION SYSTEM USED FOR TESTING
POROUS COOLING LINER

Figure 7-20



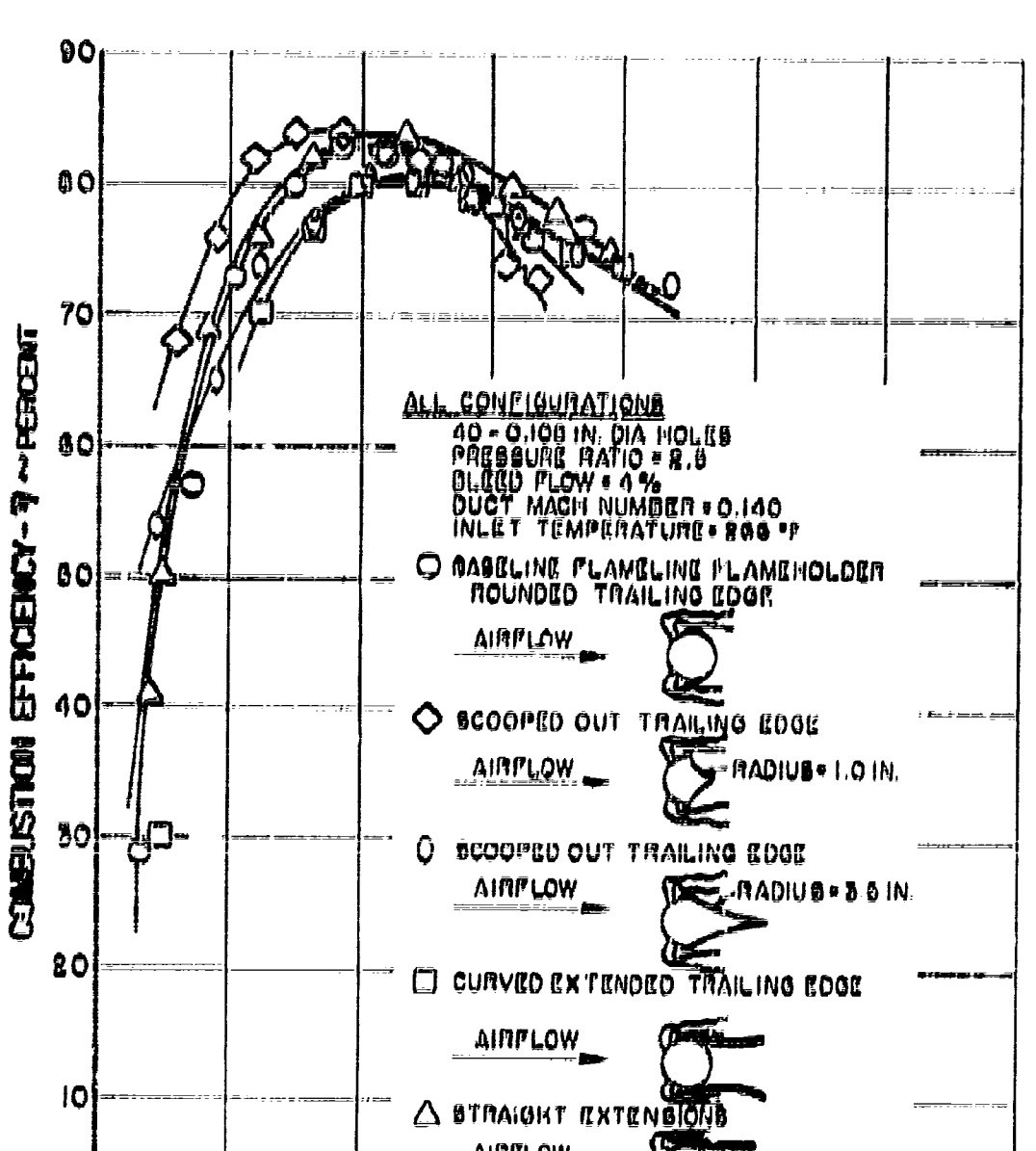
WATER TABLE USED TO DETERMINE
JET FLAMEHOLDER FLOW

Figure 6-21



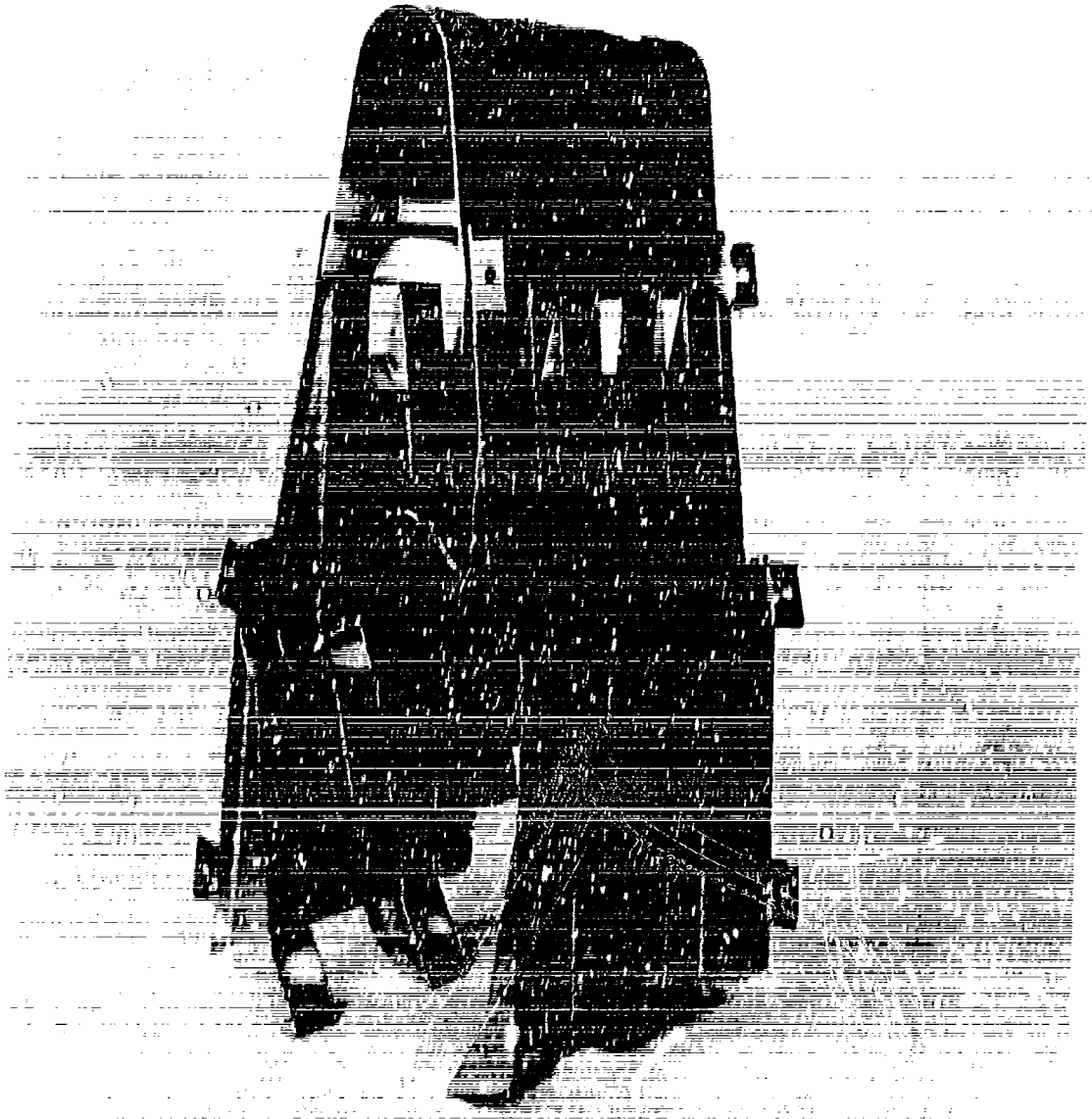
WATER TABLE STREAM LINES
AROUND FLAMEHOLDERS

Figure 6-22



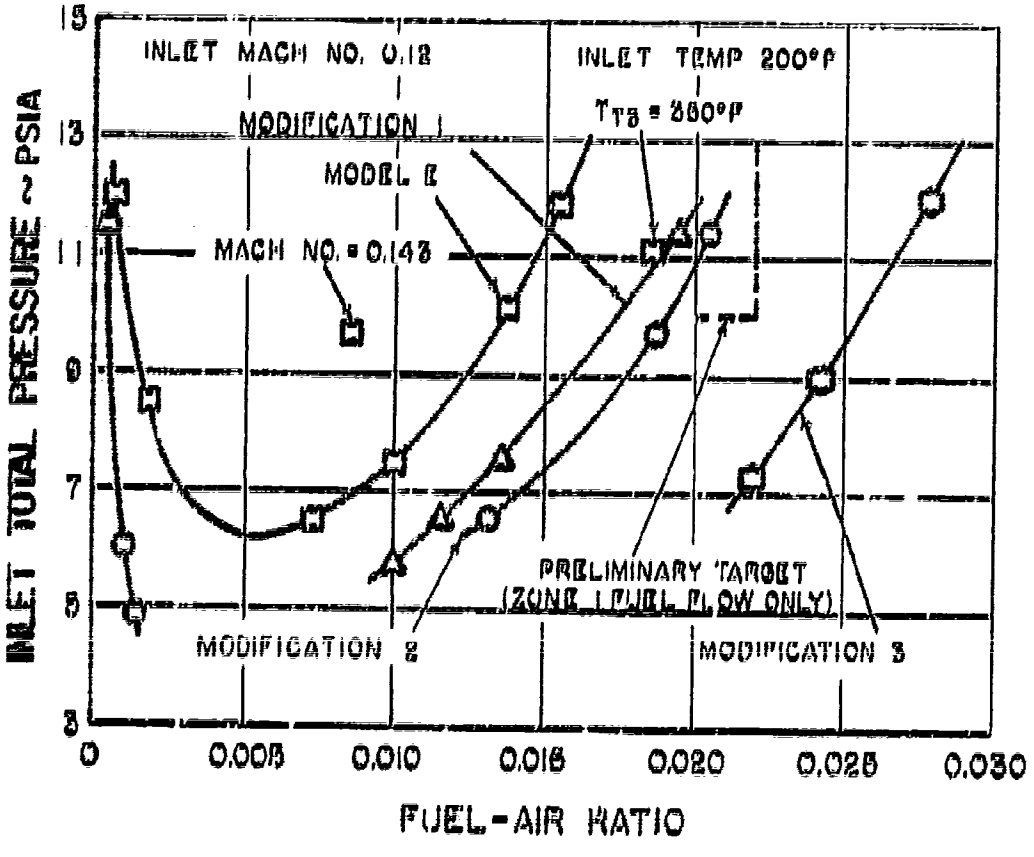
EFFECT OF TRAILING EDGE GEOMETRY
ON COMBUSTION EFFICIENCY

Figure 6-24



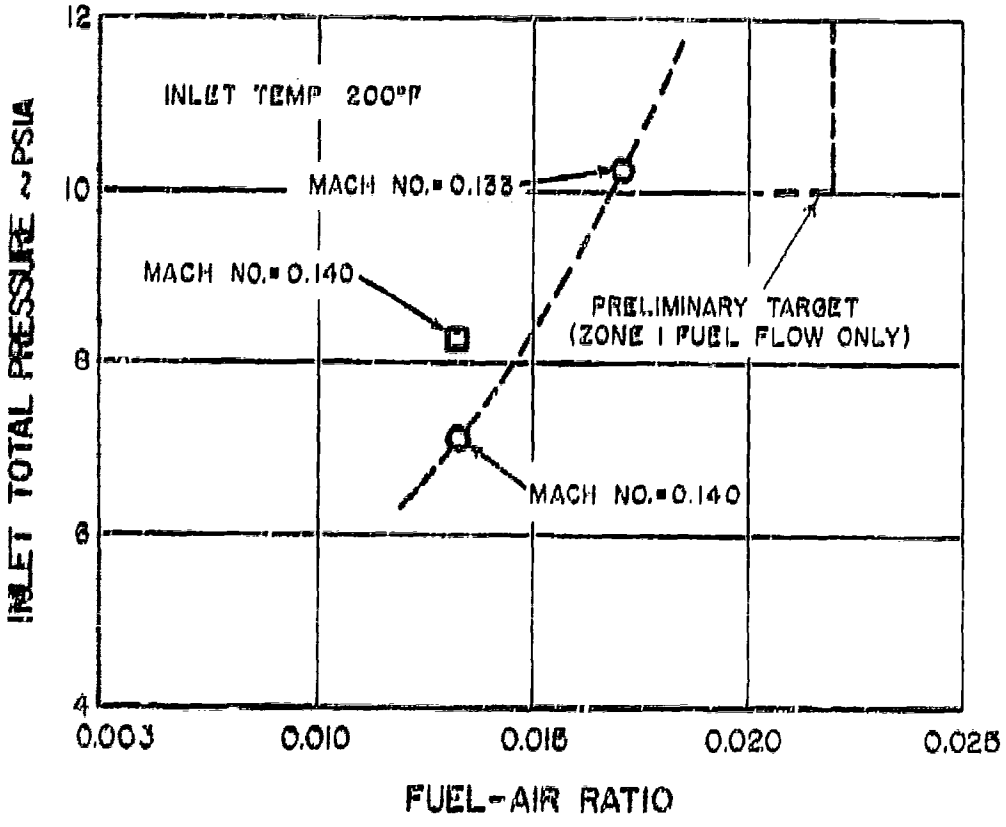
MODEL E RAM INDUCTION DUCT BURNER

Figure C-24



BLOW-OUT CHARACTERISTICS OF MODEL E
RAM INDUCTION DUCT BURNER

Figure 6-25

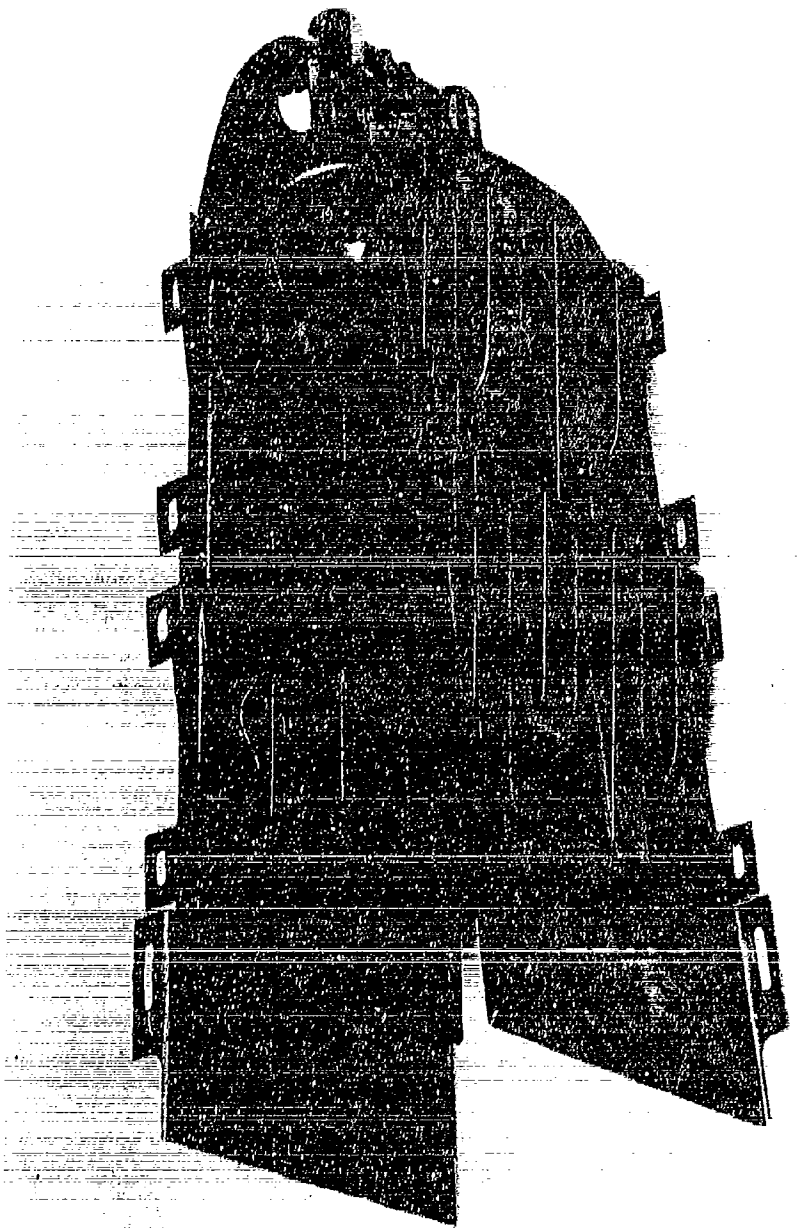


EFFECT OF MACH NUMBER ON BLOW-OUT CHARACTERISTICS OF MODEL E RAM INDUCTION DUCT BURNER

Figure 6-26

DOWNGRADED AT 3 YEAR INTERVALS
DECLASSIFIED AFTER 12 YEARS
DOD DIR 5200.10

THIS DOCUMENT CONTAINS INFORMATION AFFECTING THE NATIONAL DEFENSE OF THE UNITED STATES WITHIN THE MEANING OF THE ESPIONAGE LAWS, TITLE 18, U.S.C., SECTIONS 793 AND 794. THE TRANSMISSION OR THE REVELATION OF ITS CONTENTS IN ANY MANNER TO AN UNAUTHORIZED PERSON IS PROHIBITED BY LAW.

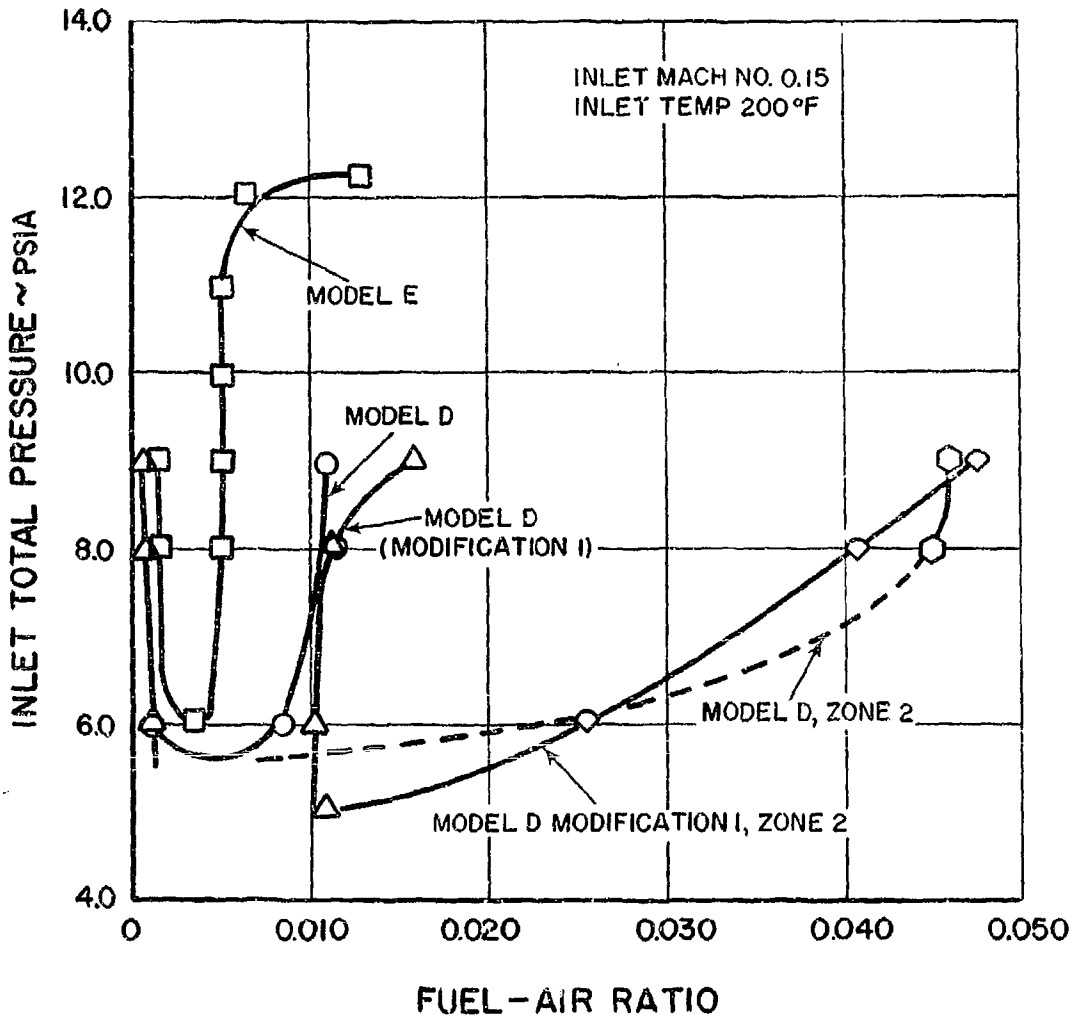


MODEL D RAM INDUCTION DUCT BURNER

Figure 6-27

DOWNGRADED AT 3 YEAR INTERVALS
DECLASSIFIED AFTER 12 YEARS
DOD DIR 5200.10

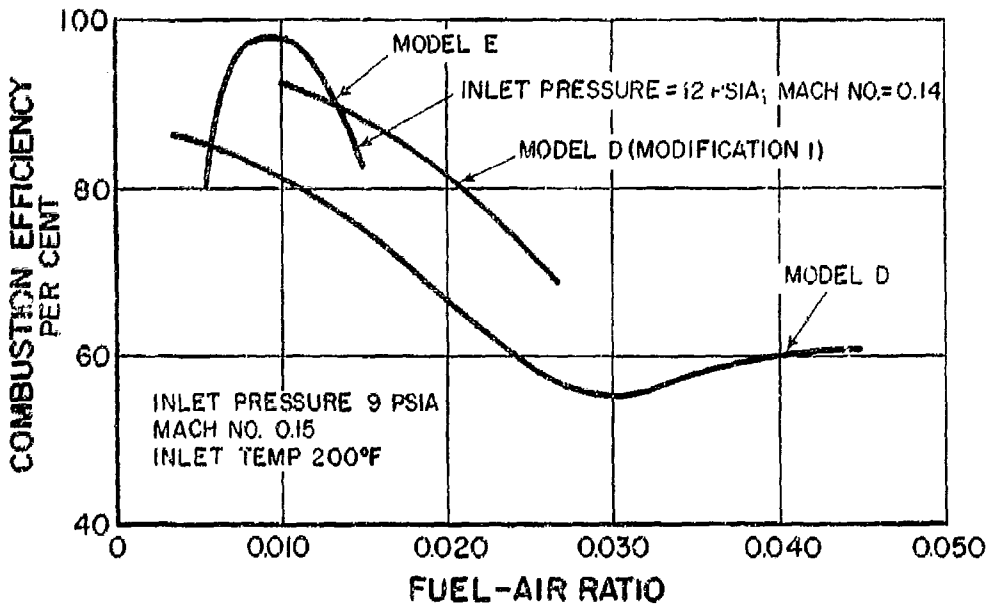
THIS DOCUMENT CONTAINS INFORMATION AFFECTING THE NATIONAL DEFENSE OF THE UNITED STATES WITHIN THE MEANING OF THE ESPIONAGE LAWS, TITLE 18, U.S.C. SECTIONS 793 AND 794. THE TRANSMISSION OR THE REVELATION OF ITS CONTENTS IN ANY MANNER TO AN UNAUTHORIZED PERSON IS PROHIBITED BY LAW.



BLOW-OUT CHARACTERISTICS OF MODEL D RAM INDUCTION DUCT BURNER

Figure 6-28

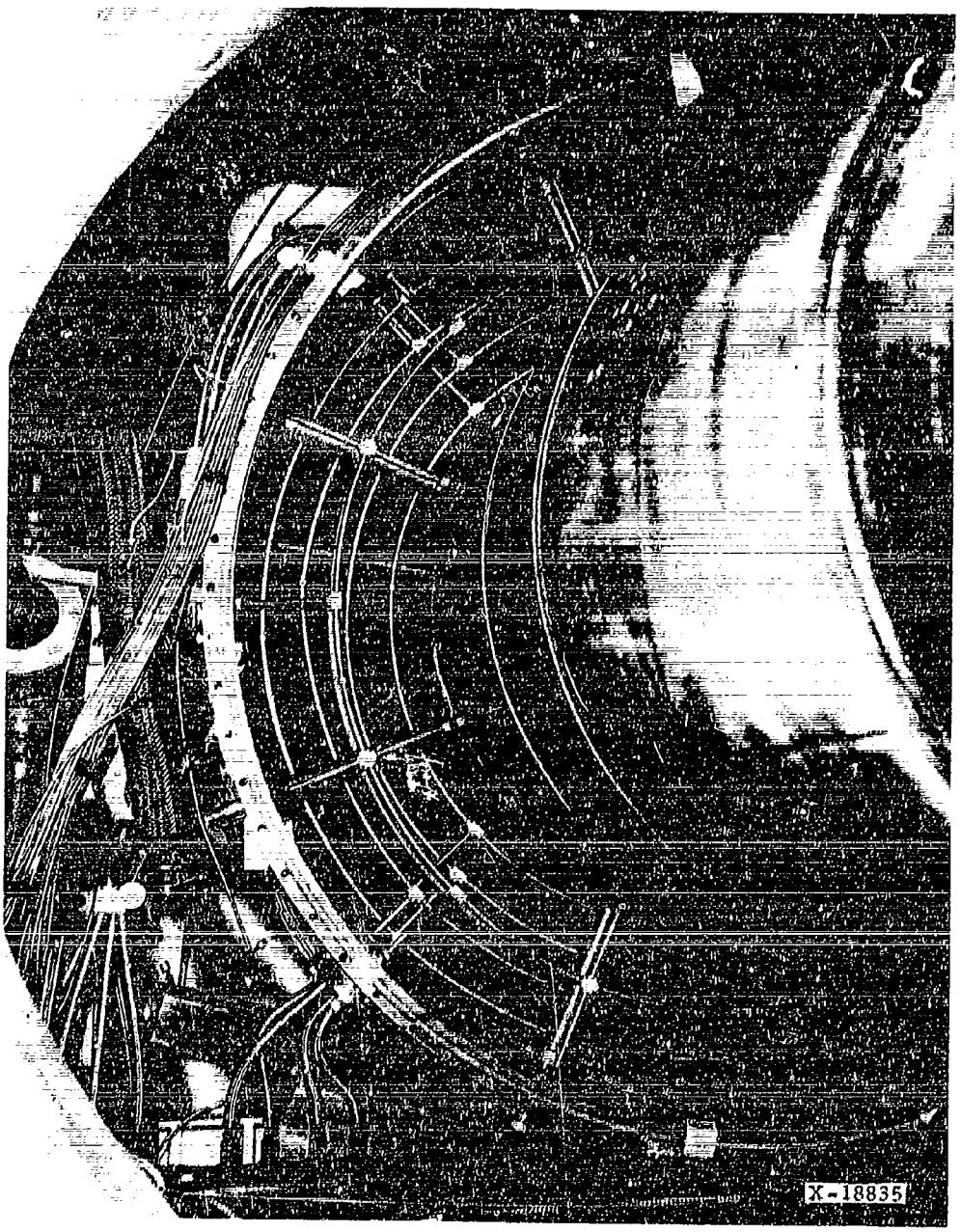
DOWNGRADED AT 3 YEAR INTERVALS
DECLASSIFIED AFTER 12 YEARS
DOD DIR 5200.10



COMBUSTION EFFICIENCY OF RAM
INDUCTION DUCT BURNERS

Figure 6-29

DOWNGRADED AT 3 YEAR INTERVALS
DECLASSIFIED AFTER 12 YEARS
DOD DIR 5200.10

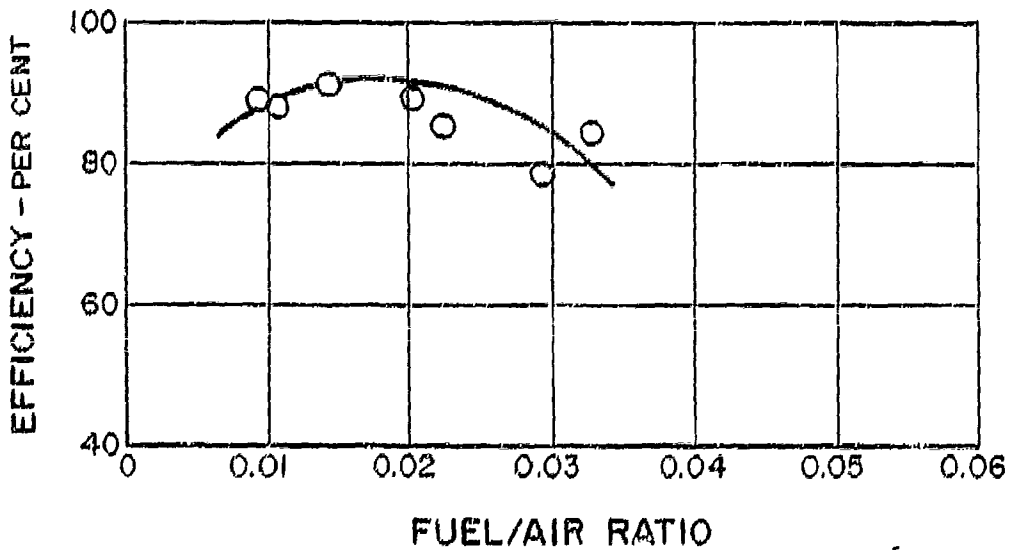


CROSS-JET FLAMEHOLDER TESTED IN FULL-SCALE DUCT HEATER RIG

Figure 6-30

DOWNGRADED AT 3 YEAR INTERVALS
DECLASSIFIED AFTER 12 YEARS

INLET TEMPERATURE = 600°F
PERCENT BLEED FLOW = 5.5%
JET FLAMEHOLDER
PRESSURE RATIO = 2.0
$P_{f_{INLET}}$ = 36 IN. Hg A



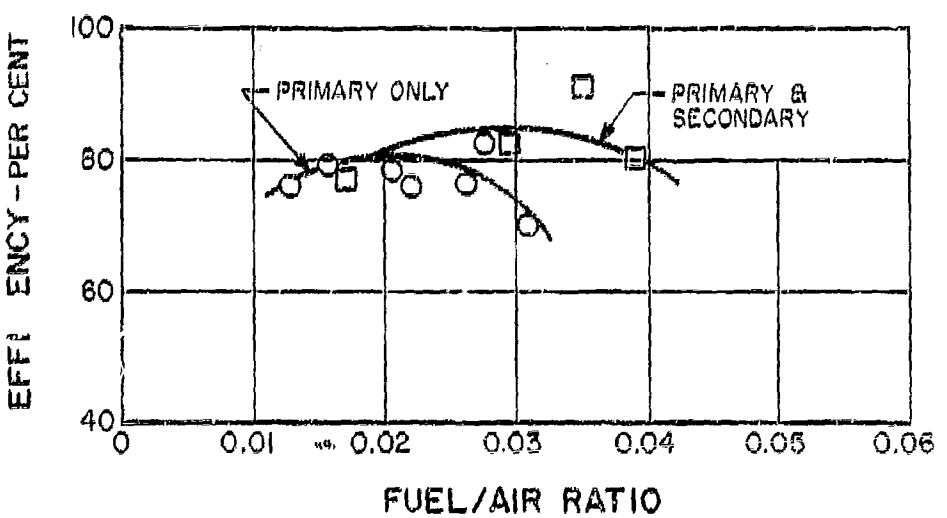
FULL-SCALE DUCT HEATER RIG TEST RESULTS WITH PRIMARY FUEL INJECTION

Figure 6-31

DOWNGRADED AT 3 YEAR INTERVALS
DECLASSIFIED AFTER 12 YEARS
DOD DIR 5200.10

THIS DOCUMENT CONTAINS INFORMATION AFFECTING THE NATIONAL DEFENSE OF THE UNITED STATES WITHIN THE MEANING OF THE ESPIONAGE LAWS, TITLE 18, U.S.C., SECTIONS 793 AND 794. ITS TRANSMISSION OR THE REVELATION OF ITS CONTENTS IN ANY MANNER TO AN UNAUTHORIZED PERSON IS PROHIBITED BY LAW.

INLET TEMPERATURE = 300°F
PER CENT BLEED FLOW = 3%
JET FLAMEHOLDER PRESSURE RATIO = 2.0
$P_{t_{INLET}}$ = 36 IN. Hg A

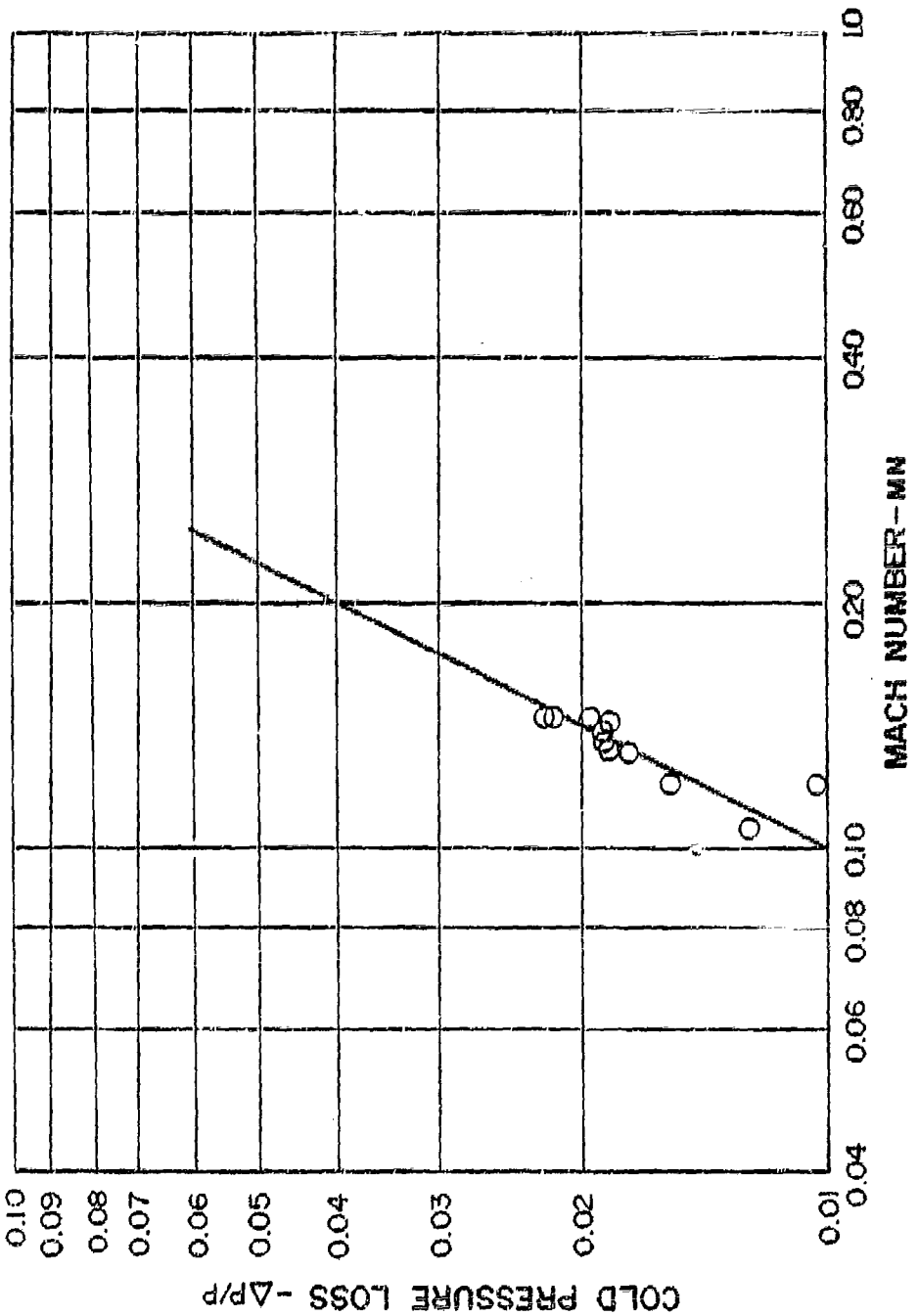


FULL-SCALE DUCT HEATER RIG TEST RESULTS WITH PRIMARY AND SECONDARY FUEL INJECTION

Figure 6-32

DOWNGRADED AT 3 YEAR INTERVALS
DECLASSIFIED AFTER 12 YEARS
DOD DIR 5200.10

THIS DOCUMENT CONTAINS INFORMATION AFFECTING THE NATIONAL DEFENSE OF THE UNITED STATES WITHIN THE MEANING OF THE ESPIONAGE LAWS, TITLE 18, U.S.C., SECTIONS 793 AND 794. THE TRANSMISSION OR THE REVELATION OF ITS CONTENTS IN ANY MANNER TO AN UNAUTHORIZED PERSON IS PROHIBITED BY LAW.

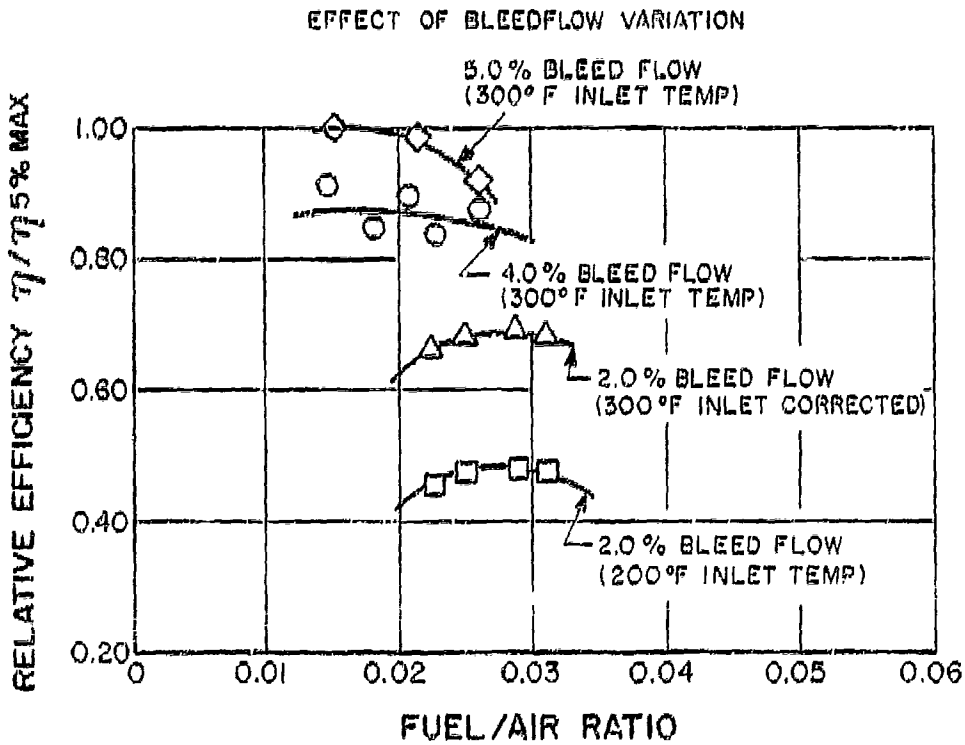


COLD PRESSURE LOSS OF FULL-SCALE DUCT HEATER RIG

Figure 6-33

DOWNGRADED AT 3 YEAR INTERVALS
DECLASSIFIED AFTER 12 YEARS
DOD DIR 5200.10

THIS DOCUMENT CONTAINS INFORMATION AFFECTING THE NATIONAL DEFENSE OF THE UNITED STATES WITHIN THE MEANING OF THE ESPIONAGE LAWS, TITLE 18, U.S.C., SECTIONS 793 AND 794. ITS TRANSMISSION OR THE REVELATION OF ITS CONTENTS IN ANY MANNER TO AN UNAUTHORIZED PERSON IS PROHIBITED BY LAW.

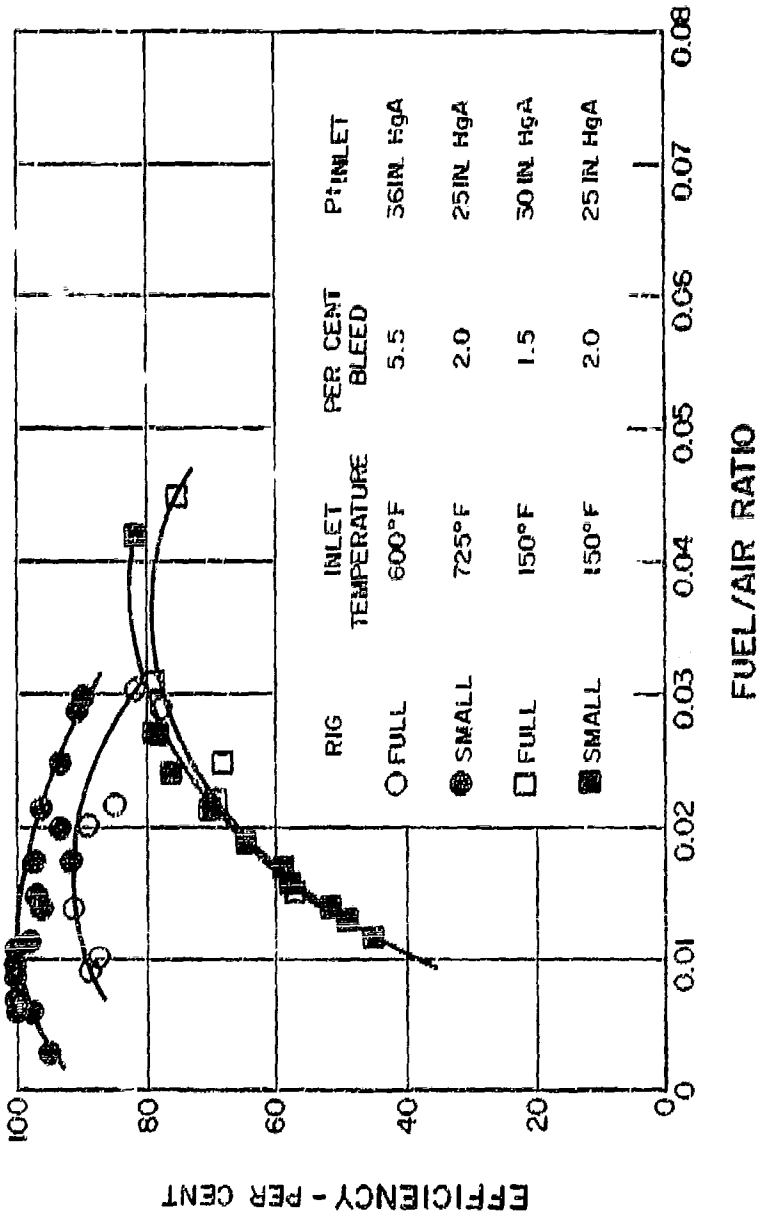


EFFECT OF BLEED FLOW ON EFFICIENCY OF FULL-SCALE DUCT HEATER RIG

Figure 6-34

DOWNGRADED AT 3 YEAR INTERVALS
DECLASSIFIED AFTER 12 YEARS
DOD DIR 5200.10

THIS DOCUMENT CONTAINS INFORMATION AFFECTING THE NATIONAL DEFENSE OF THE UNITED STATES WITHIN THE MEANING OF THE ESPIONAGE LAWS, TITLE 18, U.S.C., SECTIONS 793 AND 794. ITS TRANSMISSION OR THE REVELATION OF ITS CONTENTS IN ANY MANNER TO AN UNAUTHORIZED PERSON IS PROHIBITED BY LAW.

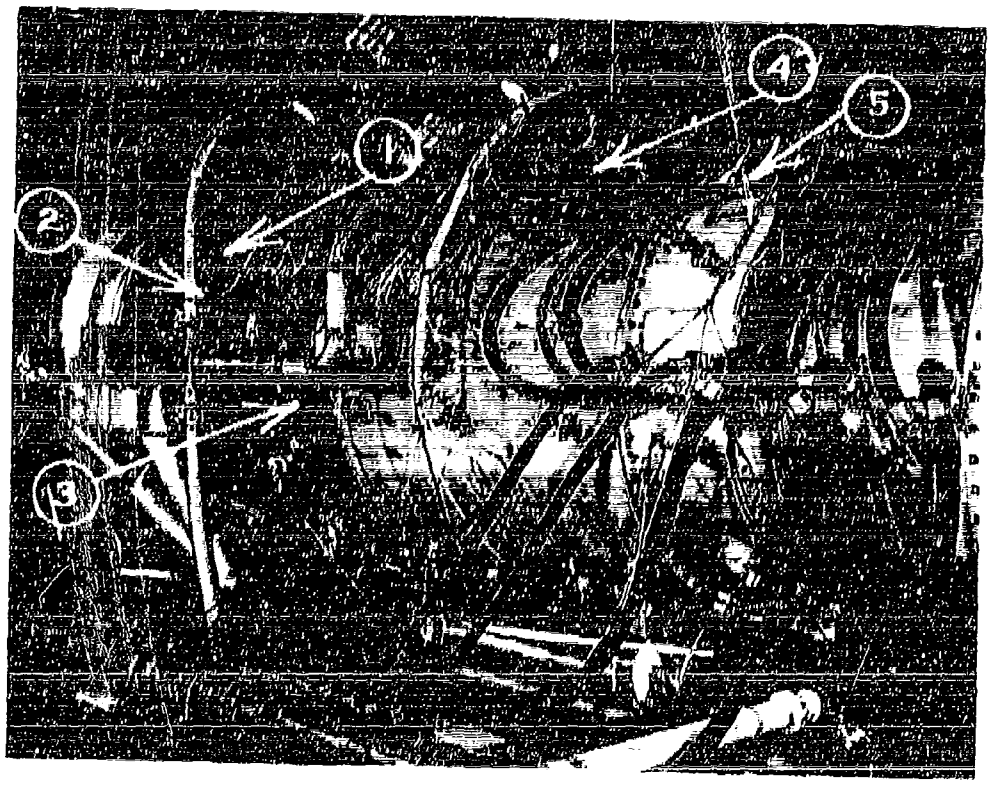


DUCT HEATER TEST RESULTS OBTAINED WITH FULL-SCALE AND SMALL-SCALE RIGS

Figure 6-35

DOWNGRADED AT 3 YEAR INTERVALS
DECLASSIFIED AFTER 12 YEARS
DOD Dir 5200.10

THIS DOCUMENT CONTAINS INFORMATION AFFECTING THE NATIONAL DEFENSE OF THE UNITED STATES WITHIN THE MEANING OF THE ESPIONAGE LAWS, TITLE 18, U.S.C., SECTIONS 793 AND 794. ITS TRANSMISSION OR THE REVELATION OF ITS CONTENTS IN ANY MANNER TO AN UNAUTHORIZED PERSON IS PROHIBITED BY LAW.



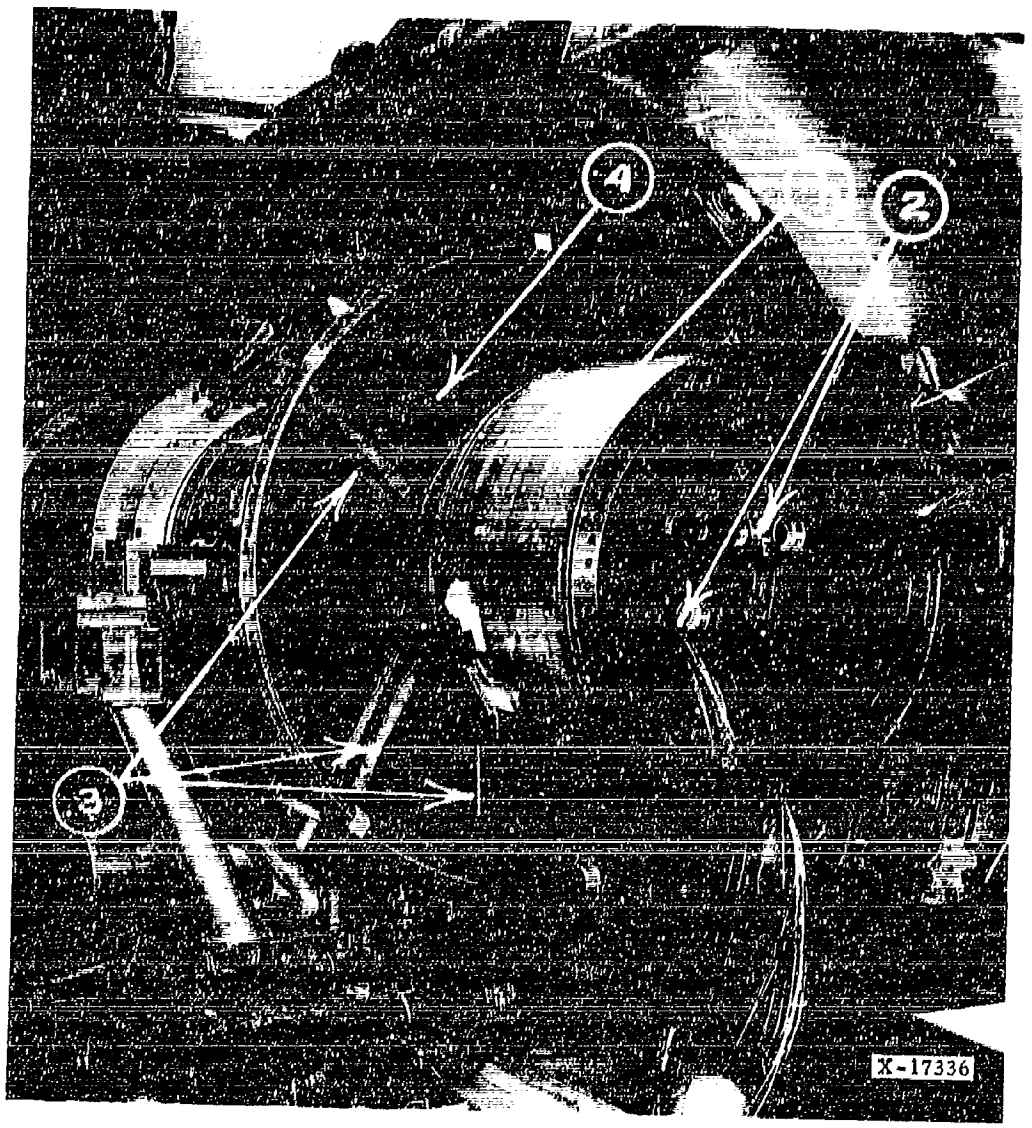
FULL-SCALE DUCT HEATER RIG

1 - Inlet Diffuser
2 - Jet Flameholder Manifold
3 - Jet Flameholder Section
4 - Combustion Chamber
5 - Exit Nozzles

Figure 6-36

DOWNGRADED AT 3 YEAR INTERVALS
DECLASSIFIED AFTER 12 YEARS
DOD DIR 5200.10

THIS DOCUMENT CONTAINS INFORMATION AFFECTING THE NATIONAL DEFENSE OF THE UNITED STATES WITHIN THE MEANING OF THE ESPIONAGE LAWS, TITLE 18, U.S.C., SECTIONS 793 AND 794. THE TRANSMISSION OR THE REVELATION OF ITS CONTENTS IN ANY MANNER TO AN UNAUTHORIZED PERSON IS PROHIBITED BY LAW.



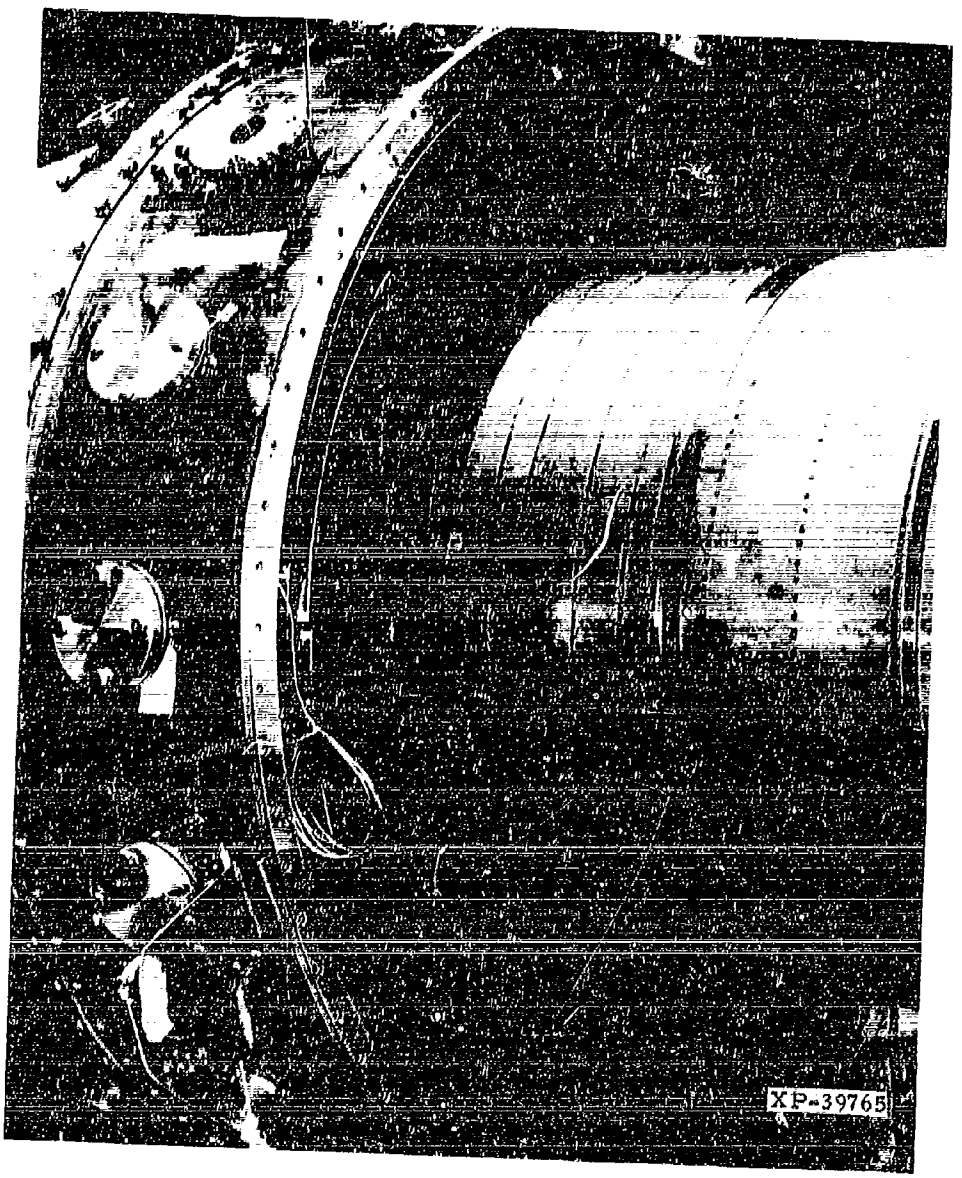
FULL-SCALE DUCT HEATER RIG INLET DIFFUSER ASSEMBLY

1 - Inner Body Fuel Baffle
2 - Water Pipes
3 - Inner Body Instrumentation Tubes
4 - Inner Body Support

Figure 6-37

DOWNGRADED AT 3 YEAR INTERVALS
DECLASSIFIED AFTER 12 YEARS
DOD DIR 5200.10

THIS DOCUMENT CONTAINS INFORMATION AFFECTING THE NATIONAL DEFENSE OF THE UNITED STATES WITHIN THE MEANING OF THE ESPIONAGE LAWS, TITLE 18, U.S.C., SECTIONS 793 AND 794. ITS TRANSMISSION OR THE REVELATION OF ITS CONTENTS IN ANY MANNER TO AN UNAUTHORIZED PERSON IS PROHIBITED BY LAW.

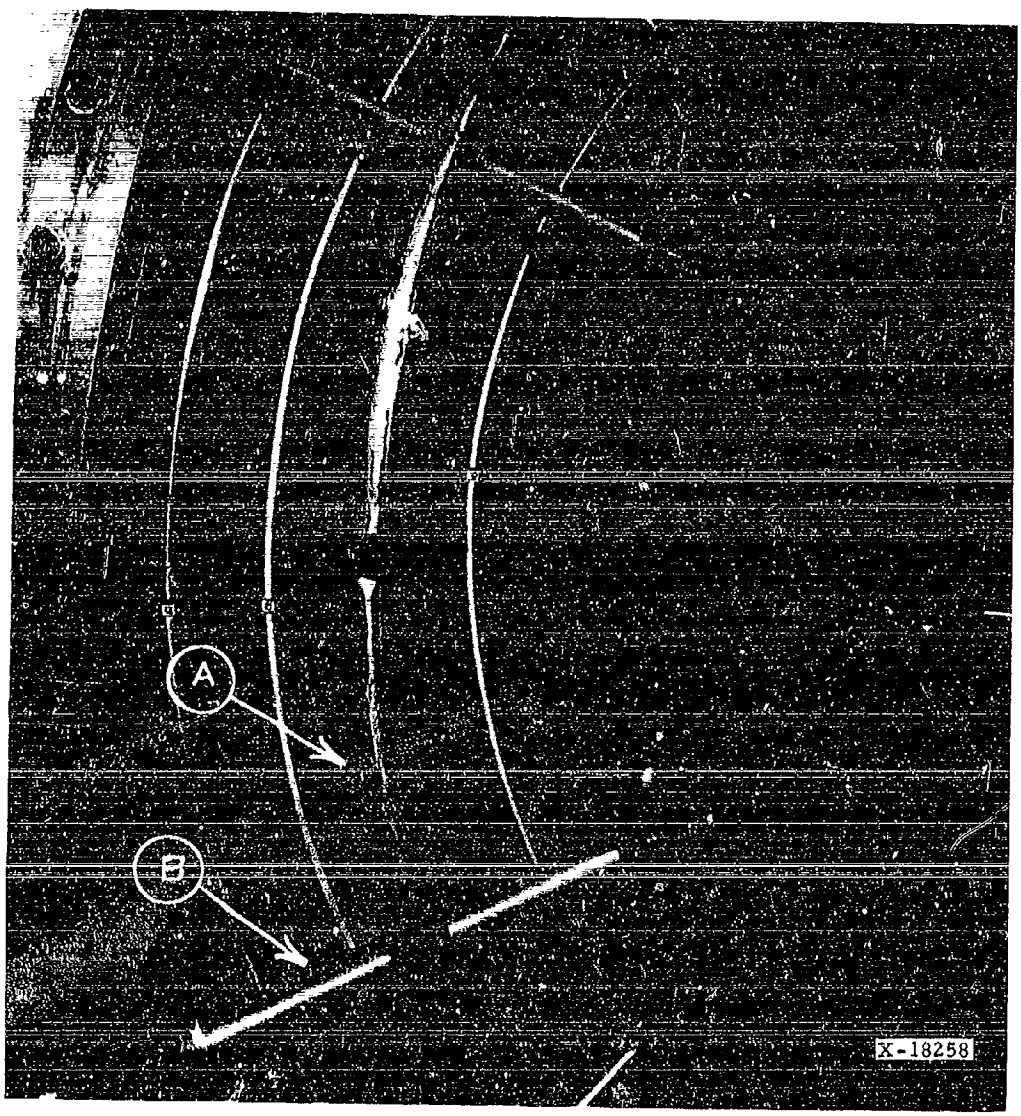


FULL-SCALE DUCT HEATER RIG SHOWING JET FLAMEHOLDER

Figure 6-38

DOWNGRADED AT 3 YEAR INTERVALS
DECLASSIFIED AFTER 12 YEARS
DOD DIR 5200.10

THIS DOCUMENT CONTAINS INFORMATION AFFECTING THE NATIONAL DEFENSE OF THE UNITED STATES WITHIN THE MEANING OF THE ESPIONAGE LAWS, TITLE 18, U.S.C., SECTIONS 793 AND 794. THE TRANSMISSION OR THE REVELATION OF ITS CONTENTS IN ANY MANNER TO AN UNAUTHORIZED PERSON IS PROHIBITED BY LAW.



JET FLAMEHOLDER AND SPRAY RINGS IN FULL-SCALE DUCT HEATER RIG

A - Flameholder Ring B - Spoke

Figure 6-39

DOWNGRADED AT 3 YEAR INTERVALS
DECLASSIFIED AFTER 12 YEARS
DOD DIR 5200.10

THIS DOCUMENT CONTAINS INFORMATION AFFECTING THE NATIONAL DEFENSE OF THE UNITED STATES WITHIN THE MEANING OF THE ESPIONAGE LAWS, TITLE 18, U.S.C., SECTIONS 793 AND 794. THE TRANSMISSION OR THE REVELATION OF ITS CONTENTS IN ANY MANNER TO AN UNAUTHORIZED PERSON IS PROHIBITED BY LAW.

ITEM 7

EXHAUST SYSTEM

ITEM 7 - EXHAUST SYSTEM

OBJECTIVES

Pratt & Whitney Aircraft has conducted static (internal flow only) and wind tunnel (internal and external flow) tests of scale models of the engine exhaust system, including thrust reverser, directed toward verification of the exhaust system performance.

A. INTRODUCTION

The goal of this program was to meet or exceed the following exhaust system performance specifications expressed in terms of the thrust-minus-drag coefficient (C_{FP}) at typical power settings for the following flight conditions:

Number	Condition	C_{FP} With 2% Secondary Air Flow
3.0	Cruise	0.999
2.7	Cruise	0.999
1.2	Acceleration	0.962
0.9	Cruise to Alternate	0.935
0	Sea-Level Take-Off	0.980

C_{FP} = [(Gross Thrust of Primary Flow and any Secondary Air) - (External Wave Drag and All Internal Losses)] / (Ideal Gross Thrust of Primary Flow)

The goal for thrust reversing is a minimum of 40 percent reverse thrust with no significant engine airflow suppression.

B. DISCUSSION

A systematic program, began in Phase IIA, to select and develop an operationally flexible and efficient exhaust nozzle system was continued in this contract period. Studies were aimed at optimization of a blow-in-door ejector for one version of the STF-219 turbofan engine cycle. All the originally predicted performance levels were met. Satisfactory nozzle performance for similar STF-219 versions could be achieved with the same general approach and available information.

DOWNGRADED AT 3 YEAR INTERVALS
DECLASSIFIED AFTER 12 YEARS
DOD DIR. 5200.10

1. FORWARD FLIGHT INVESTIGATIONS

The key simulated engine operating conditions, including take-off, subsonic cruise, transonic acceleration, and supersonic cruise, are summarized in Figure 7-1. A typical model is shown schematically in Figure 7-2. The experimental studies were conducted in the 17" x 17" transonic tunnel, the eight-foot main wind tunnel, and the main wind tunnel static cell at the UAC Research Laboratory.

Since the supersonic cruise condition is the most important operating point, the bulk of the research and development effort was concentrated on the ejector requirements for this particular case. In previous phases, the basic primary nozzle assembly, the external contour, and the exit diameter design parameters were established. The internal contour of the shroud was defined in Phase IIB by specifying the minimum diameter (D_s) and the position of this diameter (L_s) relative to the fan stream primary nozzle. These two parameters are very important since they control the initial expansion of the exhaust gases and influence the ejector's pumping characteristics. Figure 7-3, which is characteristically a "thumbprint", summarizes the results of the investigation. This figure indicates that the nozzle performance (C_{fp}) can be significantly improved if the minimum shroud diameter is optimized. Relative to a large gap ejector, having a C_{fp} of approximately 0.98, a gain of approximately two percent can be achieved by using a small gap configuration.

A small gap ejector would effectively reduce both the size and position of the minimum shroud diameter, while maintaining a certain relationship between them. A large range of geometric configurations is available for each level of desired performance. However, as the performance goal increases, the range of configurations becomes limited, but still remains multivalued.

At subsonic and transonic conditions, similar design studies were conducted to determine the off-design performance effects of the cruise requirements. The Mach 0, (max. duct heat), studies are summarized in Figure 7-4. At this condition, the blow-in-doors are open; therefore, the exit diameter strongly influences performance. Although the particular performance levels are also associated with specific geometric regions, a large area of the "thumbprint" can provide near maximum performance. Both the D_s and D_{exit} parameters are important, but a given change in the former is usually more significant. Internally cylindrical or near cylindrical shrouds generally have higher performance than the divergent configurations. The effect of spacing (L_s)

at static conditions is typically illustrated in Figure 7-5. There was essentially no spacing effect in a large part of the range considered. As the spacing ratio was reduced to very small values, a noticeable decrement in performance was obtained. This decrease was due to the severe restriction in blow-in-door area caused by the movement of L_S. These data were obtained from a statistical test program; extrapolation of the available data may be extremely critical. A fixed geometry shroud, which fulfills the supersonic cruise requirements, requires operation in the shaded region of Figure 7-4.

At subsonic cruise, the results of a similar study are shown in Figure 7-6. At Mach 0.9, the cylindrical shrouds were the best configuration. Both D_S and D_{exit} are equally important at this condition; all changes in performance are proportional to the divergence of the shroud. The influence of spacing (L_S) at these conditions is illustrated in Figure 7-5. A continuous drop in performance was experienced as the spacing ratio was reduced. This drop was attributed to the increased drag associated with the inlet geometry, which was required to provide the small spacing ratios and the severe reduction in blow-in-door area. The exact change with L_S is a function of the specific geometry being considered, but the illustrated effect is typical.

In both the static and subsonic cruise studies, the configurations were isolated models with all 12 blow-in-doors open. To evaluate the effect of blow-in-door blockage, two of the doors were blocked. The results shown in Figure 7-7 indicate that there is essentially no different between blocked and unblocked cases. The external flow being brought on board is still sufficient, and redistribution takes place internally with no losses.

At transonic acceleration, a similar test program was conducted with the blow-in-doors closed. At this condition the range of geometry required for maximum performance is somewhat smaller than the preceding cases, as illustrated in Figure 7-8. Due to the higher power setting at M = 1.2, the shrouds which provide maximum performance have divergent geometries. The improvement in C_{FP} provided by the divergent shroud as compared to a cylindrical shroud may be as high as 45%. Although testing has not been completed, it is reasonable to assume that the influence of spacing at this condition would be similar to that obtained at supersonic cruise. Unfortunately, more experimentation will be required to combine all the interactions between D_S, D_{exit}, and L_S.

These foregoing parametric studies at the four critical operating points indicate that the original performance goals are obtainable. Since the regions of high performance at each condition overlap, a practical configuration can be designed with a minimum of geometric variation to obtain the performance levels necessary for SST. The demonstrated levels for such a configuration are shown in Figure 7-9. At M = 0 and 1.2 (max. duct heat), the goals have been met. At subsonic cruise, the goal was exceeded by about one percent. At supersonic cruise, the performance of a fixed geometry ejector was below the required level by approximately one percent. However, if movable geometry is used to properly position the minimum internal shroud diameter, the goal can be achieved.

2. THRUST REVERSERS

The testing of a thrust reverser was the second major portion of the exhaust nozzle studies for the SST. The basic programs, initiated in Phase IIA and continued during Phase IIB, included the study of the reverser exit area blockage (targetting), reverser bleed flow, external flow effects, and trailing edge flap position. Figure 7-10 shows a typical configuration; Figure 7-11 illustrates the type of reverser area blockage considered.

Since targetting requirements are important in any airframe installation, a series of tests were conducted in which four, five, and six blow-in-doors out of a total of 12 were blocked as shown in Figure 7-11. The results shown in Figure 7-12 include a variation in bleed flow, both spoiled and unspoiled. (See Figure 7-10 for the spoiler configuration.) In general, the reverse thrust coefficient decreases as the blockage is increased. This decrease is due to the change in the effective discharge angle of the reversed gases, and the internal turning losses associated with redistribution of the exhaust flow. However, as the amount of bleed flow is increased, the rate of loss in performance with blockage decreases because less of the exhaust gases are discharged through the blow-in-doors. Flow coefficients were relatively unchanged with blockage.

The bleed flow associated with the reverser is another significant parameter. Bleed flow helps relieve engine suppression as well as reduces the amount of exhaust gases discharged through the blow-in-doors near the airframe. Spoiling the thrust associated with the bleed flow effectively produces a null thrust condition relative to the bleed flow. The effect of bleed flow upon reverser performance is indicated in Figure 7-13. The reverse thrust coefficient is shown to drop rapidly

as the bleed is increased. Approximately 25 percent bleed was sufficient to provide the reverser thrust coefficient goal of about 40 percent for most configurations.

The external flow effects are important in evaluating a thrust reverser due to the possibility of using inflight reversing. As shown in Figures 7-14 and 7-15, the reverse thrust coefficient increased rapidly with Mach number for the cases of both four and five doors blocked. The reverse thrust coefficient was increased as flight speeds increases since the base drag of the nozzle is increased with the reverser flaps extended. The data shown in Figures 7-14 and 7-15, were initially obtained using a configuration with the trailing edge flaps held at the maximum diameter position. To explore the effect of flap position on reverser performance, a series of tests were conducted with the flaps in both the "in" (minimum) and "out" (maximum) position. Pressure taps were installed to help establish the position to which the flaps would float. The results shown in Figure 7-16 indicate that the reverse thrust coefficient is higher when the trailing edge flaps are in the "in" position. This increase is caused by a combination of both external drag and base pressure effects in the reverser itself.

An analysis of the pressure tap data on the trailing edge flaps, indicated in Figure 7-17, revealed that the flaps tend to be completely "in" statically and move to the fully "out" position at Mach 0.4 and remain "out". The overall influence of external flow is shown in Figure 7-18, which summarizes the information in Figure 7-16 and 7-17 above Mach 0.4. A gradual performance increase at low subsonic speeds is indicated on Figure 7-18. A more rapid improvement occurs as the Mach number approaches 0.8, where the base pressure drag becomes increasingly important.

The test results conducted on the above reverser configurations indicate that a practical reverser scheme can be developed which will provide the necessary reverse thrust coefficients. Since the targetting requirements have not necessarily been finalized, large deviations from the above will necessitate further development to ensure the necessary reverser thrust levels without engine airflow suppression or inlet reingestion.

C. CONCLUSIONS

Significant advances have been made in achieving the original performance goals for the supersonic transport exhaust system during Phase IIB. The off-design performance goals at several key operating

conditions were met or exceeded; at supersonic cruise, the performance was within a fraction of one percent of the level predicted. Methods to eliminate this small supersonic cruise deficiency were sought and found. Wind tunnel testing in forward flight simulation amounted to 410 hours.

The experimental thrust reverser studies indicated that, even with rather severe targetting requirements, acceptable levels of reverse thrust coefficients with little or no engine airflow suppression could be achieved. Wind tunnel testing in reverse simulation amounted to 245 hours.

Although the overall results of the Phase IIB exhaust nozzle programs indicate excellent performance, areas still exist where additional exhaust nozzle efforts are needed to ensure a successful supersonic transport. These include:

1. A complete exhaust nozzle calibration over the entire flight spectrum using updated power settings to investigate and eliminate potentially troublesome conditions a freely floating flap co-annular blow-in door ejector has been fabricated and is available for testing to supplement this work.
2. An evaluation of thrust reversers for updated targetting requirements, and
3. An evaluation of installation effects between the exhaust system and the airframe.

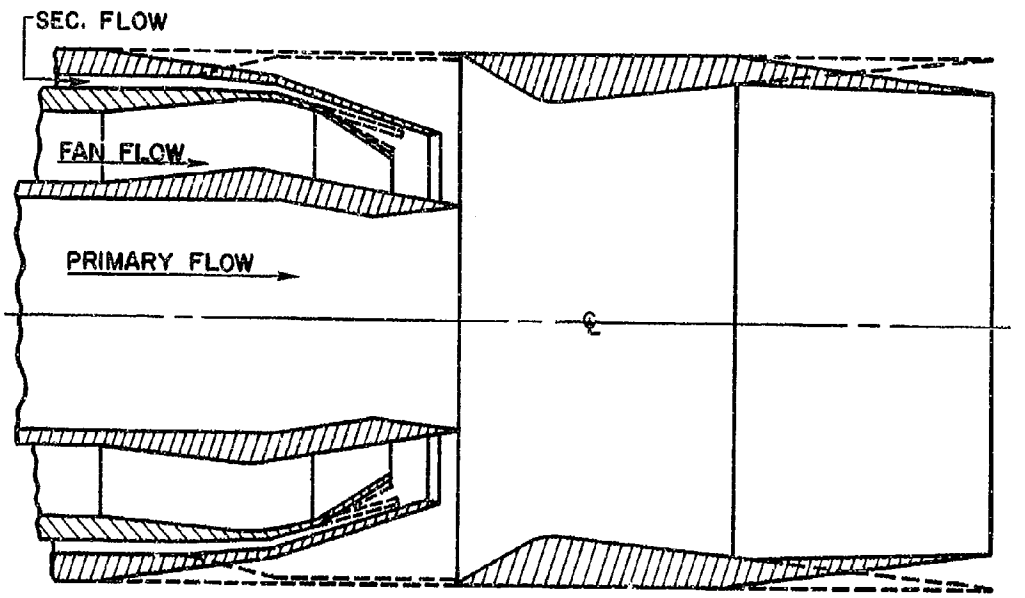
STF-219 ENGINE OPERATING CONDITIONS*
USED FOR EXHAUST NOZZLE MODELS

Nacelle Dia. = 80" (600 #/sec. Engine)

M_∞	Power	P_{te}/P_{am}	P_{tf}/P_{am}	A_iCd_e	A_iCd_f
0	S.L.T.O	2.13	2.42	4.96 ft^2	8.33 ft^2
0.9	Cruise	2.90	3.48	4.96	4.36
1.2	Max.D/H	5.19	5.84	4.96	8.47
2.7	Cruise	14.68	29.08	4.96	5.46
0	Reverse	2.00	2.10	4.96	4.00

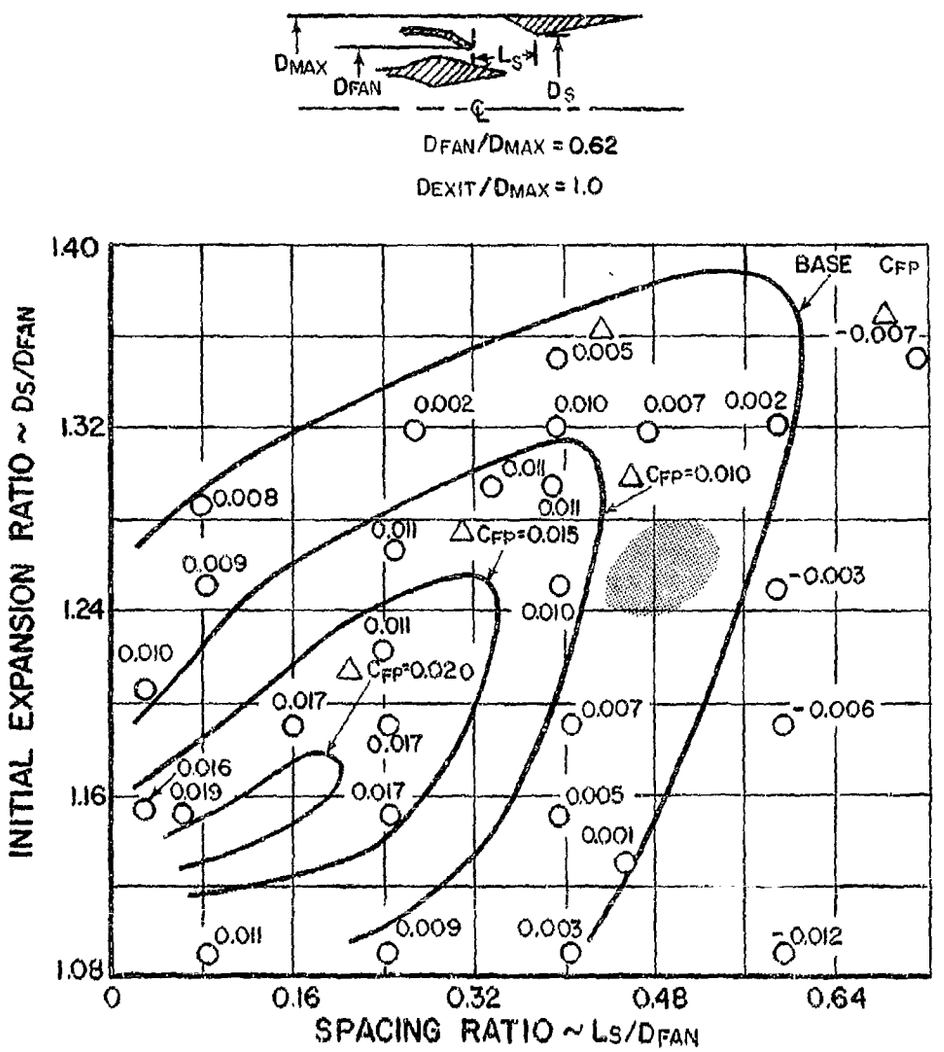
* The final engine conditions used in the model specification differ slightly from these early values.

Figure 7-1



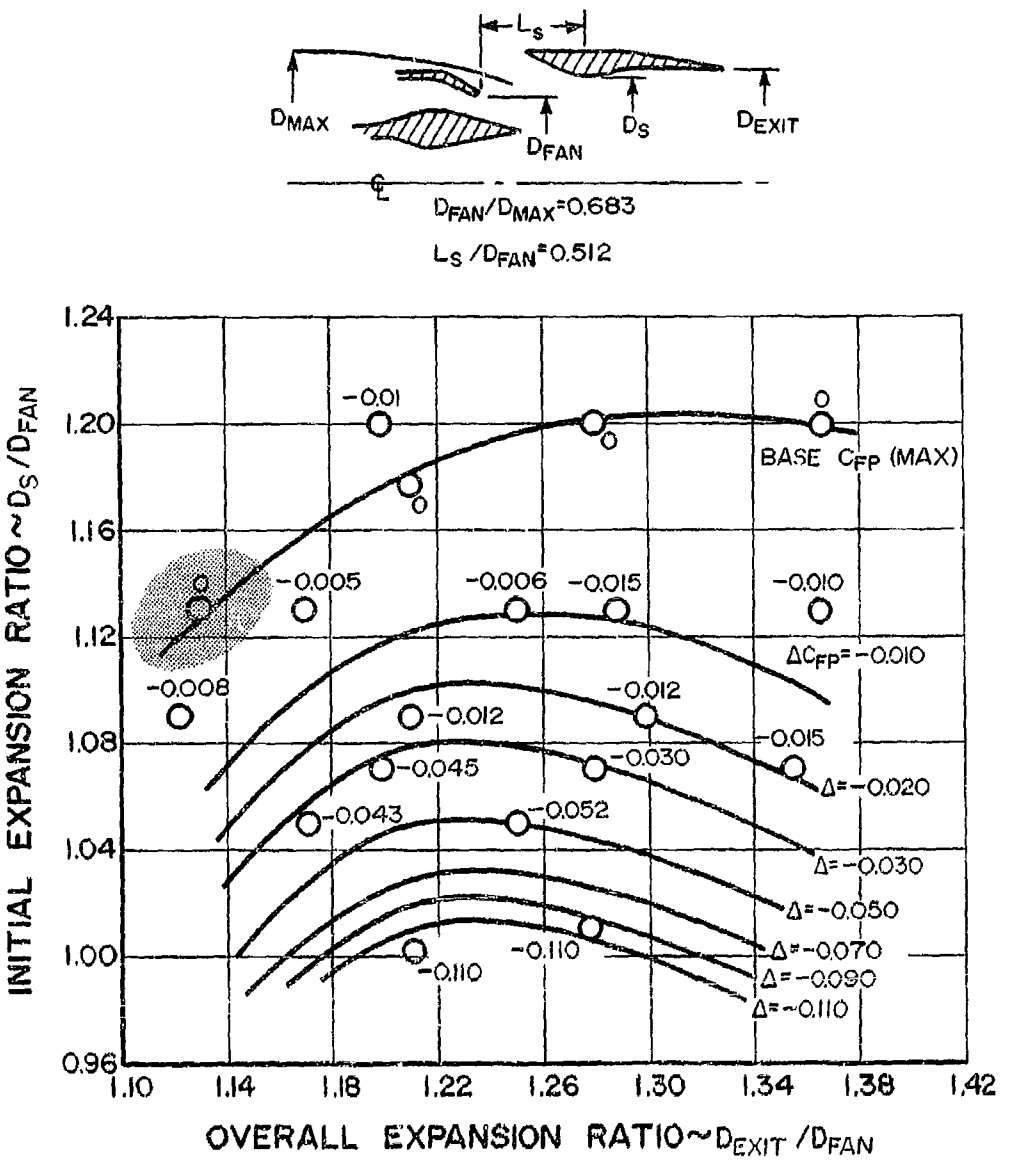
CO-ANNULAR BLOW-IN-DOOR EJECTOR

Figure 7-2



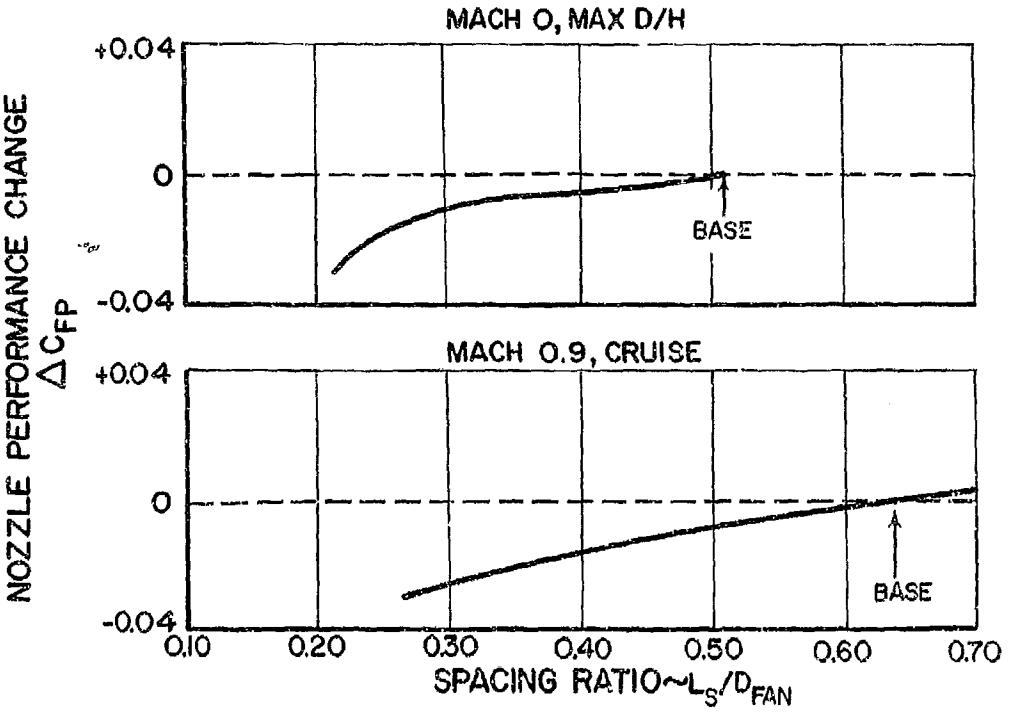
EFFECT OF INTERNAL SHROUD GEOMETRY AT SUPERSONIC CRUISE

Figure 7-3



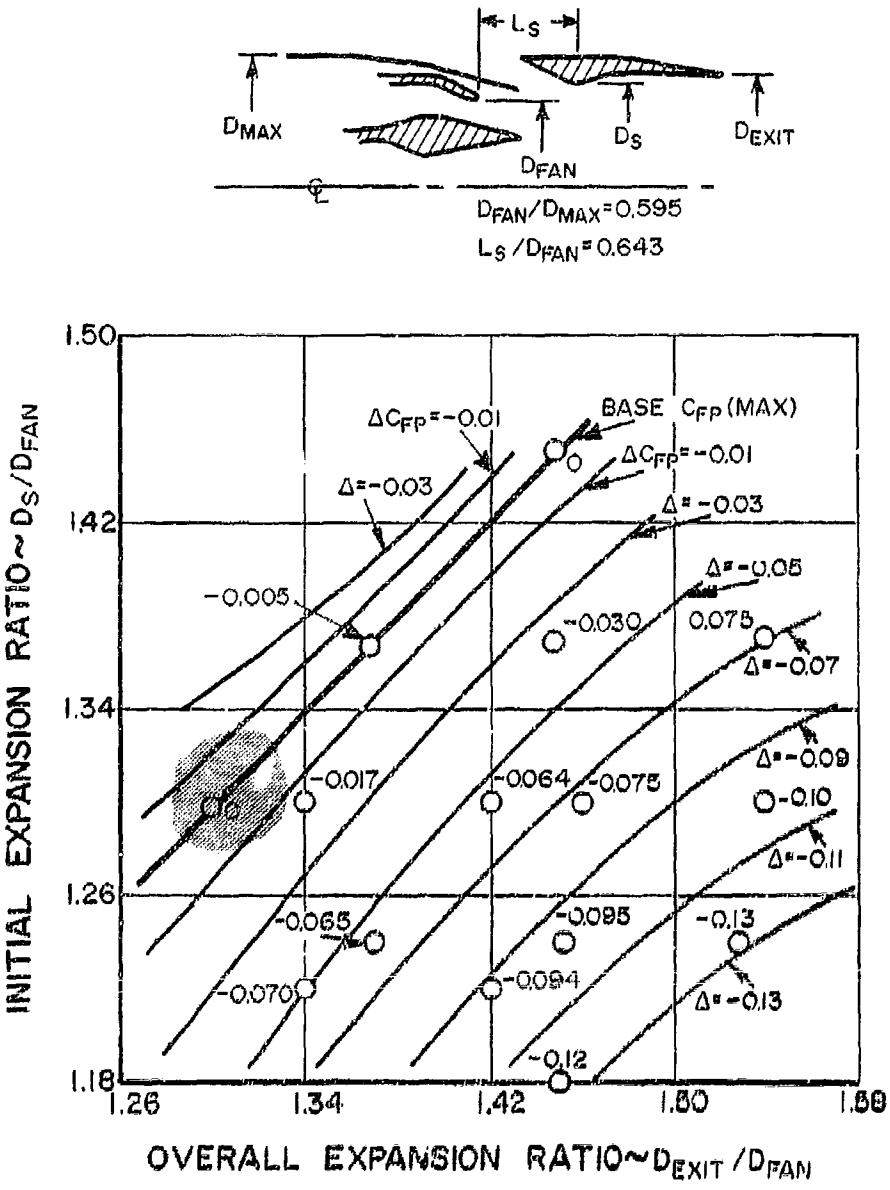
EFFECT OF INTERNAL SHROUD GEOMETRY AT SEA LEVEL STATIC WITH MAXIMUM DUCT HEAT

Figure 7-4



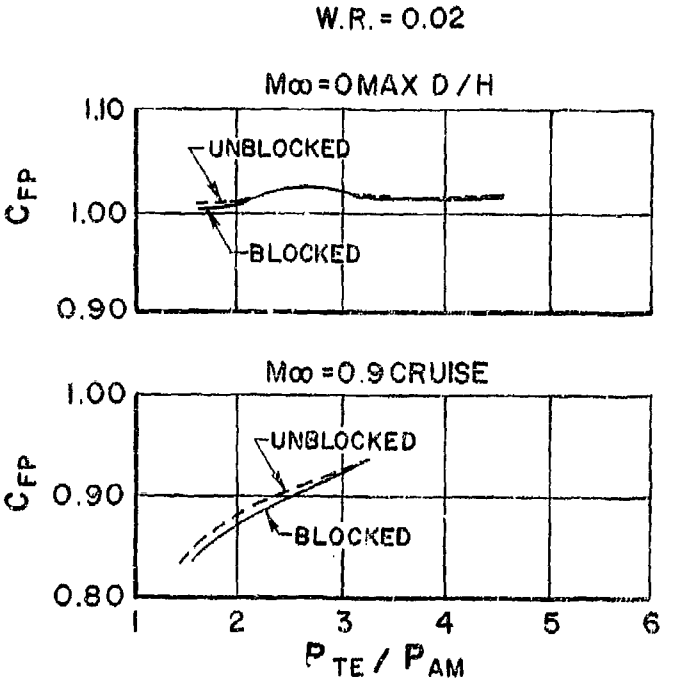
TYPICAL EFFECTS OF SHROUD SPACING RATIO FOR SUBSONIC CONDITIONS

Figure 7-5



EFFECT OF INTERNAL SHROUD GEOMETRY AT SUBSONIC CRUISE (MACH 0.9)

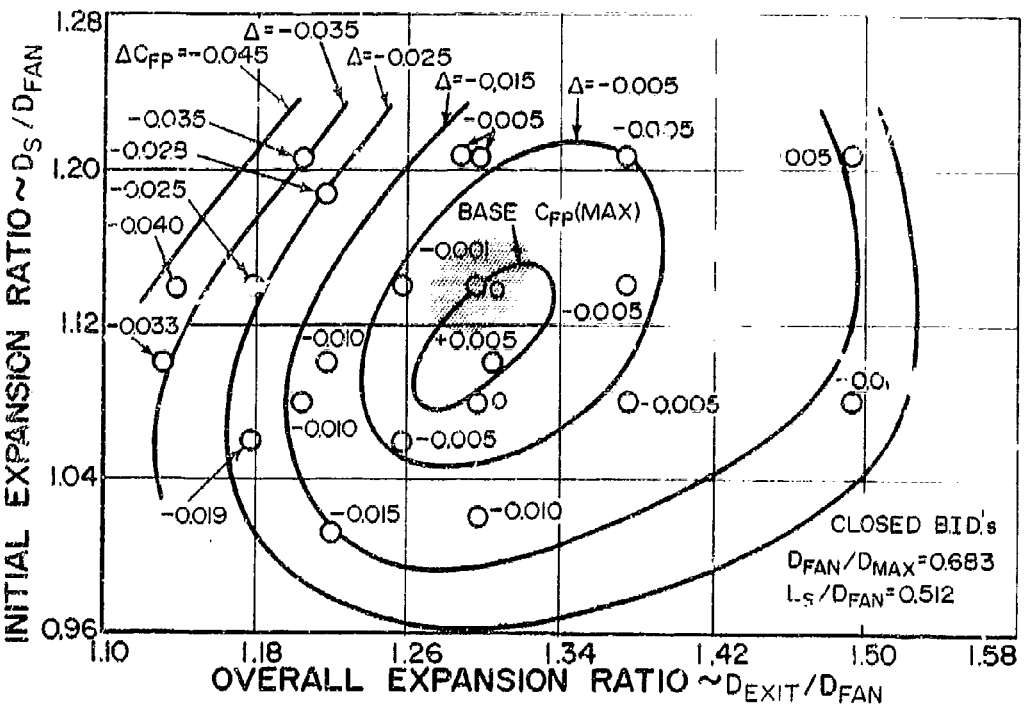
Figure 7-6



EFFECT OF BLOCKING TWO OF TWELVE BLOW-IN-DOORS

Figure 7-7

DOWNGRADED AT 3 YEAR INTERVALS
DECLASSIFIED AFTER 12 YEARS
DOD DIR 5200.10

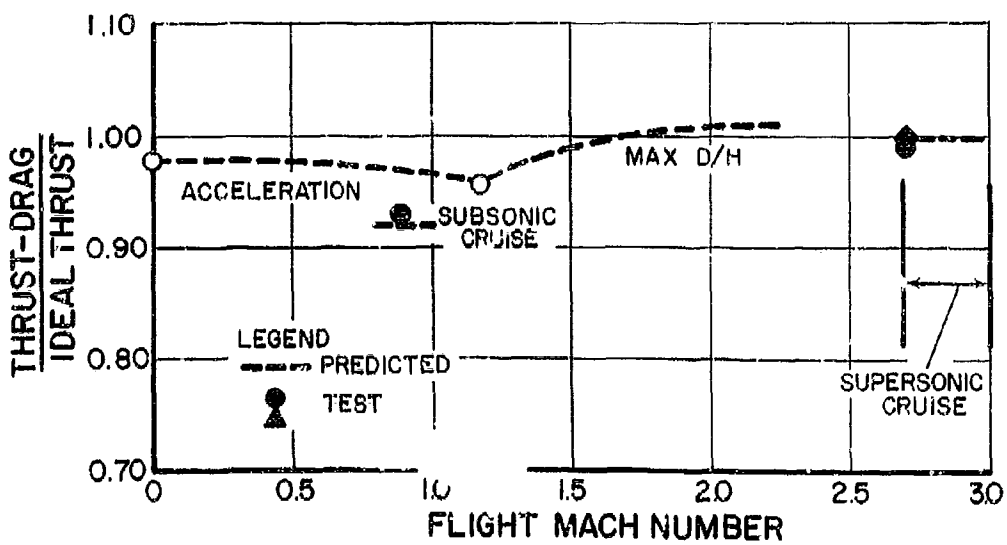


EFFECT OF INTERNAL SHROUD GEOMETRY AT TRANSONIC ACCELERATION (MACH 1.2)

Figure 7-8

DOWNGRADED AT 3 YEAR INTERVALS
DECLASSIFIED AFTER 12 YEARS
DOD DIR 5200.10

THIS DOCUMENT CONTAINS INFORMATION AFFECTING THE NATIONAL DEFENSE OF THE UNITED STATES WITHIN THE MEANING OF THE ESPIONAGE LAWS, TITLE 18, U.S.C., SECTIONS 793 AND 794. THE TRANSMISSION OR THE REVELATION OF ITS CONTENTS IN ANY MANNER TO AN UNAUTHORIZED PERSON IS PROHIBITED BY LAW.

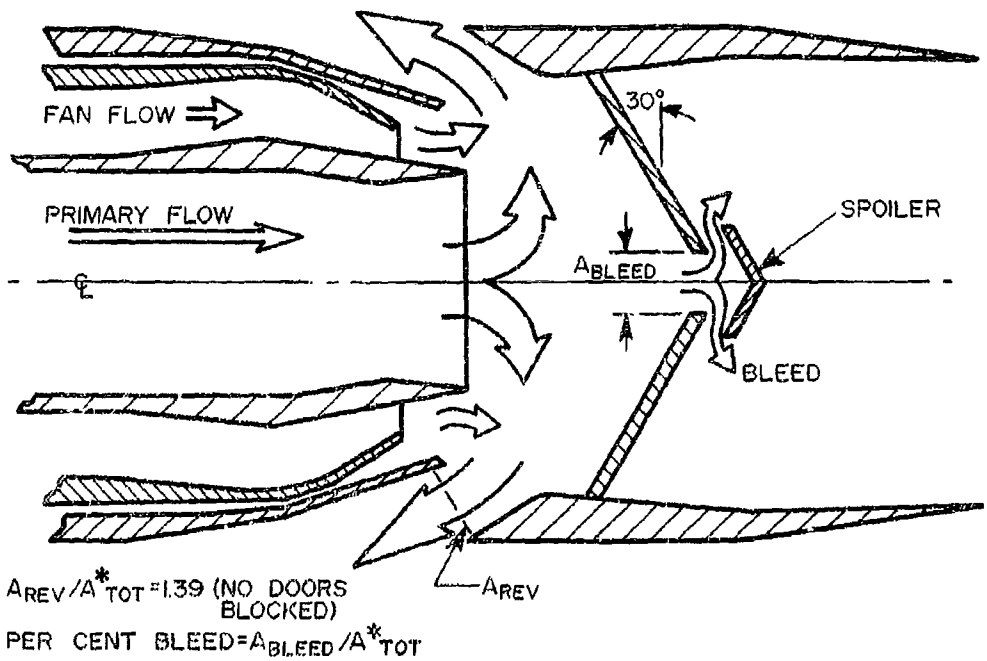


SCALE MODEL STF219 BLOW-IN-DOOR EJECTOR PERFORMANCE

Figure 7-9

DOWNGRADED AT 3 YEAR INTERVALS
DECLASSIFIED AFTER 12 YEARS
DOD DIR 5200.10

THIS DOCUMENT CONTAINS INFORMATION AFFECTING THE NATIONAL DEFENSE OF THE UNITED STATES WITHIN THE MEANING OF THE ESPIONAGE LAWS, TITLE 18, U.S.C., SECTIONS 793 AND 794. THE TRANSMISSION OR THE REVELATION OF ITS CONTENTS IN ANY MANNER TO AN UNAUTHORIZED PERSON IS PROHIBITED BY LAW.

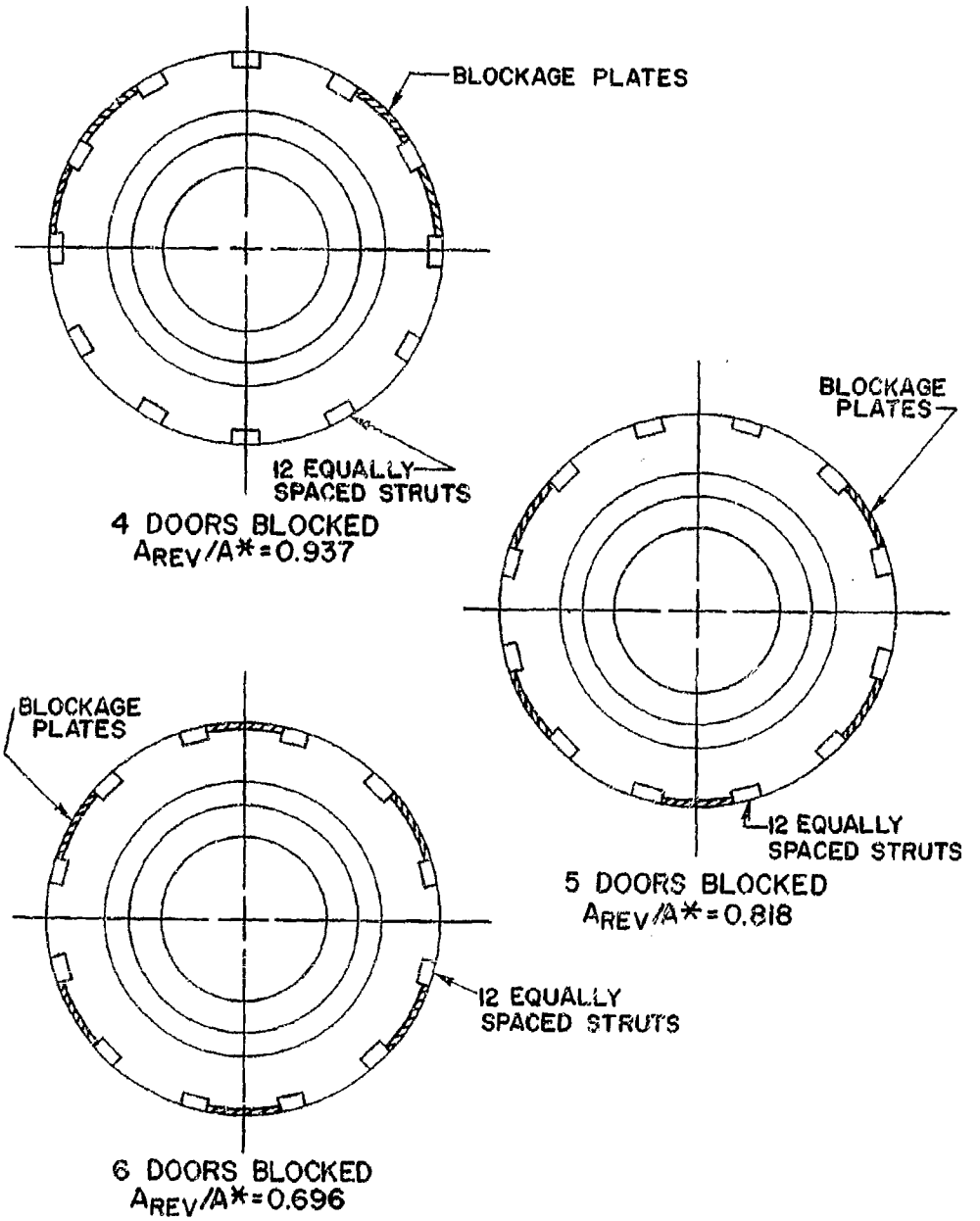


SCHEMATIC THRUST REVERSER

Figure 7-10

DOWNGRADED AT 3 YEAR INTERVALS
DECLASSIFIED AFTER 12 YEARS
DOD DIR 5200.10

THIS DOCUMENT CONTAINS INFORMATION AFFECTING THE NATIONAL DEFENSE OF THE UNITED STATES WITHIN THE MEANING OF THE ESPIONAGE LAWS, TITLE 18, U.S.C., SECS. 793 AND 794. THE TRANSMISSION OR THE REVELATION OF ITS CONTENTS IN ANY MANNER TO AN UNAUTHORIZED PERSON IS PROHIBITED BY LAW.

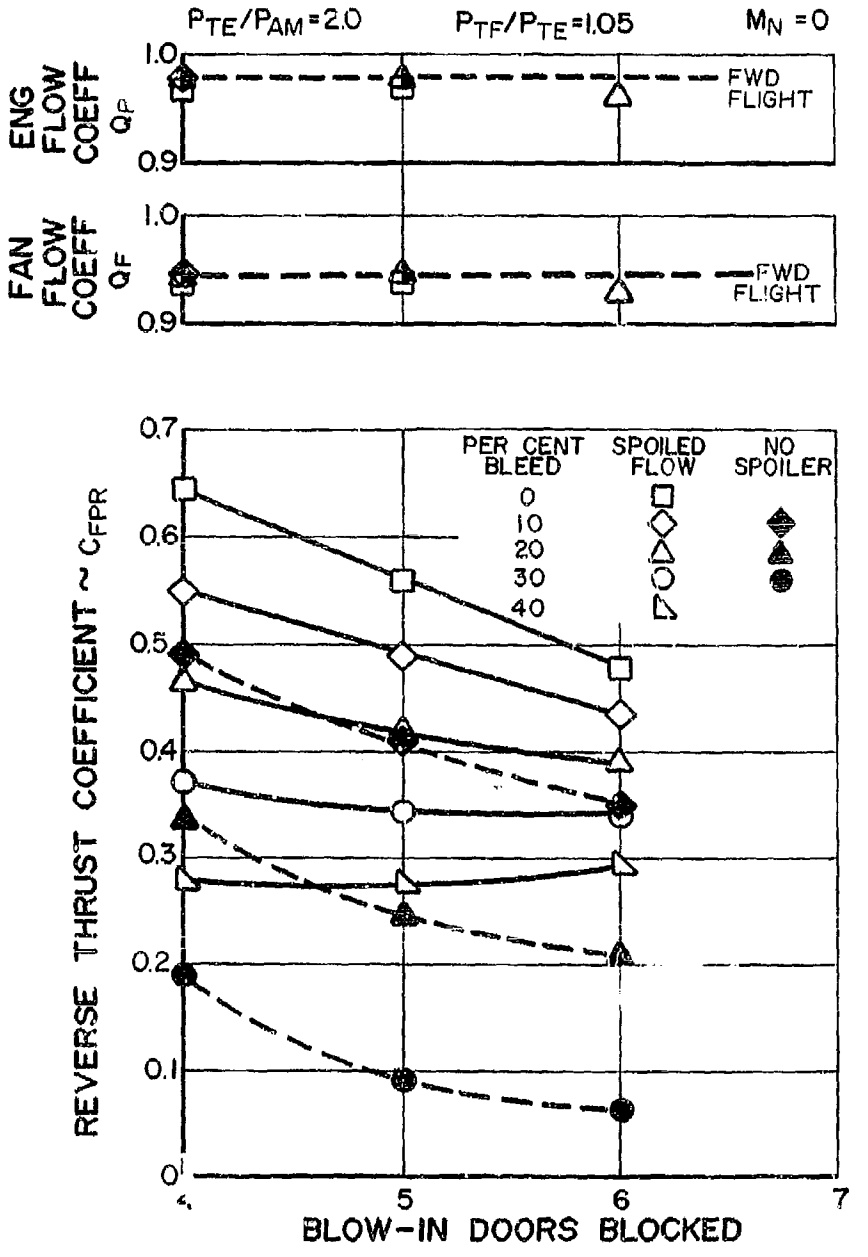


THRUST REVERSER BLOW-IN-DOOR BLOCKAGE

Figure 7-11

DOWNGRADED AT 3 YEAR INTERVALS
DECLASSIFIED AFTER 12 YEARS
DOD DIR 5200.10

THIS DOCUMENT CONTAINS INFORMATION AFFECTING THE NATIONAL DEFENSE OF THE UNITED STATES WITHIN THE MEANING OF THE ESPIONAGE LAWS, TITLE 18, U.S.C., SECTIONS 793 AND 794. THE TRANSMISSION OR THE REVELATION OF ITS CONTENTS IN ANY MANNER TO AN UNAUTHORIZED PERSON IS PROHIBITED BY LAW.

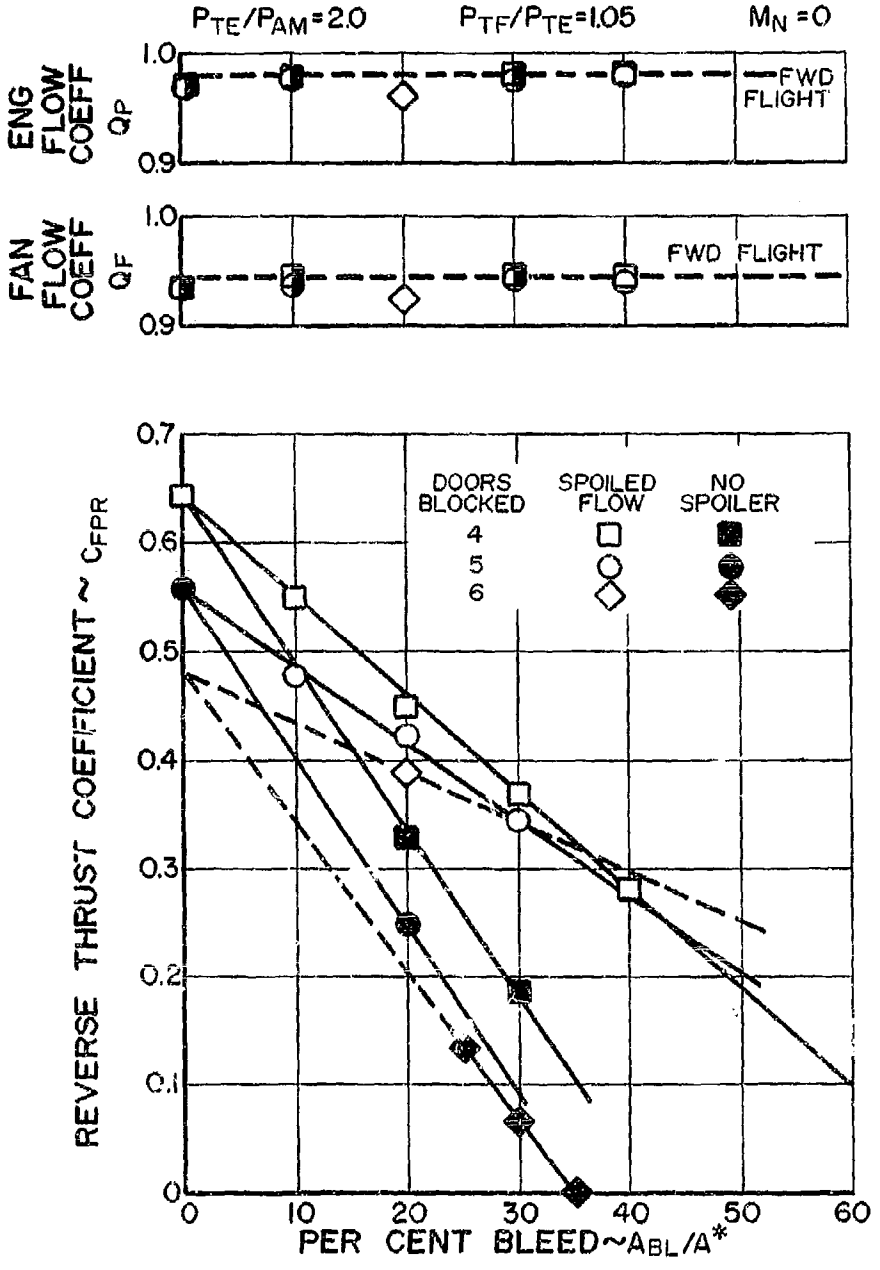


EFFECT OF BLOW-IN-DOOR BLOCKAGE

Figure 7-12

DOWNGRADED AT 3 YEAR INTERVALS
DECLASSIFIED AFTER 12 YEARS
DOD DIR 5200.10

THIS DOCUMENT CONTAINS INFORMATION AFFECTING THE NATIONAL DEFENSE OF THE UNITED STATES WITHIN THE MEANING OF THE ESPIONAGE LAWS, TITLE 18, U.S.C., SECTIONS 793 AND 794. ITS TRANSMISSION OR THE REVELATION OF ITS CONTENTS IN ANY MANNER TO AN UNAUTHORIZED PERSON IS PROHIBITED BY LAW.

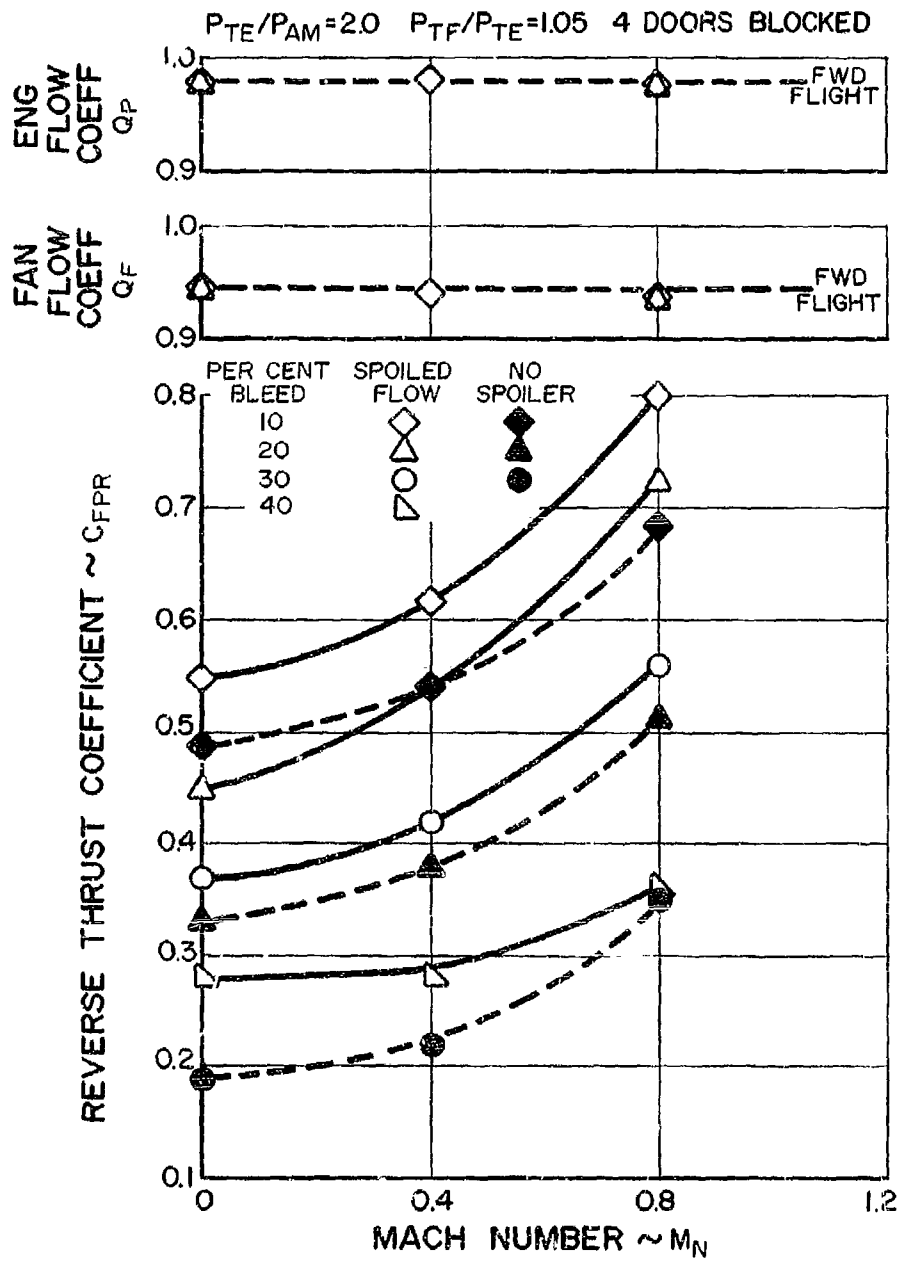


EFFECT OF REVERSER BLEED FLOW

Figure 7-13

DOWNGRADED AT 3 YEAR INTERVALS
DECLASSIFIED AFTER 12 YEARS
DOD DIR 5200.10

THIS DOCUMENT CONTAINS INFORMATION AFFECTING THE NATIONAL DEFENSE OF THE UNITED STATES WITHIN THE MEANING OF THE ESPIONAGE LAWS, TITLE 18 U.S.C. SECTIONS 793 AND 794. ITS TRANSMISSION OR THE REVELATION OF ITS CONTENTS IN ANY MANNER TO AN UNAUTHORIZED PERSON IS PROHIBITED BY LAW.

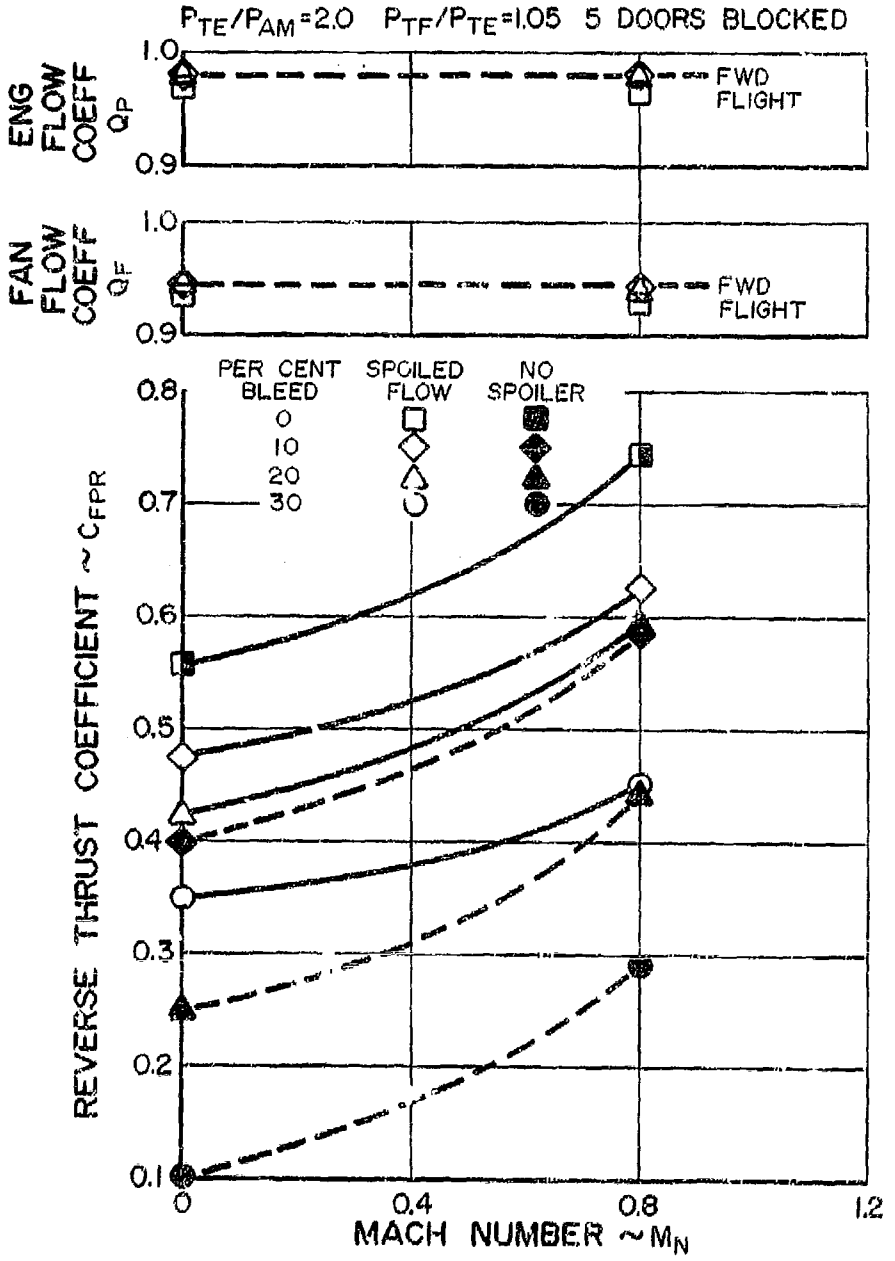


TYPICAL EFFECT OF FLIGHT MACH NUMBER WITH FOUR DOORS BLOCKED

Figure 7-14

DOWNGRADED AT 3 YEAR INTERVALS
DECLASSIFIED AFTER 12 YEARS
DOD DIR 5200.10

THIS DOCUMENT CONTAINS INFORMATION AFFECTING THE NATIONAL DEFENSE OF THE UNITED STATES WITHIN THE MEANING OF THE ESPIONAGE LAWS, TITLE 18 U.S.C. SECTIONS 793 AND 794. ITS TRANSMISSION OR THE REVELATION OF ITS CONTENTS IN ANY MANNER TO AN UNAUTHORIZED PERSON IS PROHIBITED BY LAW.

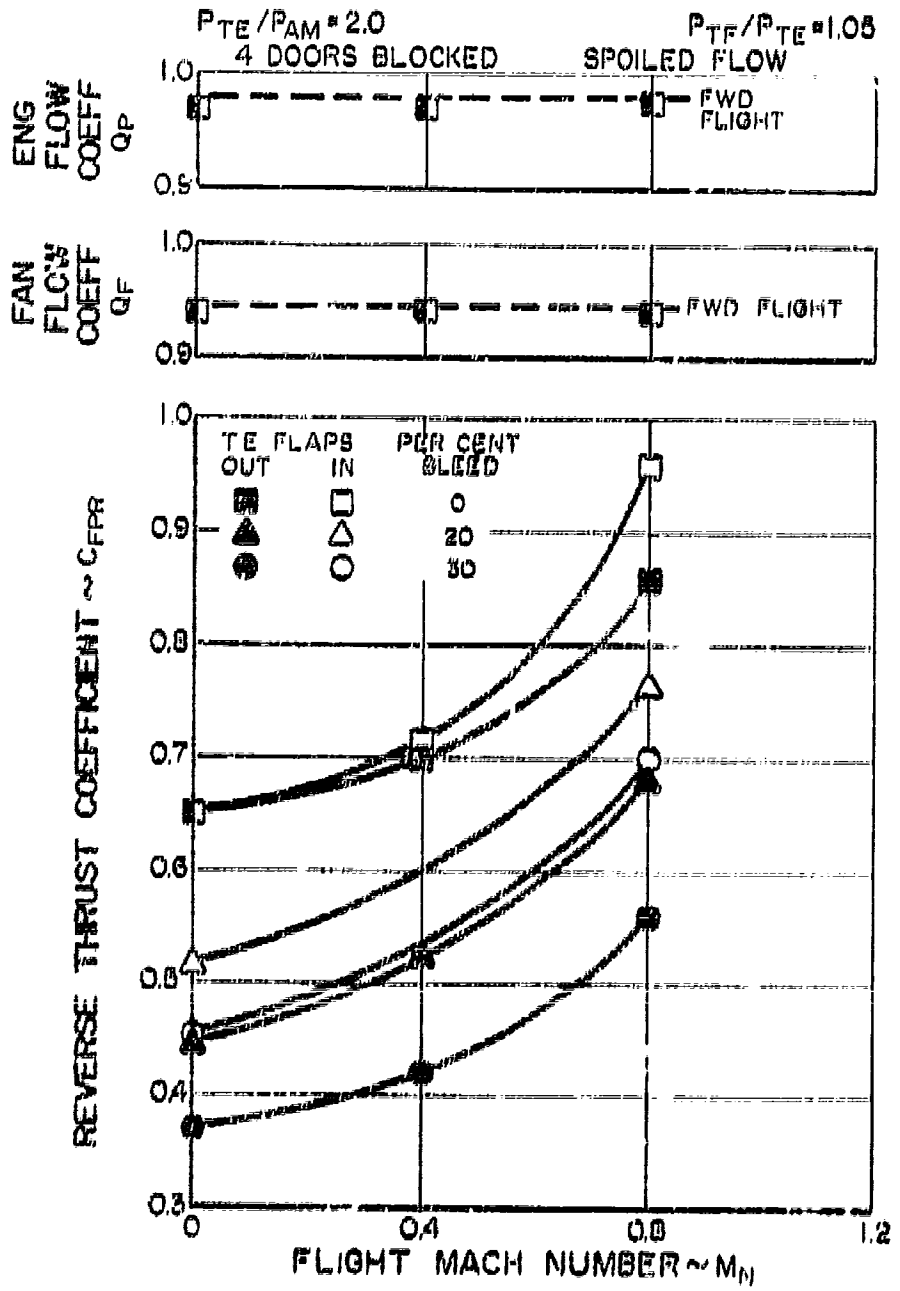


TYPICAL EFFECT OF FLIGHT MACH NUMBER WITH FIVE DOORS BLOCKED

Figure 7-15

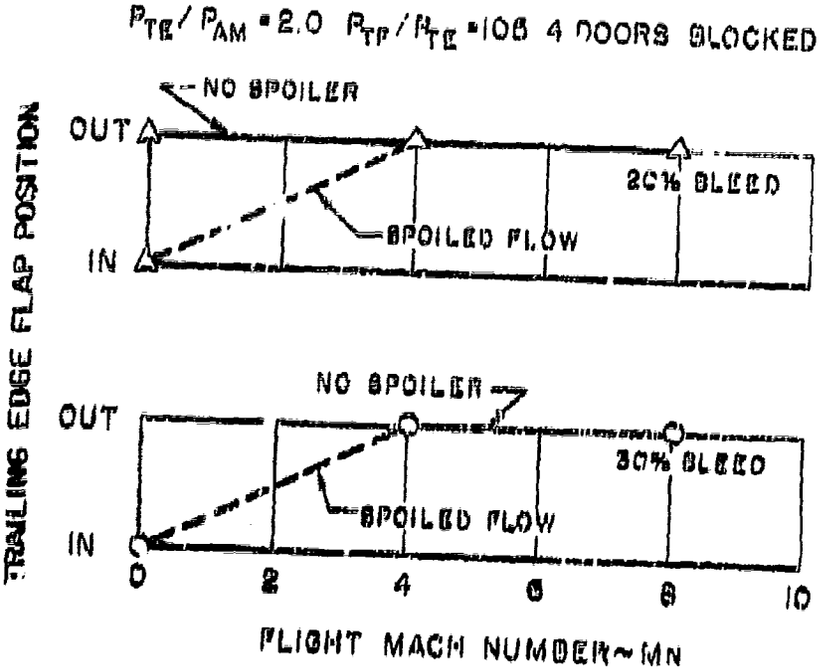
DOWNGRADED AT 3 YEAR INTERVALS
DECLASSIFIED AFTER 12 YEARS
DOD DIR 5200.10

THIS DOCUMENT CONTAINS INFORMATION AFFECTING THE NATIONAL DEFENSE OF THE UNITED STATES WITHIN THE MEANING OF THE ESPIONAGE LAWS, TITLE 18, U.S.C., SECTIONS 793 AND 794. THE TRANSMISSION OR REVELATION OF ITS CONTENTS IN ANY MANNER TO AN UNAUTHORIZED PERSON IS PROHIBITED BY LAW.



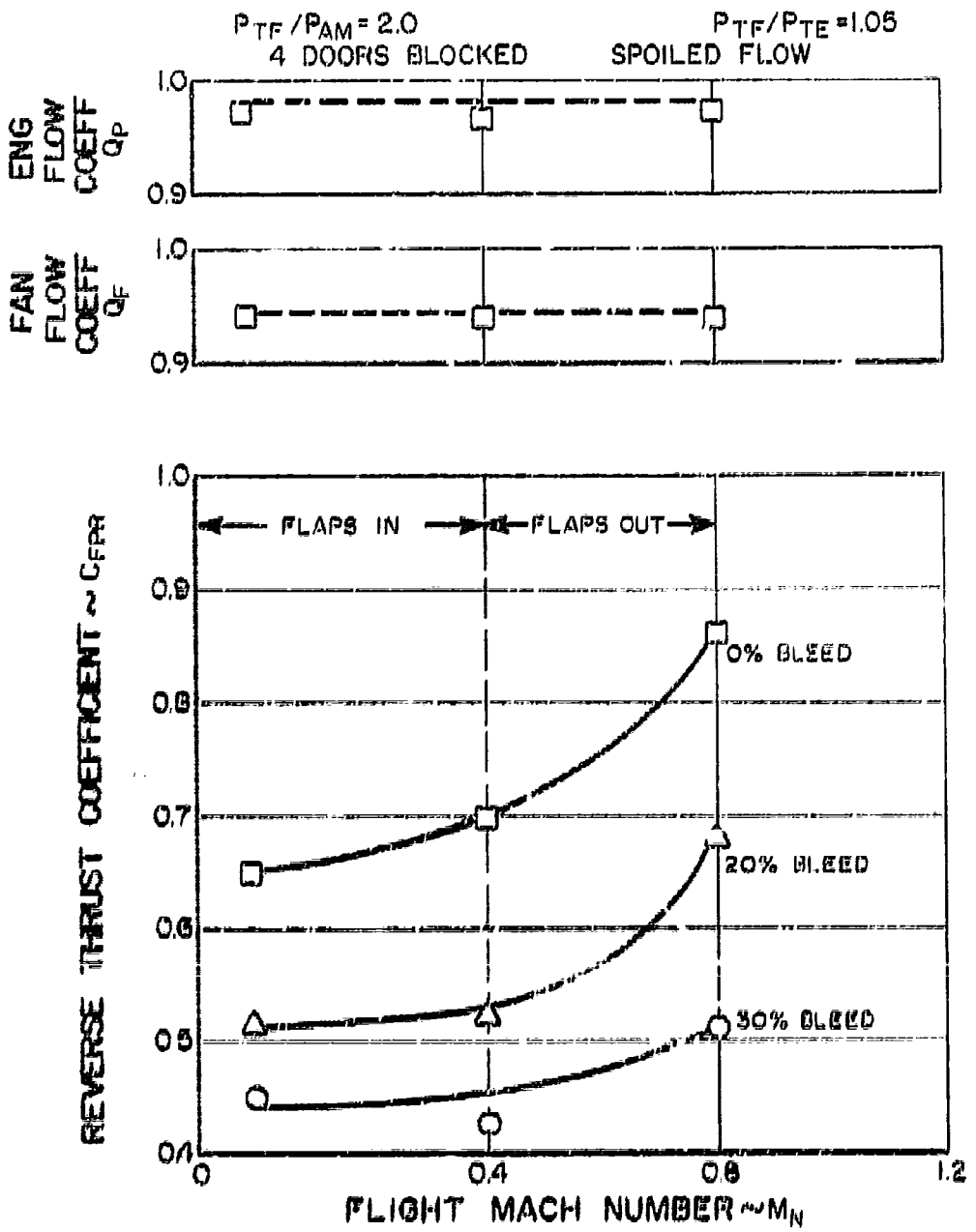
INFLUENCE OF TRAILING EDGE FLAP POSITION ON MACH NUMBER WITH SPOILED FLOW

Figure 7-16



EFFECT OF TRAILING EDGE FLAP POSITION ON MACH NUMBER FOR 20% AND 30% BLEED

Figure 7-17



SIMULATED FREE FLAP NOZZLE PERFORMANCE

Figure 7-18

ITEM 8

NOISE REDUCTIONS

ITEM 8

ITEM 8 - NOISE REDUCTION

OBJECTIVE

The objective of the noise reduction investigations was to obtain information on noise suppression devices and techniques which could be incorporated into the design of the SST airplane. During Phase II-B of the program, variations of inlets, nozzles, full-scale blow-in-door ejectors, and sound absorbing materials were tested to determine their effect on noise propagation. The specific goal of this program was to obtain information which may be used to meet or better the FAA specified noise levels of: 1) 116 PNdb at 1500 feet from the centerline of the runway during the take-off roll, 2) 105 PNdb at a point three miles from the start of the take-off roll, and 3) 109 PNdb during approach at a point one mile from the runway threshold.

A. INTRODUCTION

Since the advent of commercial aviation, there has been a trend toward noisier airplanes. This trend, coupled with large increases in population in the vicinity of most major airports, has resulted in some serious noise problems. In many instances, organized community action groups have been formed and are attempting to initiate legal actions which could adversely affect the growth of commercial air transportation. It is hoped that, through the integration of noise considerations into the design of the SST, the trend toward noisier airplanes can be halted or reversed.

Reversing this trend will be quite difficult, particularly when the important requirements for safe and economical operation are met. As shown in Figure 8-1, the basic powerplants to be used on the SST will be capable of generating substantially more noise than those used on past and current airplanes. The potentially large increase in powerplant noise production need not, however, reflect a similar increase in community noise. As the SST airplanes will be overpowered for take-off, some noise relief may be obtained from the use of special take-off procedures.

DOWNGRADED AT 3 YEAR INTERVALS
DECLASSIFIED AFTER 12 YEARS
DOD DIR 5200.10

The use of suppression devices could further reduce the noise from the SST. Test activity during Phase II-B of the SST engine study was directed toward the investigation of suppression devices which could be incorporated into the design of SST powerplant designs being developed by Pratt & Whitney Aircraft.

B. INLET DUCT SOUND PROPAGATION CHARACTERISTICS

1. GENERAL

Incorporated into the design of the forward compressor stages of the SST engines designed by Pratt & Whitney Aircraft are several features which should minimize the generation of blade passing frequency noise. Among these features are the omission of inlet guide vanes, a large number of stator vanes, and ample spacing between rotor blades and stator vanes. The effect on noise of these features has been demonstrated during previous tests conducted on a 28-inch diameter compressor rig and reported in Report No. PWA-2353. Further changes in the compressor design for low noise generation would result in very substantial increases in engine weight.

The most promising means of further reducing the compressor noise from the SST without increasing the engine weight involves development of the long supersonic inlet duct to provide noise suppression. Results of tests conducted during Phase II-A indicated that supersonic inlets provided opportunities to incorporate compressor noise control features which could not be installed in the short-length inlets used on subsonic jets. The long ducts have a large internal surface area on which acoustical treatment may be installed. Variable inlet geometry, incorporated in all supersonic inlets to ensure acceptable pressure recovery characteristics over a wide range of flight Mach numbers, provides the opportunity to choke or nearly choke the inlet during the landing approach. Phase II-A test results indicated that both these features could be employed successfully to suppress compressor noise.

Noise tests of inlet ducts were conducted during Phase II-B to further investigate the effects on noise of supersonic inlet ducts. The 28-inch diameter compressor rig, used in previous phases of the program, was used for this series of tests. A more detailed description of the facility is given in the SST Phase IIA Report No. PWA-2397.

Model inlet ducts, patterned after both the Boeing axisymmetrical design and the two-dimensional inlet planned for the Lockheed SST, were fabricated during Phase II-A. These inlets, shown in Figures 8-2 and

DOWNGRADED AT 3 YEAR INTERVALS
DECLASSIFIED AFTER 12 YEARS
DOD DIR 5200.10

8-3, were used for the Phase II-B tests. About 78 hours of running time were logged on the 28-inch diameter rig during Phase II-B inlet duct noise tests. Inlet duct configurations tested and a summary of test results are shown in Figure 8-4.

2. CONCLUSIONS

From the results of the tests, the following conclusions can be drawn:

Compressor blade and vane numbers do not significantly affect the noise attenuation with near-sonic velocity duct flow.

With all configurations tested, substantial noise reductions were measured as the duct flow velocity increased above about 0.7 Mach number.

Feltmetal is an effective sound absorbing material and is potentially useful for lining supersonic inlet ducts.

The effect on noise of boundary layer bleed is small.

Compressor whine during approach will probably be less objectional if the inlet blow-in doors are closed.

3. RECOMMENDATIONS

Results of this test series have indicated several compressor noise suppression features which can be incorporated in the design of supersonic inlets, some features which are not effective, and others which may aggravate the noise problem. Further model inlet noise studies probably would not produce significant new results. It is recommended that no further tests be conducted until full-scale hardware is available. Results of these tests will be made available to the airplane contractors for their consideration in the design of inlet ducts.

4. DISCUSSION OF RESULTS

The series of tests conducted were designed to investigate the effect on noise of four basic parameters or features which are incorporated in the design of most supersonic inlet ducts. Results from the four basic series are discussed in the following paragraphs.

DOWNGRADED AT 3 YEAR INTERVALS
DECLASSIFIED AFTER 12 YEARS
DOD DIR 5200.10

a. Effect of Duct Mach Number on Noise Attenuation

Phase II-A test results showed that a significant reduction in noise resulted from operation of the inlet duct in the near-choked flow condition. It was, however, not clear whether the sound attenuation at a given duct flow Mach number was affected by the details of the "spinning mode" sound patterns which propagate compressor noise energy out the inlet duct. The composition of these patterns is determined by the combination of blade and vane numbers used in the compressor. It was speculated that judicious choice of a blade-vane number combination could enhance the acoustical effectiveness of an inlet duct having high velocity subsonic flow.

Acoustic tests to investigate the effect on sound propagation of changes in blade-vane number were conducted using the following rig configurations.

Config.	No. of Blades	No. of Vanes	Duct Throat Area, Ft^2	Centerbody Shape	Mode Shape
3-B-0	32	18	4.3	Cylindrical	+14, -4 & -22 lobe*
3-B-1	32	18	2.51	Expanded	+14, -4 & -22 lobe
4-B-0	32	32	4.3	Cylindrical	0 lobe (plane wave)
4-B-1	32	32	2.51	Expanded	0 lobe (plane wave)
4-B-2	32	32	2.14	Expanded	0 lobe (plane wave)
5-B-0	32	46	4.3	Cylindrical	-14 lobe
5-B-1	32	46	2.51	Expanded	-14 lobe
5-B-2	32	46	2.14	Expanded	-14 lobe

* Negative lobe number indicates sound pattern rotation that is opposite to rotor rotation.

As shown by this tabulation, the selected combinations resulted in a variety of "spinning mode" patterns, including a plane wave. A plane wave was of particular interest as it propagated acoustical energy directly opposite to the direction of airflow, rather than along a helical path as was the case with all other patterns. It was expected that the plane wave noise would be the most difficult to attenuate with high subsonic velocity flow.

Attenuation as a function of duct flow Mach number is plotted in Figure 8-5 for all three blade-vane combinations and inlets tested. As shown by the curves, some change in attenuation at a given flow Mach number

DOWNGRADED AT 3 YEAR INTERVALS
DECLASSIFIED AFTER 12 YEARS
DOD DIR 5200.10

was measured with the configurations tested. At high Mach numbers, a substantial attenuation was noted for all configurations tested.

Absolute noise levels as a function of duct Mach number for the three blade-vane configurations, with and without a choked inlet duct, are shown in Figure 8-6. The 32-vane configuration which generated plane wave compressor noise was substantially more noisy than either the 18-vane configuration which generated several spinning modes or the 46-vane configuration which more nearly simulated the modal pattern incorporated in the design of the STF219 SST engine.

Also tested was the two-dimensional inlet duct with two centerbody positions which resulted in throat areas of 3.8 and 1.7 square feet. Test results shown in Figure 8-7 illustrate that compressor noise can be effectively attenuated with nearly-choked flow in a rectangular duct as well as a cylindrical duct.

b. Sound Absorbing Duct Linings

Tests of a Fiberglas-lined inlet duct were conducted during Phase II-A and a substantial noise attenuation was measured. This demonstrated that noise reduction could be achieved by the use of sound absorbing linings in an SST inlet duct. Because of the high temperatures expected in the inlet duct at cruise speeds, Fiberglas will not be satisfactory as a duct lining material. A series of tests was conducted to determine the acoustical effectiveness of Feltmetal, a potentially suitable material. This material is formed from a sintered mat of thread-like stainless steel fibers and is commercially available in a wide variety of sheet thicknesses and densities.

Noise levels were measured during several tests in which Feltmetal liners were installed on the inside of the outer duct wall. About 1 1/4 inches of space was left between the liners and the solid wall. Results of the tests indicated that:

Sound attenuation increased with the length of the liner as shown in Figure 8-8.

Attenuation decreased at higher duct flow velocities as shown in Figures 8-9 and 8-10.

The 1/8-inch thick material was about as acoustically effective as the 1/4-inch thick material.

DOWNGRADED AT 3 YEAR INTERVALS
DECLASSIFIED AFTER 12 YEARS
DOD DIR 5200.10

The material appeared to be two to three db more effective when located in the subsonic flow section of the inlet, near to the compressor.

The attenuation of the lining was not particularly sensitive to frequency as shown by Figure 8-11.

c. Boundary Layer Bleed

Boundary layer thickness control devices are incorporated in the design of most supersonic flow inlet ducts. These devices usually consist of a perforated duct wall through which the stagnant boundary layer is extracted. To investigate the effect on noise of perforated liners with various boundary layer flow rates, a series of perforated liners were installed and tested on model supersonic inlets installed on the 28-inch diameter rig. Noise levels were measured while flow was both extracted from and added to the boundary layer by connecting the bleed compartment to either a vacuum or a pressure air supply. Results of the tests showed the bleed flow to have an insignificant effect on noise.

d. Inlet Blow-In Doors

Blow-in doors are incorporated in the design of sharp-lipped supersonic inlet ducts to compensate for the poor flow recovery factors which are inherent at low speed and static operation. At a given operating condition, it was expected that compressor noise levels would increase if the doors were open, as wakes from the doors were expected to extend downstream into the pressure field of the rotor.

Results of tests with the inlet blow-in doors open were compared with results of tests conducted during Phase II-A on a similar configuration except that the doors were closed. An increase of from two to four db in the noise level was noted, and the noise was observed to have a less random quality, the discrete blade passing frequency tones becoming much more audible.

5. ANALYSIS OF RESULTS

The most effective inlet noise suppression scheme, and the least expensive in terms of added weight, appears to be a choked or nearly-choked inlet. If the requirements for fail-safe operation in the event of an aborted landing can be met, inlet noise from the SST can be reduced to levels well below that of current jet transports.

DOWNGRADED AT 3 YEAR INTERVALS
DECLASSIFIED AFTER 12 YEARS
DOD DIR 5200.10

THIS DOCUMENT CONTAINS INFORMATION AFFECTING THE NATIONAL DEFENSE OF THE UNITED STATES WITHIN THE MEANING OF THE ESPIONAGE LAWS, TITLE 18, U.S.C., SECTIONS 793 AND 794. THE TRANSMISSION OR THE REVELATION OF ITS CONTENTS IN ANY MANNER TO AN UNAUTHORIZED PERSON IS PROHIBITED BY LAW.

Duct lining is equally effective and may offer a safer solution to the inlet noise problem. Any inlet design incorporating an acoustic lining would, however, probably result in an increase in airplane weight.

The series of tests on lined inlets was conducted using the asymetrical inlet duct because its shape made configuration changes relatively simple. It is safe to assume that equally satisfactory noise attenuation would result from properly installing the lining material in a two-dimensional inlet duct.

C. SOUND ABSORBING MATERIALS

1. OBJECTIVES OF TESTS

Previous testing has shown that significant sound attenuation can be achieved in the fan duct of the STF219 engine using sound absorbing materials.

The object of the Phase II-B test program was to investigate the sound absorbing properties of a wider variety of constructions in which the weight of the absorption treatment might be less than that of the Felt-metal configurations previously reported during Phase II-A. It was also intended to study the practicability of these treatments from the standpoint of durability under engine operating conditions.

2. DESCRIPTION OF FACILITIES

The test rig facility consisted of an upstream reverberation chamber, the test duct, and a downstream reverberation chamber. The upstream chamber housed a model pulse-jet engine which served as a sound source. Airflow velocities of up to 300 feet per second through the duct were attained utilizing a 300 horsepower low-pressure blower. A more detailed description of the test facility and the theory of reverberation-chamber sound measurement techniques can be found in the Phase II-A Final Report, number PWA-2397. Photographs of the facility and a typical treated duct are shown in Figures 8-12 and 8-13.

3. METHOD OF TEST

Tests were conducted in the same manner as that reported for Phase II-A with the exception of the sound data-taking procedure. A two-channel Magnacord tape recorder was utilized to obtain simultaneous readings of the two microphones. This modification eliminated he

DOWNGRADED AT 3 YEAR INTERVALS
DECLASSIFIED AFTER 12 YEARS
DOD DIR 5200.10

THIS DOCUMENT CONTAINS INFORMATION AFFECTING THE NATIONAL DEFENSE OF THE UNITED STATES WITHIN THE MEANING OF THE ESPIONAGE LAWS, TITLE 18 U. S. C. SECTIONS 793 AND 794. ITS TRANSMISSION OR THE REVELATION OF ITS CONTENTS IN ANY MANNER TO AN UNAUTHORIZED PERSON IS PROHIBITED BY LAW.

time delay that was inherent in the graphic level recording system, and the associated possibility of slight variations in the sound pressure level of the source.

4. RESULTS

Tests were conducted on a rig model section of the STF219 fan discharge duct with the flow split into two channels, each having a width of one-half that of the full-scale engine. A photograph of the one-half width channel incorporating one of the treatments is shown in Figure 8-13. Figure 8-14 tabulates the configurations tested in this duct.

Previous tests indicated that the use of 3/8-inch thick Feltmetal gave excellent attenuation. In an effort to reduce the weight addition and yet maintain acceptable noise attenuation, a thinner layer of Feltmetal, 1/8-inch thick, was employed as the facing material. Figure 8-15, Configuration A, shows that this facing with air in the backing space gave poor results. Filling the backing space with fiberglas greatly improved the attenuation over the entire frequency spectrum, as shown by Figure 8-15, Configuration B.

Study was then centered around finding a material exhibiting the acoustic properties of fiberglas that is capable of withstanding the high temperatures existing in the STF219 fan discharge duct. Cerafelt, an alumino-silicon fiber matting produced by Johns-Manville Co. met these requirements, and Figure 8-15, Configuration C shows the result to be as good as or slightly better than the fiberglas construction.

Slitmetal is a new commercially-developed acoustic panel suitable for use as a facing material. The flow resistance through the facing is controlled by the slit width and length. Its weight is somewhat less than that of a 1/8-inch thick Feltmetal panel having a 25% density. In our tests, no significant difference was found in attenuation when the length of the rectangular slit was parallel or perpendicular to the duct flow axis. A comparison of three facing materials, using Cerafelt in the backing space, is given in Figure 8-16. It is seen that the perforated plate and wire mesh screen facing material is superior to Slitmetal, especially at the higher frequencies. The perforated plate and Slitmetal panels are of comparable weight.

DOWNGRADED AT 3 YEAR INTERVALS
DECLASSIFIED AFTER 12 YEARS
DOD DIR 5200.10

5. CONCLUSIONS

- Acceptable noise attenuation can be achieved using Feltmetal or perforated plate and wire mesh screen as the facing material, and utilizing Cerafelt in the backing space.

- Sufficient attenuation can be achieved by the use of duct liners to reduce the sound from the fan duct below the exhaust noise level under landing-approach thrust conditions.

- Attenuations comparable to those previously reported for 3/8-inch thick Feltmetal have now been achieved with treatments weighing roughly one third as much.

- Planned environmental durability studies will lead to evaluation of construction techniques that can be incorporated in more refined studies of the weight-attenuation tradeoffs that are needed to select optimum configurations.

D. MODEL EXHAUST SYSTEM NOISE TESTS

1. DESCRIPTION OF FACILITIES

An overall diagram of the anechoic chamber test facility is shown in Figure 8-17. Basically the facility consists of a compressed air supply, a natural gas fuel supply system, and a burner section in which the natural gas fuel is mixed with the compressed air and burned to be exhausted through the test nozzle. A system of ducts and valves in the burner section allows the compressed air stream to be split into two parts, each with its own burner system, the two streams of hot gas being necessary to simulate the primary stream and the duct stream in models of the STF219 engine. The pressures and temperatures of both streams are controlled independently, allowing duplication of a wide range of engine operating conditions. A more detailed description of the facility appears in the Phase II-A final report, number PWA-2397.

2. METHOD OF TEST

In evaluating model nozzle configurations it is necessary to consider both noise and performance. Accordingly, model test programs and equipment were developed to document both considerations over the range of operation for each model test. Rig operating points were selected on the basis of the engine operating schedule. For each point on the full-scale engine operating schedule, consisting of a particular tailpipe temperature and nozzle pressure ratio, a corresponding point at the same temperature and pressure ratio was set on the nozzle model. 333 hours of testing were conducted in the anechoic chamber during phase II-B.

The test rig was equipped with instrumentation to collect the necessary data for the calculation of performance parameters and a tape recording system for the collection of noise data. These data were then reduced by IBM machine computation to give predictions of full-scale noise and performance. A detailed discussion of the data collection and reduction systems was given in the Phase II-A final report, number PWA-2397.

3. DESCRIPTION OF MODEL NOZZLES

The model exhaust nozzles tested during the Phase II-B contract period are best described in two groups: nozzles without duct heat and nozzles using duct heat. Diagrams of the nozzles tested in each group are shown in Figures 8-18 and 8-19.

Considering first the group of nozzles without duct heat, Figure 8-18 (Part A) shows the so-called calibration model scaled to the STF219 engine. This model was built during the Phase II-A contract period and was used for a variety of ejector tests extending over both Phase II-A and Phase II-B contracts where engine operation with a cold duct stream was simulated. Figures 8-18 (Part B), 8-20 and 8-21 show the scalloped primary nozzle. This model is designed to use the same blow-in-door ejector configurations as the calibration model but incorporates a primary nozzle with four protrusions into the primary stream. The primary and duct nozzle throat areas are the same as in the calibration model.

The third of the models without duct heat is shown in Figure 8-18 (Parts C and D). This is a turbojet nozzle model, constructed of an alloy containing 90 percent tantalum and 10 percent tungsten, to be used when gas stream temperatures up to 3300°F are needed to simulate the engine operation. The tantalum alloy was used so that the nozzle could be operated uncooled since experience with water-cooled nozzles during the early stages of the Phase II-B contract period had shown that the heat transfer from

the gas stream to the cooling water was so excessive that the desired nozzle exit temperatures could not be reached. In the full-scale engine nozzle, wall temperatures are maintained within acceptable limits by aircooling with a very small fraction of the engine airflow. Because the heat loss is a function of the ratio of duct cross section perimeter to section area, the problems of designing an air-cooled nozzle model to run hot without wall burnout are magnified by the order of 14:1, the model scale. The problems inherent in the design of the burner system which would produce a higher gas stream temperature at the inlet to the water-cooled parts to compensate for the high temperature-drop in the gas stream are even more prohibitive. The tantalum model was designed to operate at wall temperatures near 3000°F and was cooled only by radiation. A tin-aluminum coating was applied to the tantalum alloy to prevent oxidation. Two ejectors were built to be used with this nozzle, a model of the ejector used on the YF-12A aircraft (Figure 8-18, Part C) and a geometrically scaled model of the BTF219 ejector (Figure 8-18, Part D). Photographs of the nozzle and these assemblies appear in Figures 8-22 through 8-26.

The duct-heating nozzles were two in number, a water-cooled model shown in Figure 8-19 (Parts A and B) and an uncooled tantalum alloy model shown in Figure 8-19 (Part C). The water-cooled model was designed and constructed during the Phase II-A program for testing at all duct-heat operating points. As pointed out previously, the water cooling produced excessive temperature drops in the gas stream, limiting the maximum tailpipe temperature obtainable with this model. The nozzle was, however, used as shown in Figure 8-19 (Part A) to study partial duct-heat operation, and with a series of four water-cooled channel ejectors as shown in Figures 8-19 (Part B) and 8-27. The channels are provided to introduce ambient air and mix it with the nozzle streams in the ejector.

The tantalum model of the BTF219 was built during Phase II-B to test over the high-temperature range of duct heat operation when the water-cooled model was found to be inadequate. This model allows the use of the present burner system to obtain gas stream temperatures up to 3100°F. Photos of the primary and duct nozzles and their assemblies are shown in Figures 8-28 through 8-31.

4. RESULTS

a. Nozzles Without Duct Heating

Model exhaust noise results are presented for the configurations listed below. In the three-digit identification code that is used, the first digit

refers to the primary nozzle, the second digit identifies the secondary or duct nozzle, and the last digit identifies the ejector. A zero digit denotes absence of the relevent component.

Designation	Identification
(1, 6, 0)	Basic primary nozzle assembly for use without duct heating. Secondary nozzle identical with nozzle without duct heating designated as 2 in Phase II-A report except mounted with forebody supports for a variety of ejectors. No ejector used.
(1, 6, 1)	Same as (1, 6, 0) with addition of basic STF219 ejector.
(1, 6, 3)	First of series of four configurations using channel ejectors providing for induction of ambient air through six channels protruding from the ejector surface into the gas streams. This ejector, last digit 3, has channels protruding the maximum distance into the gas stream.
(1, 6, 4)	Incorporating a channel ejector with less protrusion.
(1, 6, 5)	Incorporating a channel ejector with still less protrusion.
(1, 6, 6)	Incorporating a channel ejector with the minimum protrusion.
(3, 5, 0)	Four-lobe scalloped primary nozzle and concentric circular secondary nozzle. No ejector.
(3, 5, 1)	Same as (3, 5, 0) with addition of basic STF219 ejector.
(8, 0, 0)	Model of turbojet nozzle.
(8, 0, 7)	Turbojet nozzle with model of ejector used in the YF-12A aircraft.
(8, 0, 8)	Turbojet nozzle with ejector geometrically similar to STF219 ejector, but scaled to turbojet nozzle size.

Sound data on this group of nozzles are presented in the form of maximum overall sound pressure level (OASPL) and maximum PNdb as a function of primary jet velocity. Primary jet velocity is a convenient coordinate since, in the absence of duct heating, the secondary velocity is sufficiently low that it will generate negligible noise. The levels presented are computed for a full-scale nozzle at a constant altitude or sideline distance of 200 feet.

Basic nozzle results without duct heating are shown in Figure 8-32 for configurations (1, 6, 0) and (1, 6, 1) and form a reference for comparing other nozzles. It is seen that there is no significant difference attributable to the addition of the basic STF219 ejector over the primary velocity range tested, confirming the results reported during Phase II-A.

Figures 8-33 and 8-34 present the noise characteristics of the four channel ejectors, configurations (1, 6, 3), (1, 6, 4), (1, 6, 5) and (1, 6, 6). These ejectors are constructed with six equiangularly-spaced channels protruding inwardly from the outer surface of the ejector shroud to allow the induction and mixing of ambient air with the gas streams. Ejector 3 has channels protruding the maximum distance into the interior, ejectors designated 4 and 5 have successively less protrusion, and the final member, 6, has the minimum channel protrusion. Figure 8-33 compares ejectors (1, 6, 3) and (1, 6, 4) with the standard ejector, (1, 6, 1). The results for the other channel ejectors, (1, 6, 5) and (1, 6, 6), are compared with the standard in Figure 8-34. In these figures, lines have been drawn to fit the standard ejector data points. Because of the relatively large scatter of the channel ejector data, no curves were drawn for these data. It will be noted that no significant reduction is achieved on a maximum OASPL basis by these special ejectors, and that on a PNdb basis they actually generated somewhat higher levels of noise. Examination of the detailed acoustic data reveals that the increased levels are due to a slight forward shift in the radiation pattern and to some increase in the high frequency noise content.

The next group of results concerns performance of a special primary nozzle having four lobes or scallops in the exit plane. The outer boundary of the duct nozzle is a coplanar concentric circle, so that the exhaust streams emerge as alternating primary and secondary lobe regions. Overall sound pressure level and PNdb for this nozzle by itself, (3, 5, 0), and with the standard ejector, (3, 5, 1), are shown in Figure 8-35, and disclose no significant ejector effect. Figure 8-36 compares this scalloped nozzle with the basic nozzle, (1, 6, 0), both without ejector. The OASPL curve in Figure 8-36 shows the progressively increasing suppression of a multilobe nozzle as velocity increases. A sound pressure level

reduction of about six db at 2000 feet per second jet velocity results for the scalloped nozzle. On a PNdb basis at 2000 feet per second, a three PNdb reduction is achieved; this is reduced to zero at a jet velocity of 1700 feet per second, where the PNbd from the two nozzles is the same. Figure 8-37 compares the basic and scalloped nozzle configurations incorporating ejectors, and shows the same effect.

A model of a turbojet converging nozzle was designed and fabricated from tantalum-10W alloy to permit running at simulated afterburner conditions with ejectors. Due to restrictions of the test schedule, it was not possible to obtain data with the special high-temperature burner required, the results are limited to about 2200 feet per second. Three configurations were evaluated: (8, 0, 0), the basic nozzle, and two configurations incorporating ejectors, (8, 0, 7) and (8, 0, 8). The ejector designated by 7 was patterned after the design used in the YF-12A for which full-scale sound data were previously given in the Phase II-A report. The other model ejector used in these tests, number , was geometrically similar to the STF219 basic ejector, number , a scale such that the ratio of ejector throat diameter to total nozzle diameter was the same.

Examination of Figure 8-38 shows that on a PNdb basis there was little significant distinction between the turbojet nozzle when running by itself or with either of the two ejectors in the jet velocity range up to 2200 feet per second. On the basis of maximum OASPL, Figure 8-38, the three configurations were also essentially the same at the high end of this velocity range. As jet velocity was reduced, however, the sound pressure levels of ejector number 8 did not decrease as much as those of the basic nozzle by itself or with ejector number 7. A study of the noise spectra of the configurations revealed that the higher OASPL values for ejector 7 were due to a relative increase of the first two or three octaves, the higher octave levels corresponding quite closely with those of the other configurations. This circumstance accounted for the lack of a significant difference among the three configurations in the PNdb comparison. From the amount of information presently available, it was not possible to find a cause for the increased low frequency characteristics of the number 7 ejector which is geometrically similar to the model used with the turbofan configuration (1, 6, 1). On the turbofan model, this ejector did not materially change the basic nozzle noise characteristics.

These ejectors were made to provide for variations of position with respect to the exit plane of the nozzle, and further testing in which this feature is examined would be a first step in continued studies.

DOWNGRADED AT 3 YEAR INTERVALS
DECLASSIFIED AFTER 12 YEARS
DOD DIR 5200.10

b. Nozzles With Duct Heating

A water-cooled model of the STF219 exhaust nozzle system was fabricated during Phase II-A to provide noise information in the operating range where duct heating is used. The engine cycle calls for a variation of the duct nozzle area as the amount of duct heat is changed. Since a variable area nozzle would have been excessively difficult to fabricate in small scale, two separate duct nozzles were made to run interchangeably with a common primary. Of these, the one with the greatest area, corresponding to the maximum duct heat condition, was used together with the primary nozzle for tests reported here. Model noise studies were made for the following configurations:

Designation	Identification
(2, 3, 0)	Water-cooled primary. Water-cooled secondary or duct nozzle having max area. No ejector.
(2, 3, 1)	The basic (2, 3, 0) configuration with the addition of the basic ejector, 1.
(2, 3, 3)	Using the maximum protrusion channel ejector, 3, in place of the basic ejector. This part was described in the previous section.
(2, 3, 4) (2, 3, 5) (2, 3, 6)	Configurations using channel ejectors described in the previous section.

During checkout of the basic (2, 3, 0) configuration, it was found that heat loss to the water-cooled wall surfaces of the model and rig prevented attainment of the desired high duct temperatures. This condition led to the redesign of certain rig parts and construction of a new model using tantalum-10W alloy which was previously described. While awaiting completion of the tantalum parts, the original water-cooled model was run within a limited range. With primary velocity held at approximately 1950 feet per second, the duct velocity was successively set at approximately 1900, 2100, and 2400, feet per second.

Since both streams were operating in the same general velocity range and thus generating noise levels that were not very far apart, the observed noise levels could not very well be related to a single stream velocity such as was done for the test program without duct heat. Also, since the actual velocities measured during operation at a particular

[illegible]

test condition departed randomly from the nominal target values, a tabular presentation of the noise of different configurations did not provide the best means of comparison. Accordingly, a data presentation procedure was evolved wherein the observed maximum OASPL and PNdb values were plotted against a parameter incorporating the two stream conditions. This parameter was the predicted maximum OASPL that would result from the superposition of the two sound fields if each jet generated a noise level calculated for a standard circular nozzle of appropriate area at the corresponding stream conditions.

Specifically, the performance data taken during the running of each sound survey determined the velocity and density of each stream. The standard procedure given in the SAE-A21 report, "Procedures for Jet Noise Prediction", was used to obtain the predicted maximum OASPL for each stream, and the two levels were combined to give the total predicted maximum OASPL, against which the observed values were plotted.

Figure 8-39 presents observed versus predicted sound pressure levels for the basic water-cooled model. The three upper points, shown as circles, are for the three operating points (duct velocity values) mentioned above on the configuration (2, 3, 0) without ejector. Addition of the ejector, configuration (2, 3, 1), generated the points represented by squares; the ejector was shown to produce a noise reduction of about three db. If the corresponding circle and square symbols are examined on a PNdb basis in Figure 8-39, a similar three PNdb reduction may be credited to the standard ejector.

A unit slope line through equal predicted and computed OASPL points was drawn in Figure 8-39, and it is seen that the data for the model without the ejector fall within two to three db of their predicted values. Four other points are shown as triangles. The solid triangle represents a single condition with the duct burner turned off and unheated secondary air flowing around the hot primary. This point falls about four db below the predicted OASPL and may reflect a slight beneficial interaction effect. The other three unfilled triangles represent conditions with the primary stream burner turned off and the secondary stream operated at the three duct stream velocities. This mode of operation does not correspond to any full-scale condition, but it may be of some interest to note that these points fall about nine db below their predicted sound pressure levels. Parenthetically, a unit slope line was not drawn on Figure 8-39 for the PNdb data, since there is no unique correspondence between PNdb and OASPL.

This basic model was also operated with the channel ejectors previously run without duct heat. Figure 8-40 compares the configurations (2, 3, 3)

DOWNGRADED AT 3 YEAR INTERVALS
DECLASSIFIED AFTER 12 YEARS
DOD DIR 5200.10

THIS DOCUMENT CONTAINS INFORMATION AFFECTING THE NATIONAL DEFENSE OF THE UNITED STATES WITHIN THE MEANING OF THE ESPIONAGE LAWS, TITLE 18, U.S.C., SECTIONS 793 AND 794. THE TRANSMISSION OR THE REVELATION OF ITS CONTENTS IN ANY MANNER TO AN UNAUTHORIZED PERSON IS PROHIBITED BY LAW.

and (2, 3, 4) with the nozzle without an ejector, configuration (2, 3, 0), and shows about eight db OASPL reduction but a PNdb drop of only about two db. A more significant comparison is shown in Figure 8-41 which shows the performance of the channel ejectors and the basic ejector. Whereas either of the channel ejectors reduced the basic ejector sound pressure level by about five db, there was a total lack of reduction in the associated preceived noise level. While this is hardly a desirable result, it is of interest to compare the performance of these ejectors under duct heat conditions with the corresponding results without duct heat, Figure 8-33. Without duct heat there was no significant change in OASPL for any of the ejectors. On a PNdb basis, while the basic ejector produced no change, the channel ejectors actually tended to raise the noise levels. Increasing the secondary stream velocity by partial duct heating apparently allowed the basic ejector to produce a modest suppression of three db and three PNdb. The auxiliary air channels in the special ejectors begin to produce the desired effect, but further work is needed to clarify their performance.

The tantalum-10W alloy model of the STF219 nozzle, configuration (7, 9, 0), was assembled and mounted for running up to the maximum duct heat operating conditions. After a brief checkout, a sound run was being conducted when a failure occurred in a water-cooled spacer ring connecting the tantalum portion of the primary nozzle to the burner rig. This assembly showed significant damage, and, although the major tantalum components are reusable with little or no repair, it was not possible to restore the model to operable condition in time for completion of this phase of the program.

5. CONCLUSIONS

Over the jet velocity range attained during this program, none of the special nozzles or ejectors demonstrated impressive noise reductions.

Small noise reductions were obtained at the highest jet velocities reached, the most significant trend being shown by the scalloped nozzle. For this nozzle, a progressive increase in suppression resulted with jet velocity increase. It is expected that this trend would continue with attainment of maximum velocities.

The acoustic performance of the standard ejector and the channel ejectors is less clear than the case of the scalloped nozzle. For operation without duct heat, the basic ejector did not change the sound pattern of the basic nozzle; however, with the duct stream partially heated and discharging from the larger secondary nozzle designed for the maximum duct heat point, a slight suppression was achieved by this ejector in the velocity range tested. The special channel ejectors that were tested showed

DOWNGRADED AT 4 YEAR INTERVALS
DECLASSIFIED AFTER 12 YEARS
DOD DIR 5200.10

no advantage over the standard ejector, but they tended to improve with the use of duct heating and may become attractive for higher duct heat conditions.

It is concluded that further work is needed in the high jet velocity range to properly evaluate these suppression systems, and that more extensive study of the effect of changing nozzle and ejector shape can be expected to lead to improved suppression results.

E. FULL-SCALE BLOW-IN-DOOR EJECTOR NOISE TESTS

1. GENERAL

Analysis of noise data recorded during fly-overs of the YF-12A airplane suggested that the blow-in-door ejector nozzles used on the airplane were providing some exhaust noise suppression. Because of the manner in which the data were obtained, it was not possible to obtain a direct comparison of the effect on noise of the ejector nozzle. To obtain a direct comparison of the effect of the ejector, a boiler-plate model of the STF219 ejector was built and noise tested on a full-scale J57 afterburning jet engine. 30 hours of testing were conducted on this engine during Phase II-B.

2. RESULTS

A series of tests were conducted on the J57 engine at the Pratt & Whitney Aircraft outdoor noise test facility. Included in the test series were three baseline tests of the engine with a standard circular nozzle, two tests with the basic ejector, and tests of five variations of the ejector nozzle. The following table provides an index to the test results.

Configuration	Photograph	Plotted Results
Baseline	Figure 8-42	Figure 8-43
Basic Ejector	Figure 8-44	Figure 8-45
Ejector with Airscoops	Figure 8-46	Figure 8-47
Ejector with Mixers Fully Extended	Figure 8-48	Figure 8-49

DOWNGRADED AT 3 YEAR INTERVALS
DECLASSIFIED AFTER 12 YEARS
DOD DIR 5200.10

Configuration	Photograph	Plotted Results
Ejector with Mixers Partially Extended	None	Figure 8-49
Ejector Relocated 8" Forward	Figure 8-50	Figure 8-51
Ejector Relocated 5" Forward	None	Figure 8-52
Ejector with Blow-in-Door Area Half Blocked	None	Figure 8-53
Ejector with Blow-in-Door Area One-Quarter Blocked	Figure 8-54	Figure 8-55

Significant engine performance parameters are summarized on Figure 8-56. Results of the noise tests showed that only a small reduction in noise was measured with the basic ejector installed. Typical spectra are shown in Figure 8-57.

Noise data from tests with the eight U-shaped mixers in the exhaust gas stream are shown in Figure 8-49. The mixers were fully extended during nonafterburning operation with the exhaust nozzle closed. During afterburning operation, with the exhaust nozzle open, the mixers were only partially extended. Although the noise at maximum powere was reduced by about five PNdb by the mixers, the thrust loss was large enough to completely offset the noise suppression achieved by mechanically mixing the engine gas stream with the blow-in-door airflow. At all engine power settings below the maximum dry rating, a noise increase was measured when the mixers were extended into the gas stream.

Airflow through the ejector as a function of engine power setting is shown in Figure 8-58. Although substantial reductions in ejector flow resulted from relocating the ejector nearer to the engine nozzle, the noise levels at a given engine power setting were not affected significantly.

DOWNGRADED AT 3 YEAR INTERVALS
DECLASSIFIED AFTER 12 YEARS
DOD DIR 5200.10

THIS DOCUMENT CONTAINS INFORMATION AFFECTING THE NATIONAL DEFENSE OF THE UNITED STATES WITHIN THE MEANING OF THE ESPIONAGE LAWS, TITLE 18 U.S.C. SECTIONS 793 AND 794. THE TRANSMISSION OR THE REVELATION OF ITS CONTENTS IN ANY MANNER TO AN UNAUTHORIZED PERSON IS PROHIBITED BY LAW.

Blockage of the blow-in-door areas to create noncircular cross sectional growth of the jet exhaust plume apparently had no significant effect on noise as shown on Figures 8-53 and 8-55. Near-field noise levels with and without the ejector are shown in Figure 8-59.

3. CONCLUSIONS

- No significant reduction in noise resulted from installation of an ejector nozzle on the test engine.
- Mechanically mixing the jet exhaust gasses with the ejector flow did result in significant noise reductions. However, the performance losses of the crude device tested was excessive, and better results may be obtainable with other type mixers.
- Closing some of the blow-in doors would not enhance the noise suppression from an ejector.
- Noise generation is not sensitive to ejector airflow.

4. RECOMMENDATIONS

Further development of the SST engine exhaust system to provide noise suppression is required. The development of noncircular fan discharge nozzles, which would increase the outside perimeter of the fan stream, appears to be a more satisfactory approach than the installation of mixers in the ejector shroud.

5. DESCRIPTION OF TEST EQUIPMENT

The engine used for the test series was a standard J57-P-55 afterburning turbojet engine. This engine is the type used to power the F-101 airplane. The exhaust stream diameter at the ejector throat for maximum engine power was used as the reference dimension in scaling the STF219 engine ejector design to J57 engine size. The ratio of ejector throat area to engine stream area was held to scale, and linear dimensions were scaled based on the exhaust stream diameter.

Although the ejector was not physically attached to the engine, it was mounted so that any thrust changes which resulted from its installation were reflected in the stand thrust-meter reading. The structure used to support the weight of the ejector shroud section did not constrain motion in the fore and aft direction, so thrust loads were not affected.

DOWNGRADED AT 3 YEAR INTERVALS
DECLASSIFIED AFTER 12 YEARS
DOD DIR 5200.10

THIS DOCUMENT CONTAINS INFORMATION AFFECTING THE NATIONAL DEFENSE OF THE UNITED STATES WITHIN THE MEANING OF THE ESPIONAGE LAWS, TITLE 18 U.S.C. SECTIONS 793 AND 794. ITS TRANSMISSION OR THE REVELATION OF ITS CONTENTS IN ANY MANNER TO AN UNAUTHORIZED PERSON IS PROHIBITED BY LAW.

6. METHOD OF TEST

Outdoor noise tests on the full-scale engine were conducted at an outdoor test stand located in a remote area at Bradley Field airport near Windsor Locks, Connecticut. Several features of this stand which make it ideally suited for noise tests are:

- Low ambient noise levels.
- Carefully graded and cleared ground surface.
- Facilities and instrumentation for engine performance measurement.
- Permanently installed instrumentation for monitoring meteorological conditions.
- A permanently installed system of 20 microphones spaced along a 150-foot arc centered on the engine exhaust nozzle. This system is used for far-field noise measurements.
- Provisions for the installation of microphones in any desired pattern in the near-field of the engine.
- A permanently-installe ound data recording console which includes a 14-channel magnetic tape recorder, microphone power supplies, and system calibration equipment.

An aerial view of this facility is shown in Figure 8-60. Figure 8-61 shows the exact microphone locations. The sound data recording console is shown in Figure 8-62. During the last five years, near' 200 engine sound tests have been conducted using this facility.

Noise levels were measured at several engine power settings from idle thrust to maximum afterburner thrust. Operation of the engine over only a small range of afterburning powers was possible because the engine had only a two-position exhaust nozzle. After the engine operation was stabilized, signals from each microphone were tape recorded for at least 30 seconds. Readings of engine performance

DOWNGRADED AT 3 YEAR INTERVALS
DECLASSIFIED AFTER 12 YEARS
DOD DIR 5200.10

parameters which are of interest to the analysis of noise data were also logged at each point.

In order to ensure that the noise data were not invalidated by adverse meteorological conditions, testing was conducted only during conditions of low wind and no precipitation. Measurements of ambient temperature, barometric pressure, and relative himidity were made periodically during each noise test.

7. DATA ANALYSIS

Reduction of the tape recorded noise data was accomplished using the octave band analysis console shown in Figure 8-63. This console sampled and analyzed for at least 20 seconds the noise level in each of the eight octave bands between 37.5 and 9600 cps, and provided a digital read-out which was recorded on punched computer cards. This console was specially designed and built by the electronics section of Pratt & Whitney Aircraft to satisfy requirements for the rapid reduction of noise data, and has been in continuous use since 1960.

The punched cards containing the octave-band noise levels were used as the input to digital computers which were programmed to apply factors to correct for the electrical response of the measuring system and tape recorder, and for the acoustical response of the microphones. The corrected far-field data were then extrapolated by other computer programs from the 150-foot radius at which they are measured to a parallel line at a distance of 200 feet from the engine. Noise levels along a parallel line are more meaningful for the analysis of take-off and landing noise as they better indicate fly-over noise peaks.

8. CALIBRATION OF ACOUSTIC INSTRUMENTATION

Figure 8-64 shows some of the equipment used in the periodic frequency-response calibration of the capacitance-type microphones used for full-scale engine sound tests. The small anechoic chamber is used to calibrate periodically the response of a transfer standard microphone against our standard (a Western Electric Co. condenser microphone, type 640AA) which was calibrated by the National Bureau of Standards. Each of the 20 test microphones was calibrated prior to this series of ejector-nozzle noise tests against the transfer standard using a pressure calibration technique which covered the frequency range from 20 to 10,000 cps

The sensitivity of each test microphone was determined daily during the test series by the use of a transistor oscillator driven acoustic calibrator. The output level of this calibrator was adjusted using the primary standard microphone.

Electrical losses in the microphone systems were determined by inserting electrical test signals at the microphone and monitoring the output level of the inserted signals at the recording console. The response of the recording and play-back tape recorders and the octave band analysis console were determined from recordings of both broad-band random and sine wave test signals on each magnetic tape used during the test. Results of these calibrations determined the factors which were used in the computer program to correct the noise data in each of the eight octave bands from 37.5 to 9600 cps.

9. DISCUSSION

The mixers used through the ejector shroud for this series of tests were formed from steel tubes through which cooling water was flowed. However, water was not discharged into the exhaust stream. It is quite possible that mixers of other shapes could have provided better mixing with less thrust loss, but the ones used should be representative of the type of results obtainable. In general, a high thrust loss can be expected to result from placing devices in the jet exhaust stream through the ejector shroud.

As the model ejector was fabricated with fixed-position blow-in-doors, metal plates were installed over the door openings to simulate operation with some of the doors closed.

Noise levels measured during take-off fly-overs of the YF-12A airplane were the basis for expecting a reduction in noise from a blow-in-door ejector. At the time these data were obtained, no other data were available to indicate the effect on noise of an ejector during afterburning engine operation. Results of this series of noise tests, which involved an ejector which was not markedly dis-similar from that used on the YF-12A, have, in general, not confirmed the expected suppression characteristics of the ejector.

It has recently come to light that other details of the engine exhaust system may have been responsible for the noise reduction attributed to the ejector. Four of the five take-off fly-overs were recorded from airplanes powered by engines having "toothed" primary nozzles. These airplanes were less noisy than the one with the circular nozzle, and less noisy than would be

predicted from the SAE noise calculating procedure. This comparison is shown on Figure 8-65.

Further data to substantiate the belief that the toothed nozzle may have provided the noise suppression observed from the YF-12A airplane exhaust system are shown in NACA Technical Note 4261. Included in this note, entitled "Acoustic, Thrust, and Drag Characteristics of Several Full-Scale Noise Suppressors for Turbojet Engines", are data on a nozzle configuration incorporating a "flapped" primary nozzle and ejector. This configuration, shown in Figure 8-66, was reported to provide a reduction in noise of about the magnitude originally attributed to the YF-12A blow-in-door ejector. It was also mentioned that the use of the ejector without the flap nozzle showed no significant noise suppression.

F. ANALYSIS OF TOTAL SST AIRPLANE NOISE

1. GENERAL

Analytical studies were conducted to determine the potential community noise problems which may result from operation of SST-type airplanes. Results indicated that take-off noise, rather than approach noise, is the cause for greatest concern. Noise during take-off is generated largely by the high velocity exhaust wake from the duct-burning turbofan or afterburning turbojet SST powerplants. As shown in Figure 8-1, the engines designed for use on SST airplanes will be capable of producing substantially more noise energy than those used on any current commercial jet transport, and somewhat more noise than the unsuppressed jet engines used on many military airplanes. This figure points up the fact that the SST airplane will not reverse the unfortunate long-time trend toward more powerful engines which inherently generate more noise. The SST has one noise advantage, however, which is not shared by most of the other airplanes shown in Figure 8-1. This is an excess of take-off thrust which will allow reduced power take-off operating procedures which will result in lower take-off noise levels.

2. DISCUSSION

a. Take-off Noise

In order to ensure that noise was considered in the basic design of the SST, noise goals were established by the FAA. Take-off goals were established for both sideline noise and noise at a point three miles from the start of the take-off roll. As airplane design studies have progressed and improvements in airplane performance have been made, the noise goal levels have been reduced.

b. Sideline Noise

Noise levels at 1500 feet from and parallel to the SST airplane on the ground are shown as a function of engine thrust in Figure 8-67. As shown by the figure, the turbofan cycle engine at maximum power without duct heat can meet the current 116 PNdb sideline noise goal. The turbojet cycle engines must be operated at considerably less than maximum nonafterburning power to meet the goal. It should also be noted that the goal noise level is in excess of the noise from current jet airplanes.

c. Three-Mile Point Noise

Peak noise levels both beneath and to the side of the flight path of SST airplanes are shown in Figure 8-68 and 8-69. The levels shown are for the angle of peak noise, usually 135 degrees, to the rear of the airplane. The width of the bands was established by the differences in performance of current SST airplane designs. A large variation in noise level due to airplane altitude variations results directly beneath the flight path, with a lesser variation to the side.

Noise levels just prior to power cutback for a maximum power take-off are shown in Figure 8-68. Figure 8-69 shows the noise levels for a reduced power take-off, the power being reduced to that required to just meet the 1500-foot sideline noise goal. Noise levels directly beneath the flight path are not affected greatly by the take-off method used because the airplane having the lower power setting, and therefore generating less exhaust noise, has gained less altitude than the airplane which has used maximum power. A substantial difference in noise is noted, however, when areas to the side of the flight path are considered, the reduced power take-off being less noisy.

After power cutback to a 500-foot per minute climb rate at the three-mile point, the noise from the SST compares favorably with subsonic jets as shown on Figure 8-70. The large spread in levels beneath the flight path of the SST is the result of several variables such as airplane performance, engine type, and flight procedure used.

With a duct-burning turbofan cycle engine, potential for further noise reduction exists from the use of low levels of duct heat in the range of powers needed for a climb rate of 500 feet per minute. Lower noise at a given reduced thrust may result from decreasing the exit velocity of the primary engine and increasing the velocity of the duct stream by burning fuel in the duct. A net noise reduction of about 2.5 PNdb should result as the noise decrease resulting from the reduction in primary jet velocity is offset only partially by the increase in fan duct exhaust noise. An additional engine control lever would be required to allow this type of operation.

After the SST has reduced power to meet the three-mile point noise goal, it must at some point resume climb by increasing power. This can be done in several ways. One way would be to increase power gradually with time, to keep the noise beneath the airplane about constant at 105 PNdb until climb power is reached. The method of resuming power after the airplane has passed beyond the three-mile point so as to affect adversely the fewest people will probably be different for each airport to be used by the SST.

d. Approach Noise

At the start of Phase II-B, the approach noise goal established for a point one mile from touch-down beneath the approach flight path was reduced from 118 to 109 PNdb. The estimated noise levels for both fan and jet engine powered SST airplanes as well as several subsonic jets are shown on Figure 8-71. As shown on the figure, compressor noise must be almost completely eliminated for either of the SST powerplants to meet the new noise goal, which is substantially lower than the nominal noise levels of current jets. With a ten db reduction in compressor noise, which appears to be practically achievable within the present state of the art, the SST will be less noisy than current jets but will not meet the goal levels.

The differences in the width of the path beneath the airplane which is influenced by approach noise as compared with that affected by take-off

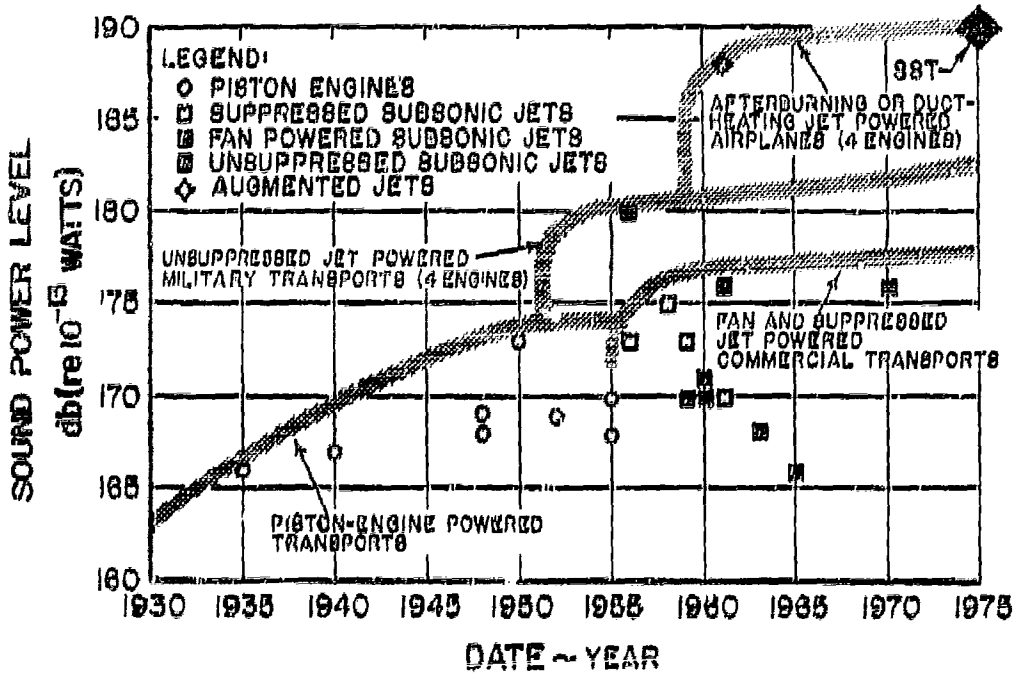
noise is illustrated by Figure 8-72. Because of the low aircraft altitude at the one-mile point, the peak levels directly beneath the approach flight path are nearly equal to take-off levels, but the noise levels to the side of the flight path are much less because of the low altitude during approach. This curve was plotted for an engine with the fan-compressor noise attenuated by ten db, and for a three-degree approach flight path.

3. CONCLUSIONS

- SST airplanes will probably be less objectionable during approach than current jet transports, but the goal level of 109 PNdb will be difficult if not impossible to meet.
- The turbofan cycle engine has more acceptable take-off noise than turbojet cycle engines.

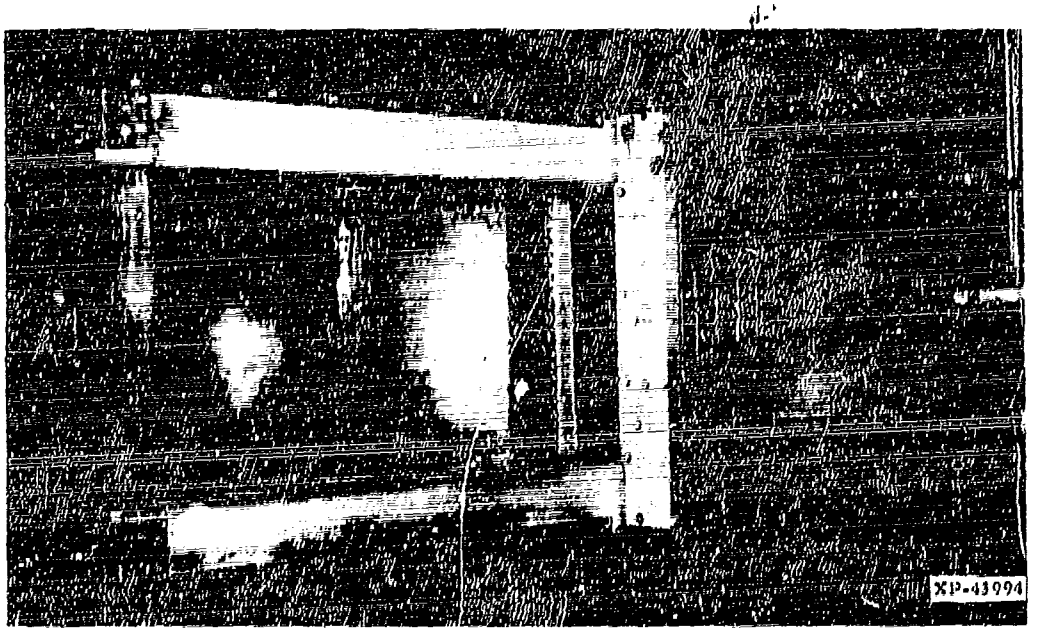
4. RECOMMENDATIONS

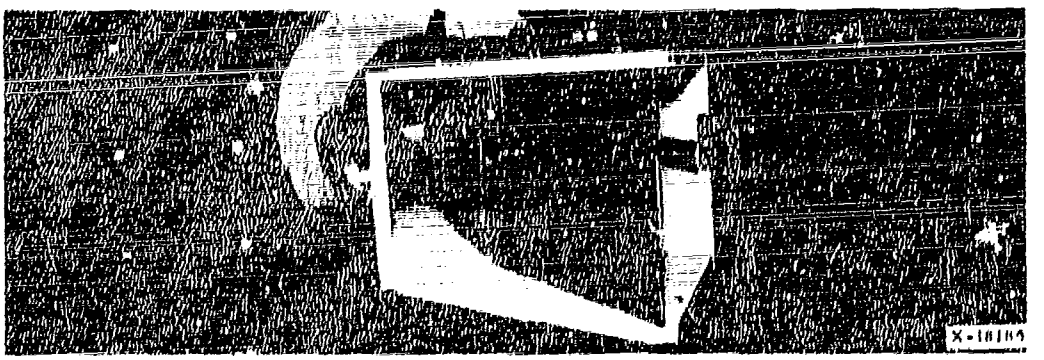
- The development of exhaust noise suppressors which are effective during high power operation should be further investigated.
- The trade between engine size and operating economy is one which should be thoroughly investigated to ensure that the engine size chosen for the SST is as large as is practical.
- Various airplane take-off procedures should be investigated without regard for noise goals to determine which method would affect adversely the fewest people. Perhaps different take-off procedures should be investigated for different airports, based on the population distribution around each of the major airports to be served by the SST.
- As approach noise from the SST will probably be lower than that from current jets, the approach noise goal should be reviewed to ensure that the design of the airplanes is not complicated by the requirements for excessive sound treatment. Little community noise relief will result from having a few SST airplanes which are far quieter than all other airplanes during approach.



AIRPLANE ENGINE NOISE POWER (WATTS) GENERATED AT MAXIMUM STATIC THRUST

Figure 8-1





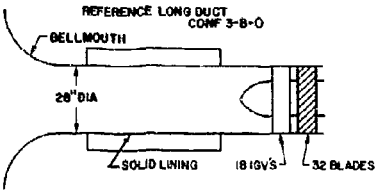
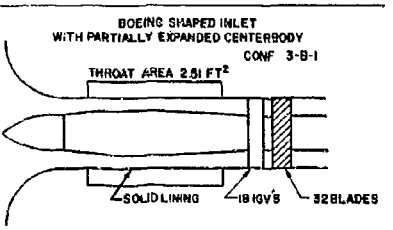
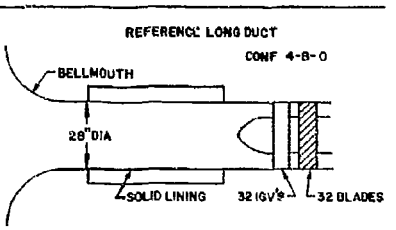
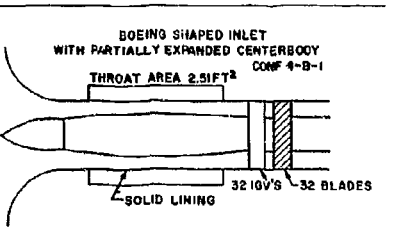
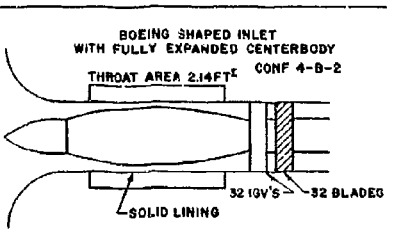
LOCKHEED TWO-DIMENSIONAL INLET

Figure 8-2



BOEING AXISYMMETRIC INLET WITH PARTIALLY EXPANDED CENTERBODY

Figure 8-3

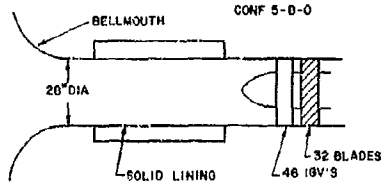
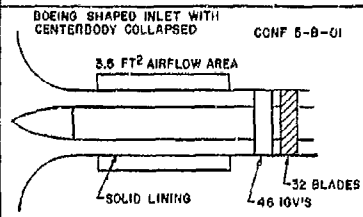
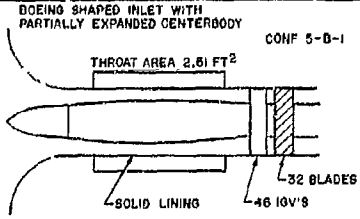
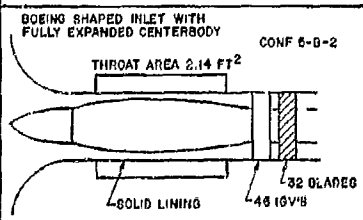
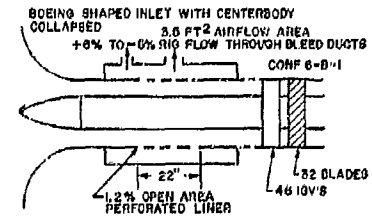
OBJECT OF TEST	RESULT OF TEST	TEST CONFIGURATION
To obtain a baseline for tests to determine the effect on noise of inlet duct flow velocity on a rig with 18 inlet guide vanes.	Baseline Configuration Noise documented over rig operating range	
To determine the effect on noise of centerbody shape and inlet duct flow velocity	Compared with 3-B-0 No significant changes when throat Mach number was below 0.50. Substantial attenuation of compressor noise noted at a throat Mach number of 0.7. Essentially no discrete noise propagated when throat Mach number exceeded 0.8.	
To obtain a baseline for test of the effect on noise of inlet duct flow velocity on a rig with 32 inlet guide vanes.	Baseline Configuration Sound documented over rig operating range. This 32-vane configuration was found to be more noisy than either the 18-vane or the 32-vane configuration.	
To determine the effect on noise of centerbody shape and inlet duct flow velocity.	Compared With 4-B-0 No significant changes when throat Mach number was below 0.50. Substantial attenuation of compressor noise noted at a throat Mach number of 0.75. Essentially no discrete noise propagated when the throat Mach number exceeded 0.85.	
To determine the effect on noise of centerbody shape and inlet duct flow velocity.	Compared with 4-B-0 No significant changes when throat Mach number was below 0.5. Substantial attenuation of compressor noise noted at a throat Mach number of 0.80. Essentially no discrete noise propagated when throat Mach number exceeded 0.88.	

RESULTS OF NOISE TESTS

Figure 8-4
Sheet 1 of 5

DOWNGRADED AT 3 YEAR INTERVALS
DECLASSIFIED AFTER 12 YEARS
DOD DIR 5200.10

THIS DOCUMENT CONTAINS INFORMATION AFFECTING THE NATIONAL DEFENSE OF THE UNITED STATES WITHIN THE MEANING OF THE ESPIONAGE LAWS, TITLE 18 U.S.C. SECTIONS 793 AND 794. ITS TRANSMISSION OR THE REVELATION OF ITS CONTENTS IN ANY MANNER TO AN UNAUTHORIZED PERSON IS PROHIBITED BY LAW.

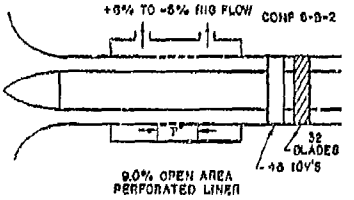
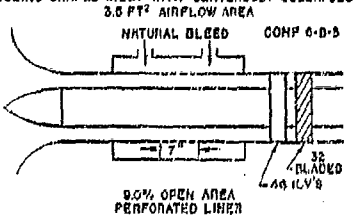
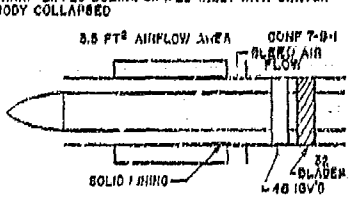
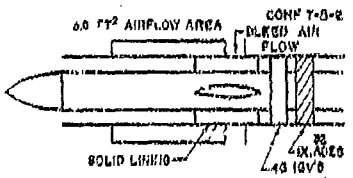
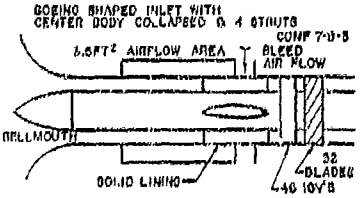
OBJECT OF TEST	RESULT OF TEST	TEST CONFIGURATION
To obtain a baseline for test of the effect on noise of inlet duct flow velocity on a rig with 46 inlet guide vanes.	Baseline Configuration Noise documented over rig operating range. This 46 inlet guide vane configuration was found to be less noisy than either the 18-vane or the 32-vane configuration.	REFERENCE LONG DUCT CONF 5-B-0 
To determine the effect on noise of the cylindrical centerbody.	Compared with 5-B-0 No significant change in either level or directivity pattern.	BOEING SHAPED INLET WITH CENTERBODY COLLAPSED CONF 5-B-01 
To determine the effect on noise of centerbody shape and inlet duct flow velocity.	Compared with 5-B-0 & 5-B-01 No significant change when the throat Mach number was below 0.80. Substantial attenuation of compressor noise noted at a throat Mach number of 0.80. Essentially no discrete noise propagated when throat Mach number exceeded 0.88.	BOEING SHAPED INLET WITH PARTIALLY EXPANDED CENTERBODY CONF 5-B-1 
To determine the effect on noise of centerbody shape and inlet duct flow velocity.	Compared with 5-B-1 & 5-B-0 No significant changes when throat Mach number was below 0.80. Substantial attenuation of compressor noise noted at a throat Mach number of 0.84. Essentially no discrete noise propagated when throat Mach number exceeded 0.88.	BOEING SHAPED INLET WITH FULLY EXPANDED CENTERBODY CONF 5-B-2 
To determine the effect on noise of a combination of 1.2% open area perforated liners and a bleed airflow range from +6% to -5% of rig flow.	Compared with 5-B-01 Both blowing air into the duct and drawing air out of the duct through the perforated liner showed no significant reduction in compressor noise.	BOEING SHAPED INLET WITH CENTERBODY COLLAPSED 3.6 FT² AIRFLOW AREA +6% TO -5% RIG FLOW THROUGH BLEED DUCTS CONF 6-B-1 

RESULTS OF NOISE TESTS

Figure 8-4
Sheet 2 of 5

DOWNGRADED AT 3 YEAR INTERVALS
DECLASSIFIED AFTER 12 YEARS
DOD DIR 5200.10

THIS DOCUMENT CONTAINS INFORMATION AFFECTING THE NATIONAL DEFENSE OF THE UNITED STATES, WITHIN THE MEANING OF THE ESPIONAGE LAWS, TITLE 18, U.S.C., SECTIONS 793 AND 794. THE TRANSMISSION OR THE REVELATION OF ITS CONTENTS IN ANY MANNER TO AN UNAUTHORIZED PERSON IS PROHIBITED BY LAW.

OBJECT OF TEST	RESULT OF TEST	TEST CONFIGURATION
To determine the effects on noise of a combination of 9.0% open area perforated liners and a bleed air flow from +6% to -5% of rig flow.	Compared With 5-B-01 No significant reduction in compressor noise was detected. With the 9% open area perforated liner.	BOEING SHAPED INLET WITH CENTERBODY COLLAPSED 3.5 FT² AIRFLOW AREA +6% TO -5% RIG FLOW CONF 5-B-2  9.0% OPEN AREA PERFORATED LINER
To determine the effect on noise of natural bleed flow through the 9.0% Open Area perforated liner.	Compared With 5-B-01 No significant change in noise was noted with natural bleed flow (venting the bleed ducts directly to the atmosphere).	BOEING SHAPED INLET WITH CENTERBODY COLLAPSED 3.5 FT² AIRFLOW AREA NATURAL BLEED CONF 6-B-5  9.0% OPEN AREA PERFORATED LINER
To determine the effect on noise of a sharp-lipped inlet and bleed airflow through wide open inlet blow-in doors.	Compared With Conf. 2-B-0A Tested During Phase II-A (Same Conf. Except Blow-In-Doors Were Closed) Discrete frequency compressor whine became much more audible when the inlet doors were opened, as contrasted with the random quality of the noise when the doors were closed.	SHARP-LIPPED BOEING SHAPED INLET WITH CENTER-BODY COLLAPSED 3.5 FT² AIRFLOW AREA CONF 7-B-1  INLET BLOW-IN DOORS WIDE OPEN
To evaluate the effect on noise of a sharp-lipped air intake and the bleed airflow through partially open inlet blow-in-doors.	Compared With 7-B-1 No significant change in compressor noise was detected. Once again, as with Conf. 7-B-1, Discrete frequencies were quite audible.	SHARP-LIPPED BOEING SHAPED INLET WITH CENTER-BODY COLLAPSED & 4 STRUTS 3.5 FT² AIRFLOW AREA CONF 7-B-2  INLET BLOW-IN DOORS 1/8 OPEN
To determine the effects of bleed airflow through partially opened inlet blow-in doors with a rig bell-mouth.	Compared With 7-B-2 and 5-B-01 No significant change in either noise level or directivity pattern.	BOEING SHAPED INLET WITH CENTER BODY COLLAPSED & 4 STRUTS 3.5FT² AIRFLOW AREA CONF 7-B-3  INLET BLOW-IN DOORS 1/8 OPEN

RESULTS OF NOISE TESTS

Figure 8-4
Sheet 3 of 5

DOWNGRADED AT 3 YEAR INTERVALS
DECLASSIFIED AFTER 12 YEARS
DOD DIR 5200.10

THIS DOCUMENT CONTAINS INFORMATION AFFECTING THE NATIONAL DEFENSE OF THE UNITED STATES WITHIN THE MEANING OF THE ESPIONAGE LAWS, TITLE 18, U.S.C., SECTIONS 793 AND 794. THE TRANSMISSION OR THE REVELATION OF ITS CONTENTS IN ANY MANNER TO AN UNAUTHORIZED PERSON IS PROHIBITED BY LAW.

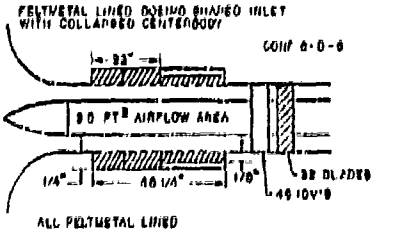
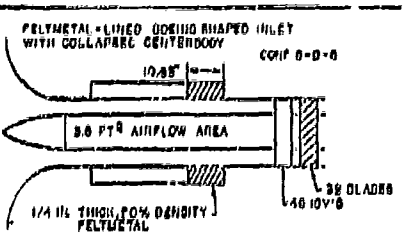
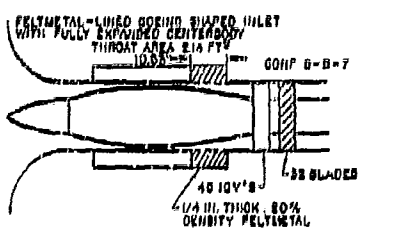
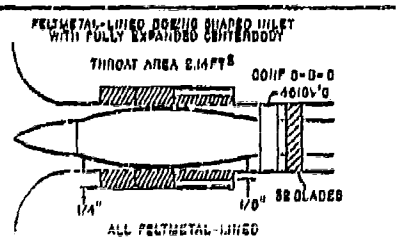
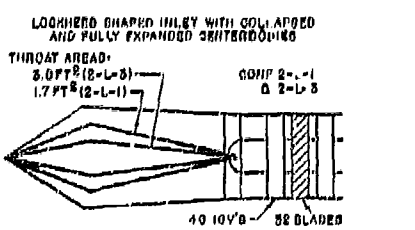
OBJECT OF TEST	RESULT OF TEST	TEST CONFIGURATION
To obtain a baseline for tests with acoustical linings installed.	Baseline Configuration Sound documented over rig operating range.	BOEING SHAPED INLET WITH COLLAPSED CENTERBODY AND NO SOUND TREATMENT CONF 0-0-0 46 1/4" 3.6 FT² AIRFLOW AREA 46 IGV'S SOLID LINERS 22 BLADES
To determine the noise attenuation from lining the front half of the inlet duct with 1/8" thick Feltmetal.	Compared With 0-0-0 Discrete noise levels at angles of 30 to 90 degrees from the compressor centerline were reduced from 5 to 12 db at rig speeds up to 75% of maximum, and by 4 to 10 db at 85% of maximum to maximum rig speeds.	FELTMETAL-LINED BOEING SHAPED INLET WITH COLLAPSED CENTERBODY CONF 0-0-1 24 1/4" 3.6 FT² AIRFLOW AREA 46 IGV'S 1/8 IN. THICK, 20% DENSITY FELTMETAL 22 BLADES
To determine whether a given length of Feltmetal lining is more effective in the rear of the inlet rather than in the front.	Compared with 0-0-0 & 0-0-1 Lining the rear of the duct resulted in from 3 to 5 db more noise attenuation.	FELTMETAL-LINED BOEING SHAPED INLET WITH COLLAPSED CENTERBODY CONF 0-0-2 24 1/4" 3.6 FT² AIRFLOW AREA 22 BLADES 46 IGV'S 1/8 IN. THICK, 20% DENSITY FELTMETAL
To determine the acoustical effectiveness of doubling the thickness of the Feltmetal lining.	Compared with 0-0-0 & 0-0-1 The thicker lining appeared to be no more effective than the 1/8" thick lining.	FELTMETAL-LINED BOEING SHAPED INLET WITH COLLAPSED CENTERBODY CONF 0-0-3 22" 3.6 FT² AIRFLOW AREA 46 IGV'S 22 BLADES 1/4 IN. THICK, 20% DENSITY FELTMETAL
To determine the noise attenuation from lining the rear half of the inlet duct with 1/4" thick Feltmetal.	Compared with 0-0-0 & 0-0-2 Lining the rear of the duct appeared to be more effective than lining the front. The thicker lining appeared to be no more effective than an equal length of 1/8" lining in the same location.	FELTMETAL-LINED BOEING SHAPED INLET WITH COLLAPSED CENTERBODY CONF 0-0-4 22" 3.6 FT.² AIRFLOW AREA 46 IGV'S 22 BLADES 1/4 IN. THICK, 20% DENSITY FELTMETAL

RESULTS OF NOISE TESTS

Figure 8-4
Sheet 4 of 5

DOWNGRADED AT 3 YEAR INTERVALS
DECLASSIFIED AFTER 12 YEARS
DOD DIR 5200.10

THIS DOCUMENT CONTAINS INFORMATION AFFECTING THE NATIONAL DEFENSE OF THE UNITED STATES WITHIN THE MEANING OF THE ESPIONAGE LAWS, TITLE 18 U.S.C. SECTIONS 793 AND 794. THE TRANSMISSION OR THE REVELATION OF ITS CONTENTS IN ANY MANNER TO AN UNAUTHORIZED PERSON IS PROHIBITED BY LAW.

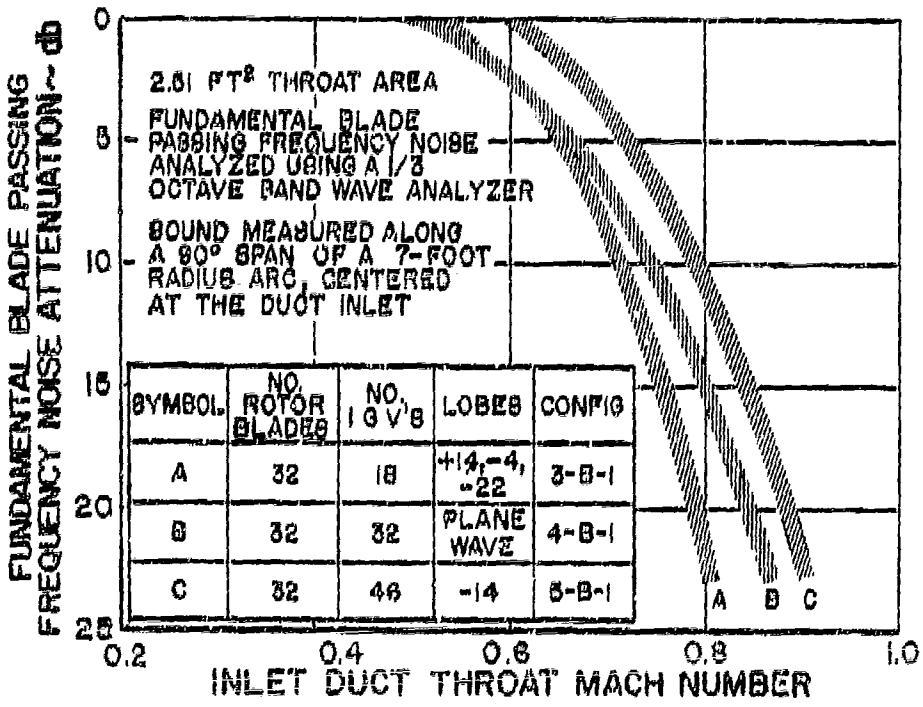
OBJECT OF TEST	RESULT OF TEST	TEST CONFIGURATION
To determine the effect of length of inlet duct lining on noise attenuation.	Compared with 0-D-0 Discrete noise levels at angles of 30 to 90 degrees from the compressor centerline were reduced by 15 to 18 db at rig speeds up to 74% of maximum, and by 7 to 15 db at 84% of maximum to maximum rig speeds, indicating that noise attenuation increased as the length of lining increased.	
To determine the effect of length of inlet duct lining on noise attenuation.	Compared with 0-D-0 Discrete noise levels at angles of 30 to 90 degrees from the compressor centerline were reduced by 5 to 7 db at rig speeds up to 74% of maximum, and by 3 to 5 db at 84% of maximum to maximum rig speeds	
To determine whether the effectiveness of an acoustical lining is enhanced when combined with an expanded centerbody.	Compared to 0-D-0 This short length of acoustical treatment combined with the expanded centerbody produced a slightly greater attenuation than the configuration of equal lining length but with a collapsed centerbody.	
To determine whether the effectiveness of a full acoustical lining is enhanced when combined with an expanded centerbody.	Compared with 0-D-0 The combination of full acoustical treatment and expanded centerbody shape produced a greater attenuation than the configuration of full acoustical lining with a collapsed centerbody.	
To determine the effect of choking on the noise from a two-dimensional inlet.	Compared with 5-D-0, 5-D-1 & 5-D-2 Acoustic results were similar to those obtained with the Dobiid shaped axisymmetric inlets.	

RESULTS OF NOISE TESTS

Figure 8-4
Sheet 5 of 5

DOWNGRADED AT 6 YEAR INTERVALS
DECLASSIFIED AFTER 12 YEARS
DOD DIR 5200.10

THIS DOCUMENT CONTAINS INFORMATION AFFECTING THE NATIONAL DEFENSE OF THE UNITED STATES WITHIN THE MEANING OF THE ESPIONAGE LAWS, TITLE 18, U.S.C., SECTIONS 793 AND 794. THE TRANSMISSION OR THE REVELATION OF ITS CONTENTS IN ANY MANNER TO AN UNAUTHORIZED PERSON IS PROHIBITED BY LAW.

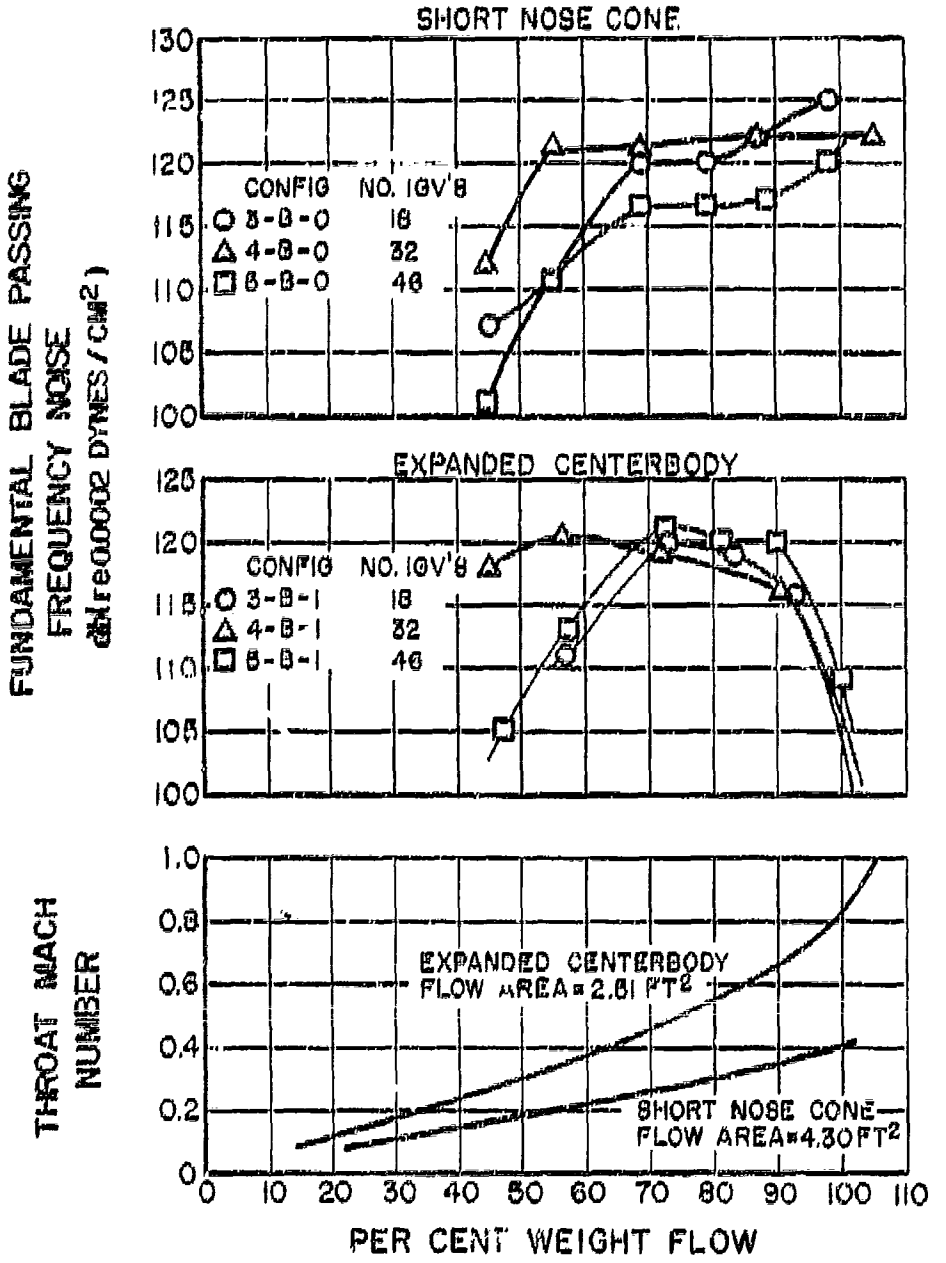


EFFECT OF DUCT FLOW MACH NUMBER ON INLET NOISE FOR AXISYMMETRIC DUCTS

Figure 8-5

DOWNGRADED AT 3 YEAR INTERVALS
DECLASSIFIED AFTER 12 YEARS
DOD DIR 5200.10

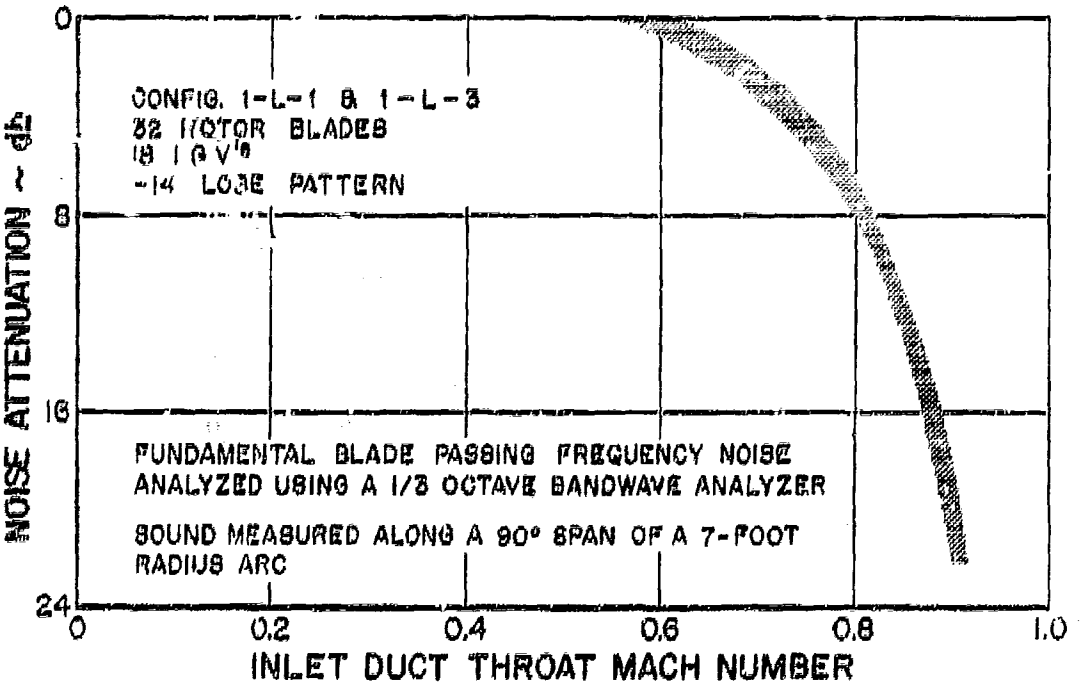
THIS DOCUMENT CONTAINS INFORMATION AFFECTING THE NATIONAL DEFENSE OF THE UNITED STATES WITHIN THE MEANING OF THE ESPIONAGE LAWS, TITLE 18, U.S.C., SECTIONS 793 AND 794. THE TRANSMISSION OR THE REVELATION OF ITS CONTENTS IN ANY MANNER TO AN UNAUTHORIZED PERSON IS PROHIBITED BY LAW.



INLET NOISE AND THROAT MACH NUMBER AS A FUNCTION OF DUCT AIRFLOW

Figure 8-6

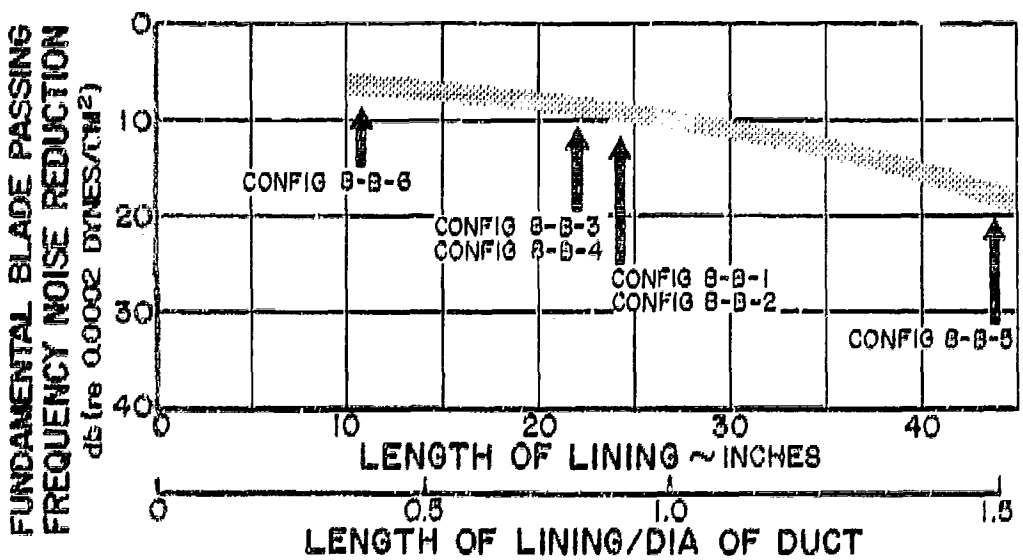
DOWNGRADED AT 3 YEAR INTERVALS
DECLASSIFIED AFTER 12 YEARS
DOD DIR 5200.10



EFFECT OF DUCT FLOW MACH NUMBER ON INLET NOISE FOR TWO-DIMENSIONAL INLETS

Figure 8-7

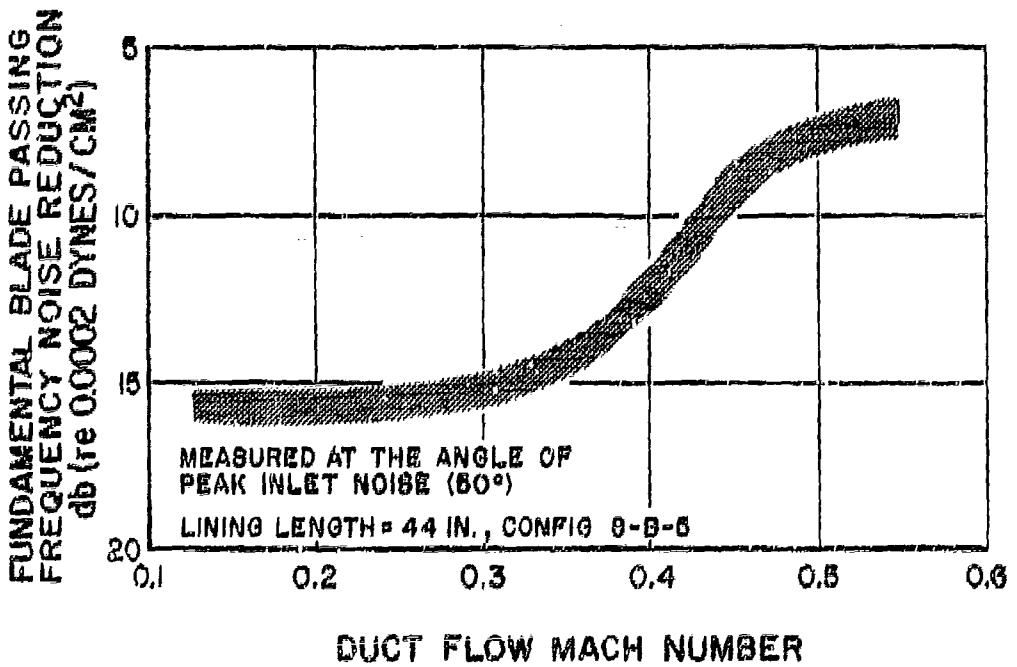
DOWNGRADED AT 3 YEAR INTERVALS
DECLASSIFIED AFTER 12 YEARS
DOD DIR 5200.10



EFFECT OF FELTMETAL ACOUSTIC LINING LENGTH ON INLET NOISE REDUCTION

Figure 8-8

DOWNGRADED AT 3 YEAR INTERVALS
DECLASSIFIED AFTER 12 YEARS
DOD DIR 5200.10

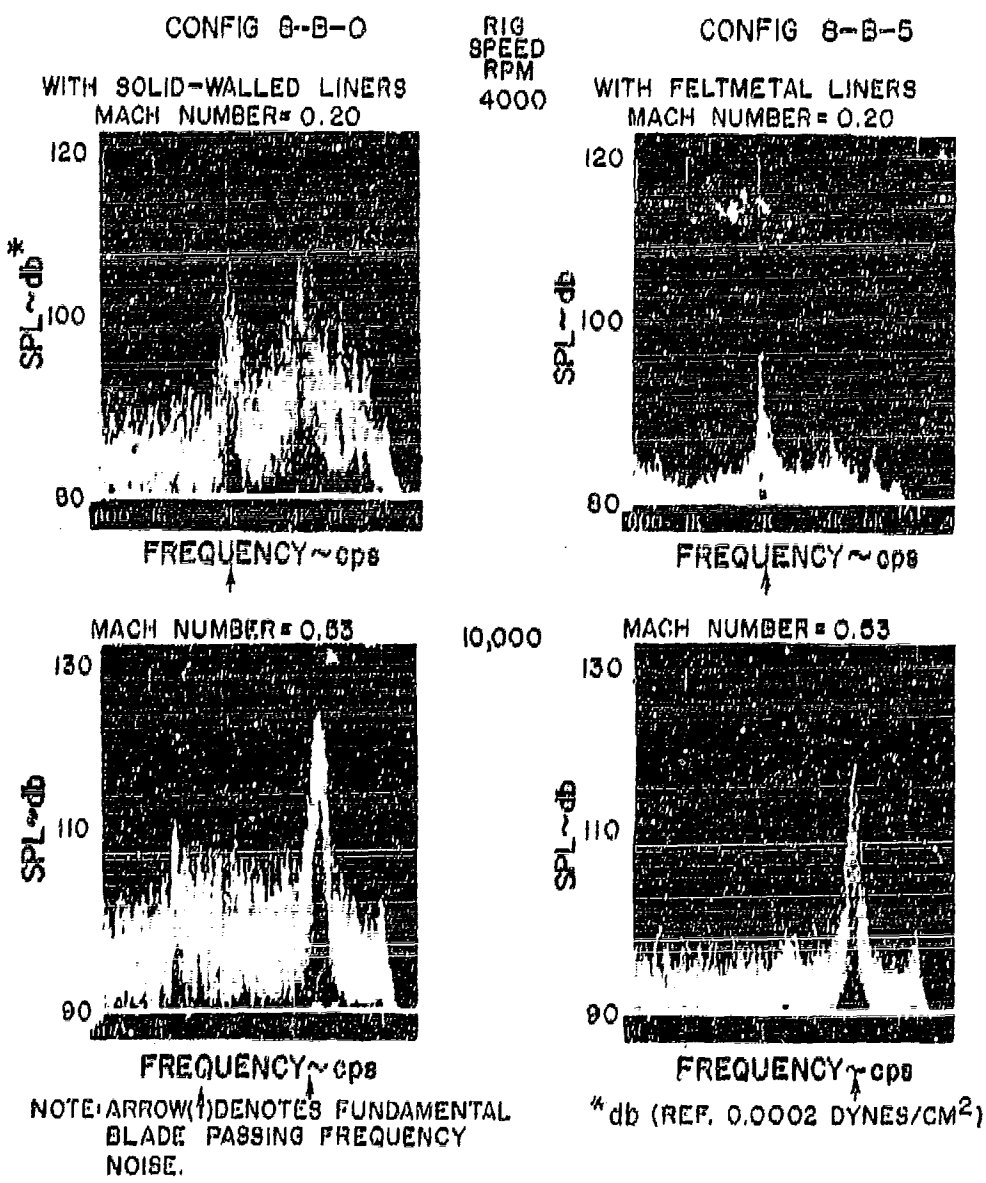


EFFECT OF INLET DUCT AIRFLOW MACH NUMBER ON THE ACOUSTIC EFFECTIVENESS OF FELTMETAL DUCT LINING

Figure 8-9

DOWNGRADED AT 3 YEAR INTERVALS
DECLASSIFIED AFTER 12 YEARS
DOD DIR 5200.10

THIS DOCUMENT CONTAINS INFORMATION AFFECTING THE NATIONAL DEFENSE OF THE UNITED STATES WITHIN THE MEANING OF THE ESPIONAGE LAWS, TITLE 18, U.S.C., SECTIONS 793 AND 794. THE TRANSMISSION OR THE REVELATION OF ITS CONTENTS IN ANY MANNER TO AN UNAUTHORIZED PERSON IS PROHIBITED BY LAW.



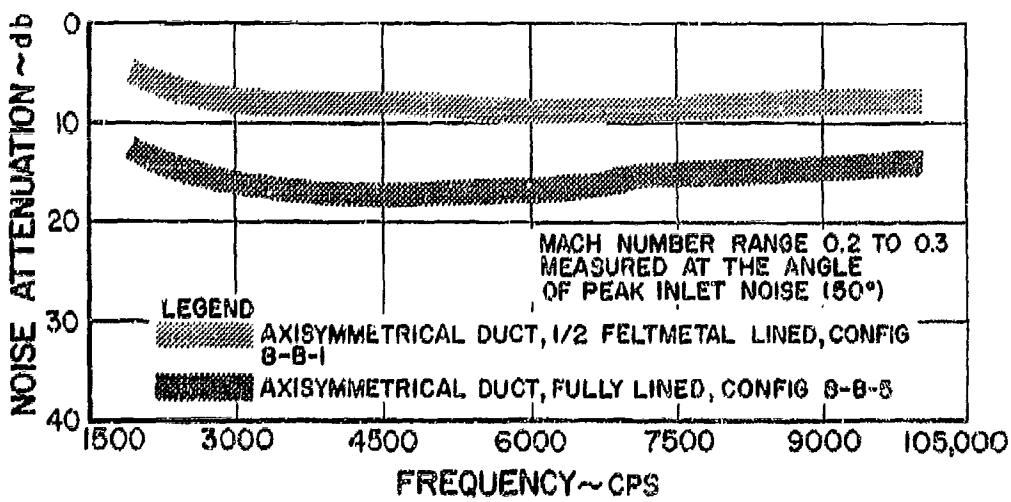
NOTE: ARROW(↑) DENOTES FUNDAMENTAL BLADE PASSING FREQUENCY NOISE.

* db (REF. 0.0002 DYNES/CM^2)

COMPARISON OF INLET NOISE SPECTRA FOR FELTMETAL LINERS AND SOLID-WALLED LINERS

Figure 8-10

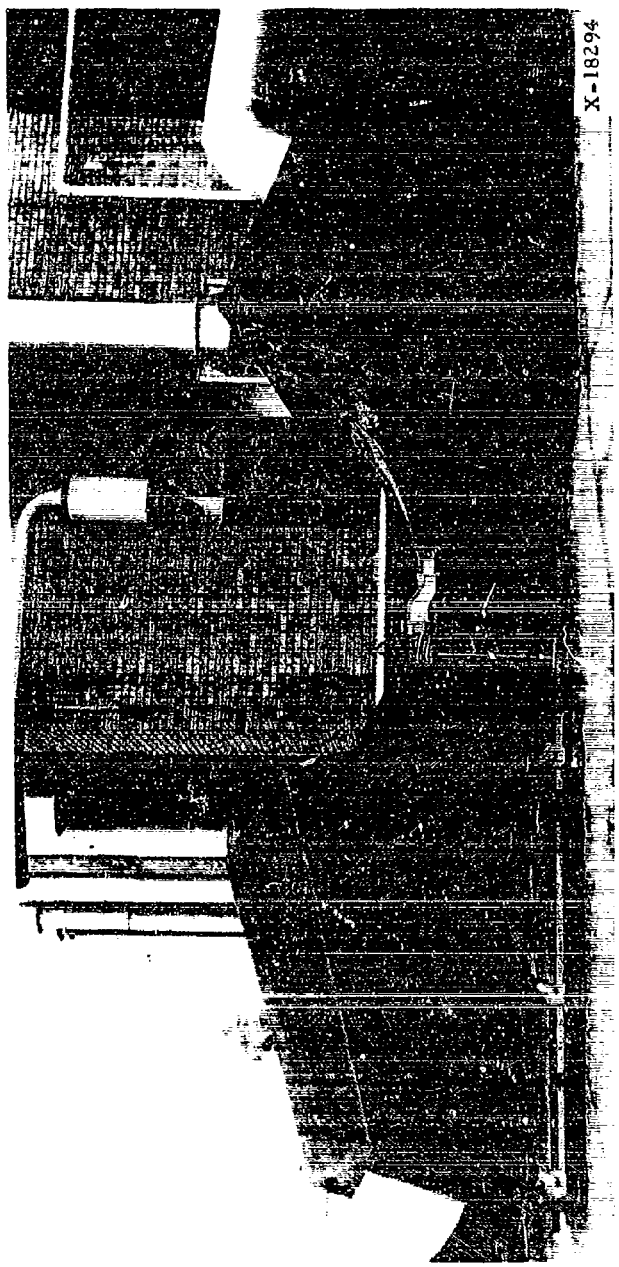
DOWNGRADED AT 3 YEAR INTERVALS
DECLASSIFIED AFTER 12 YEARS
DOD DIR 5200.10



NOISE ATTENUATION VS. FREQUENCY FOR A FELTMETAL LINED INLET DUCT

Figure 8-11

DOWNGRADED AT 3 YEAR INTERVALS
DECLASSIFIED AFTER 12 YEARS
DOD DIR 5200.10



REVERBERATION CHAMBER TEST FACILITY

Figure 8-12

DOWNGRADED AT 3 YEAR INTERVALS
DECLASSIFIED AFTER 12 YEARS
DOD DIR 5200.10



FAN DISCHARGE DUCT MODEL FOR TESTING SOUND ABSORPTION MATERIALS

Figure 8-13

DOWNGRADED AT 3 YEAR INTERVALS
DECLASSIFIED AFTER 12 YEARS
DOD DIR 5200.10

SPECIFICATIONS FOR NOISE ATTENUATION TREATMENTS TESTED IN FAN DISCHARGE DUCT MODEL

Configuration	Facing	Backing Material	Total Thickness, inch
A	0.125" Feltmetal	Air, Segmented by Splitters Spaced 5" Apart Axially	0.50
B	0.125" Feltmetal	0.375" Fiberglas	0.50
C	0.125" Feltmetal	Cerafelt	0.50
D	Slitmetal	Cerafelt	0.50
E	Perforated Plate & Wire Mesh Screen	Cerafelt	0.50

Slitmetal: Type 347 SS, 0.040" Thick, 30-70 Rayls Flow Resistance, Slits 0.010" Wide And 0.25" Long, 3000 Slits/ft^2

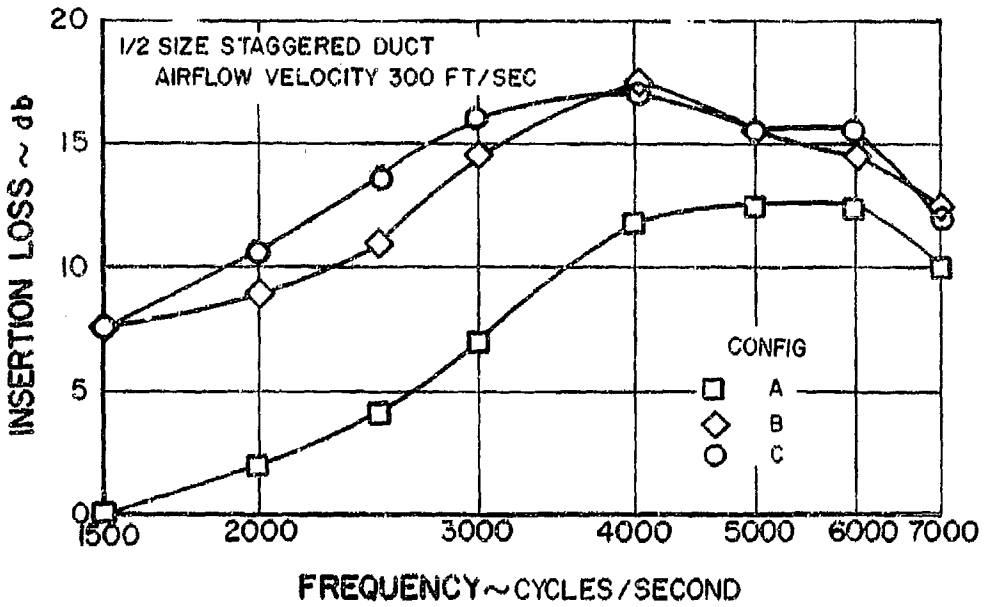
Feltmetal: Type 302 SS Sin[illegible]d Fiber Matting, Fiber Dia. ≈ 15 Microns, Pore Size ≈ 15 to 37 microns, Density ≈ 20%

Perforated Plate & Wire Mesh Screen: 3/32" Dia. Holes Staggered on 3/16" Centers, 22% Open Area, 0.037" Thick SS; Screen has 20 x 100 wires/in^2

Figure 8-14

DOWNGRADED AT 3 YEAR INTERVALS
DECLASSIFIED AFTER 12 YEARS
DOD DIR 5200.10

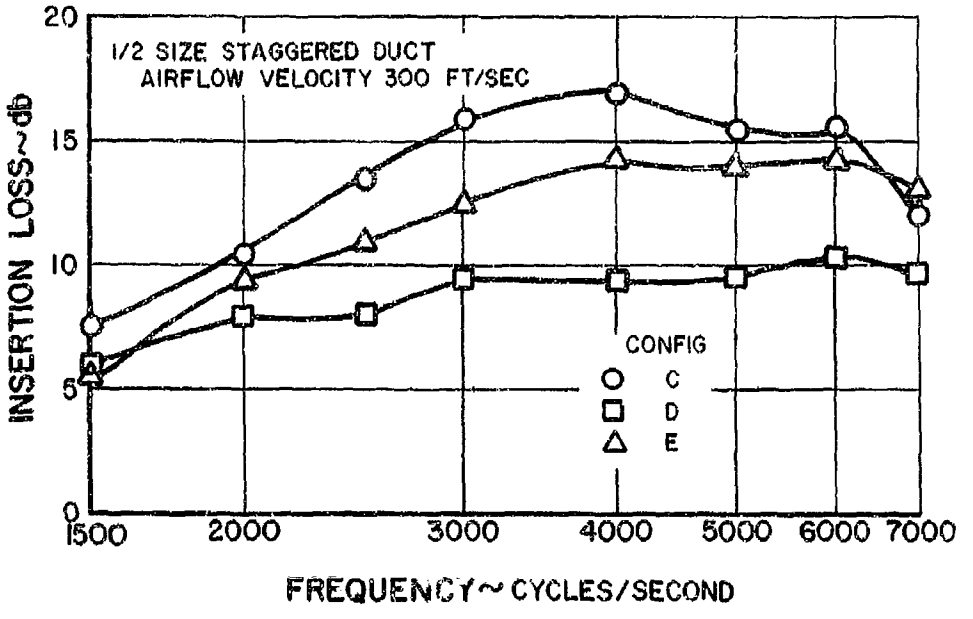
This document contains information affecting the national defense of the United States within the meaning of the espionage laws, Title 18, U.S.C., Sections 793 and 794. The transmission or revelation of its contents in any manner to an unauthorized person is prohibited by law.



INSERTION LOSS WITH FAN DUCT TREATMENTS A, B AND C

Figure 8-15

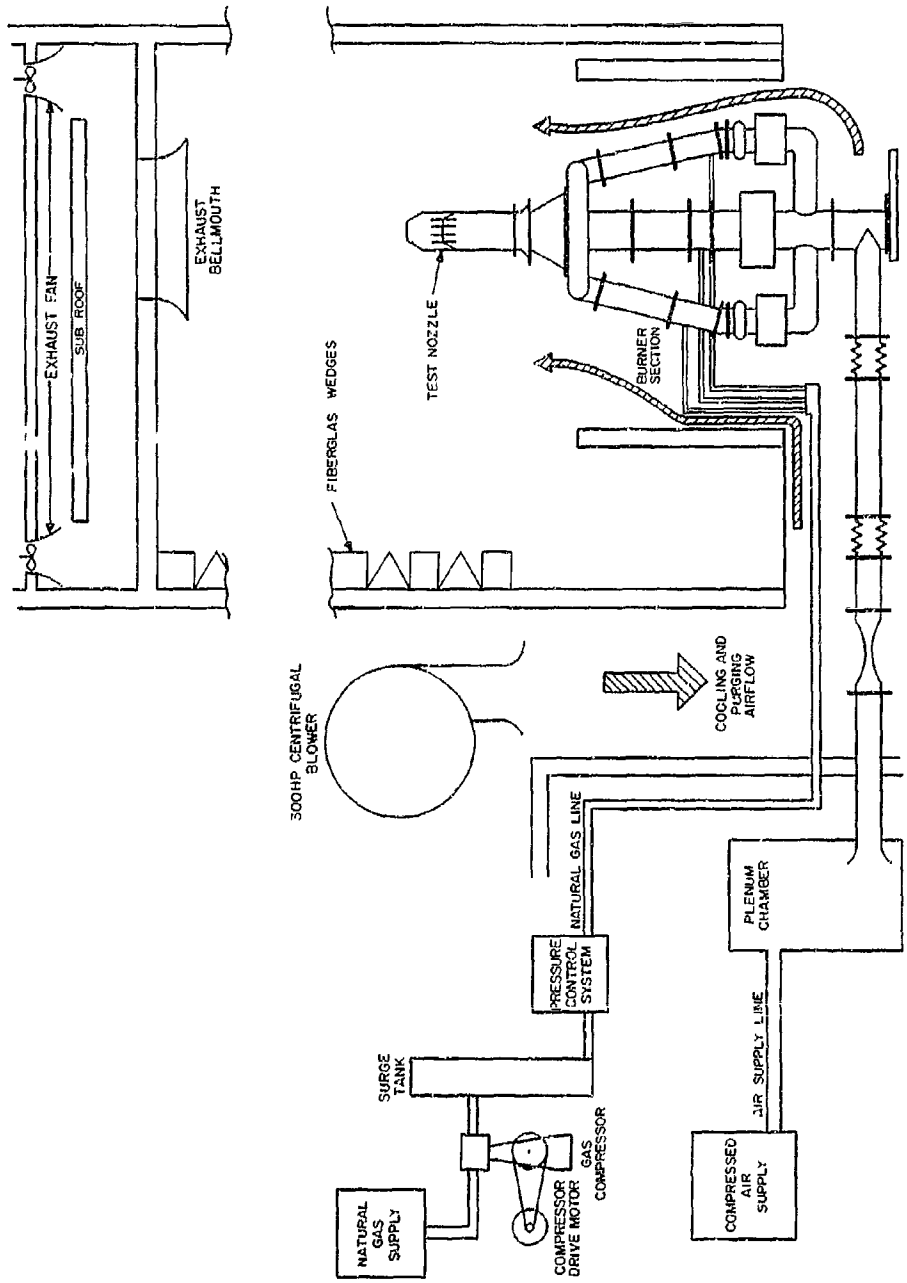
DOWNGRADED AT 3 YEAR INTERVALS
DECLASSIFIED AFTER 12 YEARS
DOD DIR 5200.10



INSERTION LOSS WITH FAN DUCT TREATMENTS C, D AND E

Figure 8-16

DOWNGRADED AT 3 YEAR INTERVALS
DECLASSIFIED AFTER 12 YEARS
DOD DIR 5200.10

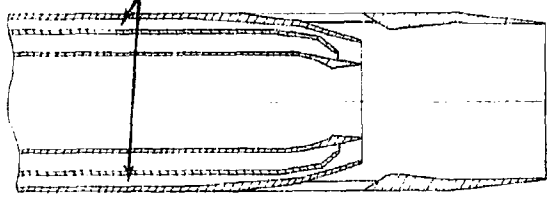


OVERALL DIAGRAM OF ANECHOIC CHAMBER TEST FACILITY

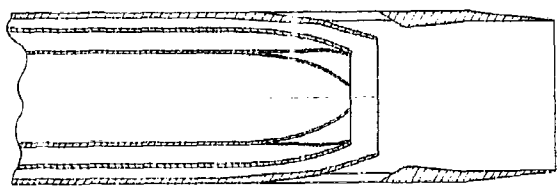
Figure 8-17

DOWNGRADED AT 3 YEAR INTERVALS
DECLASSIFIED AFTER 12 YEARS
DOD DIR 5200.10

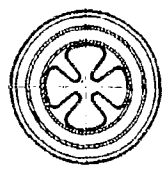
BLOCKED COOLING PASSAGE

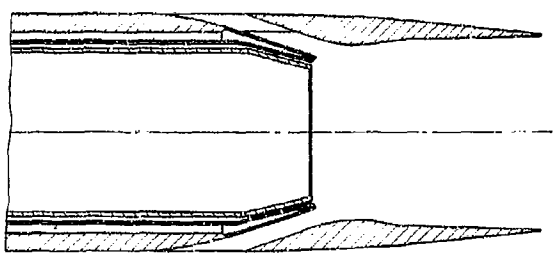


CALIBRATION
CONFIGURATION 1,6,1

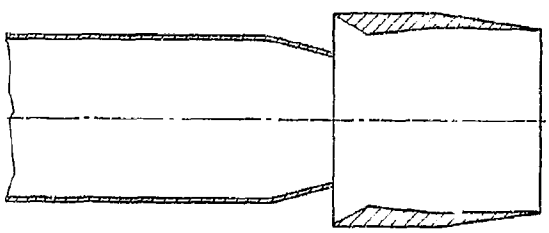


SCALLOPED PRIMARY NOZZLE
CONFIGURATION 3,5,1





TURBOJET NOZZLE
WITH MODEL OF EJECTOR
USED ON YF-12A AIRCRAFT
CONFIGURATION 8,0,7



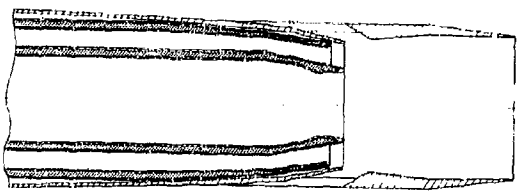
TURBOJET NOZZLE
WITH EJECTOR GEOMETRICALLY
SIMILAR TO STF219 BUT SCALED
TO THE TURBOJET MODEL
CONFIGURATION 8,0,8

BLOW-IN-DOOR EJECTOR NOZZLE MODELS FOR NOISE TESTS
WITHOUT DUCT HEATING

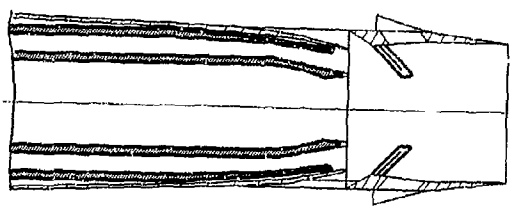
Figure 8-18

DOWNGRADED AT 3 YEAR INTERVALS
DECLASSIFIED AFTER 12 YEARS
DOD DIR 5200.10

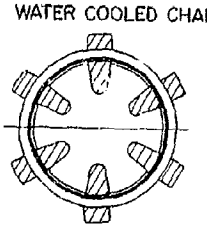
THIS DOCUMENT CONTAINS INFORMATION AFFECTING THE NATIONAL DEFENSE OF THE UNITED STATES WITHIN THE MEANING OF THE ESPIONAGE LAWS, TITLE 18 U.S.C. SECTIONS 793 AND 794. THE TRANSMISSION OR THE REVELATION OF ITS CONTENTS IN ANY MANNER TO AN UNAUTHORIZED PERSON IS PROHIBITED BY LAW



WATER COOLED MODEL
OF STF219 NOZZLE
CONFIGURATION 2,3,1

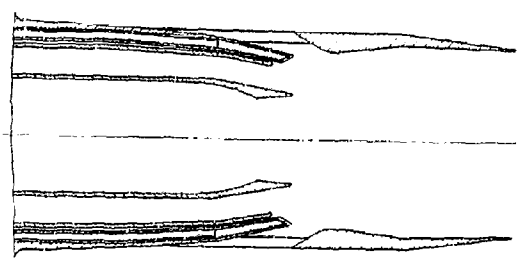


WATER COOLED CHANNEL EJECTOR



CONFIGURATION 2,3,3

CHANNELS SHOWN
FOR MAXIMUM
PROTRUSION INTO
THE STREAM



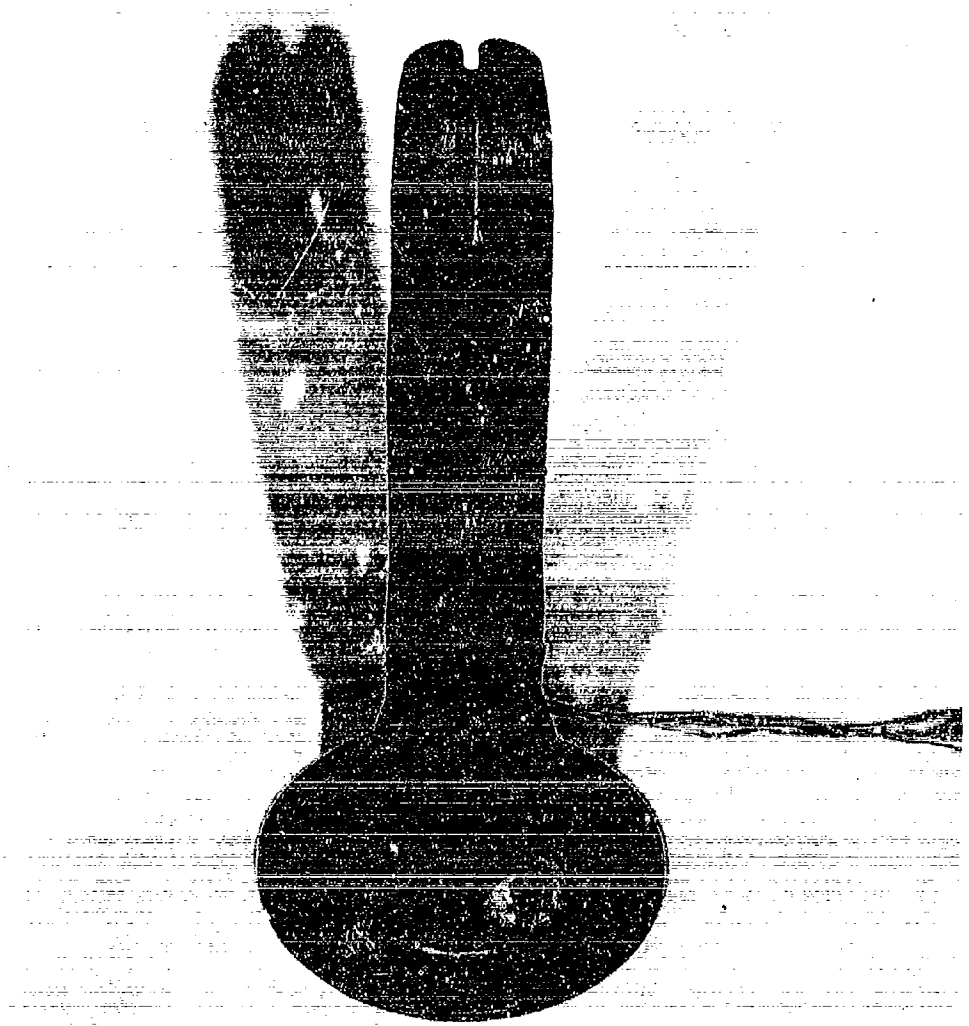
TANTALUM ALLOY MODEL
OF STF219 NOZZLE
CONFIGURATION 9,7,1

BLOW-IN-DOOR EJECTOR NOZZLE MODELS FOR NOISE TESTS WITH DUCT HEATING

Figure 8-19

DOWNGRADED AT 3 YEAR INTERVALS
DECLASSIFIED AFTER 12 YEARS
DOD DIR 5200.10

THIS DOCUMENT CONTAINS INFORMATION AFFECTING THE NATIONAL DEFENSE OF THE UNITED STATES WITHIN THE MEANING OF THE ESPIONAGE LAWS, TITLE 18 U.S.C. SECTIONS 793 AND 794. ITS TRANSMISSION OR THE REVELATION OF ITS CONTENTS IN ANY MANNER TO AN UNAUTHORIZED PERSON IS PROHIBITED BY LAW.



SCALLOPED PRIMARY NOZZLE

Figure 8-20

DOWNGRADED AT 3 YEAR INTERVALS
DECLASSIFIED AFTER 12 YEARS
DOD DIR 5200.10

THIS DOCUMENT CONTAINS INFORMATION AFFECTING THE NATIONAL DEFENSE OF THE UNITED STATES WITHIN THE MEANING OF THE ESPIONAGE LAWS, TITLE 18, U.S.C., SECTIONS 793 AND 794. THE TRANSMISSION OR THE REVELATION OF ITS CONTENTS IN ANY MANNER TO AN UNAUTHORIZED PERSON IS PROHIBITED BY LAW.

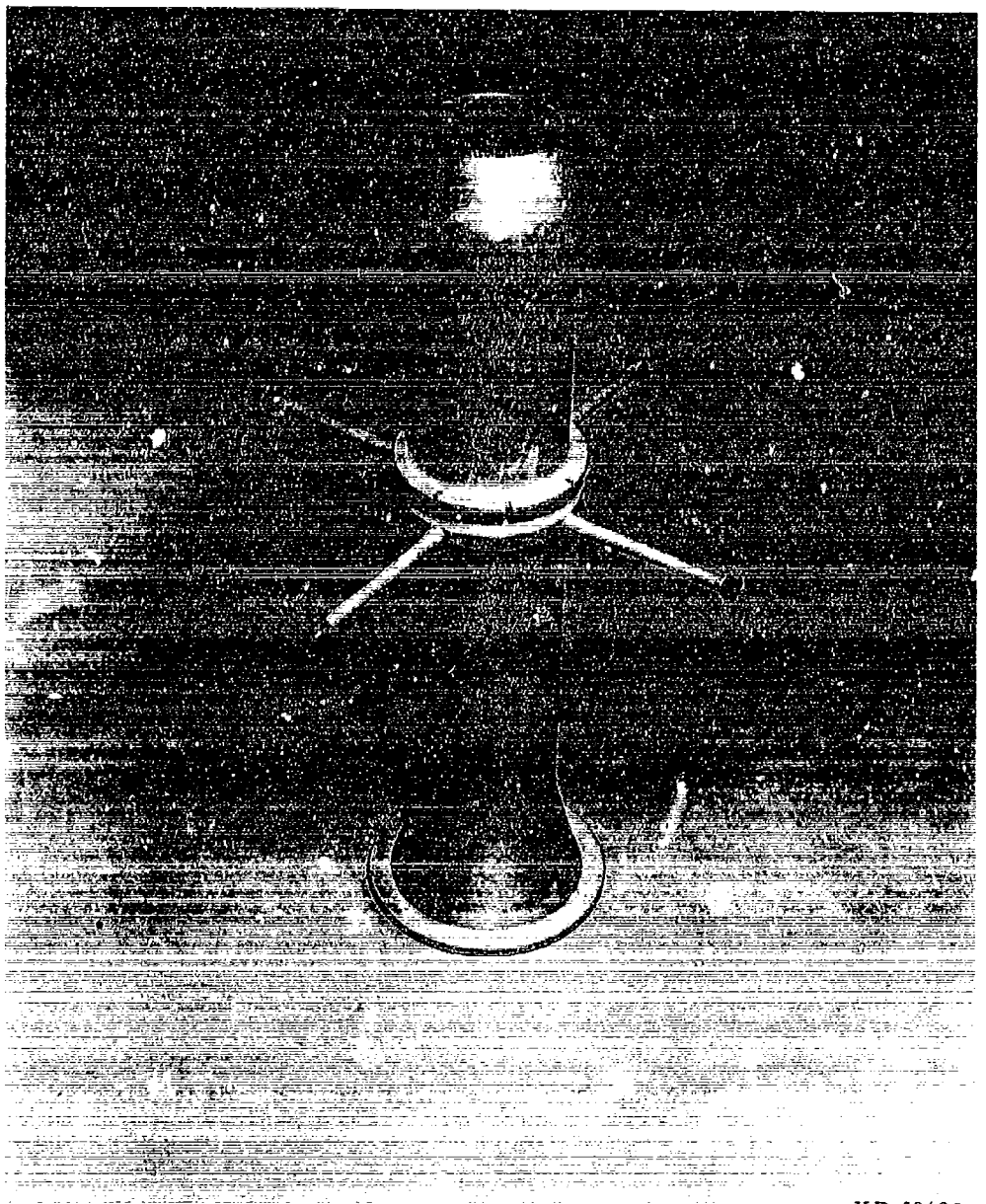


SCALLOPED PRIMARY NOZZLE AND DUCT NOZZLE ASSEMBLY

Figure 8-21

DOWNGRADED AT 3 YEAR INTERVALS
DECLASSIFIED AFTER 12 YEARS
DOD DIR 5200.10

THIS DOCUMENT CONTAINS INFORMATION AFFECTING THE NATIONAL DEFENSE OF THE UNITED STATES WITHIN THE MEANING OF THE ESPIONAGE LAWS, TITLE 18, U.S.C. SECTIONS 793 AND 794. ITS TRANSMISSION OR THE REVELATION OF ITS CONTENTS IN ANY MANNER TO AN UNAUTHORIZED PERSON IS PROHIBITED BY LAW.



XP-52620

TANTALUM ALLOY TURBOJET NOZZLE MODEL

Figure 8-22

DOWNGRADED AT 3 YEAR INTERVALS
DECLASSIFIED AFTER 12 YEARS
DOD DIR 5200.10

THIS DOCUMENT CONTAINS INFORMATION AFFECTING THE NATIONAL DEFENSE OF THE UNITED STATES WITHIN THE MEANING OF THE ESPIONAGE LAWS, TITLE 18, U.S.C., SECTIONS 793 AND 794. THE TRANSMISSION OR THE REVELATION OF ITS CONTENTS IN ANY MANNER TO AN UNAUTHORIZED PERSON IS PROHIBITED BY LAW.



XP-52618

TURBOJET NOZZLE MODEL WITH WATER-COOLED JACKET SIMULATING BLOW-IN DOORS

Figure 8-23

DOWNGRADED AT 3 YEAR INTERVALS
DECLASSIFIED AFTER 12 YEARS
DOD DIR 5200.10

THIS DOCUMENT CONTAINS INFORMATION AFFECTING THE NATIONAL DEFENSE OF THE UNITED STATES WITHIN THE MEANING OF THE ESPIONAGE LAWS, TITLE 18, U.S.C., SECTIONS 793 AND 794. ITS TRANSMISSION OR THE REVELATION OF ITS CONTENTS IN ANY MANNER TO AN UNAUTHORIZED PERSON IS PROHIBITED BY LAW.



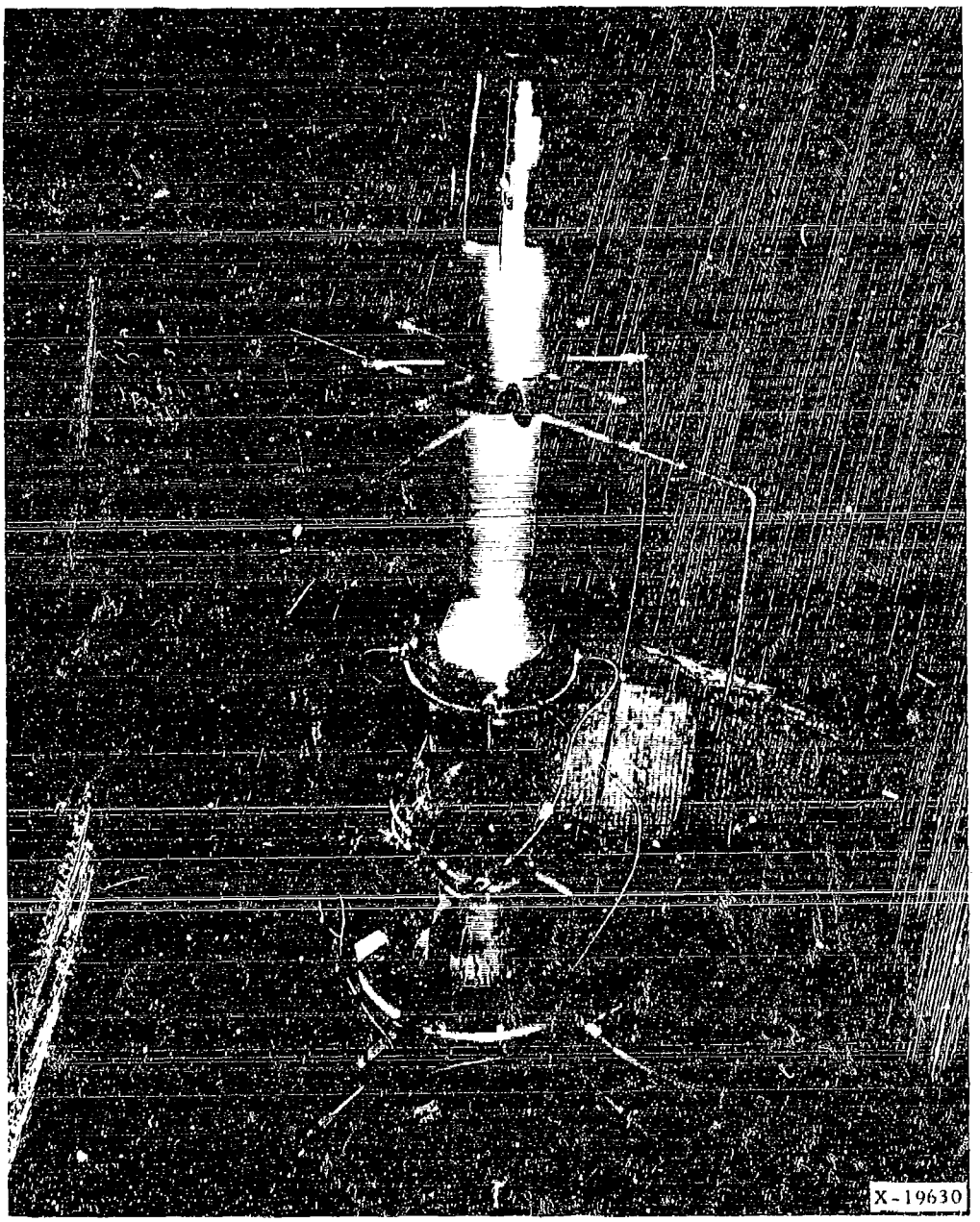
XP-52622

TURBOJET NOZZLE WITH MODEL OF EJECTOR USED ON YT-12A AIRCRAFT

Figure 8-24

DOWNGRADED AT 3 YEAR INTERVALS
DECLASSIFIED AFTER 12 YEARS
DOD DIR 5200.10

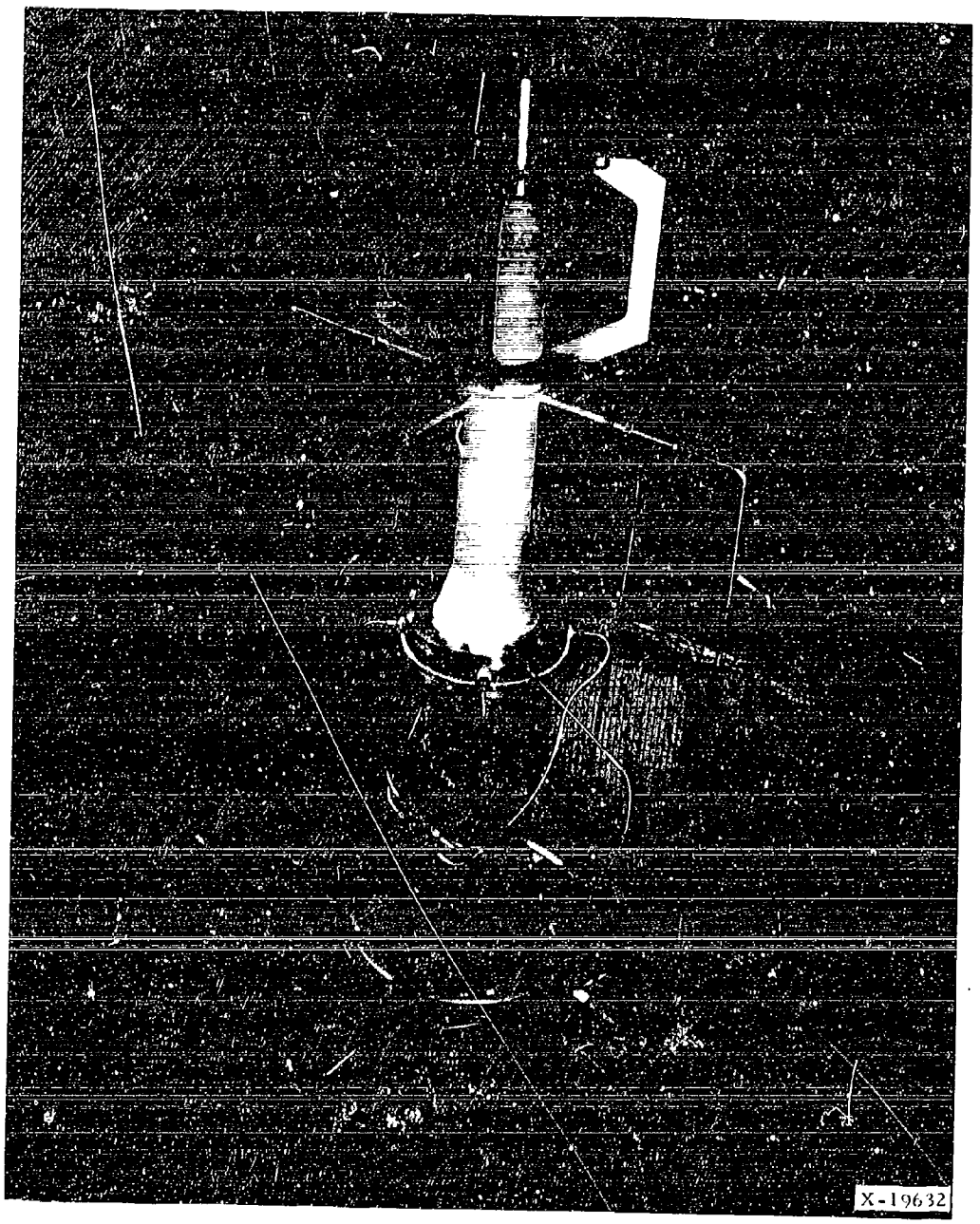
THIS DOCUMENT CONTAINS INFORMATION AFFECTING THE NATIONAL DEFENSE OF THE UNITED STATES WITHIN THE MEANING OF THE ESPIONAGE LAWS, TITLE 18, U.S.C., SECTIONS 793 AND 794. ITS TRANSMISSION OR THE REVELATION OF ITS CONTENTS IN ANY MANNER TO AN UNAUTHORIZED PERSON IS PROHIBITED BY LAW.



TEST STAND INSTALLATION OF TURBOJET NOZZLE WITH MODEL OF EJECTOR USED ON YF-12A AIRCRAFT

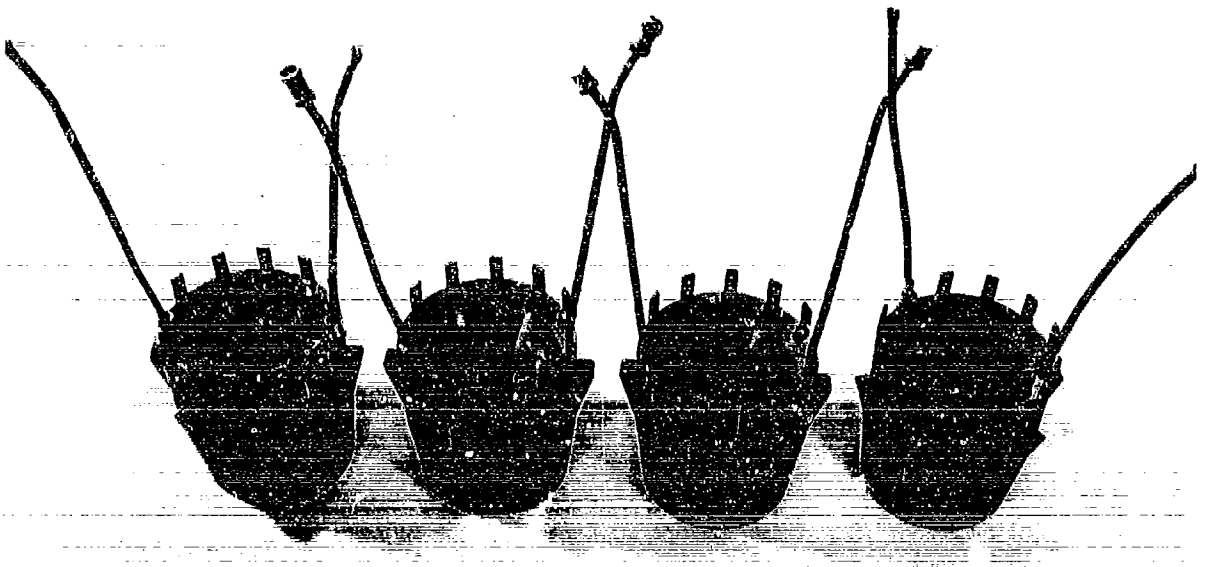
Figure 8-25

DOWNGRADED AT 3 YEAR INTERVALS
DECLASSIFIED AFTER 12 YEARS
DOD DIR 5200.10

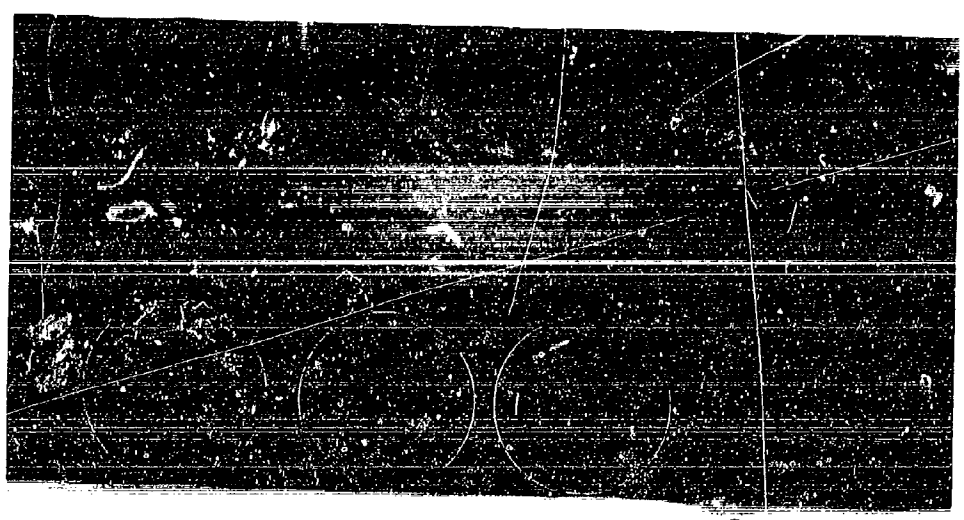


TEST STAND INSTALLATION OF TURBOJET NOZZLE WITH EJECTOR GEOMETRICALLY SIMILAR TO STF219 BUT SCALED TO THE TURBOJET MODEL

Figure 8-26



X-19678

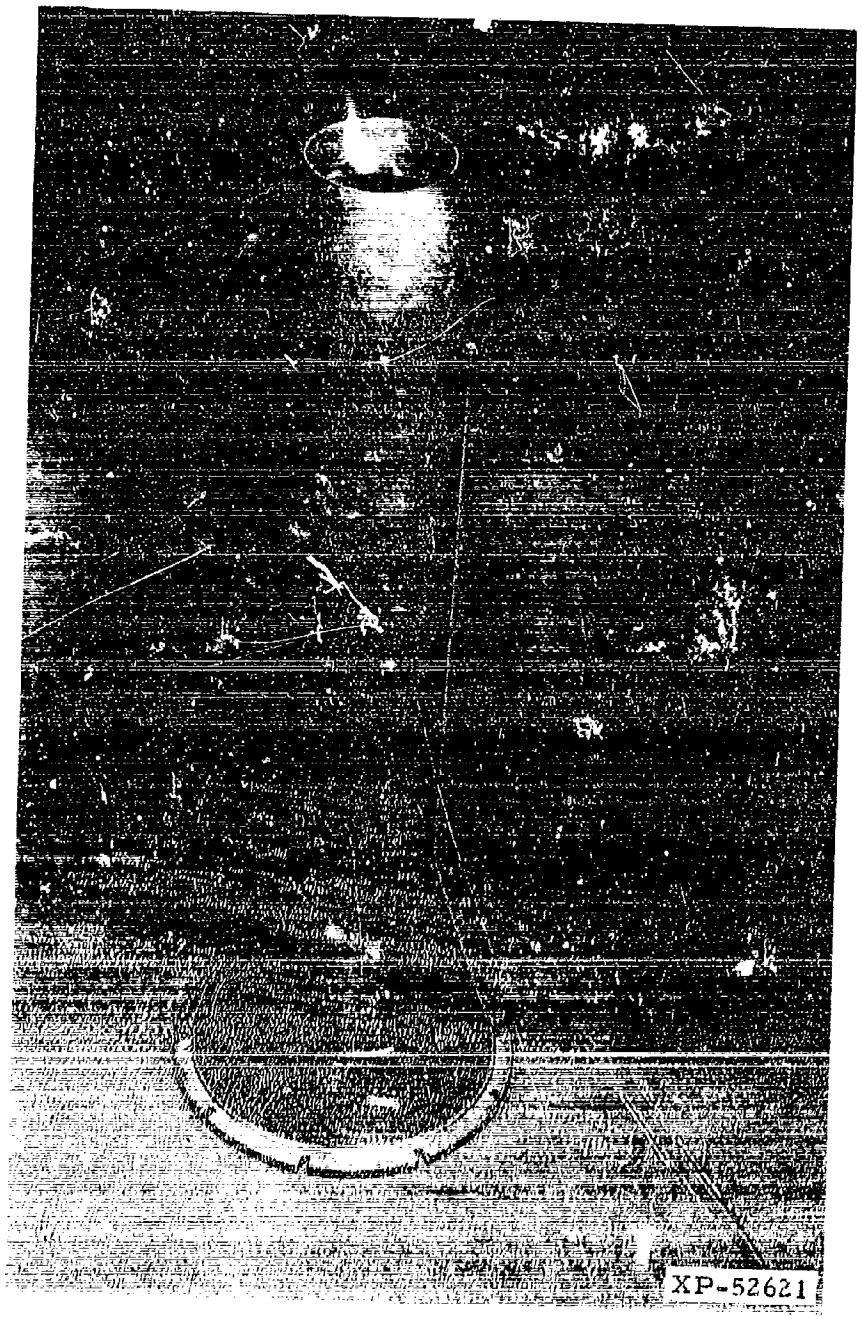


X-19673

WATER-COOLED CHANNEL EJECTORS

Figure 8-27

DOWNGRADED AT 3 YEAR INTERVALS
DECLASSIFIED AFTER 12 YEARS
DOD DIR 5200.10



STF219 TANTALUM-ALLOY PRIMARY NOZZLE MODEL

Figure 8-28

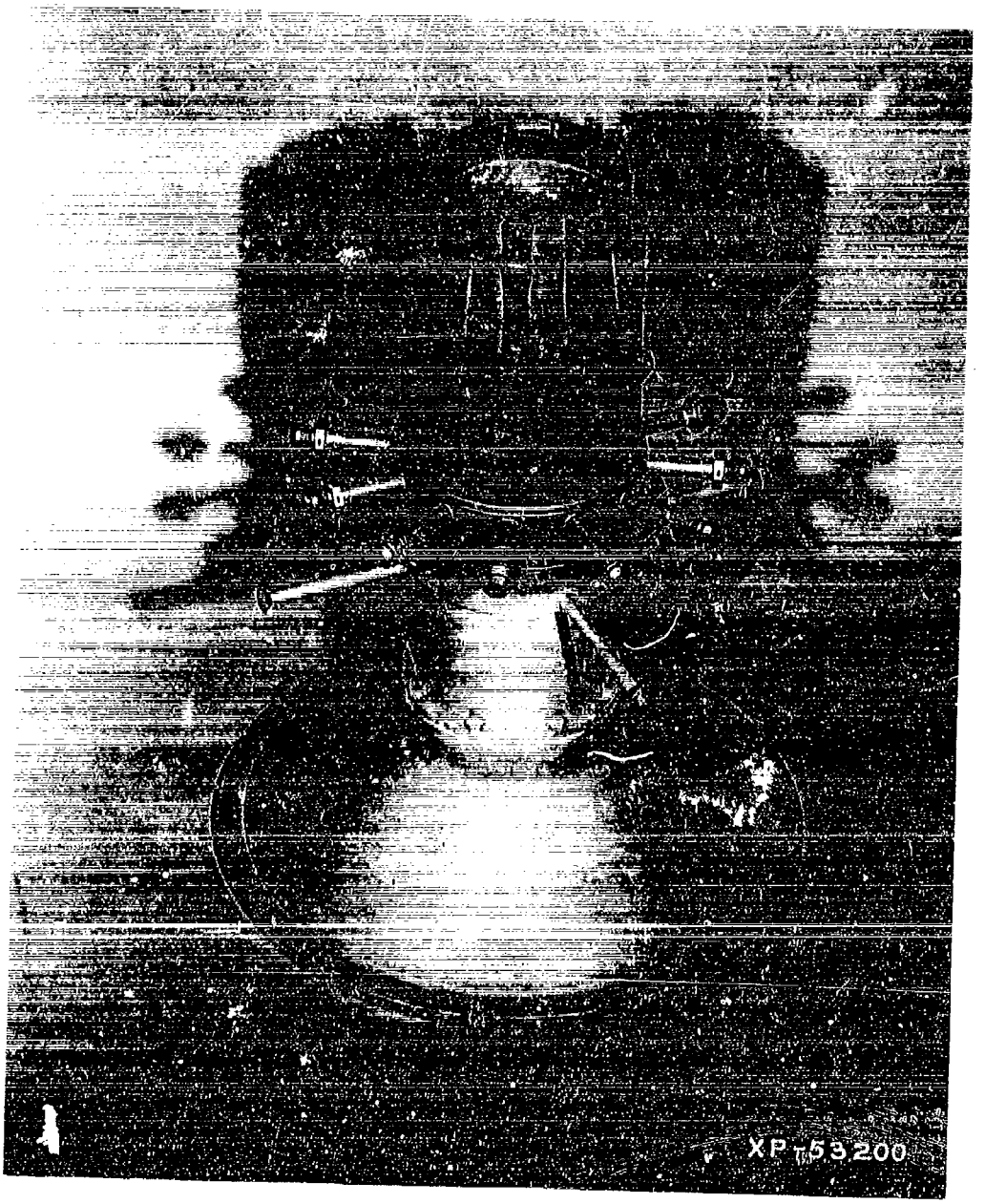


STF219 TANTALUM-ALLOY DUCT NOZZLE MODEL

Figure 8-29

DOWNGRADED AT 3 YEAR INTERVALS
DECLASSIFIED AFTER 12 YEARS
DOD DIR 5200.10

THIS DOCUMENT CONTAINS INFORMATION AFFECTING THE NATIONAL DEFENSE OF THE UNITED STATES WITHIN THE MEANING OF THE ESPIONAGE LAWS, TITLE 18, U.S.C., SECTIONS 793 AND 794. THE TRANSMISSION OR THE REVELATION OF ITS CONTENTS IN ANY MANNER TO AN UNAUTHORIZED PERSON IS PROHIBITED BY LAW.

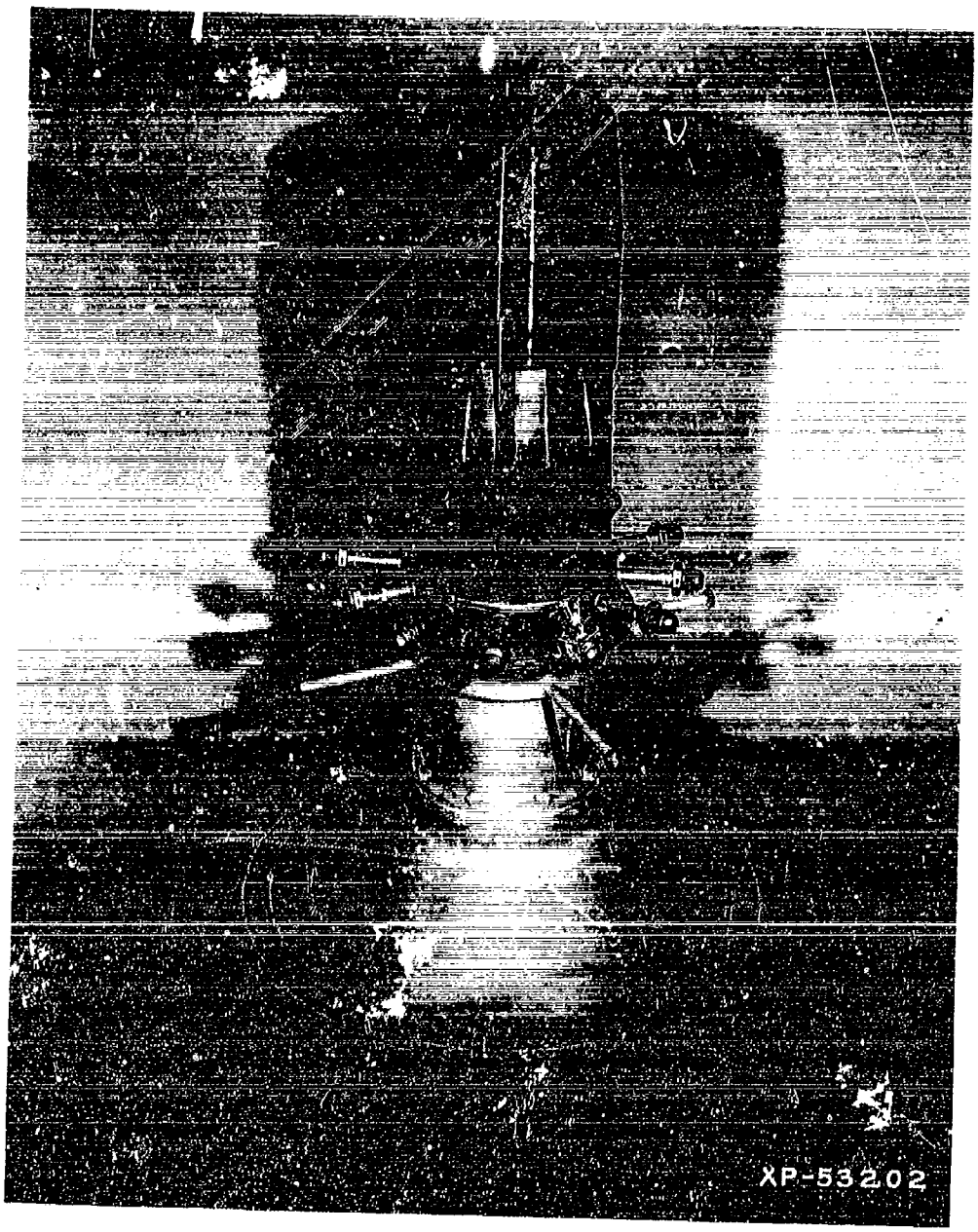


STF219 NOZZLE MODEL WITH WATER JACKET SIMULATING BLOW-IN DOORS

Figure 8-30

DOWNGRADED AT 3 YEAR INTERVALS
DECLASSIFIED AFTER 12 YEARS
DOD DIR 5200.10

THIS DOCUMENT CONTAINS INFORMATION AFFECTING THE NATIONAL DEFENSE OF THE UNITED STATES WITHIN THE MEANING OF THE ESPIONAGE LAWS, TITLE 18, U.S.C. SECTIONS 793 AND 794. THE TRANSMISSION OR THE REVELATION OF ITS CONTENTS IN ANY MANNER TO AN UNAUTHORIZED PERSON IS PROHIBITED BY LAW.

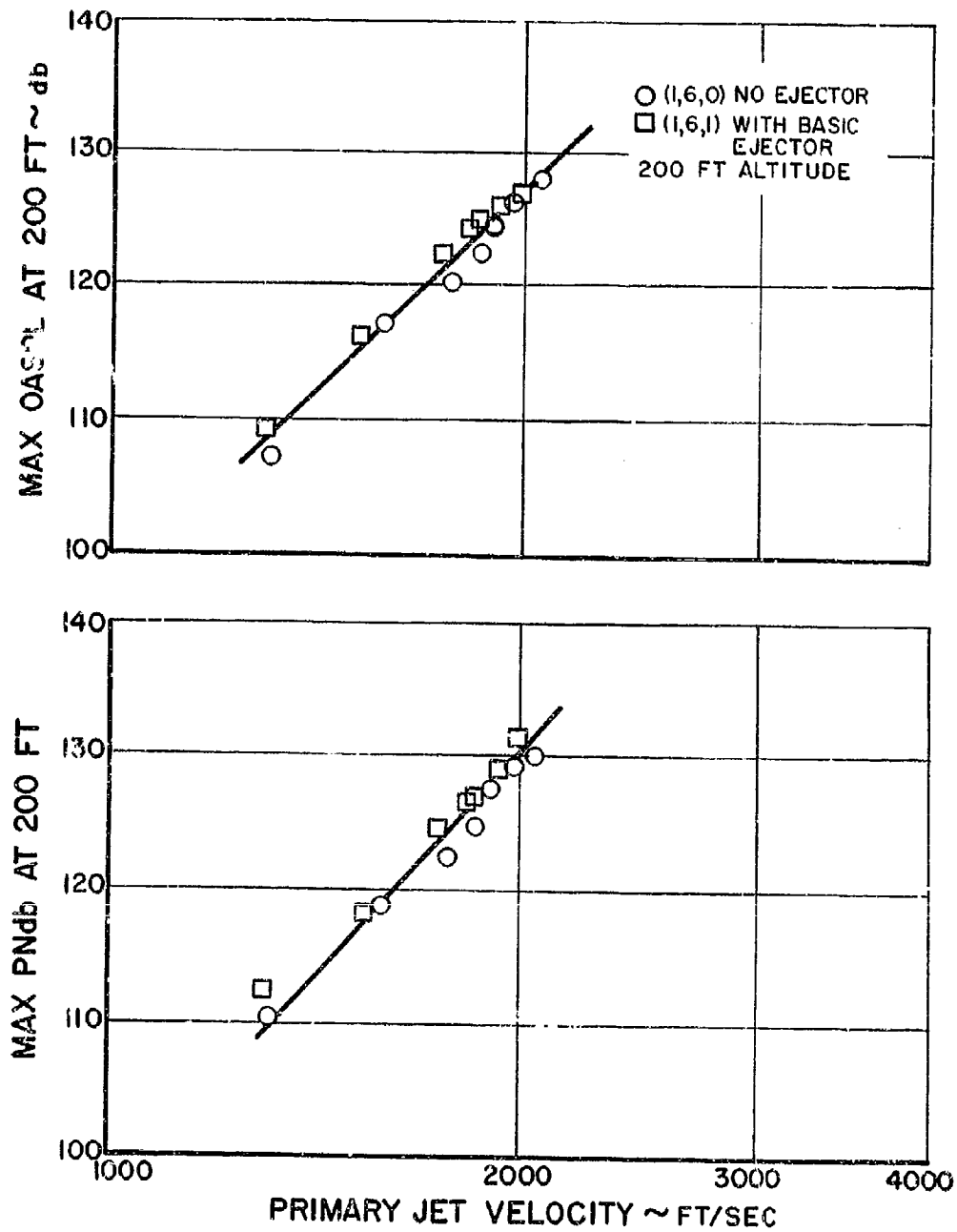


STF219 NOZZLE MODEL ASSEMBLY WITH EJECTOR

Figure 8-31

DOWNGRADED AT 3 YEAR INTERVALS
DECLASSIFIED AFTER 12 YEARS
DOD DIR 5200.10

THIS DOCUMENT CONTAINS INFORMATION AFFECTING THE NATIONAL DEFENSE OF THE UNITED STATES WITHIN THE MEANING OF THE ESPIONAGE LAWS, TITLE 18, U.S.C., SECTIONS 793 AND 794. THE TRANSMISSION OR REVELATION OF ITS CONTENTS IN ANY MANNER TO AN UNAUTHORIZED PERSON IS PROHIBITED BY LAW.

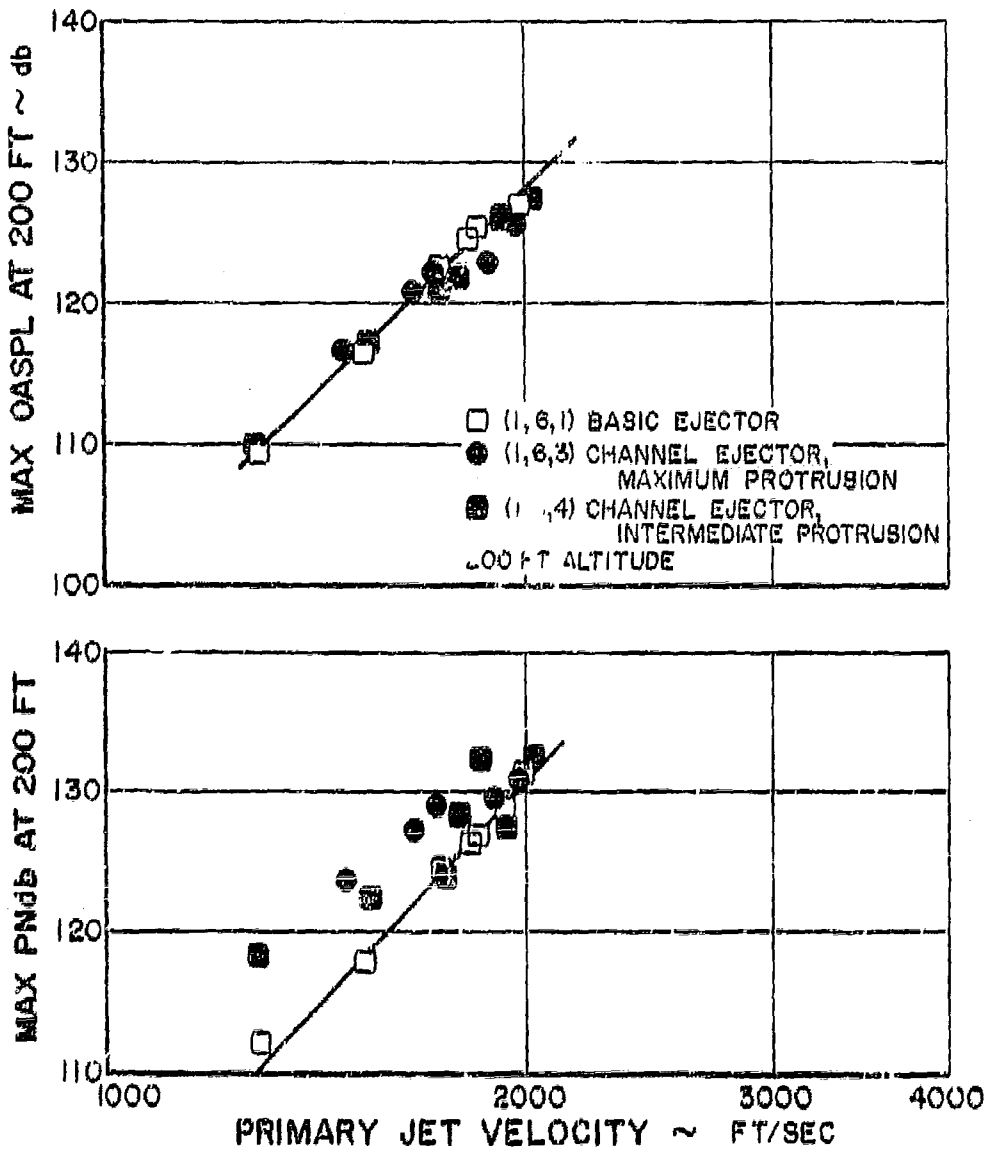


MODEL TURBOFAN NOZZLE NOISE TEST RESULTS WITHOUT DUCT HEATING FOR CONFIGURATIONS (1, 6, 0) AND (1, 6, 1)

Figure 8-32

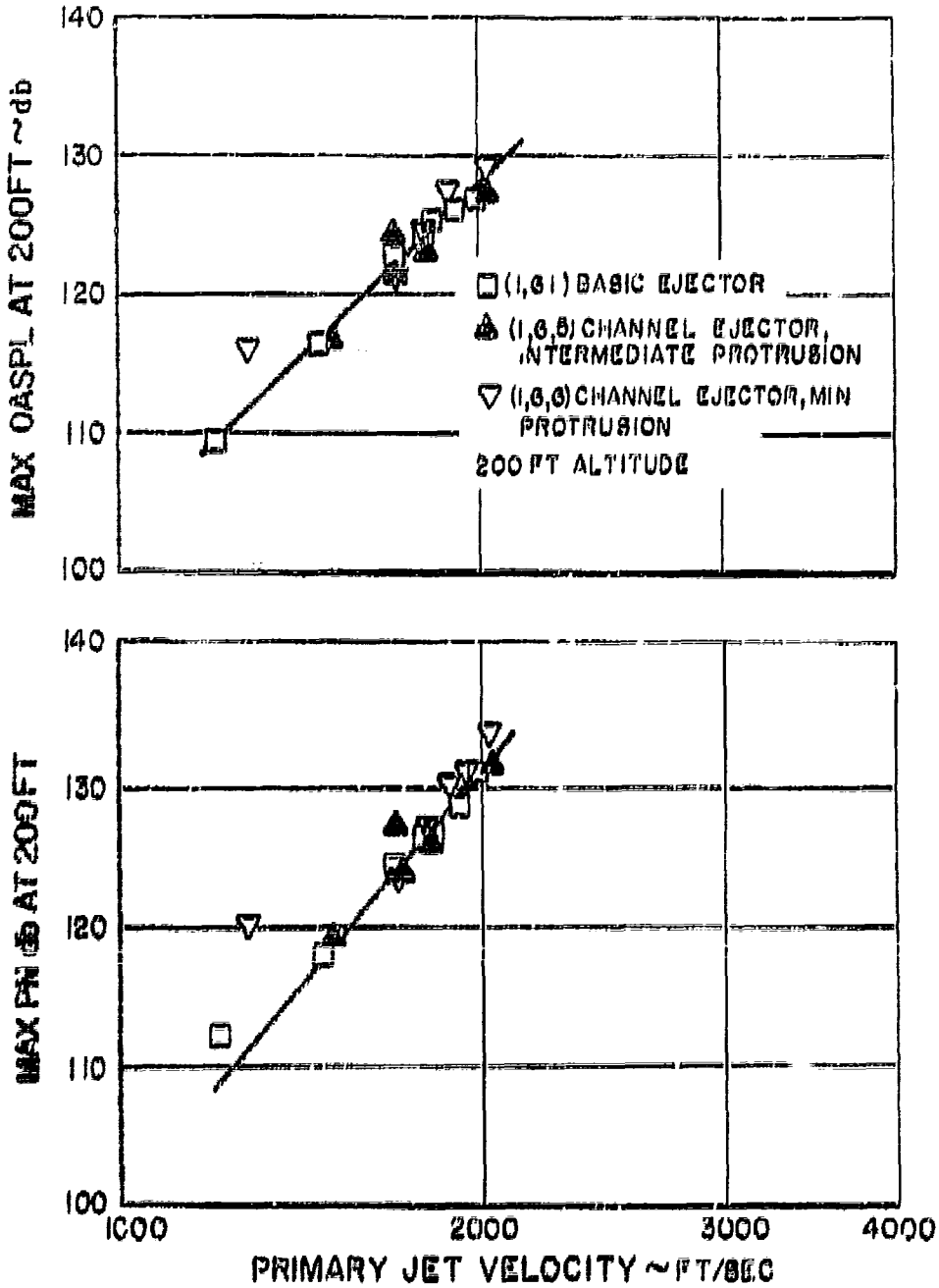
DOWNGRADED AT 3 YEAR INTERVALS
DECLASSIFIED AFTER 12 YEARS
DOD DIR 5200.10

THIS DOCUMENT CONTAINS INFORMATION AFFECTING THE NATIONAL DEFENSE OF THE UNITED STATES WITHIN THE MEANING OF THE ESPIONAGE LAWS, TITLE 18, U.S.C., SECTIONS 793 AND 794. THE TRANSMISSION OR THE REVELATION OF ITS CONTENTS IN ANY MANNER TO AN UNAUTHORIZED PERSON IS PROHIBITED BY LAW.



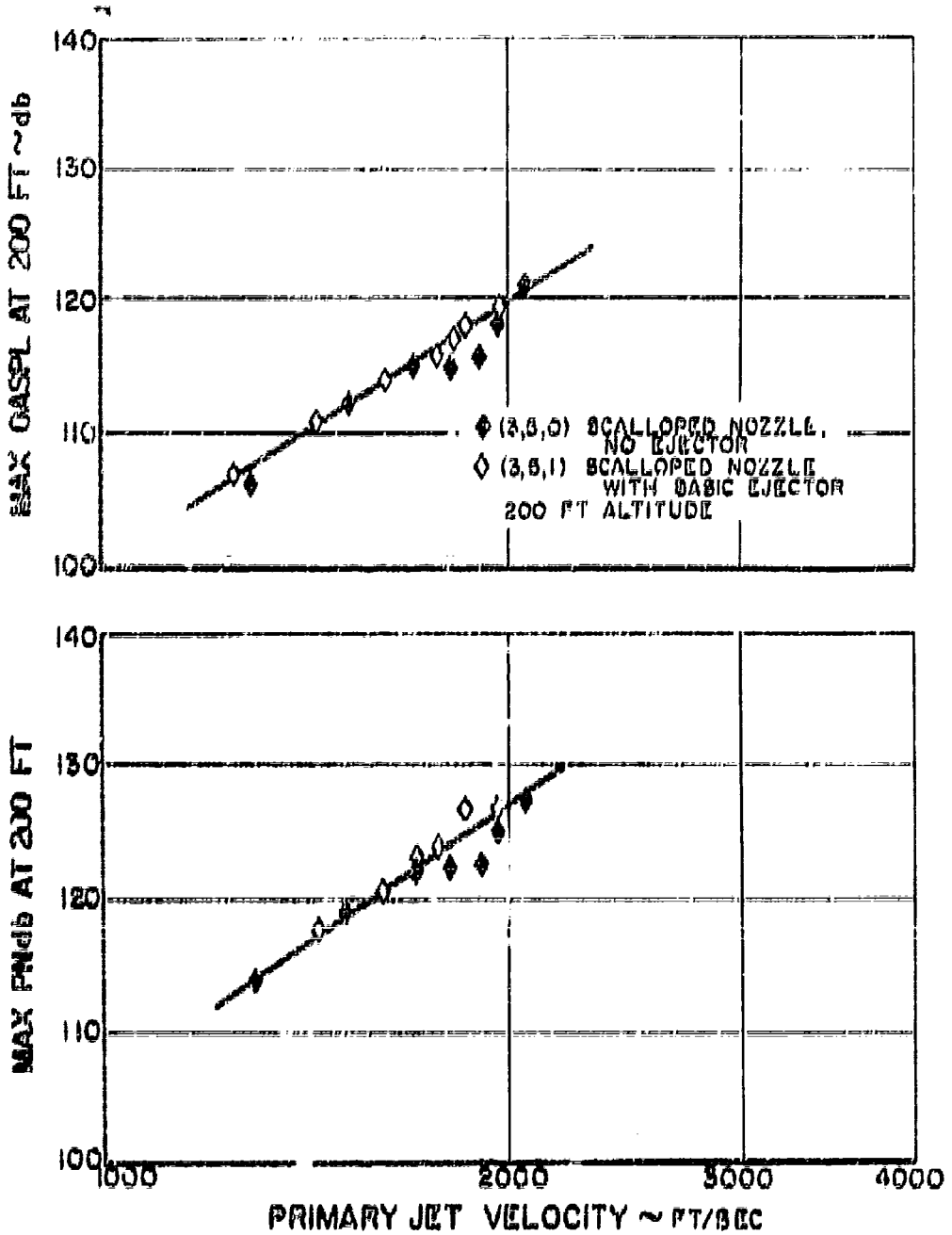
MODEL TURBOFAN NOZZLE NOISE TEST RESULTS WITHOUT DUCT HEATING FOR CONFIGURATIONS (1, 6, 1), (1, 6, 3) AND (1, 6, 4)

Figure 8-33



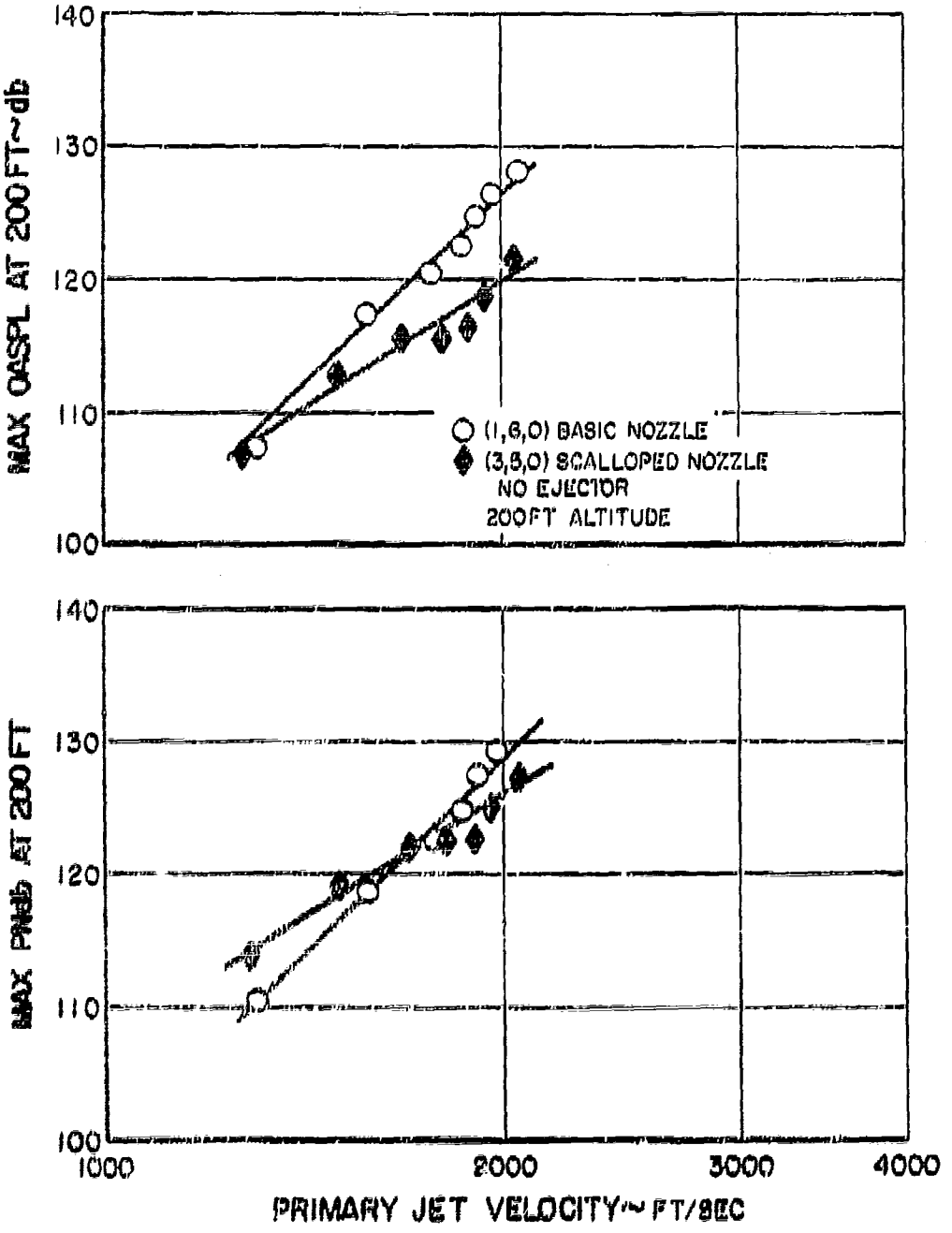
MODEL TURBOFAN NOZZLE NOISE TEST RESULTS WITHOUT DUCT HEATING FOR CONFIGURATIONS (1, 6, 1), (1, 6, 5) AND (1, 6, 6)

Figure 8-14



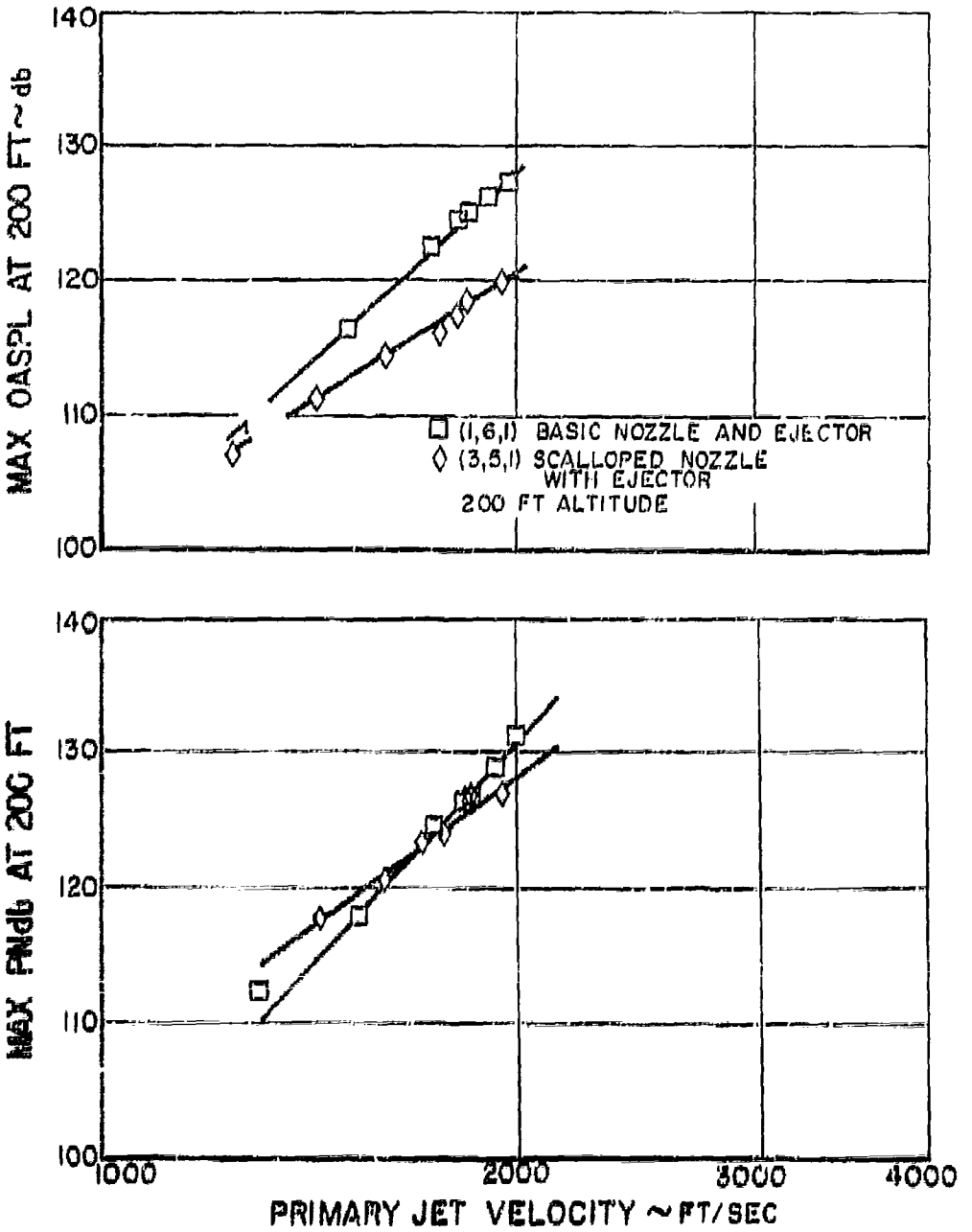
MODEL TURBOFAN NOZZLE NOISE TEST RESULTS WITHOUT DUCT HEATING FOR CONFIGURATIONS (3, 5, 0) AND (3, 5, 1)

Figure 6-35



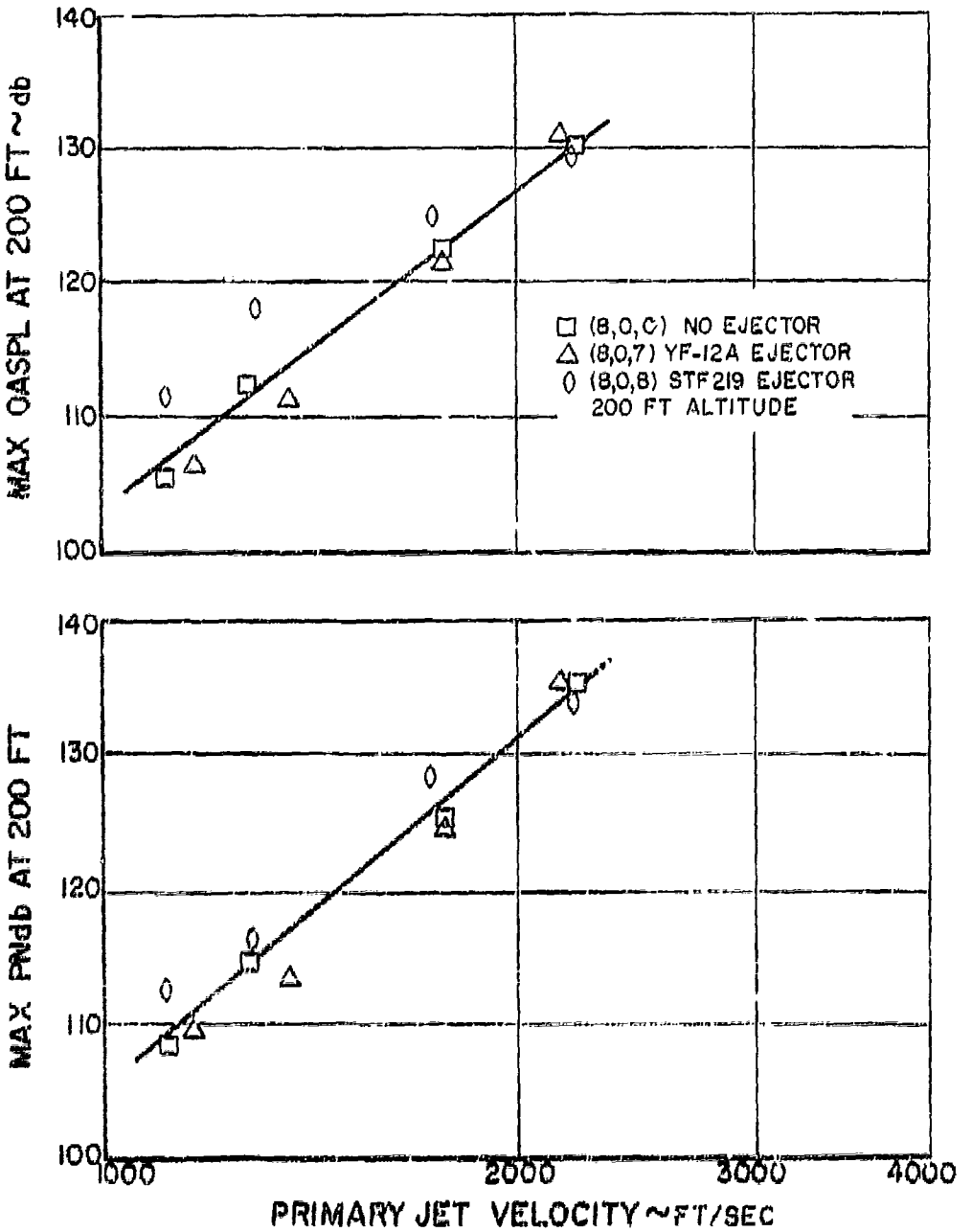
MODEL TURBOFAN NOZZLE NOISE TEST RESULTS WITHOUT DUCT HEATING FOR CONFIGURATIONS (1, 6, 0) AND (3, 5, 0)

Figure 8-36



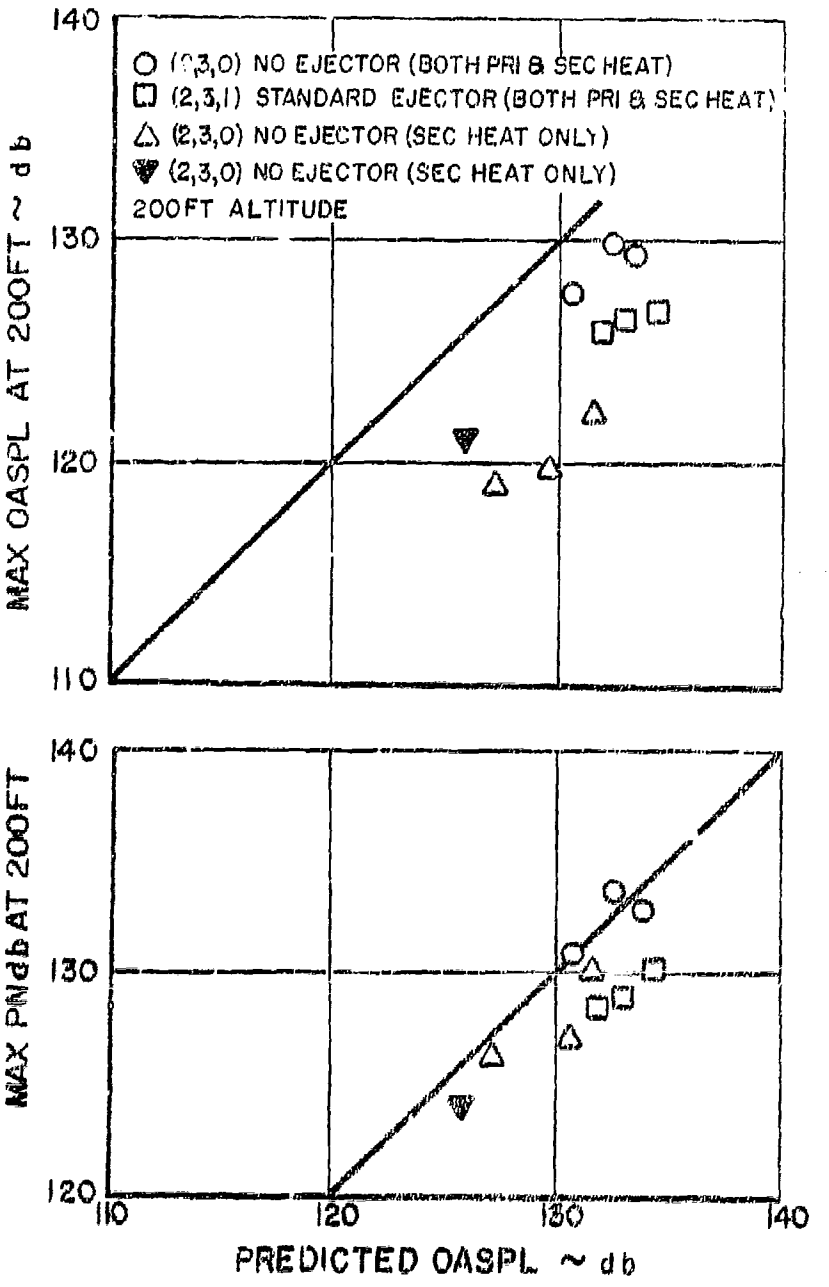
MODEL TURBOFAN NOZZLE NOISE TEST RESULTS WITHOUT DUCT HEATING FOR CONFIGURATIONS (1, 6, 1) AND (3, 5, 1)

Figure 8-37



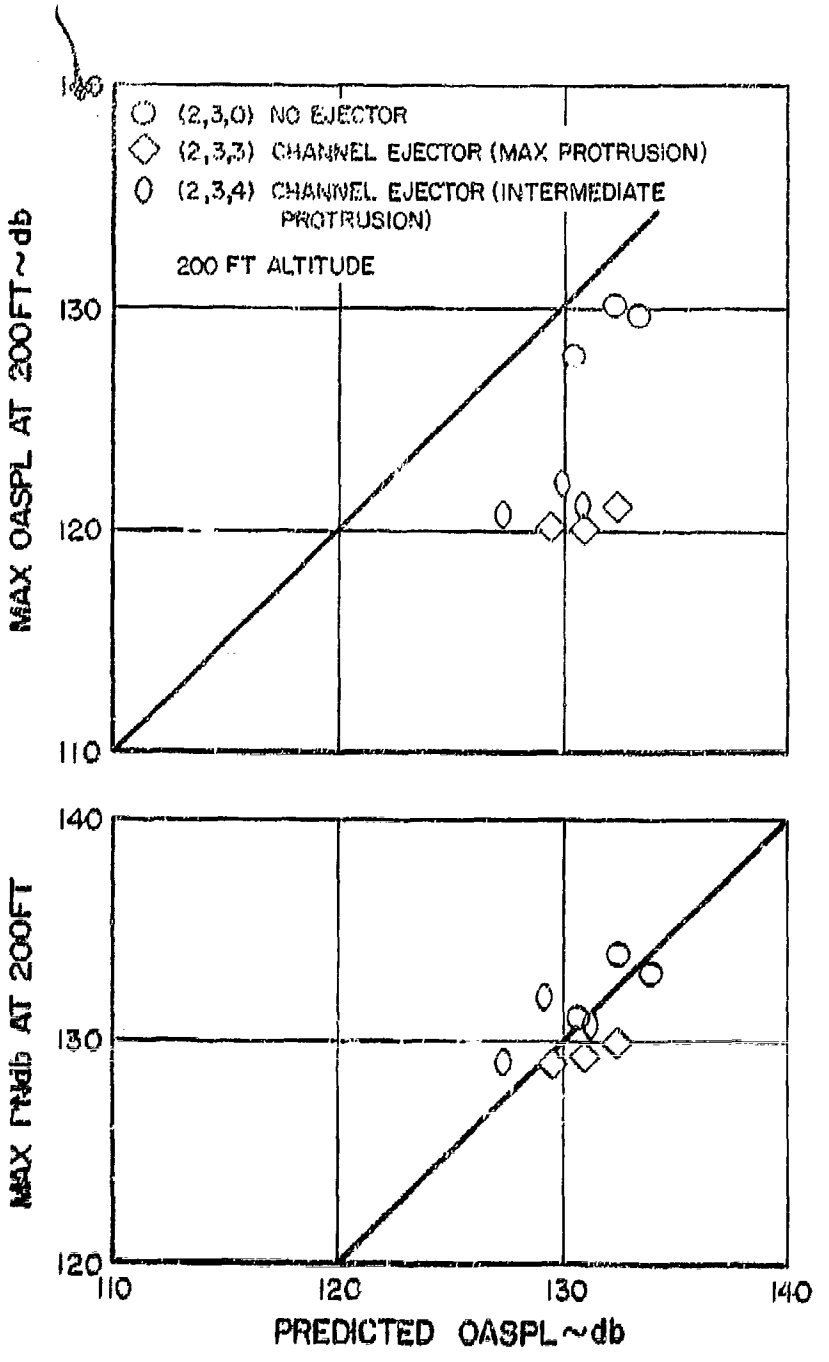
MODEL TURBOJET NOZZLE NOISE TEST RESULTS FOR CONFIGURATIONS (8, 0, 0), (8, 0, 7) AND (8, 0, 8)

Figure 8-38



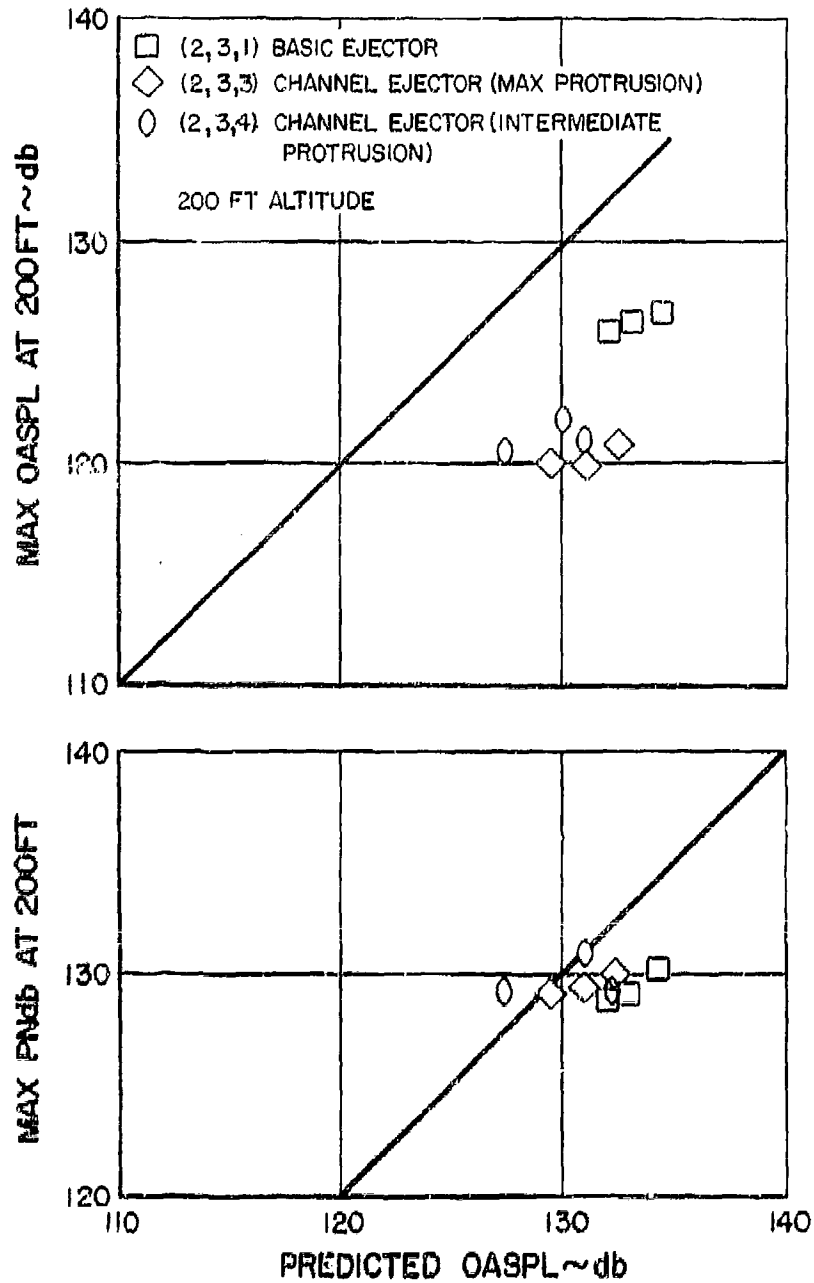
MODEL TURBOFAN NOZZLE NOISE TEST RESULTS WITH DUCT HEATING FOR CONFIGURATIONS (2, 3, 0) AND (2, 3, 1)

Figure 8-39



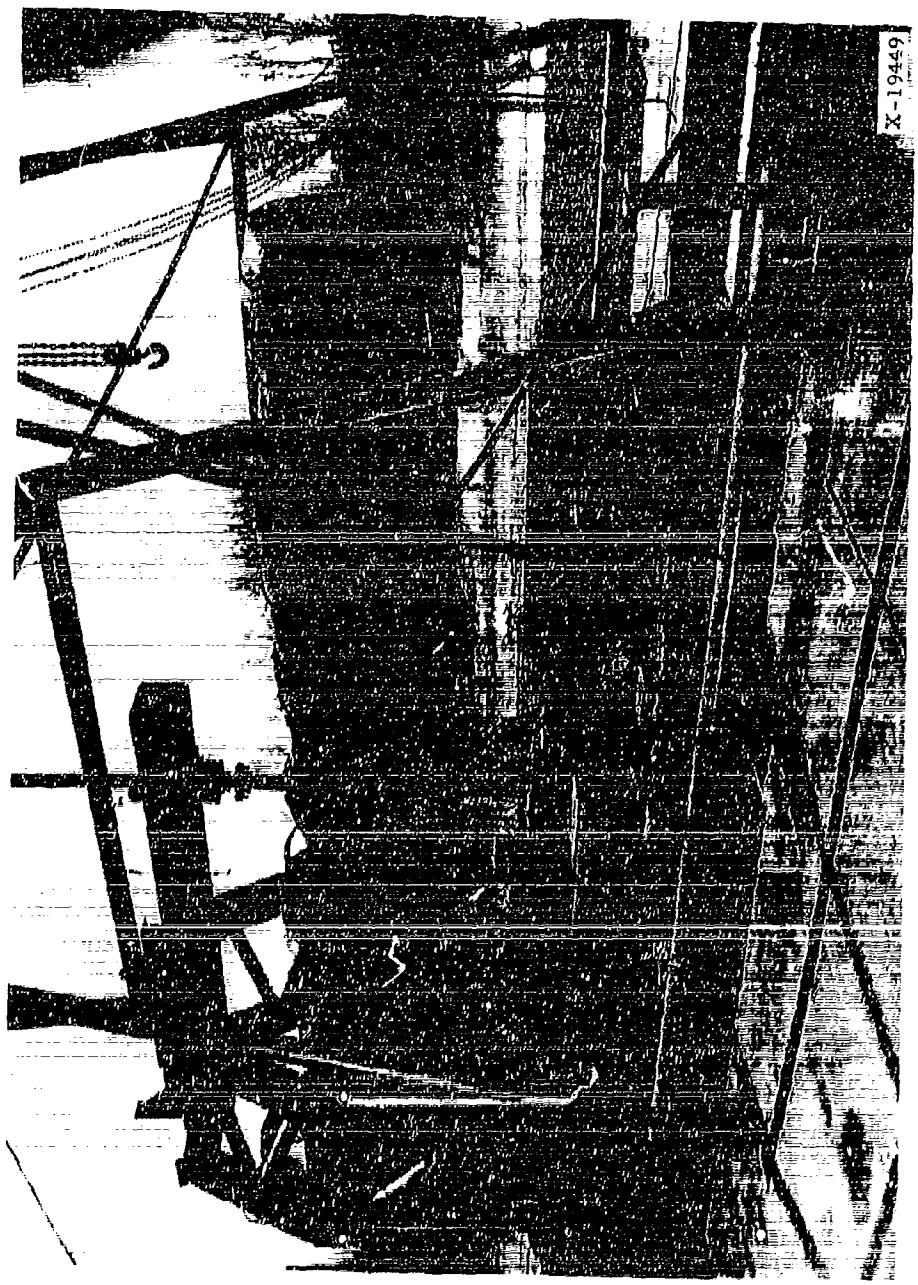
MODEL TURBOFAN NOZZLE NOISE TEST RESULTS WITH DUCT HEATING FOR CONFIGURATIONS (2, 3, 0), (2, 3, 3) AND (2, 3, 4)

Figure 8-40



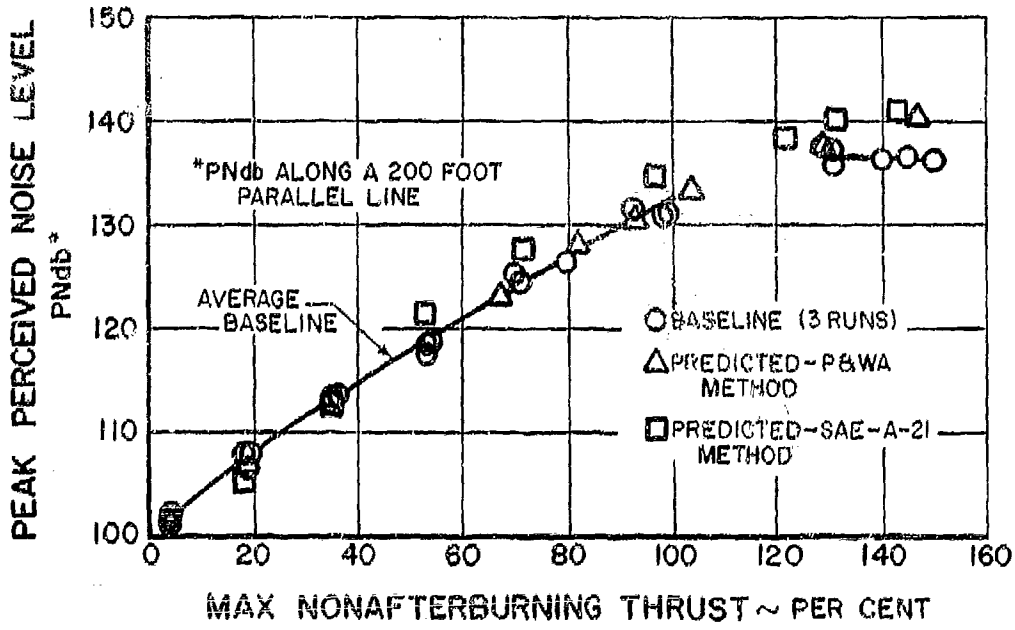
MODEL TURBOFAN NOZZLE NOISE TEST RESULTS WITH DUCT HEATING FOR CONFIGURATIONS (2, 3, 1), (2, 3, 3) AND (2, 3, 4)

Figure 8-41



J57 AFTERBURNING ENGINE USED FOR BASELINE TESTS

Figure 8-42

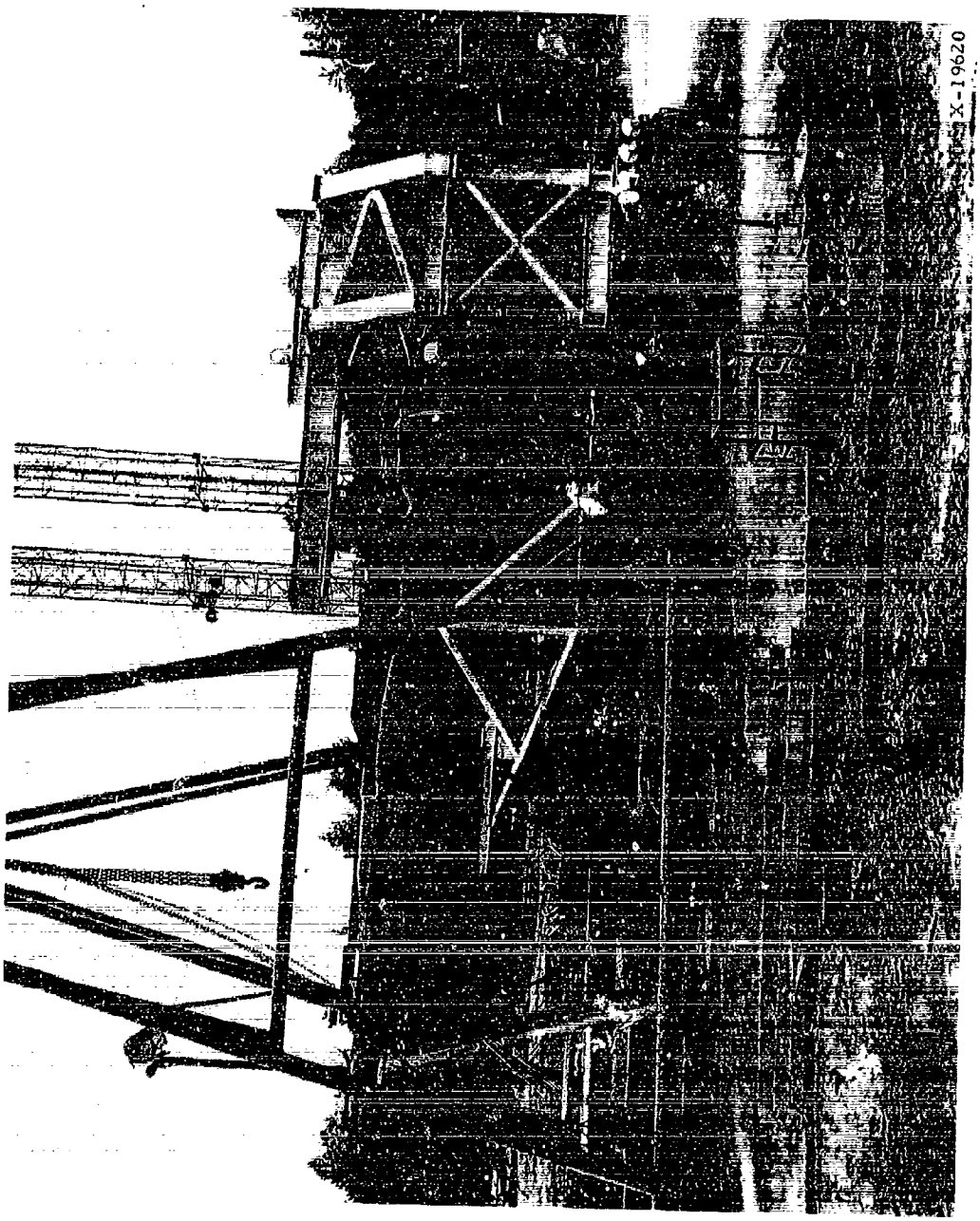


RESULTS OF J57 AFTERBURNING ENGINE NOISE TESTS; BASELINE VERSUS PREDICTED NOISE LEVELS

Figure 8-43

DOWNGRADED AT 3 YEAR INTERVALS
DECLASSIFIED AFTER 12 YEARS
DOD DIR 5200.10

THIS DOCUMENT CONTAINS INFORMATION AFFECTING THE NATIONAL DEFENSE OF THE UNITED STATES WITHIN THE MEANING OF THE ESPIONAGE LAWS, TITLE 18, U.S.C. SECTIONS 793 AND 794. THE TRANSMISSION OR THE REVELATION OF ITS CONTENTS IN ANY MANNER TO AN UNAUTHORIZED PERSON IS PROHIBITED BY LAW.

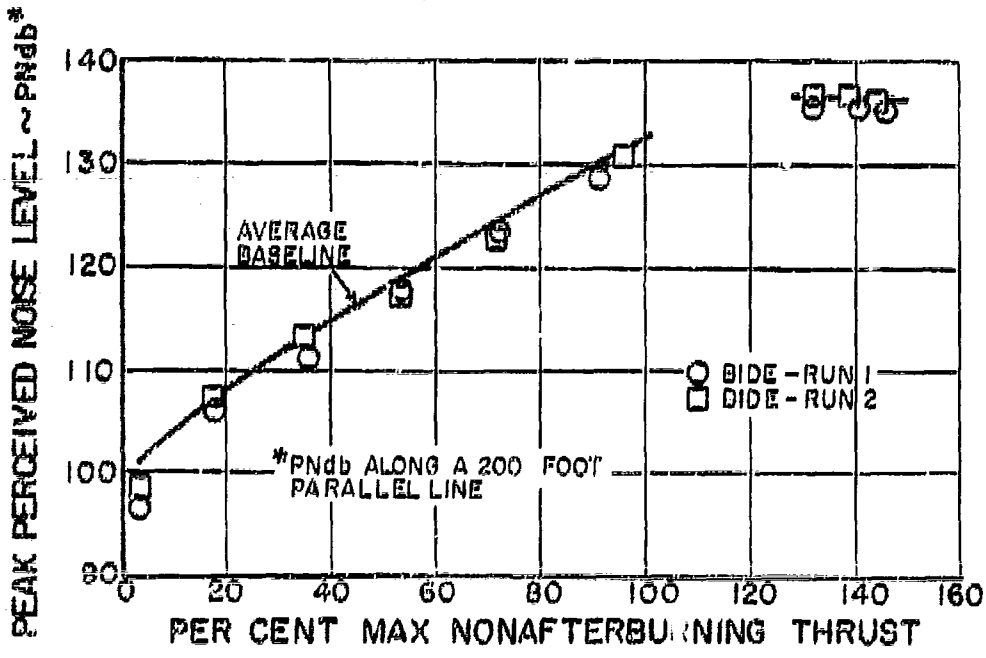


FULL-SCALE J57 AFTERBURNING ENGINE WITH BASIC STF219-TYPE BLOW-IN-DOOR EJECTOR

Figure 8-44

DOWNGRADED AT 3 YEAR INTERVALS
DECLASSIFIED AFTER 12 YEARS
DOD DIR 5200.10

THIS DOCUMENT CONTAINS INFORMATION AFFECTING THE NATIONAL DEFENSE OF THE UNITED STATES WITHIN THE MEANING OF THE ESPIONAGE LAWS, TITLE 18 U. S. C. SECTIONS 793 AND 794. ITS TRANSMISSION OR THE REVELATION OF ITS CONTENTS IN ANY MANNER TO AN UNAUTHORIZED PERSON IS PROHIBITED BY LAW.



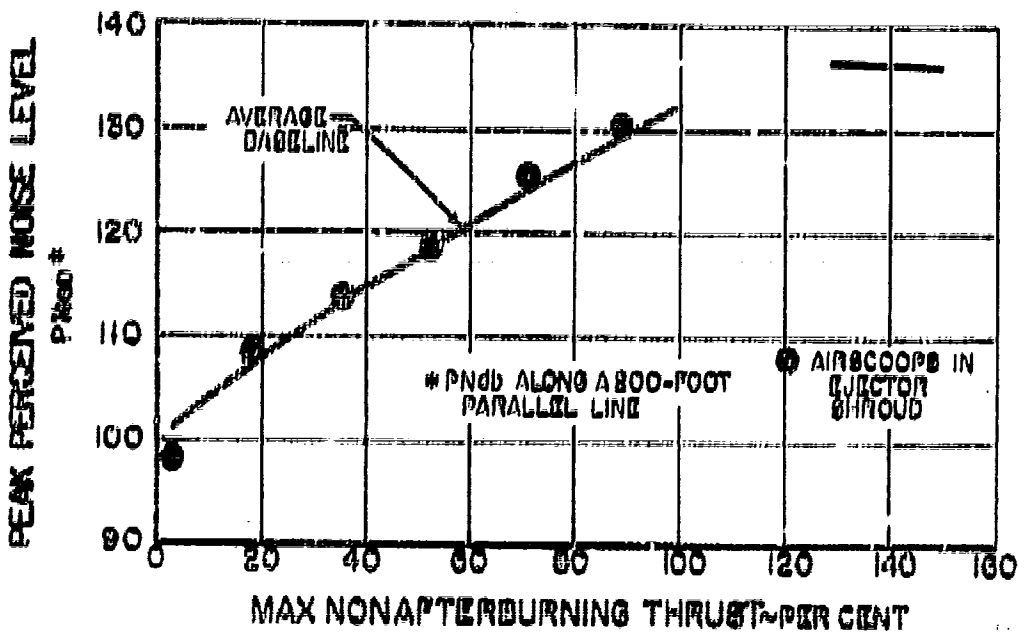
RESULTS OF FULL-SCALE BLOW-IN-DOOR EJECTOR NOISE TESTS; BASIC STF219-TYPE EJECTOR

Figure 8-45



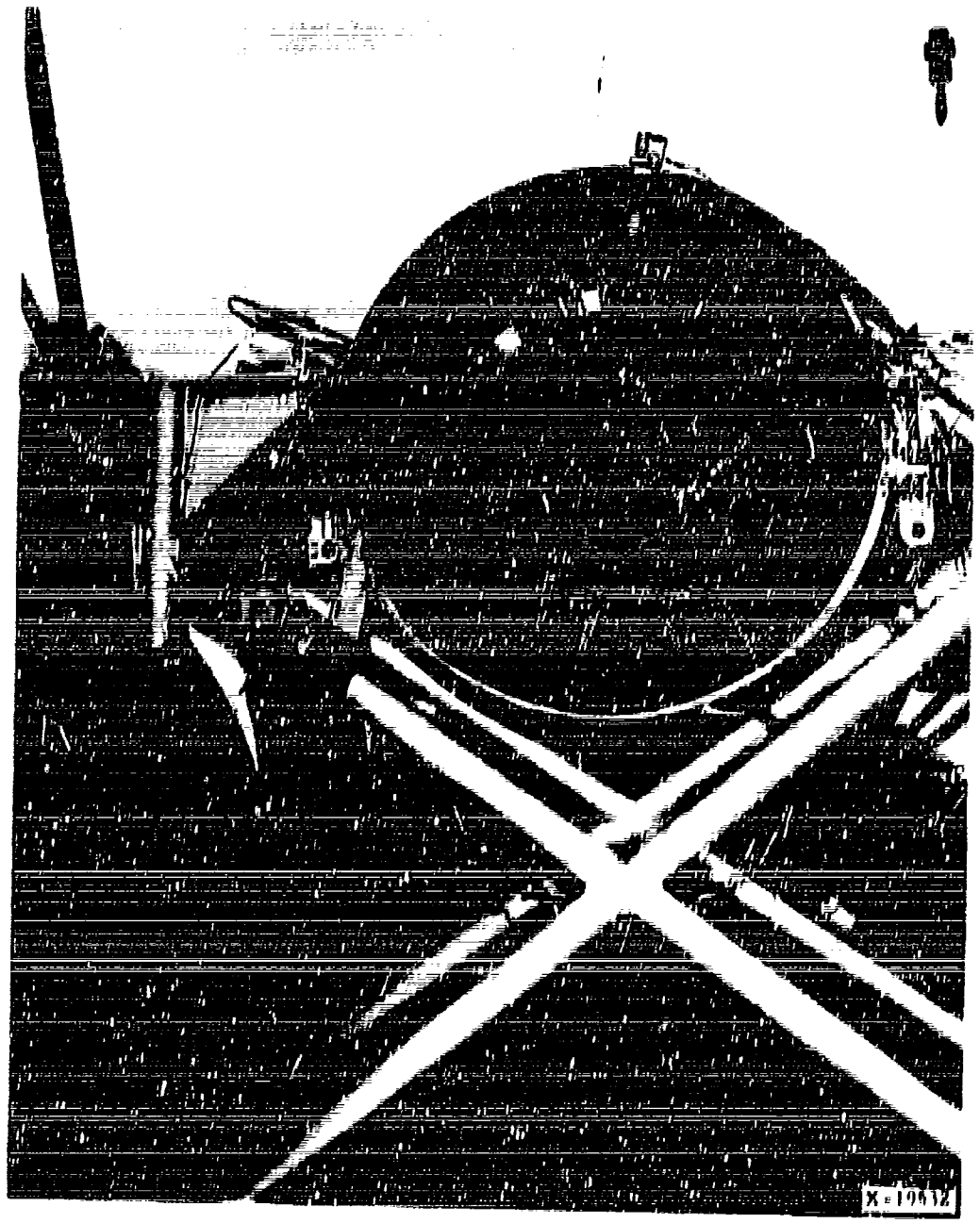
FULL-SCALE BLOW-IN-DOOR EJECTOR WITH AIR-SCOOPS IN EJECTOR SHROUD

Figure 8-46



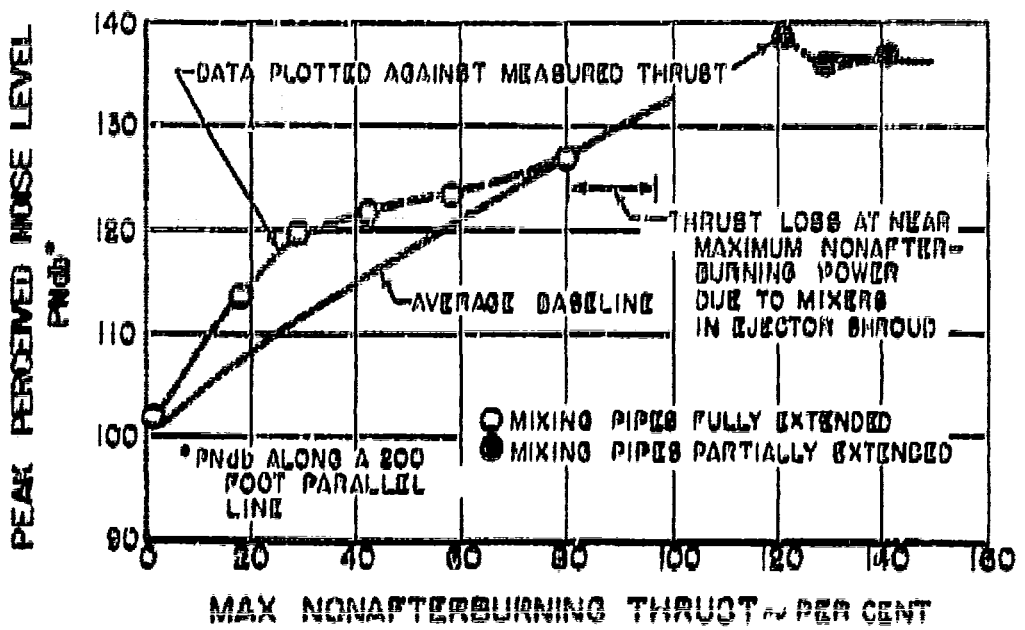
RESULTS OF FULL-SCALE BLOW-IN-DOOR EJECTOR NOISE TESTS; AIR-SCOOPS IN EJECTOR SHROUD

Figure 6-47



FULL-SCALE BLOW-IN-DOOR EJECTOR WITH MIXERS FULLY EXTENDED

Figure 8-48



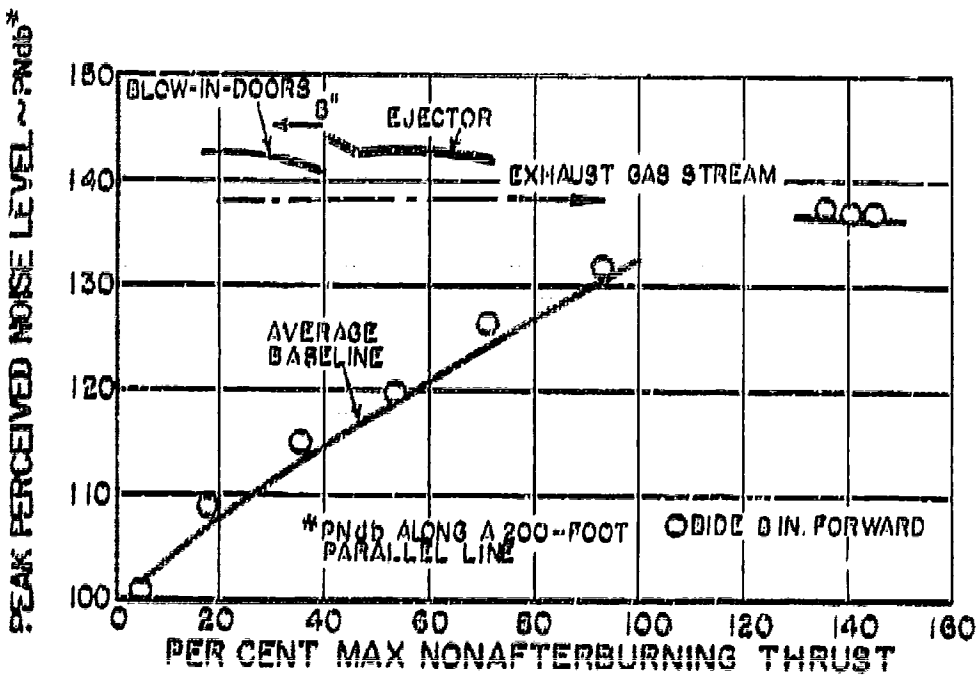
RESULTS OF FULL-SCALE BLOW-IN-DOOR EJECTOR NOISE TESTS, EJECTOR WITH MIXERS EXTENDED

Figure 8-49



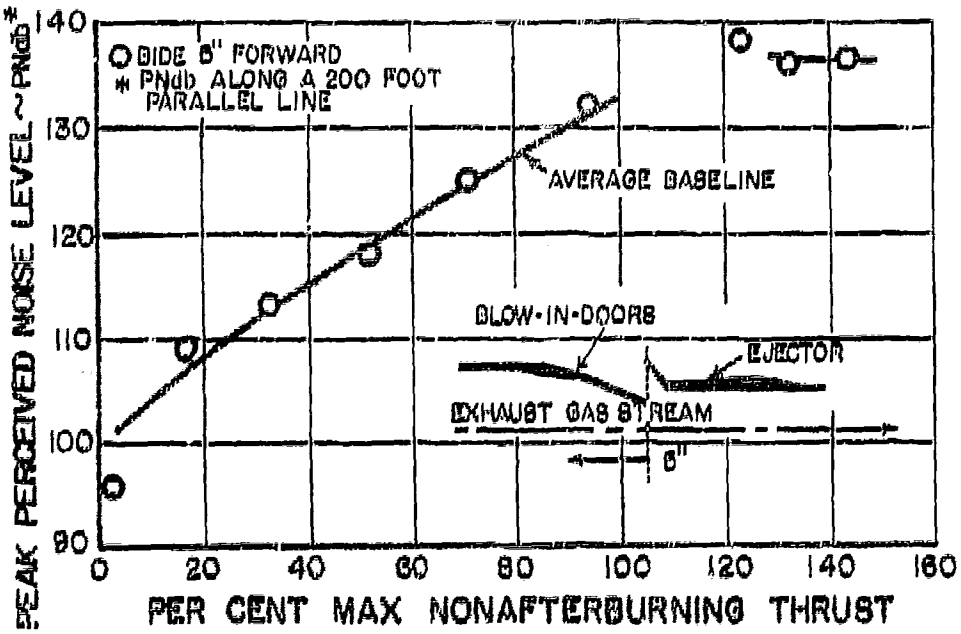
FULL-SCALE BLOW-IN-DOOR EJECTOR RELOCATED EIGHT INCHES FORWARD

Figure 8-50



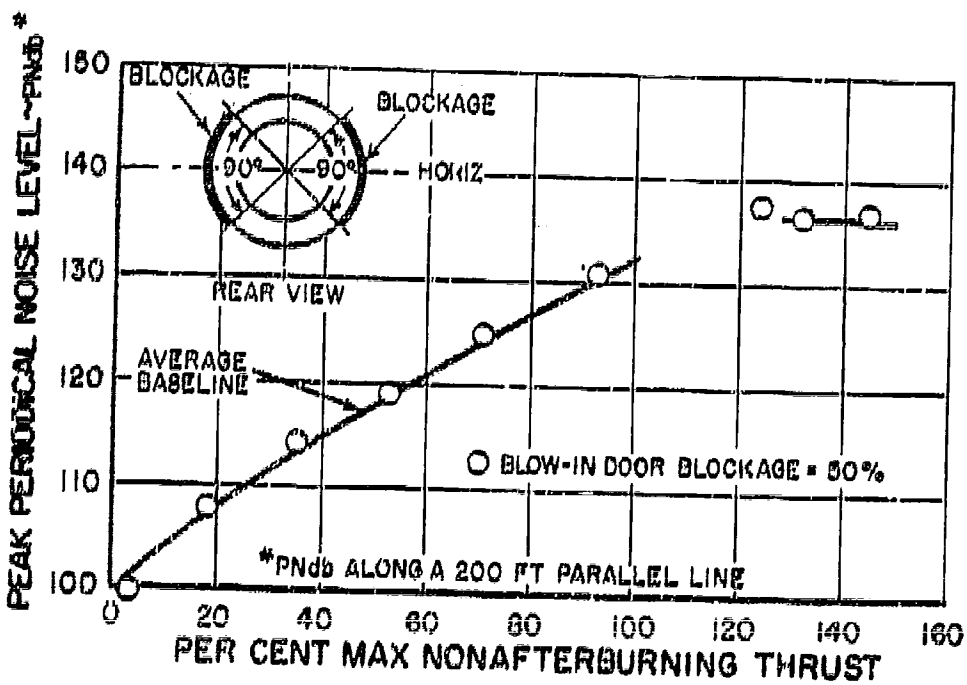
RESULTS OF FULL-SCALE BLOW-IN-DOOR EJECTOR NOISE TESTS; EJECTOR RELOCATED EIGHT INCHES FORWARD

Figure 8-51



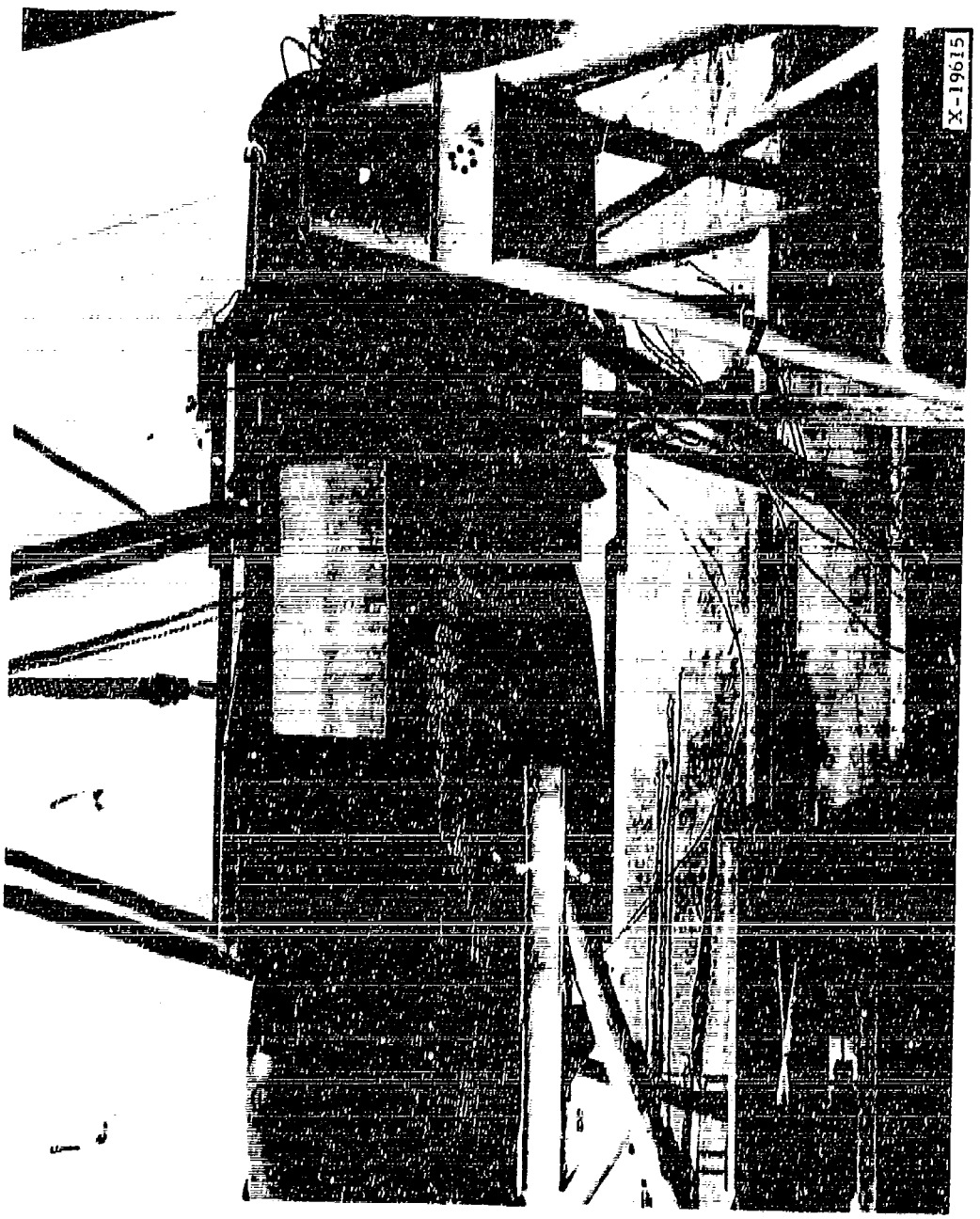
RESULTS OF FULL-SCALE BLOW-IN-DOOR EJECTOR NOISE TESTS; EJECTOR RELOCATED FIVE INCHES FORWARD

Figure 8-52



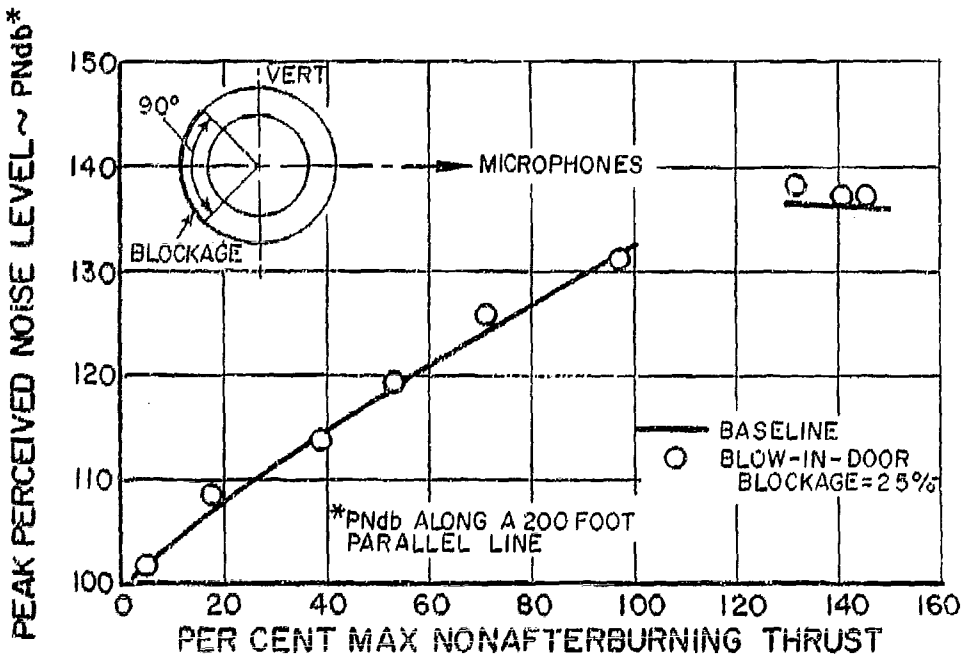
RESULTS OF FULL-SCALE BLOW-IN-DOOR EJECTOR NOISE TESTS; EJECTOR WITH ONE-HALF BLOCKAGE OF BLOW-IN-DOOR AREA

Figure 8-53



FULL-SCALE BLOW-IN-DOOR EJECTOR WITH ONE-QUARTER BLOCKAGE OF BLOW-IN-DOOR AREA

Figure 8-54

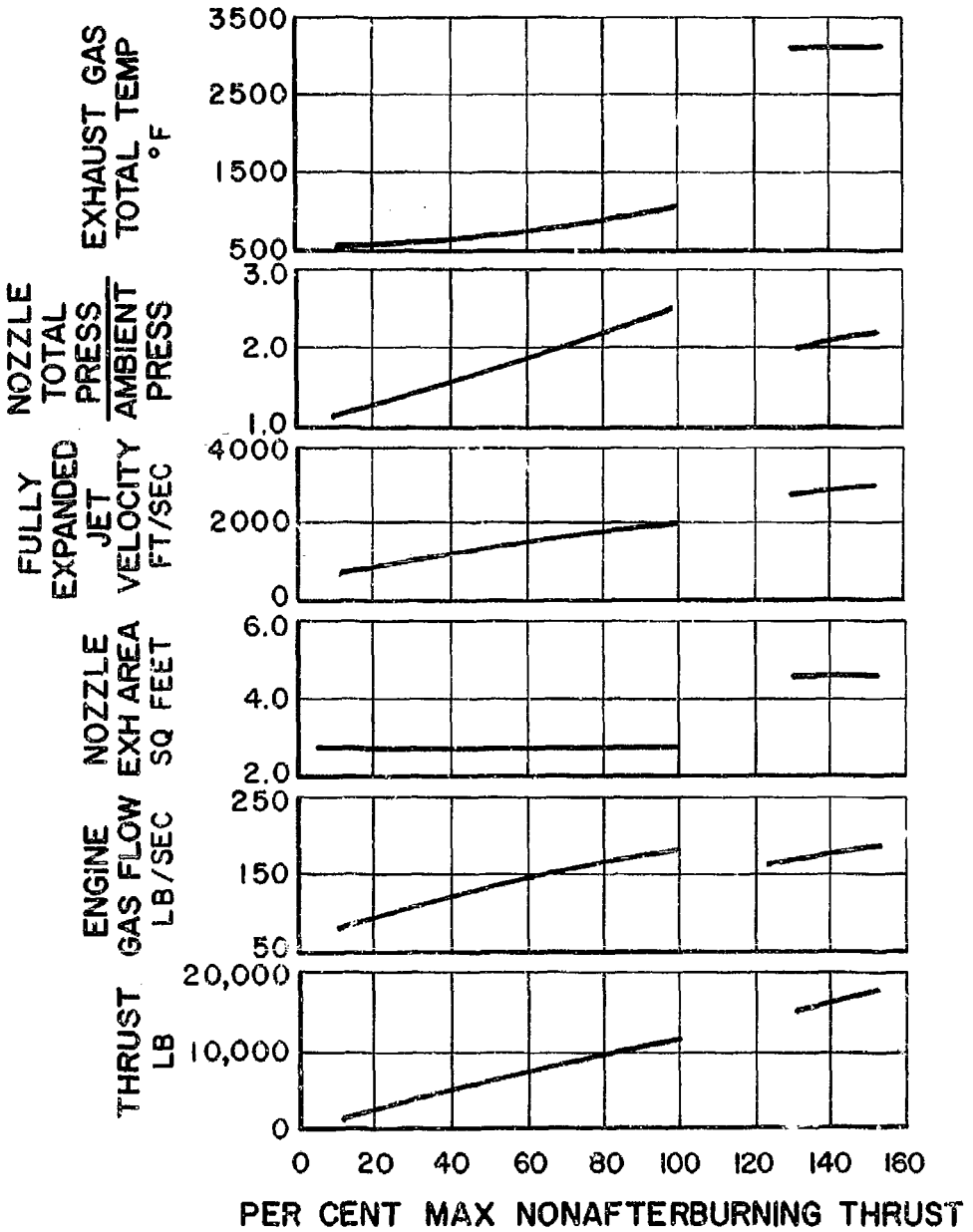


RESULTS OF FULL-SCALE BLOW-IN-DOOR EJECTOR NOISE TESTS; EJECTOR WITH ONE-QUARTER BLOCKAGE OF BLOW-IN-DOOR AREA

Figure 8-55

DOWNGRADED AT 3 YEAR INTERVALS
DECLASSIFIED AFTER 12 YEARS
DOD DIR 5200.10

THIS DOCUMENT CONTAINS INFORMATION AFFECTING THE NATIONAL DEFENSE OF THE UNITED STATES WITHIN THE MEANING OF THE ESPIONAGE LAWS, TITLE 18, U.S.C., SECTIONS 793 AND 794. THE TRANSMISSION OR THE REVELATION OF ITS CONTENTS IN ANY MANNER TO AN UNAUTHORIZED PERSON IS PROHIBITED BY LAW.

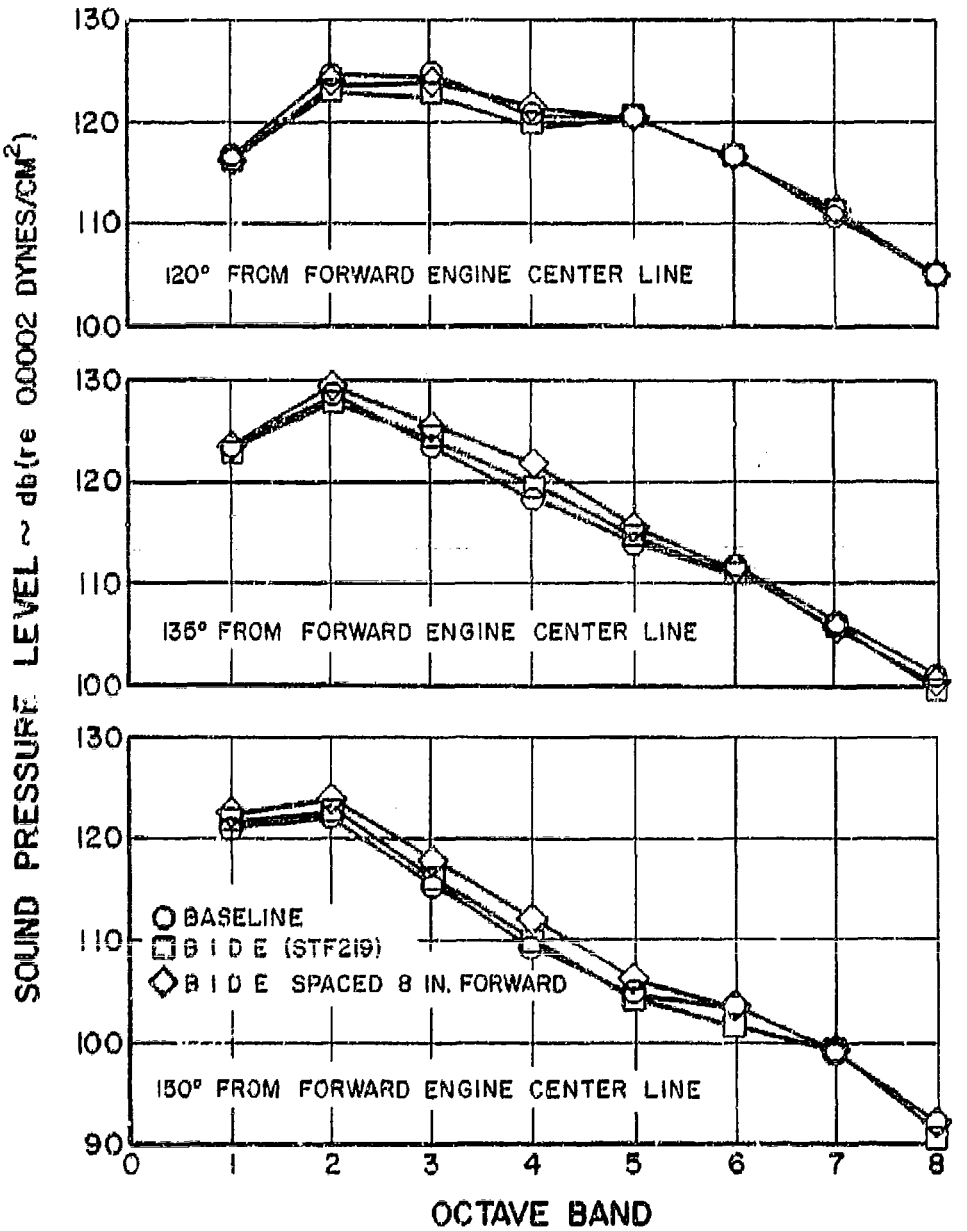


J57-P-55 ENGINE PERFORMANCE PARAMETERS

Figure 3-56

DOWNGRADED AT 3 YEAR INTERVALS
DECLASSIFIED AFTER 12 YEARS
DOD DIR 5200.10

THIS DOCUMENT CONTAINS INFORMATION AFFECTING THE NATIONAL DEFENSE OF THE UNITED STATES WITHIN THE MEANING OF THE ESPIONAGE LAWS, TITLE 18, U.S.C., SECTIONS 793 AND 794. THE TRANSMISSION OR THE REVELATION OF ITS CONTENTS IN ANY MANNER TO AN UNAUTHORIZED PERSON IS PROHIBITED BY LAW.

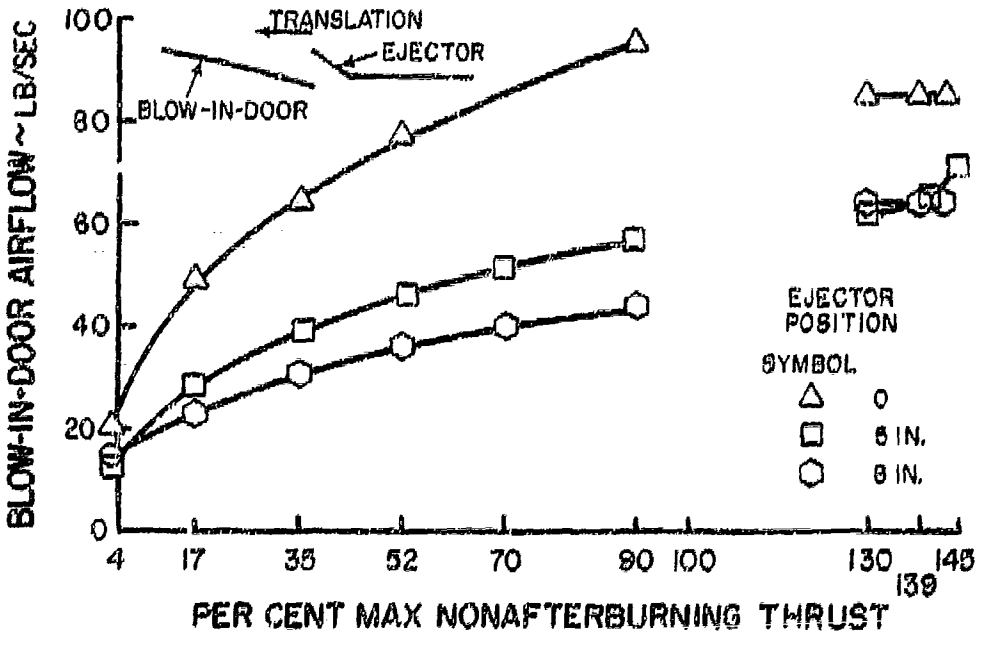


FULL-SCALE BLOW-IN-DOOR EJECTOR NOISE TESTS; TYPICAL EXHAUST NOISE SPECTRA AT MAXIMUM A/B POWER

Figure 8-57

DOWNGRADED AT 3 YEAR INTERVALS
DECLASSIFIED AFTER 12 YEARS
DOD DIR 5200.10

THIS DOCUMENT CONTAINS INFORMATION AFFECTING THE NATIONAL DEFENSE OF THE UNITED STATES WITHIN THE MEANING OF THE ESPIONAGE LAWS, TITLE 18, U.S.C., SECTIONS 793 AND 794. ITS TRANSMISSION OR THE REVELATION OF ITS CONTENTS IN ANY MANNER TO AN UNAUTHORIZED PERSON IS PROHIBITED BY LAW.

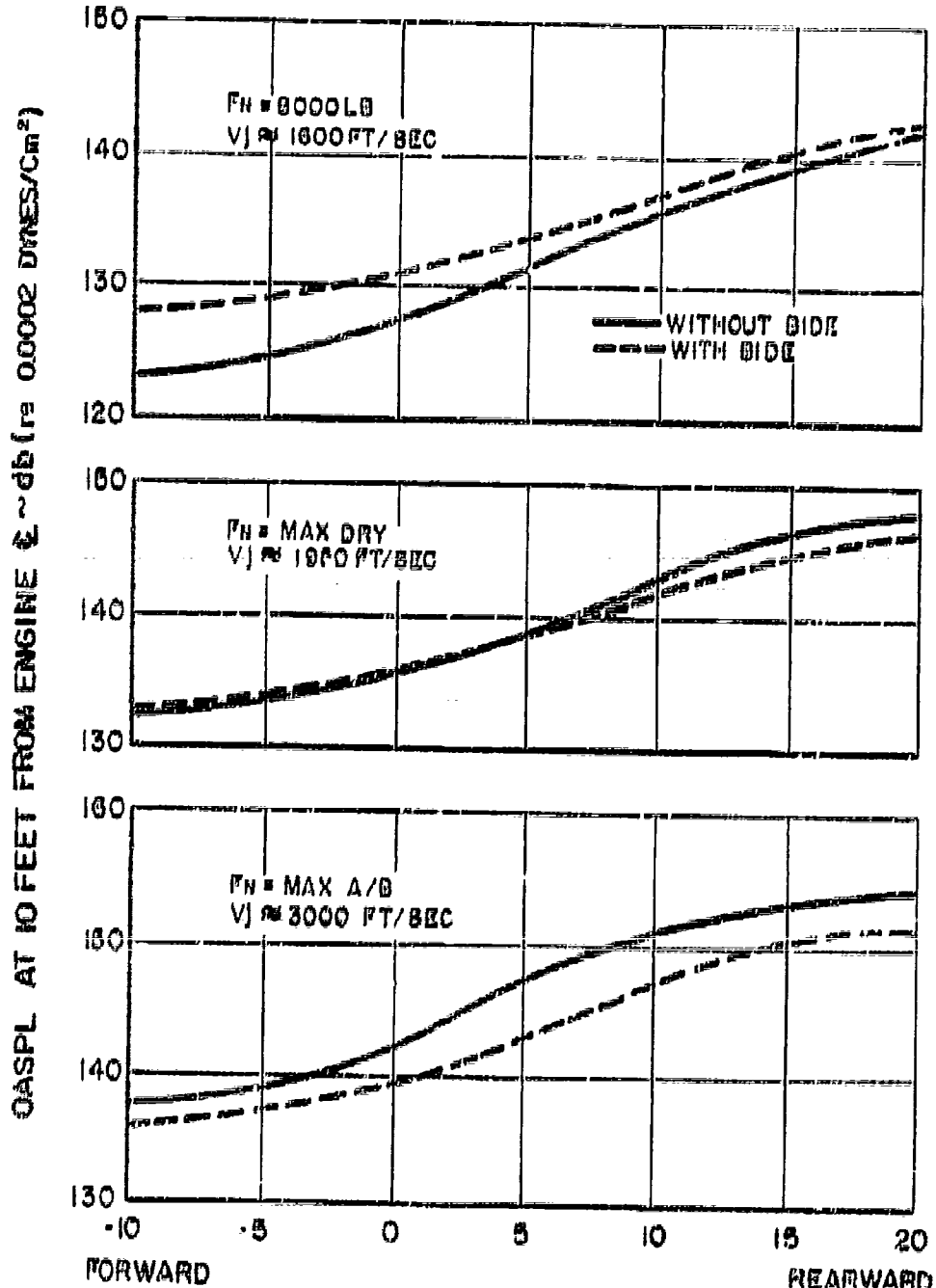


BLOW-IN-DOOR AIRFLOW AS A FUNCTION OF ENGINE THRUST

Figure 8-58

DOWNGRADED AT 3 YEAR INTERVALS
DECLASSIFIED AFTER 12 YEARS
DOD DIR 5200.10

THIS DOCUMENT CONTAINS INFORMATION AFFECTING THE NATIONAL DEFENSE OF THE UNITED STATES WITHIN THE MEANING OF THE ESPIONAGE LAWS, TITLE 18, U.S.C., SECTIONS 793 AND 794. ITS TRANSMISSION OR THE REVELATION OF ITS CONTENTS IN ANY MANNER TO AN UNAUTHORIZED PERSON IS PROHIBITED BY LAW.



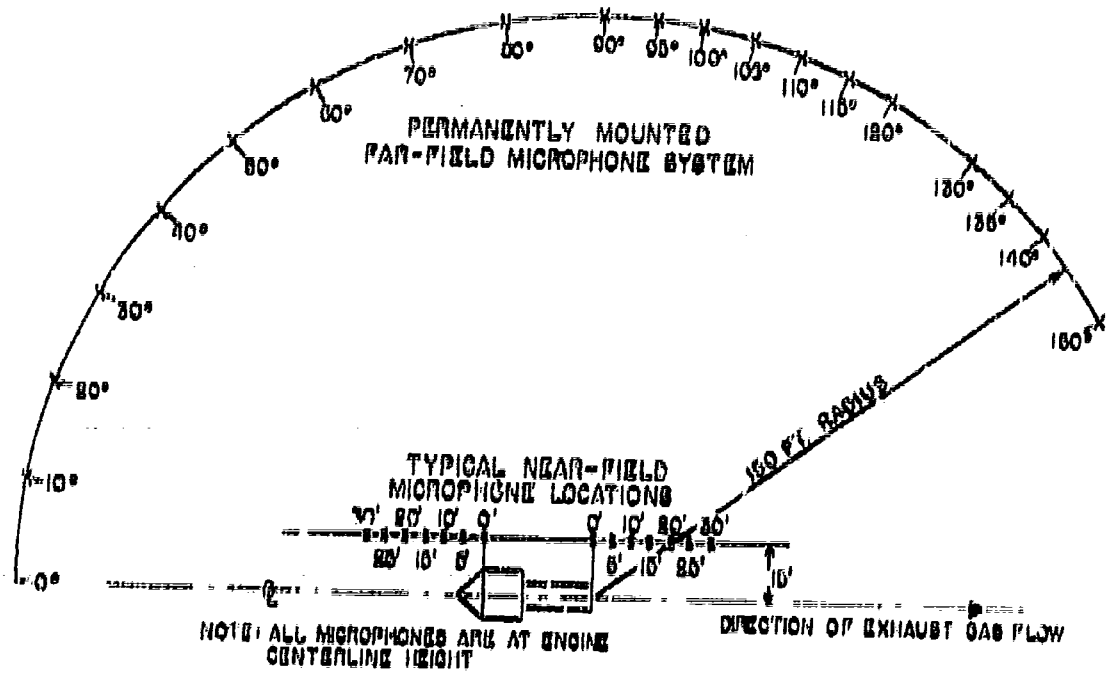
EFFECT OF BLOW-IN-DOOR EJECTOR ON NEAR-FIELD NOISE

Figure 8-99



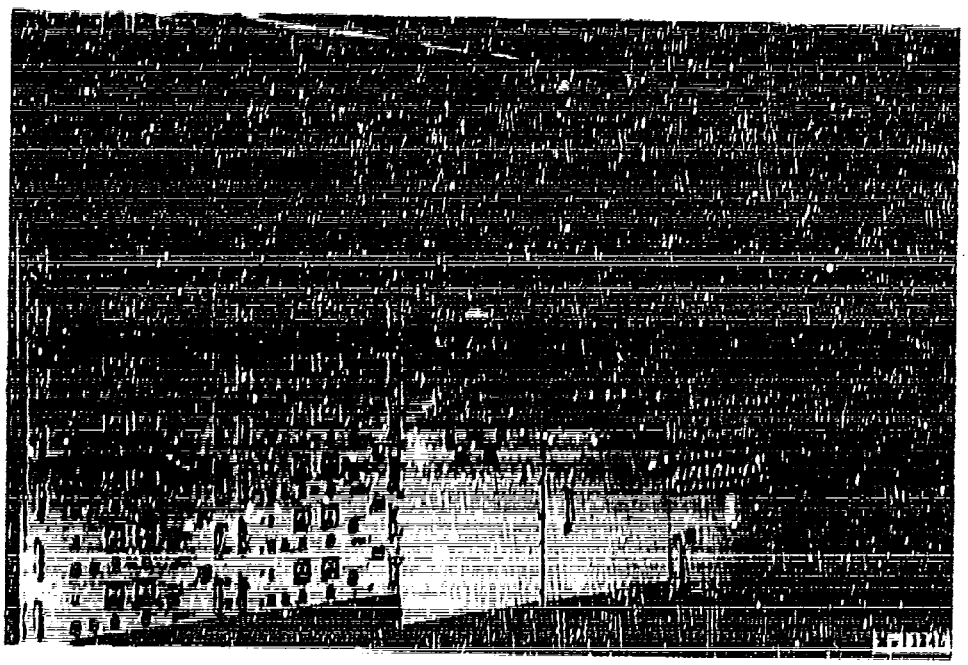
AERIAL VIEW OF BRADLEY FIELD FULL-SCALE ENGINE NOISE TEST FACILITY

Figure 8-60



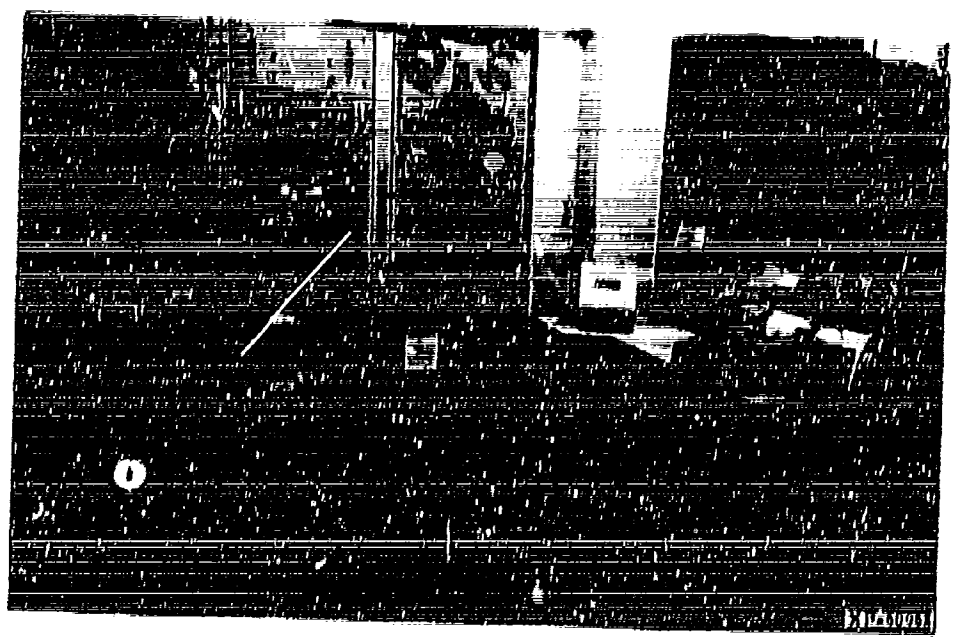
MICROPHONE LOCATIONS AT BRADLEY FIELD FULL-SCALE ENGINE NOISE TEST FACILITY

Figure 8-61



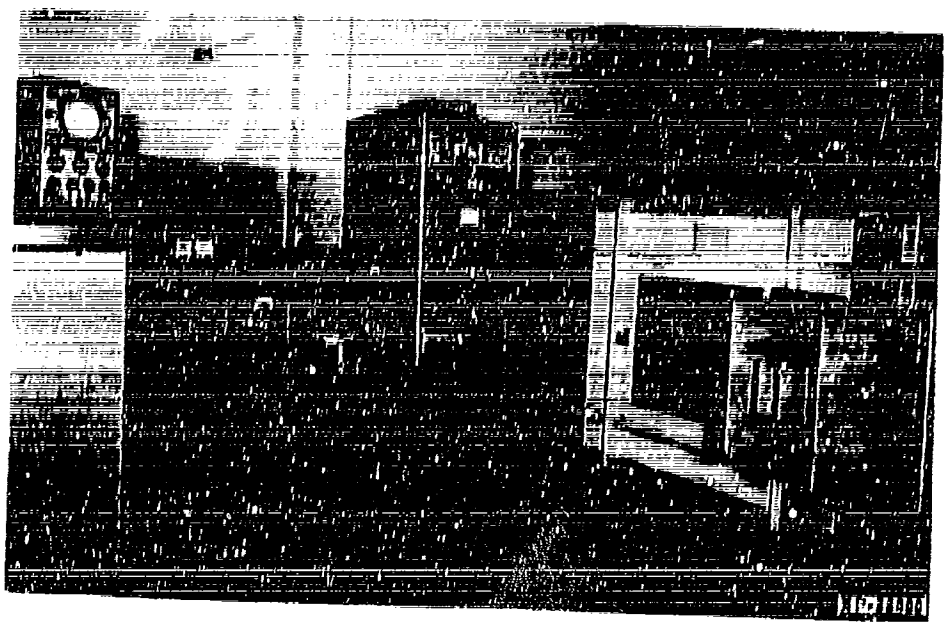
SOUND RECORDING CONSOLE AT BRADLEY FIELD FULL-SCALE ENGINE NOISE TEST FACILITY

Figure 8-62



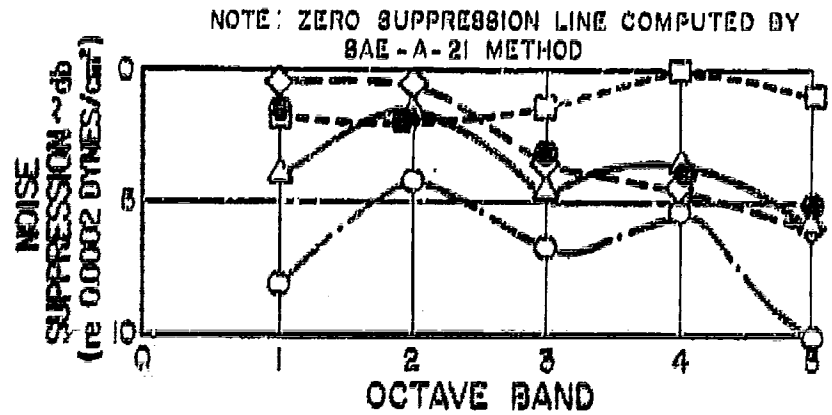
AUTOMATIC SOUND SPECTRUM ANALYZER

Figure 8-63



PRIMARY ACOUSTIC CALIBRATION EQUIPMENT

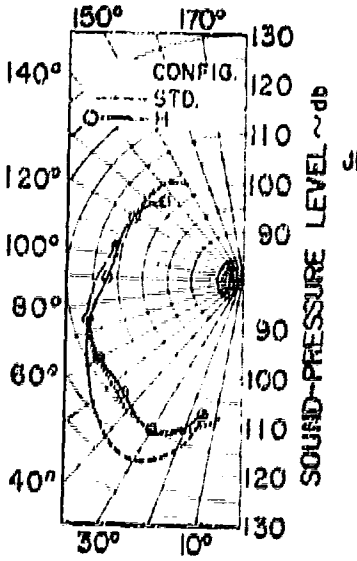
Figure 8-64



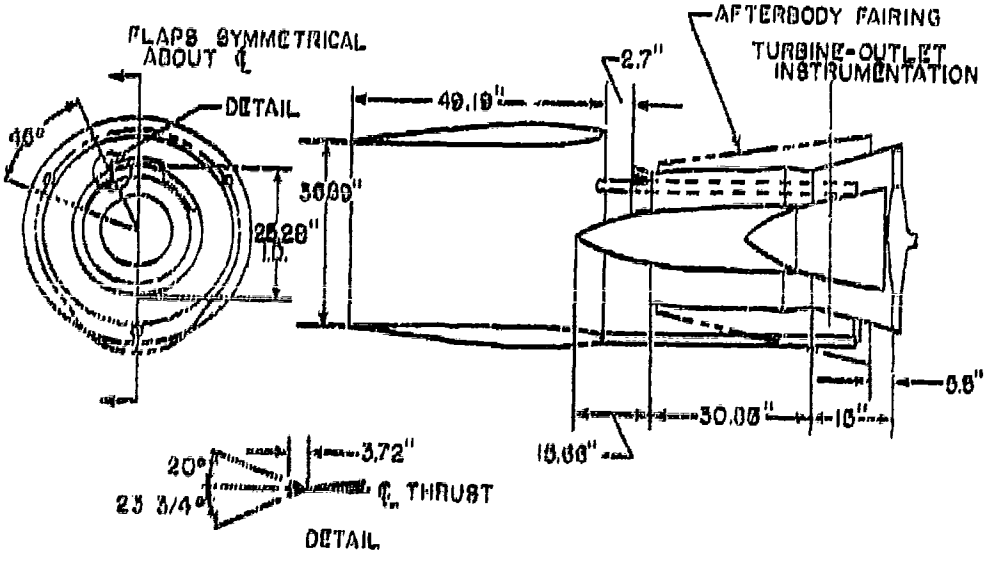
SYMBOL	IAS MACH NO	ALTITUDE FEET	TEMP °F	RELATIVE HUMIDITY %	NOZZLE
●	0.35	250	92	26	TOOTHED
◇	0.525	965	95	12	TOOTHED
○	0.51	490	96	12	TOOTHED
□	0.55	320	97	12	CIRCULAR
△	0.37	600	92	35	TOOTHED

SUPPRESSION OF TAKE-OFF NOISE BY BLOW-IN-DOOR EJECTOR; YF-12A FLY-OVER MEASUREMENTS

Figure 6-65

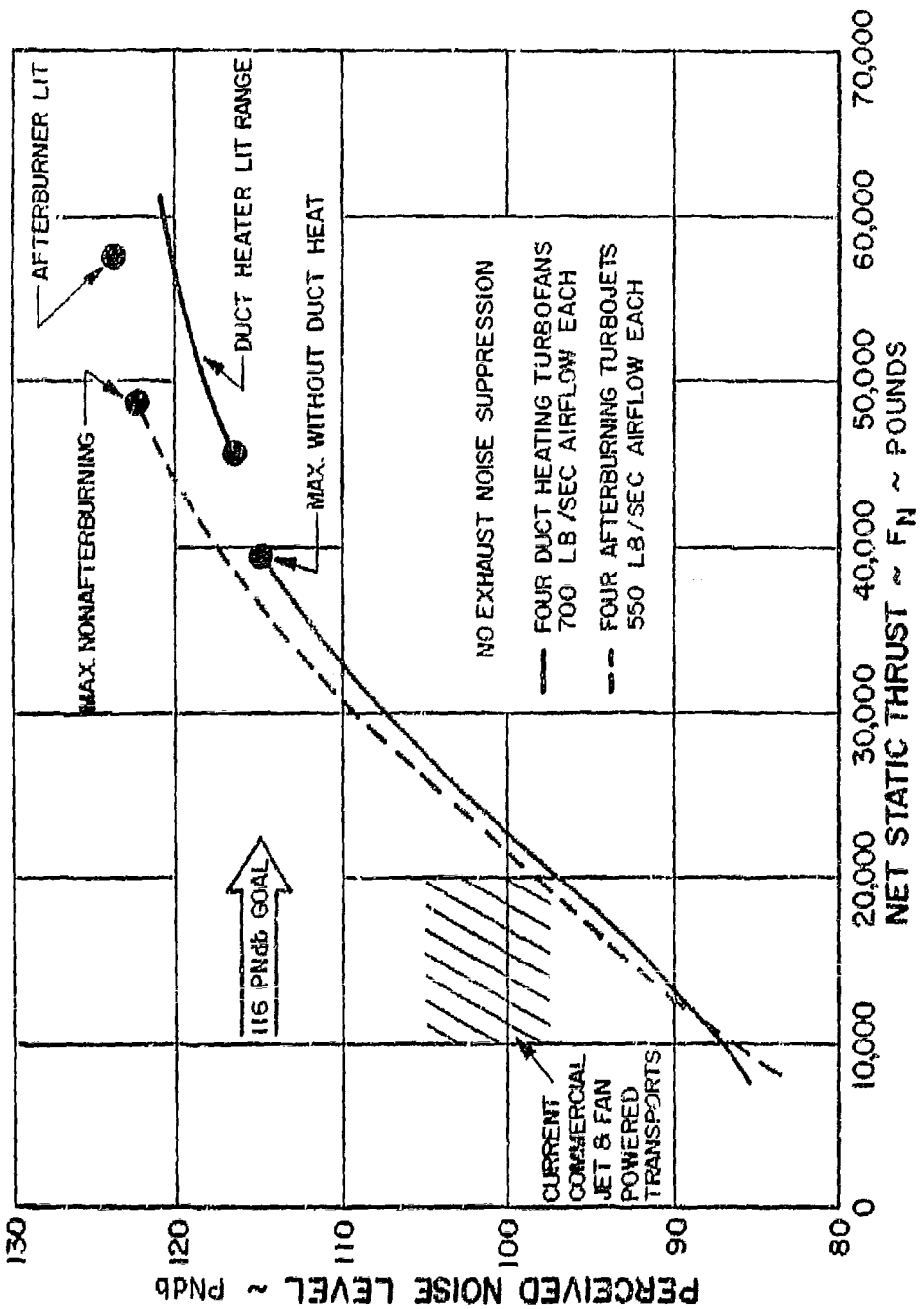


POLAR SOUND-PRESSURE LEVELS



"FLAPPED" NOZZLE AND EJECTOR ASSEMBLY TESTED BY NACA

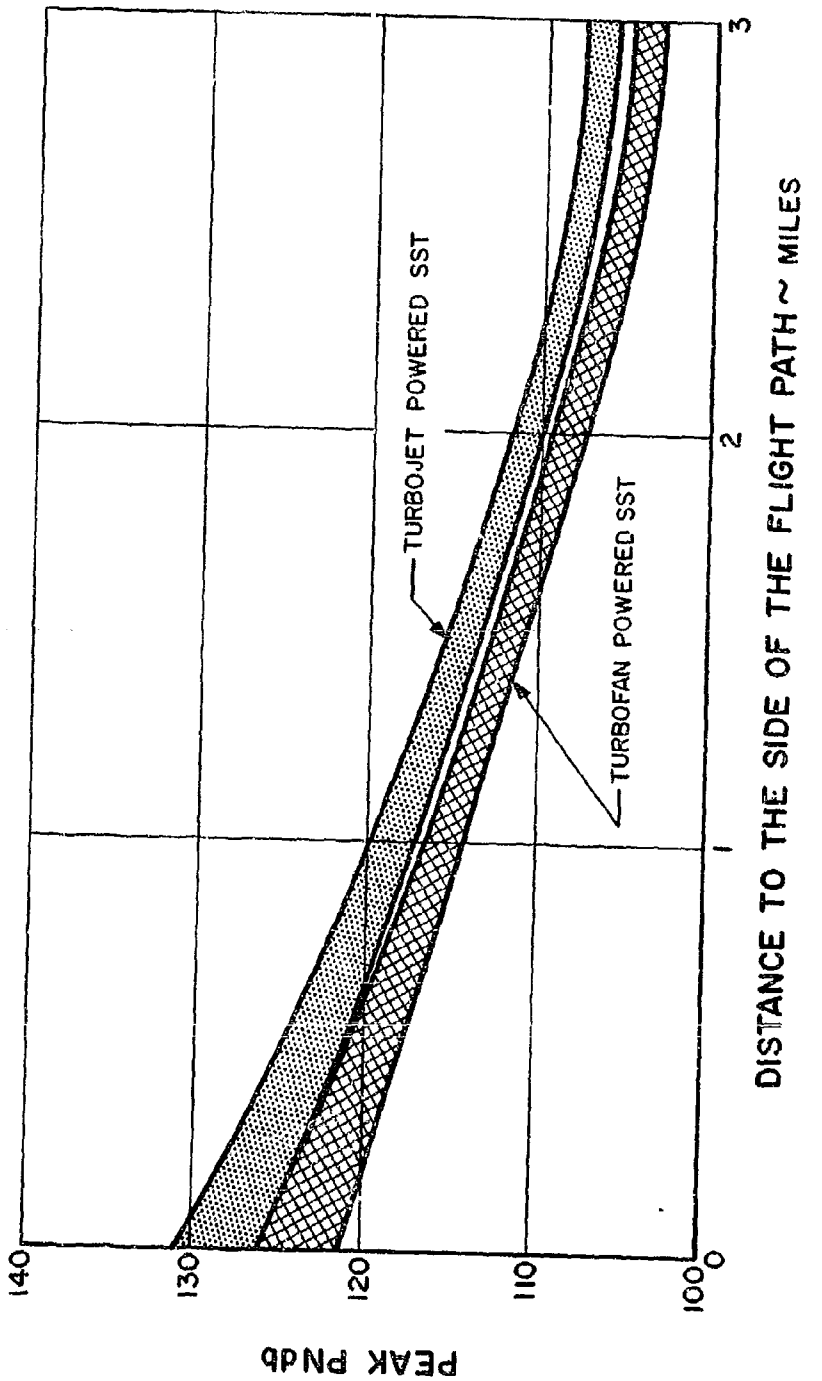
Figure 8-66



COMPARISON OF 1500-FOOT SIDELINE NOISE FROM SST ENGINES

Figure 8-67

DOWNGRADED AT 3 YEAR INTERVALS
DECLASSIFIED AFTER 12 YEARS
DOD DIR 5200.10

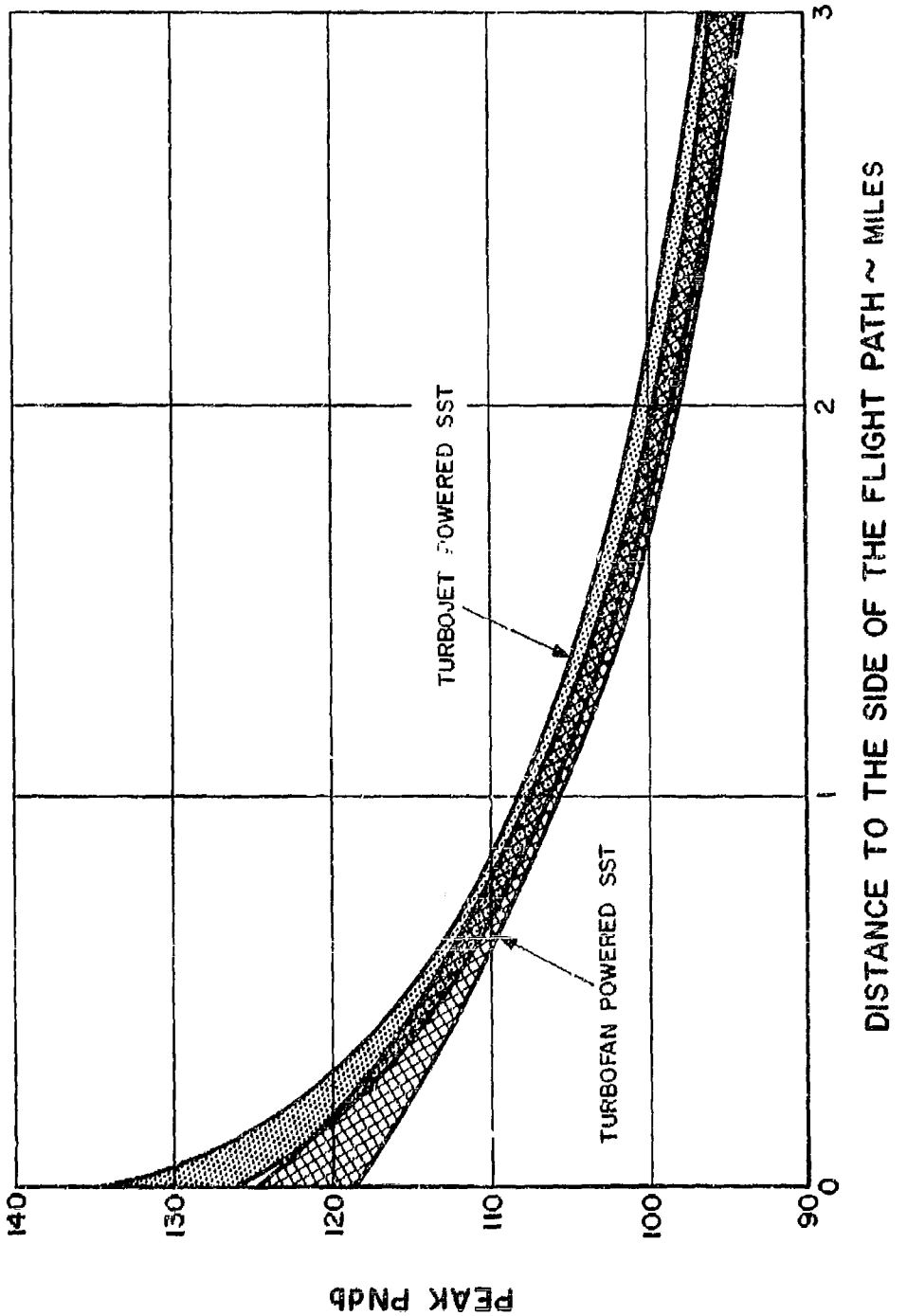


MAXIMUM POWER TAKE-OFF NOISE FROM SST AIRPLANES AT THE THREE-MILE POINT BEFORE POWER CUT-BACK

Figure 8-68

DOWNGRADED AT 3 YEAR INTERVALS
DECLASSIFIED AFTER 12 YEARS
DOD DIR 5200.10

THIS DOCUMENT CONTAINS INFORMATION AFFECTING THE NATIONAL DEFENSE OF THE UNITED STATES WITHIN THE MEANING OF THE ESPIONAGE LAWS, TITLE 18, U.S.C., SECTIONS 793 AND 794. ITS TRANSMISSION OR THE REVELATION OF ITS CONTENTS IN ANY MANNER TO AN UNAUTHORIZED PERSON IS PROHIBITED BY LAW.

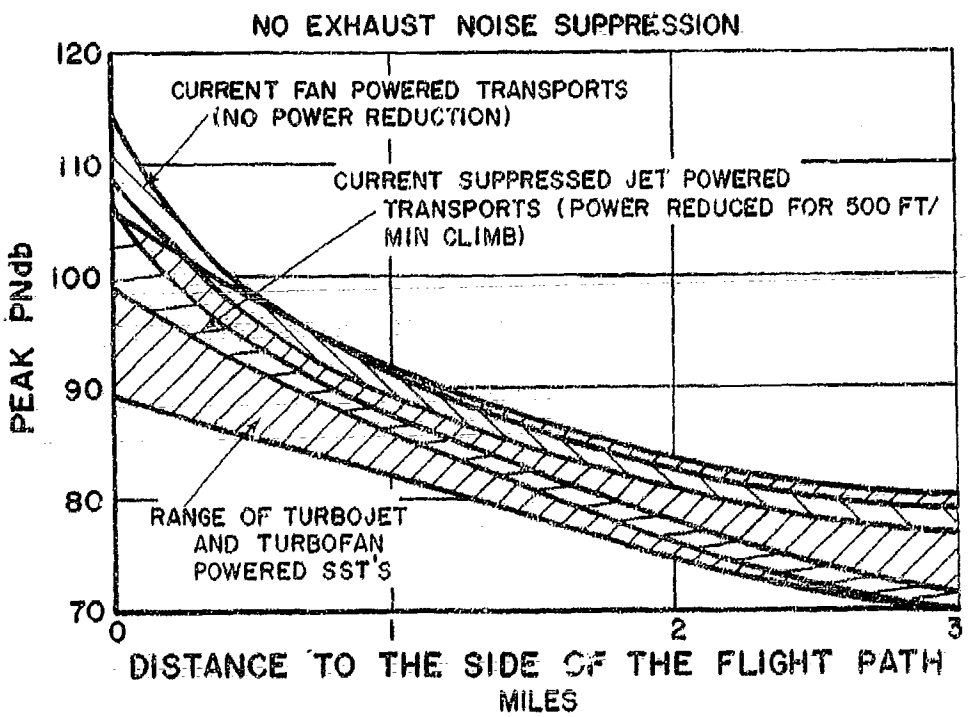


REDUCED POWER TAKE-OFF NOISE FROM SST AIRPLANES AT THE THREE-MILE POINT BEFORE POWER CUT-BACK

Figure 8-69

DOWNGRADED AT 3 YEAR INTERVALS
DECLASSIFIED AFTER 12 YEARS
DOD DIR 5200.10

THIS DOCUMENT CONTAINS INFORMATION AFFECTING THE NATIONAL DEFENSE OF THE UNITED STATES WITHIN THE MEANING OF THE ESPIONAGE LAWS, TITLE 18, U.S.C., SECTIONS 793 AND 794. THE TRANSMISSION OR THE REVELATION OF ITS CONTENTS IN ANY MANNER TO AN UNAUTHORIZED PERSON IS PROHIBITED BY LAW.

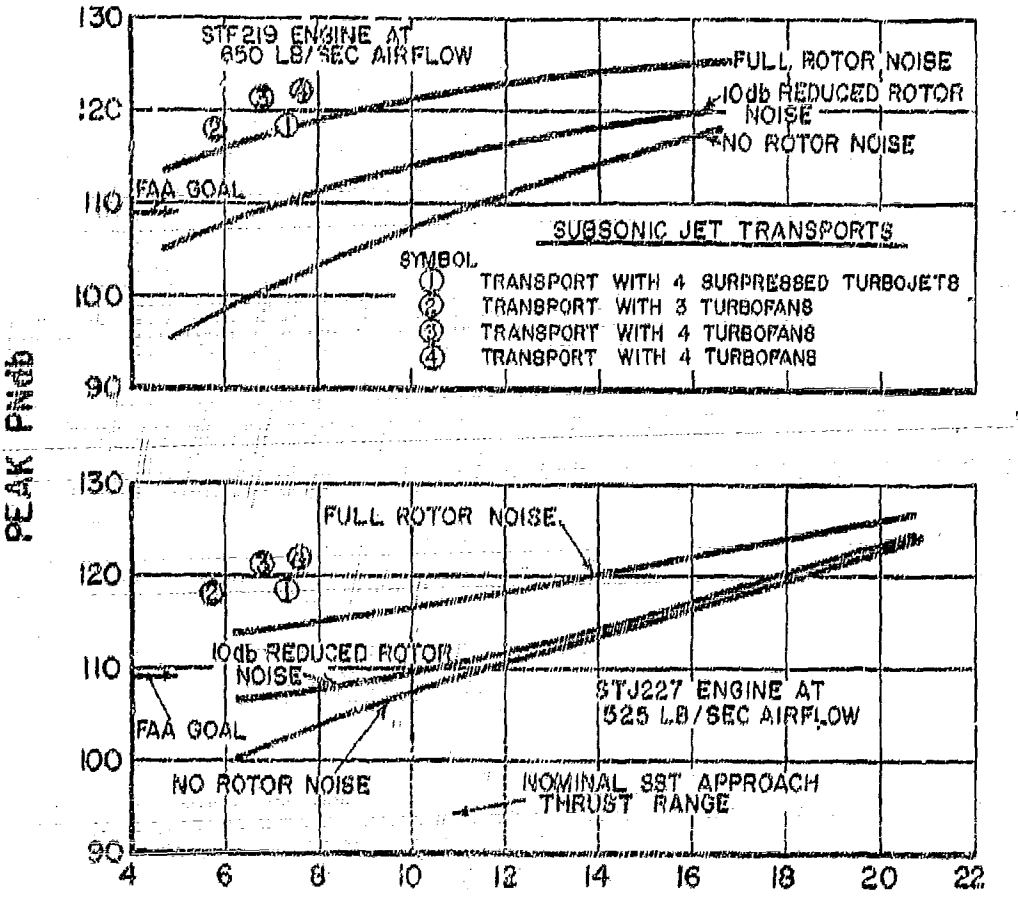


COMPARISON OF TAKE-OFF NOISE FROM SST AIRPLANES AND SUBSONIC JETS AT THE THREE-MILE POINT AFTER POWER CUT-BACK

Figure 8-70

DOWNGRADED AT 3 YEAR INTERVALS
DECLASSIFIED AFTER 12 YEARS
DOD DIR 5200.10

THIS DOCUMENT CONTAINS INFORMATION AFFECTING THE NATIONAL DEFENSE OF THE UNITED STATES WITHIN THE MEANING OF THE ESPIONAGE LAWS, TITLE 18 U.S.C. SECTIONS 793 AND 794. THE TRANSMISSION OR THE REVELATION OF ITS CONTENTS IN ANY MANNER TO AN UNAUTHORIZED PERSON IS PROHIBITED BY LAW.

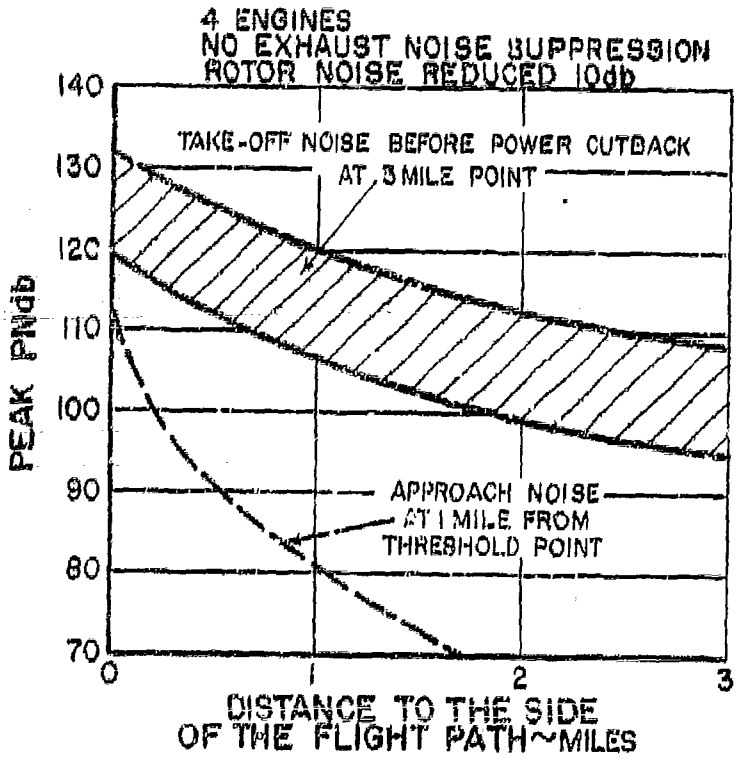


SST LANDING APPROACH NOISE LEVELS BY SAE-A-21 CALCULATION PROCEDURE FOR 327 FEET ALTITUDE

Figure 8-71

DOWNGRADED AT 3 YEAR INTERVALS
DECLASSIFIED AFTER 12 YEARS
DOD DIR 5200.10

THIS DOCUMENT CONTAINS INFORMATION AFFECTING THE NATIONAL DEFENSE OF THE UNITED STATES WITHIN THE MEANING OF THE ESPIONAGE LAWS, TITLE 18, U.S.C., SECTIONS 793 AND 794. THE TRANSMISSION OR THE REVELATION OF ITS CONTENTS IN ANY MANNER TO AN UNAUTHORIZED PERSON IS PROHIBITED BY LAW.



COMPARISON OF SST TAKE-OFF AND APPROACH NOISE LEVELS

Figure 5. 72

DOWNGRADED AT 3 YEAR INTERVALS
DECLASSIFIED AFTER 12 YEARS
DOD DIR 5200.10

THIS DOCUMENT CONTAINS INFORMATION AFFECTING THE NATIONAL DEFENSE OF THE UNITED STATES WITHIN THE MEANING OF THE ESPIONAGE LAWS, TITLE 18, U.S.C., SECTIONS 793 AND 794. THE TRANSMISSION OR THE REVELATION OF ITS CONTENTS IN ANY MANNER TO AN UNAUTHORIZED PERSON IS PROHIBITED BY LAW.

ITEM 9

CONTROLS AND ACCESSORIES

ITEM 9

CONTROLS AND ACCESSORIES

OBJECTIVE

This program was conducted to determine the controls and accessories requirements of the engine and to establish the design requirements with the subcontractors.

A. CONTROLS

1. INTRODUCTION

The fuel control system for the STF219 engine is a hydromechanical system employing the same fundamental principles outlined in the Supersonic Transport Aircraft Engine Phase II A-Development Program Final Report, (PWA-2397 Item 10).

The control system has four basic functions:

- Controls the engine speed between idle and maximum gas generator power.
- Schedules the main engine fuel flow within the desired limits during transient operation.
- Sequences the scheduled duct burner flow, supplied from an air driven turbopump, over the operating envelope between augmentation cut-off and maximum augmentation to individual fuel manifolds.
- Positions the exhaust nozzle area to maintain the desired engine operating condition.

The phase II B study effort was primarily devoted to simplifying the control system as presented in phase II A, and optimizing bias schedules. The objective was to improve reliability and obtain a superior control system.

Control vendor studies were continued with emphasis on design, analytical and associated component testing in the areas found to be deficient during the phase II A study.

DOWNGRADED AT 3 YEAR INTERVALS
DECLASSIFIED AFTER 12 YEARS
DOD DIR 5200.10

THIS DOCUMENT CONTAINS INFORMATION AFFECTING THE NATIONAL DEFENSE OF THE UNITED STATES WITHIN THE MEANING OF THE ESPIONAGE LAWS, TITLE 18, U.S.C., SECTIONS 793 AND 794. ITS TRANSMISSION OR THE REVELATION OF ITS CONTENTS IN ANY MANNER TO AN UNAUTHORIZED PERSON IS PROHIBITED BY LAW.

Simulation studies were continued to represent the aircraft inlet, the engine and each vendors control system. A program was conducted by each vendor to refine the control modes further improving the system's ability to meet aircraft requirements.

2. ENGINE SIMULATION STUDIES

The hybrid analog-digital computer has been utilized to continue the simulation of the STF219 SST engine, the aircraft inlet and each vendors control. The engine simulation remained basically as it was in Phase I' A. The inlet computer program used in Phase II A was a representation received from Lockheed. However, the Phase II B inlet program was written to allow change of flight condition, and with modifications would operate either as a Lockheed inlet or a Boeing inlet.

Each control simulation was connected to the aircraft inlet and engine system, and a program was run by each vendor to refine the control modes to further improve the system ability to meet aircraft requirements.

a. Performance Program

It was required that the vendors perform similar analog transients to permit consistent evaluation of the results. The following paragraphs outline a program designed to describe the engine transient operating conditions at sea level static and cruise flight conditions. In each case the power lever movement was 100 degrees per second for each vendors control. The following is a definition of the terms used in describing the program.

Idle - The minimum engine power setting obtainable from the computer program, except at the cruise flight conditions where minimum flow represents the idle setting.

Rated Power - The maximum gas generator power setting without augmentation.

Maximum Power - Maximum gas generator power setting with maximum augmentation.

(1) Sea Level Static Transients

- Acceleration from idle to maximum power and deceleration back to idle.

DOWNGRADED AT 3 YEAR INTERVALS
DECLASSIFIED AFTER 12 YEARS
DOD DIR 5200.10

THIS DOCUMENT CONTAINS INFORMATION AFFECTING THE NATIONAL DEFENSE OF THE UNITED STATES WITHIN THE MEANING OF THE ESPIONAGE LAWS, TITLE 18, U.S.C., SECTIONS 793 AND 794. THE TRANSMISSION OR REVELATION OF ITS CONTENTS IN ANY MANNER TO AN UNAUTHORIZED PERSON IS PROHIBITED BY LAW.

- Acceleration from idle to rated power and deceleration back to idle.
- Acceleration from rated power to maximum power and deceleration back to rated power.
- Light up of Zone I only and back to rated power.
- Blow out at maximum fuel flow in Zone II.

(2) Cruise Transients

- Acceleration from idle to maximum power and deceleration back to idle.
- Acceleration from idle to rated power and deceleration back to idle.
- Acceleration from rated power to maximum power and deceleration back to rated power.
- Light up of Zone I only and back to rated power.
- Blow out at cruise level of duct fuel flow. (Approximately $T_{td} = 2500°R.$)

Zone transients were made at each flight condition. This was accomplished by acceleration from minimum duct heating of each zone to maximum duct heating of each zone.

The results of each vendors computer effort is presented in Appendices A and B of this report.

b. Aircraft Inlet Simulation

Air inlets for supersonic engines must satisfy two important requirements. The first is that the inlet must provide as high a stagnation pressure (P_{t2}) as possible at the engine interface; the second is that their external surfaces must produce as low a drag as possible. The Pratt & Whitney Aircraft simulation is not concerned with the second requirement but is primarily concerned with the accurate calculations of engine inlet total pressure (P_{t2}).

The primary requirement in obtaining an accurate calculation of P_{t2} is to know the velocity and position of the internal normal shock. For a transient program the supersonic diffuser pressure loss may be considered constant as a first approximation. This leaves the shock total pressure loss and the subsonic diffuser pressure loss as the

DOWNGRADED AT 3 YEAR INTERVALS
DECLASSIFIED AFTER 12 YEARS
DOD DIR 5200.10

THIS DOCUMENT CONTAINS INFORMATION AFFECTING THE NATIONAL DEFENSE OF THE UNITED STATES WITHIN THE MEANING OF THE ESPIONAGE LAWS, TITLE 18, U.S.C., SECTIONS 793 AND 794. THE TRANSMISSION OR THE REVELATION OF ITS CONTENTS IN ANY MANNER TO AN UNAUTHORIZED PERSON IS PROHIBITED BY LAW.

variables in calculating the value of P_{t2}. An additional requirement of a transient inlet program is the calculation of the bypass door area.

Figures 9-1 through 9-4 show the calculation procedure for the inlet program. The first figure is the airflow balance downstream of the shock. It is the airflow contained between the shock position and the inlet boundaries which determines the subsonic stream static pressure that positions the shock. It is this airflow calculation procedure which distinguishes the Lockheed inlet from the Boeing inlet. The Lockheed inlet has a system of "educated" bleeds (W_{bly}) which have a stabilizing effect on the shock when it is positioned in the converging supersonic diffuser section.

During Phase II A Pratt & Whitney Aircraft received from Lockheed a program simulating a two-dimensional mixed compression inlet and a bypass door control. The Phase II B Pratt & Whitney Aircraft inlet was studied under various disturbance conditions and it was concluded that the results were similar to the Phase II A Lockheed inlet and it was used throughout the Phase II B control vendor studies.

The Lockheed bypass area control was used during the current study. The control senses shock position with a pressure ratio sensor and the bypass door area is changed to position the shock at the desired terminal position.

(1) Lockheed Inlet Operation

To obtain optimum inlet operation the shock is positioned at the throat by a combination of proper scheduling of engine airflow and bleed door operation. In the Lockheed installation the engine airflow is controlled by adjusting the duct exhaust nozzle area as a function of flight Mach number, high speed rotor speed, and engine inlet total temperature during engine operation in the cruise regime.

The control vendor computer program was conducted using the Lockheed inlet configuration.

(2) Boeing Inlet Operation

The Boeing inlet operates with optimum pressure recovery and minimum distortion when the shock is in the desired position which is slightly downstream of the throat, and when the bypass doors are closed. To position the shock at the optimum position the engine airflow must be adjusted. When the shock is slightly downstream of the optimum

position the engine airflow must be adjusted by closing the duct exhaust nozzle area. A block diagram of the Boeing inlet shock position control is shown on Figure 9-5. This scheme was put on the computer with the Pratt & Whitney Aircraft inlet representation modified to resemble the Boeing configuration, the STF219 engine and a vendors control.

It was determined that the system was feasible, however, the program should be run with the actual Boeing inlet and control characteristics. It will be necessary to establish the proper relationship between the K_0, K_1 and K_2 gains in order to provide a system whose stability is acceptable.

(3) Inlet Distortion

To fully appreciate the interaction between the inlet and the engine it was necessary to determine the effect of distortion on the engine. It was also necessary to define inlet distortion and to determine a relationship that would allow the inlet program to result in a distortion parameter.

Inlet distortion was grossly defined as $(P_{t2\ avg} - P_{t2\ min}) / P_{t2\ avg}$. There was no distinction made between radial or circumferential distortion since the entire distortion routine was approximate due to insufficient inlet data especially during transient operation. A relationship was obtained for the change in the low compressor and high compressor surge line with inlet distortion.

Inlet distortion appears to be caused by two conditions in the inlet. Shock interaction with the boundary layer in the subsonic diffuser section and bypass area door position both cause changes in inlet distortion. Minimum distortion occurs with the bypass doors closed and the shock located at the throat. It appears that there exists a steady state level of distortion in the inlet even when these two conditions are satisfied. The available data allowed for an approximate relationship between inlet distortion and the percentage amount P_{t2} is lower than the steady state or critical value (percent supercritical). The relationship between percent supercritical and the percentage change in the surge pressure ratio for each compressor was input to the engine program as is shown on Figures 10-9 and 10-11 of the engine program as presented in the SST Phase IIA Final Report (PWA 2397).

The effect of adding the distortion routine to the engine program was to reduce the surge margin of the match points of each compressor.

DOWNGRADED AT 3 YEAR INTERVALS
NOT AUTOMATICALLY DECLASSIFIED AFTER 12 YEARS
DOD DIR 5200.10

THIS DOCUMENT CONTAINS INFORMATION AFFECTING THE NATIONAL DEFENSE OF THE UNITED STATES WITHIN THE MEANING OF THE ESPIONAGE LAWS, TITLE 18, U.S.C., SECTIONS 793 AND 794. THE TRANSMISSION OR THE REVELATION OF ITS CONTENTS IN ANY MANNER TO AN UNAUTHORIZED PERSON IS PROHIBITED BY LAW.

Ignition of the duct heater raises the back pressure on the fan and the match point is moved toward the surge region. Protection against surge is obtained by increasing the duct exhaust nozzle area before lighting the duct burner in the same manner as when at the sea level static point. Operating in this manner produces adequate surge margin during light-off of the duct burner. The transient operation of the engine and inlet during this disturbance is presented on the computer traces presented by the vendors in Appendices A and B.

3. ENGINE CONTROL STUDIES

The STF219 engine control studies were separated into two areas. One area is the engine control function which would simplify aircraft operation such as constant velocity of approach control. The other area of engine control study is directly associated with engine control parameters.

a. Constant Aircraft Approach Velocity Control

Lockheed requested that the feasibility of controlling engine thrust to provide a constant approach velocity for a landing be studied. The Phase II A conclusion was that such a feature was feasible. The Phase II B study was to demonstrate the control concept and check the stability of the system when coupled with the aircraft. The study was performed with the computer program. It was demonstrated that the approach velocity coupler is feasible; however, further evaluation would be required using Lockheed supplied approach velocity control characteristics and aircraft dynamics.

As a first approximation Pratt & Whitney Aircraft has assumed that the aircraft altitude remains constant during the landing approach. This assumption reduces the aircraft simulation to a single degree of freedom, where the velocity is a function of the forces acting on the aircraft as follows:

$$v = \int \frac{(4 F_{nt} \cos \alpha - D)}{W/g} \, dt$$

where,

v = velocity of aircraft at constant altitude
F_{nt} = net thrust delivered by one engine
α = aircraft angle of attack
D = aircraft drag
W = 265,000 lbs.

DOWNGRADED AT 3 YEAR INTERVALS
DECLASSIFIED AFTER 12 YEARS
DOD DIR 5200.10

THIS DOCUMENT CONTAINS INFORMATION AFFECTING THE NATIONAL DEFENSE OF THE UNITED STATES WITHIN THE MEANING OF THE ESPIONAGE LAWS, TITLE 18, U.S.C., SECTIONS 793 AND 794. ITS TRANSMISSION OR THE REVELATION OF ITS CONTENTS IN ANY MANNER TO AN UNAUTHORIZED PERSON IS PROHIBITED BY LAW.

The aircraft drag has been determined from the Lockheed CL-823 Approach Thrust Requirements curve received at Pratt & Whitney Aircraft in July, 1964. The curve has been reduced by the weight component which is opposite in direction to the drag. A block diagram of the aircraft representation is shown in Figure 9-6.

The engine control has been simulated to adjust engine thrust with a change in approach control lever position. It is anticipated that Lockheed would supply this signal with a proportional velocity sensor control. The simplified control block diagram is shown at the bottom of Figure 9-6.

During steady operation the aircraft drag, D, equals the sum of the thrust delivered by the four engines. This is shown on Figure 9-7 at the point just prior to the input disturbance.

To demonstrate the control response, a force disturbance was imposed upon the aircraft. The magnitude of the force disturbance was relatively high. It may be considered as a step change in approach angle from minus three degrees to plus six degrees which results in doubling the aircraft drag. The immediate response was to reduce aircraft speed, which increases drag to further slow down the aircraft. However, the change in velocity will be sensed by the aircraft approach control system and an approach control lever angle signal sent to the engine fuel control. As a result engine speed setting (turbine inlet temperature) will automatically increase to allow the engine thrust to compensate for the force disturbance and allow the aircraft to settle out at the new velocity level.

The band of velocity control is a function of the proportional gain in the aircraft approach control and the gain in the fuel control between approach control lever angle and engine speed setting. Several runs were made with various proportional gains and the resultant final approach velocity is shown on Figure 9-8. It should be noted that the higher gains in the vicinity of K/Ko = 2.0 result in a marginally stable system.

If it is desired to hold a constant approach velocity, it would be necessary for the aircraft approach control to contain an integrator which would continue to change engine thrust until a zero velocity error is obtained. It is suggested that a proportional plus integral control be used with a fairly high ratio of proportional to integral gain.

DOWNGRADED AT 3 YEAR INTERVALS
DECLASSIFIED AFTER 12 YEARS
DOD DIR 5200.10

THIS DOCUMENT CONTAINS INFORMATION AFFECTING THE NATIONAL DEFENSE OF THE UNITED STATES WITHIN THE MEANING OF THE ESPIONAGE LAWS, TITLE 18, U.S.C., SECTIONS 793 AND 794. THE TRANSMISSION OR THE REVELATION OF ITS CONTENTS IN ANY MANNER TO AN UNAUTHORIZED PERSON IS PROHIBITED BY LAW.

b. Engine Control Parameter Study

The STF219 SST engine control parameter study was primarily directed toward the duct burner operation with emphasis placed upon improving simplicity and increasing reliability. The parameter study of the main gas generator was directed toward simplifying and determining the accuracy of the bias schedules which set turbine inlet temperature during acceleration and cruise.

(1) Duct Fuel Flow Bias Simplification

The duct fuel flow bias schedules were investigated, and it was determined that the fan inlet total pressure (P_{t2}) bias could be eliminated from the Zone I and Zone II fuel schedules. Figures 7, 8, and 9 of PWA Purchase Specification 819D, as shown in Appendix 10-A of the Phase IIA Report (PWA 2397), show that duct fuel flow ratio (W_{fd}/P_{t4}) is biased by fan inlet total temperature (T_{t2}) and pressure (P_{t2}). The elimination of the P_{t2} bias results in a control computer simplification and increases the reliability of the duct fuel system. However, some error is introduced into the fuel flow delivered to the duct.

(a) Zone I - During Zone I selection, the lighting fuel flow would be scheduled as shown on Figure 9-9. This figure shall supersede Figure 7 of PPS 819D. The error in lighting Zone I with this schedule will be approximately ±5 percent of the nominal lighting value of .008 fuel air ratio units.

The maximum fuel-air ratio in Zone I has been determined to be .025, however, to comply with Lockheed and Boeing's request for a constant cruise flight condition control [1], the fuel-air ratio was reduced linearly from .025 at Mach 2 to .020 at Mach 3. This fuel-air schedule for Zone I maximum was satisfied by Figure 8 of PPS 819D. However, it has since been determined that the P_{t2} bias can be removed and still remain within ±6 percent of the desired fuel-air for various flight conditions. The revised curve is shown in Figure 9-10. This figure supersedes Figure 8 of PPS 819D.

1. The constant cruise flight condition control modulates engine thrust to hold the Mach number constant and provide cruise speed stability. This control scheme was discussed in the Phase IIA Report PWA 2397, Item 10.

DOWNGRADED AT 3 YEAR INTERVALS
DECLASSIFIED AFTER 12 YEARS
DOD DIR 5200.10

(b) Zone II - The maximum augmentation point is defined by a duct temperature of 3560°R. However, the Zone II maximum fuel flow ratio schedule on Figure 9 of PPS 819D has been altered to schedule the duct temperature to be reduced linearly from 3560°R at Mach 2 to 3000°R at Mach 3. This cut back is to occur simultaneously with the Zone I cut back to control the cruise flight condition as desired by Lockheed and Boeing. It has since been determined that the P_{t2} can be removed and still allow the standard day maximum net thrust to remain approximately within ± 1.0 percent. A slightly greater penalty is obtained during cold day operation. The percentage change in maximum net thrust for a minus 30 degree day may be as high as minus three percent, the worst condition being sea-level, Mach 0.6. The percentage change in maximum net thrust for a minus 60 degree day may be as high as minus five percent, again the worse condition being sea-level, Mach 0.6. The revised Zone II maximum schedule is shown on Figure 9-11. This figure supersedes Figure 9 of PPS 819D.

(2) Optimum Zone I Operation During Acceleration

During aircraft acceleration, it is expected that the main gas generator turbine inlet temperature will be 2760°R and the duct burner will be operating with both Zone I and Zone II. To obtain minimum fuel expenditure for any climb path it would be necessary for Zone I to operate at its most efficient fuel-air ratio of .015. The fuel flow schedule as shown on Figure 6 of the PWA Purchase Specification 819D in the Phase II A final report allows the fuel air ratio to vary from .012 to .025.

The schedule has been revised and is shown on Figure 9-12. This curve schedules W_{fd}/P_{t4} as a function of power lever angle for sea-level static day operation. This figure supersedes Figure 6 of PPS 819D. It is noted that for this flight condition the fuel-air ratio in Zone I is held constant at approximately .016 when Zone II is in operation. Zone I fuel flow is scheduled to allow ignition at a fuel-air ratio of .008 and is increased to .025 at maximum Zone I fuel flow. As Zone II is selected, Zone I "gearshifts" from a fuel flow ratio of W_{fd}/P_{t4} = 190 down to a constant fuel flow ratio of 110, and Zone II is scheduled to deliver the gearshifted amount of 80 ratio units. Zone II is subsequently scheduled to deliver fuel flow up to a maximum augmentation fuel air ratio of .054.

As the flight condition is varied, the fuel flow ratio level in Zone I during Zone II operation must be biased to deliver the desired fuel-air ratio. This is accomplished by "gearshifting" Zone I by a constant 80 ratio units regardless of flight condition. The result is that the

DOWNGRADED AT 3 YEAR INTERVALS
DECLASSIFIED AFTER 12 YEARS
DOD DIR 5200.10

Zone I bias during Zone II operation is the same bias as Zone I maximum, with the level of fuel flow ratio units reduced by the amount of the gearshift.

This results in the Zone I fuel-air ratio deviating from the optimum by ± 8 percent during the majority of the aircraft flight conditions. A couple of flight conditions in the Mach 1.8 to Mach 2.0 region result in the fuel-air ratio going as high as .018 which is still less than one duct burner efficiency point deviation from the optimum.

(3) Constant Duct Area Operation at Low Part Power

Each vendor subcontracted for component development during the SST R&D contract and IIA has decided to use a closed loop control on the duct exhaust nozzle area. They both have selected a $\Delta P/P$ "duct area control parameter" which is a function of the Mach number at the exit of the fan. A scheduled value of $\Delta P/P$ (Bendix uses $(P_{t3}-P_{s3})/P_{s3}$, and Hamilton Standard uses $(P_{t3}-P_{s3})/P_{t2}$ is obtained as a function of rotor speed, N_2, and flight condition, Mach number or T_{t2}. A measured value is obtained from a series of probes which measure P_{t3} and P_{s3} at the exit of the fan. The difference between the scheduled value and the measured value is the error which is used to open or close the area as required, using a proportional plus integral control.

The problem anticipated with this type of control would result from the measured value of P_{t3} and P_{s3} when the engine is operating at low part power, idle or during the starting transient. During these conditions it is expected that the noise level of the measured parameter could exceed the signal level for the operating point. If this should happen, it would be impossible to set the desired area, and most likely the area would tend to follow the noise signal in a fluctuating pattern.

Therefore the vendors were strongly advised to develop a control scheme which would schedule area independent of any measured parameter when operating at low part power. During the early performance stages it was deliberately decided upon to operate all part power points at a constant area of four square feet for a 600 PPS size engine.

Both vendors have designed a new control mode for the control of area during this low part power operation. The new control mode operates with the duct area control parameter setting the nozzle area at high engine power settings and during augmentation. As the engine power is reduced, the duct area control parameter operates to set nozzle area until four square feet is obtained. Further reduction in engine power results in the area remaining locked at this constant value.

DOWNGRADED AT 3 YEAR INTERVALS
DECLASSIFIED AFTER 12 YEARS
DOD DIR 5200.10

Each vendor has demonstrated the new control scheme on the computer and no unusual interactions have resulted.

(4) Alternate Duct Area Control Parameter

The final report written for SST R&D Contract Number AF33 (657) - 11189 discussed several duct area control parameters. However, the engine in reference at the time was a single spool duct burning turbofan. The conversion to a twin spool duct burning turbofan leaves one parameter not discussed. This parameter is fan rotor speed, N_1. The following is a discussion of the problem of using N_1 as a direct area control parameter.

The duct area control parameter must have the ability to adjust the exhaust nozzle area to its desired position in response to disturbances either externally or internally generated; and secondly must have the capacity to permit the system to recover from stall if encountered.

The choice of N_1 as a control parameter seems to be a natural one for this engine since one would normally expect there to be a strong influence between the duct area and low compressor rotor speed. However, such is not the case. For a twin spool engine of the SST configuration, there is only a weak interaction between these two parameters since the characteristic of the fan is such that a line of constant corrected rotor speed is nearly coincident with a line of constant input horsepower especially at the lower corrected speed operating points. Thus changes in back pressure, due to changes in the exhaust nozzle area, result in a change of fan airflow opposite to the pressure change so that the inlet horsepower remains nearly constant. The result is that there is not a strong enough interaction between the parameters to make N_1 a suitable controlling choice.

The second problem area is that during an inadvertent fan stall, it is desirable to have a system which will recover from the stall. During fan stall, at a constant area, the rotor speed remains nearly constant. As a result the duct area control parameter will remain unchanged and no corrective action would occur to help the system recover from fan stall.

(5) Duct Light-off Signal

A characteristic of each vendors control system is that the fuel flow added to the duct cannot be advanced from the light-off value without receiving a light-off signal from the duct.

For values of lighting fuel-air ratio of .008 there does not appear to be any problems. The duct light-off detector would simply be the duct area control parameter $\Delta P/P$, which decreases by at least 5 percent at all flight conditions when duct burning initiates. This change is

DOWNGRADED AT 3 YEAR INTERVALS
DECLASSIFIED AFTER 12 YEARS
DOD DIR 5200.10

sufficiently strong to be detected above the noise of the measuring apparatus. However, if the light up fuel-air ratio were .003, a problem would exist. A study was made of the various methods which would indicate a duct burner light-off under these circumstances. At a fuel-air ratio of .003, the engine disturbance would be difficult to sense, particularly above the normal noise levels of the various sensors. Based upon durability, reliability, and signal to noise ratio criteria, it appeared that the most promising parameter would be the time rate of change of the duct area control parameter, $d(\Delta P/P)/dt$.

In view of the complexity involved to sense a light-off at a fuel-air ratio of .003 it appeared reasonable that a lighting fuel-air ratio of .008 was justified.

(6) Speed Bias Simplification and Accuracy Analysis

The primary burner speed bias schedules were studied with emphasis placed upon simplifying the system, and to determine how accurately the schedule would set turbine inlet temperature during various aircraft flight conditions.

The control of turbine inlet temperature is performed by scheduling high rotor speed with power lever position, P_{t2} and T_{t2} and comparing with actual rotor speed. The error provides the input to a proportional control system (droop governor) which delivers the desired amount of fuel to the primary burner. In the STF219, the most important engine power level settings are maximum rated power and cruise rated power. To obtain the greatest accuracy a separate speed bias schedule (variation of speed setting with P_{t2} and T_{t2}) for each power level setting was provided. This was the program as presented in Phase II A. However, in monitoring the progress of the vendors it was decided that the control schemes to execute the two separate biases was very complex.

A study was made to simplify the speed bias system. The conclusion was to make the cruise bias exactly the same as the maximum rated power bias. The change in engine power level setting would be accomplished by the change in power lever position only. The new speed bias curve is shown on Figure 9-13 which replaces Figures 4 and 5 of PWA Purchase Specification 819D.

An accuracy analysis was performed to demonstrate that the revised schedule would satisfy the desired turbine inlet temperature for various flight conditions during aircraft acceleration. Figure 9-14 shows what the turbine inlet temperature is expected to be when the power

DOWNGRADED AT 3 YEAR INTERVALS
DECLASSIFIED AFTER 12 YEARS
DOD DIR 5200.10

lever is positioned in the maximum rated power position. Each point is identified with a specific flight condition on the representative climb path shown at the bottom of the figure.

A similar study was made for flight conditions during the cruise regime of operation. The turbine inlet temperatures obtained are shown in the following Table:

Control of T_{t5} During Cruise Flight Conditions

Altitude	M_n	T_{t5} Desired	T_{t5} Obtained
55,000	2.0	2660°R	2664°R
65,000	2.0	2660°R	2669°R
55,000	2.2	2600°R	2669°R
60,000	2.5	2660°R	2660°R
75,000	2.5	2660°R	2653°R
62,000	2.7	2660°R	2651°R
65,000	2.7	2660°R	2655°R
75,000	2.7	2660°R	2650°R
65,000	3.0	2660°R	2666°R
70,000	3.0	2660°R	2657°R
75,000	3.0	2660°R	2660°R

At low values to T_{t2}, the turbine inlet temperature is limited to prevent aerodynamic overspeed. The following Table shows several flight conditions along with their desired turbine inlet temperatures. The table is presented for two power lever positions, maximum rated power which is used for aircraft acceleration, and cruise, along with the turbine inlet temperatures obtained at each setting. It is noted that the bias schedule would control T.I.T. to within ±2% of the desired setting at the maximum rated power lever position. At the cruise power lever position T.I.T. never exceeds the limit, but may be about 5% low. It is not anticipated that this is a problem since the pilot may select the maximum rated power lever position to obtain the desired T.I.T.

Control of T_{t5} During Aerodynamic Overspeed Limitation

Altitude	M_n	T_{t5} Desired	Power Lever Position	T_{t5} Obtained
25,000	.2	2640°R	Max. Rated	2600°R
25,000	.2	2640°R	Cruise	2500°R

DOWNGRADED AT 3 YEAR INTERVALS
DECLASSIFIED AFTER 12 YEARS
DOD DIR 5200.10

Altitude	M_n	T_{t5} Desired	Power Lever Position	T_{t5} Obtained
25,000	.4	2700°R	Max. Rated	2680°R
25,000	.4	2660°R	Cruise	2550°R
36,000	.4	2450°R	Max. Rated	2440°R
36,000	.4	2450°R	Cruise	2350°R
36,000	.6	2550°R	Max. Rated	2540°R
36,000	.6	2550°R	Cruise	2410°R
45,000	.5	2500°R	M x. Rated	2550°R
45,000	.5	2500°R	Cruise	2430°R
45,000	.8	2680°R	Max. Rated	2710°R
45,000	.8	2660°R	Cruise	2605°R

The control of turbine inlet temperature during flat rating take-off is presented in terms of thrust deviations from the desired value for several flight conditions on Figures 9-15, 9-16 and 9-17. In each case the power lever is in the maximum rated position. It is noted that the thrust deviation from the desired normal rated value does not exceed ±5.0% with the higher deviations occurring at the colder day conditions.

Figure 9-18 is a descriptive explanation of flat rating during part power operation. The speed schedule varies with power lever to adjust turbine inlet temperature so as to modulate thrust linearly from maximum rated power to idle for any given atmospheric day operation. The linear thrust schedule is maintained whether the engine is flat rated or not. Since the flat rating is accomplished by the P_{t2} and T_{t2} bias schedule, it follows that the engine would be flat rated not only at the maximum rated power setting but also at the idle power setting.

4. VENDOR ACTIVITY

a. Control Vendor Studies

Contracts for the continuation of the work funded by the Phase II A study contract were placed with the Bendix Product Aerospace Division and with the Hamilton Standard Division. The contracts provided for each vendor to perform design and analytical studies and associated component testing with emphasis placed on those areas which were found to be deficient during the Phase II A study.

The vendors have completed their studies and have submitted their

DOWNGRADED AT 3 YEAR INTERVALS
DECLASSIFIED AFTER 12 YEARS
DOD DIR 5200.10

THIS DOCUMENT CONTAINS INFORMATION AFFECTING THE NATIONAL DEFENSE OF THE UNITED STATES WITHIN THE MEANING OF THE ESPIONAGE LAWS, TITLE 18, U.S.C., SECTIONS 793 AND 794. ITS TRANSMISSION OR THE REVELATION OF ITS CONTENTS IN ANY MANNER TO AN UNAUTHORIZED PERSON IS PROHIBITED BY LAW.

final reports. The reports are included in this report as Appendices A and B and contain the results of design, analytical and experimental efforts conducted to develop a control system which will meet the requirements of the engine and aircraft inlet system and provide optimum engine performance. The trust levels shown on the computer times are primarily for the purpose of determining relative levels, they may, or may not, agree with steady state performance. Included are the results of packaging and arranging of components in the control computer section and layouts of the metering section along with the coordinated installation designs of the complete system. The reports also contain results of the studies made of the pressure ratio sensor, including some experimental results. Also included are the results of control mode studies and analog computer control simulation studies.

b. Pump Vendor Studies

Designs for the main fuel, hydraulic actuation, and duct heater fuel pumps have been obtained based upon the proposals submitted by the various pump vendors. The pump vendors submitting designs are Chandler Evans Co., Tapco division of Thompson-Ramo-Wooldridge, Vickers, Hamilton Standard Division of United Aircraft Corporation and Pesco division of Borg-Warner. These designs were studied to determine conformance to the desired envelopes of each of the fuel pump types. Each vendor was able to design a unit which would meet the required envelope restrictions. Similarly evaluations of the weight of each proposed unit was compared to the weight estimates used in the engine weight estimates to determine that the original estimates were reasonable.

Performance of each of the proposed units was compared to specification requirements. The main and hydraulic actuation fuel pumps had adequate performance margins while one version of the duct fuel pump also had adequat margin. The other proposed duct heater fuel pump was lacking required performance by a substantial amount which would require, if this pump were employed on the engine, an increase in allowable fuel inlet pressure of 15 to 20 psi.

DOWNGRADED AT 3 YEAR INTERVALS
DECLASSIFIED AFTER 12 YEARS
DOD DIR 5200.10

THIS DOCUMENT CONTAINS INFORMATION AFFECTING THE NATIONAL DEFENSE OF THE UNITED STATES WITHIN THE MEANING OF THE ESPIONAGE LAWS, TITLE 18 U.S.C. SECTIONS 793 AND 794. ITS TRANSMISSION OR THE REVELATION OF ITS CONTENTS IN ANY MANNER TO AN UNAUTHORIZED PERSON IS PROHIBITED BY LAW.

B. ACCESSORIES - IGNITION SYSTEM

1. INTRODUCTION

The design of the SST engine ignition system was predicated on requirements for high reliability and long life under extreme environmental conditions. Careful consideration was given during design and testing to reducing system complexity, weight and cost where such reductions could be made without sacrificing performance or reliability. The Pratt & Whitney Aircraft program conducted during Phase IIB consisted of the endurance testing of vendor supplied components.

Vendor effort during this report phase included additional performance testing and further development of some of the components for both the low tension and high tension systems. The Scintilla Division of Bendix Corporation subjected their annular cooled low tension exciter to heat transfer performance testing using 300°F fuel as the coolant. The results of that test are contained in Scintilla Division's engineering report number 12-4439 dated May 11, 1965 and titled "Preliminary Testing, Bendix 10-370925-1 Exciter for Pratt & Whitney Aircraft SST Using PWA 523B Coolant" the results are summarized in this report. In addition to the hot fuel tests, Scintilla continued development of a high temperature high tension lead which would permit incorporation of a high tension transformer in the fuel cooled housing of the low tension exciter; one of the schemes suggested in the Phase II A report for achieving a high tension ignition system. Two methods of constructing this lead were attempted; one, a chemical treatment to maintain a high dielectric at high temperature, was abandoned due to chemical instability, and fabrication of the second, which consists of a sufficient buildup of new insulating materials to prevent arcing at high temperature, is continuing. The second vendor, General Laboratories Associates, have concentrated on improving the heat transfer capabilities of their low tension exciter. GLA has corrected some deficiencies in their initial model which prevented efficient heat transfer from the end plates to the spiral wrapped cooling tube. Their revised low tension exciter weighs approximately 3.3 lbs. less than the original model, and preliminary heat transfer test of this revised unit have been conducted.

2. COMPONENTS

The low tension ignition system consisted of two independent AC powered 4-joule low tension capacitance discharge type ignition circuits designed to fire two igniters continuously. Both circuits were contained in a single exciter package.

DOWNGRADED AT 3 YEAR INTERVALS
DECLASSIFIED AFTER 12 YEARS
DOD DIR 5200.10

THIS DOCUMENT CONTAINS INFORMATION AFFECTING THE NATIONAL DEFENSE OF THE UNITED STATES WITHIN THE MEANING OF THE ESPIONAGE LAWS, TITLE 18 U.S.C. SECTIONS 793 AND 794. THE TRANSMISSION OR THE REVELATION OF ITS CONTENTS IN ANY MANNER TO AN UNAUTHORIZED PERSON IS PROHIBITED BY LAW.

Studies were made of two cooling systems. The first is shown in Figure 9-19 and is spiral-wrapped and the second, shown in Figure 9-20, is peripherally cooled. In both designs a thermal insulation blanket was used. These were the same exciters used during the performance evaluation testing program conducted during the Phase IIA program. Testing was conducted on each of the systems.

The exciter used by Scintilla during the heat transfer testing using heated fuel was the same as the units previously tested at Pratt & Whitney Aircraft and endurance tested during Phase II B, with the exception that during some of the tests by Scintilla the exciter was further protected by an insulation layer to reduce ambient heat transfer to the cooling fuel.

The exciter tested by GLA was a revision to the unit tested at Pratt & Whitney Aircraft in that the heat transferred through the end plate of the exciter was extracted by providing cooling coils closer to the end plates and by a more efficient heat flow path from the end plate to the cooling coil. In addition, in response to a Pratt & Whitney Aircraft request to consider using fuel at 300°F, GLA elected to replace the glass tube rectifiers with solid state rectifiers rated at 347°F for continuous duty operation. The resulting GLA exciter weighed 13 lbs. without an insulation blanket, a reduction of approximately 3.3 lbs.

Two high-tension ignition systems were designed. The first consisted of a low tension exciter, similar to that used for the low tension system driving two separate voltage transformer-capacitor-igniter packages as shown in Figure 9-21. The transformer-igniter system is designed to operate in environments up to 1000°F and provision made for the replacement of the igniter plug in the field. For the second system, the high-tension transformer is housed in the cooled exciter package. High temperature, high tension leads, still in the development stage, will connect the exciter to the igniters.

3. FACILITIES

The endurance tests at Pratt & Whitney Aircraft were conducted in a thermostatically controlled oven. Exciter skin and internal temperatures were monitored using thermocouples. The exciters were electrically loaded using low tension leads and igniter plugs.

DOWNGRADED AT 3 YEAR INTERVALS
DECLASSIFIED AFTER 12 YEARS
DOD DIR 5200.10

THIS DOCUMENT CONTAINS INFORMATION AFFECTING THE NATIONAL DEFENSE OF THE UNITED STATES WITHIN THE MEANING OF THE ESPIONAGE LAWS, TITLE 18, U.S.C., SECTIONS 793 AND 794. ITS TRANSMISSION OR THE REVELATION OF ITS CONTENTS IN ANY MANNER TO AN UNAUTHORIZED PERSON IS PROHIBITED BY LAW.

The heat transfer testing of the Scintilla exciter was conducted at the facilities of the Bendix Products Aerospace Division and consisted basically of a hot fuel source using PWA 523B fuel at 300°F to provide cooling for the exciter mounted in a 750°F air chamber with suitable fluid flow, temperature, and pressure instrumentation. Testing of the spiral wrapped tube design by GLA was conducted at their own facility using water as the cooling fluid.

4. TEST PROCEDURE

a. Endurance Tests at Pratt & Whitney Aircraft

The exciter units, one each of the annular cooled exciters supplied by Scintilla and the spiral wound tube cooled exciters supplied by GLA, were mounted in the oven and the temperature set at 350°F, which established the exciter skin temperature estimated to exist when the exciters are cooled with 300°F fuel in a 750°F ambient. Controlling the oven temperature in this fashion eliminated the need for supplying a cooling fluid during the endurance testing of the exciter internal components. It was necessary to establish a low volume flow of air through the annular cooled exciter to eliminate the insulating effect of a stagnant air volume in this unit.

The units were then operated for 16 hours continuously and allowed to soak for 8 hours, and this cycle repeated until the conclusion of testing. Condition of the units was monitored hourly during the test.

b. Scintilla Heat Transfer Tests

Heat transfer studies conducted by Scintilla using heated fuel, PWA 523B, are summarized in the following table which lists the variations in parameters for each of the test conditions.

	Test Number						
Variable	1	2	3	4	5	5A	5B
Ambient Temp °F	750	750	750	750	750	750	750
Fuel Temp °F	300	300	300	300	300	300	300
Fuel Flow, pph	500	400	350	500	500	500	400
Fuel Pres, psig	6	3	3	200	200	200	200
Insulation Blanket	yes	yes	yes	yes	no	no	no
*Operating Cycle	Duty	Duty	Duty	Duty	Duty	Cont.	Cont.

* The SST ignition system duty cycle consists of operation for 2 minutes ON, 3 minutes OFF, 2 minutes ON, 23 minutes OFF.

DOWNGRADED AT 3 YEAR INTERVALS
DECLASSIFIED AFTER 12 YEARS
DOD DIR 5200.10

THIS DOCUMENT CONTAINS INFORMATION AFFECTING THE NATIONAL DEFENSE OF THE UNITED STATES WITHIN THE MEANING OF THE ESPIONAGE LAWS, TITLE 18 U.S.C. SECTIONS 793 AND 794. ITS TRANSMISSION OR THE REVELATION OF ITS CONTENTS IN ANY MANNER TO AN UNAUTHORIZED PERSON IS PROHIBITED BY LAW.

During these tests, the internal exciter wall temperature was monitored near the electrical input and output connections which are two areas of greatest heat transfer from ambient to the interior of the exciter. Fuel temperature and exciter skin temperatures were also monitored. The test data was taken after temperatures were stabilized.

c. GLA Heat Transfer Tests

The heat transfer testing conducted by GLA was accomplished in a 515°F forced air oven with water circulating through the exciter at a rate of 233 pph to simulate the heat removal ability of fuel at a 500 pph rate. The exciter temperature data obtained during this test was then used to verify the electrical analog model of the heat transfer mechanism. The model can then be used to predict exciter temperatures for other operating conditions.

5. DISCUSSION OF RESULTS

a. Endurance Tests at Pratt & Whitney Aircraft

Endurance testing with internal components operating at approximately 380°F max. for the GLA unit and 390°F max. for the Scintilla unit, revealed that both systems are capable of long term operation in the SST environment. One GLA unit operated for 668 hours of continuous ignition and 256 hours of soaking at 350°F before the tests were concluded with the unit still satisfactory (this unit was subjected to continuous operation in excess of the 16 hours ON, 8 hours OFF cycle). One Scintilla unit sustained a failure of all the rectifier tubes in both electrically separate circuits at approximately the same time, at 170 hours of continuous operation. The failure has not been explained and investigation by Scintilla is continuing at the writing of this report. The second Scintilla unit had satisfactorily completed 350 hours of continuous ignition and 151 hours of soaking at 350°F at the conclusion of testing.

b. Scintilla Heat Transfer Tests

The Scintilla heat transfer tests indicated that the unit internal temperatures were maintained well within operating limits without an exciter insulating blanket although without the blanket, undesirable heat transfer from ambient to the fuel coolant occurred. The test results are summarized in the following table:

DOWNGRADED AT 3 YEAR INTERVALS
DECLASSIFIED AFTER 12 YEARS
DOD DIR 5200.10

THIS DOCUMENT CONTAINS INFORMATION AFFECTING THE NATIONAL DEFENSE OF THE UNITED STATES WITHIN THE MEANING OF THE ESPIONAGE LAWS, TITLE 18 U.S.C. SECTIONS 793 AND 794. ITS TRANSMISSION OR THE REVELATION OF ITS CONTENTS IN ANY MANNER TO AN UNAUTHORIZED PERSON IS PROHIBITED BY LAW.

Location of Temperature Reading	Analog Predicted Temperature	Actual Test Temperature
Exciter cylindrical case at 6 locations	306°F to 385°F	303°F to 395°F
Heat transfer bulkheads inside each end plate	329°F	339°F
End Covers at 4 locations	460°F to 480°F	362°F to 423°F
Fuel in at 500 pph[2]	300°F	300°F
Fuel out[2]	303°F	less than 302°F

The GLA unit on the basis of these water cooled exciter heat transfer tests passes less heat into the cooling fluid than the Scintilla unit, but it must always use an insulation blanket. It is to be noted in the GLA unit that less heat is generated by the power transformer than predicted. The oven temperature for this test was maintained at 450°F above the cooling water temperature resulting in a lower actual ambient temperature than will be encountered in service. While this lower temperature correctly simulates the heat transfer through the insulation to the cooling fluid, it does not correctly simulate the heat flow through exposed connectors and brackets to the end plates and probably accounts for the lower than predicted end cover temperatures. Correcting for this condition would probably result in a higher fuel OUT temperature but still below the predicted value. The component closest to its temperature limit is the solid state rectifier operating 24°F below its rated temperature of 347°F. It is expected that operation of the exciter to the duty cycle will result in a slight reduction in the rectifier temperature.

d. Glow Plug Tests

Development effort on the augmentor ignition system glow plug should continue to be directed toward improving durability and warm-up time and to determine the configuration necessary to provide effective ignition of the fuel. Testing during Phase II A had indicated that the augmentor combustor rig described could not be consistently lit using the glow plug in its present location. Additional effort in optimizing size and shape of the glow plug coil consistent with acceptable warm-up time, and determination of the glow plug mounting and fuel requirements is needed. Vendor effort to find an improved material over the platinum wire currently used has not been successful and should be continued.

2 - Fuel IN and fuel OUT temperatures are calculated on the basis of the actual rise in water temperature at a flow rate chosen to simulate the heat sink properties of fuel at 500 pph.

DOWNGRADED AT 3 YEAR INTERVALS
DECLASSIFIED AFTER 12 YEARS
DOD DIR 5200.10

THIS DOCUMENT CONTAINS INFORMATION AFFECTING THE NATIONAL DEFENSE OF THE UNITED STATES WITHIN THE MEANING OF THE ESPIONAGE LAWS, TITLE 18, U.S.C., SECTIONS 793 AND 794. ITS TRANSMISSION OR THE REVELATION OF ITS CONTENTS IN ANY MANNER TO AN UNAUTHORIZED PERSON IS PROHIBITED BY LAW.

6. RECOMMENDATIONS

Pratt & Whitney Aircraft and vendor testing has demonstrated the basic durability of the components and their compatibility of the design with the SST engine requirements.

Development of the low tension system should be directed toward:

- Possible weight reduction in the Scintilla design based on the temperature safety margin which exists in the present model.
- Continued endurance testing of the units to demonstrate long term reliability. Failure of the Scintilla rectifier tubes is thought to be an easily correctable problem.
- Demonstration of actual ignition capabilities in combustion rig testing.
- Hot fuel heat transfer tests of the GLA exciter.

Development of high tension system:

Although construction of a high tension lead is in process, the effects of high temperature on this component and on a satisfactory high tension transformer remain to be evaluated. The development problems of the more costly and complex high tension system will require high temperature endurance testing to demonstrate reliability.

DOWNGRADED AT 3 YEAR INTERVALS
DECLASSIFIED AFTER 12 YEARS
DOD DIR 5200.10

THIS DOCUMENT CONTAINS INFORMATION AFFECTING THE NATIONAL DEFENSE OF THE UNITED STATES WITHIN THE MEANING OF THE ESPIONAGE LAWS, TITLE 18, U.S.C., SECTIONS 793 AND 794. ITS TRANSMISSION OR THE REVELATION OF ITS CONTENTS IN ANY MANNER TO AN UNAUTHORIZED PERSON IS PROHIBITED BY LAW.

INLET PROGRAM NOMENCLATURE

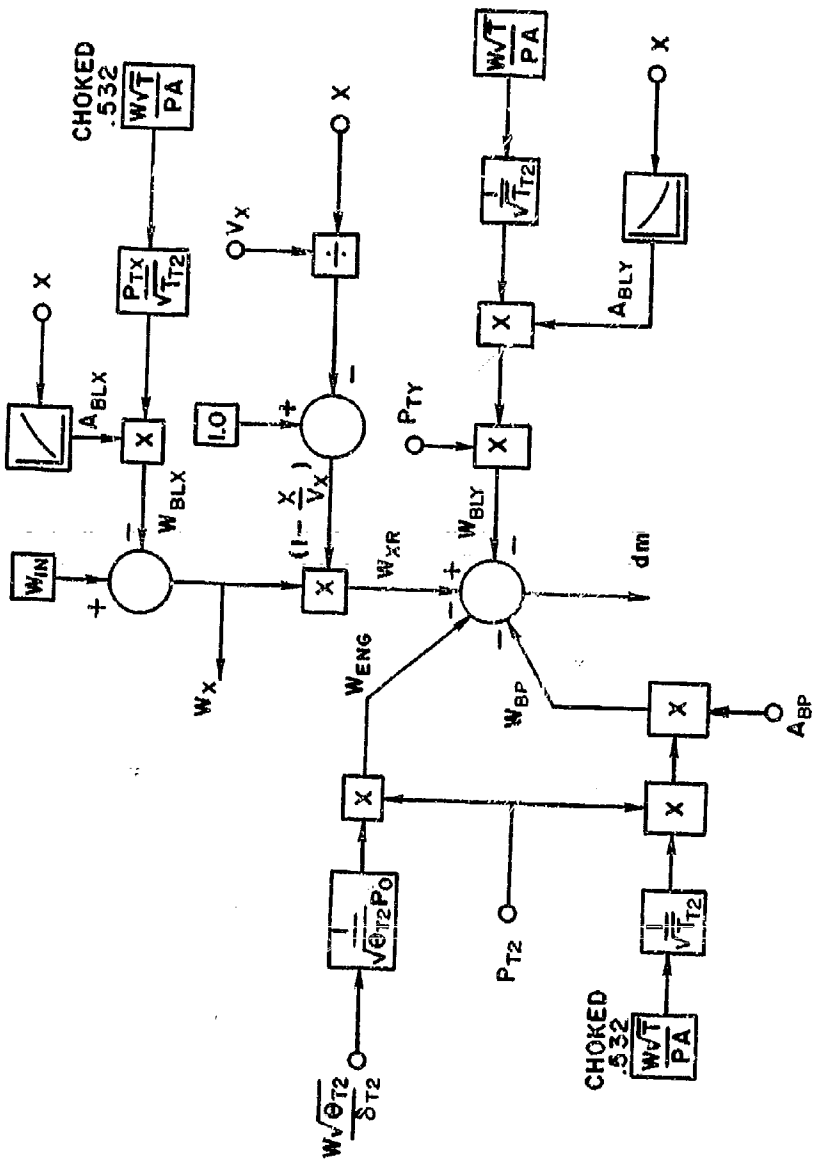
a	speed of sound	ft/sec
A	area	ft^2
M	Mach Number	
P_t	pressure, total	lbs/ft^2
T	temperature	°R
C	density	lbs/ft^3
W	weight flow	lbs/sec
V	volume	ft^3
X	shock position	ft
V_x	gas velocity	ft/sec
S	Laplace Complex Operator	1/sec
$\dot{X}$	shock velocity	ft/sec
W_{blx}	boundary layer bleed upstream of shock	lbs/sec
W_{bly}	Educated Bleed downstream of shock	lbs/sec

Subscripts

av	average
e	engine compressor face
bl	bleed
x	location of parameter at the shock position
y	location of parameter immediately downstream of shock
r	relative to shock position
in	inlet to diffuser
t	total to diffuser
o	reference

DOWNGRADED AT 3 YEAR INTERVALS
DECLASSIFIED AFTER 12 YEARS
DOD DIR 5200.10

THIS DOCUMENT CONTAINS INFORMATION AFFECTING THE NATIONAL DEFENSE OF THE UNITED STATES WITHIN THE MEANING OF THE ESPIONAGE LAWS, TITLE 18 U.S.C. SECTIONS 793 AND 794. ITS TRANSMISSION OR THE REVELATION OF ITS CONTENTS IN ANY MANNER TO AN UNAUTHORIZED PERSON IS PROHIBITED BY LAW.

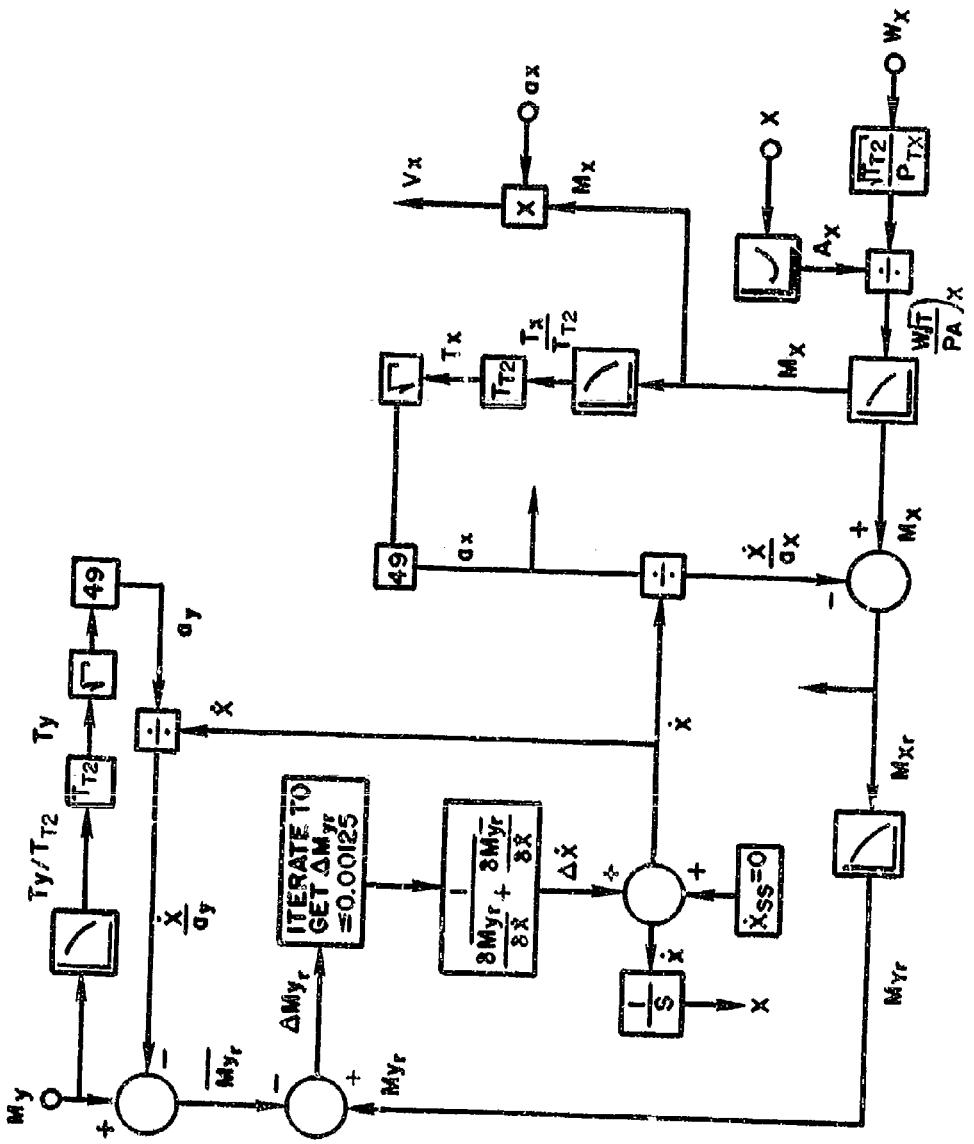


AIRFLOW BALANCE DOWNSTREAM OF SHOCK - AIRCRAFT INLET PROGRAM

Figure 9-1

DOWNGRADED AT 3 YEAR INTERVALS
DECLASSIFIED AFTER 12 YEARS
DOD DIR 5200.10

THIS DOCUMENT CONTAINS INFORMATION AFFECTING THE NATIONAL DEFENSE OF THE UNITED STATES WITHIN THE MEANING OF THE ESPIONAGE LAWS, TITLE 18, U.S.C., SECTIONS 793 AND 794. ITS TRANSMISSION OR REVELATION OF ITS CONTENTS IN ANY MANNER TO AN UNAUTHORIZED PERSON IS PROHIBITED BY LAW.



CALCULATION OF SHOCK POSITION - AIRCRAFT INLET PROGRAM

Figure 9-2

DOWNGRADED AT 3 YEAR INTERVALS
DECLASSIFIED AFTER 12 YEARS
DOD DIR 5200.10

CALCULATION OF SUBSONIC MACH NUMBER AFTER SHOCK - AIRCRAFT INLET PROGRAM

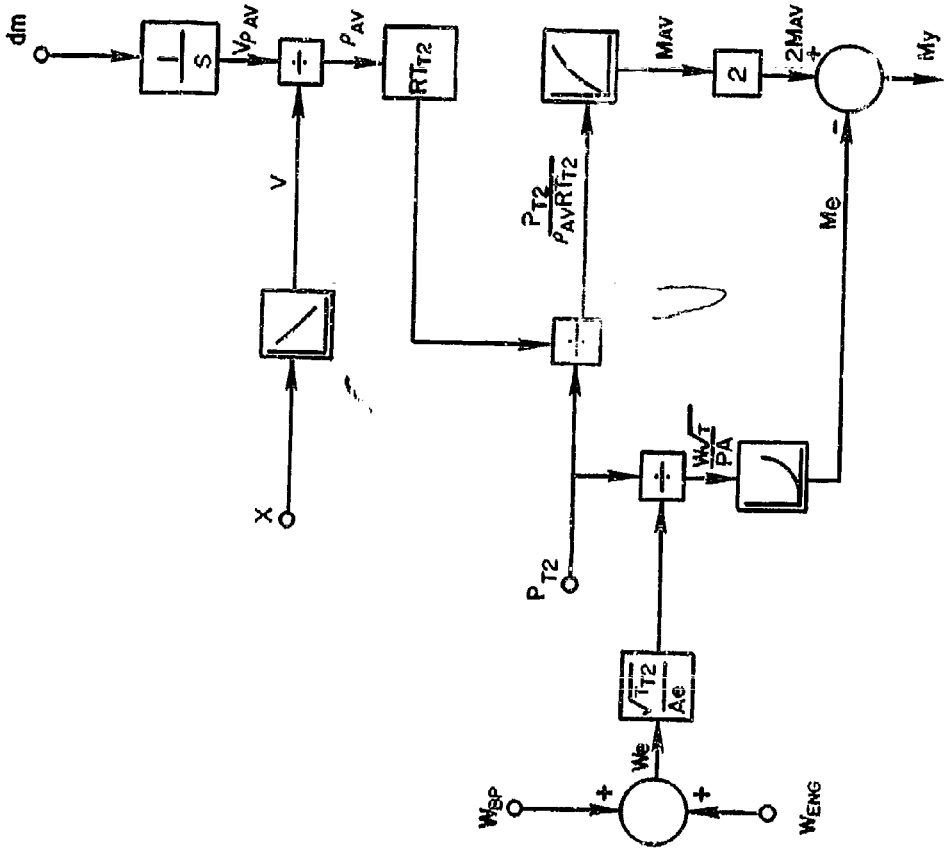
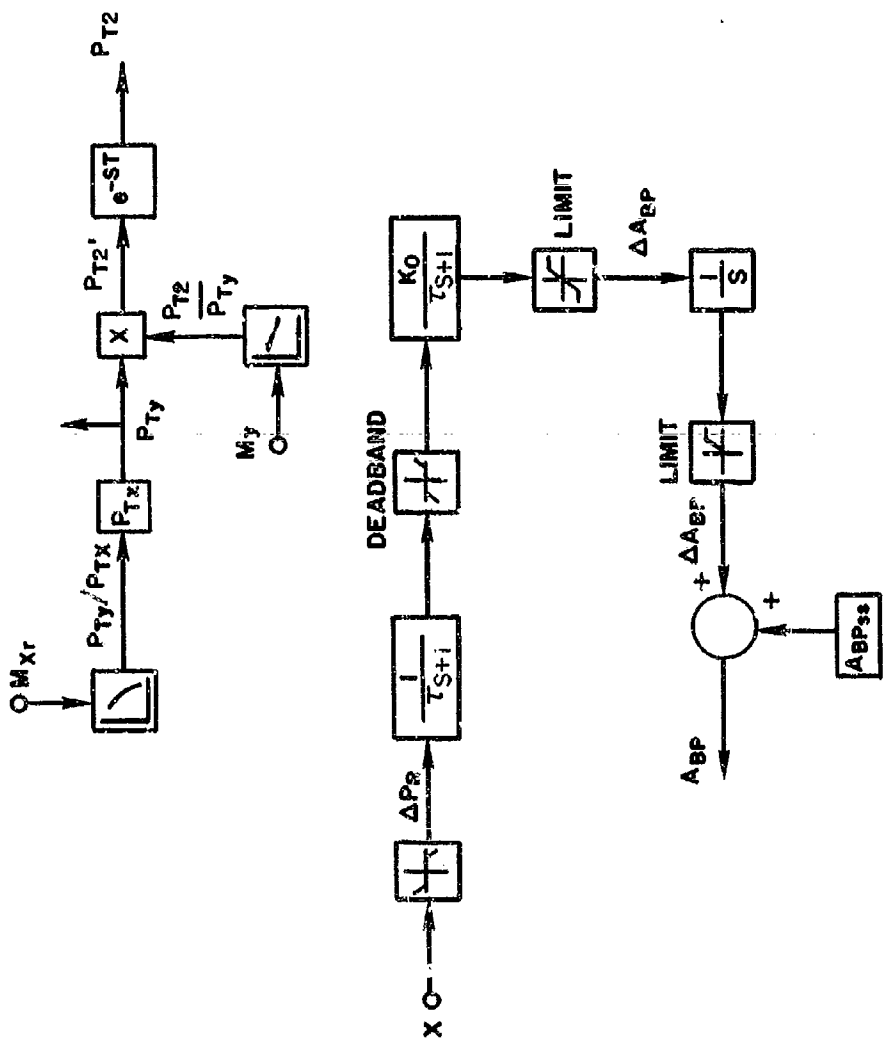


Figure 9-3

DOWNGRADED AT 3 YEAR INTERVALS
DECLASSIFIED AFTER 12 YEARS
DOD DIR 5200.10

THIS DOCUMENT CONTAINS INFORMATION AFFECTING THE NATIONAL DEFENSE OF THE UNITED STATES WITHIN THE MEANING OF THE ESPIONAGE LAWS, TITLE 18, U.S.C., SECTIONS 793 AND 794. ITS TRANSMISSION OR THE REVELATION OF ITS CONTENTS IN ANY MANNER TO AN UNAUTHORIZED PERSON IS PROHIBITED BY LAW.

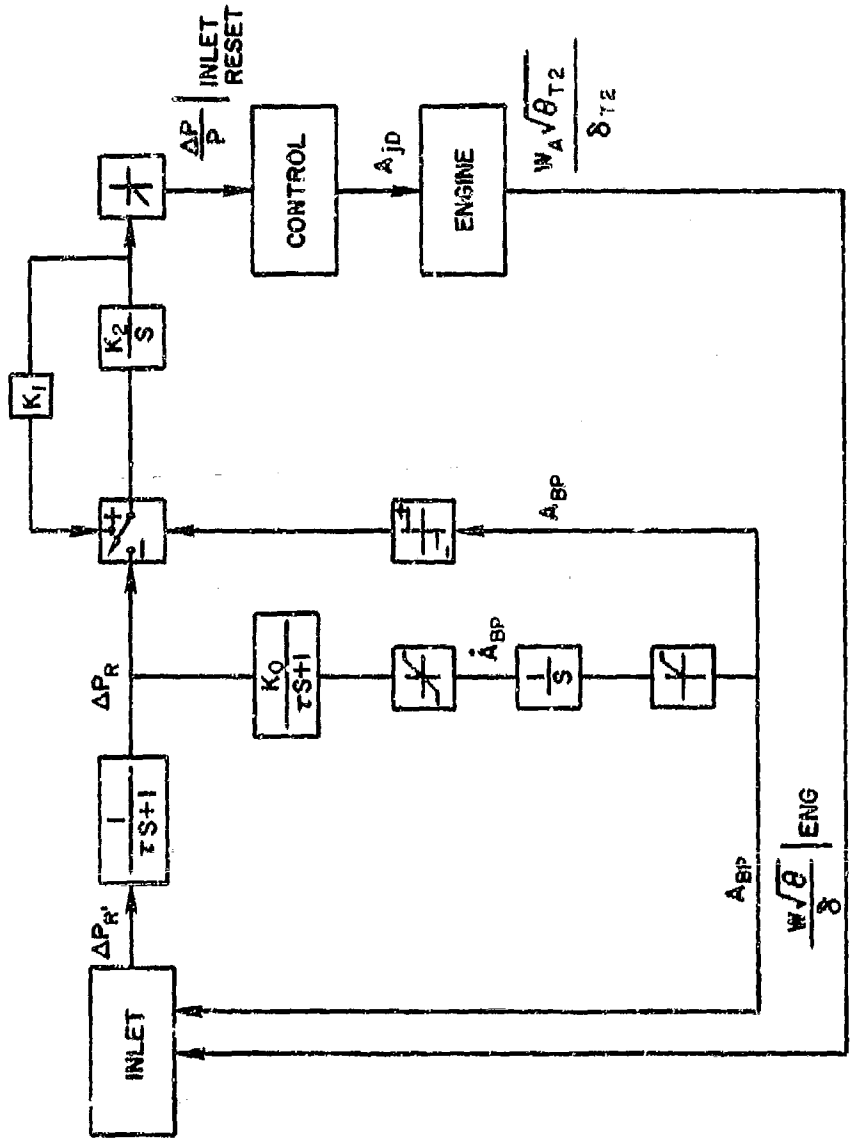


CALCULATION OF TOTAL PRESSURE LOSSES AND BYPASS AREA CONTROL - AIRCRAFT INLET PROGRAM

Figure 9-4

DOWNGRADED AT 3 YEAR INTERVALS
DECLASSIFIED AFTER 12 YEARS
DOD DIR 5200.10

THIS DOCUMENT CONTAINS INFORMATION AFFECTING THE NATIONAL DEFENSE OF THE UNITED STATES WITHIN THE MEANING OF THE ESPIONAGE LAWS, TITLE 18 U. S. C. SECTIONS 793 AND 794. ITS TRANSMISSION OR THE REVELATION OF ITS CONTENTS IN ANY MANNER TO AN UNAUTHORIZED PERSON IS PROHIBITED BY LAW

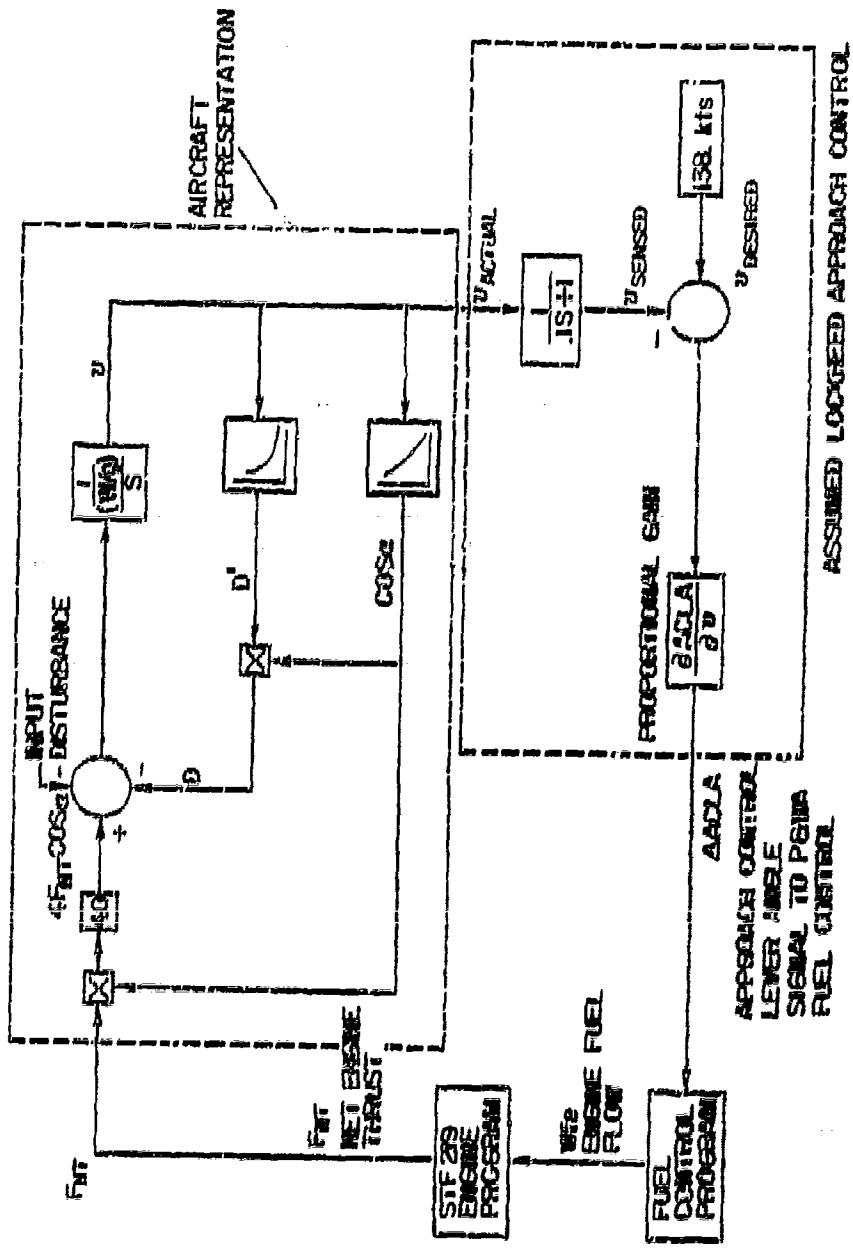


BLOCK DIAGRAM OF BOEING INLET SHOCK POSITION CONTROL

Figure 9-5

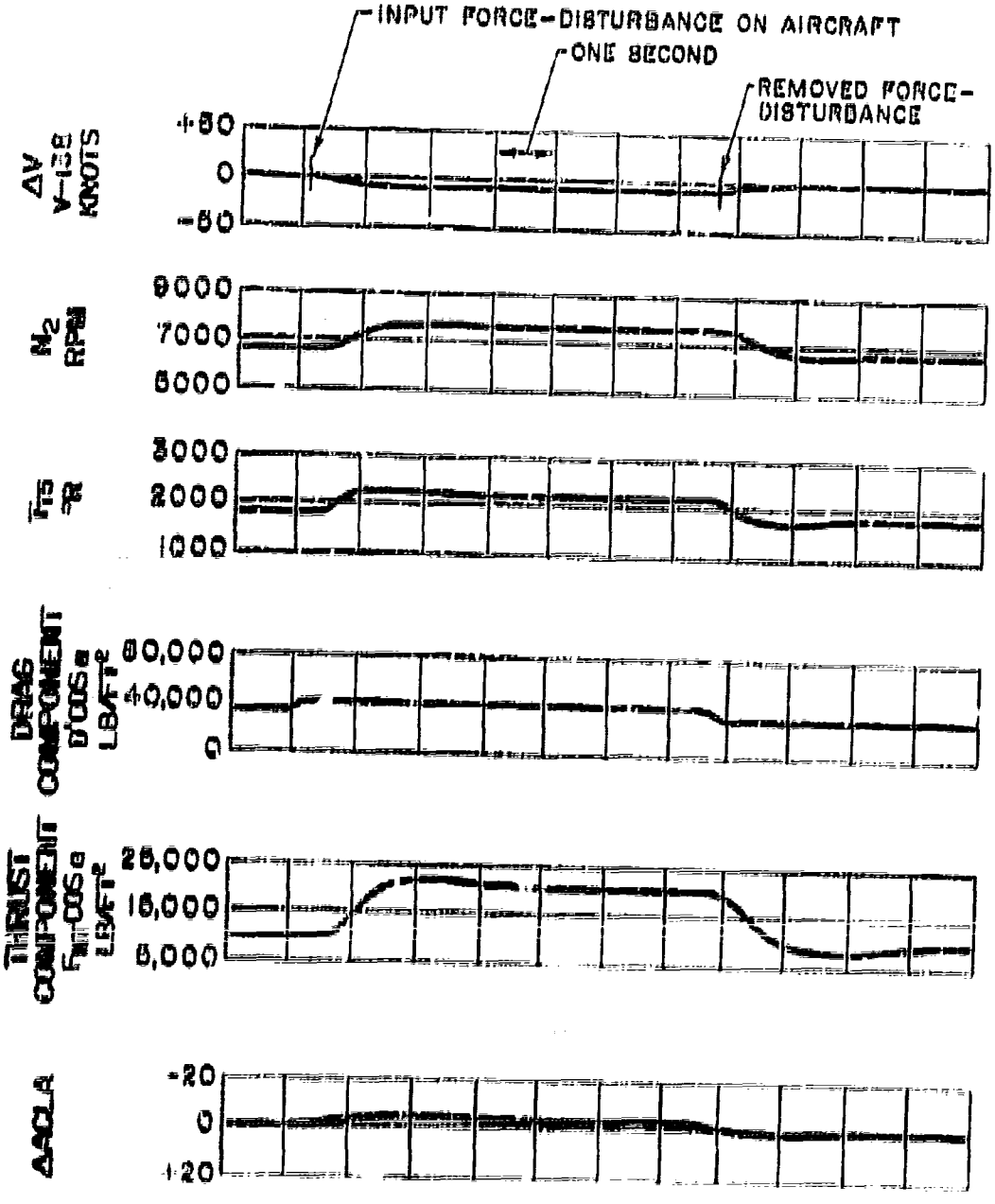
DOWNGRADED AT 3 YEAR INTERVALS
DECLASSIFIED AFTER 12 YEARS
DOD DIR 5200.10

THIS DOCUMENT CONTAINS INFORMATION AFFECTING THE NATIONAL DEFENSE OF THE UNITED STATES WITHIN THE MEANING OF THE ESPIONAGE LAWS, TITLE 18 U.S.C. SECTIONS 793 AND 794. ITS TRANSMISSION OR THE REVELATION OF ITS CONTENTS IN ANY MANNER TO AN UNAUTHORIZED PERSON IS PROHIBITED BY LAW.



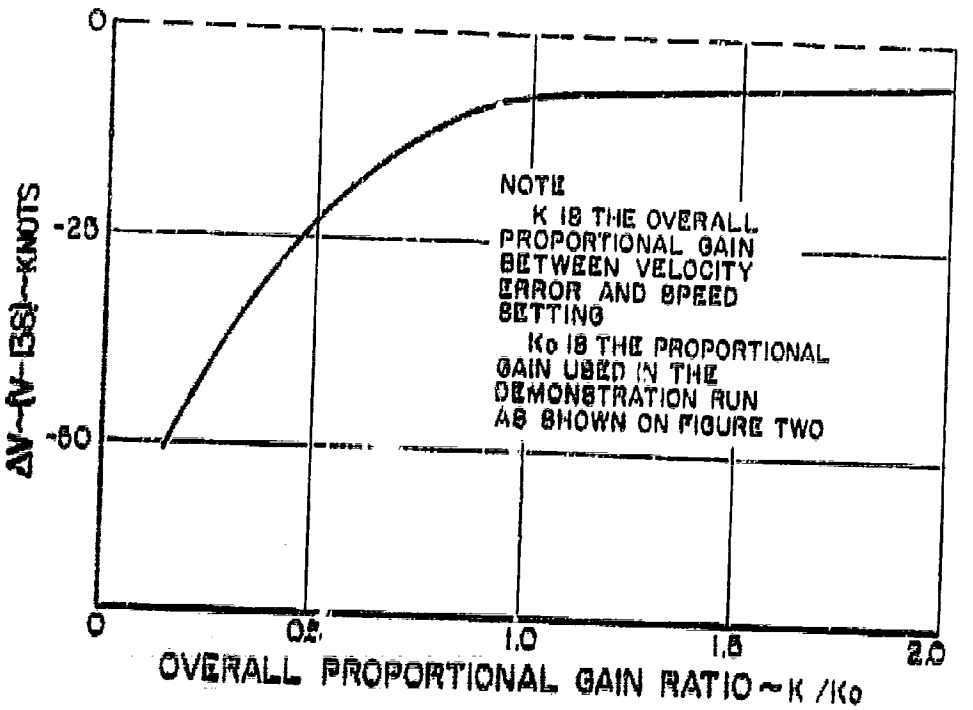
BLOCK DIAGRAM OF LOCKHEED APPROACH CONTROL STUDY

Figure 9-6



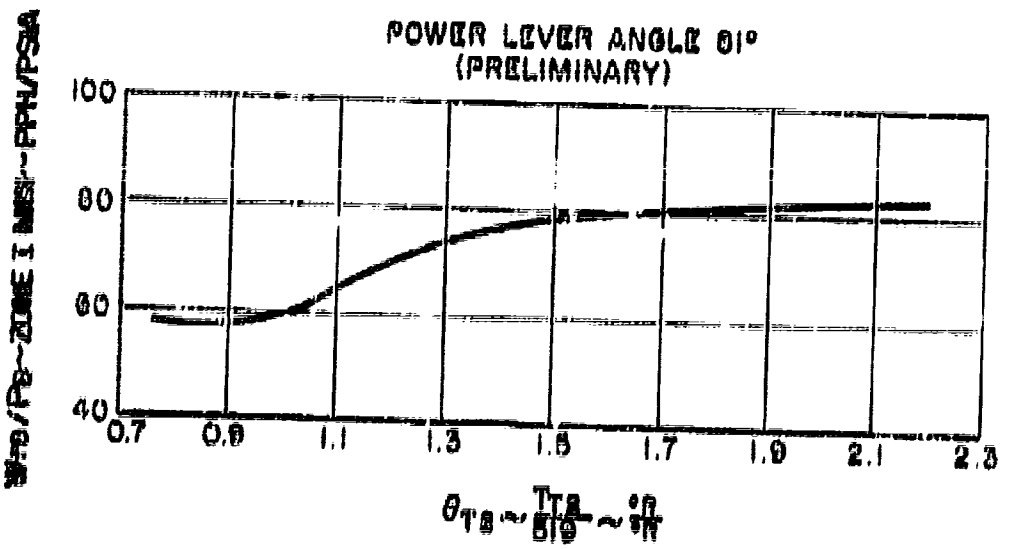
STF219 SST ENGINE OPERATION WITH APPROACH CONTROL

Figure 9-7



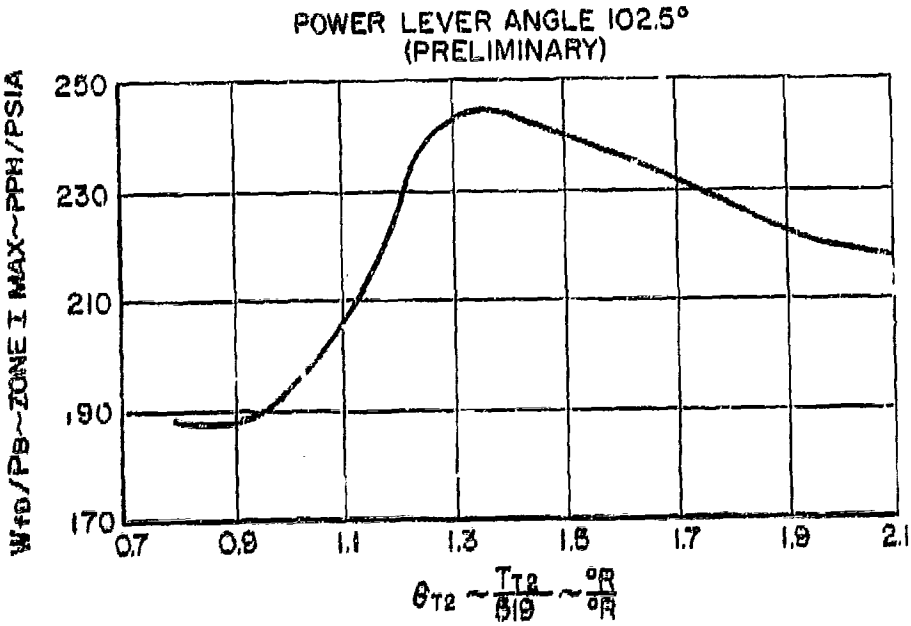
STF219 SST ENGINE APPROACH CONTROL

Figure 9-8



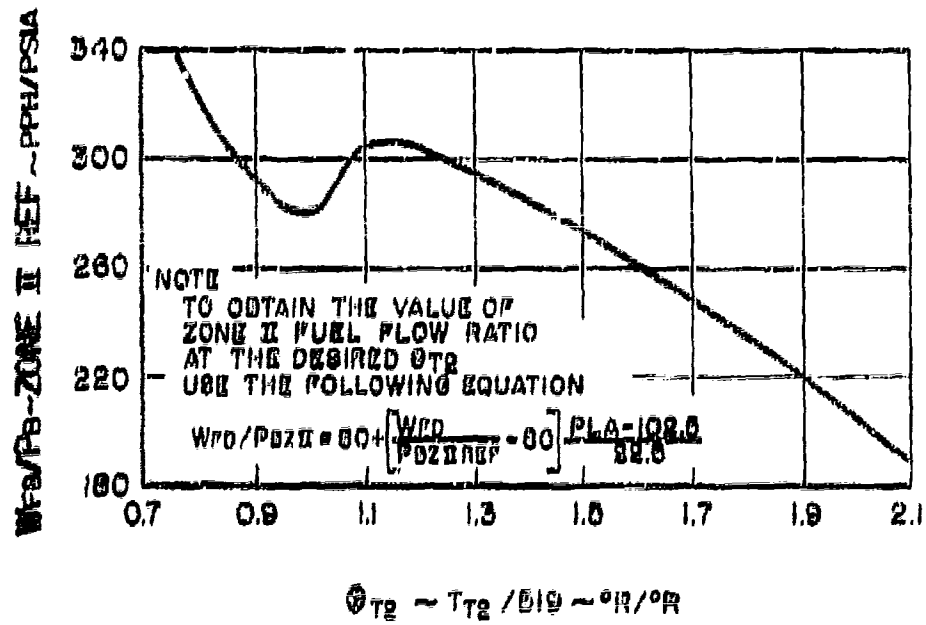
ESTIMATED θ_{T2} BIASING OF ZONE I MINIMUM FUEL FLOW RATIO

Figure 9-9



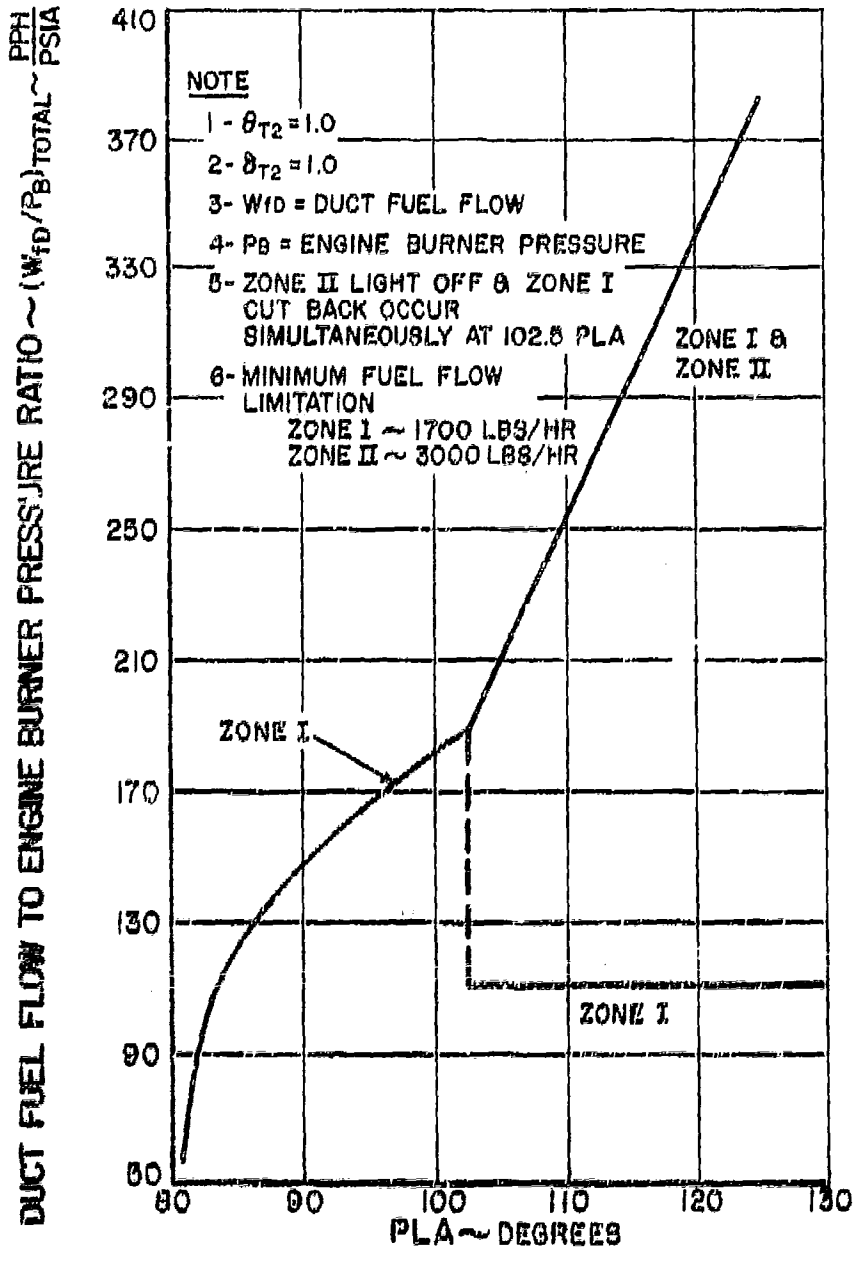
ESTIMATED θ_{T2} BIASING OF ZONE I MAXIMUM FUEL RATIO

Figure 9-10



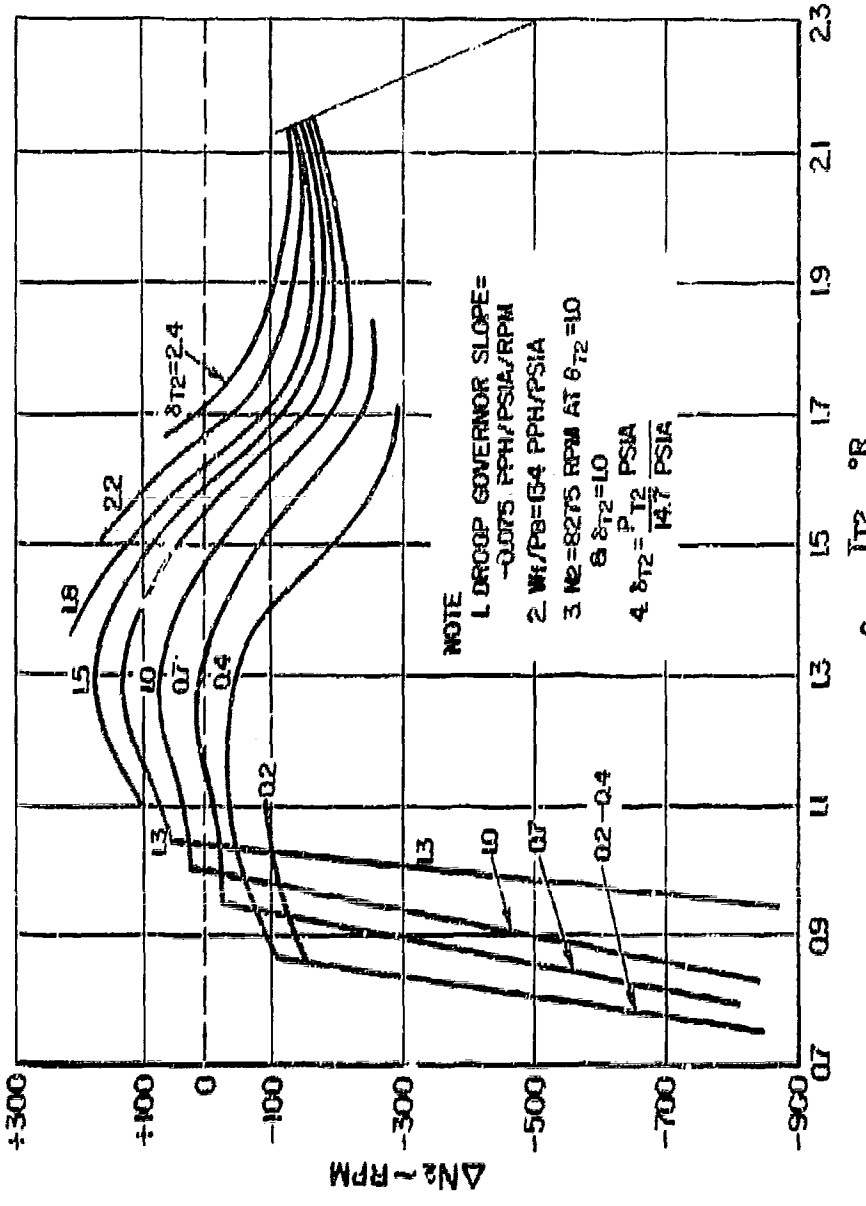
ESTIMATED θ_{T2} BIASING OF ZONE II FUEL FLOW RATIO

Figure 9-11



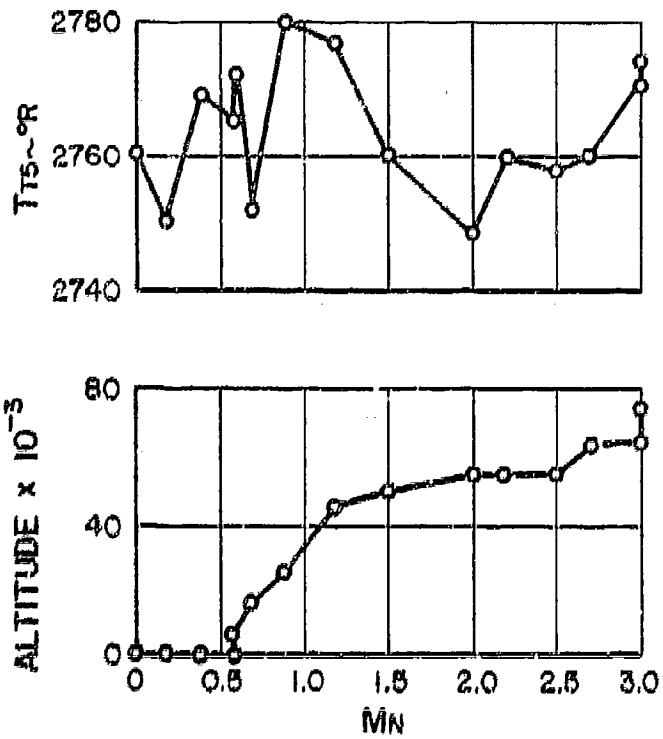
ESTIMATED FUEL FLOW REQUIREMENTS FOR THE DUCT BURNER

Figure 9-12



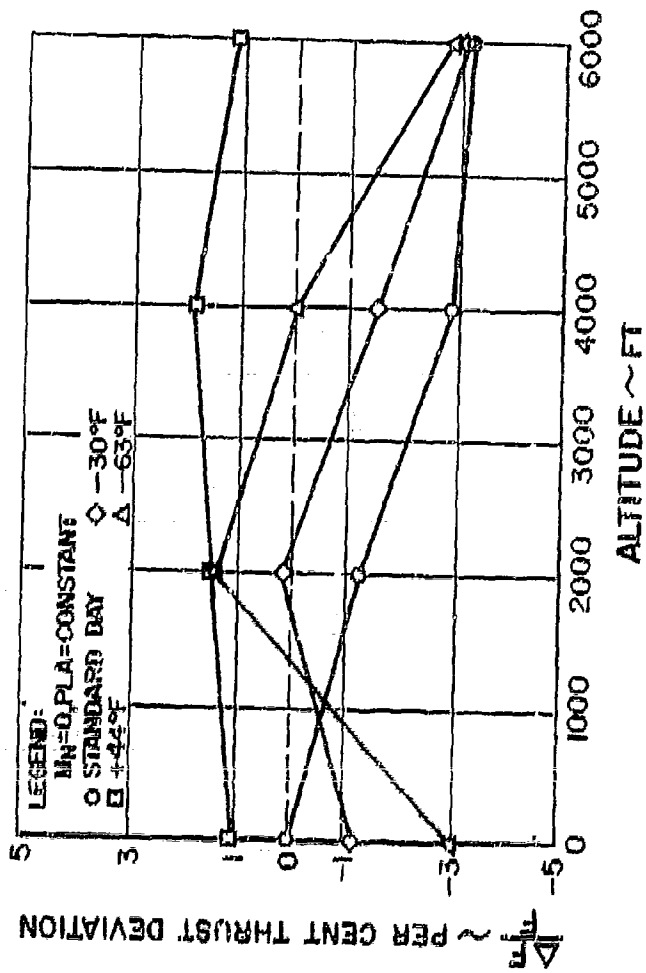
ESTIMATED θ_{T2} AND δ_{T2} BIASING OF N_2 FOR MAXIMUM RATED AND CRUISE POWER

Figure 9-13



ESTIMATED CONTROL OF T_{t5} DURING AIRCRAFT ACCELERATION

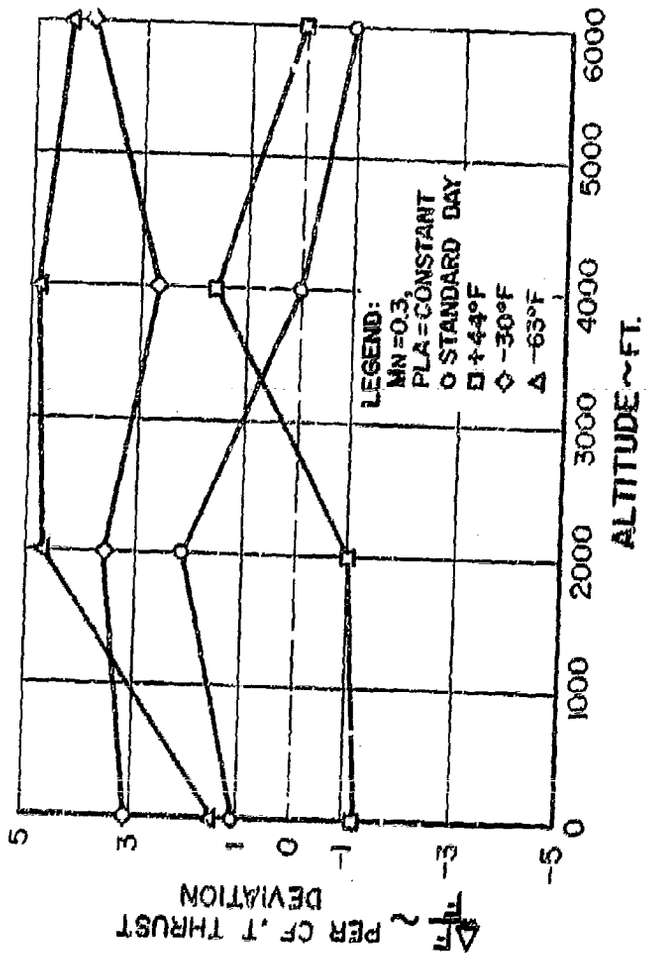
Figure 9-14



PERCENT THRUST DEVIATION FROM DESIRED NORMAL RATED VALUE VS. ALTITUDE AT $M_N = 0$

Figure 9-15

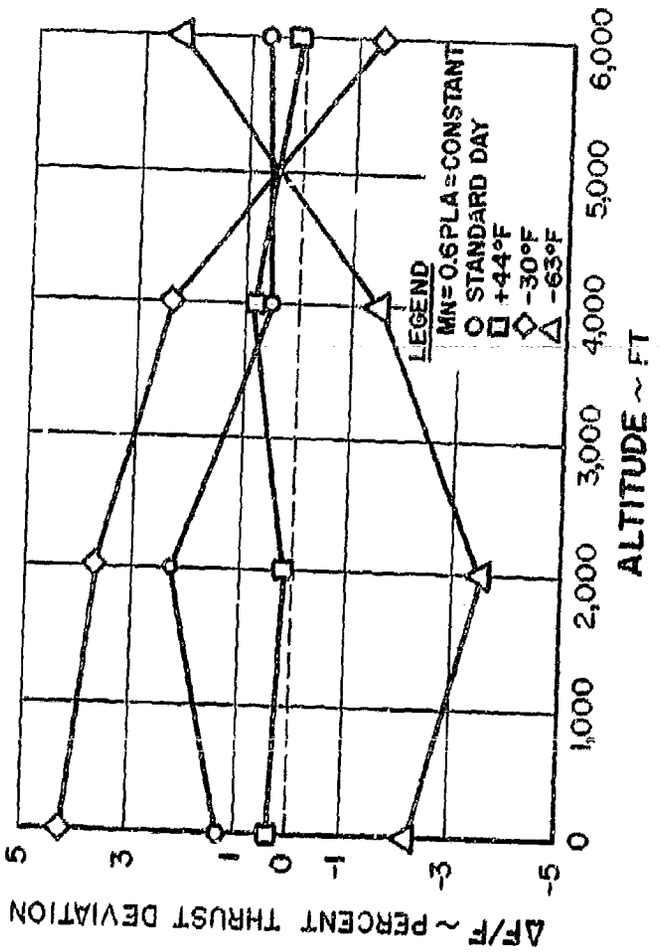
CONFIDENTIAL



PERCENT THRUST DEVIATION FROM DESIRED NORMAL RATED VALUE VS. ALTITUDE AT $M_n = 0.3$

Figure 9-16

DOWNGRADED AT 3 YEAR INTERVALS
DECLASSIFIED AFTER 12 YEARS
DOD DIR 5200.10

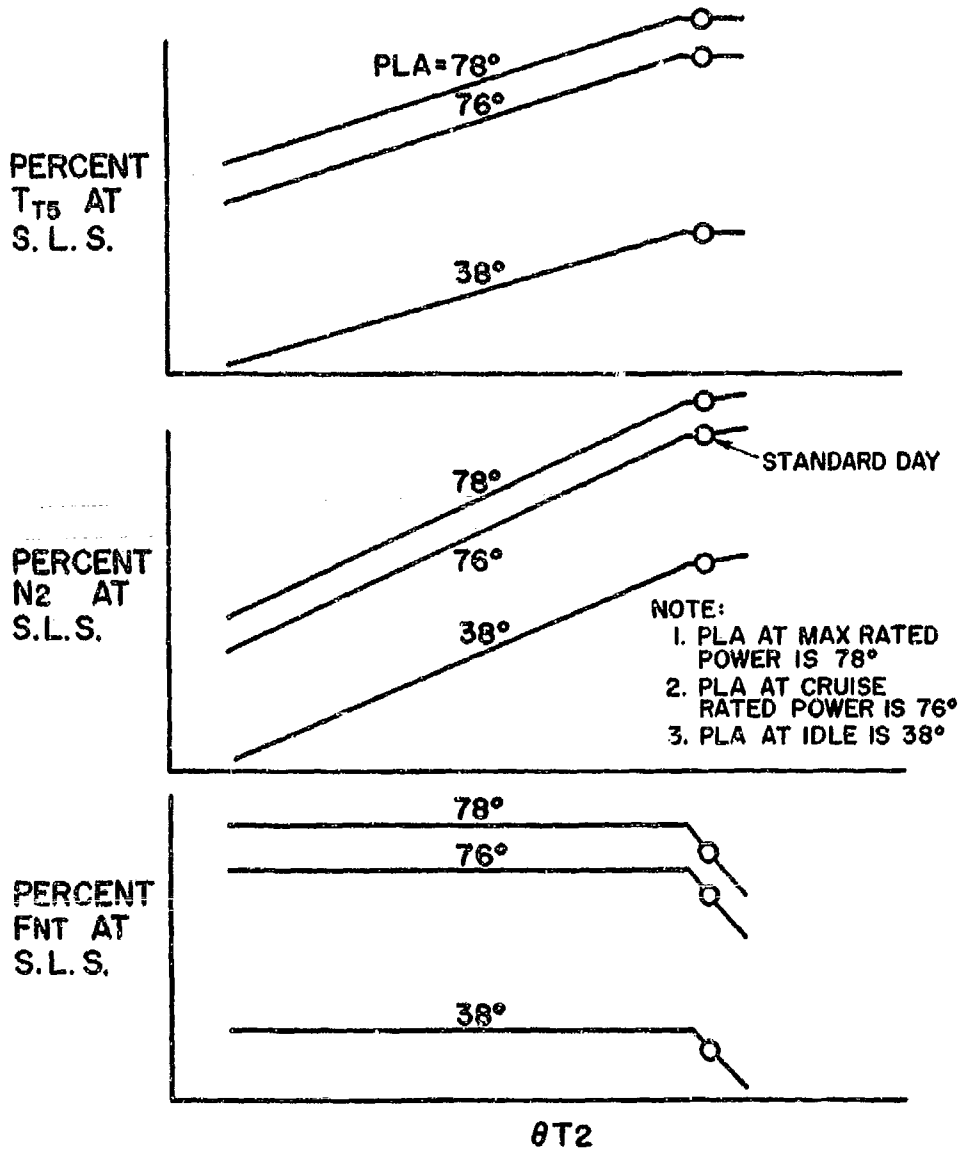


PERCENT THRUST DEVIATION FROM DESIRED NORMAL RATED VALUE VS. ALTITUDE AT $M_n = 0.6$

Figure 9-17

DOWNGRADED AT 3 YEAR INTERVALS
DECLASSIFIED AFTER 12 YEARS
DOD DIR 5200.10

THIS DOCUMENT CONTAINS INFORMATION AFFECTING THE NATIONAL DEFENSE OF THE UNITED STATES WITHIN THE MEANING OF THE ESPIONAGE LAWS, TITLE 18, U.S.C., SECTIONS 793 AND 794. ITS TRANSMISSION OR THE REVELATION OF ITS CONTENTS IN ANY MANNER TO AN UNAUTHORIZED PERSON IS PROHIBITED BY LAW.

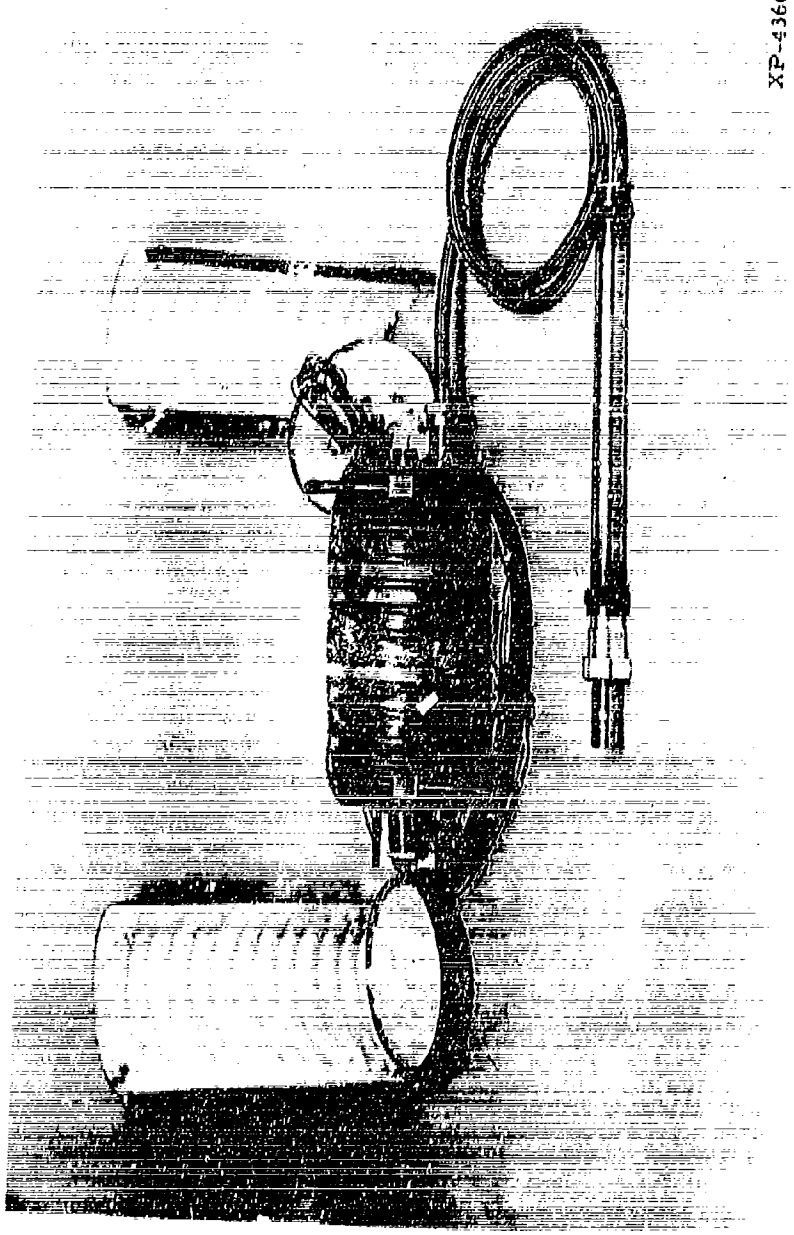


DESCRIPTIVE EXPLANATION OF FLAT RATING CONTROL DURING PART POWER

Figure 9-18

DOWNGRADED AT 3 YEAR INTERVALS
DECLASSIFIED AFTER 12 YEARS
DOD DIR 5200.10

THIS DOCUMENT CONTAINS INFORMATION AFFECTING THE NATIONAL DEFENSE OF THE UNITED STATES WITHIN THE MEANING OF THE ESPIONAGE LAWS, TITLE 18 U. S. C. SECTIONS 793 AND 794. ITS TRANSMISSION OR THE REVELATION OF ITS CONTENTS IN ANY MANNER TO AN UNAUTHORIZED PERSON IS PROHIBITED BY LAW.



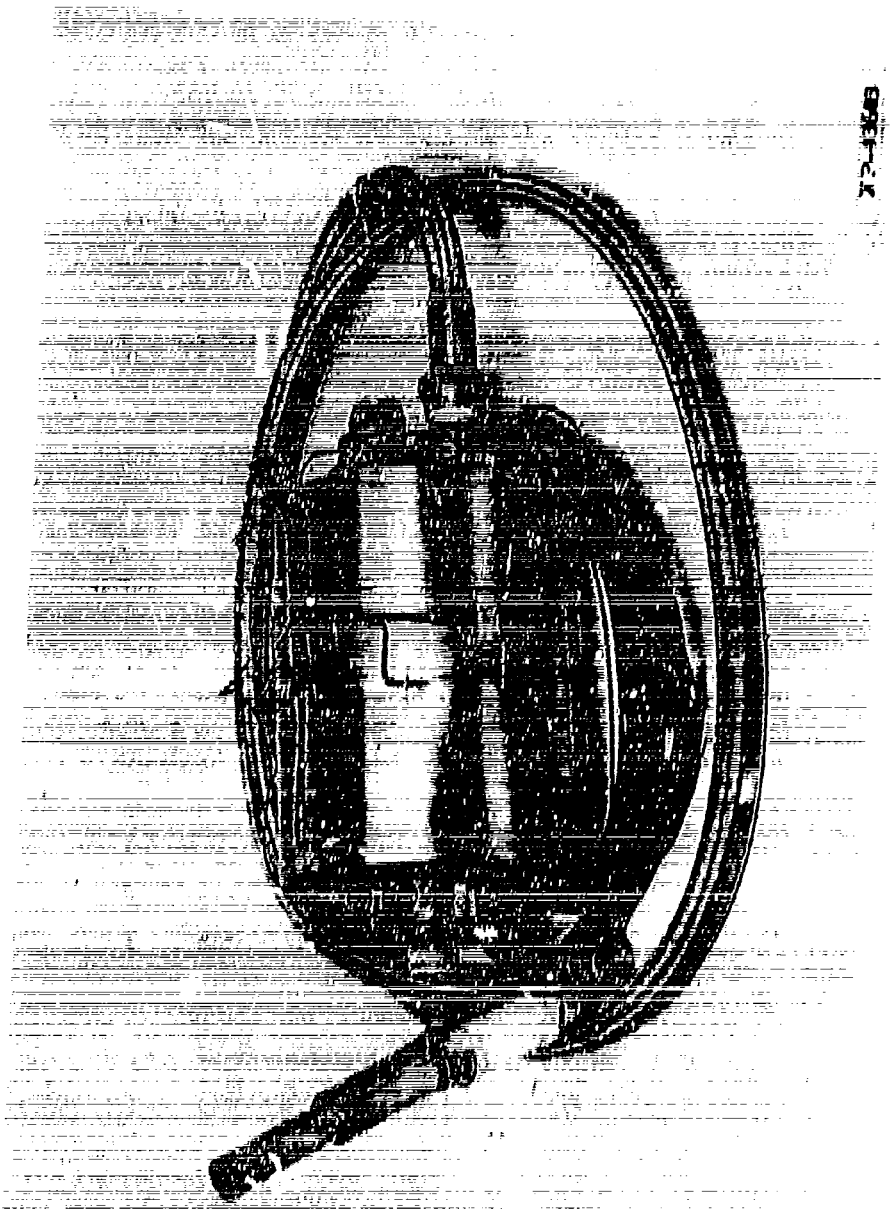
XP-43606

SST LOW TENSION SPIRAL WRAPPED COOLED EXCITER

Figure 9-19

DOWNGRADED AT 3 YEAR INTERVALS
DECLASSIFIED AFTER 12 YEARS
DOD DIR 5200.10

THIS DOCUMENT CONTAINS INFORMATION AFFECTING THE NATIONAL DEFENSE OF THE UNITED STATES WITHIN THE MEANING OF THE ESPIONAGE LAWS, TITLE 18 U.S.C., SECTIONS 793 AND 794. ITS TRANSMISSION OR THE REVELATION OF ITS CONTENTS IN ANY MANNER TO AN UNAUTHORIZED PERSON IS PROHIBITED BY LAW.



72-4368

SST PERIPHERALLY COOLED EXCITER

Figure 9-20

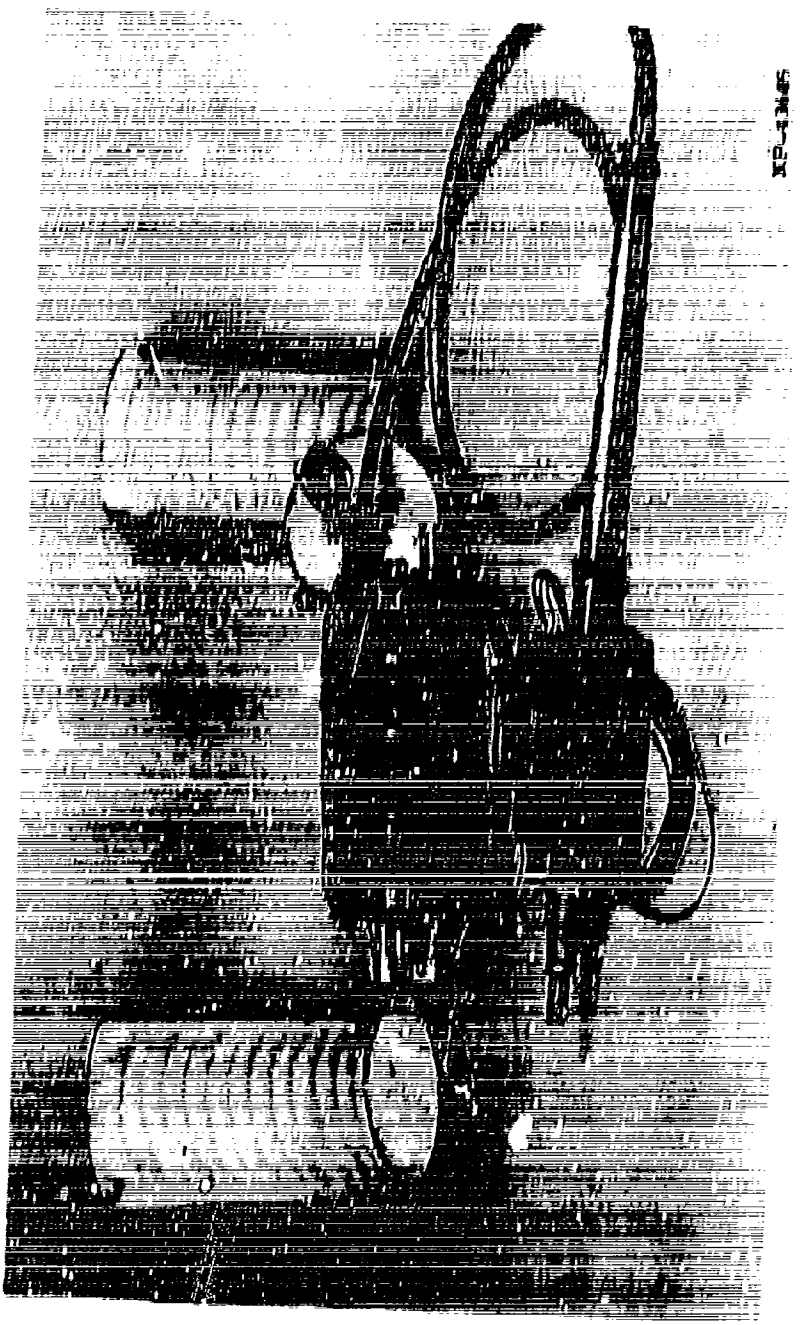


Figure 9-21

ITEM 10

BEARING AND SEAL DEVELOPMENT

ITEM 10 - BEARING AND SEAL DEVELOPMENT

OBJECTIVE

This item of the contract required that Pratt & Whitney Aircraft conduct bearing and seal development testing, and determine the design suitability of these components.

The specific goals of the bearing program were to study the performance and fatigue characteristics of candidate bearings and bearing materials in order to determine the effect of applied loads, temperature environments, and lubricants, on bearing life expectancy. This information was to be used to finalize bearing materials selection and bearing compartment design for optimum performance and long life.

The goal of the seal program was to determine the design parameters necessary to provide reliable operation and long life at SST operating conditions.

A. BEARING DEVELOPMENT

1. ENDURANCE AND CALIBRATION TESTS

a. Introduction

The endurance and calibration programs conducted by Pratt & Whitney Aircraft under the Phase II-B contract included the following:

- An endurance test program to determine the fatigue life of Vantro-3 bearing material.
- A continued endurance test program to determine the fatigue life of M-50 CVM bearing material (125 mm bore size).

- An accelerated endurance test program to determine the relative fatigue life of M-50 CVM bearing material in both 125 mm and 170 bore size bearings.

- A calibration program to determine the operating characteristics of the 125 mm and 170 mm bore size bearings plus two special bearings incorporating a modified cage design and different plating.

The 170 mm bore size bearings were chosen for the Phase II-B test program because of availability. Bearings made from WD-65 material, as tested during the Phase II-A test program, were in process of revision at the vendor during the Phase II-B test program.

b. Description

(1) Components

The 125 mm bore size bearing design selected for fatigue failure testing under Phase II-B was an ABEC No. 7 duplexed angular-contact ball thrust bearing with balls and races made of PWA-725 (M-50) steel, melted by the consumable-vacuum melt process and stabilized for 600°F operation. The bearing retainers were machined in one piece from AMS 6415 steel, plated with 0.001 to 0.002 inches of silver. The bearing geometry included a 125 mm bore x 190 mm O.D. x 32.5 mm width, with a split-inner race construction. The bearing incorporated 21 balls of 0.8125 inch diameter with a contact angle of 23 to 27 degrees. The "Ventro-A" bearings were similar in size; however, the balls and races were made with a special Vanadium material.

The 170 mm bore-size bearings contained the same (as above) materials in the balls, races and retainer; the geometry being 170 mm bore x 260 mm O.D. x 43.8 mm width. These bearings contained 21 balls of 1.125 inch diameter with a convact angle of 27 to 30 degrees. The 170 mm bore-size bearings were stabilized for 1000°F operation.

(2) Rig

The test rig used for the evaluation of bearing endurance was designed to permit the simulation of speeds, thrust loads and temperatures representative of SST engine operation. The major components of the rig include a drive shaft, hydraulic piston load cylinder, front and rear bearing housings, a thrust ring, front and rear covers and exterior case.

The desired load is applied to the bearings through a hydraulic load cylinder built into the rear cover. The pressurized piston applies load to both bearings, one opposing the other, through a strain-gaged thrust ring. The rear housing is free to move forward and load the front bearing against the stationary front housing.

Bearing lubrication is accomplished by directing a jet of oil at rotating scoops which feed the oil to the split in the bearing inner races through axial grooves in the hubs. This method duplicates engine design. The oil is drained from the rig through a series of holes located at the bottom of the bearing cavity.

(3) Facility

The bearing endurance test rig was driven by a variable-speed electric motor through a step-up 7:1 ratio gearbox. The rig and gearbox were coupled by quill shaft to accommodate minor misalignment.

Thermocouples were installed in the oil-in and the oil-out lines and on the bearing races to monitor temperatures. Accelerometers were mounted in the horizontal and vertical plane on both end covers to monitor for bearing failures. The read outs for these units were calibrated to record a fatigue failure at full-scale deflection. Pressure gages, speed counters, and other instrumentation normally associated with a test facility were used as required. Heating of the bearing lubricant was done with immersed-rod heater units. The heater supplied the required quantity of PWA-524 oil to the rig test machine at 500°F.

c. Method of Test

The method used to induce bearing fatigue failure consisted of running the bearing at a speed and thrust load using PWA-524 oil at an average oil-in temperature of 500°F. A 5900-pound thrust level was established by assuming a 10 percent life of 100 hours and then calculating the corresponding load by AFBMA formula; higher thrust loads were established by assuming a B-10 life of 20 hours. The rig speed was established at relatively high levels to account for the use of test bearings which had a smaller diameter than that of the SST engine bearing. The oil temperature was established at 500°F as an approximation of the peak expected bulk oil temperature in the SST engine. The end product of the test methodology was a number which designated the ratio of the test bearing life to the bearing life predicted by the AFBMA method. The two major readings recorded during the endurance test program were bearing race temperature and accelerometer readings. The race temperatures were monitored to protect against possible overtemperaturing due to oil starvation or other cause; the accelerometers were calibrated to indicate a bearing fatigue failure.

d. Test Results

Four 125 mm bore bearings made from Vantro-S material were endurance tested for a total of 3.5 hours under a 10,200 pound thrust load, the load required to provide an estimated B-10 life of 20 hours. Two bearing failures occurred; one at 1.5 hours and the second at 0.25 hours. Analysis of the bearings indicated that the material had subsurface voids due to overheating of the steel in the heat treating procedure. The Vantro-S material bearings were returned to the vendor to be refurbished in preparation for future re-test evaluation.

Two M-50 CVM material bearings were endurance-tested for an additional 285 hours under the Phase II-A contract program(B-10 life of 100 hours, 5900 pound thrust load) again without producing any fatigue failures. Because of the method of establishing Weibull distribution, the additional running time did not substantially increase the statistical fatigue life of the subject bearings; however, as shown on Figure 10-1, the additional time gives further indication that the life expectancy of the bearings will be higher than the predicted life. This test was suspended so that the third phase of the contract could be achieved. The endurance times are tabulated below:

M-50 CVM 125 mm Bore Bearings
5,900 pound thrust load, 12,000 rpm Rig Speed

Serial Number	Total Hours	Remarks
4-1	332.75	Stopped *
4-2	332.75	" *
6-1	58.0	Misaligned
6-2	58.0	"
7-1	100.0	Stopped
7-2	100.0	"
8-1	104.0	"
8-2	104.0	"
18-1	455.0	"
18-2	455.0	"
19-1	100.0	"
19-2	100.0	"
21-1	246.0	"
21-2	246.0	"
	2791.50	

*Phase II-B additional running time accomplished on these two bearings without producing any failures.

In the third phase of the endurance and calibration program, eight 125 mm bore and eight 178 mm bore M-50 material bearings were tested at a B-10 life of 20 hours for a total of 2,820 hours without fatigue failure. The Weibull plot (Figure 10-2) based on the 125 mm bore M-50 bearings tested to date shows them to have a minimum life expectancy of 184 hours or 9.2 times the predicted (calculated) life. Secondly, the Weibull plot (Figure 10-3) based on the 178 mm bore M-50 bearings tested shows them to have a minimum expected life of 120 hours or 6.0 times the predicted (calculated) life. Further testing, especially by running ten bearings of each size out to 200 hours each, would increase the expected life of these bearings. Figure 10-4 illustrates a typical 125 mm bearing after test. The endurance time accumulated on the M-50 CVM bearings, at the B-10 life program of 20 hours, is tabulated below:

M-50 CVM 125 mm Bore Bearings
10,200 pound Thrust Load 12,000 rpm Rig Speed

S/N	Total Time (hours)	Remarks
F3-1	197.5	Stopped
F3-2	197.5	Stopped
F4-1	208.5	Stopped
F4-2	208.5	Stopped
F1-1	201.25	Stopped
F1-2	201.25	Stopped
G1-1	190	Stopped
G1-2	190	Stopped
H1-1	77	Stopped
H1-2	77	Stopped
	1748.50	

M-50 CVM 178 mm Bore Bearings
21,600 pound Thrust Load 7,000 rpm Rig Speed

S/N	Total Time (hours)	Remarks
200-1	200.0	Stopped
200-2	200.0	Stopped
203-1	192.0	Stopped
203-2	192.0	Stopped
279-1	200.0	Stopped
279-2	200.0	Stopped
283-1	100.0	Stopped
283-2	100.0	Stopped
	1384.0	

DOWNGRADED AT 3 YEAR INTERVALS
DECLASSIFIED AFTER 12 YEARS
DOD DIR 5200.10

The calibration programs run on both size bearings and the experimental M-50 bearing with the new cage design and two platings were completed without incident. Figures 10-5 through 10-10 are the results obtained from these programs. Figures 10-11 and 10-12 illustrate the typical experimental calibration M-50 bearings. Examination of the bearings at the completion of the calibration program showed that:

- The general condition of all bearings was good,
- The cage land riding surfaces of the bearing contained light rubbing,
- The oil cooling grooves were generally clean,
- All bearings could be used in further test programs.

e. Discussion of Results

The accumulation of more than 3100 hours of endurance testing on the M-50 CVM material main shaft bearings during the Phase II-B program has increased the confidence level in the feasibility of operating these bearings at high loads and speeds using a high-temperature lubricant. The testing has verified that serious consideration may be given to the use of these bearings in an SST engine with the expectation that after additional development, the bearing durability will be commensurate with those in present production engines. The endurance programs have also shown the necessity for an adequate fail-safe type lubrication system, operable, with an oil or at a temperature level which will not produce sludge or cause oxidation of the lubricant.

The completion of the calibrations on the M-50 thrust bearings has given insight into two possible problems of operation with bearings of these sizes: the first concerning cage balance, and the second associated with the formation of coke. The calibration program on the bearings with the modified cage designs also indicated that cage plating affects bearing race temperatures. Future programs will be directed toward establishing optimum materials combinations for this application.

f. Recommendations

As the results of the bearing development testing noted above, future program recommendations are as follows:

- Continuation of endurance testing until actual B-10 bearing lives are determined.

- Improvement of lubrication for longer sludge-free operation.

DOWNGRADED AT 3 YEAR INTERVALS
DECLASSIFIED AFTER 12 YEARS
DOD DIR 5200.10

- Development of fail-safe systems for lubrication of bearings.
- Continuation of cage development work to obtain a reliable retainer design which will be tolerant to sludge and low oil flow, and strong enough to survive operation under misalignment or other adverse condition.
- Conduct work to optimize cage balance requirements.
- Evaluate actual SST bearing designs for performance and durability.

2. SINGLE-BALL MATERIAL TESTS

a. Introduction

An investigation was undertaken to determine the effect of mid-temperature range lubricants on the fatigue life of bearing ball materials.

The investigation was considered significant to the SST program as a means of determining the most-promising candidate oils for operation at predicted high lubricant temperature.

b. Description

(1) Materials

The testing was conducted with half-inch diameter M-50 (CVM) and standard AISI-52100 (CVM) material balls. The fatigue life of the M-50 balls in MIL-L-7808D oil was used as a baseline.

The lubricants tested during Phase II-B are listed below in order of test use:

- Cellutherm 2712-C - This lubricant met requirements of both MIL-L-7808E, and MIL-L-7808F specifications, and was tested first with M-50 (CVM) and then with 52100 (CVM) ball material.
- Humble 4040 - This lubricant met the requirements of both MIL-L-7808E and MIL-L-7808F specifications and was subjected to two identical tests in order to substantiate the data. The tests were run with M-50 CVM ball material.
- Esso Humble WS5251 (PWA 521B Type II) - Tested with M-50 CVM ball material.

DOWNGRADED AT 3 YEAR INTERVALS
DECLASSIFIED AFTER 12 YEARS
DOD DIR 5200.10

THIS DOCUMENT CONTAINS INFORMATION AFFECTING THE NATIONAL DEFENSE OF THE UNITED STATES WITHIN THE MEANING OF THE ESPIONAGE LAWS, TITLE 18 U.S.C. SECTIONS 793 AND 794. ITS TRANSMISSION OR THE REVELATION OF ITS CONTENTS IN ANY MANNER TO AN UNAUTHORIZED PERSON IS PROHIBITED BY LAW.

- PWA 524R (Polyphenyl-Ether Skylube 600 Reclaimed) - Tested with M-50 CVM ball material.

- PWA 521A (MIL-L-7808D) - A rig calibration was made using this lubricant and 52100 CVM material to determine accuracy and repeatability of rig results.

(2) Rig

A ball fatigue test rig is shown in Figure 10-13. The test ball was held between two 130° V-groove MVI (M-50 equivalent) races by a flat-plate bronze cage and loaded through the upper race by a hydraulic load piston on top of the rig. See Figure 10-14. The rig was belt-driven at approximately 7,600 rpm by an electric motor. Lubricating oil was supplied to the test specimen by means of two multiple-orifice oil jets. The oil-in temperature was maintained at 300°F during all tests.

(3) Facilities

Five ball fatigue test rigs were utilized for the lubricant-material evaluation program. The five rigs had common lubricating and load-oil systems. Load-oil pressure was maintained at 60.2 psig, producing a downward force of 421 pounds on the test specimen, and thereby exerting 400,000 psi mean Hertz stress at the points of contact between the test ball and V-groove races.

c. Method of Test

For each test, a lot containing 15 balls was run until failure, or 20 hours, whichever occurred first. The rigs were equipped with accelerometers which stopped the test in response to the vibration of a ball failure.

The number of cycles for each ball in each lot was computed and plotted on Weibul curves to show B-10 life, the life expectancy of 90 percent of the balls in any given lot. Figure 10-15 shows a typical ball failure from spalling.

d. Test Results

A total test time of 972.75 hours was accumulated in ball material testing during the six-month period covered by this report.

DOWNGRADED AT 3 YEAR INTERVALS
DECLASSIFIED AFTER 12 YEARS
DOD DIR 5200.10

THIS DOCUMENT CONTAINS INFORMATION AFFECTING THE NATIONAL DEFENSE OF THE UNITED STATES WITHIN THE MEANING OF THE ESPIONAGE LAWS, TITLE 18 U.S.C. SECTIONS 793 AND 794. ITS TRANSMISSION OR THE REVELATION OF ITS CONTENTS IN ANY MANNER TO AN UNAUTHORIZED PERSON IS PROHIBITED BY LAW.

The results of this testing, in terms of B-10 life and percent of baseline standard, are tabulated below:

Oil/Ball Material	B-10 Life/Cycle	Percent of Baseline
MIL-L-7808D (PWA 521A)/ M-50 CVM	15.7×10^6	(Baseline)
Humble WS5251/M-50 CVM	9.3×10^6	59.1
Humble 4040/M-50 CVM (2nd Test)	8.1×10^6	51.6
PWA 524R (Skylube 600/M-50 CVM	6.4×10^6	40.8
Cellutherm 2712C/M-50 CVM	2.7×10^6	17.2
Humble 4040/M-50 CVM (1st test)	1.63×10^6	10.4
MIL-L-7808D (PWA 521A)/ 52100 CVM	5.7×10^6	(Baseline)
Cellutherm 2712C/52100 CVM	0.98×10^6	17.3

Figures 10-16 through 10-22 show the Weibull distributions for each of the oil and ball material tests.

e. Discussion of Results

The significance of ball material test results depends on background items in the overall test program. Pertinent background is listed below:

- Test balls are made from the same heat of steel and purchased in quantities of 10,000 to assure uniform quality.
- A baseline or standard B-10 life cycle is established with each new lot of balls, and subsequently rechecked at periodic intervals. The baseline is revised if necessary with each purchase of a new lot of balls.
- The materials tested during Phase II-B represent two stages in the state of the art: AISI 52100 CVM steel is an improved ver-

DOWNGRADED AT 3 YEAR INTERVALS
DECLASSIFIED AFTER 12 YEARS
DOD DIR 5200.10

THIS DOCUMENT CONTAINS INFORMATION AFFECTING THE NATIONAL DEFENSE OF THE UNITED STATES WITHIN THE MEANING OF THE ESPIONAGE LAWS, TITLE 18, U.S.C. SECTIONS 793 AND 794. ITS TRANSMISSION OR THE REVELATION OF ITS CONTENTS IN ANY MANNER TO AN UNAUTHORIZED PERSON IS PROHIBITED BY LAW

sion of a widely-accepted bearing steel, heat-treated and stabilized for use to temperature levels of 400°F; M-50 CVM is an advanced bearing steel, currently used in several Pratt & Whitney Aircraft production engines, normally stabilized for use to 600°F with a potential limit, through additional heat treat, of 1000°F.

The results of the Phase II-B tests were analyzed and compared with previous data to determine the relative worth of each lubricant, with special consideration for potential temperature limitations.

The results indicate that the fatigue life of PWA 524 oil is approximately half of that attributed to PWA 521 oil; however, PWA 521 appears to degrade rapidly at temperatures above 300°F, whereas PWA 524 shows a relatively unchanged fatigue life to temperatures above 500°F.

Humble 4040 oil produced a relative B-10 life of 10.4 percent during one evaluation, and a relative B-10 life of 51.6 percent during a second evaluation. These results were considered valid and the difference was attributed to a variation in the batches of oil used during test.

f. Recommendations

The performance data as noted above indicates the need for further evaluation of lubricants with special consideration for those lubricants having high-temperature capability, such as PWA-524 and Monsanto MCS 293.

3. OIL PUMP AND JET TESTS

a. Introduction

The purpose of this work was to 1) design, fabricate and test at elevated temperatures, an oil pump having rolling elements rather than journal bearings, and 2) to establish design parameters for development of more-efficient oil jets.

b. Description

(1) Component

The pump tested was a gear pump having four roller bearings for shaft support. A schematic of the pump is shown in Figure 10-23.

DOWNGRADED AT 3 YEAR INTERVALS
DECLASSIFIED AFTER 12 YEARS
DOD DIR 5200.10

A typical orifice and inlet jet test configuration is shown in Figure 10-24.

(2) Test Facility

The pump was mounted directly to a 5:1 ratio gearbox driven by a 15 hp reversible electric drive. Oil was supplied from a separate tank and heated with electric heaters. Oil temperatures and flows were read and recorded.

The various jet configurations were tested in the stand facility shown in Figure 10-25.

c. Method of Test

The pump was scheduled for calibration in a 441-point program consisting of combinations of the following variables:

- Inlet Pressures (in Hg abs.): 30, 25, 20, 15, 10, 8, 6, 4, and 2,
- Speeds (rpm): 1000, 2000, 2500, 3000, 3500, 4000 and 4500,
- Outlet Pressures (psi): 10, 20, 30, 40, 50, 100 and 150.

Oil flows and temperatures are recorded at each point.

Twenty-eight oil jets, with diameters from 0.040 to 0.140 inch, were tested during the Phase II-B program. Each jet configuration was tested with three diameters of flow straighteners (0.150, 0.200, and 0.250 in.) located immediately upstream of the jet. The test fluid in all tests was PWA 521A oil at ambient temperature and at pressures ranging from 10 to 140 psig. Pressure losses were recorded and photographs of spray patterns were taken for each jet configuration.

d. Test Results

Flow calibrations with PWA 521 oil at a temperature of 250°F totaled 55 hours of running time. The rolling element bearings performed satisfactorily through the test program. Data were directly comparable with current pump test data. Stand modifications were scheduled in an effort to improve overall pump performance prior to endurance test evaluations.

Four-hundred and thirty hours of testing were completed in the oil jet study program.

B. SEAL DEVELOPMENT

1. FACE SEAL TESTS

a. Introduction

A three-phase program of testing face seals was conducted under the Phase II-B contract to obtain data on major sealing variables. The first phase was directed towards optimization of the spring load used in the seal assembly; the second phase was conducted to evaluate the geometric unbalance on the carbon seal face while using the optimum spring load determined from previous tests; the third phase aimed at optimization of seal lip width. These phases were completed in the prescribed time period.

b. Description

The seals tested in this program were of the wet face type with conventional piston ring type secondary seals to accommodate axial excursions of the seal. The seal plates were of the flamoplated, oil-cooled type, which allows cooling oil to be directed to the sealing interface for cooling and to provide the necessary oil film to create a hydrodynamic bearing.

(1) Rig

The rig used for this program was designed so that simulated SST engine environmental and operating conditions could be imposed on the seal. The component parts of the rig are shown in Figure 10-26. Instrumentation necessary for recording pressures and temperatures was installed in the rig in the appropriate areas.

(2) Facility

The rig mounted in the test stand is shown in Figure 10-27. This stand had the equipment necessary to supply an adequate quantity of oil and air to the rig at the proper temperatures and pressures.

c. Method of Test

The air was heated by a hot wire heater to a 1600°F limit. A rotating-drum-induction-type oil heater was installed replacing the cal-rod heaters used previously; this heater raised the temperature of the oil, out of the first-stage steam heater from 200 to 400°F. The oil used was PWA 524. The rig was driven by a piston engine through a 12:1 ratio step-up gearbox. The rig instrumentation was furnished as part of the stand or supplied as special equipment.

The first phase consisted of testing seals with varied spring loads from nine to 30 pounds. The second phase was to test seals with unbalance configurations while using the optimum spring load. Tests were conducted on seals having unbalances of 75 percent, 65 percent and 55 percent. The third phase run was to determine ideal lip width while using the optimum parameters. Seals with lip widths of 0.100, 0.150 and 0.200 and 0.250 inches were run.

All testing in these phases were conducted at rig speeds of 12,500 rpm, 600°F air temperature, 400°F oil temperature using PWA-524 oil, and varied air pressures of 50, 30, 20 and 10 psig.

d. Test Results

Seventeen builds were completed and a total of 27 tests were run. A total of 661.75 test hours were accumulated during this period.

The test data are tabulated in Table 10-I following.

The general trend of the data indicates that a seal with a 15 lb. spring load, 65 percent unbalance, and seal lip width of 0.150 or 0.200 inch wide will function properly at the conditions stated.

e. Discussion of Results

The tests conducted during this report period contributed to the general SST development program by establishing the seal design requirements that can be used under the present SST conditions.

Data from the spring load tests indicates that a 15 lb. load gave the

TABLE 10-1
FACE SEAL TEST DATA

Seals Number	Carbon	Pressure psi	Temp. °F	Speed rpm	Spring Load	Time Hours	MILS per 100 hours	Figure Number	Remarks
67	CDJ-83 coated.	25	850°	10,000	35 lb.	7.25	no change		Pops open. Special plate
68	CDJ-83 .200 lip	40	850°	12,500	27 lb.	57.5	179.00	10-28 10-29	Dry Face Seal Plate
69	CDJ-83 .150 lip	150	850°	12,500	36 lb.	3.75	—		Overloaded.
70	POSSET .200 lip	40 15 10	850°	12,500	35 lb.	38.50 19.25 28.00	22.8 3.1 15.8	10-30	Oil fluctuating.
71	CDJ-83 .150 lip	50 30 20 10 10	850°	12,500 12,500 12,500 11,500 6,000	27 lb.	28.00 28.00 28.00 28.00 28.00	8.90 3.22 4.50 2.50 Grew	10-31	13 oil holes plugged. Oil soaked.
72	POSSET .200 lip	50	850°	12,500	27 lb.	22.75	35.10	10-32	Typical wear rate as per previous runs.
73	CDJ-83 .150 lip	50	850°	12,500	27 lb.	22.75	1.76	10-33 10-34	—
74	CDJ-83 .150 lip	50 30 20 10	830° 800° 700° 700°	12,500 12,500 12,500 12,500	15 lb.	23.00 28.00 28.00 26.75	no change 2.00 2.00 Grew	10-35 10-36	— —

CONFIDENTIAL

TABLE 10-I (Cont'd)

Seal Number	Carbon	Pressure psi	Temp. °F	Speed rpm	Spring Load	Time Hours	MILS per 100 hours	Figure Number	Remarks
75	CDJ-83 .150 Hp	50	850°	12,500	9 lb.	23.00	.9	10-37	Unstable.
76	CDJ-83	50 30 20 10	850° 825° 800° 700°	12,500 12,500 12,500 12,500	15 lb.	23.00 28.30 28.00 20.00	no change 1.50 2.00 no change	10-38	75% unbalance.
77	CDJ-83 .150 Hp	50	850°	12,500	15 lb.	23.00	no change	10-39 10-40	55% unbal. unstable.
78	CDJ-83 .250 Hp	50	850°	12,500	15 lb.	15.50	7.74	--	High leakage heater.
79	CDJ-83 .250 Hp	50	850°	12,500	15 lb.	17.00	.6	--	High leakage heater.
80	CDJ-83 .200 Hp	50	850°	12,500	15 lb.	8.25	no change	--	High leakage thru oil slots.
81	CDJ-83 .250 Hp	50	850°	12,500	15 lb.	31.75	6.90	10-41	Re-run of SLD 78.
82	CDJ-83 .150 Hp	50	850°	12,500	15 lb.	13.00	no change	10-42	Standardization run.
83	CDJ-83 .200 Hp	50	850°	12,500	15 lb.	28.00	not measured	10-43	Re-run of SLD 79

Except as noted, seal embalance was 65%, and all seals were run against a wet-face seal plate having an LCBC coating.

best wear rate and still kept leakage down: a 27 lb. load caused a higher wear, and a ½ lb. load was too light, causing the seal to be unstable.

Data from the unbalance program indicated that a 65 percent unbalance gave the best results, a 75 percent unbalance tended to overload the seal, and a 55 percent unbalance caused a negative closing force which gave an unstable seal.

An 0.150 to 0.200 inch seal lip was judged to be the better seal lip width. When a 0.250 inch lip seal was run, a tracking problem evolved, creating higher leakage and uneven wear. An 0.100 inch wide lip was too narrow to be used effectively with the wet-face seal plates.

f. Recommendations

The test programs conducted during the three study contracts have definitely established the feasibility of the face seal for use at expected SST operating and environmental conditions. Variations in seal performance between tests also suggest that secondary variables have a more significant effect on the seals at the SST operating conditions than in current advanced engine seal applications.

These results point out the necessity for continuing investigation into a complete seal development program in which all the aspects of geometric variations, materials combinations, cooling and lubricants are investigated. New and advanced sealing concepts must also be studied.

Long time endurance runs are required on all potential seals for use in an SST engine in order to establish durability, reliability, and potential time between overhaul.

2. RING SEAL TESTS

a. Introduction

The purpose of this work was to develop a ring seal design that would perform satisfactorily at higher rubbing speeds required in the SST engine. The higher rubbing velocities are a result of larger diameter and high rotating speeds. The geometry must be such that the seal would fit in the allowable space, and the wear rates obtained under conditions of higher pressures and temperature must be low enough to insure long life.

b. Description

(1) Component

The components tested were made of carbon and of the ring seal configuration. The geometric variations and the designs are shown in Figure 10-44.

Type CDJ-83 carbon material ring seals of the radial groove type were designed for the statistical type program. The seal plates against which the seals mated were of Haynes Stellite 6B material. A seal plate three-fourths of an inch in thickness was provided for a suitable heat sink. The rubbing faces of the seal plates were ground and lapped to a two light-band flatness. Figures 10-45 and 10-46 show the seal components in "exploded" arrangement and as assembled, respectively.

(2) Test Rig

A schematic sketch of the test rig used to test the ring seals is shown in Figure 10-47. Two seals were mounted back to back on the rotating shaft between lapped seal plates. The stationary seal liner was chrome-plated on the internal diameter rubbing surfaces. Two seals were tested simultaneously to eliminate thrust forces due to air pressure loading within the rig. During the program two rigs and four interchangeable shafts were used. Figures 10-48 and 10-49 show two views of a ring seal test rig mounted on the test stand.

(3) Facility

The test stand used during this program was adequately supplied with equipment and instrumentation necessary to conduct the tests. Three independent rig positions were provided on the test stand for simultaneous operation.

Power was provided by 15 hp, 1750 rpm electric motors driving through variable speed pulleys. The pulleys were in turn connected to a 5:1 ratio gearbox on which the test rigs were mounted. Air was supplied to load the seals at pressures up to 120 psig. Auxiliary equipment such as lubricating and fire fighting systems were also mounted in the test stand.

Air pressure, air temperature and rig rpm were controlled from a

test bench console located at the front of the stand. Oil pressures and temperatures, breather temperatures and rotometer air flow were measured and recorded.

c. Method of Test

The standard test program shown in Table 10-2 consisted of operating seals at 200, 250 and 275 ft/sec speed level at a pressure of 40 and 60 psig using an ambient temperature air source. Two seals in addition were tested at conditions of 325 ft/sec and 90 psi.

Each test was scheduled for five hours. It was terminated prior to that time if the breather (air out) temperature reached 400°F or if the rotometer indicated more than a 15 percent increase in seal leakage between test points. The seals were considered to have failed if there was a sudden increase in seal leakage or if the leakage rate reached 100 percent on the stand flowmeter capacity (36.2 cu ft/min). High seal leakage and seal temperatures were avoided to eliminate any potential fire hazard.

Each of the test ring seals were precisely measured axially and radially both prior to and after testing. The five hour wear rate was used as the basis for an estimated 100-hour wear-rate measurement.

d. Test Results

Fifty rig hours (100 seal hours) were accumulated in tests with eight inch diameter, radial-grooved ring seals. The complete program is outlined in Table 10-2. Two other short tests were made in addition to this program. Two seals were run at conditions above those in the statistical program, but failed after two hours of running. The conditions of this test are listed at the end of the statistical program under Test "X". In addition, three runs were made in a test to evaluate circular-grooved seals. The results of this test confirmed previous results showing seals with circular grooves to be inherently weak.

All tests were made with CDJ-83 grade carbon seals against Haynes-Stellite 6B alloy plates.

DOWNGRADED AT 3 YEAR INTERVALS
DECLASSIFIED AFTER 12 YEARS
DOD DIR 5200.10

TABLE 10-2

RING SEAL TEST PROGRAM

Design Location / Test	A Thickness (Radial) (Inches)	B No. of Pads Per In. Dia.	C Groove Width (Inches)	D Speed (ft./sec)	E Outside Diameter (Inches)	F Air Pressure (Psi)	G Lip Width (Inches)
1	.2	4	.200	250	6	60	.025
2	.2	6	.155	250	6	40	.050
3	.8	6	.200	275	6	40	.050
4	.8	4	.155	200	6	40	.050
5	.2	6	.155	275	6	40	.025
6	.2	6	.155	250	6	40	.050
7	.8	6	.155	200	6	60	.050
8	.8	6	.155	250	6	60	.050
9	.2	6	.200	250	6	60	025
10	.8	6	.155	275	6	60	.050
11	.8	4	.200	275	6	60	.025
12	.8	4	.155	275	8	40	.025
13	.2	4	.155	200	8	60	.050
14	.2	4	.155	275	8	60	.025
15	.2	6	.155	275	8	40	.050
16	.2	4	.200	200	8	40	.025
17	.2	6	.155	275	8	40	.050
18	.2	4	.155	250	8	60	.050
19	.8	6	.200	200	8	60	.025
20	.2	4	.200	200	8	40	.025
21	.2	4	.200	275	8	60	.050
22	.8	4	.155	250	8	60	.025
23	.8	4	.200	250	8	40	.025
24	.8	4	.200	275	6	40	.050
25	.2	6	.200	200	6	60	.025
26	.8	4	.200	275	6	60	.025
27	.2	4	.200	250	6	40	.025
28	.8	4	.200	275	6	40	.050
29	.8	4	.200	250	6	40	.050
30	.2	6	.155	200	6	40	.025
31	.2	6	.200	200	6	60	.050
32	.8	6	.200	200	6	40	.025
33	.2	6	.200	275	6	60	.025
34	.2	4	.200	275	8	40	.050
35	.2	6	.155	250	8	40	.050
36	.8	4	.200	200	8	60	.050
37	.2	4	.155	200	8	40	.025
38	.8	6	.155	250	8	40	.050
39	.8	6	.200	200	8	60	.025
40	.8	6	.155	275	8	60	.025
41	.8	6	.200	250	8	60	.025
42	.8	4	.200	200	8	60	.050
43	.8	4	.155	200	8	40	.050
44	.2	6	.155	250	8	40	.050
X	.8	4	.125	325	8	20	.050

DOWNGRADED AT 3 YEAR INTERVALS
DECLASSIFIED AFTER 12 YEARS
DOD DIR 5200.10

THIS DOCUMENT CONTAINS INFORMATION AFFECTING THE NATIONAL DEFENSE OF THE UNITED STATES WITHIN THE MEANING OF THE ESPIONAGE LAWS, TITLE 18, U.S.C., SECTIONS 793 AND 794. THE TRANSMISSION OR THE REVELATION OF ITS CONTENTS IN ANY MANNER TO AN UNAUTHORIZED PERSON IS PROHIBITED BY LAW.

The results of the radial-grooved seal tests are tabulated below:

Radial-Groove Seal-Test Results

Test Point No.	Radial Thickness Inches	Air Pressure PSIG	Speed rpm	Test Time hours	Front Wear Mils/100 hours	Rear Wear Mils/100 hours
20	0.2	40	5730	5.0	156.0	54.0
41	0.8	60	7150	5.0	80.0	6.0
22	0.8	60	7150	5.0	36.0	26.0
38	0.8	40	7150	5.0	6.0	52.0
37	0.2	40	5730	5.0	36.0	34.0
43	0.8	40	5730	5.0	20.0	10.0
X	0.8	90	9310	2.0	Broken	Broken

e. Conclusions

- Seals with straight radial grooves are inherently stronger than those with circular grooves.
- Seals with a 0.800 inch radial width have lower wear rates than those with 0.200 inch radial width.
- Adequate sealing and low wear can be achieved with ring seals having radial grooves machined into the face.

f. Recommendations

- That future studies be made to determine the optimum radial seal width for operation at conditions at or above those expected for the SST application.
- That future studies be made to determine the effects of varying groove geometry such as taper and cross-section.

3. MATERIALS AND DESIGN TESTS

a. Introduction

This program was established to test candidate materials for carbon ring seals and seal plates. These materials are evaluated at conditions expected in the SST application and optimum seal-seal plate combinations

DOWNGRADED AT 3 YEAR INTERVALS
DECLASSIFIED AFTER 12 YEARS
DOD DIR 5200.10

THIS DOCUMENT CONTAINS INFORMATION AFFECTING THE NATIONAL DEFENSE OF THE UNITED STATES WITHIN THE MEANING OF THE ESPIONAGE LAWS, TITLE 18 U.S.C. SECTIONS 793 AND 794. ITS TRANSMISSION OR THE REVELATION OF ITS CONTENTS IN ANY MANNER TO AN UNAUTHORIZED PERSON IS PROHIBITED BY LAW.

are determined.

(1) Component

The components tested were carbon ring seals with metal seal plates. The carbon seals had an outside diameter of 4.9 inches and a radial thickness of 0.420 inch. The mating seal plates were ground and lapped to a two light band flatness.

(2) Test Rig

Two seals were mounted back-to-back on the rotating shaft between lapped seal plates. The stationery seal liner was chrome plated on the I.D. rubbing surfaces. Two seals were tested simultaneously to eliminate thrust forces due to pressure loading in a rig. Three rigs with six interchangeable shafts were used.

(3) Facility

A test stand was equipped with equipment and instrumentation to handle the program and obtain the necessary data.

Power was provided by 15 hp, 1750 rpm electric motors through variable speed pulleys. The pulleys were connected to a 5:1 ratio gearbox and the rigs were mounted on the gearboxes. Air at pressures up to 120 psig was supplied to the rigs. See Figure 10-50.

Air pressure, air temperatures and rig speed were controlled from a console mounted in front of the stand. See Figure 10-51. Oil pressures and temperatures, breather temperature and rotometer flows were read and recorded.

b. Method of Test

The test program consisted of the 16 points listed in Table 10-3. In three instances, this program was revised to include more points or different conditions, as is noted in the following discussion. Each test point was scheduled for five hours. A point was terminated prior to that time if the breather (air out) temperature amounted to 400°F or if there was more than 15 percent increase in seal leakage between each step. The seal was considered to have failed if there was a sudden increase in seal leakage or if the leakage rate reached 100 percent on the stand flowmeters (35.5 SCFM). High seal leakage or seal temperatures were avoided because of fire hazard.

DOWNGRADED AT 3 YEAR INTERVALS
DECLASSIFIED AFTER 12 YEARS
DOD DIR 5200.10

THIS DOCUMENT CONTAINS INFORMATION AFFECTING THE NATIONAL DEFENSE OF THE UNITED STATES WITHIN THE MEANING OF THE ESPIONAGE LAWS, TITLE 18, U.S.C. SECTIONS 793 AND 794. THE TRANSMISSION OR THE REVELATION OF ITS CONTENTS IN ANY MANNER TO AN UNAUTHORIZED PERSON IS PROHIBITED BY LAW.

Each of the test ring seals were precisely measured axially and radially prior to and after test. The difference in measurement was multiplied by a factor of 20 to give wear rate in mils/100 hours.

TABLE 10-3

SEAL MATERIAL EVALUATION

STANDARD PROGRAM

Point No.	Air Press. Psig	Air Temp. °F	Speed Rpm
1	30	500	6000
2	50	500	6000
3	80	500	6000
4	30	500	9000
5	50	500	9000
6	80	500	9000
7	30	1000	6000
8	50	1000	6000
9	80	1000	6000
10	30	1000	9000
11	50	1000	9000
12	80	1000	9000
13	80	500	6000
14	80	500	9000
15	80	1000	6000
16	80	1000	9000

Each point is run for 5.0 hours unless terminated by carbon or seal plate failure.

c. Method of Test

Tests totaling 729.75 rig hours (1459.5 seal hours) were made to evaluate eight carbon grades and six seal plate materials. The 4.9-inch diameter ring seals were tested in the standard program outlined in Table 10-3. Unless otherwise specified, each carbon-seal plate combination was subjected to this 16-point program. Two experimental carbon grades and one seal plate material were subjected to conditions higher than those in the standard program, as noted in the following discussion. Baseline carbon grade was National Carbon CDJ-83 and

DOWNGRADED AT 3 YEAR INTERVALS
DECLASSIFIED AFTER 12 YEARS
DOD DIR 5200.10

THIS DOCUMENT CONTAINS INFORMATION AFFECTING THE NATIONAL DEFENSE OF THE UNITED STATES WITHIN THE MEANING OF THE ESPIONAGE LAWS, TITLE 18, U.S.C., SECTIONS 793 AND 794. THE TRANSMISSION OR THE REVELATION OF ITS CONTENTS IN ANY MANNER TO AN UNAUTHORIZED PERSON IS PROHIBITED BY LAW.

baseline seal plate material was Haynes Stellite 6B. Figure 10-52 presents a curve summarizing previous test results of the baseline CDJ-83 vs. Stellite 6B material for reference. Data curves from all tests are included in Figure 10-53 through 10-81.

d. Test Results

A summary of seal vs. plate combination test results follows:

Carbon P2239 vs. Stellite 6B

This was one of the two carbon grades which showed better performance than the baseline grade. Wear rates were 25 to 40 mils/100 hrs. lower than CDJ-83 carbon against Stellite 6B plates at the same conditions. A carbon failure occurred in one of the 16 test points. See Figures 10-53 and 10-54.

Speer 9341 vs. Stellite 6K

Wear Rates were 50 to 75 mils/100 hours higher than standard CDJ-83 vs. Stellite 6B. No carbon breakage occurred in the 16-point program. See Figures 10-55 and 10-56.

Speer 9341 vs. Stellite 6B

Wear rates for this assembly were 50 mils/100 hours higher than CDJ-83 vs. Stellite 6B. The standard program was altered to include additional testing at air pressures of 90, 100, and 110 psig. Extreme wear rates were experienced at these higher air pressures. See Figures 10-57 and 10-58.

Pure Carbon PO3XHT vs. Linde LCIC Flamsplate

High breakage occurred at 9000 RPM. Extra repeat points were run and carbons failed in seven of the 19 total points run. Wear rates for those specimens which completed the five hours of running were moderate. Refer to Figures 10-59 and 10-60.

Pure Carbon PO3XHT vs. Chromeplate on AMS 6323

Highest wear rates were below 100 mils/100 hours on carbons that completed five hours of running. Carbons failed during four of the 15 points run. (Point 4 was omitted). Refer to Figures 10-61 and 10-62.

DOWNGRADED AT 3 YEAR INTERVALS
DECLASSIFIED AFTER 12 YEARS
DOD DIR 5200.10

Pure Carbon PO3XHT vs. Stellite 6B

High seal wear and breakage occurred at a temperature of 1000°F. Wear rates were also excessive at 9000 rpm at both temperature conditions. The failure rate was 38 percent at 1000°F and 13 percent at 500°F air temperature. Refer to Figures 10-63 and 10-64.

National Carbon B-2936 vs. Stellite 6K

Tests were made at speeds and air pressures exceeding those in the standard 16-point program. B-2936 carbon material out-performed National Carbon CDJ-83 at speeds from 9000 to 11700 rpm and air pressures from 70 psi to 90 psi. A seven point program at the above conditions resulted in three carbon failures and a maximum wear rate of 140 mils/100 hours. See Figure 10-65. A 16-point program was conducted at higher speeds and pressures with one CDJ-83 seal and one B-2936 seal run simultaneously in the test rig at each point. (Refer to Figures 10-66 and 10-67. Five CDJ-83 seals failed in the 16 point program and no failures occurred with B-2936 seals. Wear rates of B-2936 were 50% less than for CDJ-83 at 11,700 rpm, 100 psig, and 500°F.

USG 2800 vs. Stellite 6K

Wear rates were excessive at high air pressures: carbon failure rate was 50 percent. Refer to Figures 10-68 and 10-69.

USG 2803 vs. Stellite 6K

Carbon wear rates were excessive and 10 carbon failures occurred in the 14 points run. (Two points were omitted.) Refer to Figures 10-70 and 10-71.

USG 2777 vs. Linde LCIC Flameplate

Wear rates compared favorably with CDJ-83 carbon. Four of the 16 points were terminated by carbon failures at 80 psi. See Figures 10-72 and 10-73.

Seal Plate Material Evaluations

Three new seal plate materials (Brush Beryllium $NiBe$, Haynes No. 25, and Clevite 300) were tested with baseline CDJ-83 carbon seals. The programs varied from the standard 16-point program as noted in the following discussion. None of the seal plate materials

DOWNGRADED AT 3 YEAR INTERVALS
DECLASSIFIED AFTER 12 YEARS
DOD DIR 5200.10

performed better than the baseline Stellite 6B seal plates below 1000°F.

Although the performance of cast Ni_4B_9 plates was below that of Stellite 6B plates at temperatures up to 1000°F, this material was superior to all other materials, including Stellite 6B, at temperatures in the 1200°F range. Only three CDJ-83 carbons failed during the 31 total points run. The seals were tested at temperatures of 500°, 1000° and 1200°F; air pressures of 30, 50, 80 and 100 psig; and speeds of 6000 and 9000 rpm. Refer to Figures 10-74 through 10-77.

The sintered Clevite 300 seal plates lacked the strength necessary to withstand the conditions of the nine point program. Wear and carbon breakage rates were high. One seal plate fractured radially. See Figures 10-78 and 10-79.

Haynes No. 25 seal plates had the best performance below 1000°F of the three materials tested. Wear rates of the CDJ-83 seals were all below 150 mils/100 hours at 500°F. Maximum wear rate was 200 mils/100 hours at the 1000°F temperature condition. One carbon failed in the 16 point standard program. See Figures 10-80 and 10-81.

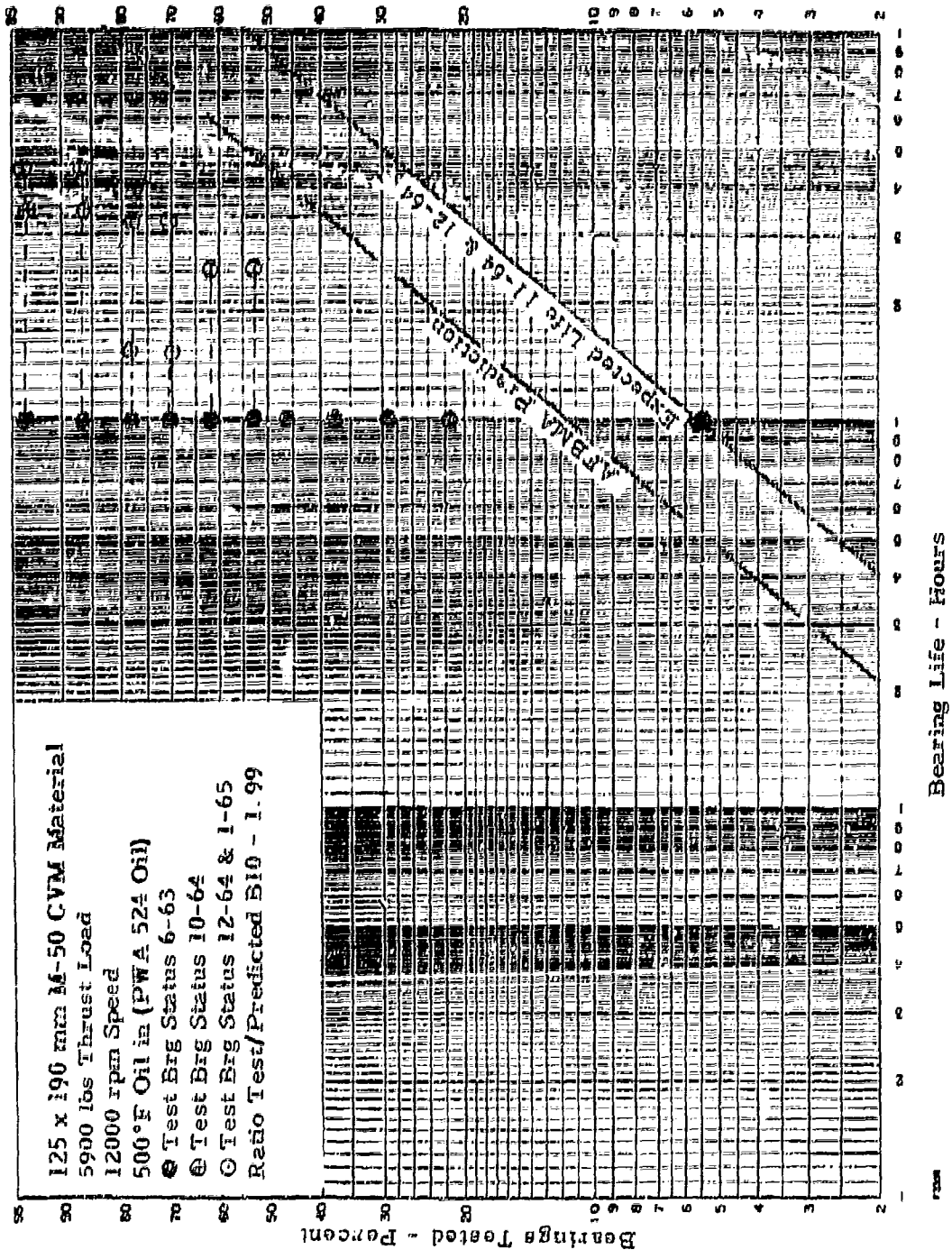
d. Discussion of Results

These tests represent a preliminary screening of potential seal materials combinations for severe applications. Results were generally less successful than baseline; however, indications were that some of the carbon grades, particularly B-2936 and USC 2777, were strong candidates for these conditions and that their performance and life can be comparable to seals in use in current high performance engines.

e. Recommendations

Screening tests of the better materials tested in this program should be continued along with evaluation of newer materials as they become available. Subsequent to the screening tests, the better materials should be fully evaluated in full-scale face and ring seal assemblies to complete the component portion of the program prior to engine test.

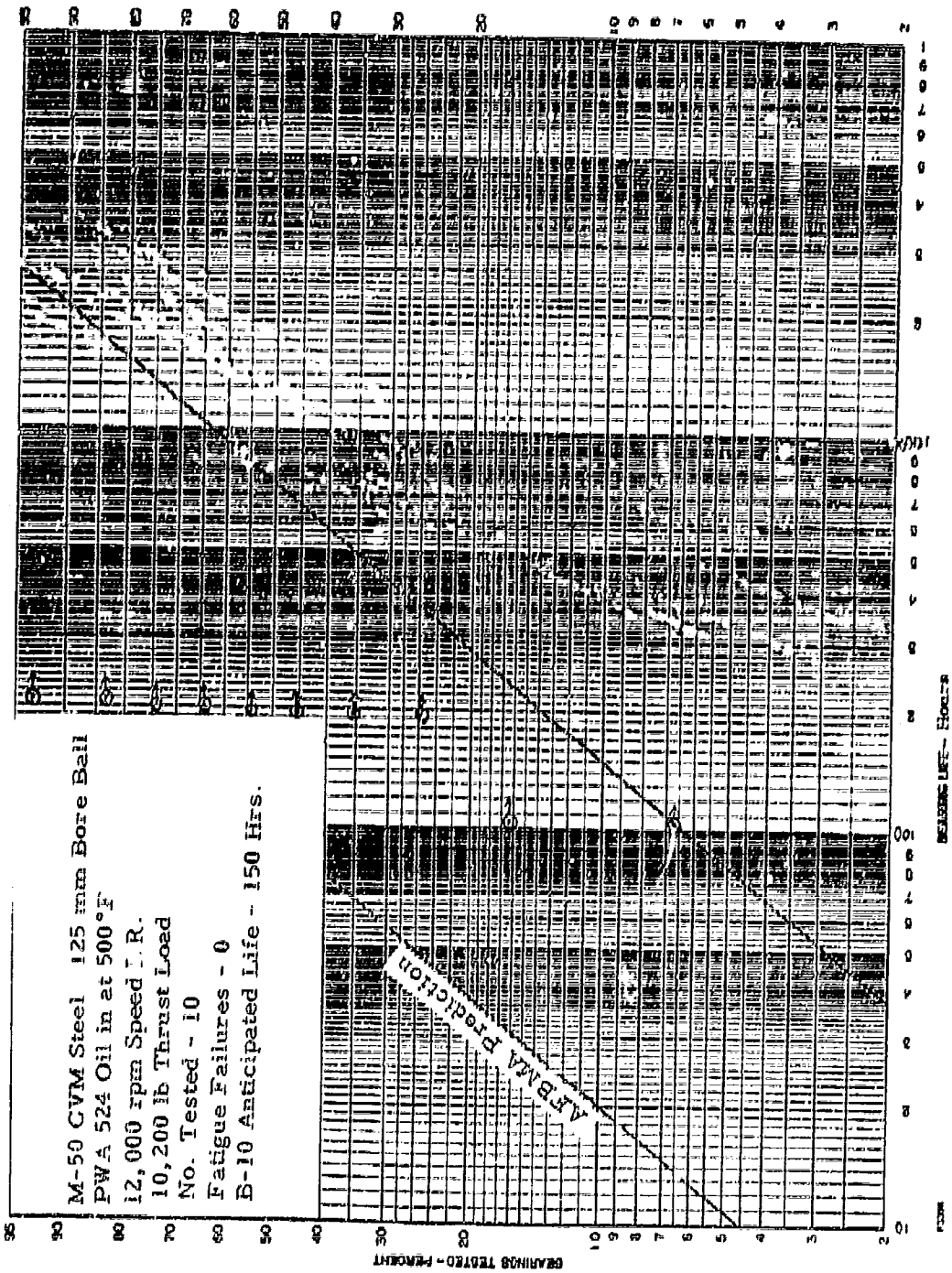
DOWNGRADED AT 3 YEAR INTERVALS
DECLASSIFIED AFTER 12 YEARS
DOD DIR 5200.10



WEIBULL DISTRIBUTION OF TEST DATA FROM M-50 CVM BALL BEARING (125 MM BORE)

Figure 10-1

DOWNGRADED AT 3 YEAR INTERVALS
DECLASSIFIED AFTER 12 YEARS
DOD DIR 5200.10

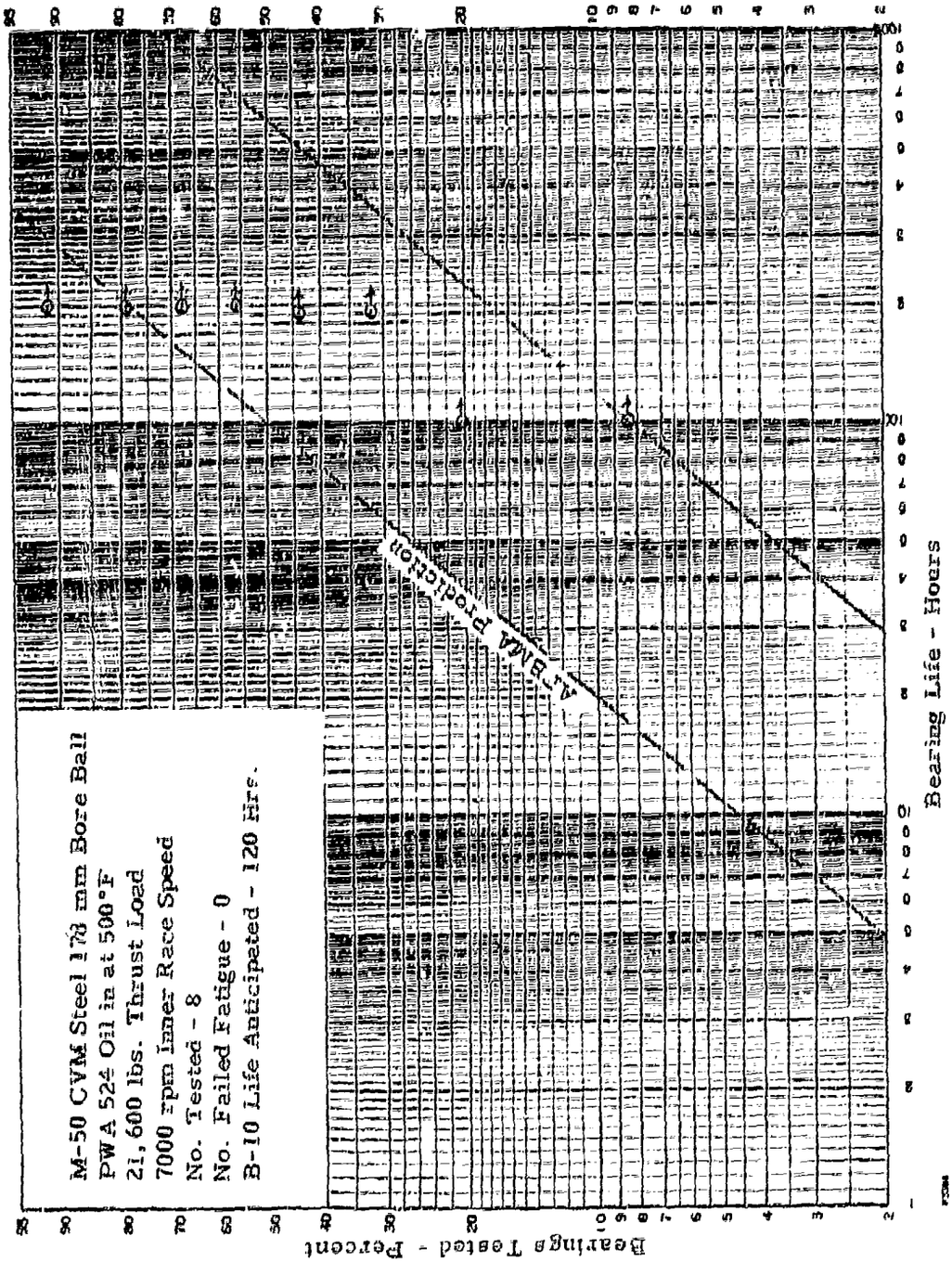


WEIBULL DISTRIBUTION OF TEST DATA FROM M-50 CVM BALL BEARING (125 MM BORE)

Figure 10-2

DOWNGRADED AT 3 YR INTERVALS
DECLASSIFIED AFTER 12 YEARS
DOD DIR 5200.10

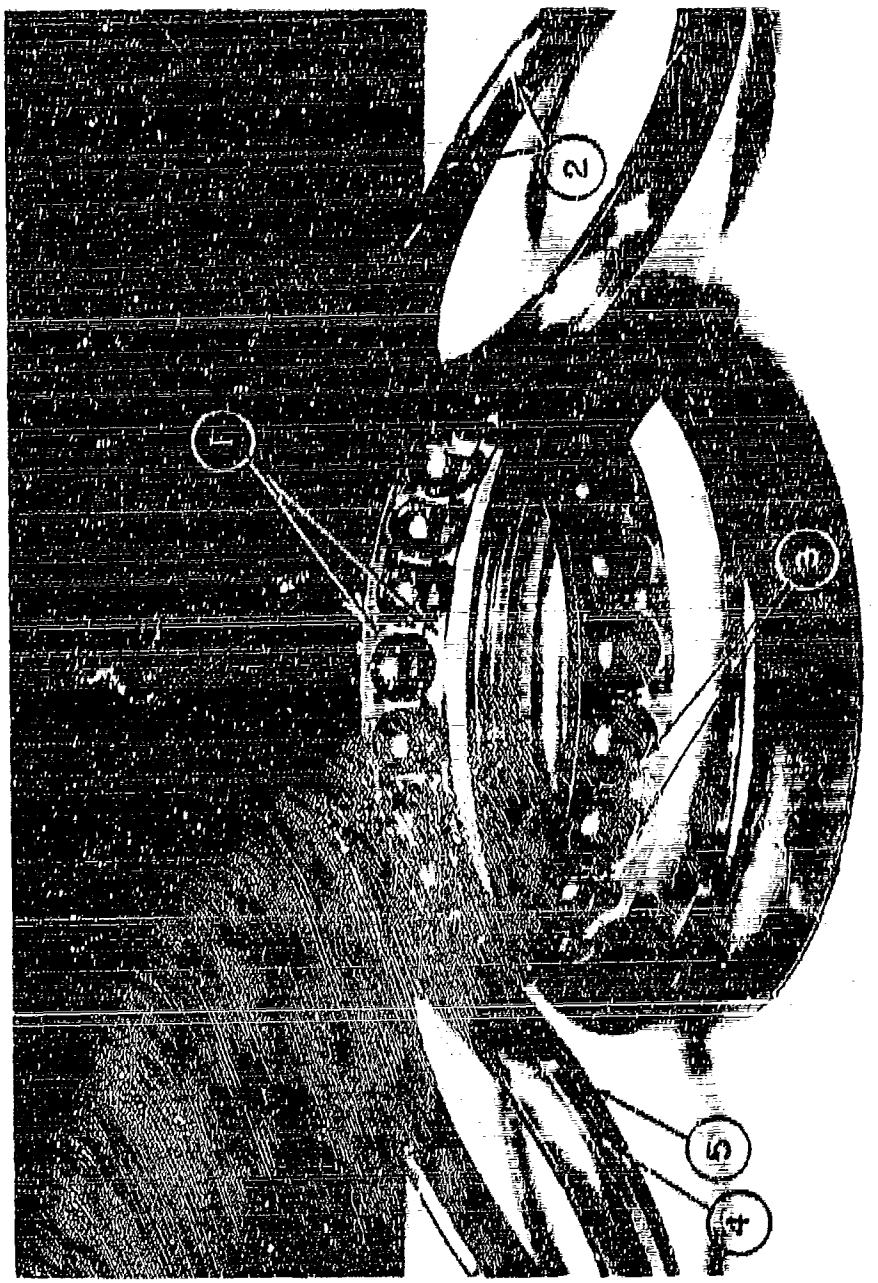
THIS DOCUMENT CONTAINS INFORMATION AFFECTING THE NATIONAL DEFENSE OF THE UNITED STATES WITHIN THE MEANING OF THE ESPIONAGE LAWS, TITLE 18, U.S.C., SECTIONS 793 AND 794. THE TRANSMISSION OR THE REVELATION OF ITS CONTENTS IN ANY MANNER TO AN UNAUTHORIZED PERSON IS PROHIBITED BY LAW.



WEIBULL DISTRIBUTION OF TEST DATA FROM M-50 CVM BALL BEARING (178 MM BORE)

Figure 10-3

DOWNGRADED AT 3 YEAR INTERVALS
DECLASSIFIED AFTER 12 YEARS
DOD DIR 5200.10



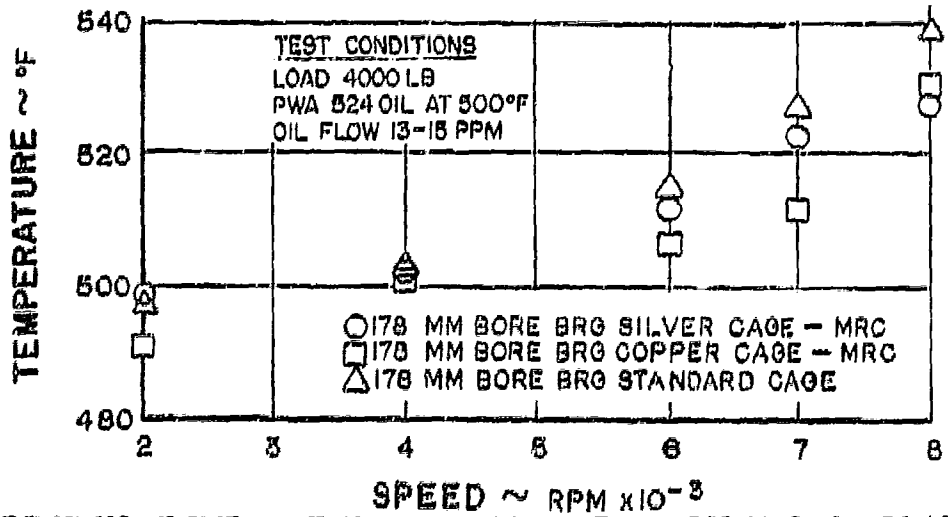
6188-4-PX

VIEW OF 125 MM BORE M-50 CVM BEARING AFTER 150-HOUR ENDURANCE USING PWA-524 OIL AT 500°F FOR COOLING. ARROWS 1-4 INDICATE EXCELLENT CONDITION OF (1) CAGE LANDS, (2) COOLING GROOVES, (3) BALL POCKETS, AND (4) INNER RACE LANDS. ARROW (5) POINTS TO SLIGHT COKING IN THE PULLER GROOVE.

Figure 10-4

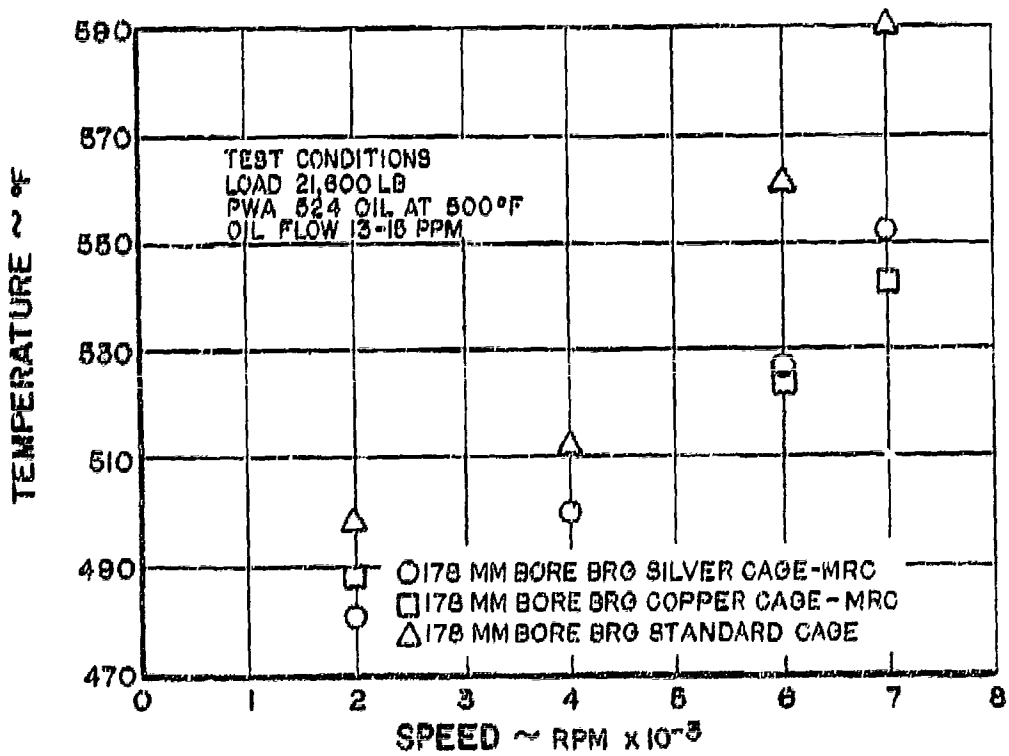
DOWNGRADED AT 3 YEAR INTERVALS
DECLASSIFIED AFTER 12 YEARS
DOD DIR 5200.10

THIS DOCUMENT CONTAINS INFORMATION AFFECTING THE NATIONAL DEFENSE OF THE UNITED STATES WITHIN THE MEANING OF THE ESPIONAGE LAWS, TITLE 18 U.S.C. SECTIONS 793 AND 794. ITS TRANSMISSION OR THE REVELATION OF ITS CONTENTS IN ANY MANNER TO AN UNAUTHORIZED PERSON IS PROHIBITED BY LAW.



SPEED VS. TEMPERATURE EFFECTS WITH VARIOUS CAGE PLATING IN THREE 178 MM BORE BEARINGS.

Figure 10-5

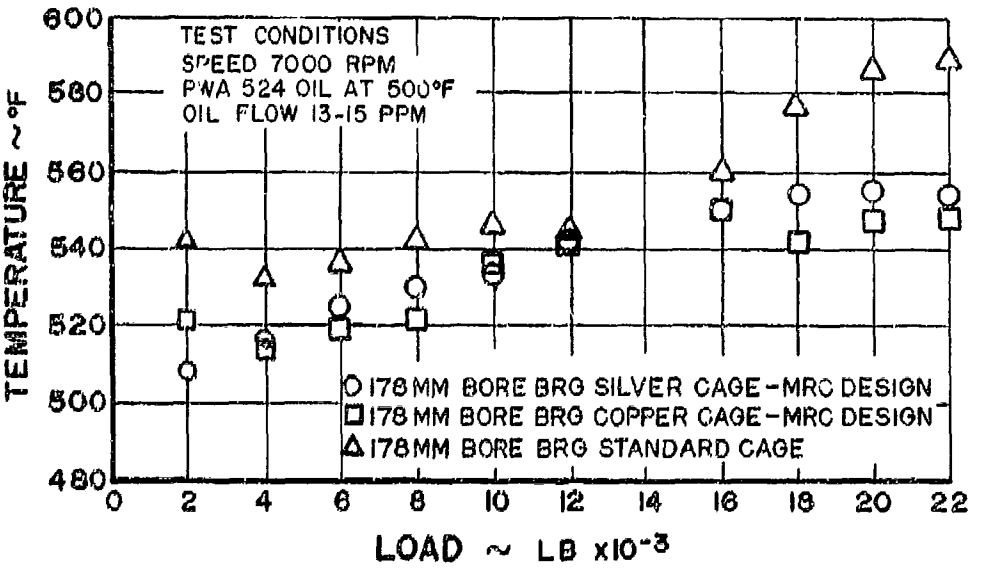


SPEED VS. TEMPERATURE EFFECTS WITH VARIOUS CAGE PLATING IN THREE 178 MM BORE BEARINGS.

Figure 10-6

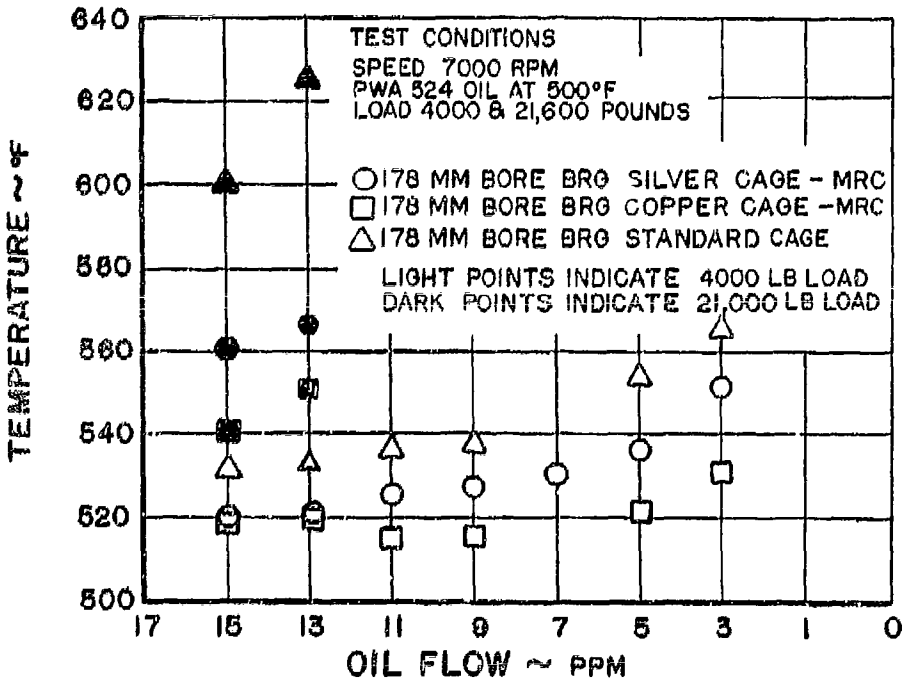
DOWNGRADED AT 3 YEAR INTERVALS
DECLASSIFIED AFTER 12 YEARS
DOD DIR 5200.10

THIS DOCUMENT CONTAINS INFORMATION AFFECTING THE NATIONAL DEFENSE OF THE UNITED STATES WITHIN THE MEANING OF THE ESPIONAGE LAWS, TITLE 18, U.S.C. SECTIONS 793 AND 794. THE TRANSMISSION OR THE REVELATION OF ITS CONTENTS IN ANY MANNER TO AN UNAUTHORIZED PERSON IS PROHIBITED BY LAW.



LOAD VS. TEMPERATURE EFFECTS WITH VARIOUS CAGE PLATING IN THREE 178 MM BORE BEARINGS.

Figure 10-7

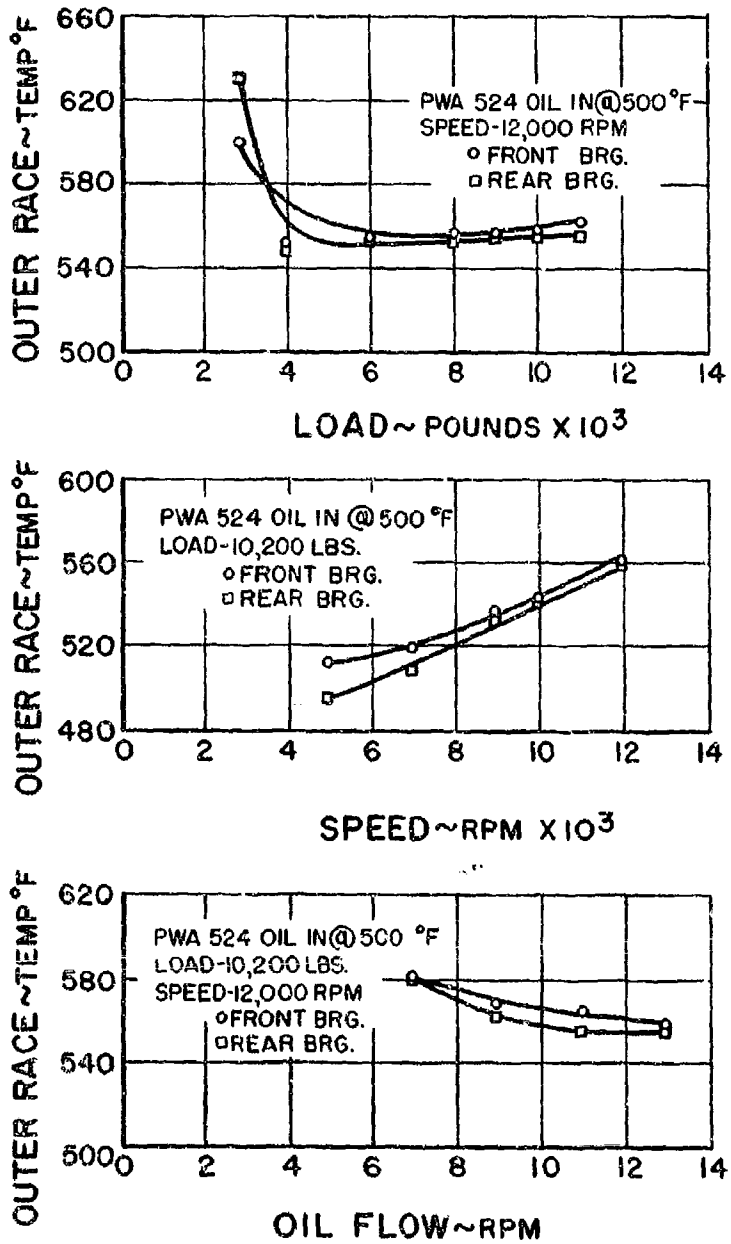


OIL FLOW VS. TEMPERATURE EFFECTS WITH THREE 178 MM BORE BEARINGS CONTAINING DIFFERENT CAGE PLATING UNDER TWO LOAD CONDITIONS.

Figure 10-8

DOWNGRADED AT 3 YEAR INTERVALS
DECLASSIFIED AFTER 12 YEARS
DOD DIR 5200.10

THIS DOCUMENT CONTAINS INFORMATION AFFECTING THE NATIONAL DEFENSE OF THE UNITED STATES WITHIN THE MEANING OF THE ESPIONAGE LAWS, TITLE 18, U.S.C., SECTIONS 793 AND 794. ITS TRANSMISSION OR THE REVELATION OF ITS CONTENTS IN ANY MANNER TO AN UNAUTHORIZED PERSON IS PROHIBITED BY LAW.

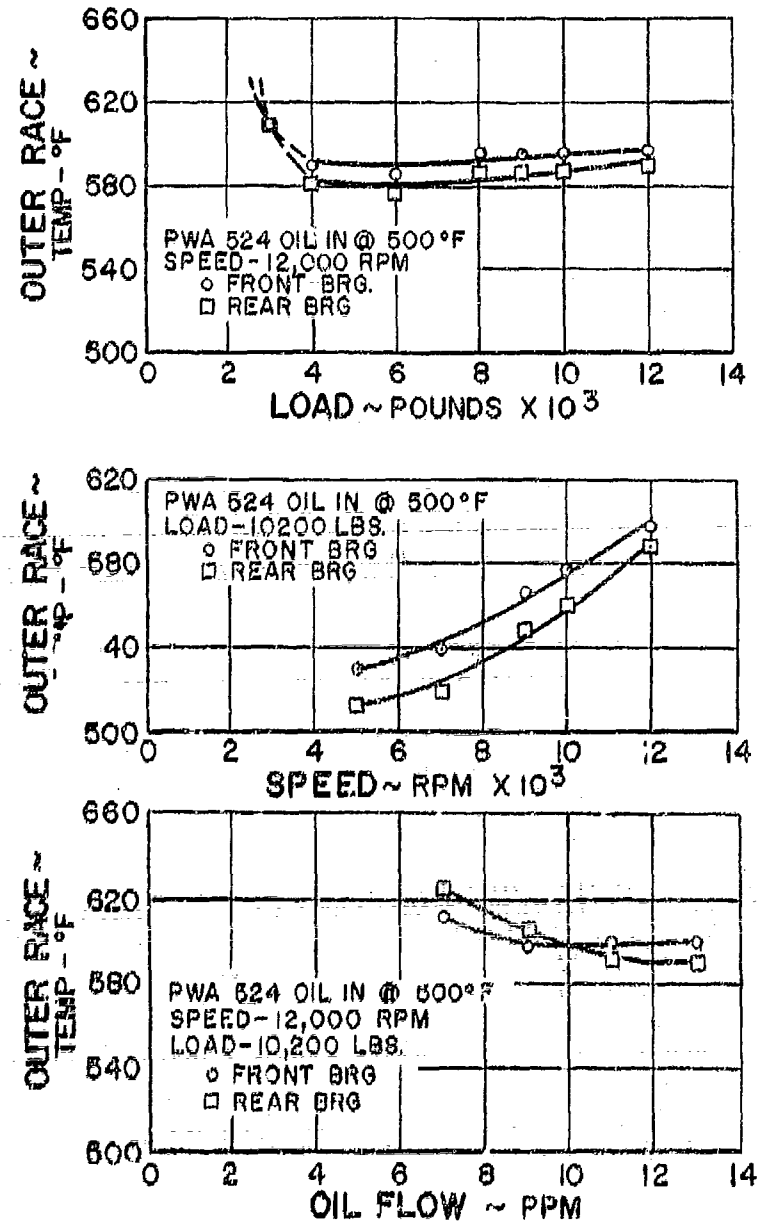


LOAD, SPEED AND OIL FLOW VS. TEMPERATURE EFFECTS WITH FAFNIR 125 MM BORE BEARINGS.

Figure 10-9

DOWNGRADED AT 3 YEAR INTERVALS
DECLASSIFIED AFTER 12 YEARS
DOD DIR 5200.10

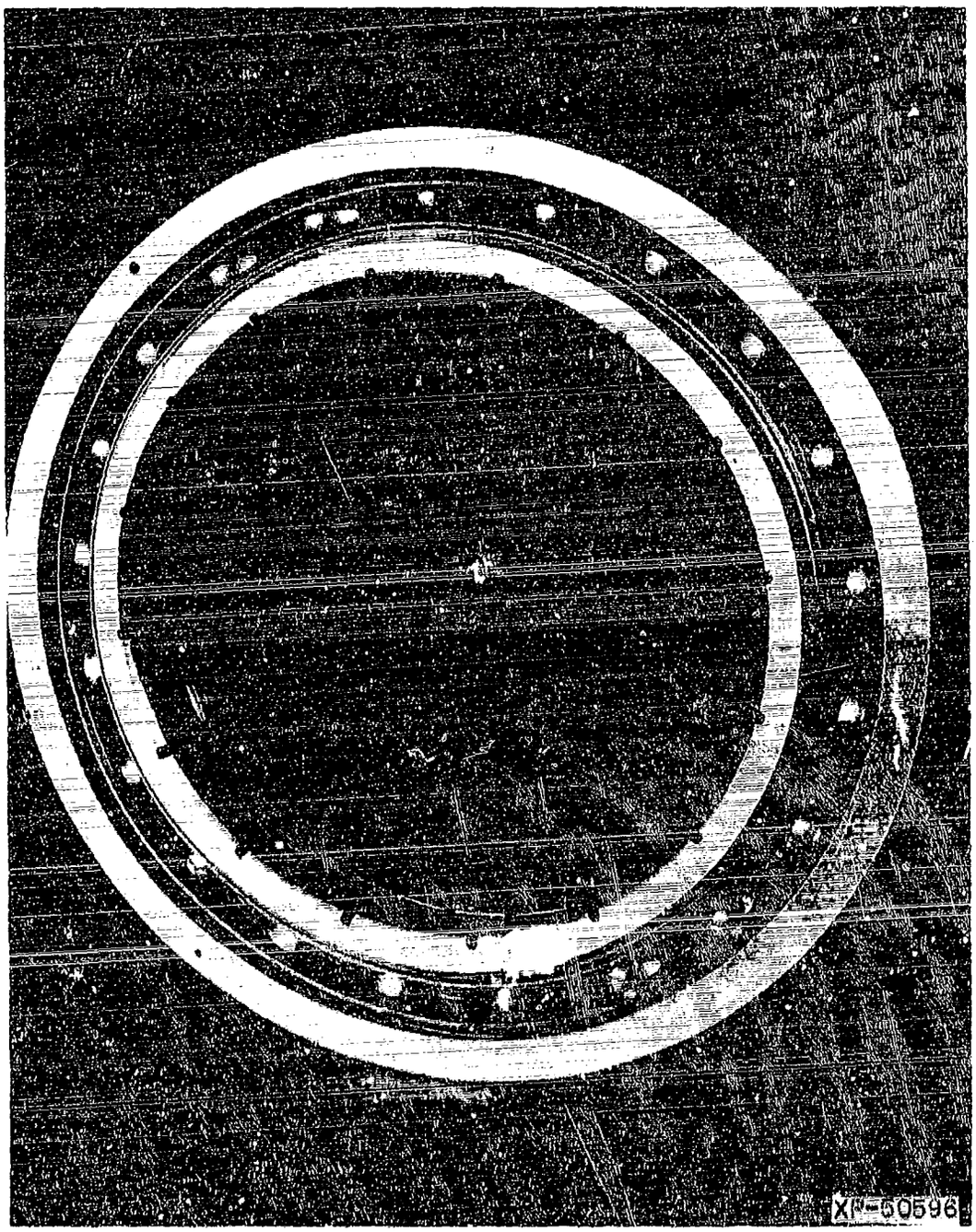
THIS DOCUMENT CONTAINS INFORMATION AFFECTING THE NATIONAL DEFENSE OF THE UNITED STATES WITHIN THE MEANING OF THE ESPIONAGE LAWS, TITLE 18 U.S.C. SECTIONS 793 AND 794. ITS TRANSMISSION OR THE REVELATION OF ITS CONTENTS IN ANY MANNER TO AN UNAUTHORIZED PERSON IS PROHIBITED BY LAW.



LOAD, SPEED AND OIL FLOW VS. TEMPERATURE EFFECTS WITH SKF 125 MM BORE BEARINGS.

Figure 10-10

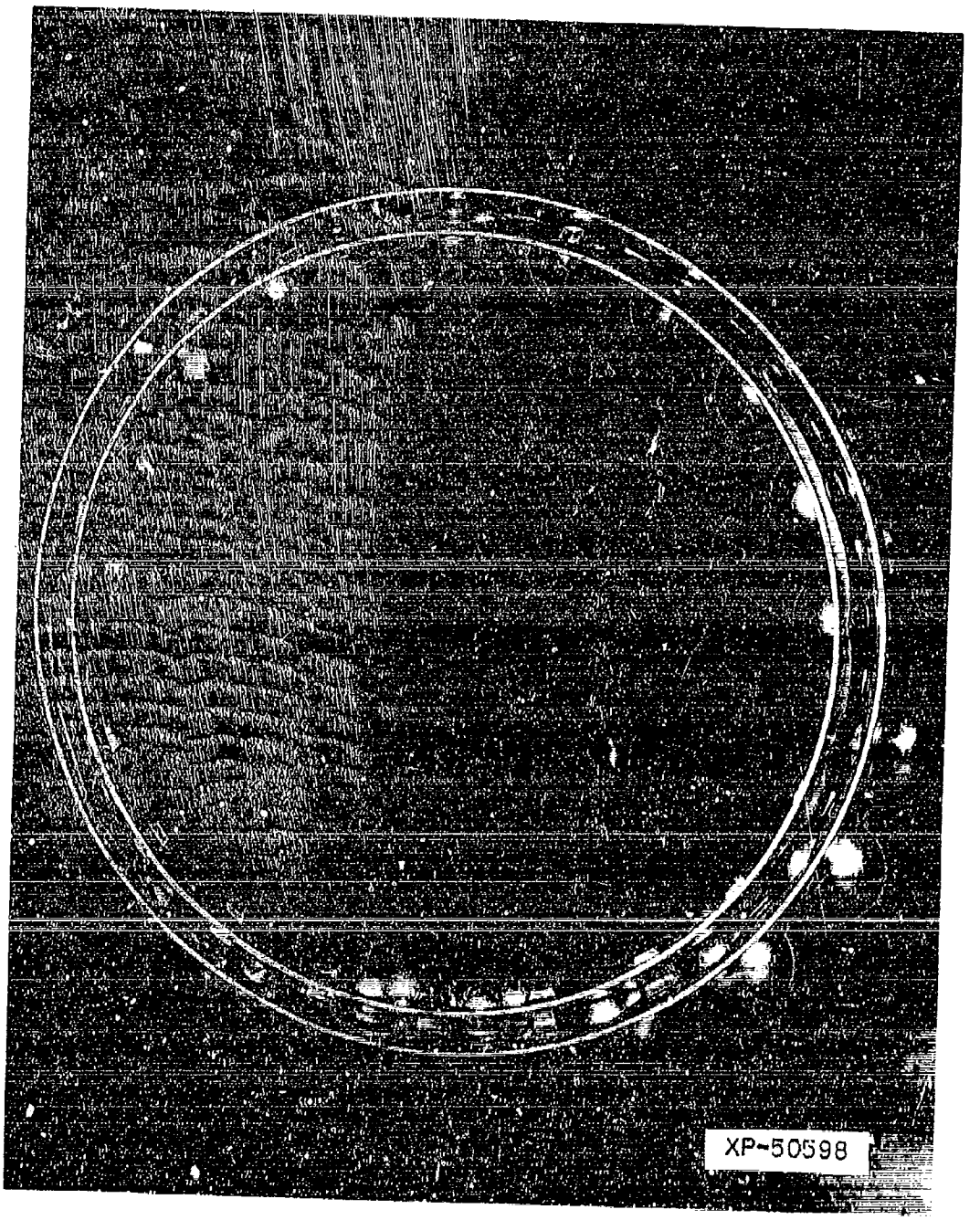
DOWNGRADED AT 3 YEAR INTERVALS
DECLASSIFIED AFTER 12 YEARS
DOD DIR 5200.10



VIEW OF 178 MM BORE M-50 CVM BALL BEARING TESTED IN PWA-524 OIL AT 500°F.

Figure 10-11

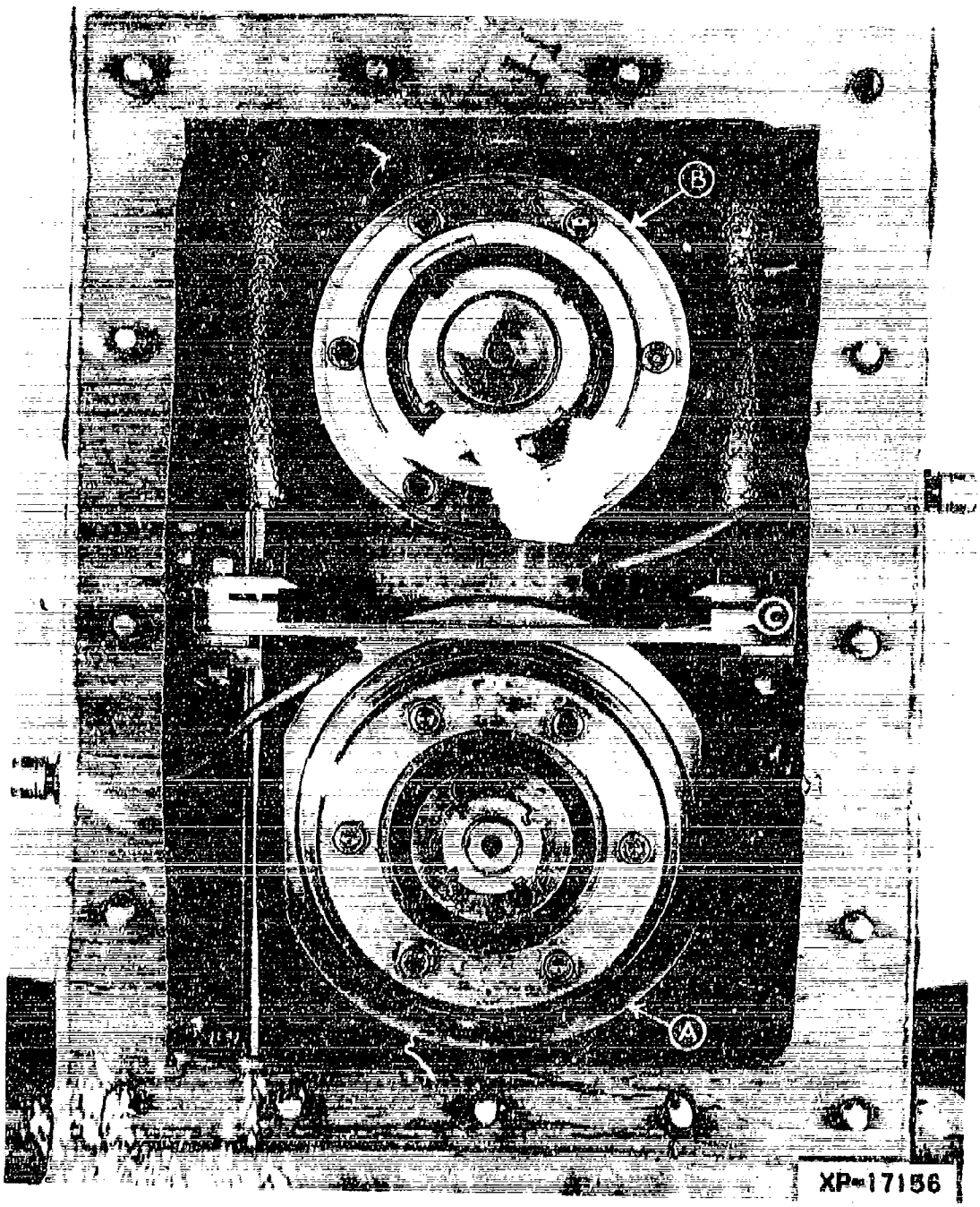
DOWNGRADED AT 3 YEAR INTERVALS
DECLASSIFIED AFTER 12 YEARS
DOD DIR 5200.10



CAGE FROM 178 MM BORE M-50 CVM BALL BEARING TESTED IN PWA-524 OIL AT 500°F.

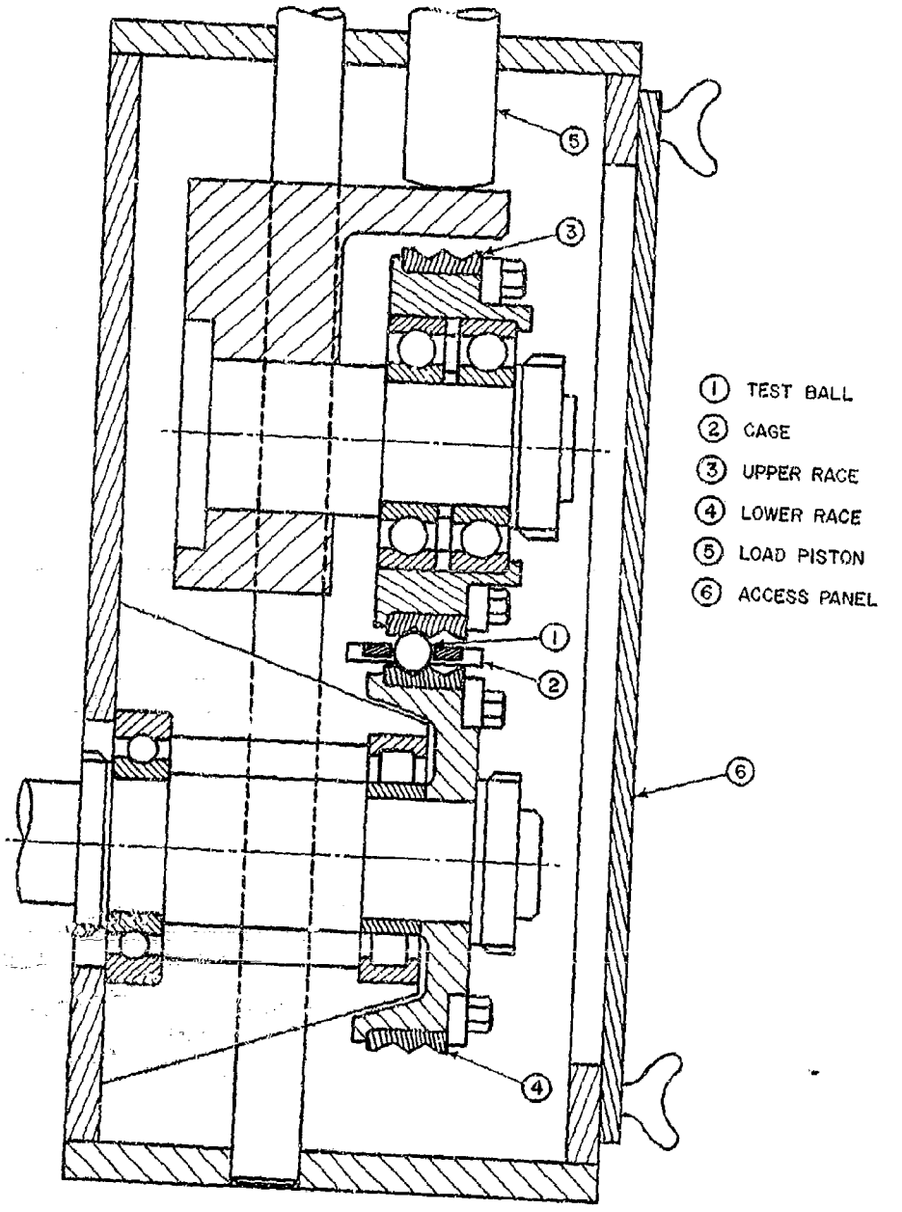
Figure 10-12

DOWNGRADED AT 3 YEAR INTERVALS
DECLASSIFIED AFTER 12 YEARS
DOD DIR 5200.10



BALL-FATIGUE TEST RIG INCLUDING (A) LOWER RACE, (B) UPPER RACE IN UP POSITION, AND (C) CAGE HOLDER.

Figure 10-13

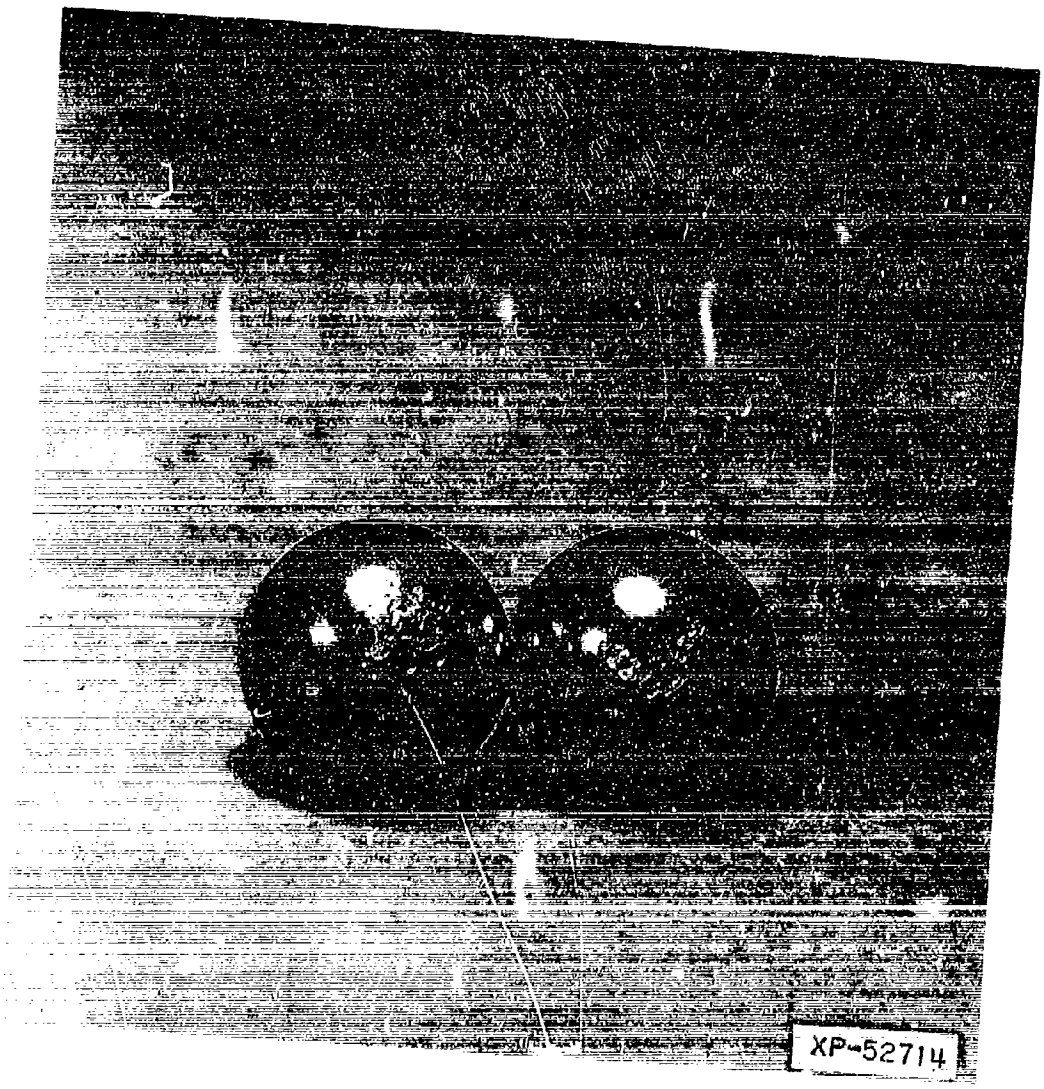


SCHEMATIC OF BALL-FATIGUE TEST RIG

Figure 10-14

DOWNGRADED AT 3 YEAR INTERVALS
DECLASSIFIED AFTER 12 YEARS
DOD DIR 5200.10

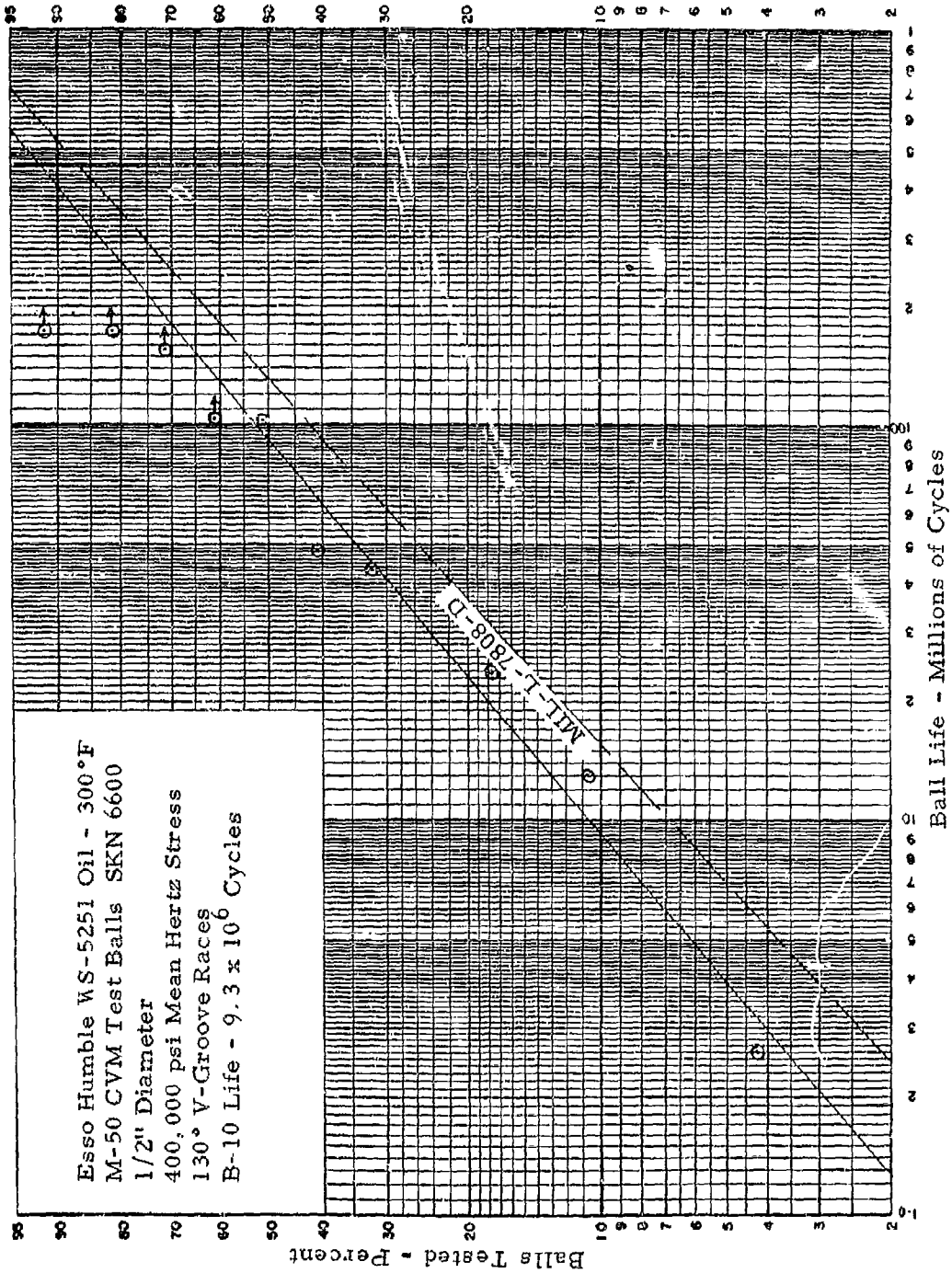
THIS DOCUMENT CONTAINS INFORMATION AFFECTING THE NATIONAL DEFENSE OF THE UNITED STATES WITHIN THE MEANING OF THE ESPIONAGE LAWS, TITLE 18, U.S.C., SECTIONS 793 AND 794. ITS TRANSMISSION OR THE REVELATION OF ITS CONTENTS IN ANY MANNER TO AN UNAUTHORIZED PERSON IS PROHIBITED BY LAW.



HALF-INCH DIAMETER M-50 CVM MATERIAL TEST BALLS SHOWING TYPICAL SPALL FAILURE OBTAINED IN BALL-FATIGUE TEST RIG.

Figure 10-15

DOWNGRADED AT 3 YEAR INTERVALS
DECLASSIFIED AFTER 12 YEARS
DOD DIR 5200.10

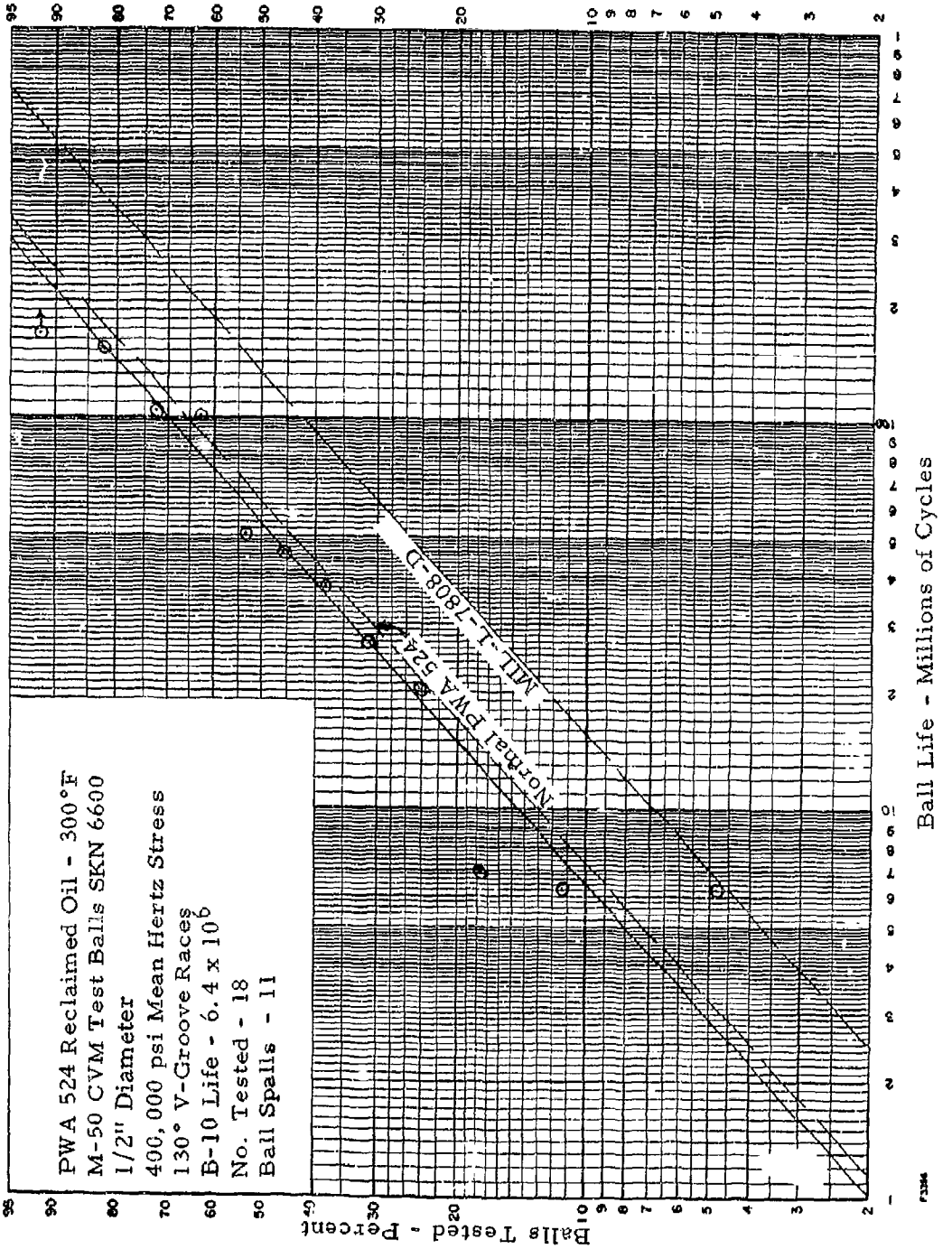


WEIBULL DISTRIBUTION OF TEST DATA FROM M-50 CVM BALLS IN HUMBLE WS-5251 OIL.

Figure 10-16

DOWNGRADED AT 3 YEAR INTERVALS
DECLASSIFIED AFTER 12 YEARS
DOD DIR 5200.10

THIS DOCUMENT CONTAINS INFORMATION AFFECTING THE NATIONAL DEFENSE OF THE UNITED STATES WITHIN THE MEANING OF THE ESPIONAGE LAWS, TITLE 18, U.S.C., SECTIONS 793 AND 794. THE TRANSMISSION OR THE REVELATION OF ITS CONTENTS IN ANY MANNER TO AN UNAUTHORIZED PERSON IS PROHIBITED BY LAW.

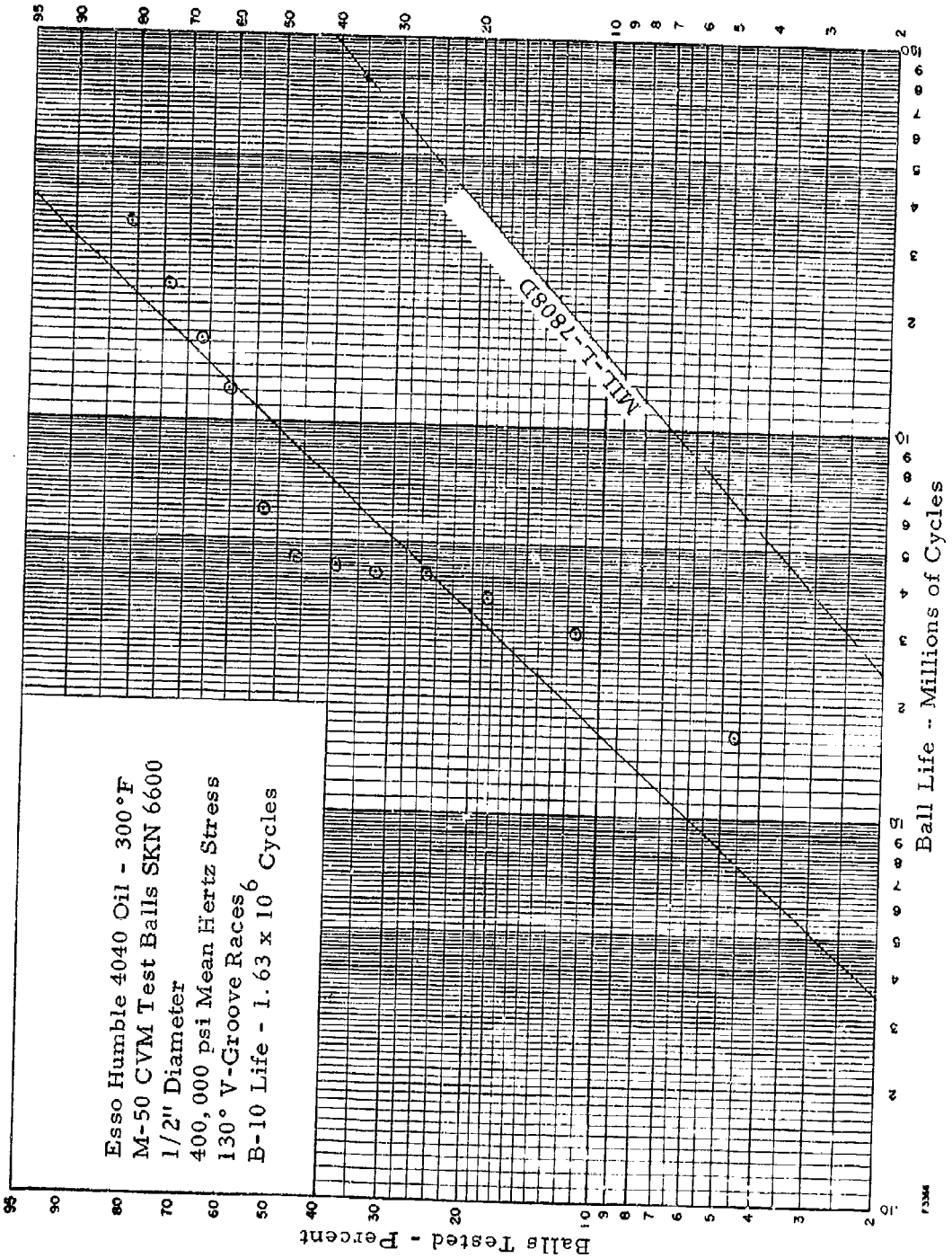


WEIBULL DISTRIBUTION OF TEST DATA FROM M-50 CVM BALLS IN PWA -524R OIL.

Figure 10-17

DOWNGRADED AT 3 YEAR INTERVALS
DECLASSIFIED AFTER 12 YEARS
DOD DIR 5200.10

THIS DOCUMENT CONTAINS INFORMATION AFFECTING THE NATIONAL DEFENSE OF THE UNITED STATES WITHIN THE MEANING OF THE ESPIONAGE LAWS, TITLE 18, U.S.C., SECTIONS 793 AND 794. ITS TRANSMISSION OR THE REVELATION OF ITS CONTENTS IN ANY MANNER TO AN UNAUTHORIZED PERSON IS PROHIBITED BY LAW.

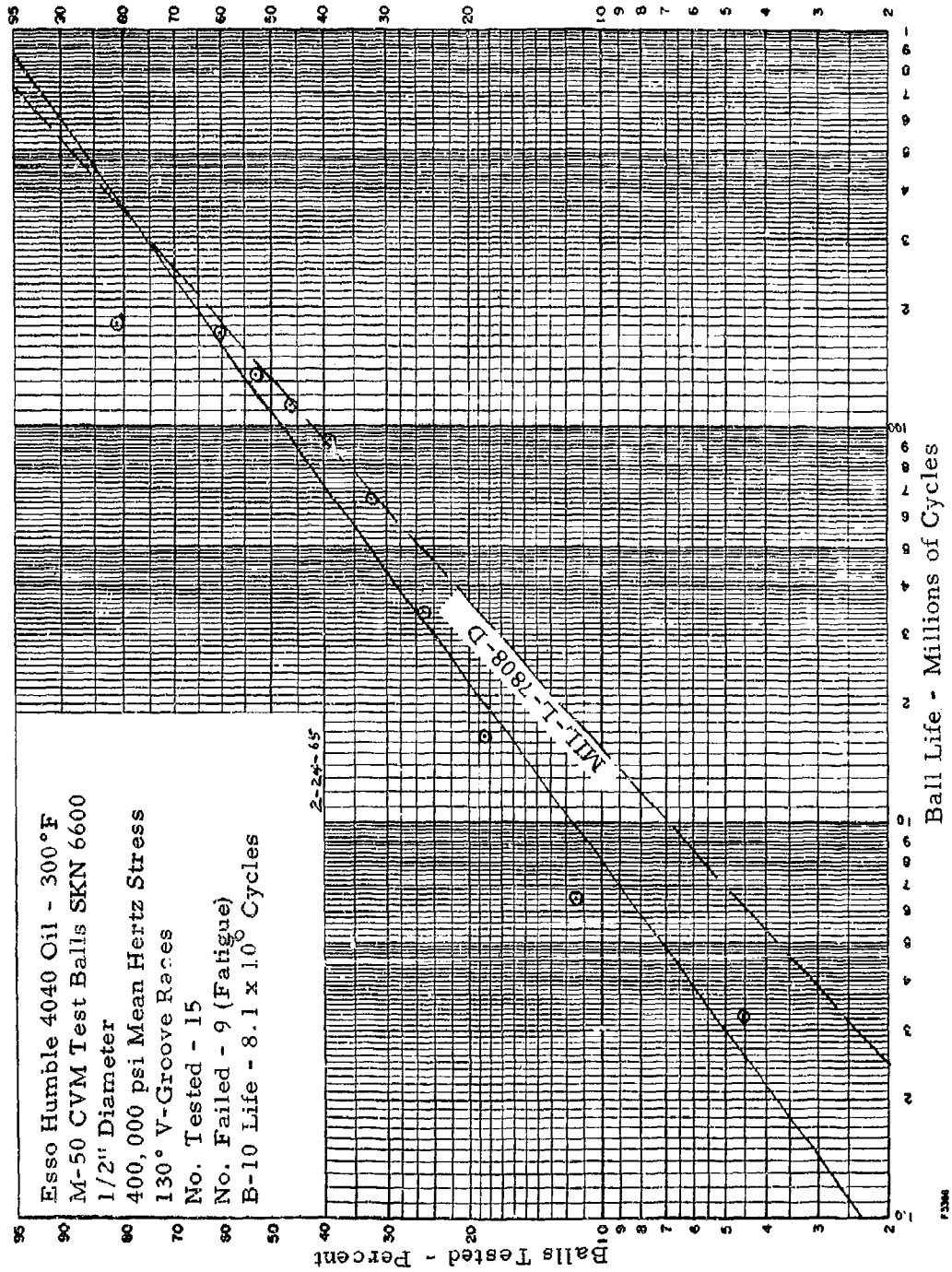


WEIBULL DISTRIBUTION OF TEST DATA FROM M-50 CVM BALLS IN HUMBLE 4040E OIL.

Figure 10-18

DOWNGRADED AT 3 YEAR INTERVALS
DECLASSIFIED AFTER 12 YEARS
DOD DIR 5200.10

THIS DOCUMENT CONTAINS INFORMATION AFFECTING THE NATIONAL DEFENSE OF THE UNITED STATES WITHIN THE MEANING OF THE ESPIONAGE LAWS, TITLE 18 U.S.C. SECTIONS 793 AND 794. ITS TRANSMISSION OR THE REVELATION OF ITS CONTENTS IN ANY MANNER TO AN UNAUTHORIZED PERSON IS PROHIBITED BY LAW

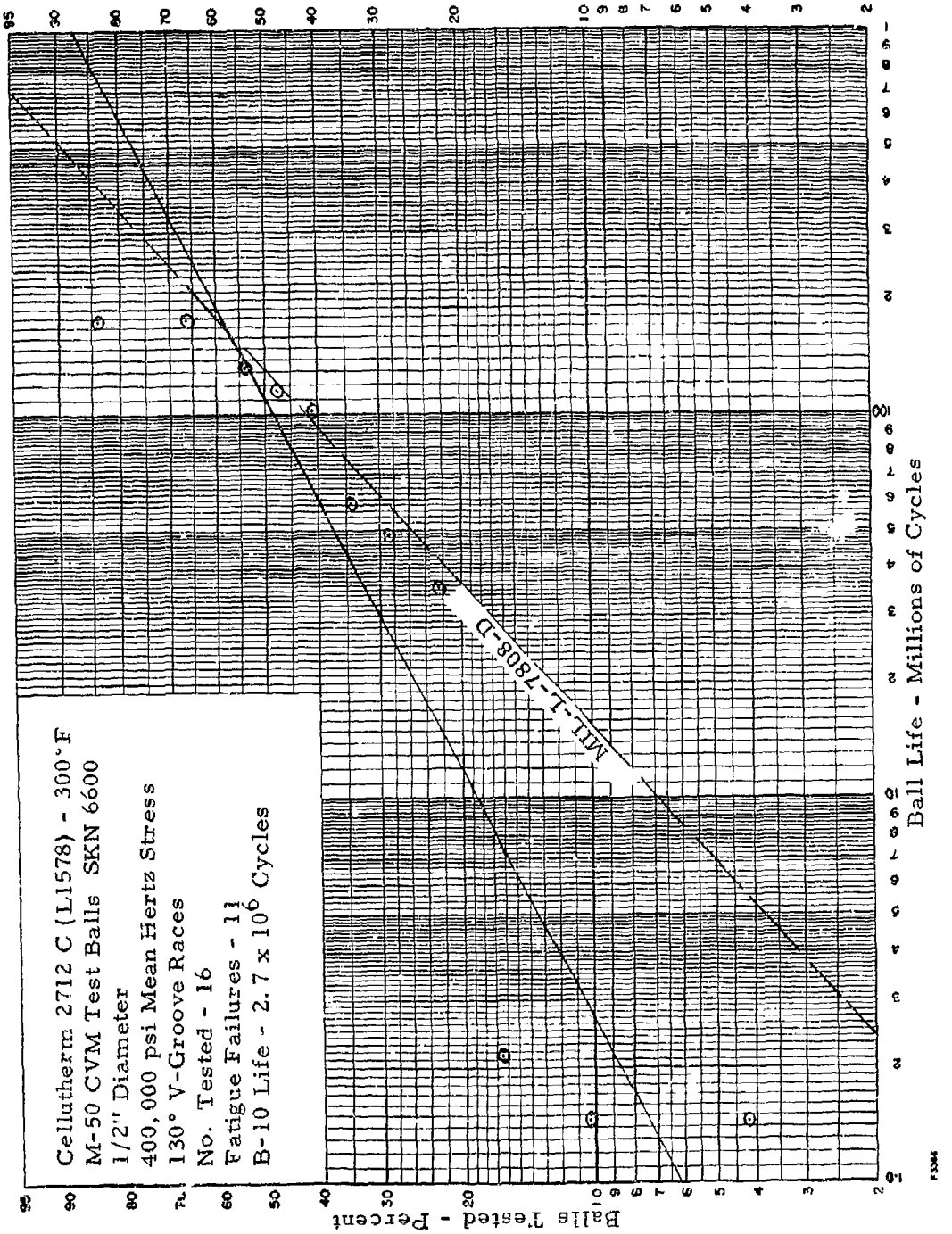


WEIBULL DISTRIBUTION OF TEST DATA FROM M-50 CVM BALLS IN HUMBLE 4040 OIL.

Figure 10-19

DECLASSIFIED AFTER 12 YEARS
DOD DIR 5200.10

THIS DOCUMENT CONTAINS INFORMATION AFFECTING THE NATIONAL DEFENSE OF THE UNITED STATES WITHIN THE MEANING OF THE ESPIONAGE LAWS, TITLE 18 U.S.C. SECTIONS 793 AND 794. THE TRANSMISSION OR THE REVELATION OF ITS CONTENTS IN ANY MANNER TO AN UNAUTHORIZED PERSON IS PROHIBITED BY LAW.

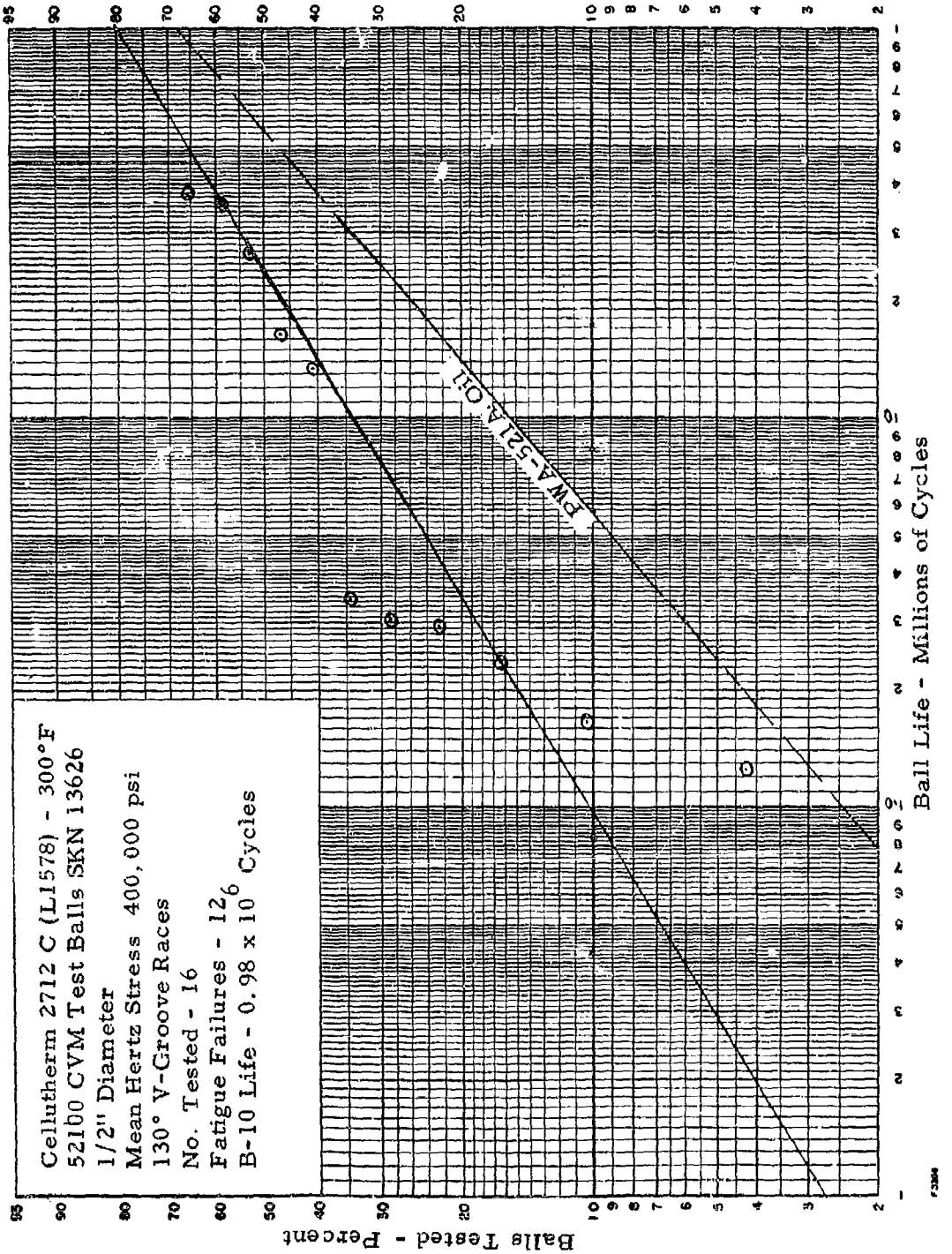


WEIBULL DISTRIBUTION OF TEST DATA FROM M-50 CVM BALLS IN CELLUTHERM 2712C OIL.

Figure 10-20

DOWNGRADED AT 3 YEAR INTERVALS
DECLASSIFIED AFTER 12 YEARS
DOD DIR 5200.10

THIS DOCUMENT CONTAINS INFORMATION AFFECTING THE NATIONAL DEFENSE OF THE UNITED STATES WITHIN THE MEANING OF THE ESPIONAGE LAWS, TITLE 18, U.S.C., SECTIONS 793 AND 794. ITS TRANSMISSION OR THE REVELATION OF ITS CONTENTS IN ANY MANNER TO AN UNAUTHORIZED PERSON IS PROHIBITED BY LAW.

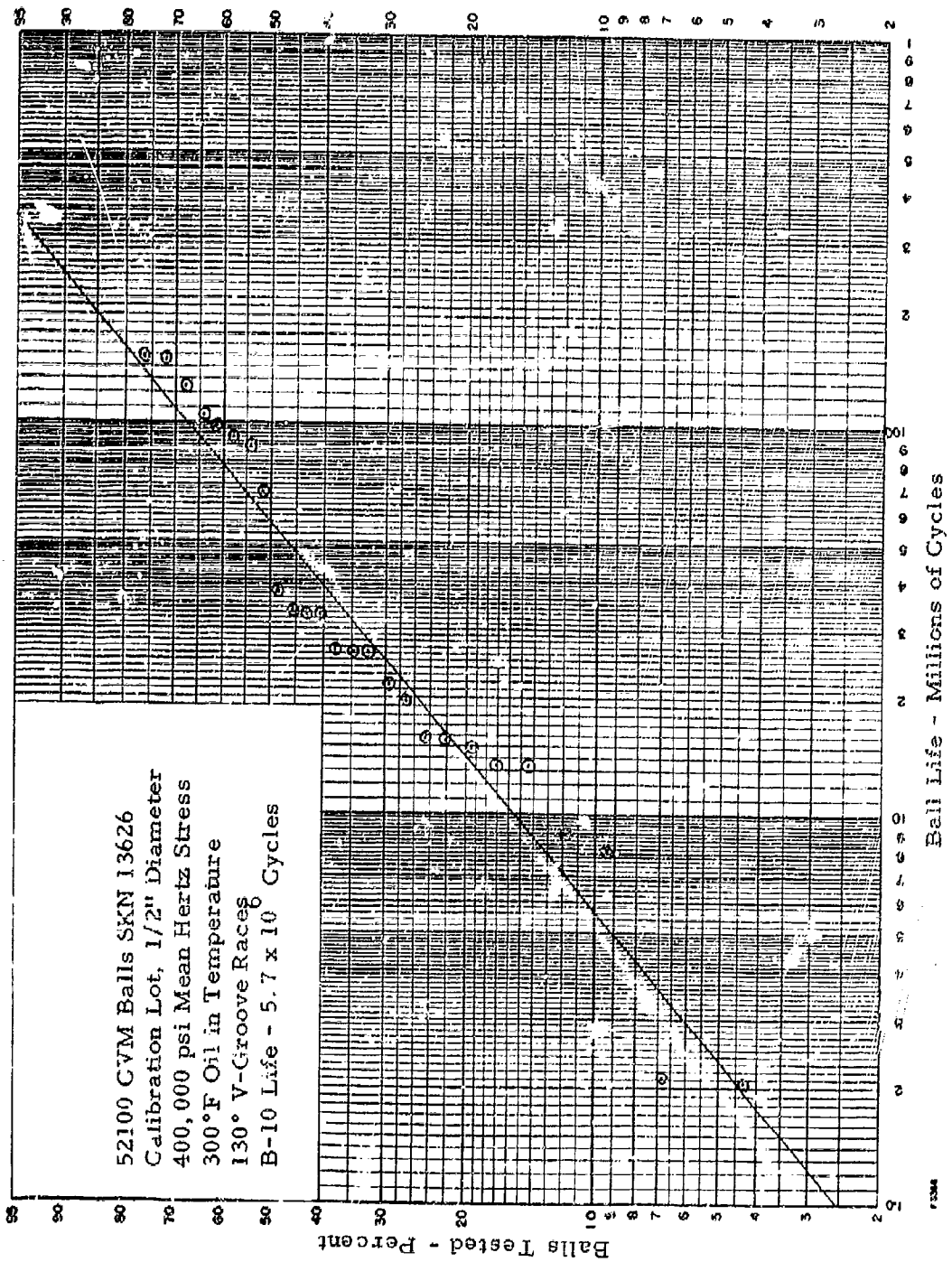


WEIBULL DISTRIBUTION OF TEST DATA FROM AISI 52100 CVM BALLS IN CELLUTHERM 2712C OIL.

Figure 10-21

DOWNGRADED AT 3 YEAR INTERVALS
DECLASSIFIED AFTER 12 YEARS
DOD DIR 5200.10

THIS DOCUMENT CONTAINS INFORMATION AFFECTING THE NATIONAL DEFENSE OF THE UNITED STATES WITHIN THE MEANING OF THE ESPIONAGE LAWS, TITLE 18 U.S.C. SECTIONS 793 AND 794. ITS TRANSMISSION OR THE REVELATION OF ITS CONTENTS IN ANY MANNER TO AN UNAUTHORIZED PERSON IS PROHIBITED BY LAW.



WEIBULL DISTRIBUTION OF TEST DATA FROM AISI 52100 CVM BALLS IN MIL-L-7808D (PWA 521A) OIL.

Figure 10-22

DOWNGRADED AT 3 YEAR INTERVALS
DECLASSIFIED AFTER 12 YEARS
DOD DIR 5200.10

THIS DOCUMENT CONTAINS INFORMATION AFFECTING THE NATIONAL DEFENSE OF THE UNITED STATES WITHIN THE MEANING OF THE ESPIONAGE LAWS, TITLE 18, U.S.C., SECTIONS 793 AND 794. ITS TRANSMISSION OR REVELATION OF ITS CONTENTS IN ANY MANNER TO AN UNAUTHORIZED PERSON IS PROHIBITED BY LAW.

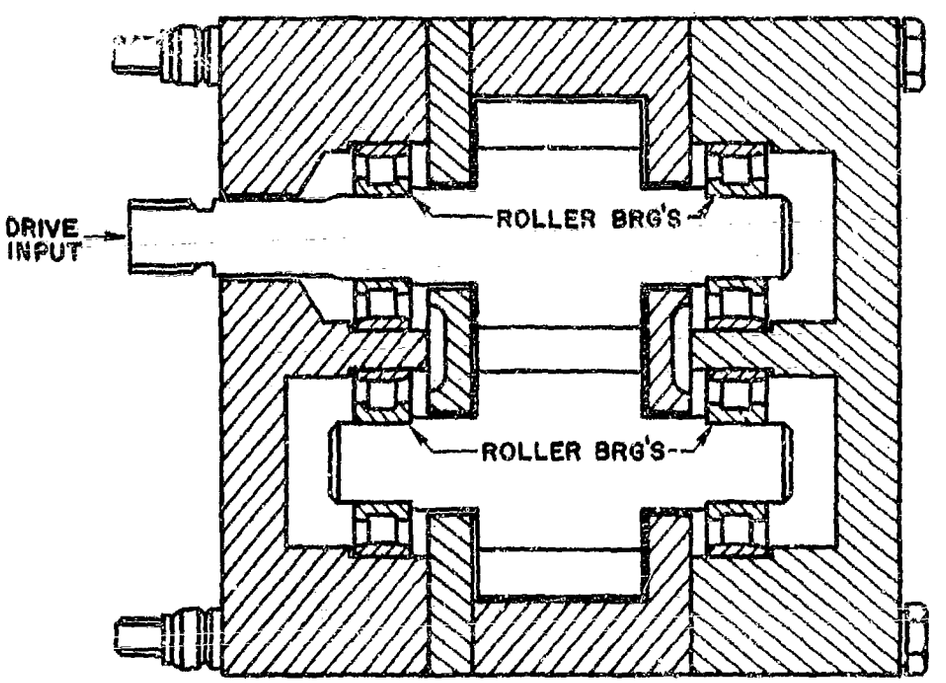
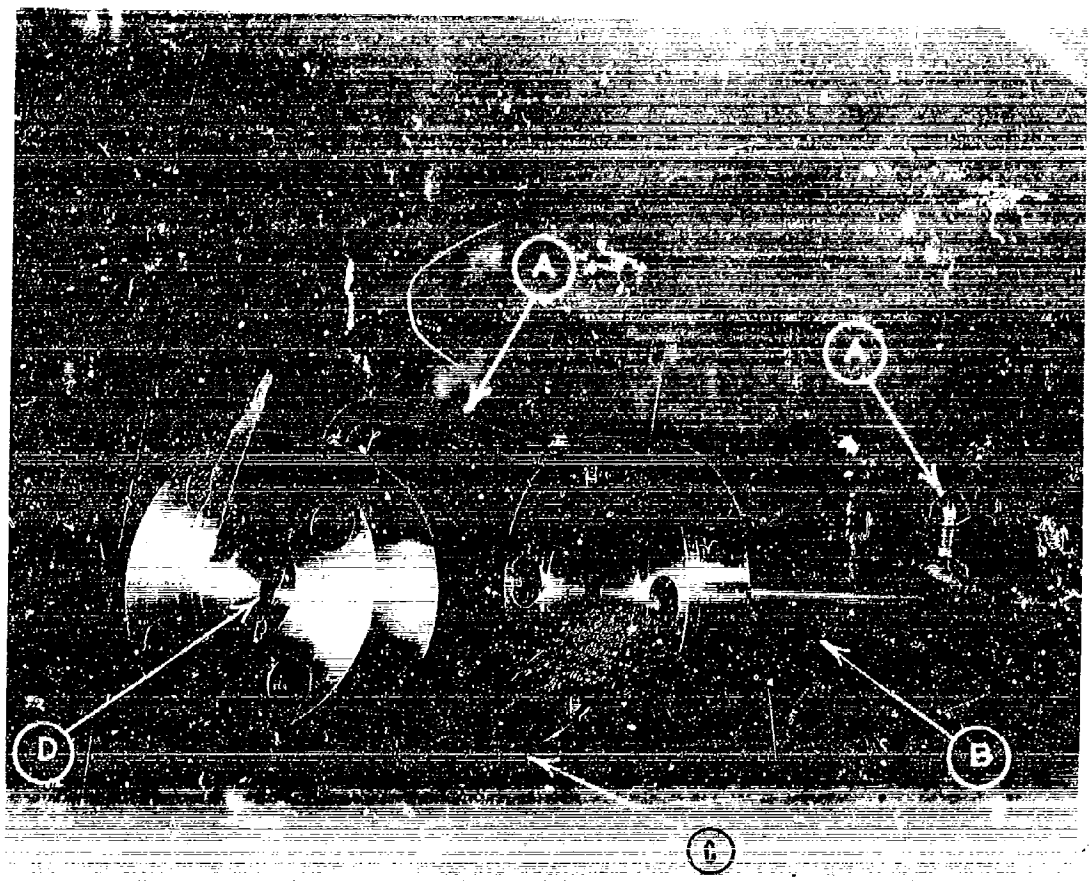


DIAGRAM OF EXPERIMENTAL OIL PUMP FEATURING ROLLER BEARINGS

Figure 10-23

DOWNGRADED AT 3 YEAR INTERVALS
DECLASSIFIED AFTER 12 YEARS
DOD DIR 5200.10

THIS DOCUMENT CONTAINS INFORMATION AFFECTING THE NATIONAL DEFENSE OF THE UNITED STATES WITHIN THE MEANING OF THE ESPIONAGE LAWS, TITLE 18 U.S.C. SECTIONS 793 AND 794. THE TRANSMISSION OR THE REVELATION OF ITS CONTENTS IN ANY MANNER TO AN UNAUTHORIZED PERSON IS PROHIBITED BY LAW.



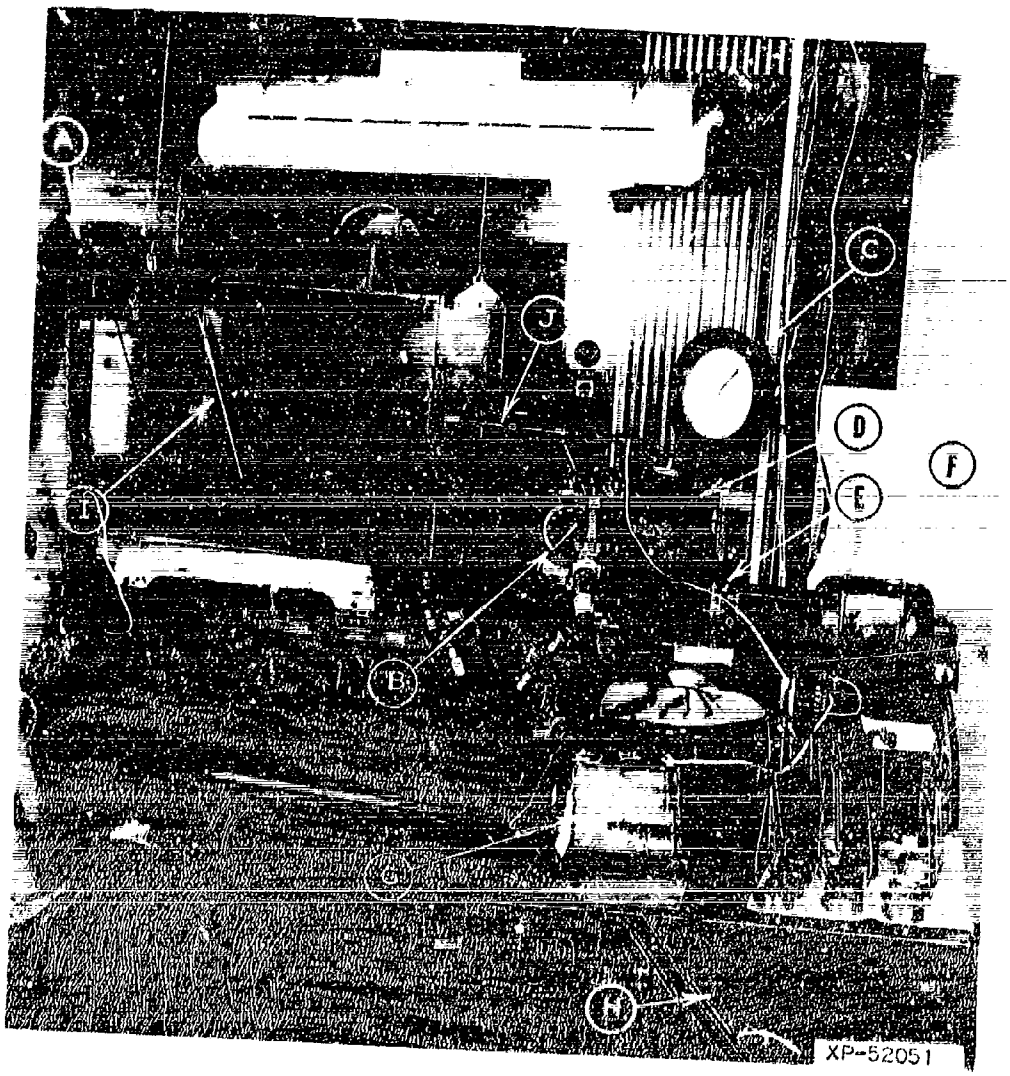
XP-52008

OIL JET TEST CONFIGURATION SHOWING (A) PRESSURE TAPS (B) INLET JET, (C) O-RING SEAL, AND (D) ORIFICE

Figure 10-24

DOWNGRADED AT 3 YEAR INTERVALS
DECLASSIFIED AFTER 12 YEARS
DOD DIR 5200.10

THIS DOCUMENT CONTAINS INFORMATION AFFECTING THE NATIONAL DEFENSE OF THE UNITED STATES WITHIN THE MEANING OF THE ESPIONAGE LAWS, TITLE 18, U.S.C., SECTIONS 793 AND 794. ITS TRANSMISSION OR THE REVELATION OF ITS CONTENTS IN ANY MANNER TO AN UNAUTHORIZED PERSON IS PROHIBITED BY LAW.



OIL JET TEST RIG SHOWING (A) SCALE FOR FLOW MEASUREMENT, (B) PRESSURE DROP GAUGE, (C) PRESSURE GAUGE, (D) ACCUMULATOR (E) PUMP, (F) MOTOR, (G) TEMPERATURE METER, (H) OIL TANK, (I) SHIELD AND (J) OIL JET.

Figure 10-25

DOWNGRADED AT 3 YEAR INTERVALS
DECLASSIFIED AFTER 12 YEARS
DOD DIR 5200.10

THIS DOCUMENT CONTAINS INFORMATION AFFECTING THE NATIONAL DEFENSE OF THE UNITED STATES WITHIN THE MEANING OF THE ESPIONAGE LAWS, TITLE 18, U.S.C. SECTIONS 793 AND 794. ITS TRANSMISSION OR THE REVELATION OF ITS CONTENTS IN ANY MANNER TO AN UNAUTHORIZED PERSON IS PROHIBITED BY LAW.

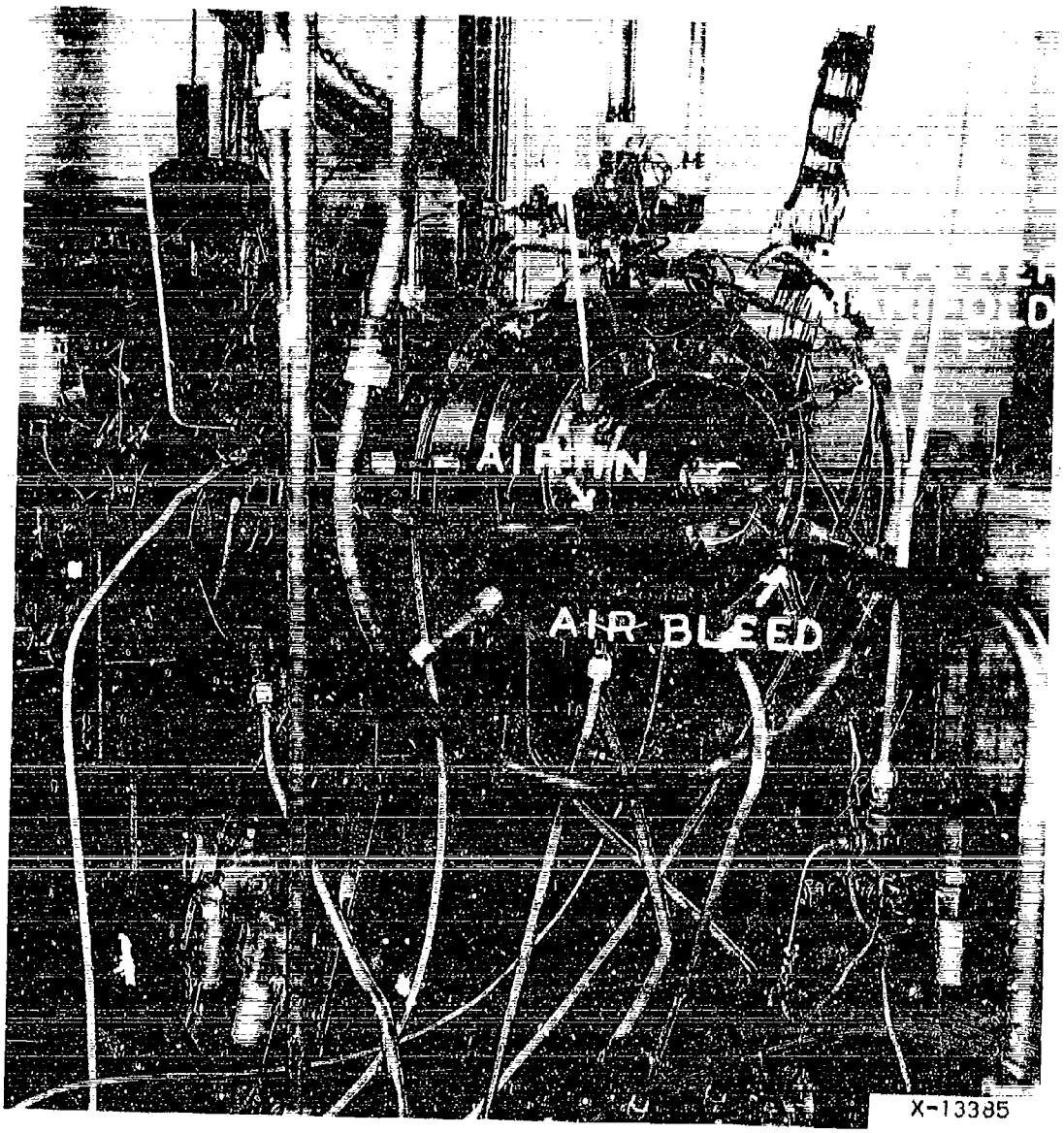


COMPONENT PARTS OF OIL SEAL TESTING RIG INCLUDING (A) FRONT COVER, (B) RIG BEARING, (C) HUB, (D) OIL JET TO SEAL PLATE, (E) BREATHER MANIFOLD, AND (F) SHAFT

Figure 10-26

DOWNGRADED AT 3 YEAR INTERVALS
DECLASSIFIED AFTER 12 YEARS
DOD DIR 5200.10

THIS DOCUMENT CONTAINS INFORMATION AFFECTING THE NATIONAL DEFENSE OF THE UNITED STATES WITHIN THE MEANING OF THE ESPIONAGE LAWS, TITLE 18, U.S.C., SECTIONS 793 AND 794. ITS TRANSMISSION OR THE REVELATION OF ITS CONTENTS IN ANY MANNER TO AN UNAUTHORIZED PERSON IS PROHIBITED BY LAW.

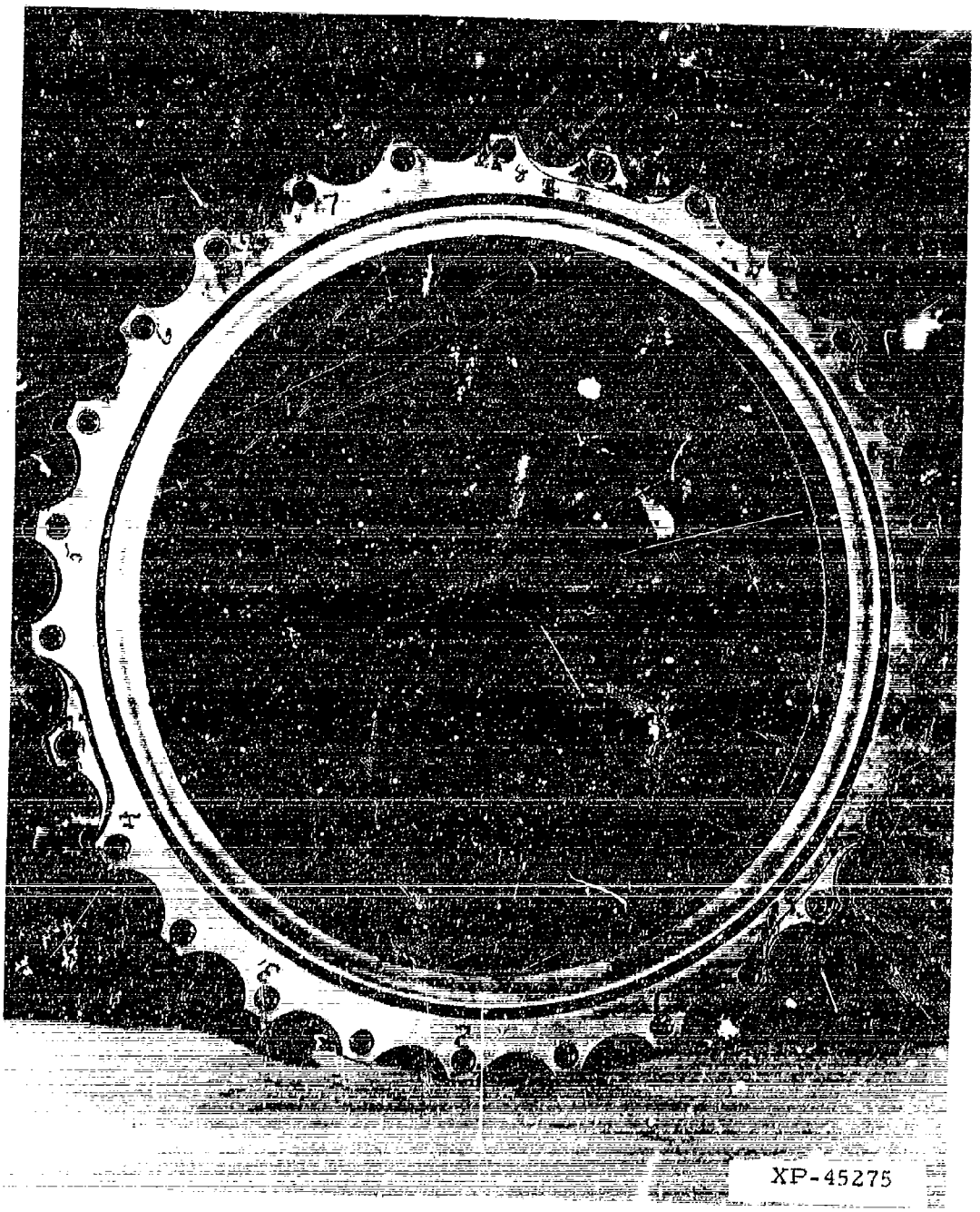


FACE SEAL HIGH-TEMPERATURE TEST RIG INSTALLATION.

Figure 10-27

DOWNGRADED AT 3 YEAR INTERVALS
DECLASSIFIED AFTER 12 YEARS
DOD DIR 5200.10

THIS DOCUMENT CONTAINS INFORMATION AFFECTING THE NATIONAL DEFENSE OF THE UNITED STATES WITHIN THE MEANING OF THE ESPIONAGE LAWS, TITLE 18, U.S.C., SECTIONS 793 AND 794. ITS TRANSMISSION OR THE REVELATION OF ITS CONTENTS IN ANY MANNER TO AN UNAUTHORIZED PERSON IS PROHIBITED BY LAW.

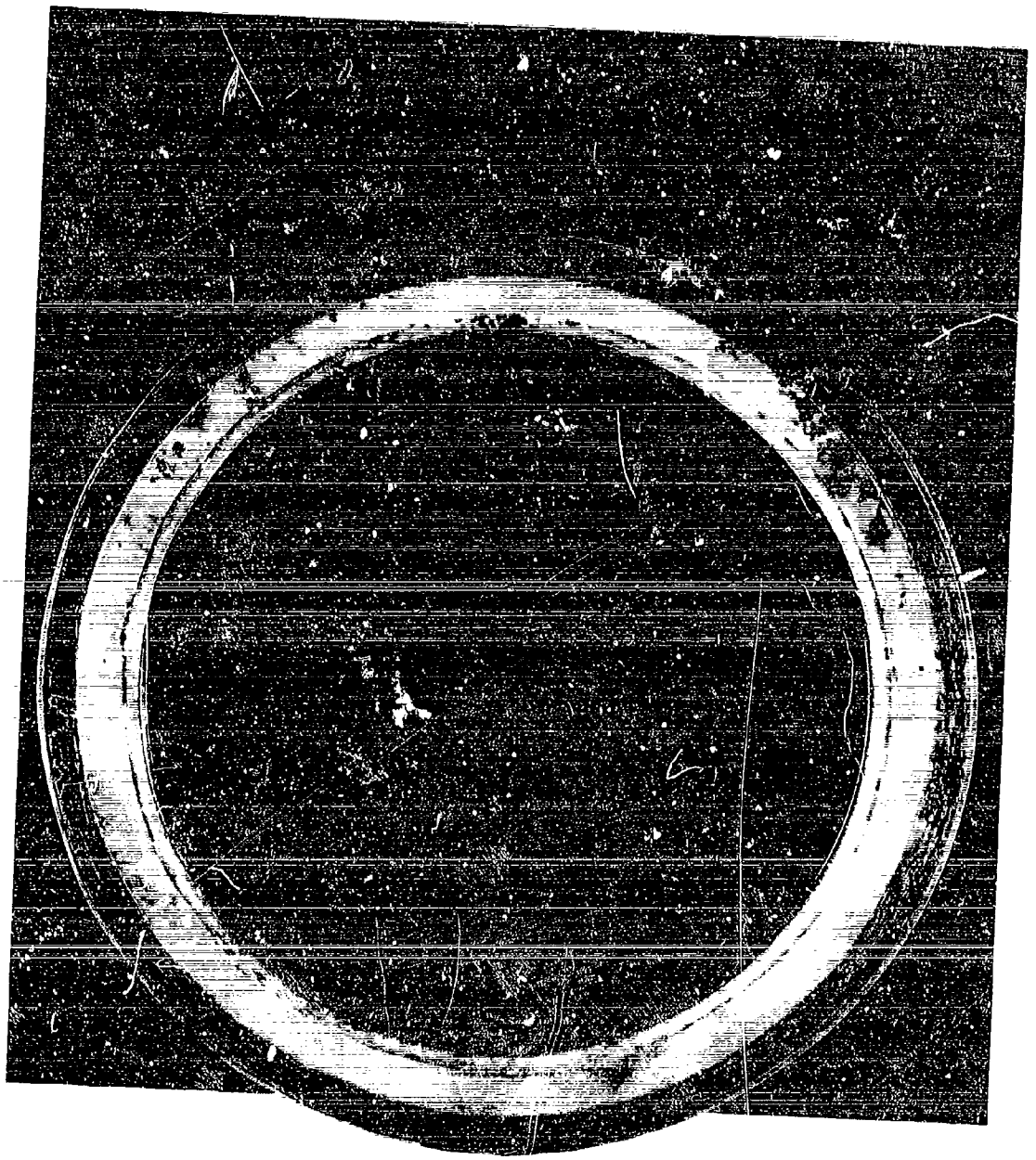


CDJ-83 MATERIAL CARBON RUN FOR 57.5 HOURS AT 40 PSI, 400°F, AND 12,500 RPM.

Figure 10-28

DOWNGRADED AT 3 YEAR INTERVALS
DECLASSIFIED AFTER 12 YEARS
DOD DIR 5200.10

THIS DOCUMENT CONTAINS INFORMATION AFFECTING THE NATIONAL DEFENSE OF THE UNITED STATES WITHIN THE MEANING OF THE ESPIONAGE LAWS, TITLE 18, U.S.C., SECTIONS 793 AND 794. THE TRANSMISSION OR THE REVELATION OF ITS CONTENTS IN ANY MANNER TO AN UNAUTHORIZED PERSON IS PROHIBITED BY LAW.

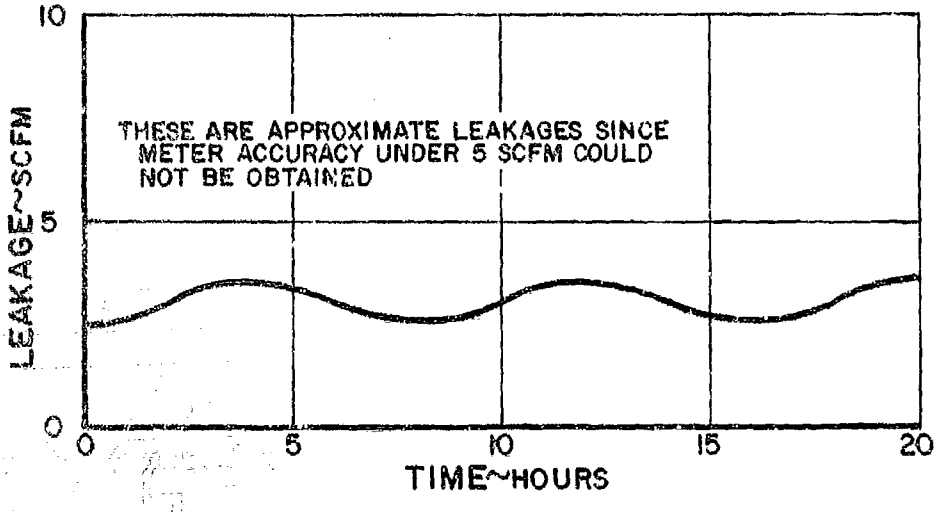


DRY-FACE SEAL PLATE RUN FOR 57.5 HOURS AT 40 PSI, 400°F AND 12,500 RPM.

Figure 10-29

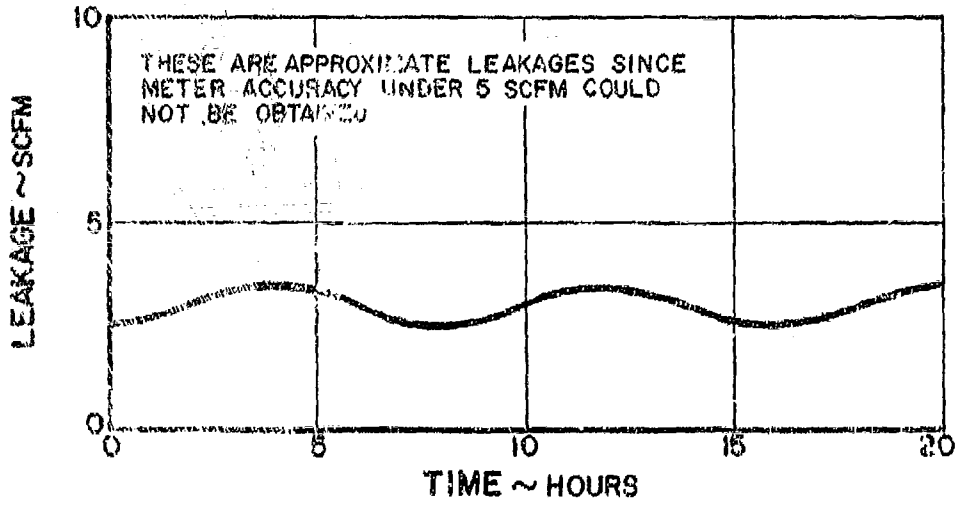
DOWNGRADED AT 3 YEAR INTERVALS
DECLASSIFIED AFTER 12 YEARS
DOD DIR 5200.10

THIS DOCUMENT CONTAINS INFORMATION AFFECTING THE NATIONAL DEFENSE OF THE UNITED STATES WITHIN THE MEANING OF THE ESPIONAGE LAWS, TITLE 18 U.S.C. SECTIONS 793 AND 794. ITS TRANSMISSION OR THE REVELATION OF ITS CONTENTS IN ANY MANNER TO AN UNAUTHORIZED PERSON IS PROHIBITED BY LAW.



TIME VS. LEAKAGE EFFECTS WITH A PO3XHT CARBON (.200 LIP) AND WET-FACE PLATE COMBINATION.

Figure 10-30

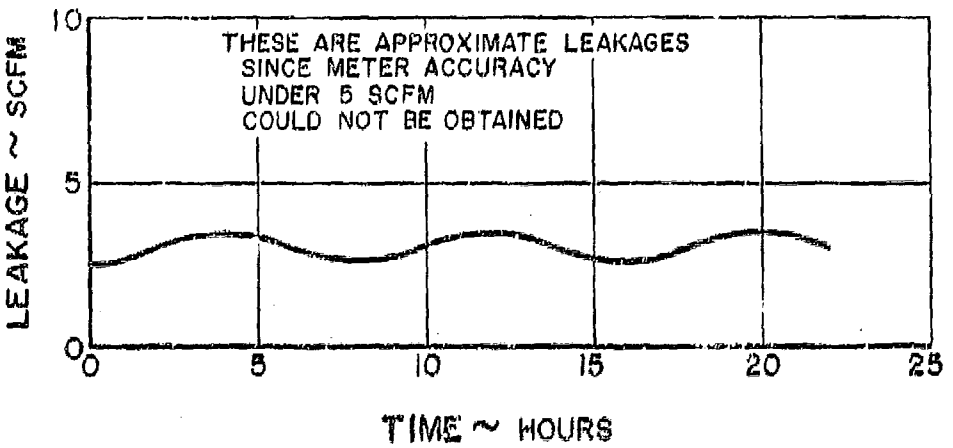


TIME VS. LEAKAGE EFFECTS WITH A CDJ-83 CARBON (.150 LIP) AND WET-FACE PLATE COMBINATION.

Figure 10-31

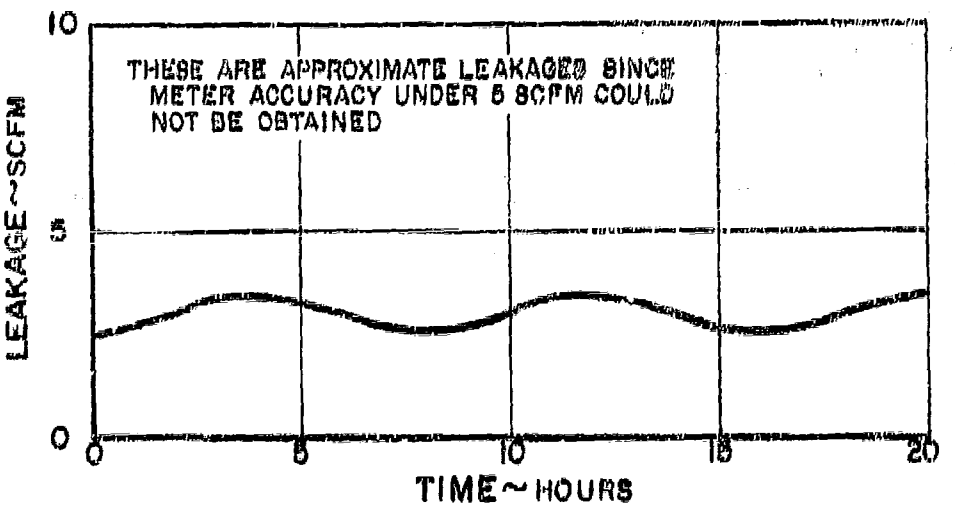
DOWNGRADED AT 3 YEAR INTERVALS
DECLASSIFIED AFTER 12 YEARS
DOD DIR 5200.10

THIS DOCUMENT CONTAINS INFORMATION AFFECTING THE NATIONAL DEFENSE OF THE UNITED STATES WITHIN THE MEANING OF THE ESPIONAGE LAWS, TITLE 18, U.S.C., SECTIONS 793 AND 794. THE TRANSMISSION OR THE REVELATION OF ITS CONTENTS IN ANY MANNER TO AN UNAUTHORIZED PERSON IS PROHIBITED BY LAW.



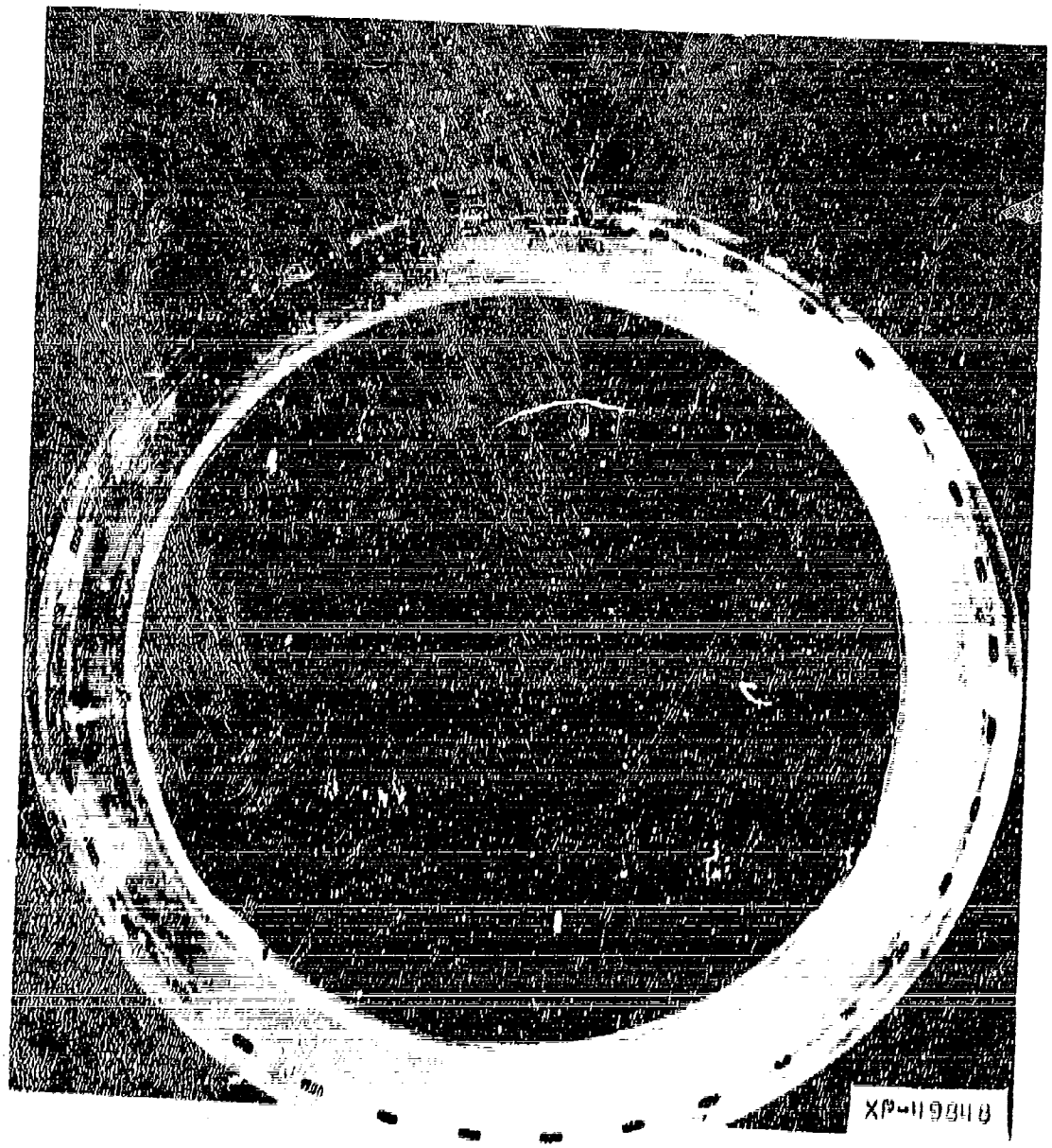
TIME VS. LEAKAGE EFFECTS WITH A PO3XHT CARBON (.200 LIP) AND WET-FACE PLATE COMBINATION.

Figure 10-32



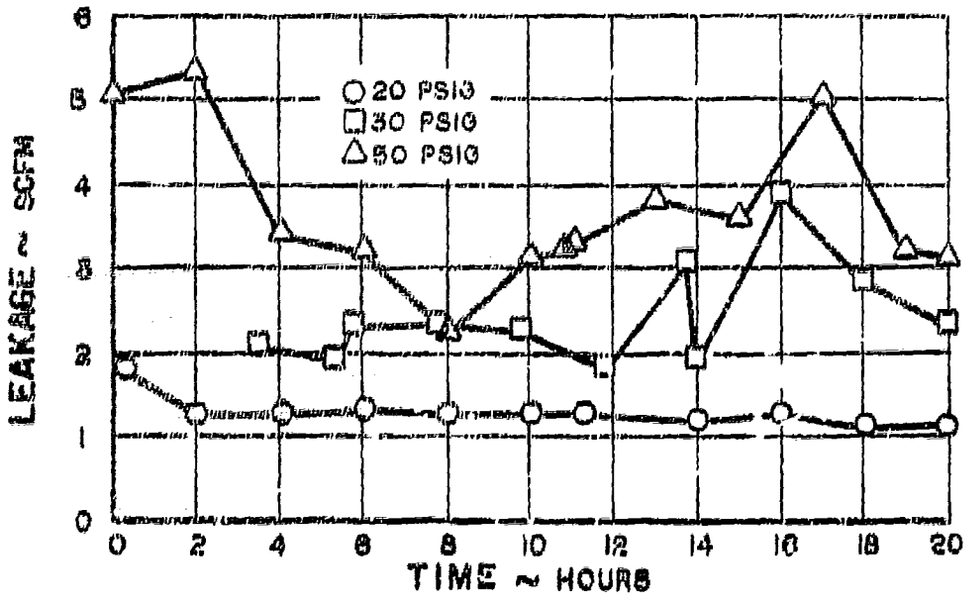
TIME VS. LEAKAGE EFFECTS WITH A CDJ-83 CARBON (.150 LIP) AND WET-FACE PLATE COMBINATION.

Figure 10-33



WET-FACE SEAL PLATE RUN FOR 45.5 HOURS AT 50 PSI, 400°F and 12,500 RPM.

Figure 10-34



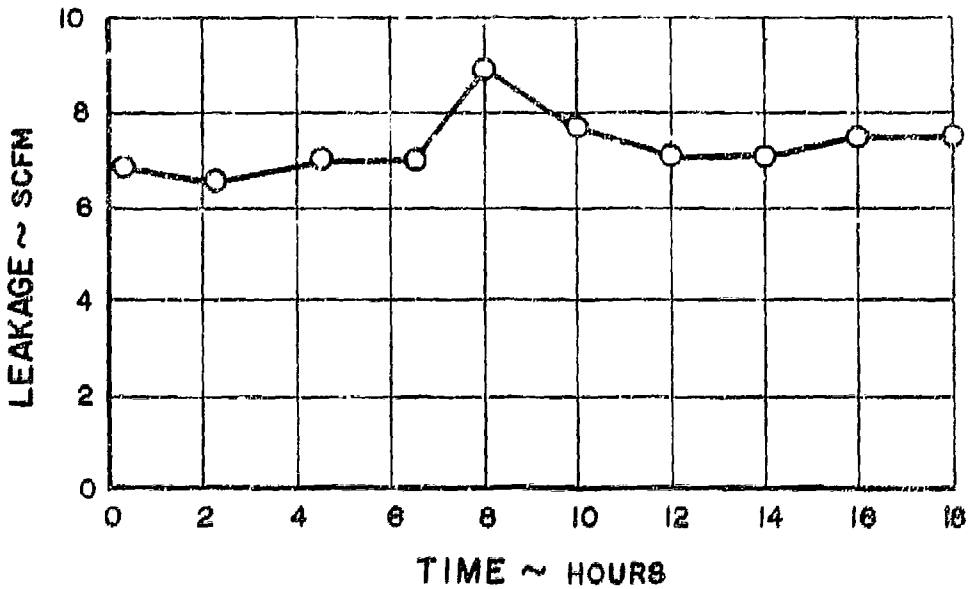
TIME VS. LEAKAGE EFFECT WITH A CDJ-63 (.150 LIP) CARBON SEAL AND WET-FACE SEAL PLATE COMBINATION AT VARIED PRESSURES.

Figure 10-35



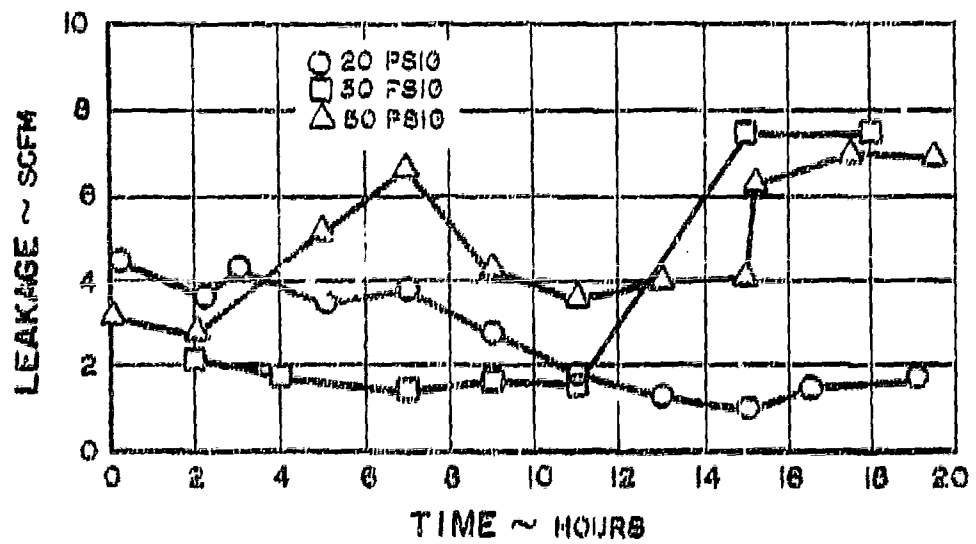
WET-FACE SEAL PLATE RUN FOR 89.75 HOURS AT 10-50 PSI, 400°F AND 12,500 RPM.

Figure 10-36



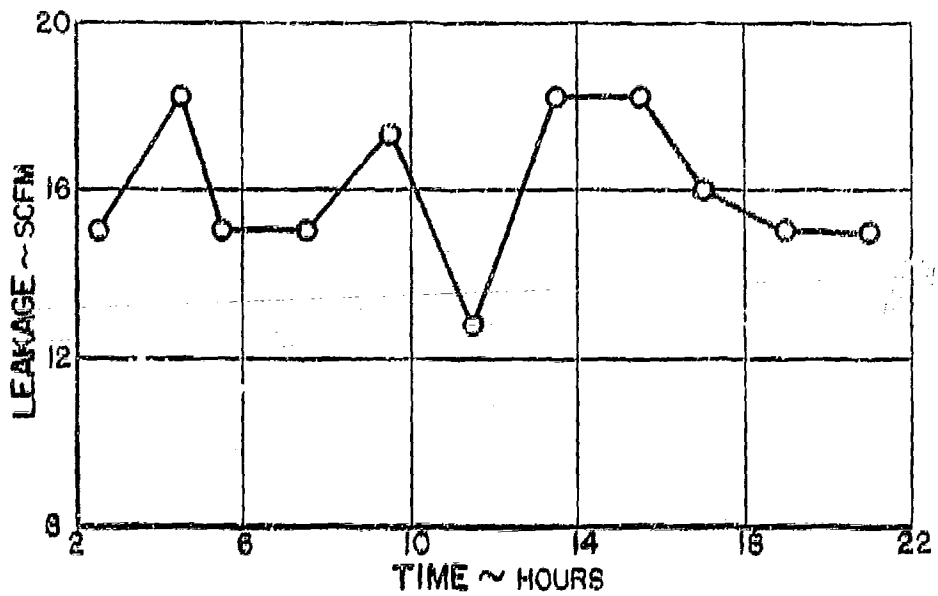
TIME VS. LEAKAGE EFFECT WITH A CDJ-83 (.150 LIP) CARBON SEAL AND WET-FACE PLATE COMBINATION

Figure 10-37



TIME VS. LEAKAGE EFFECT WITH A CDJ-8 (75% UNBALANCE) CARBON SEAL AND WET FACE PLATE COMBINATION.

Figure 10-38



TIME VS. LEAKAGE EFFECT WITH A CDJ-83 (55% UNBALANCE) CARBON SEAL AND WET-FACE SEAL PLATE COMBINATION.

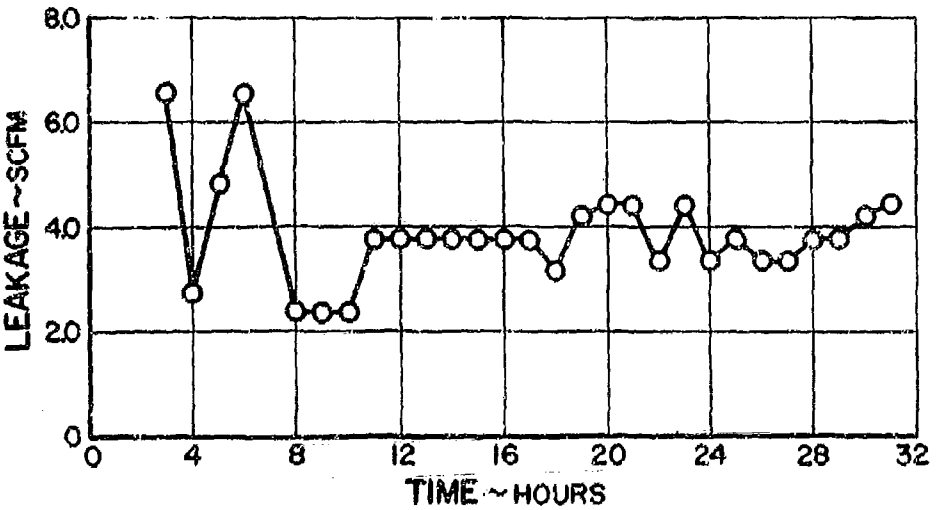
Figure 10-39



XP-51849

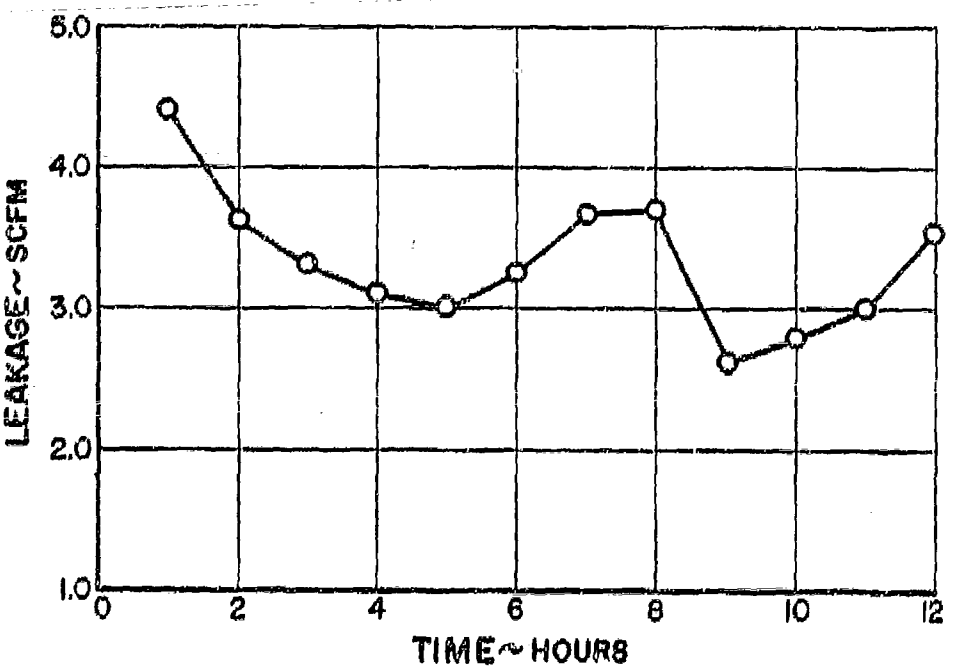
WET-FACE SEAL PLATE RUN FOR 129 HOURS AT 10-50 PSI, 400°F, AND 12,500 RPM.

Figure 10-40



TIME VS. LEAKAGE EFFECTS WITH A CDJ-83 (.250 LIP) CARBON SEAL AND WET-FACE PLATE COMBINATION.

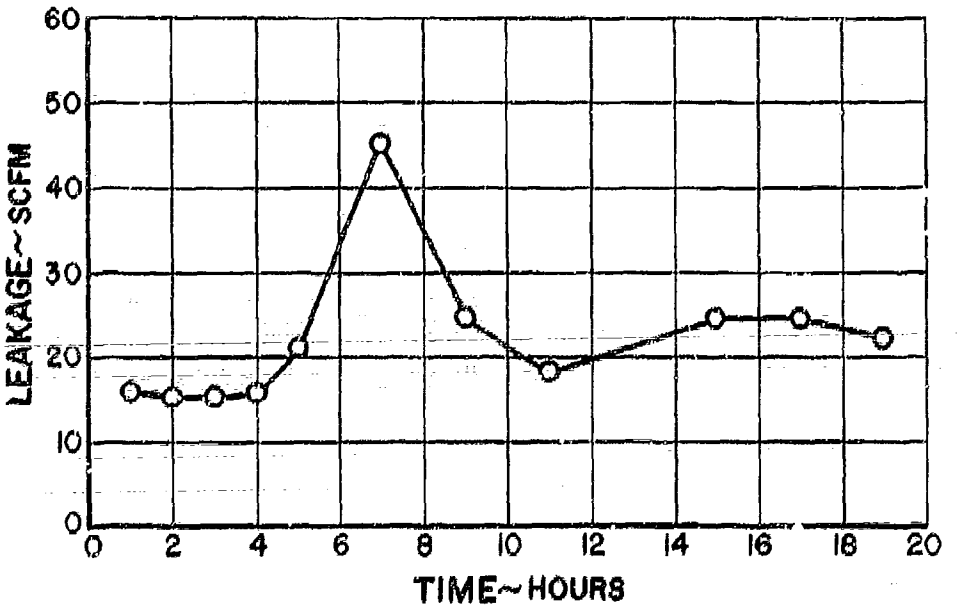
Figure 10-41



TIME VS. LEAKAGE EFFECTS WITH A CDJ-83 (.150 LIP) CARBON SEAL AND WET-FACE PLATE COMBINATION.

Figure 10-42

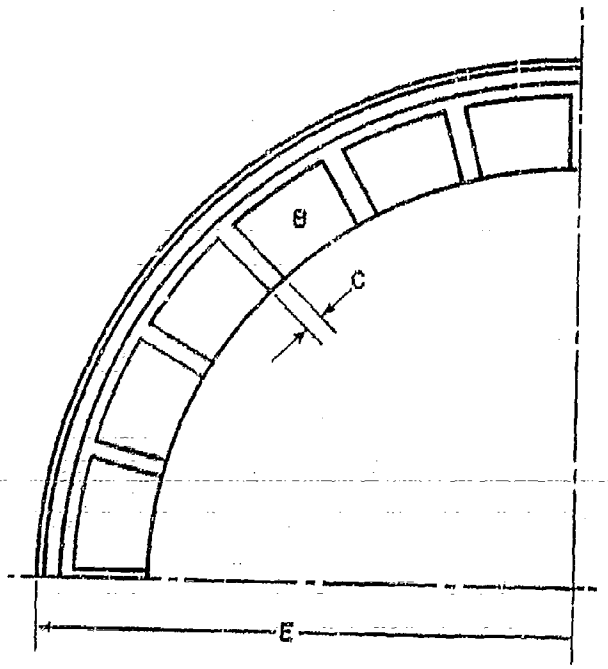
DOWNGRADED AT 3 YEAR INTERVALS
DECLASSIFIED AFTER 12 YEARS
DOD DIR 5200.10

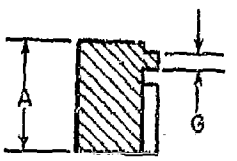


TIME VS. LEAKAGE EFFECT WITH A CDJ-83 (.200 LIP) CARBON SEAL AND WET-FACE PLATE COMBINATION.

Figure 10-43

DOWNGRADED AT 3 YEAR INTERVALS
DECLASSIFIED AFTER 12 YEARS
DOD DIR 5200.10





VARIABLES AND LEVELS

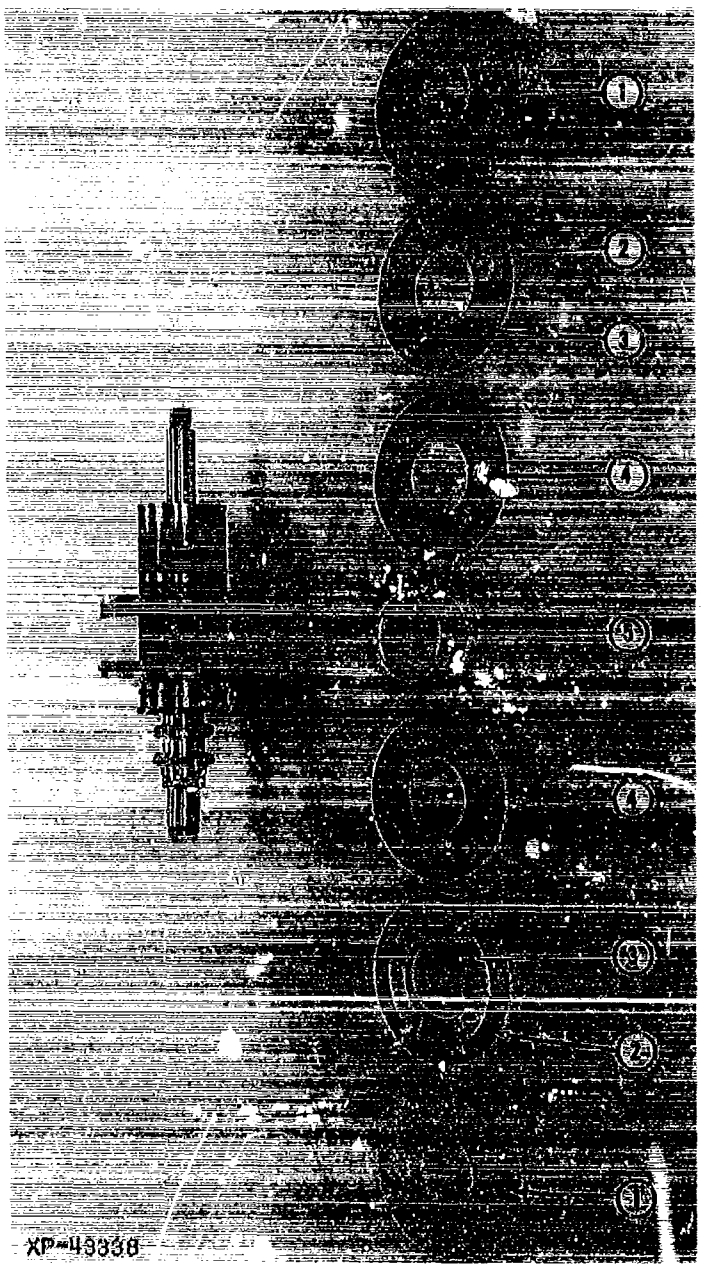
A – THICKNESS: 0.2, 0.8 INCH
B – NO. OF PADS PER INCH OF DIA: 4, 6
C – GROOVE WIDTH: 0.125, 0.200 INCH
E – OUTSIDE DIA: 6, 8 INCHES
G – LIP WIDTH: 0.025, 0.050 INCH

RADIAL GROOVE-TYPE RING SEAL LAYOUT.

Figure 10-44

DOWNGRADED AT 3 YEAR INTERVALS
DECLASSIFIED AFTER 12 YEARS
DOD DIR 5200.10

THIS DOCUMENT CONTAINS INFORMATION AFFECTING THE NATIONAL DEFENSE OF THE UNITED STATES WITHIN THE MEANING OF THE ESPIONAGE LAWS, TITLE 18, U.S.C., SECTIONS 793 AND 794. THE TRANSMISSION OR THE REVELATION OF ITS CONTENTS IN ANY MANNER TO AN UNAUTHORIZED PERSON IS PROHIBITED BY LAW.

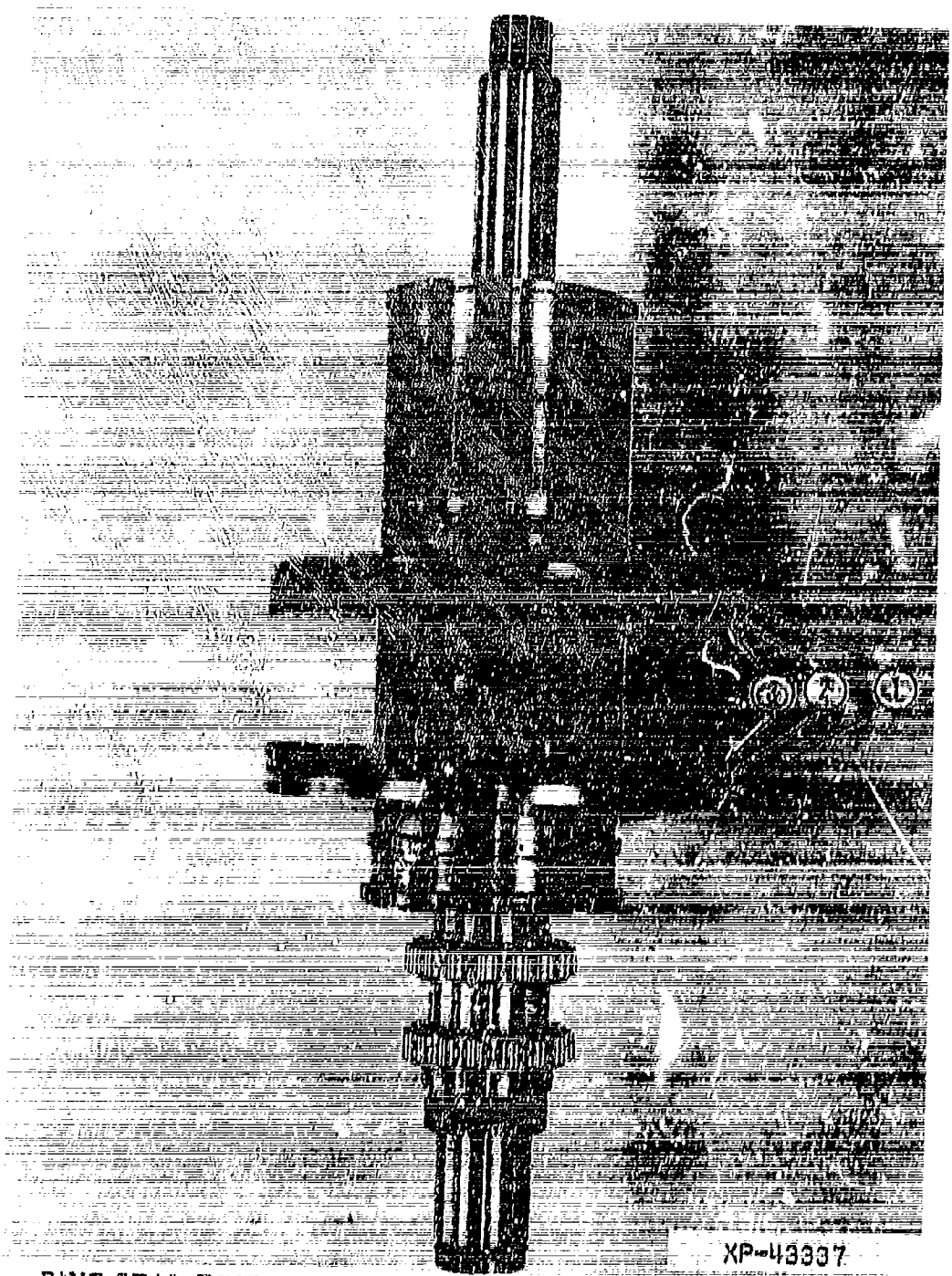


RING SEAL TEST SHAFT AND DETAILS, INCLUDING (1) SEAL PLATE, (2) TEST CARBON RING SEAL, (3) SPACER, (4) BACK-UP PLATE, AND (5) SPACER.

Figure 10-45

DOWNGRADED AT 3 YEAR INTERVALS
DECLASSIFIED AFTER 12 YEARS
DOD DIR 5200.10

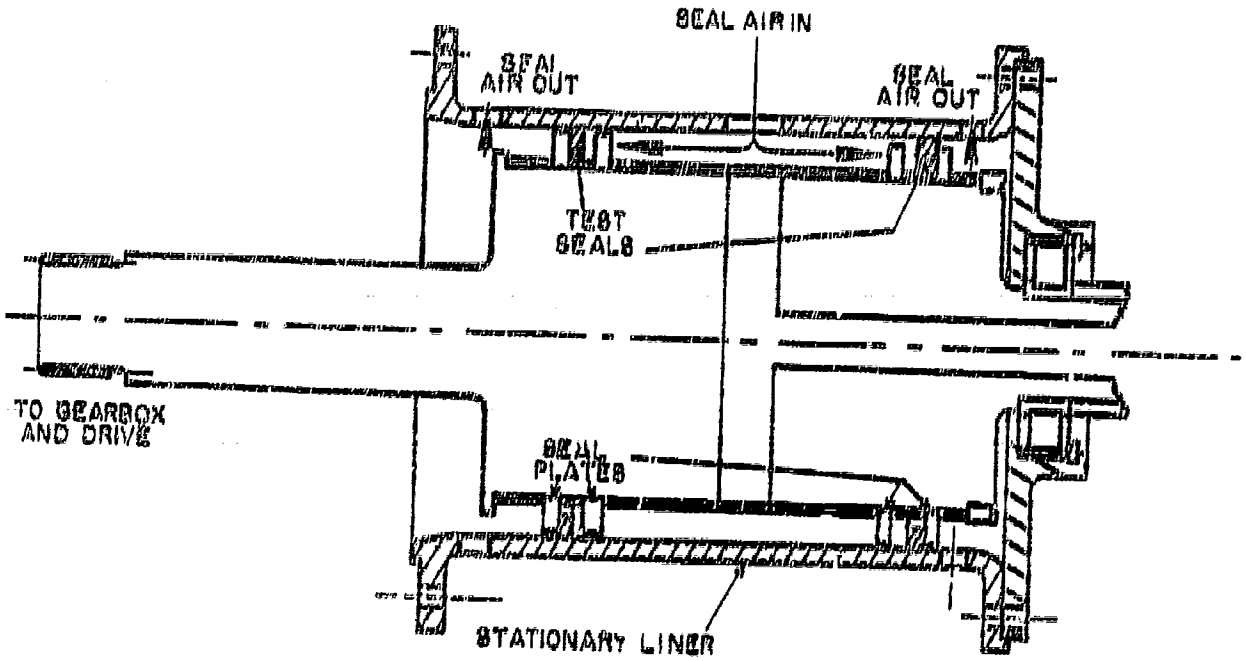
THIS DOCUMENT CONTAINS INFORMATION AFFECTING THE NATIONAL DEFENSE OF THE UNITED STATES WITHIN THE MEANING OF THE ESPIONAGE LAWS, TITLE 18 U. S. C. SECTIONS 793 AND 794. ITS TRANSMISSION OR THE REVELATION OF ITS CONTENTS IN ANY MANNER TO AN UNAUTHORIZED PERSON IS PROHIBITED BY LAW



RING SEAL TEST SHAFT ASSEMBLED, SHOWING (1) BACK-UP PLATE, (2) TEST CARBON RING SEAL, AND (3) SEAL PLATE.

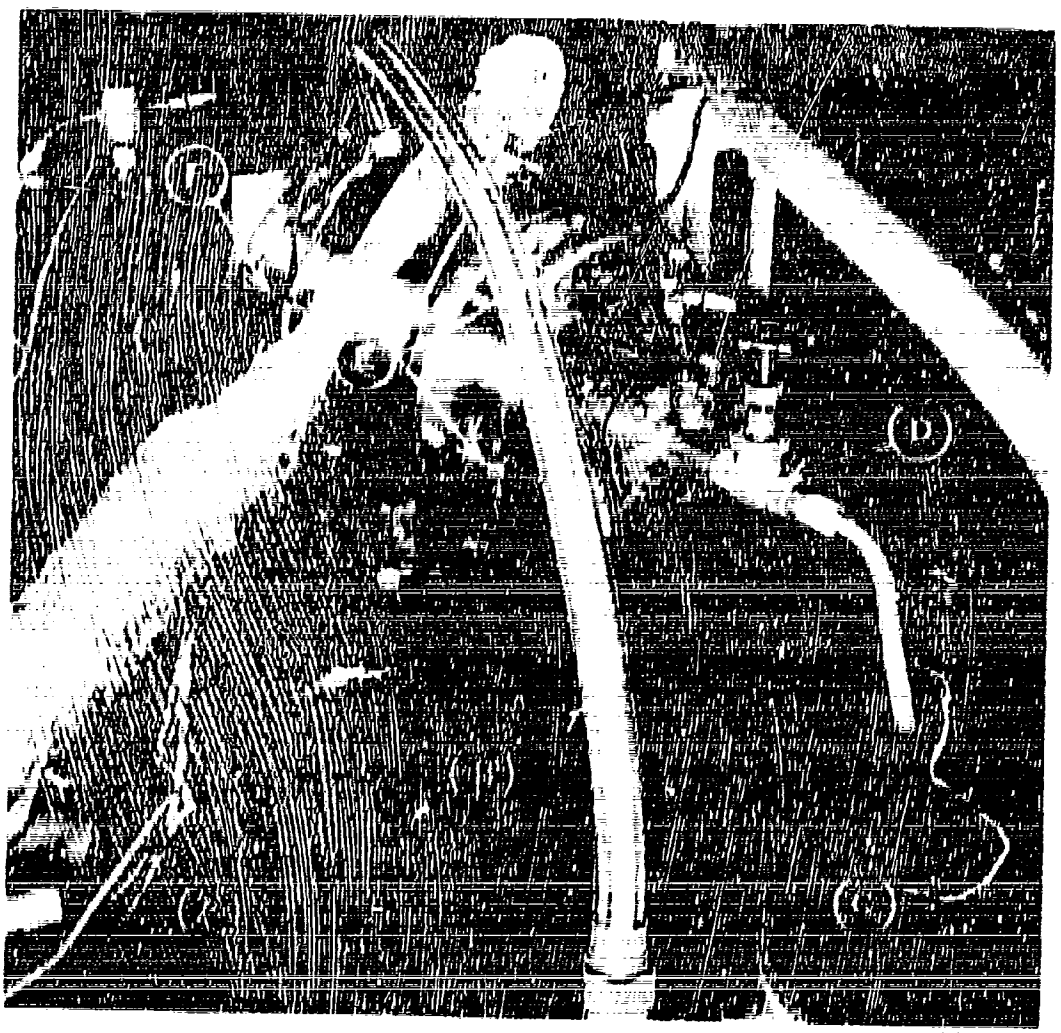
Figure 10-46

DOWNGRADED AT 3 YEAR INTERVALS
DECLASSIFIED AFTER 12 YEARS
DOD DIR 5200.10



SCHEMATIC DIAGRAM OF SEAL MATERIAL EVALUATION RIG

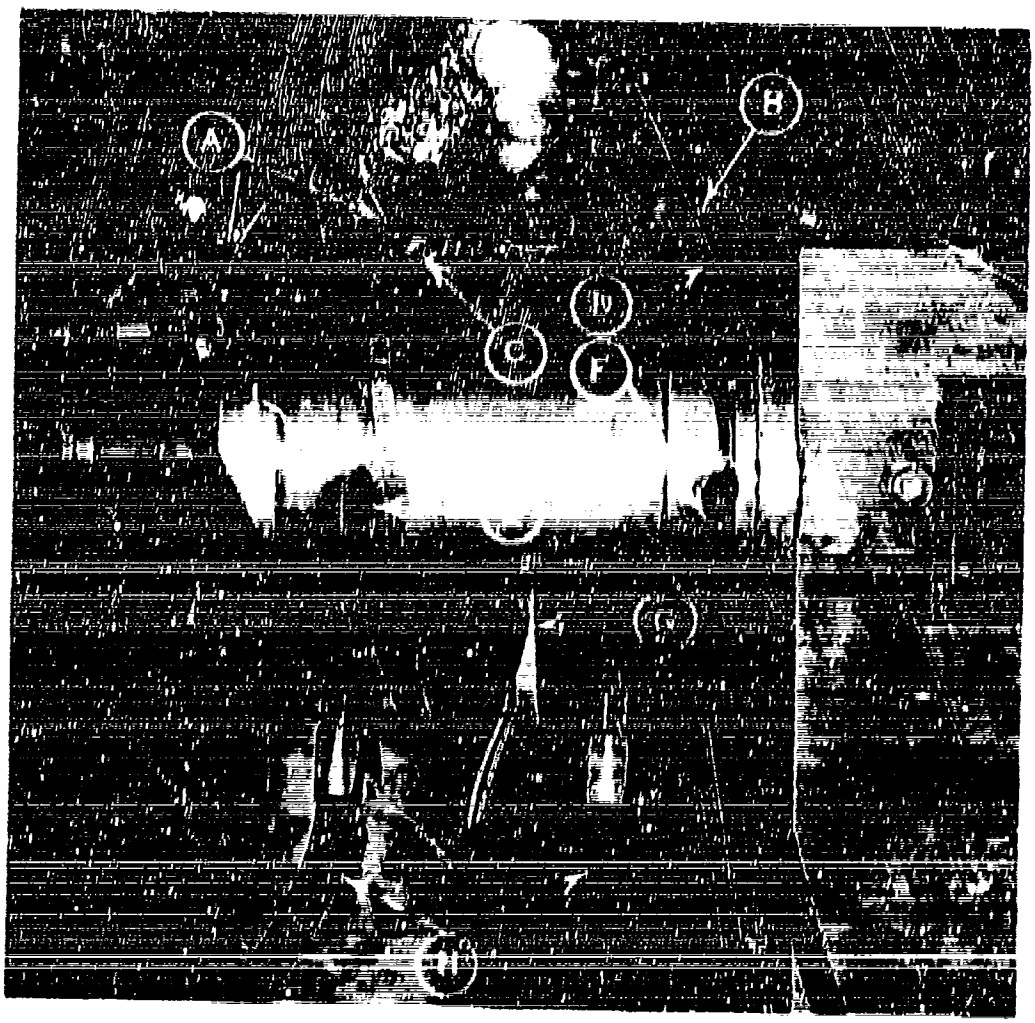
Figure 10-47



XP-30162

SEAL MATERIAL TEST RIG INSTALLATION SHOWING (A) HOT AIR SUPPLY LINE, (B) RIG BREATHER LINE, (C) BREATHER SETTLEMENT TANK, (D) BLEED CONTROL VALVE, (E) BEARING OIL LINES, AND (F) SEAL AIR TEMPERATURE PROBE.

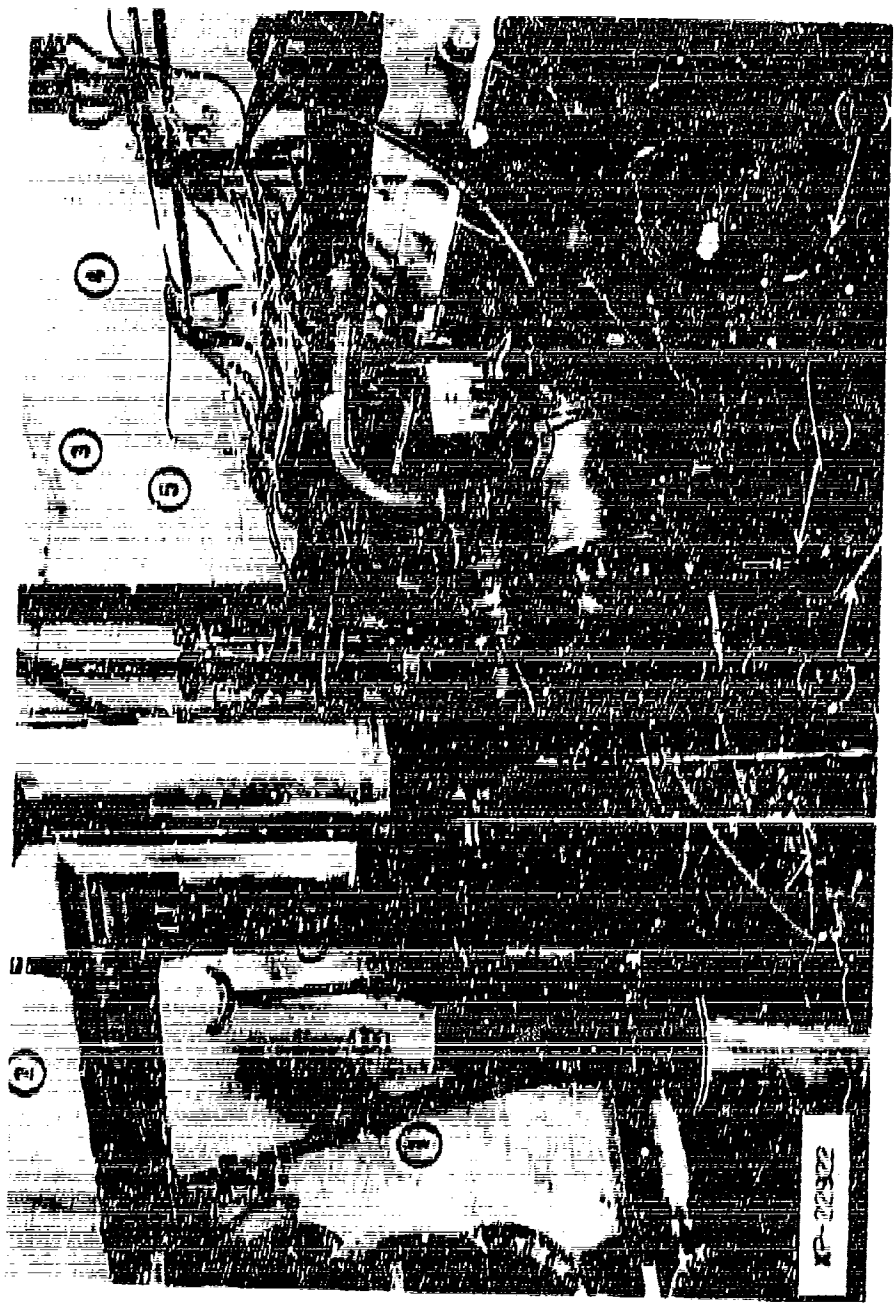
Figure 10-48



XP-30163

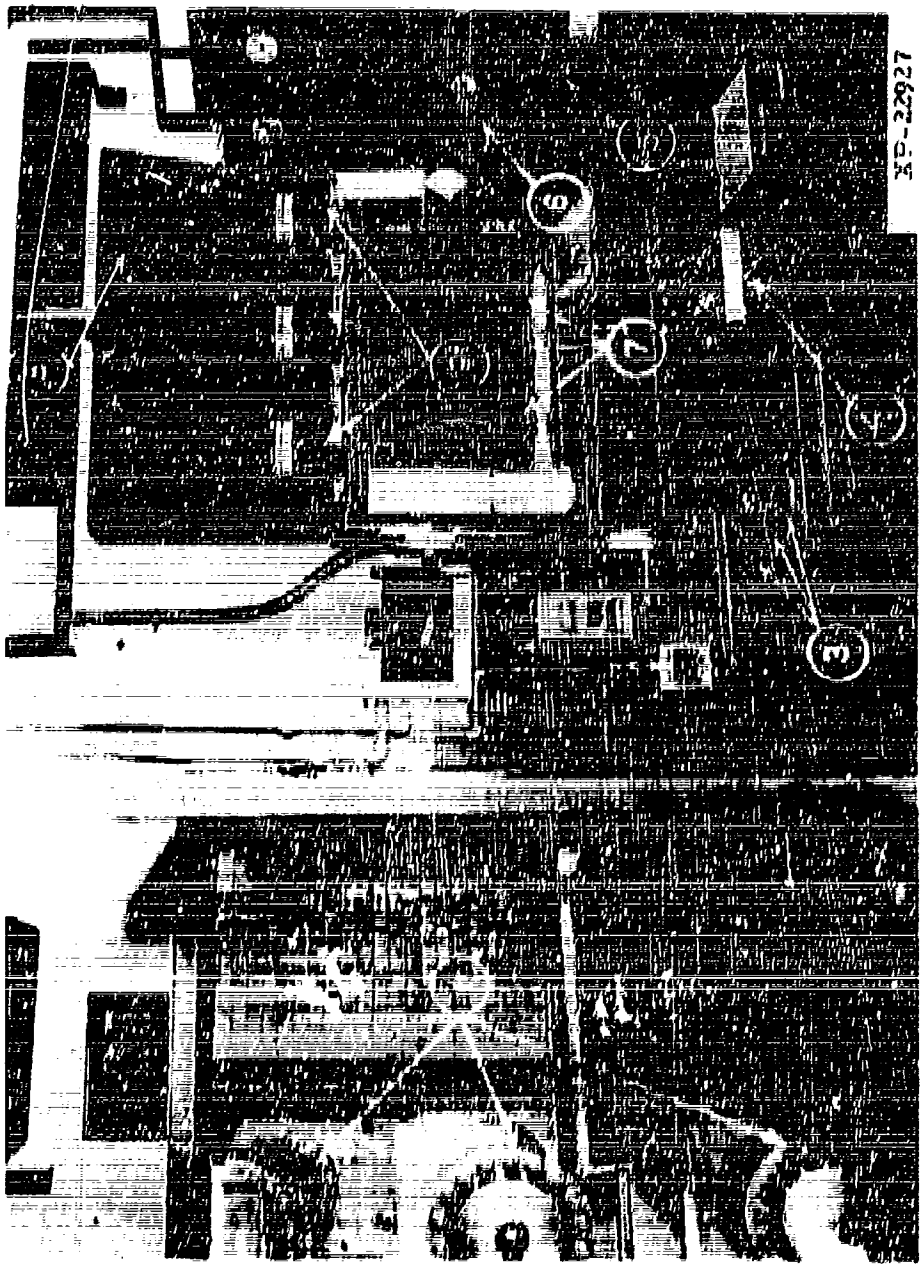
SEAL MATERIAL TEST RIG INSTALLATION SHOWING (A) FRONT BREATHER THERMOCOUPLE, (B) REAR BREATHER THERMOCOUPLE, (C) FRONT BREATHER PRESSURE, (D) REAR BREATHER PRESSURE, (E) FRONT SEAL OIL, (F) REAR SEAL OIL, (G) SEAL AIR PRESSURE, AND (H) OIL DRAINS.

Figure 10-49



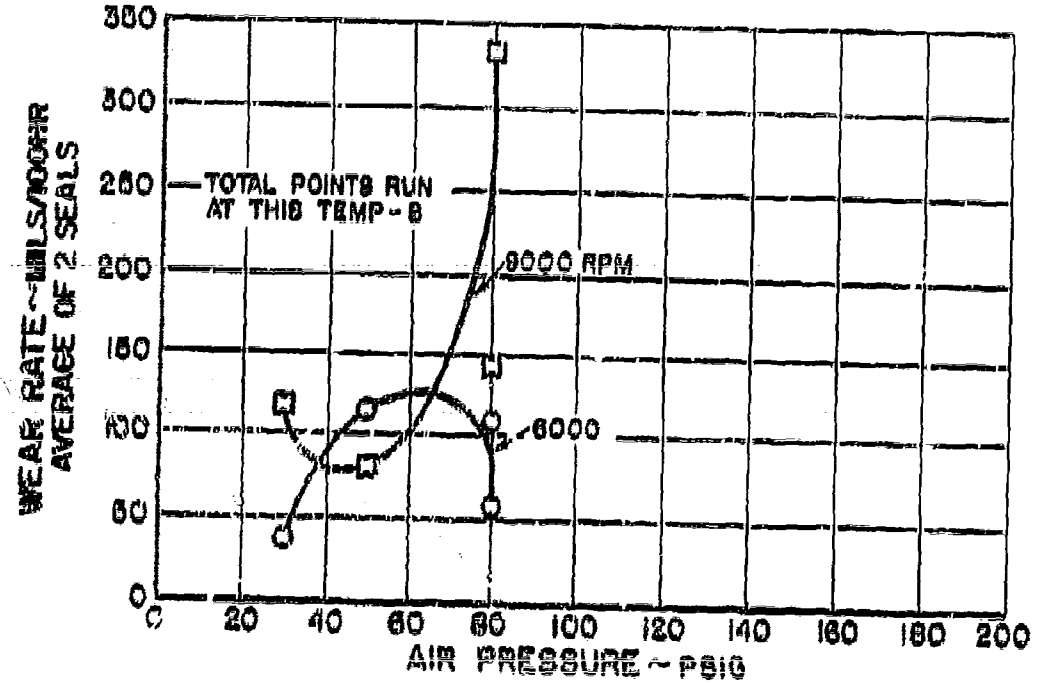
RING SEAL RIG INCLUDING (1) AIR HEATERS, (2) HIGH PRESSURE AIR LINES, (3) STAND BREATHER LINE, (4) THERMOCOUPLE CONDUIT, (5) RIG BREATHER, (6) DRIVE MOTORS (THREE 14 HP), (7) GEARBOX OIL DRAIN, (8) TWO-SPEED GEARBOXES, (9) RIG DRAIN, (10) RIG OIL SUPPLY MANIFOLD

Figure 10-50



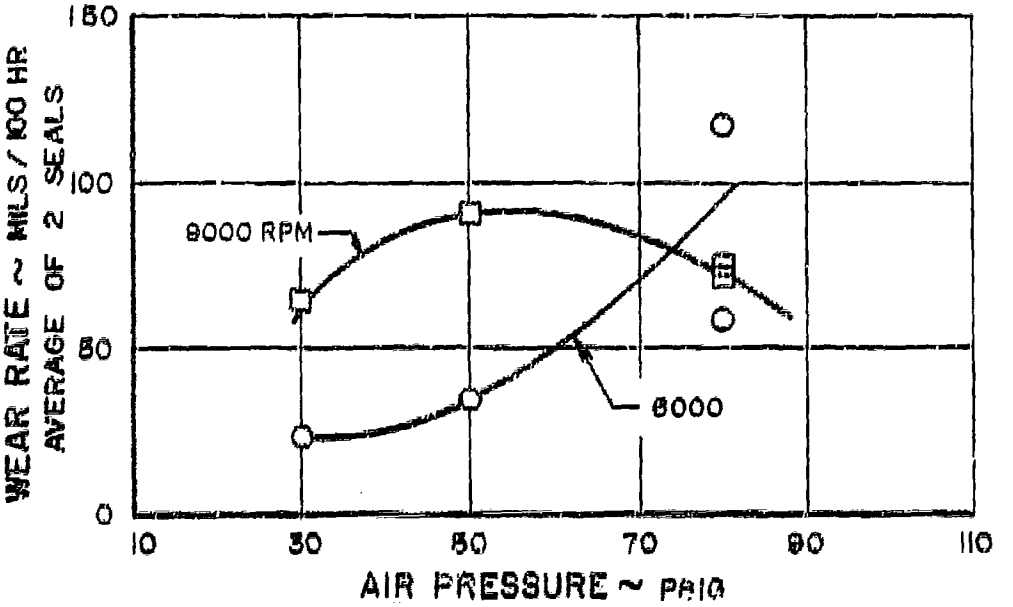
RIG TEST CONTROL STAND INCLUDING (1) AIR HEATER, (2) FIRE CONTROL, (3) POWER STATION TO CONTROL HEATER, (4) LEWIS SWITCH, (5) POTENTIOMETER, (6) PRESSURE GAUGES, (7) ROTOMETERS, (8) PRESSURE GAGES, (9) HEATER TEMPERATURE CONTROLS.

Figure 10-51



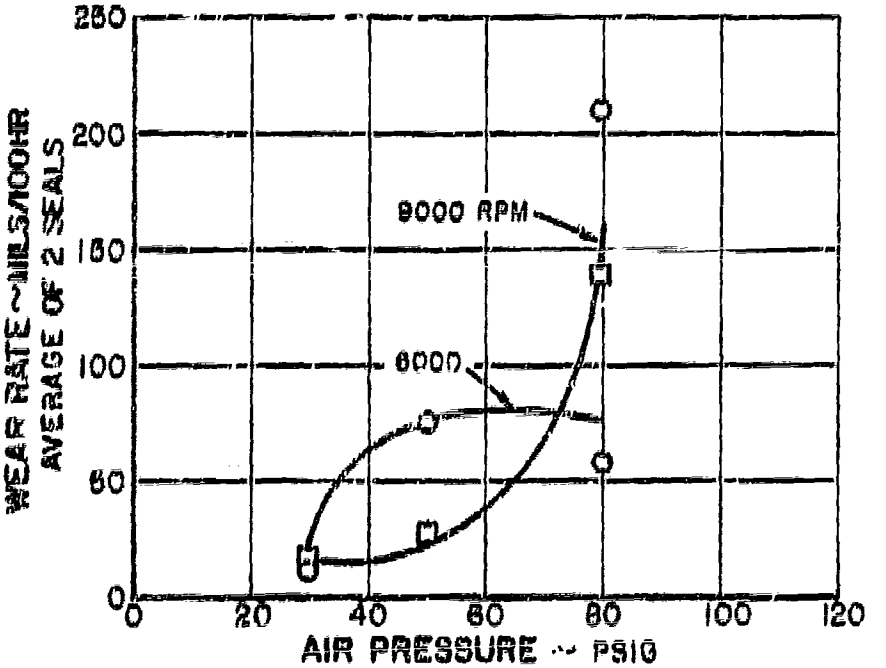
AIR PRESSURE VS. WEAR RATE OF A CDJ-83 CARBON-STELLITE 6B PLATE COMBINATION AT 500°F.

Figure 10-52



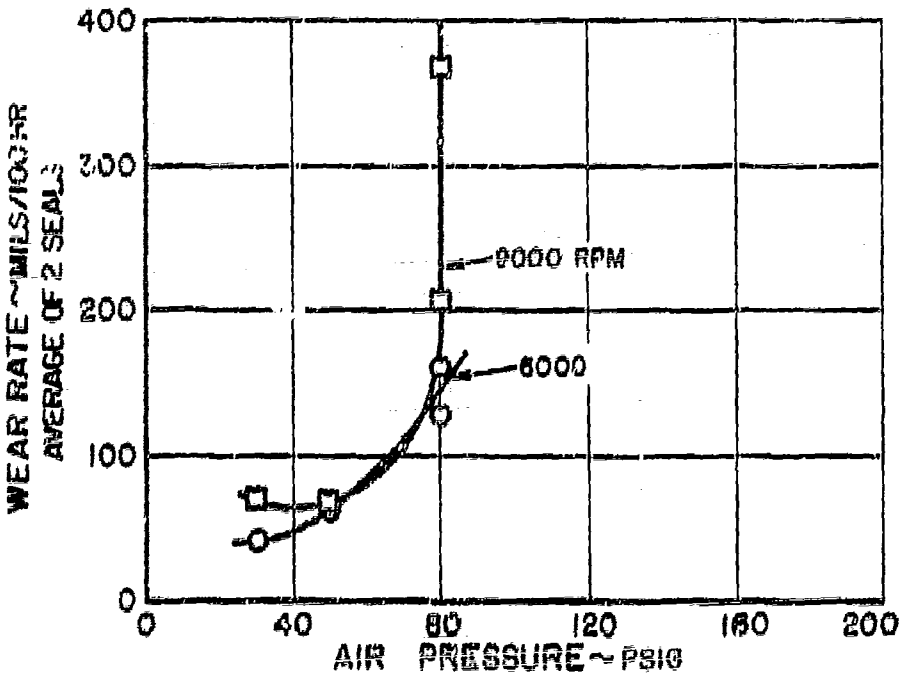
AIR PRESSURE VS. WEAR RATE WITH A P-2239 CARBON-STELLITE 6B PLATE COMBINATION AT 500°F.

Figure 10-53



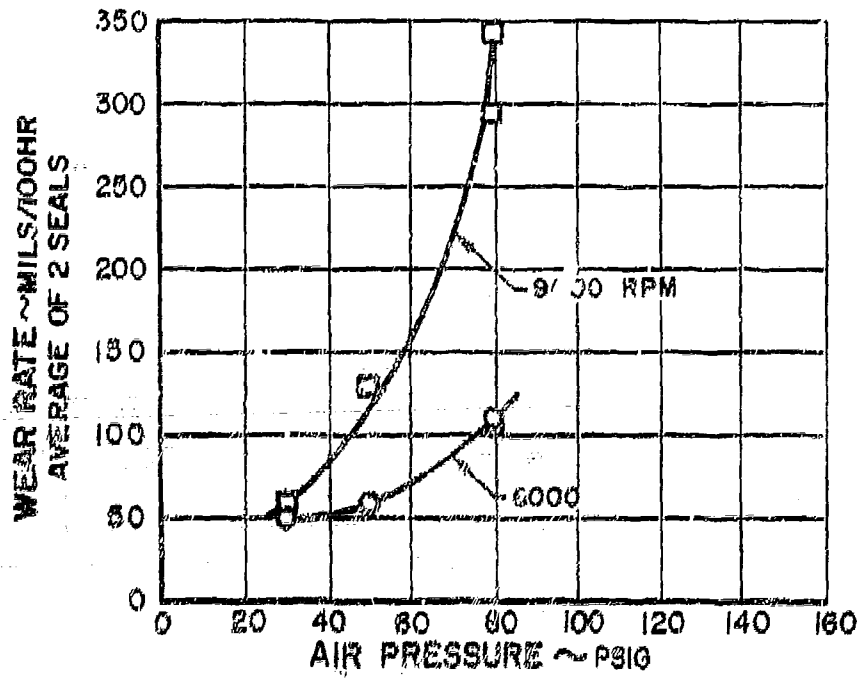
AIR PRESSURE VS. WEAR RATE OF A P-2239 CARBON-STELLITE 6B PLATE COMBINATION AT 1000°F.

Figure 10-54



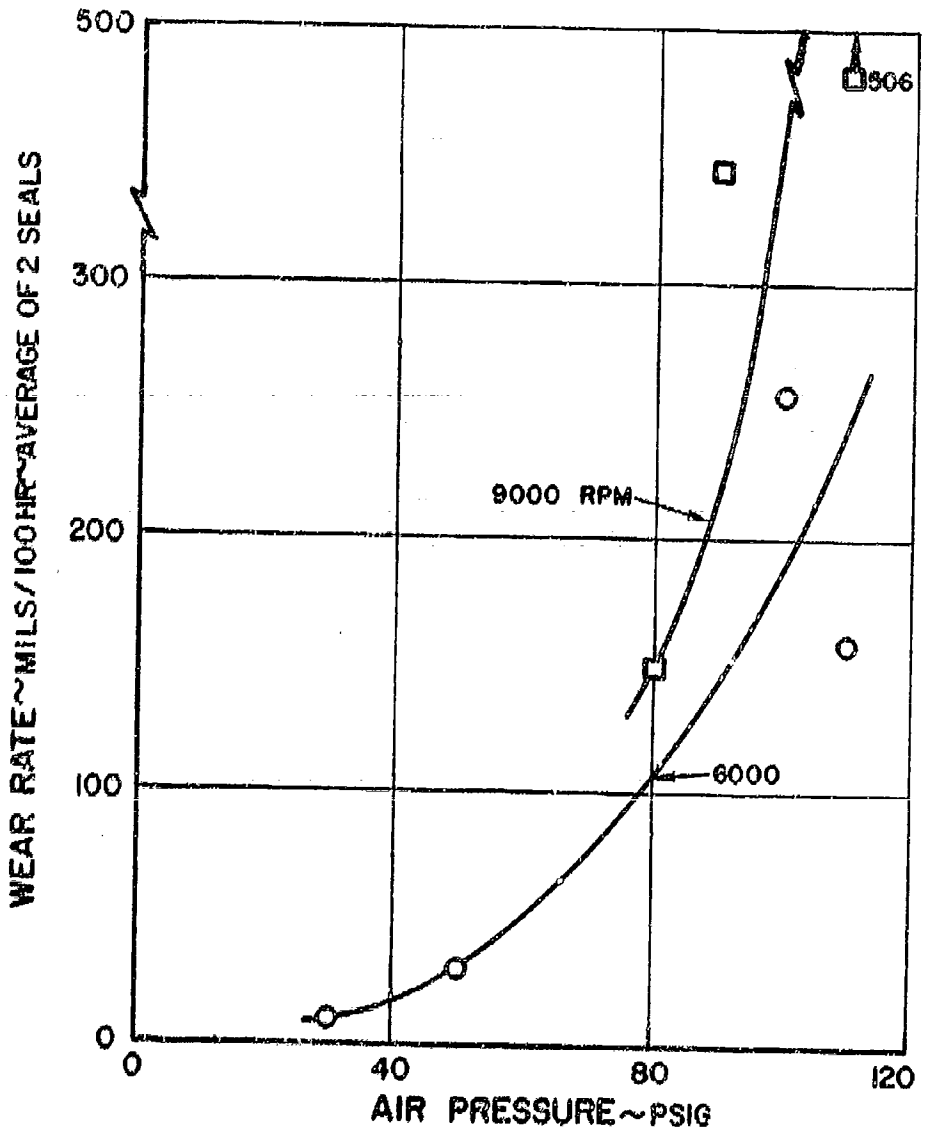
AIR PRESSURE VS. WEAR RATE OF A SPEER 9341 CARBON - STELLITE 6K PLATE COMBINATION AT 500°F.

Figure 10-55



AIR PRESSURE VS. WEAR RATE OF A SPEER 9341 CARBON - STELLITE 6K PLATE COMBINATION AT 1000°F.

Figure 10-56

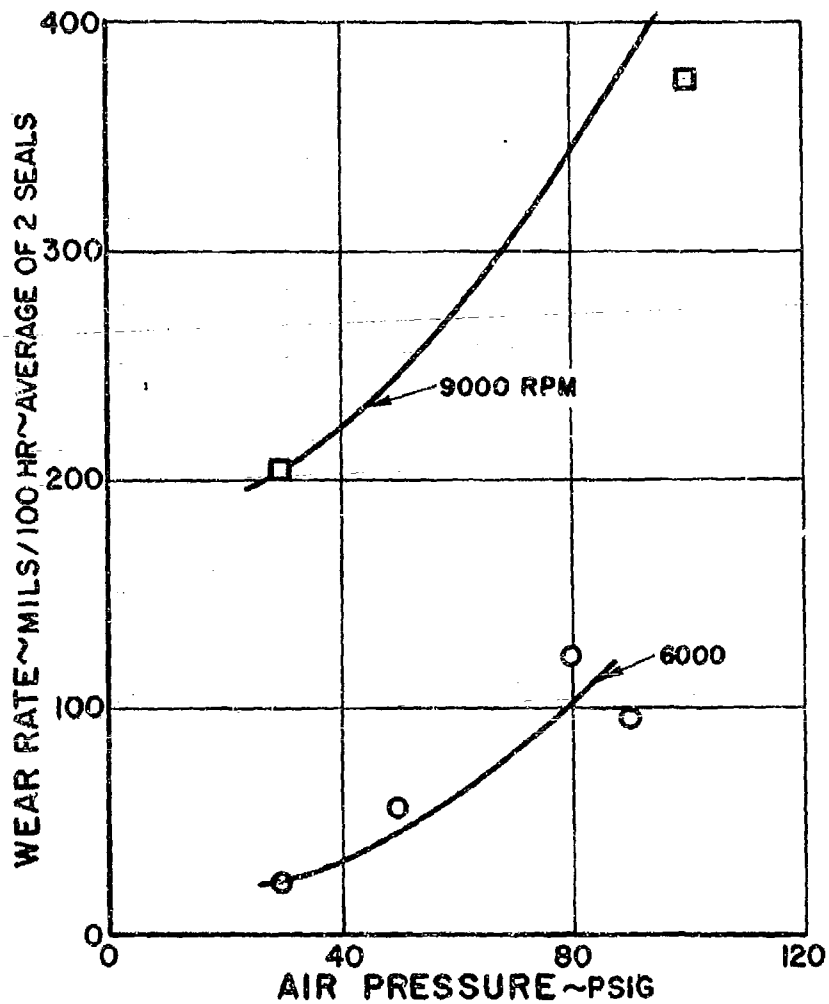


AIR PRESSURE VS. WEAR RATE OF A SPEER 9341 CARBON-STELLITE 6B PLATE COMBINATION AT 1000°F.

Figure 10-57

DOWNGRADED AT 3 YEAR INTERVALS
DECLASSIFIED AFTER 12 YEARS
DOD DIR 5200.10

THIS DOCUMENT CONTAINS INFORMATION AFFECTING THE NATIONAL DEFENSE OF THE UNITED STATES WITHIN THE MEANING OF THE ESPIONAGE LAWS, TITLE 18, U.S.C., SECTIONS 793 AND 794. ITS TRANSMISSION OR THE REVELATION OF ITS CONTENTS IN ANY MANNER TO AN UNAUTHORIZED PERSON IS PROHIBITED BY LAW.

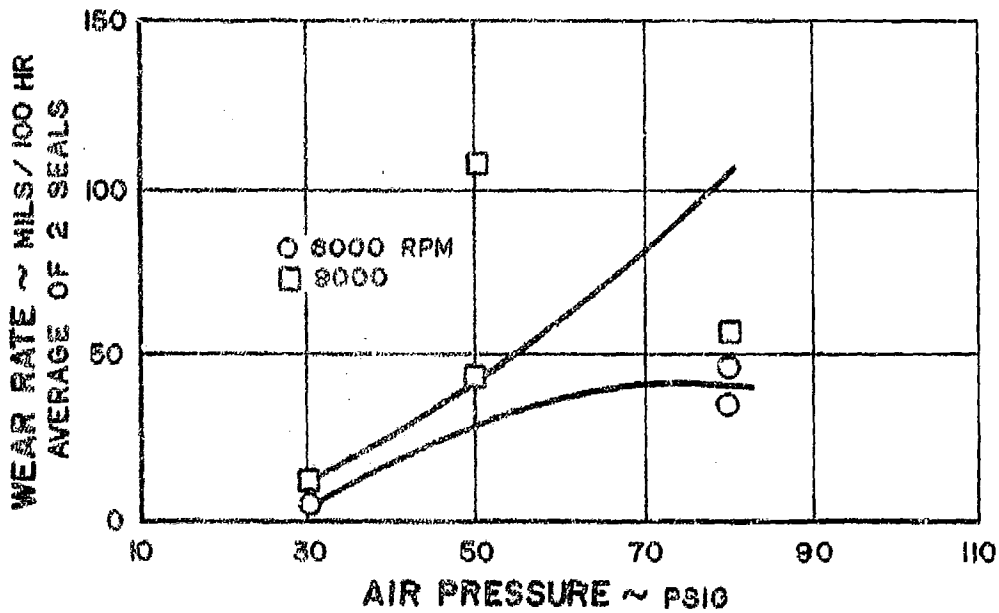


AIR PRESSURE VS. WEAR RATE OF A SPEER 9341 CARBON-STELLITE 6B PLATE COMBINATION AT 500°F.

Figure 10-58

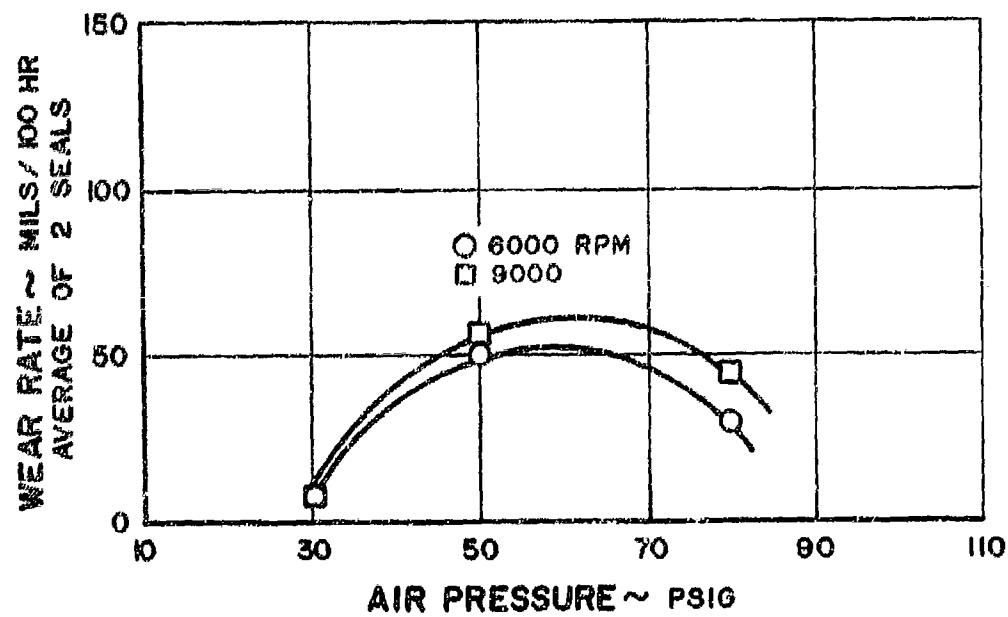
DOWNGRADED AT 3 YEAR INTERVALS
DECLASSIFIED AFTER 12 YEARS
DOD DIR 5200.10

THIS DOCUMENT CONTAINS INFORMATION AFFECTING THE NATIONAL DEFENSE OF THE UNITED STATES WITHIN THE MEANING OF THE ESPIONAGE LAWS, TITLE 18 U.S.C. SECTIONS 793 AND 794. ITS TRANSMISSION OR THE REVELATION OF ITS CONTENTS IN ANY MANNER TO AN UNAUTHORIZED PERSON IS PROHIBITED BY LAW.



AIR PRESSURE VS. WEAR RATE OF A PO3XHT CARBON-LINDE LCIC PLATE COMBINATION AT 1000°F.

Figure 10-59

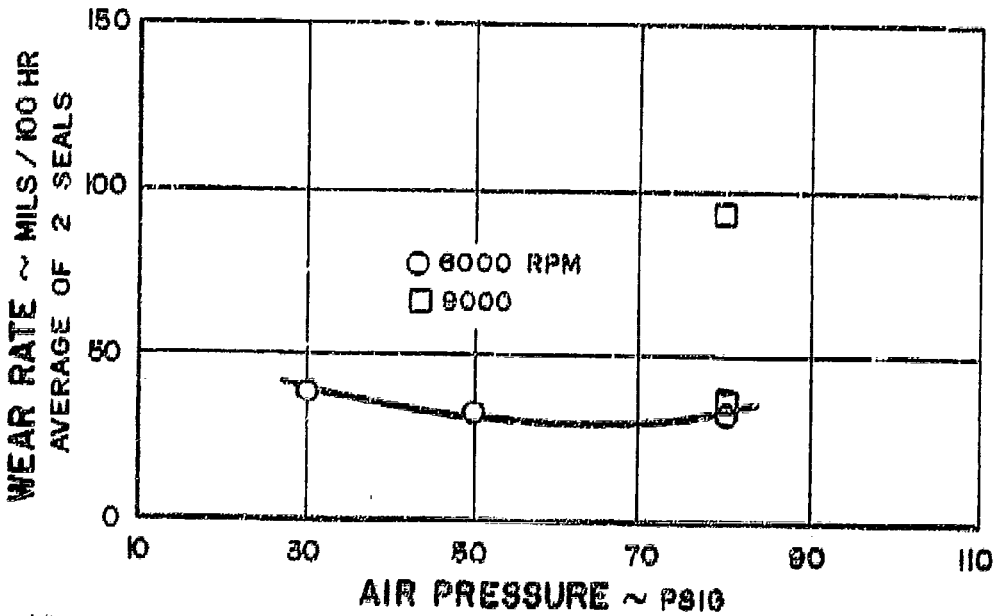


AIR PRESSURE VS. WEAR RATE OF A PO3XHT CARBON-LINDE LCIC PLATE COMBINATION AT 500°F.

Figure 10-60

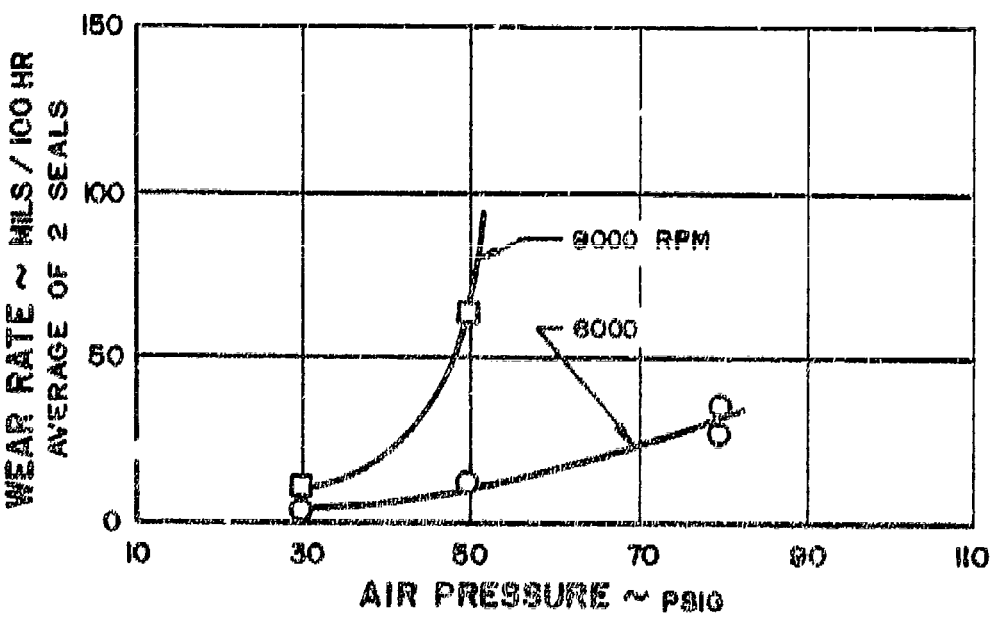
DOWNGRADED AT 3 YEAR INTERVALS
DECLASSIFIED AFTER 12 YEARS
DOD DIR 5200.10

THIS DOCUMENT CONTAINS INFORMATION AFFECTING THE NATIONAL DEFENSE OF THE UNITED STATES WITHIN THE MEANING OF THE ESPIONAGE LAWS, TITLE 18, U.S.C. SECTIONS 793 AND 794. THE TRANSMISSION OR THE REVELATION OF ITS CONTENTS IN ANY MANNER TO AN UNAUTHORIZED PERSON IS PROHIBITED BY LAW.



AIR PRESSURE VS. WEAR RATE OF A PO3XMT CARBON-CHROME-PLATE AMS 6323 PLATE COMBINATION AT 500°F.

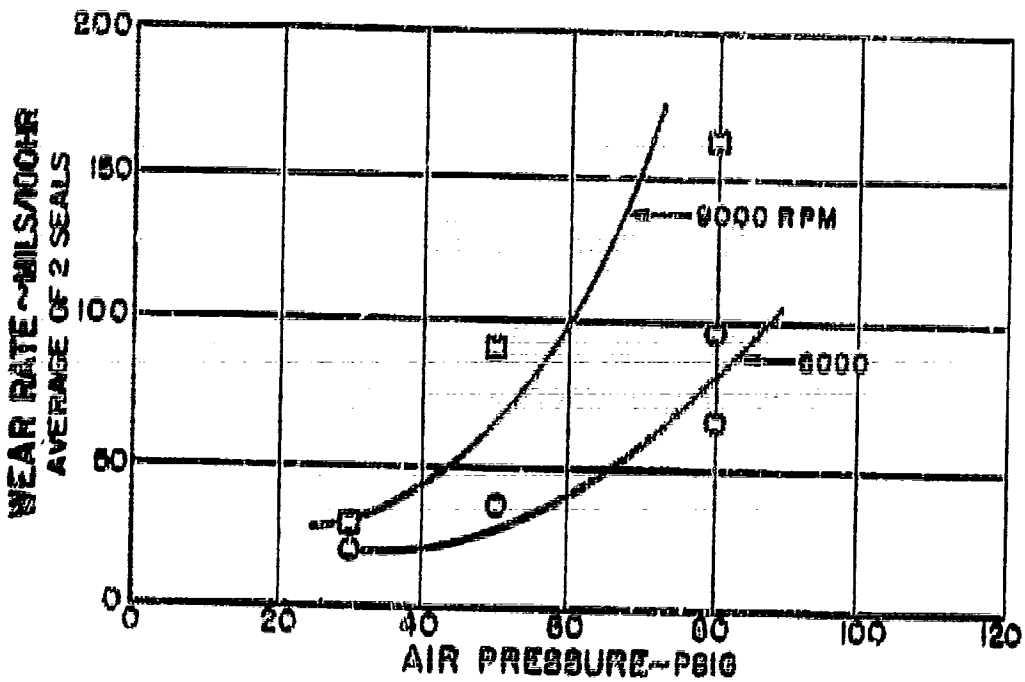
Figure 10-61



AIR PRESSURE VS. WEAR RATE OF A PO3XHT CARBON-CHROME-PLATED AMS 6323 PLATE COMBINATION AT 1000°F.

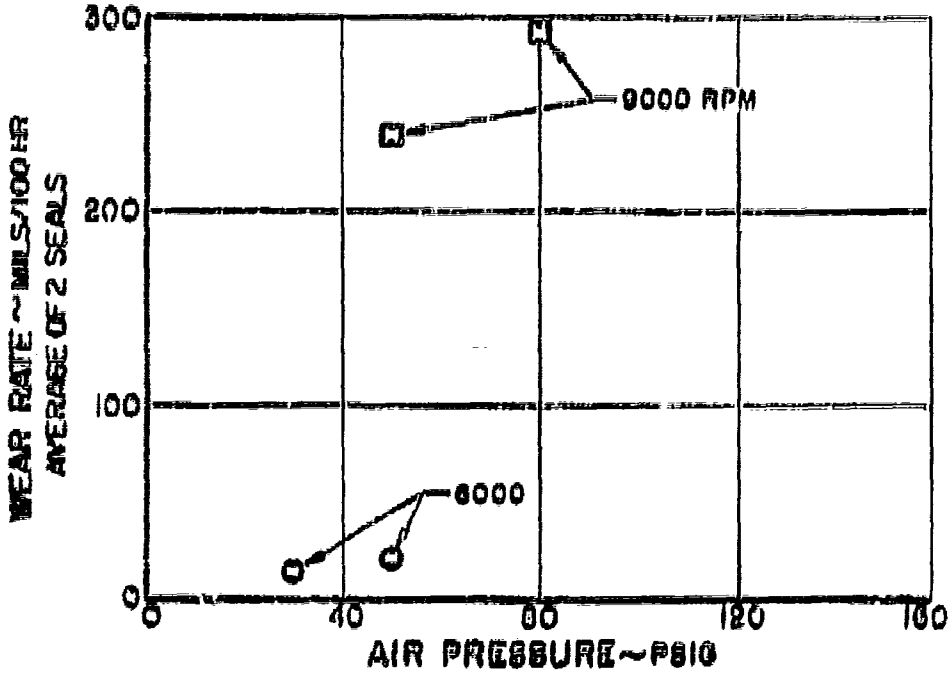
Figure 10-62

DOWNGRADED AT 3 YEAR INTERVALS
DECLASSIFIED AFTER 12 YEARS
DOD DIR 5200.10



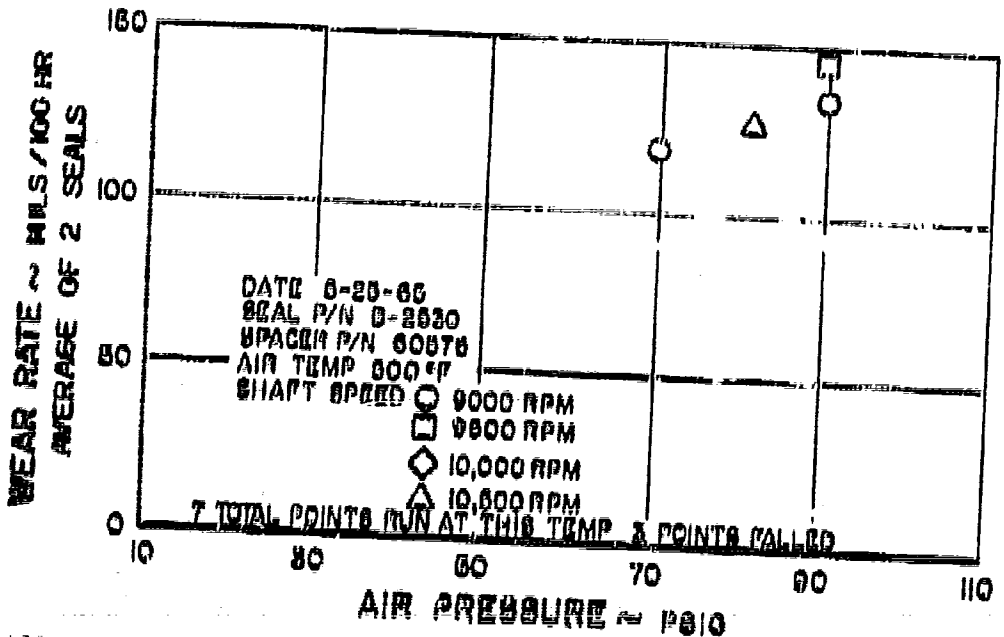
AIR PRESSURE VS. WEAR RATE OF A POSITT CARBON-STELLITE 6B PLATE COMBINATION AT 500°F.

Figure 10-63



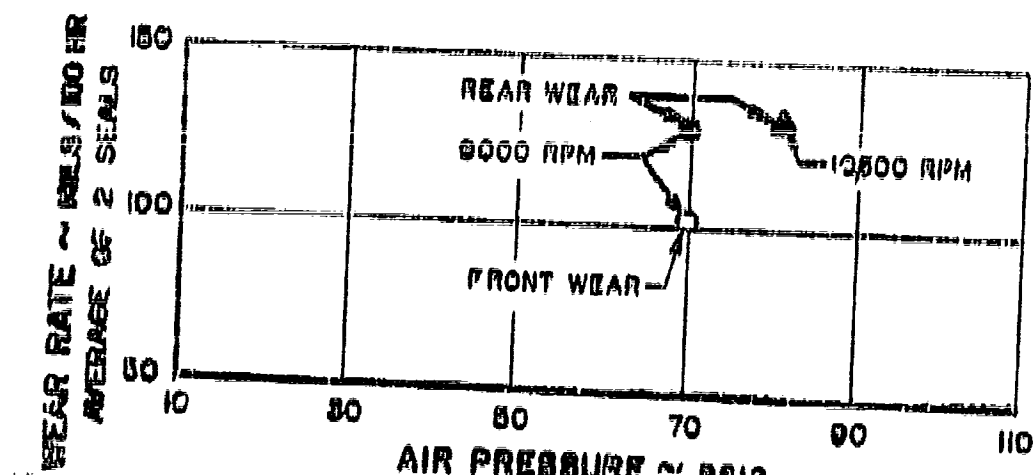
AIR PRESSURE VS. WEAR RATE OF A POSHT CARBON-STELLITE 6B PLATE COMBINATION AT 1000°F.

Figure 10-64



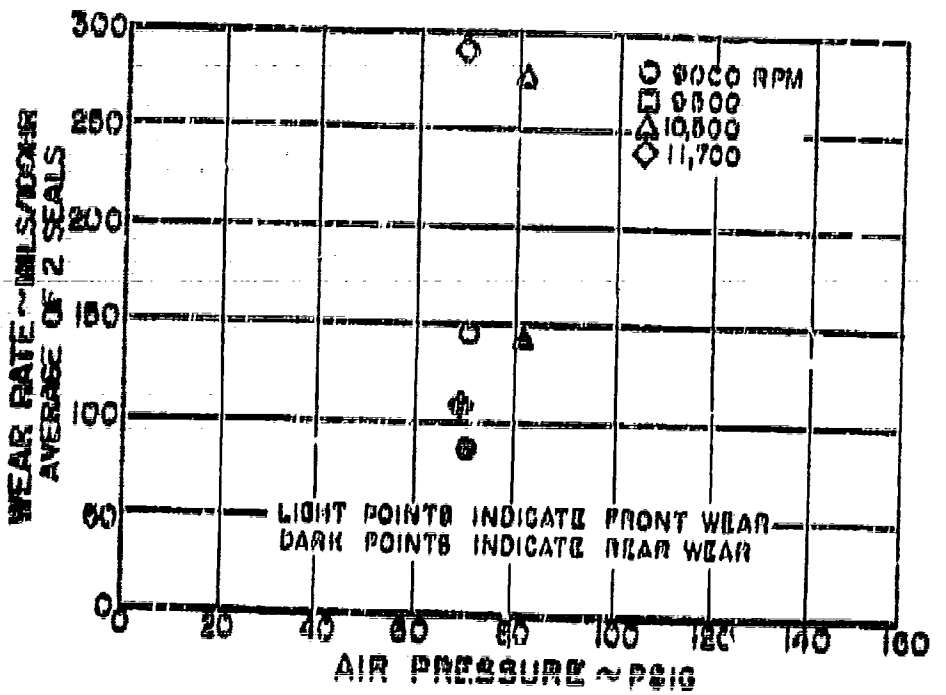
AIR PRESSURE VS. WEAR RATE OF A B-2936 CARBON-STELLITE 6K PLATE COMBINATION AT 500°F.

Figure 10-65



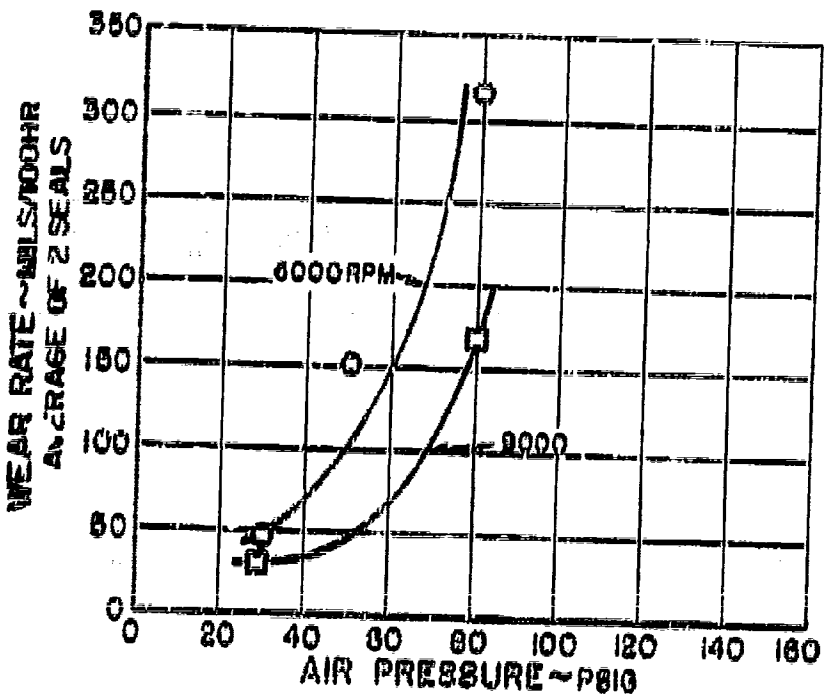
AIR PRESSURE VS. WEAR RATE OF A B-2936 AND CDJ-63 CARBON-STELLITE 6K PLATE COMBINATION AT 1000°F.

Figure 10-66



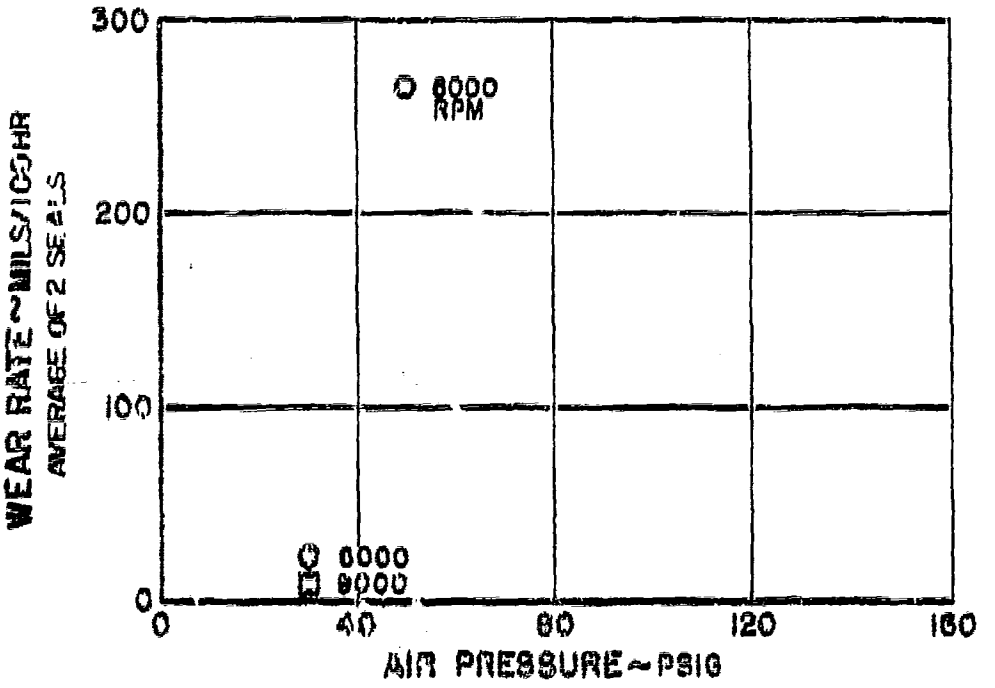
AIR PRESSURE VS. WEAR RATE OF A B-2936 AND CDJ-83 CARBON-STELLITE 6K PLATE COMBINATION AT 500°F.

Figure 10-67



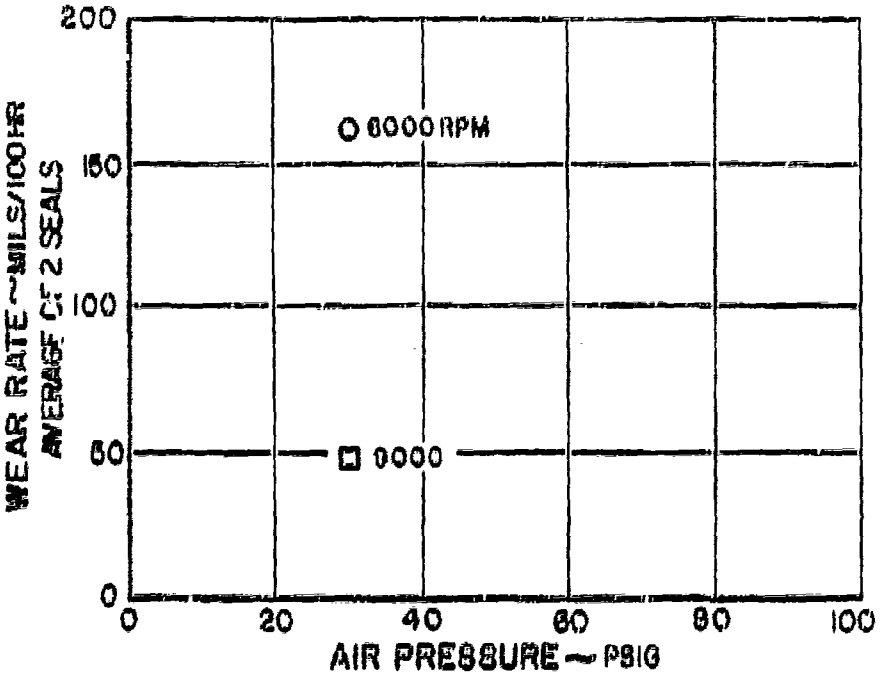
AIR PRESSURE VS. WEAR RATE OF A USC 2800 CARBON-STELLITE 6K PLATE COMBINATION AT 900°F.

Figure 10-68



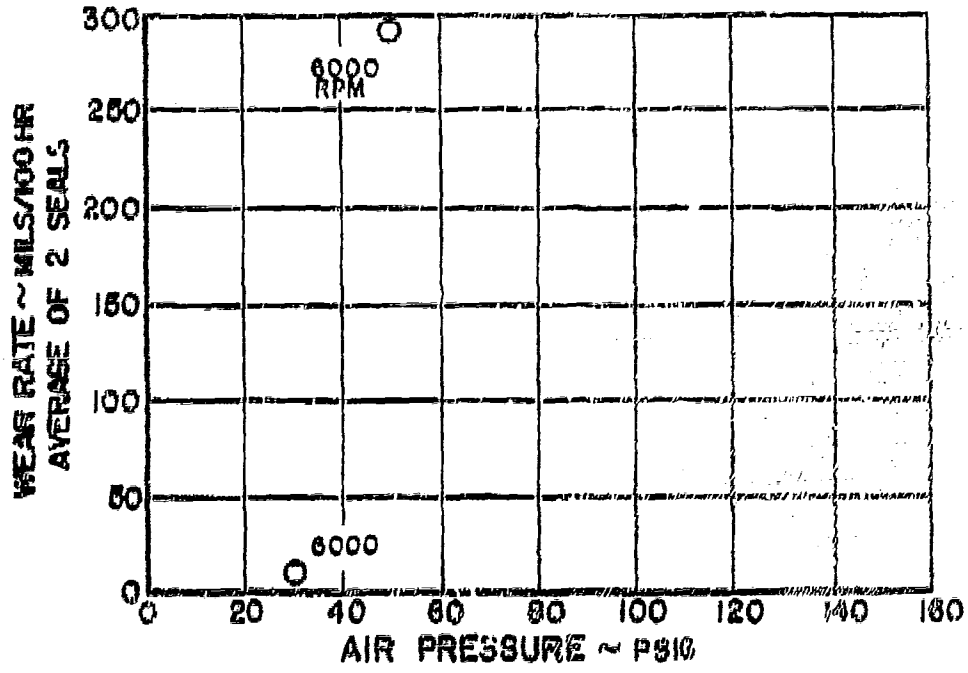
AIR PRESSURE VS. WEAR RATE OF A USG 2800 CARBON-STELLITE 6K PLATE COMBINATION AT 1000°F.

Figure 10-69



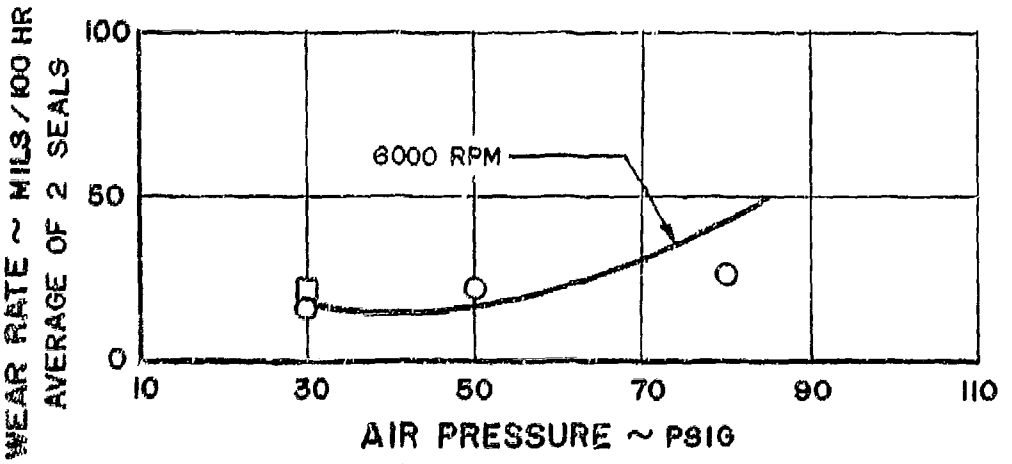
AIR PRESSURE VS. WEAR RATE OF A USG 2803 CARBON-STELLITE 6K PLATE COMBINATION AT 1000°F.

Figure 10-70



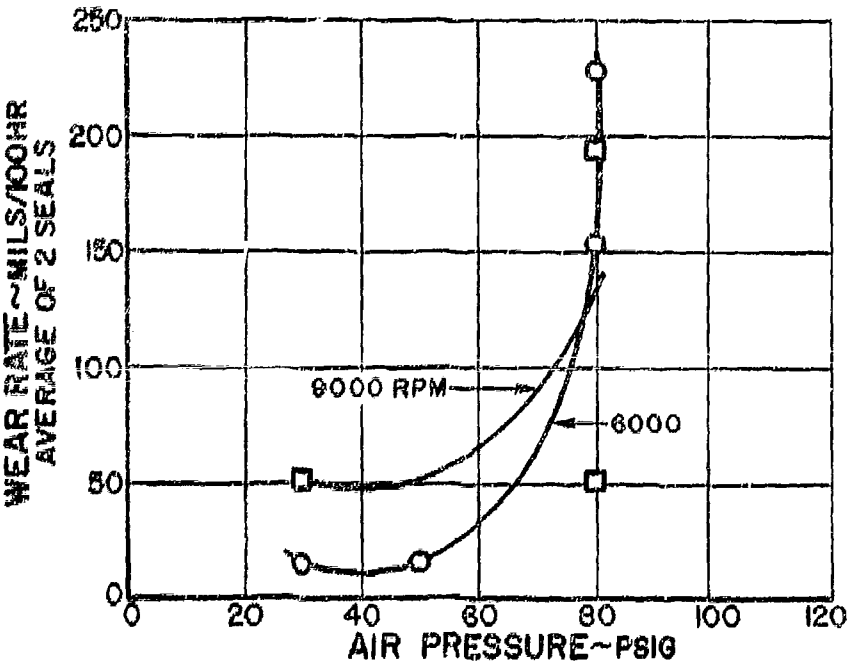
AIR PRESSURE VS. WEAR RATE OF A USG 2003 CARBON-STELLITE 6K PLATE COMBINATION AT 500°F.

Figure 10-71



AIR PRESSURE VS. WEAR RATE OF A USG 2777 CARBON-LINDE LCIC PLATE COMBINATION AT 500°F.

Figure 10-72

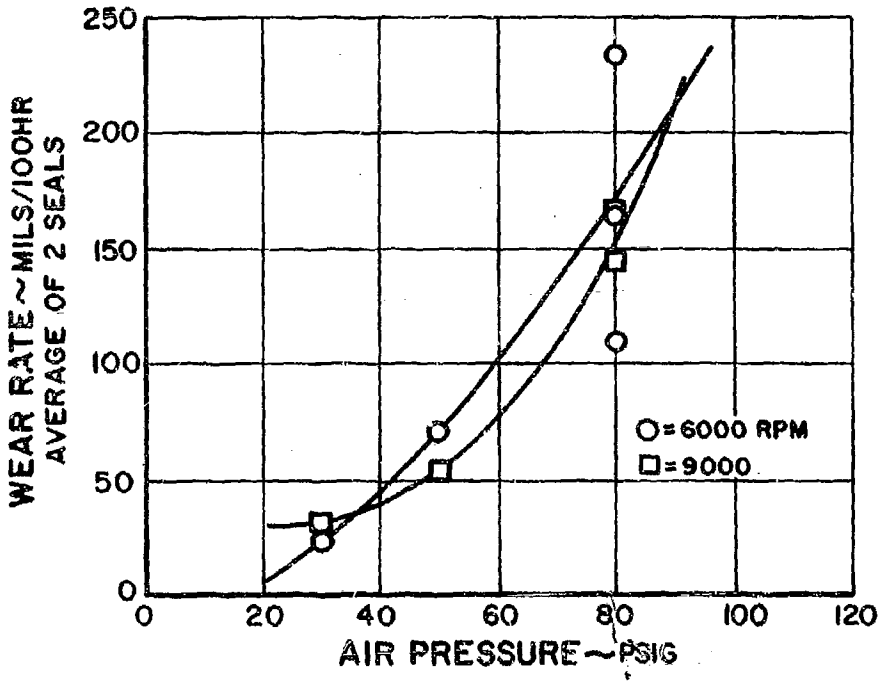


AIR PRESSURE VS. WEAR RATE OF A USG 2777 CARBON-LINDE LCIC PLATE COMBINATION AT 1000°F.

Figure 10-73

DOWNGRADED AT 3 YEAR INTERVALS
DECLASSIFIED AFTER 12 YEARS
DOD DIR 5200.10

THIS DOCUMENT CONTAINS INFORMATION AFFECTING THE NATIONAL DEFENSE OF THE UNITED STATES WITHIN THE MEANING OF THE ESPIONAGE LAWS, TITLE 18 U.S.C. SECTIONS 793 AND 794. ITS TRANSMISSION OR THE REVELATION OF ITS CONTENTS IN ANY MANNER TO AN UNAUTHORIZED PERSON IS PROHIBITED BY LAW.

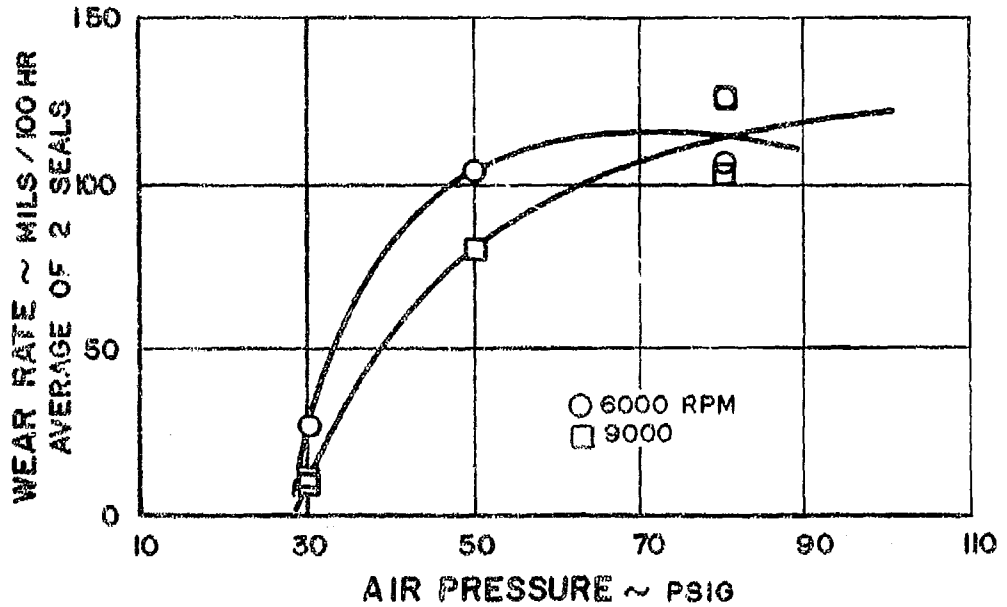


AIR PRESSURE VS. WEAR RATE OF A CDJ-83 CARBON-BRUSH NIBE PLATE COMBINATION AT 500°F.

Figure 10-74

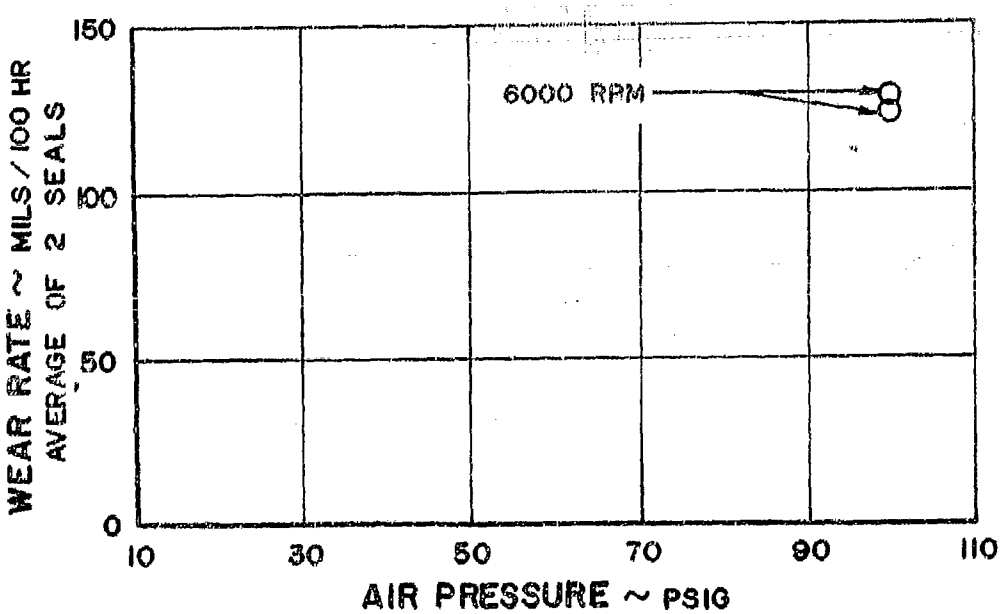
DOWNGRADED AT 3 YEAR INTERVALS
DECLASSIFIED AFTER 12 YEARS
DOD DIR 5200.10

THIS DOCUMENT CONTAINS INFORMATION AFFECTING THE NATIONAL DEFENSE OF THE UNITED STATES WITHIN THE MEANING OF THE ESPIONAGE LAWS, TITLE 18, U.S.C., SECTIONS 793 AND 794. THE TRANSMISSION OR THE REVELATION OF ITS CONTENTS IN ANY MANNER TO AN UNAUTHORIZED PERSON IS PROHIBITED BY LAW.



AIR PRESSURE VS. WEAR RATE OF A CDJ-83 CARBON-BRUSH NIBE PLATE COMBINATION AT 1000°F.

Figure 10-75

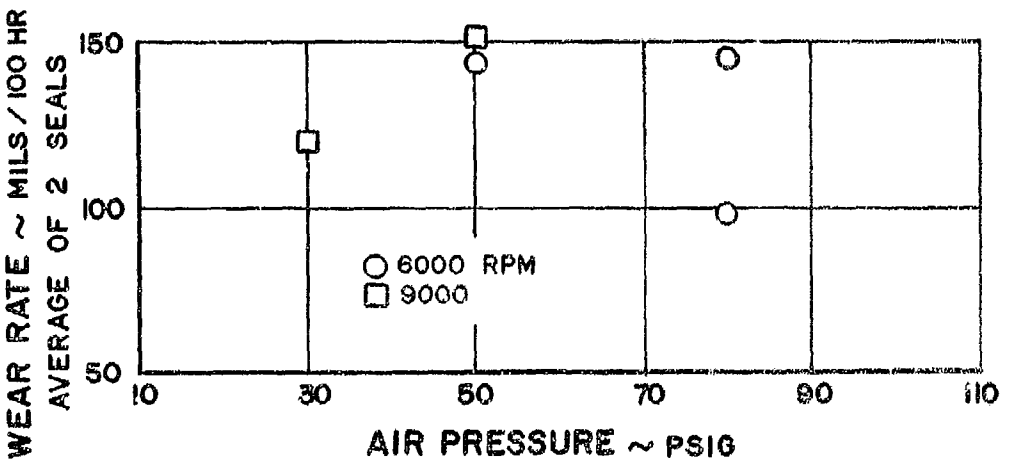


AIR PRESSURE VS. WEAR RATE OF A CDJ-83 CARBON-BRUSH NIBE PLATE COMBINATION AT 1000°F.

Figure 10-76

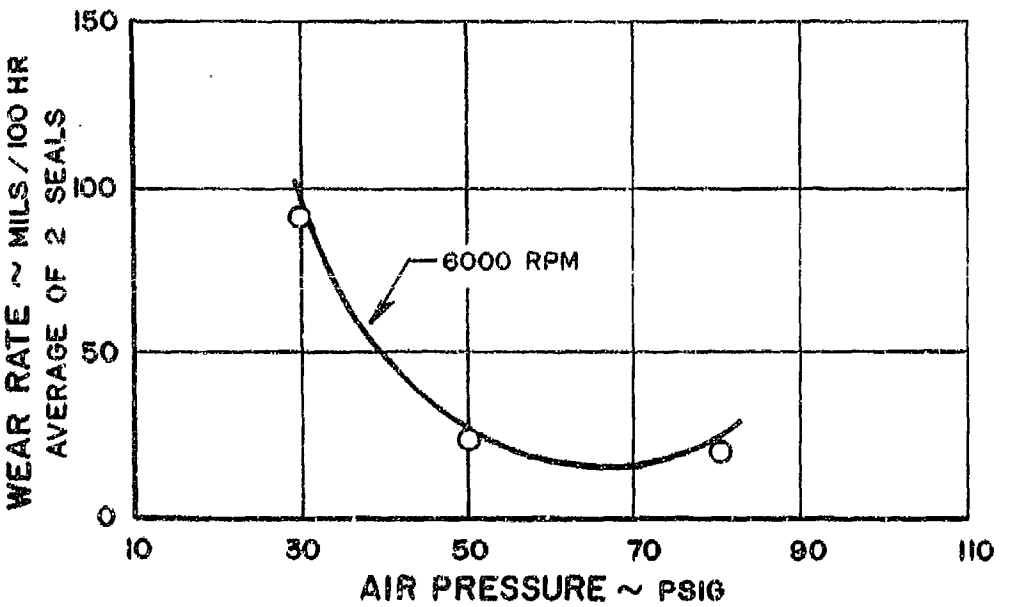
DOWNGRADED AT 3 YEAR INTERVALS
DECLASSIFIED AFTER 12 YEARS
DOD DIR 5200.10

THIS DOCUMENT CONTAINS INFORMATION AFFECTING THE NATIONAL DEFENSE OF THE UNITED STATES WITHIN THE MEANING OF THE ESPIONAGE LAWS, TITLE 18 U.S.C. SECTIONS 793 AND 794. THE TRANSMISSION OR THE REVELATION OF ITS CONTENTS IN ANY MANNER TO AN UNAUTHORIZED PERSON IS PROHIBITED BY LAW.



AIR PRESSURE VS. WEAR RATE OF A CDJ-83 CARBON-BRUSH NiBe PLATE COMBINATION AT 1200°F.

Figure 10-77

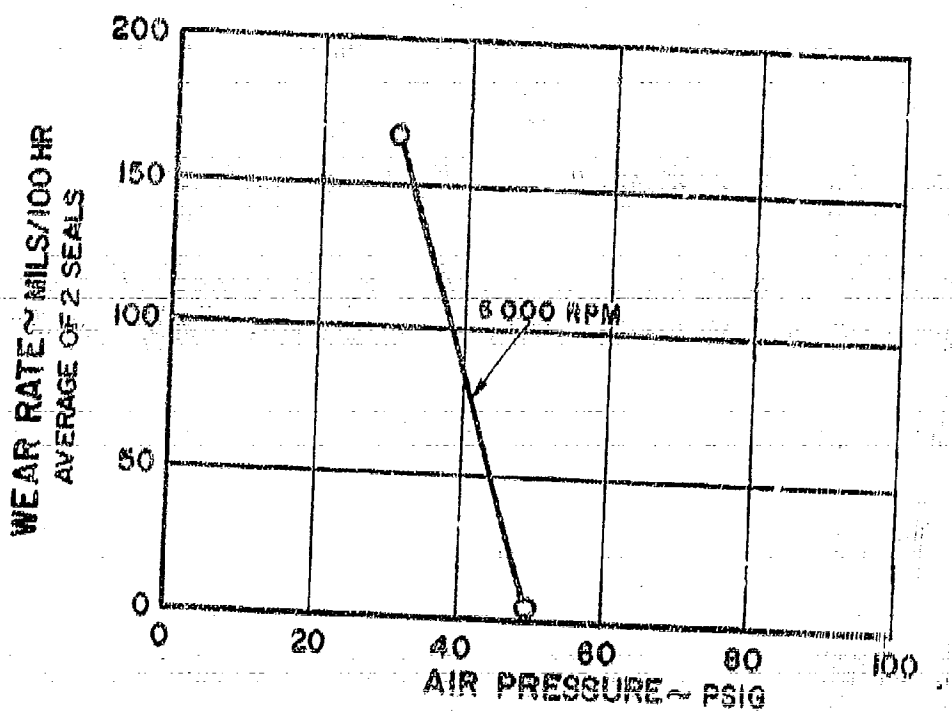


AIR PRESSURE VS. WEAR RATE OF A CDJ-83 CARBON-CLEVITE 300 PLATE COMBINATION AT 500°F.

Figure 10-78

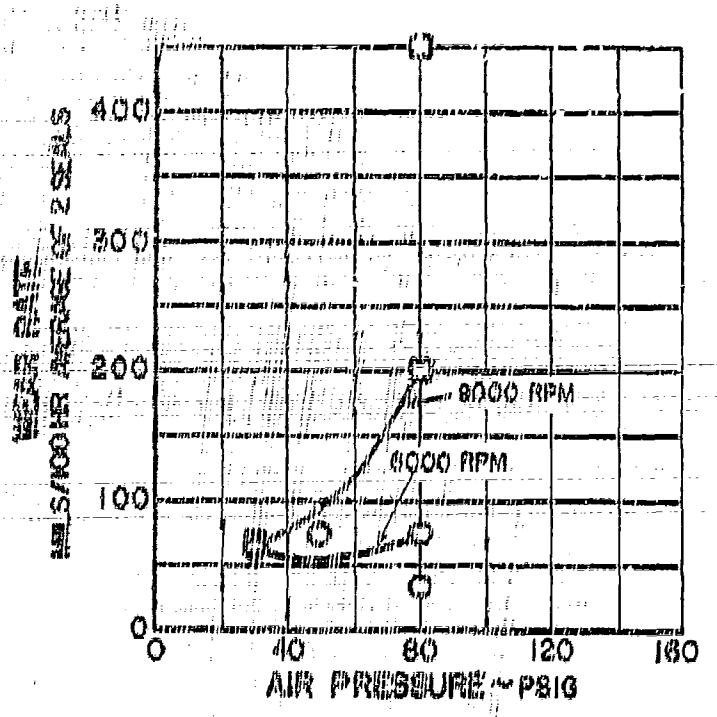
DOWNGRADED AT 3 YEAR INTERVALS
DECLASSIFIED AFTER 12 YEARS
DOD DIR 5200.10

THIS DOCUMENT CONTAINS INFORMATION AFFECTING THE NATIONAL DEFENSE OF THE UNITED STATES WITHIN THE MEANING OF THE ESPIONAGE LAWS, TITLE 18, U.S.C. SECTIONS 793 AND 794. ITS TRANSMISSION OR THE REVELATION OF ITS CONTENTS IN ANY MANNER TO AN UNAUTHORIZED PERSON IS PROHIBITED BY LAW.



AIR PRESSURE VS. WEAR RATE OF A CDJ-83 CARBON-CLEVITE 300 PLATE COMBINATION AT 1000°F.

Figure 10-79

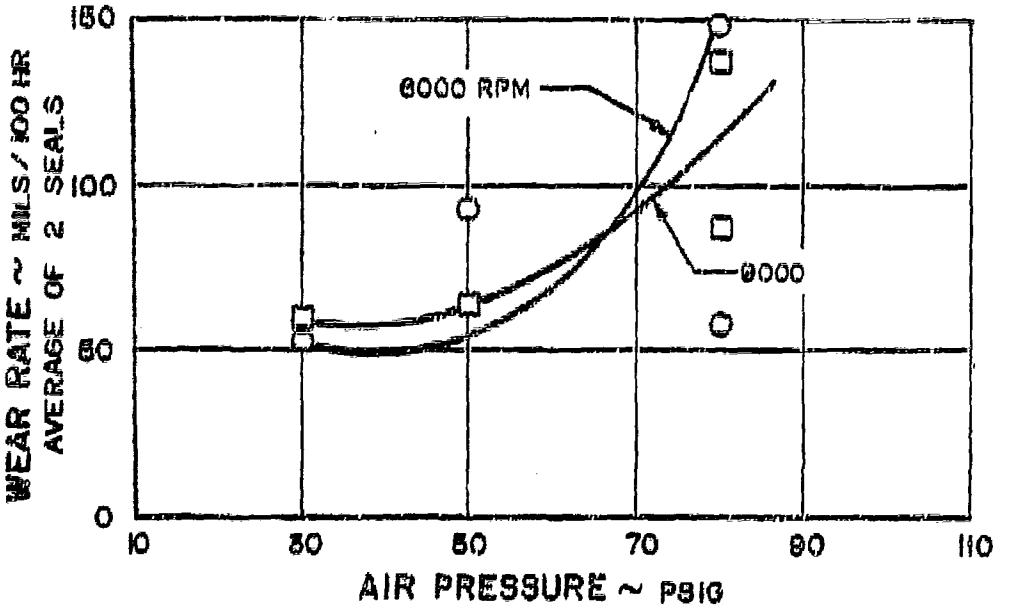


AIR PRESSURE VS. WEAR RATE OF A CDJ-83 CARBON-HAYNES NO. 25 PLATE COMBINATION AT 1000°F.

Figure 10-80

DOWNGRADED AT 3 YEAR INTERVALS
DECLASSIFIED AFTER 12 YEARS
DOD DIR 5200.10

THIS DOCUMENT CONTAINS INFORMATION AFFECTING THE NATIONAL DEFENSE OF THE UNITED STATES WITHIN THE MEANING OF THE ESPIONAGE LAWS, TITLE 18, U.S.C., SECTIONS 793 AND 794. THE TRANSMISSION OR THE REVELATION OF ITS CONTENTS IN ANY MANNER TO AN UNAUTHORIZED PERSON IS PROHIBITED BY LAW.



AIR PRESSURE VS. WEAR RATE OF A CDJ-83 CARBON-HAYNES NO. 25 PLATE COMBINATION AT 500°F.

Figure 10-81

DOWNGRADED AT 3 YEAR INTERVALS
DECLASSIFIED AFTER 12 YEARS
DOD DIR 5200.10

This document contains information affecting the national defense of the United States within the meaning of the espionage laws, Title 18, U.S.C., Sections 793 and 794. The transmission or the revelation of its contents in any manner to an unauthorized person is prohibited by law.

ITEM 11

FUELS

ITEM 11 - FUELS

OBJECTIVE

This item of the contract required that Pratt & Whitney Aircraft continue to work with major oil companies to investigate fuels suitable for use in the engine of a supersonic transport aircraft. The goal of this program was to obtain a satisfactory compromise between engine design parameters and engine fuel delivery temperatures, to establish the capability of, and improvement required, to make "Jet A" kerosene satisfy the requirements for economical supersonic transport operation.

A. INTRODUCTION

During the previous phase of the supersonic transport development program it was determined that the environmental conditions of the SST powerplant required that the Jet A fuel have a thermal stability, determined in the ASTM-CFR Fuel Coker, of 350/450°F. This level of fuel thermal stability was based on a fuel delivery temperature of 250°F maximum at the airframe/engine interface and a resulting fuel temperature of 325°F maximum entering the engine fuel manifold. Continued reviews of the fuel environment conducted during Phase II B indicated that these fuel thermal stability requirements have remained unchanged.

During phase IIB a further investigation of the effect of oxygen dissolved in fuel on fuel thermal stability was conducted to determine if this phenomenon could permit the use of present Jet A fuels having minimum thermal stability quality.

B. INVESTIGATION OF THE EFFECT OF FUEL OXYGEN CONTENT ON THERMAL STABILITY

A survey of Jet A and Jet A-1 fuels, comprising 49 samples, conducted during Phase IIA of the supersonic transport program established that about 80 percent of present day domestic fuel of the above type could meet the thermal stability level of 350/450 determined as necessary for the SST powerplant and that the average fuel had an ASTM-CFR Fuel

Coker breakpoint temperature of 350-375°F. Also during Phase IIA a test program was conducted to investigate the thermal stability breakpoint temperatures of three representative aviation kerosene fuels in the CRC Research Fuel Coker at a reservoir temperature of 175°F and at low fuel oxygen contents equivalent to pressure altitudes of 1.0 psia and 1.5 psia (4 ppm and 9 ppm fuel oxygen content respectively). Test results on these fuels did not show any consistent improvement in fuel thermal performance.

During Phase IIB these investigations were broadened to test a wider sampling of Jet A and A-1 fuels at low oxygen contents. Eleven fuels of the Jet A and Jet A-1 type which were expected to have ASTM-CFR Fuel Coker breakpoint temperatures at or below the 350-375°F range were submitted for testing by several major oil companies. The sample identification, vendor code and fuel type for each of these fuels are shown in Figure 11-1. Physical properties of these fuels are shown in Figure 11-2.

Each fuel was tested in the ASTM-CFR Fuel Coker at several levels of preheater/filter temperature to determine a threshold failure temperature. These tests were conducted at 25°F increments of preheater/filter temperature. Threshold failure temperature was defined as the highest preheater/filter temperature at which the fuel would pass present specification criteria, i.e., a Code 2 maximum preheater deposit and a maximum filter pressure rise of 12" Hg. Summarized ASTM-CFR Fuel Coker test results for each fuel are shown in Figure 11-3.

Tests to evaluate the effect of low fuel oxygen content on thermal stability were conducted on the test fuels in the CRC Research Fuel Coker at a reservoir temperature of 175°F. Threshold failure temperatures were initially determined in the CRC Research Fuel Coker at this reservoir temperature under a fully saturated fuel oxygen condition to serve as a baseline. Coker tests were then conducted with low fuel oxygen content by drawing a vacuum of 0.9 ± 0.1 psia on the coker reservoir prior to the start of testing. A magnetic stirrer was operated in the fuel reservoir during each test to hasten oxygen elimination. Thirty minutes were allowed to precondition the reservoir fuel to lower oxygen content and to stabilize the pressure. At this point reservoir heating was initiated and continued for approximately 30 minutes, at which time a reservoir temperature of 175°F was attained and the coker test started.

The 1.0 psia tank pressure represented a typical cruise altitude for a supersonic transport flying at Mach 2.7 cruise with open tank vents and is equivalent to an equilibrium fuel oxygen content of 4 ppm (0.25% by volume). Tests with oxygen contents equivalent to 1.5 ± 0.1 psia (50,000 ft. altitude) and 9 ppm oxygen content (0.5% by volume) were also conducted. A Beckman Model 777 Oxygen Sensor was located in the fuel inlet line to the fuel coker pump to monitor fuel oxygen content during each test; the sensor probe was calibrated in air prior to each test.

Fuel oxygen contents were determined for each test fuel under fully air-saturated conditions prior to coker testing samples of each fuel by sending to a testing laboratory having gas analysis capabilities. The test fuels were air saturated at 80°F by bubbling air through them, duplicating the air saturation occurring prior to coker testing. They were subsequently degassed by a thin film vacuum technique and the gas composition analyzed in a chromatograph. Oxygen saturation values determined for the test fuels are listed below. These are the dissolved oxygen values for the test fuels at the start of each coker test and are the basis on which fuel oxygen contents are calculated during each coker test by means of the Beckman Oxygen Sensor probe which basically indicates a read-out in percent of saturation.

Fuel	Saturated Dissolved Oxygen Content at 80°F
1564	4.41 % by volume
1565	3.41 "
1566	4.45 "
1567	4.27 "
1568	4.47 "
1569	4.48 "
1573	4.60 "
1595	5.03 "
1596	4.48 "
1597	4.40 "
1598	4.15 "

Test results obtained in the CRC Research Fuel Coker at 175°F reservoir temperature with ambient reservoir pressures (fuel air saturated), reservoir pressures of 1.0 psia (approximately 4 ppm oxygen) and reservoir pressures 1.5 psia (approximately 9 ppm oxygen) are shown in Figure 11-4. Fuel oxygen contents during tests at a reservoir pressure of 1.0 psia and 1.5 psia are shown respectively in Figures 11-5 and 11-6.

Threshold failure temperatures determined for the test fuels in the ASTM-CFR Fuel Coker and in the CRC Research Fuel Coker under air saturated and low fuel oxygen contents are summarized in Figure 5-7. With the exception of Sample 1595 which had a standard coker threshold failure temperature (TFT) of 375°F, the test fuels had threshold failure temperatures in the 300-350°F range and thus represented the lower quality spectrum of domestic Jet A thermal stability.

At reduced fuel oxygen contents equivalent to 1.0 psia tank pressure (approximately 4 ppm oxygen content) all of the test fuels showed gains in threshold failure temperature ranging from 25°F to 175+°F. At a 1.5 psia tank pressure (approximately 9 ppm oxygen) no consistent improvement in fuel thermal stability performance was noted. Inasmuch as coker test reproducibility is about ±25°F, only gains in TFT equaling or exceeding 50°F can be assumed as meaningful. It can be concluded from the above that fuels vary in their susceptibility to oxygen, even at very low oxygen contents. Therefore, it appears that no benefits from this phenomenon can be applied against the presently-specified level of fuel thermal stability required for the SST powerplant.

IDENTIFICATION OF DOMESTIC JET A AND JET A-1 FUEL SAMPLES USED IN LOW OXYGEN-FUEL COKER TESTS

PWA Sample Number	Vendor Code	ASTM Fuel Type
1564	A	A-1
1565	A	A-1
1566	B	A
1567	B	A
1573	B	A-1
1568	C	A
1569	C	A-1
1595	D	A-1
1596	D	A
1597	E	A
1598	E	A-1

Figure 11-1

INSPECTION DATA ON TEST FUELS

	ASTM Method	Fuel Number 1564	1565	1566	1567	1568	1569	1573	1595	1596	1597	1598
API Gravity	D-287	43.1	43.7	44.0	44.0	43.0	41.1	42.9	43.7	45.3	42.4	45.8
Specific Gravity 60/60F	D-287	.8104	.8076	.8063	.8063	.8109	.8198	.8114	.8076	.8003	.8137	.7981
Flash Point, °F	D-56	120	108	120	118	132	126	128	116	115	116	116
Freeze Point, °F	D-1477	-66	-65	-58	-55	-57	-57	-64	-67	-60	-47	-62
Pour Point, °F	D-77	-76	-65	-71	-56	-56	-60	-61	-68	-57	-50	-60
Viscosity @ 100°F cs	D-445	1.40	1.45	1.44	1.51	1.43	1.63	1.43	1.38	1.32	1.66	1.23
@ -30°F cs	D-445	7.83	8.04	8.28	8.92	8.05	11.24	8.27	7.73	6.93	11.55	5.95
Aniline Point, °F	D-611	137.8	142.5	144.1	146.1	140.0	143.6	140.0	143.4	144.5	147.2	141.1
Water Tolerance, ML	D-1094	0	0.1	0	0	0	0	0	0	1.0	2.0	2.0
Sulphur, %	D-1266	0.03	0.03	0.08	0.07	0.02	0.01	0.04	0.02	0.08	0.07	0.13
Mercaptan Sulphur, %	D-1323	<0.0001	0.0002	<0.0001	0.0002	0.0001	<0.0001	0.0001	<0.0001	0.0001	<0.0001	0.0002
Copper Corrosion 3 Hr. @ 212°F	D-130	1A	1A	1B	2C	1A	1A	1A	1B	1B	1B	1B
Hydrocarbon Type	D-1319											
Aromatics, %		19.8	11.8	13.3	13.6	17.4	14.0	15.0	13.5	13.5	15.0	14.5
Olefins, %		1.6	2.3	2.2	2.2	1.9	1.0	2.1	1.0	1.0	1.5	1.5
Paraffins & Naphthenes, %		78.6	85.9	84.5	84.2	80.7	85.0	82.9	85.5	85.5	83.5	84.0
Smoke Point, MM	D-1322	22.1	23.6	26.4	25.1	22.8	20.1	24.0	24.3	19.5	22.7	25.1
Existent Gum, Mg/100 ML	D-381	2.2	<1.0	2.4	<1.0	<1.0	1.0	<1.0	1.0	<1.0	<1.0	1.0
Net Heat of Combustion, BTU/Lb.	D-240	18,597	18,476	18,636	18,538	18,560	18,532	18,541	18,575	18,614	18,638	18,578(1)
Luminometer Number	D-1740	43.3	54.3	51.0	59.7	50.1	50.0	48.4	56.5	55.3	57.4	55.0
Distillation, °F	D-86											
1 BP		320	286	306	316	322	318	318	325	294	356	312
20 %		379	364	371	377	374	386	364	372	363	406	356
50 %		401	410	402	420	408	427	406	402	400	436	379
90 %		462	469	481	477	491	490	475	466	465	484	464
EP		503	490	528	505	522	516	505	489	500	510	494
Residue, %		1.5	1.0	1.5	1.5	1.5	1.3	1.9	2.0	1.5	1.8	2.0
Loss, %		1.5	3.0	1.0	1.5	2.0	1.1	1.1	1.0	0.5	1.4	0.5

(1) ASTM Method D1405

Figure 11-2

SUMMARY OF TESTS TO DETERMINE THRESHOLD FAILURE TEMPERATURE OF JET A AND JET A-1 FUEL SAMPLES IN ASTM-CFR FUEL COKER

PWA Sample Number	Temperature Conditions Preheater/Filter	Filter ΔP/Minutes	Tube Deposit Cold											Hot
1564	300/400	2.5/300	2	2	2	2	2	2	2	2	0	0	0	0	0
	325/425	11.9/300	2	2	1	1	1	1	1	1	1	1	1	1	1
	350/450	19/300	0	2	0	0	0	0	0	0	1	2	4	1	1
1565	325/425	0.1/300	1	1	1	1	1	1	1	1	1	1	1	1	1
	350/450	0.3/300	1	1	1	1	1	1	1	1	1	1	4	4	4
	375/475	25/263	1	1	1	1	1	1	1	1	1	6	6	5	6
1566	350/450	0.5/300	1	2	2	1	1	1	1	1	1	1	1	1	1
	375/475	14.7/300	1	2	2	1	1	1	1	1	1	1	2	2	2
	400/500	25/245	1	2	2	1	1	1	1	1	1	1	3	3	3
1567	325/425	5.8/300	1	1	1	1	1	1	1	1	1	1	1	1	1
	350/450	14.9/300	1	1	1	1	1	2	2	2	2	2	3	3	1
	375/475	25/204	1	1	1	1	1	1	1	1	1	1	2	2	1
	400/500	25/166	1	2	2	1	1	1	1	1	2	3	3	3	3
1568	350/450	12.2/300	1	2	2	1	1	1	1	1	1	1	2	2	1
	375/475	25/131	1	2	2	2	1	1	1	1	1	2	6	6	6
1569	350/450	14.6/300	1	1	1	1	1	1	1	1	1	1	1	1	1
	3 475	25/215	1	1	1	1	1	1	1	1	1	2	2	2	1
	400/500	25/242	1	2	2	2	2	2	2	3	3	3	3	3	3
1573	325/425	9.0/300	1	2	2	2	2	2	2	2	2	2	2	2	1
	350/450	25/274	1	2	2	1	1	2	2	2	2	2	2	2	1
	375/475	25/149	1	2	1	1	1	1	1	1	1	2	4	4	2
1595	350/450	0.3/300	1	2	1	1	1	1	1	1	2	2	2	1	1
	375/475	0.9/300	1	2	2	2	1	1	2	2	2	2	2	1	1
	400/500	25/142	1	1	1	1	1	1	1	1	4	4	5	5	4
1596	350/450	8.3/300	1	1	1	1	1	1	1	1	1	1	1	1	1
	375/475	25/239	1	2	2	1	1	1	1	1	1	1	1	1	1
	400/500	25/210	1	1	1	1	1	1	1	2	3	3	3	3	2
1597	300/400	2.6/300	1	1	1	1	1	1	1	1	1	1	2	2	1
	325/425	25/273	1	1	1	1	1	1	1	1	1	1	1	1	1
	350/450	18.3/300	1	1	1	1	1	1	1	1	1	1	1	1	1
	375/475	9.9/300	2	2	2	2	2	2	1	1	1	1	1	1	1
	400/500	25/222	1	1	1	1	1	1	1	1	1	3	4	4	4
1598	350/450	1.9/300	1	1	1	1	1	1	1	1	1	1	1	1	1
	375/475	25/253	0	1	1	1	1	1	1	1	1	2	2	2	1
	400/500	25/99	1	1	1	1	1	1	1	2	3	6	5	5	4

Figure 11-3

SUMMARY OF TESTS TO DETERMINE THRESHOLD FAILURE TEMPERATURE OF TEST FUELS IN CRC RESEARCH FUEL COKER AT CONTROLLED FUEL OXYGEN CONDITIONS WITH 175 °F RESERVOIR FUEL TEMPERATURE

PWA Sample Number	Reservoir Pressure PSIA	Test No.	P/F Temp. °F	Filter ΔP/Minutes	Tube Deposit Cold → Hot
1564	ATM	2267	350/450	12.5/300	2 2 2 2 2 2 1 1 1 1 1 1 1
		2279	375/475	25/236	1 1 1 2 2 2 2 2 2 1 1 1 1
		2276	400/500	25/123	1 1 1 1 1 1 1 1 1 1 4 4 4
	1.0	2269	375/475	21/300	1 1 1 1 1 1 1 2 2 2 2 2 2
		2270	400/500	6.5/300	1 1 1 1 1 1 1 1 2 2 2 2 2
		2271	425/525	2.4/300	1 1 1 1 1 1 1 2 2 2 2 2 2
		2272	450/550	25/250	0 2 2 2 2 2 2 3 4 4 4 4 4
	1.5	2292	325/425	2.0/300	1 1 1 1 1 1 1 1 1 1 1 1 1
		2280	350/450	25/295	1 1 1 1 1 1 1 2 2 2 2 2 2
		2275	375/475	25/224	1 1 1 1 1 1 1 1 1 2 3 3 3
		2274	400/500	25/300	1 1 1 1 1 1 1 1 2 2 3 3 3
		2273	425/525	25/288	1 1 1 1 1 2 2 2 3 3 3 3 2
1565	ATM	2289	325/425	0.45/300	1 1 1 1 1 1 1 1 1 1 1 1 1
		2302	350/450	0.9/300	1 1 1 1 1 1 1 1 1 1 1 1 1
		2346	375/475	25/178	1 1 1 1 1 1 1 1 1 6 6 6 6
	1.0	2290	350/450	0.35/300	1 1 1 1 1 1 1 1 1 1 1 1 1
		2294	375/475	0.2/300	0 1 1 1 1 1 1 1 1 2 2 2 2
		2295	400/500	0.2/300	0 1 1 1 1 1 1 1 2 2 2 2 2
		2296	425/525	0/300	0 1 1 2 2 2 2 2 2 2 2 2 2
		2297	450/550	0.2/300	1 1 1 1 1 1 1 3 3 2 2 1 1
	1.5	2299	325/425	0.2/300	1 1 1 1 1 1 1 1 2 2 1 1 1
		2298	350/450	0.2/300	2 2 2 2 2 2 2 2 2 3 3 3 3
		2352	375/475	15.4/300	1 1 1 1 1 1 1 1 2 3 3 3 3
		2347	475/575	0.8/300	1 1 1 1 1 1 5 5 5 1 1 1 1
1566	ATM	2255	350/450	2.0/300	1 1 1 1 1 1 1 1 1 1 1 1 1
		2256	375/475	25/230	1 1 1 1 1 1 1 1 1 2 2 2 2
		2257	400/500	25/140	1 1 1 1 1 1 1 2 2 2 3 3 3
	1.0	2258	400/500	/300	0 0 1 1 1 1 1 1 1 2 2 2 1
		2260	425/525	0.0/300	1 1 1 1 1 1 1 1 1 2 2 2 2
		2263	450/550	14.1/300	1 1 1 1 1 2 2 2 2 2 2 2 1
		2264	475/575	6.1/300	1 1 1 1 1 1 2 2 2 3 3 2 1
	1.5	2353	375/475	1.25/300	1 1 1 1 1 1 1 1 2 2 2 2 2
		2372	400/500	9.6/300	0 1 1 1 1 1 1 1 1 2 2 2 2
		2266	425/525	25/217	0 0 1 1 1 1 1 2 2 2 2 2 2
		2265	450/550	20/300	1 1 1 1 1 2 3 3 3 3 2 2 2

Figure 11-4
(sheet 1 of 4)

SUMMARY OF TESTS TO DETERMINE THRESHOLD FAILURE TEMPERATURE OF TEST FUELS IN CRC RESEARCH FUEL COKER AT CONTROLLED FUEL OXYGEN CONDITIONS WITH 175°F RESERVOIR FUEL TEMPERATURE

(Continued)

PWA Sample Number	Reservoir Pressure PSIA	Test No.	P/F Temp. °F	Filter ΔP/Minutes	Tube Deposit Cold → Hot
1567	ATM	2318	350/450	7.7/300	1 2 1 1 1 1 1 1 1 1 2 1
		2317	375/475	18/300	1 2 2 1 1 1 1 1 2 2 2 3 3
		2316	400/500	25/215	1 1 2 2 1 1 1 1 1 3 3 3 3
	1.0	2319	350/450	4.7/300	1 1 1 1 1 1 1 1 1 2 2 2 2
		2320	375/475	4.8/300	1 1 1 1 1 1 1 1 1 1 1 1 1
		2321	400/500	8.7/300	1 1 1 1 1 1 2 2 2 2 2 2
		2322	425/525	0.4/300	1 1 1 1 1 1 1 2 2 2 2 2 2
		2323	450/550	2.9/300	1 1 1 1 1 1 1 1 2 2 1 1 1
		2324	475/575	3.0/300	1 1 1 1 1 1 1 1 1 2 2 2 2
		2325	500/600	1.7/300	1 1 1 1 1 1 1 1 1 2 2 2 2
	1.5	2345	325/425	18.3/300	1 1 1 1 1 1 1 1 1 1 1 1 1
		2343	350/450	25/276	1 1 1 1 1 1 1 1 1 1 1 1 1
		2336	400/500	25/226	0 1 1 1 1 1 1 2 2 2 2 2 1
		2326	450/550	25/176	1 1 1 1 1 1 1 2 2 2 2 2 2
		2330	500/600	25/163	1 1 1 1 1 1 1 2 2 2 2 1 1
		2333	550/650	25/160	1 1 1 1 1 2 2 3 3 3 2 2 1
1568	ATM	2408	325/425	4.4/300	0 1 1 1 1 1 1 1 1 1 1 1 1
		2384	350/450	18.6/300	1 1 2 2 2 2 2 2 2 2 2 2 2
		2385	375/475	25/182	1 2 2 2 2 2 2 2 2 2 2 3 3
	1.0	2386	350/450	2.8/300	1 1 1 1 1 1 1 1 2 2 2 2 2
		2387	375/475	11.9/300	1 1 1 1 1 1 1 2 2 2 2 2 2
		2388	400/500	3.6/300	1 1 1 1 1 1 1 1 2 2 2 2 2
		2389	425/525	7.2/300	1 1 1 1 1 1 1 1 2 2 2 2 2
		2390	450/550	5.1/300	1 1 1 1 1 1 2 2 2 2 2 2 2
		2391	475/575	2.0/300	1 1 1 2 1 1 2 2 2 2 2 2 2
		2392	500/600	1.6/300	1 1 1 1 1 2 2 2 2 2 2 2 2
	1.5	2399	450/550	6.4/300	1 1 1 1 1 1 1 2 2 2 2 2 2
		2400	475/575	5.1/300	0 1 1 1 1 1 1 2 2 2 3 3 3
1569	ATM	2432	375/475	12.6/300	1 1 1 1 1 1 1 1 1 2 2 2 2
		2433	400/500	25/198	1 1 1 1 1 2 2 2 2 3 5 5 3
	1.0	2440	375/475	14.8/300	1 1 1 1 1 1 1 2 2 2 2 2 1
		2446	400/500	1.8/300	1 1 1 1 1 1 1 1 1 1 2 2 1
		2439	425/525	25/290	1 1 1 1 1 1 3 4 4 4 4 3 2
		2434	450/550	10.8/300	1 1 1 1 2 2 3 4 4 4 3 2 2
	1.5	2452	350/450	25/225	1 1 1 1 1 2 2 2 3 3 3 3 3
		2474	350/450	25/114	1 2 2 2 2 2 2 2 3 3 3 3 3
		2441	375/475	8.3/300	1 1 1 1 1 1 1 1 2 2 5 5 4
		2445	375/475	4.8/300	1 1 1 1 1 1 1 1 1 2 3 3 2

Figure 11-4
(sheet 2 of 4)

SUMMARY OF TESTS TO DETERMINE THRESHOLD FAILURE TEMPERATURE OF TEST FUELS IN CRC RESEARCH FUEL COKER AT CONTROLLED FUEL OXYGEN CONDITIONS WITH 175°F RESERVOIR FUEL TEMPERATURE
(Continued)

PWA Sample Number	Reservoir Pressure PSIA	Test No.	P/F Temp. °F	Filter ΔP/Minutes	Tube Deposit Cold → Hot
1573	ATM	2410	300/400	1.7/300	2 2 2 2 2 2 2 2 2 2 2 2 2
		2361	325/425	14.3/300	1 2 2 2 2 2 1 1 1 1 1 2 2
		2348	350/450	25/257	2 2 2 2 2 2 2 2 1 1 1 1 1
		2355	375/475	25/102	2 2 2 2 2 2 2 2 2 2 2 5 6
	1.0	2366	325/425	7.4/300	1 1 1 1 1 1 1 1 1 1 1 1 1
		2349	350/450	25/243	1 1 1 1 1 1 2 2 2 2 2 2 2
		2356	375/475	25/175	1 1 1 1 1 1 1 1 2 2 2 2 2
		2362	400/500	3.7/300	1 1 1 1 1 1 1 1 1 1 1 2 2
		2363	425/525	2.8/300	1 1 1 1 2 2 2 2 1 1 1 2 2
		2365	450/550	19.2/300	1 1 1 1 1 1 1 1 2 2 2 2 2
		2367	475/575	15.5/300	1 1 1 1 1 1 1 1 2 2 2 2 2
	1.5	2376	325/425	6.0/300	1 1 1 1 1 1 2 2 2 2 2 2 1
		2374	350/450	25/216	1 1 1 1 1 1 1 1 1 2 2 2 2
		2373	375/475	25/114	1 1 1 1 1 1 1 1 3 6 3 3 6
1595	ATM	2484	350/450	3.4/300	2 2 2 2 2 2 2 2 2 2 2 2 2
		2525	375/475	4.4/300	2 2 2 2 2 2 2 2 2 2 2 2 2
		2485	400/500	25/230	1 1 1 1 1 1 1 1 1 2 4 5 4
	1.0	2488	400/500	1.1/300	1 1 1 1 1 1 1 1 1 1 1 1 1
		2489	425/525	0.3/300	1 1 1 1 1 1 1 1 1 1 1 1 1
		2490	450/550	0.6/300	1 1 1 1 1 1 1 1 1 1 1 1 1
		2491	500/600	3.2/300	1 1 1 1 1 2 2 2 1 1 1 1 1
		2492	525/625	4.9/300	1 1 1 1 1 2 2 2 2 2 2 1 1
		2493	550/650	11.2/300	1 1 1 1 2 2 2 2 2 2 2 2 2
	1.5	2499	350/450	0.3/300	1 1 1 1 1 1 1 1 1 1 1 1 1
		2487	375/475	14/300	1 1 1 1 1 1 1 1 1 1 1 2 1
		2486	400/500	25/290	1 2 2 2 1 1 1 1 2 2 3 3 3
1596	ATM	2516	350/450	6.3/300	0 1 1 1 1 1 1 1 1 1 1 1 1
		2517	375/475	25/157	1 1 1 1 1 2 2 2 2 2 2 2 2
		2518	400/500	25/192	0 1 1 1 1 1 1 2 2 3 3 3 3
	1.0	2519	400/500	1.1/300	1 1 1 1 1 1 1 1 1 1 1 1 1
		2521	425/525	0.8/300	0 0 1 1 1 1 1 1 1 1 1 1 1
		2522	500/600	1.1/300	1 1 1 1 1 1 1 1 1 1 1 1 1
	1.5	2527	400/500	23.6/300	1 1 1 1 1 1 1 2 2 2 2 2 2
		2528	450/550	23.7/300	0 1 1 1 1 1 1 2 2 2 2 2 2
		2523	500/600	1.7/300	1 1 1 1 1 2 2 2 2 2 2 2 2

Figure 11-4
(sheet 3 of 4)

SUMMARY OF TESTS TO DETERMINE THRESHOLD FAILURE TEMPERATURE OF TEST FUELS IN CRC RESEARCH FUEL COKER AT CONTROLLED FUEL OXYGEN CONDITIONS WITH 175°F RESERVOIR FUEL TEMPERATURE

(Continued)

PWA Sample Number	Reservoir Pressure PSIA	Test No.	P/F Temp. °F	Filter ΔP/Minutes	Tube Deposit Cold → Hot
1597	ATM	2453	350/450	7.9/300	1 1 1 1 1 1 1 1 1 1 1 1 1
		2435	375/475	25/219	1 1 1 1 1 1 1 1 1 1 1 1 1
		2436	400/500	25/143	1 2 2 2 2 2 2 2 1 1 1 1 1
		2442	425/525	25/78	1 1 1 1 1 1 1 2 2 3 4 4 4 3
		2447	450/550	25/110	1 1 1 1 1 1 1 1 2 3 5 5 4
	1.0	2443	425/525	6.2/300	1 1 1 1 1 1 1 1 2 2 2 2 2 2
		2444	450/550	8.3/300	1 1 1 1 1 1 1 1 1 1 1 1 1 1
		2460	500/600	3.6/300	0 1 1 1 1 1 1 1 2 2 2 2 2 2
	1.5	2479	325/425	4.6/300	1 1 1 1 1 1 1 1 1 1 1 1 1 1
		2473	350/450	21/300	1 1 1 1 1 1 1 1 1 1 1 1 1 1
		2468	375/475	25/146	1 2 2 2 1 2 2 2 2 2 2 2 2 2
		2464	400/500	7.5/300	1 1 1 3 3 3 1 1 3 3 3 2 2 2
		2459	425/525	25/211	1 1 1 2 2 2 2 3 3 3 3 3 3 3
		2455	450/550	25/142	1 1 3 1 1 1 1 2 2 2 2 2 2 2
1598	ATM	2494	350/450	0.15/300	1 1 1 1 1 1 1 1 1 1 1 1 1 1
		2497	375/475	25/154	1 1 2 2 1 1 1 1 2 2 2 2 2 2
		2498	400/500	25/68	1 1 1 1 1 1 1 1 2 2 3 3 3 3
	1.0	2503	400/500	0.95/300	1 1 1 1 1 1 1 1 1 1 1 1 1 1
		2509	450/550	9.7/300	1 1 1 1 1 2 2 2 2 2 2 2 1 1
		2510	475/575	3.3/300	1 1 1 1 1 2 2 2 2 2 2 2 2 2
		2508	500/600	15.4/300	1 1 1 1 2 2 2 2 3 3 3 3 2 2
	1.5	2500	400/500	8.2/300	1 1 1 1 2 2 2 2 2 2 2 2 2 2
		2501	425/525	15.7/300	1 1 1 2 2 1 1 1 1 2 2 2 2 2
		2502	450/550	23/300	1 1 1 1 1 1 1 1 2 2 2 2 2 2
		2504	475/575	25/271	1 1 1 1 1 1 1 1 2 2 2 2 2 2
		2511	500/600	20/300	0 1 1 1 1 1 1 1 2 2 2 2 2 2

Figure 11-4
(sheet 4 of 4)

FUEL OXYGEN CONTENT DURING RESEARCH COKER TESTS
WITH 1.0 PSIA RESERVOIR PRESSURE

Test Number	Fuel Oxygen Content, % Vol.							
	Heat On -0.5 Hr.	Start 0 Hr.	0.5 Hr.	1 Hr.	2 Hr.	3 Hr.	4 Hr.	End 5 Hr.
2258	0.70	0.27	0.18	0.11	0.07	0.07	0.07	0.07
2260	0.89	0.25	0.09	0.04	0.02	0.02	0.02	0.01
2263	-	0.04	0.02	0.01	0.01	0.01	0.01	0.01
2264	0.60	0.18	0.06	0.05	0.04	0.04	0.04	0.04
2269	0.99	0.32	0.16	0.08	0.04	0.04	0.04	0.04
2270	0.64	0.35	0.18	0.09	0.04	0.04	0.04	0.04
2271	0.93	0.53	0.19	0.11	0.07	0.06	0.05	0.05
2272	0.80	0.36	0.26	0.13	0.03	-	-	-
2290	-	0.17	-	-	-	-	-	-
2294	0.36	0.14	-	-	-	-	-	0.03
2295	0.55	0.26	0.09	0.05	0.03	0.03	0.03	0.03
2296	0.49	0.29	0.28	0.06	0.03	0.03	0.03	0.03
2297	0.41	0.38	0.14	0.14	0.14	0.14	0.14	0.14
2319	0.85	0.47	0.32	0.23	0.13	0.10	0.09	0.07
2320	0.77	0.38	0.29	0.19	0.13	0.09	0.07	0.06
2321	0.62	0.30	0.15	0.09	0.04	0.04	0.04	0.04
2322	0.58	0.33	0.19	0.11	0.05	0.04	0.04	0.04
2323	0.57	0.20	0.06	0.04	0.03	0.02	0.01	0.01
2324	0.16	0.11	0.07	0.04	0.03	0.02	0.02	0.02
2325	0.64	0.53	0.43	0.41	0.36	0.21	0.15	0.10
2349	0.92	0.48	0.23	0.18	0.11	0.09	0.08	0.07
2356	0.69	0.48	0.41	0.18	0.09	0.09	0.09	0.07
2362	0.68	0.39	0.25	0.15	0.08	0.06	0.05	0.05
2363	0.57	0.37	0.19	0.09	0.02	0.01	0.02	0.00
2365	0.69	0.42	0.26	0.15	0.10	0.07	0.06	0.06
2366	0.80	0.51	0.33	0.21	0.13	0.09	0.07	0.07
2367	0.69	0.35	0.21	0.12	0.07	0.05	0.04	0.04
2386	0.80	0.36	0.13	0.09	0.04	0.04	0.04	0.04
2387	0.85	0.47	0.34	0.25	0.13	0.09	0.08	0.07
2388	0.78	0.47	0.36	0.22	0.12	0.11	0.11	0.11
2389	0.69	0.38	0.21	0.19	0.09	0.05	0.04	0.04
2390	2.46	0.74	0.18	0.09	0.06	0.04	0.03	0.02
2391	0.82	0.32	0.17	0.09	0.04	0.03	0.03	0.02
2392	0.92	0.34	0.20	0.13	0.08	0.06	0.05	0.05
2434	-	0.54	0.36	0.27	0.22	0.22	0.16	0.11
2439	0.64	0.40	0.33	0.24	0.18	0.13	0.13	0.18
2440	-	0.42	0.28	0.22	0.14	0.10	0.08	0.08
2443	0.88	0.42	0.27	0.20	0.13	0.10	0.08	0.07
2444	1.43	0.55	0.37	0.18	0.13	0.11	0.09	0.09
2446	1.12	0.37	0.06	0.04	0.03	0.03	0.03	0.03
2460	-	0.46	0.33	0.26	0.16	0.11	0.11	0.11

Figure 11-5

FUEL OXYGEN CONTENT DURING RESEARCH COKER TESTS
WITH 1.0 PSIA RESERVOIR PRESSURE (CONT'D)

Test Number	Fuel Oxygen Content, % Vol. Heat On -0.5 Hr.	Start 0 Hr.	0.5 Hr.	1 Hr.	2 Hr.	3 Hr.	4 Hr.	End 5 Hr.
2488	1.06	0.45	0.18	0.13	0.11	0.11	0.10	0.08
2489	-	0.17	0.05	0.05	0.05	0.05	0.05	0.05
2490	0.62	0.30	0.06	0.05	0.05	0.05	0.05	0.05
2491	1.13	0.50	0.16	0.11	0.10	0.10	0.10	0.10
2492	-	0.40	0.21	0.14	0.08	0.07	0.06	0.06
2493	0.55	0.19	0.08	0.06	0.03	0.02	0.01	0.02
2503	0.58	0.24	0.07	0.06	0.05	0.05	0.05	0.04
2508	0.50	0.30	0.06	0.05	0.05	0.05	0.04	0.04
2509	-	0.18	0.05	0.05	0.02	0.02	0.02	0.02
2510	-	0.15	0.04	0.02	0.02	0.02	0.02	0.02
2519	0.85	0.59	0.18	0.15	0.15	0.15	0.15	0.15
2521	0.61	0.38	0.17	0.08	0.03	0.06	0.07	0.07
2522	0.59	0.32	0.04	0.04	0.03	0.03	0.03	0.03

Figure 11-5 (Continued)

FUEL OXYGEN CONTENT DURING RESEARCH COKER TESTS
WITH 1.5 PSIA RESERVOIR PRESSURE

Test Number	Fuel Oxygen Content, % Vol. Heat On -0.5 Hr.	Start 0 Hr.	0.5 Hr.	1 Hr.	2 Hr.	3 Hr.	4 Hr.	End 5 Hr.
2265	0.87	0.47	0.27	0.27	0.26	0.23	0.22	0.23
2266	0.73	0.49	0.38	0.33	0.29	0.29	0.29	0.29
2273	1.00	0.66	0.51	0.40	0.26	0.22	0.22	0.22
2274	1.08	0.68	0.50	0.39	0.28	0.26	0.26	0.26
2275	0.97	0.66	0.54	0.49	0.35	0.31	0.30	0.29
2280	0.97	0.71	0.57	0.44	0.40	0.37	0.35	0.33
2292	0.97	0.64	0.51	0.40	0.30	0.26	0.20	0.18
2298	0.60	0.51	0.39	0.13	0.09	0.08	0.08	0.08
2299	0.75	0.55	0.48	0.37	0.26	0.20	0.18	0.17
2326	0.90	0.62	0.43	0.34	0.23	0.20	0.19	0.18
2330	2.03	0.60	0.47	0.36	0.25	0.19	0.17	0.13
2333	0.98	0.60	0.47	0.41	0.27	0.22	0.20	0.19
2336	0.81	0.55	0.47	0.42	0.32	0.28	0.26	0.23
2343	-	0.53	0.43	0.36	0.26	0.22	0.19	0.26
2345	0.68	0.53	0.35	0.26	0.17	0.13	0.10	0.19
2347	0.61	0.43	0.17	0.11	0.07	0.07	0.07	0.07
2352	0.70	0.42	0.27	0.20	0.11	0.08	0.08	0.08
2353	1.05	0.64	0.47	0.36	0.26	0.22	0.20	0.20
2372	1.09	0.71	0.52	0.42	0.36	0.31	0.29	0.29
2373	-	0.78	0.53	0.44	0.38	0.32	0.30	0.30
2374	0.91	0.67	0.55	0.41	0.30	0.24	0.20	0.19
2376	1.26	0.51	0.37	0.25	0.15	0.12	0.14	0.14
2399	-	0.51	0.35	0.27	0.18	0.16	0.14	0.15
2400	0.83	0.48	0.37	0.29	0.21	0.21	0.21	0.21
2441	1.12	0.92	0.73	0.72	0.67	0.50	0.43	0.38
2445	0.90	0.67	0.57	0.56	0.41	0.31	0.27	0.26
2452	-	1.61	0.09	0.06	0.10	0.13	0.21	0.22
2455	0.88	0.57	0.51	0.47	0.36	0.29	0.27	0.22
2459	1.10	0.70	0.58	0.47	0.35	0.30	0.27	0.27
2464	0.84	0.59	0.53	0.47	0.35	0.31	0.25	0.26
2468	1.10	0.86	0.70	0.62	0.51	0.42	0.40	0.33
2473	1.08	0.66	0.56	0.51	0.42	0.33	0.31	0.29
2474	1.23	0.90	0.83	0.63	0.42	0.36	0.36	0.36
2479	0.86	0.53	0.47	0.40	0.30	0.25	0.22	0.20
2486	1.28	0.76	0.60	0.60	0.43	0.40	0.40	0.35
2487	0.90	0.53	0.48	0.36	0.25	0.21	0.21	0.21
2499	1.23	0.63	0.34	0.25	0.24	0.25	0.24	0.24
2500	-	0.50	0.34	0.28	0.23	0.23	0.23	0.24
2501	0.83	0.54	0.29	0.25	0.23	0.23	0.23	0.23
2502	-	0.61	0.30	0.25	0.21	0.20	0.19	0.19
2504	1.02	0.60	0.35	0.33	0.31	0.30	0.25	0.24
2511	0.73	0.50	0.29	0.24	0.22	0.22	0.22	0.22
2523	1.39	0.55	0.29	0.23	0.19	0.18	0.18	0.18
2527	0.99	0.63	0.36	0.25	0.25	0.24	0.24	0.27
2528	0.99	0.62	0.36	0.26	0.25	0.25	0.23	0.22

Figure 11-6

SUMMARY OF THRESHOLD FAILURE TEMPERATURES FOR TEST FUELS UNDER AIR SATURATION AND LOW FUEL OXYGEN CONTENT

Fuel	Threshold Failure Temperature, °F					
		CRC Research Coker (175F Reservoir)				
	Std. Coker	Air Saturated	1.0 PSIA (4 ppm O_2)	Gain	1.5 PSIA (9 ppm O_2)	Gain
1564	325	325	350	25	325	0
1565	325	350	425	75	325	-25
1566	350	350	425+	75+	400	50
1567	325	350	500+	150+	300	-50
1568	325	325	500+	175+	450	125
1569	(350)	375	400	25	(325)	-50
1573	325	300	325	25	325	25
1595	375	375	550	175	350	-25
1596	350	350	500+	150+	(350)	0
1597	300	350	500+	150+	325	-25
1598	350	350	475	125	400	50

Note: TFT temperatures shown in brackets could not be definitely established and are approximate only.

Figure 11-7

ITEM 12

LUBRICANTS

ITEM 12

ITEM 12 - LUBRICANTS

OBJECTIVE

The goal of this program is to obtain the most favorable compromise between engine design parameters and lubricant capability to satisfy the requirements for safe, reliable and economical operation of a supersonic transport engine.

A. INTRODUCTION

It is necessary to determine the rolling contact fatigue life of gear materials expected to be used in supersonic aircraft engines for two reasons: (1) metal fatigue is a critical problem in extended engine operation, and (2) lubricant composition and temperature levels have a significant effect on the rolling contact fatigue life of steels.

PWA 724 (Bower 315) carburized test gears were used in the metal fatigue tests. The testing of PWA 724 gears in this contract period is compared with AMS 6260 gears reported under previous contracts.

Using the latest fuel delivery temperature information supplied by the airframe contractor, the environmental conditions to be imposed on the lubricant were analytically determined. No significant changes were noted in this review relative to previous studies.

B. LUBRICANT ENVIRONMENT

Since the temperature of the fuel delivered to the engine fuel system is the predominant factor governing many temperatures throughout the oil system, the current predicted temperature data and environmental conditions are based upon the temperature of the fuel delivered from the airframe. Figure 12-1 indicates that the fuel temperature will rise sharply to a peak of 250°F. This curve is identical to one presented in the Phase IIA report. Any increase in the fuel temperatures relative to those shown in Figure 12-1 will change the expected lubricant system temperature pattern; large temperature increases could conceivably require a lubricant with properties superior to those evaluated in this contract period. Supplemental cooling, utilizing unscheduled fuel flow

DOWNGRADED AT 3 YEAR INTERVALS
DECLASSIFIED AFTER 12 YEARS
DOD DIR 5200.10

THIS DOCUMENT CONTAINS INFORMATION AFFECTING THE NATIONAL DEFENSE OF THE UNITED STATES WITHIN THE MEANING OF THE ESPIONAGE LAWS, TITLE 18 U. S. C. SECTIONS 793 AND 794. THE TRANSMISSION OR THE REVELATION OF ITS CONTENTS IN ANY MANNER TO AN UNAUTHORIZED PERSON IS PROHIBITED BY LAW.

returned to the fuel tanks, is necessary to prevent excessive temperature levels in the lubrication system during descent from the flight cruise condition. Thus, the environmental conditions must be considered as estimates.

During the contract period, additional studies were conducted of the lubricant environment. These environmental conditions are outlined below:

1. TEMPERATURE

Based on the lubricant temperatures shown in Figure 12-1, bearing temperatures are expected to reach a maximum steady-state level of 400°F at the end of the cruise, and may possibly approach 500°F during the descent portion of the flight. Local compartment wall hot spots are not expected to exceed 600°F.

2. OIL TANK CAPACITY

6 gallons nominal oil
4 gallons usable oil

3. AIR CONTACTING OIL

Flow - 0.06 lbs/sec./seal; 0.4 lb./sec./seal with seal failure
Temperature - 830°F max. at Mach 3.0

4. BEARINGS

a. Materials

Races, rollers, balls - PWA 724 CVM or AMS 6490
Cages - AMS 6415, silver-plated per AMS 2410

b. Types

Angular Contact-Split Inner Race, Single Bearing, ABEC #7
Tolerances; 170 x 260 x 42 mm at 6100 rpm and 200 x 300 x 51 mm at 8250 rpm
Roller - Preloaded, 200 x 300 x 38 mm at 8250 rpm

DOWNGRADED AT 3 YEAR INTERVALS
DECLASSIFIED AFTER 12 YEARS
DOD DIR 5200.10

5. ALLOYS IN LUBRICATING SYSTEM

Tank - AMS 5510, 5645
Oil Filter - AMS 5362, 5640
Fuel-Oil Cooler - AMS 5362, 5571, 5646
Scavenge Pumps - AMS 5362, 5640, PWA 724
Piping - AMS 5570, 5571, 5646, 6005
Bearing Compartments - AMS 5062, 5613, 5616, 5688, 6322, 6323, 7310, PWA 724

6. GEARS

Hertz Stress - 92,000 psi starting, 71,000 psi steady-state
Material - PWA 724 heat treated

7. ELASTOMERS

None in lubricating system

8. LUBRICANT VISCOSITY

Lubricating system imposes no restrictions on oil viscosity.

9. LUBRICANT VOLATILITY

Volatility requirements of the lubricating system are compatible with the volatility characteristics of MIL-L-23699 lubricants.

C. GEAR PITTING TESTS

Gear pitting fatigue tests were initiated in the previous contract period on AMS 6260 test gears to evaluate the influence of temperature and load on the gear fatigue life as affected by a MIL-L-23699 lubricant (L-919).

PWA 724 carburized test gears replaced the AMS 6260 test gears used in previous contract periods. Steady-state gear pitting fatigue tests were conducted in Ryder Gear Machines at lubricant temperatures of 300 and 350°F and at Hertz stresses up to 250,000 psi for 1250 hours. The Hertz stresses were kept at a high level to accumulate a maximum amount of data in the shortest possible time interval. Test oil flow rate and rate of stress application were maintained at constant levels. The gear pitting fatigue data are shown in Figures 12-2 and 12-3.

DOWNGRADED AT 3 YEAR INTERVALS
DECLASSIFIED AFTER 12 YEARS
DOD DIR 5200.10

The Ryder Gear Machine and the Erdco Universal Drive Test Stand, as described in Federal Test Method Standard No. 791a Method 6508 and ASTM D-1947, were used in the gear pitting fatigue tests.

In addition to the gear pitting fatigue program, two oils were subjected to cursory evaluations during this contract period using the test procedures and equipment described in the previous SST report, submitted for contract AF33(657)-11189, PWA-2353. Included in these lubricant evaluations were physical property determinations, lubricant-carbon wear, volatility and oxidation-corrosion tests and Ryder Gear load-carrying capacity as shown in Figures 12-4 through 12-7.

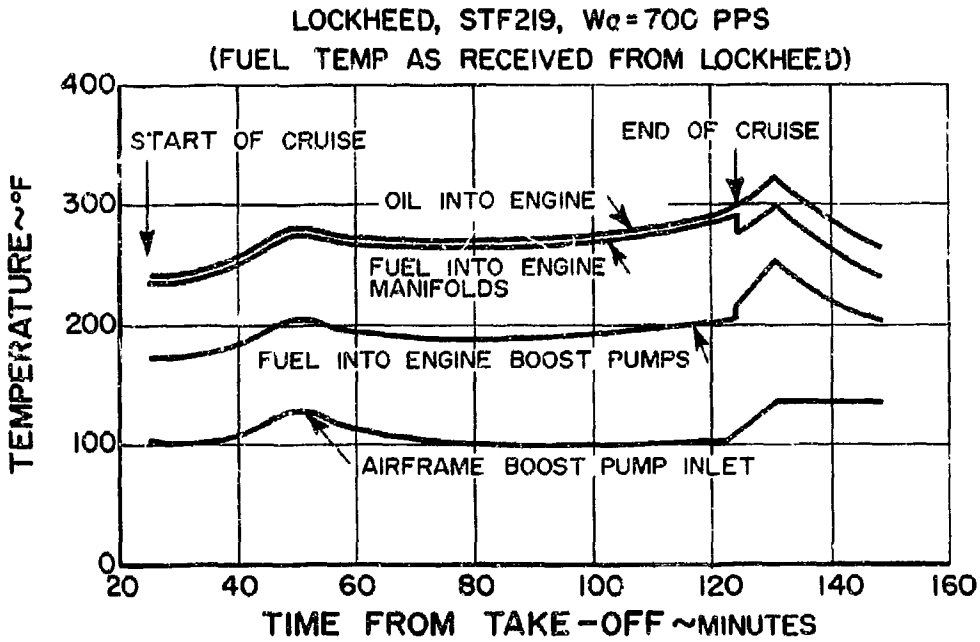
D. DISCUSSION

The supersonic transport powerplant requires a lubricant to withstand the oxidative and thermal stresses encountered in the lubricant system environment. The lubricant must demonstrate the following characteristics satisfactorily: metal rolling contact fatigue, valatility, carbon seal wear rates, gear load-carrying ability, and corrosive tendencies in oxidizing atmospheres. During previous contract periods, these characteristics were evaluated in tests covering a large range of operational severities utilizing the most recent lubrication system environmental parameters. During this contract period, effort was primarily concentrated upon rolling contact fatigue.

Due to the nature of fatigue testing, the data presented in Figure 12-2 are in bands rather than lines. Individual test results obtained during this contract period are tabulated in Figure 12-3. Figure 12-4 lists the general properties of the two lubricants tested during this contract period. Volatility characteristics of these two lubricants are shown in Figures 12-5 and 12-6. Oxidation-corrosion tendencies of lubricant L-1530 are tabulated in Figure 12-7.

DOWNGRADED AT 3 YEAR INTERVALS
DECLASSIFIED AFTER 12 YEARS
DOD DIR 5200.10

THIS DOCUMENT CONTAINS INFORMATION AFFECTING THE NATIONAL DEFENSE OF THE UNITED STATES WITHIN THE MEANING OF THE ESPIONAGE LAWS, TITLE 18 U.S.C. SECTIONS 793 AND 794. ITS TRANSMISSION OR THE REVELATION OF ITS CONTENTS IN ANY MANNER TO AN UNAUTHORIZED PERSON IS PROHIBITED BY LAW.

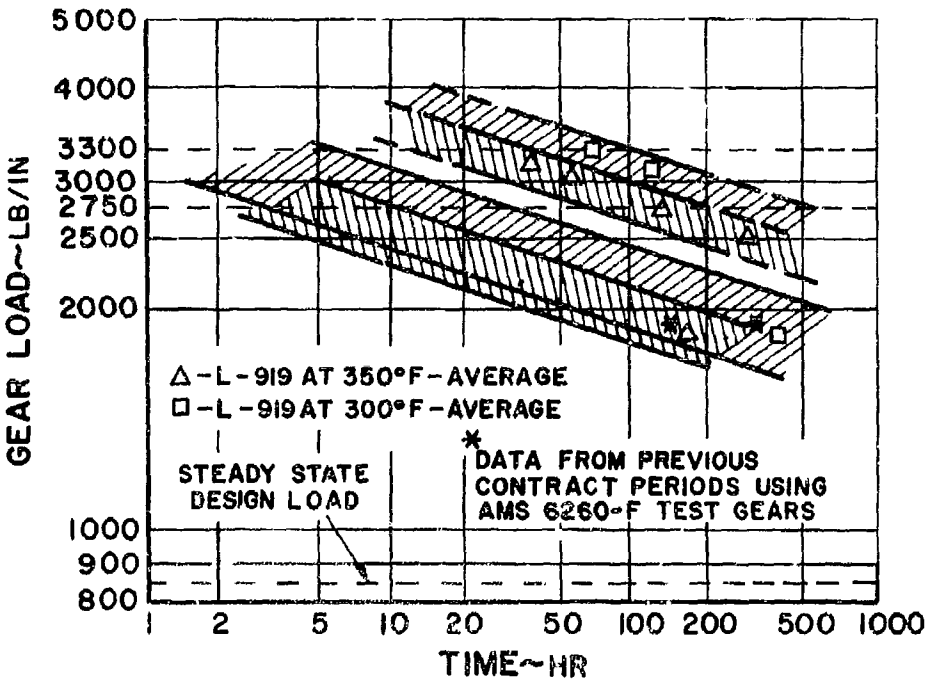


ESTIMATED FUEL AND OIL TEMPERATURES VERSUS MISSION

Figure 12-1

DOWNGRADED AT 3 YEAR INTERVALS
DECLASSIFIED AFTER 12 YEARS
DOD DIR 5200.10

THIS DOCUMENT CONTAINS INFORMATION AFFECTING THE NATIONAL DEFENSE OF THE UNITED STATES WITHIN THE MEANING OF THE ESPIONAGE LAWS, TITLE 18, U.S.C., SECTIONS 793 AND 794. ITS TRANSMISSION OR THE REVELATION OF ITS CONTENTS IN ANY MANNER TO AN UNAUTHORIZED PERSON IS PROHIBITED BY LAW.



GEAR PITTING FATIGUE LIFE IN RYDER GEAR MACHINE
WITH PWA 724 GEAR MATERIAL

Figure 12-2

DOWNGRADED AT 3 YEAR INTERVALS
DECLASSIFIED AFTER 12 YEARS
DOD DIR 5200.10

THIS DOCUMENT CONTAINS INFORMATION AFFECTING THE NATIONAL DEFENSE OF THE UNITED STATES WITHIN THE MEANING OF THE ESPIONAGE LAWS, TITLE 18 U.S.C. SECTIONS 793 AND 794. THE TRANSMISSION OR THE REVELATION OF ITS CONTENTS IN ANY MANNER TO AN UNAUTHORIZED PERSON IS PROHIBITED BY LAW.

TEST DATA SUMMARY FOR LUBRICANT L-919
GEAR PITTING FATIGUE LIFE IN RYDER GEAR
MACHINE WITH PWA 724 GEAR MATERIAL

Test Sequence	Test Oil In Temp. °F	Gear Load (pounds per inch of tooth width)	Resultant Time to Failure (hours)
1	300	3000	120
2	350	2500	250
3	350	3000	70
4	300	3300	70
5	350	3300	40
6	300	3000	120
7	350	3000	20
8	350	3300	40
9	350	3000	70
10	350	2750	150
11	300	3300	40
12	350	2750	160
13	300	3300	100

Figure 12 - 3

DOWNGRADED AT 3 YEAR INTERVALS
DECLASSIFIED AFTER 12 YEARS
DOD DIR 5200.10

THIS DOCUMENT CONTAINS INFORMATION AFFECTING THE NATIONAL DEFENSE OF THE UNITED STATES WITHIN THE MEANING OF THE ESPIONAGE LAWS, TITLE 18, U.S.C. SECTIONS 793 AND 794. THE TRANSMISSION OR THE REVELATION OF ITS CONTENTS IN ANY MANNER TO AN UNAUTHORIZED PERSON IS PROHIBITED BY LAW.

GENERAL PROPERTIES OF LUBRICANTS TESTED

Designation	L - 1530	L - 1537
Type of Lubricant	Ether	Polyester
Kinematic Viscosity:		
at 100°F, centistokes	24.34	45.50
at 210°F, centistokes	4.07	8.08
Pour Point, °F	-25	Below -65
Flash Point, °F	465	500
Fire Point, °F	540	530
Ryder Gear Test:		
Gear Scuffing Load, lb./in.	3160	----
Lubricant-Carbon Wear Test:		
Axial Wear Rate, in./min.	0.2×10^{-5}	1.4×10^{-5}
Evaporation Rate at 400°F At Sea Level, % Loss in Wgt.	9.7	3.5

Figure 12 - 4

DOWNGRADED AT 3 YEAR INTERVALS
DECLASSIFIED AFTER 12 YEARS
DOD DIR 5200.10

THIS DOCUMENT CONTAINS INFORMATION AFFECTING THE NATIONAL DEFENSE OF THE UNITED STATES WITHIN THE MEANING OF THE ESPIONAGE LAWS, TITLE 18, U.S.C., SECTIONS 793 AND 794. ITS TRANSMISSION OR THE REVELATION OF ITS CONTENTS IN ANY MANNER TO AN UNAUTHORIZED PERSON IS PROHIBITED BY LAW.

EFFECT OF TEMPERATURE AND PRESSURE ON EVAPORATION LOSS OF L-1530 LUBRICANT

Duration of Test - 6 1/2 hours

Evaporation Loss in Percent of Weight

Temp. °F	Pressure Altitude, Feet		
	Sea Level	20,000	40,000
400	9.7	14.3	---
425	17.4	19.4	---
450	30.0	40.0	---
475	37.2	47.6	---
500	50.1	---	61

Figure 12-5

EFFECT OF TEMPERATURE AND PRESSURE ON EVAPORATION LOSS OF L-1537 LUBRICANT

Duration of Test - 6 1/2 hours

Evaporation Loss in Percent of Weight

Temp., °F	Pressure Altitude, Feet			
	Sea Level	20,000	40,000	60,000
400	3.5	8.3	11.9	13.5
425	8.6	13.1	18.9	20.9
450	12.4	20.0	27.0	---

Figure 12-6

DOWNGRADED AT 3 YEAR INTERVALS
DECLASSIFIED AFTER 12 YEARS
DOD DIR 5200.10

THIS DOCUMENT CONTAINS INFORMATION AFFECTING THE NATIONAL DEFENSE OF THE UNITED STATES WITHIN THE MEANING OF THE ESPIONAGE LAWS, TITLE 18, U.S.C., SECTIONS 793 AND 794. THE TRANSMISSION OR THE REVELATION OF ITS CONTENTS IN ANY MANNER TO AN UNAUTHORIZED PERSON IS PROHIBITED BY LAW.

LUBRICANT L-1530 OXIDATION-CORROSION DATA AT CONSTANT AIRFLOW

Airflow = 5 standard liters/hour

Test Time = 48 hours

Lubricant Designation		L - 1530 (averages)	
Test Temperature, °F	425	450	500
Weight Loss, Mg/Cm^2			
for Silver	-0.70	-0.79	-1.55
Copper	-4.00	-5.60	-13.57
Steel	+0.20	+0.27	+0.30
Titanium	+0.10	+0.18	+0.09
Aluminum	+0.20	+0.22	+0.23
Magnesium	+0.40	+0.66	+0.54
% Viscosity Increase at 100°F after 12 hours		1.64	2.48
24 hours		1.44	3.32
36 hours		2.10	4.94
48 hours		1.85	4.14
Neutralization Number			
after 0 hours		0.1	0.0
12 hours		0.1	0.0
24 hours		0.0	0.0
36 hours		0.0	0.0
48 hours		0.0	0.0

Figure 12-7

DOWNGRADED AT 3 YEAR INTERVALS
DECLASSIFIED AFTER 12 YEARS
DOD DIR 5200.10

THIS DOCUMENT CONTAINS INFORMATION AFFECTING THE NATIONAL DEFENSE OF THE UNITED STATES WITHIN THE MEANING OF THE ESPIONAGE LAWS, TITLE 18, U.S.C., SECTIONS 793 AND 794. THE TRANSMISSION OR THE REVELATION OF ITS CONTENTS IN ANY MANNER TO AN UNAUTHORIZED PERSON IS PROHIBITED BY LAW.

ITEM 13

ENGINE-INLET COMPATIBILITY

ITEM 13 - ENGINE-INLET COMPATIBILITY

The contractor will conduct continued investigation in cooperation with each airframe contractor to establish engine-inlet compatibility. The steady state performance and flow distribution over both the typical engine flight conditions and the transient inlet conditions will be considered.

A. INTRODUCTION

With the exception of very limited preliminary data from Lockheed, no additional inlet distortion data were received from the airframe companies during Phase IIB. The existing data received during Phase IIA were further analyzed and converted into working curves for determining the effect of the inlet on the compressor and engine control system.

B. DISCUSSION

The Boeing inlet design has remained basically unchanged from the initial design considered in Phase IIA. Minor modifications in the subsonic diffuser length and shape and the incorporation of vortex generators, immediately downstream of the throat region on the centerbody, have been made to reduce the distortion level at the compressor face.

Typical distortion maps at Mach 1.1 and 2.5, generated from Boeing test data in Phase IIA, are presented in Figure 13-1. These plots graphically represent the total pressure distribution at the compressor face station. The distortion maps were constructed for all data received to date; they serve as a guide for studying the effect of distortion on compressor performance. It should be emphasized that this data are preliminary information from Phase IIA and do not necessarily represent Boeing's latest results.

The distortion at Mach 1.1, 0° angle of attack, and with the bypass half open is shown on Figure 13-1 (a). The highest distortion level at Mach 1.1 occurred when the bypass was half opened. The weight flow ratio for the above conditions was determined near the choke point, where the engine will probably operate. Figure 13-1 (b) represents the inlet operating at Mach 2.5, 0° angle of attack, and

peak pressure recovery without vortex generators on the centerbody. Due to the control tolerance required for safe operation of the complete powerplant system, the inlet probably cannot be operated at the above point in actual practice. The distortion pattern indicated in Figure 13-1 (b) is almost fully radial; it is a baseline reference representing the minimum distortion for the configuration. As the inlet is operated in the supercritical condition to provide the control tolerance, the distortion increases and a slight amount of circumferential distortion is introduced. Figure 13-1 (c) is a typical plot of this condition at the 3.9% supercritical point. A distortion map for the inlet at the supercritical condition with vortex generators installed on the centerbody is shown in Figure 13-1 (d). The overall distortion level was lowered approximately 1.5 percent; the radial distortion shifted, leaving the center of the passage with less distortion.

Cross plots of Figures 13-1 (a) and 13-1 (c) are shown as radial profiles in Figure 13-2. The radial distortion at Mach 2.5 is more severe than at Mach 1.1. The radial pressure profiles shown in Figure 13-2 do not reflect the use of bealing devices such as vortex generators. The distortion at Mach 2.5 would be marginal without these devices.

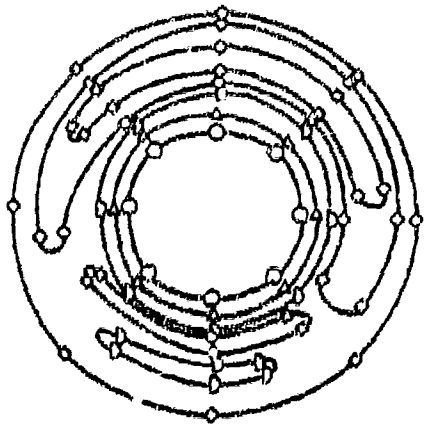
Plots of distortion versus the percent supercritical operation at Mach 2.5 and the bypass door opening are shown in Figure 13-3. This information was given to the control group for use in the inlet engine control response to airflow transients study. This work is reported in the inlet control section of this report.

C. CONCLUSIONS

Essentially no new distortion data have been received during Phase IIB from either Boeing or Lockheed. Additional evaluations of the existing data have not revealed any additional problems which supersede those previously mentioned. However, every effort is being made to continuously improve the inlet distortion and engine tolerance to insure a compatible system.

A

MACH 1.1 ALPHA=0° PRESSURE RECOVERY 0.979
BY-PASS 1/2 OPEN

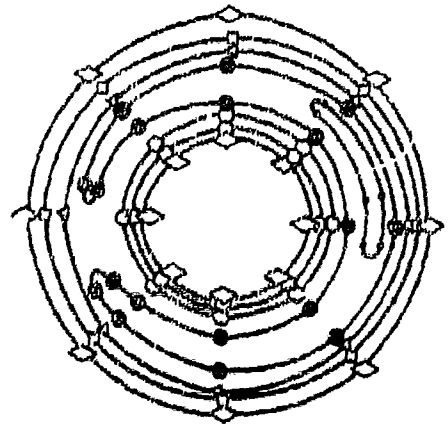


DISTORTION = 0.089 P_T LOCAL / P_T AVG

◇ 0.93
○ 0.98
△ 0.99
D 1.03

C

MACH 2.5 SUPERCRITICAL 3.9 %
PRESSURE RECOVERY 0.8750

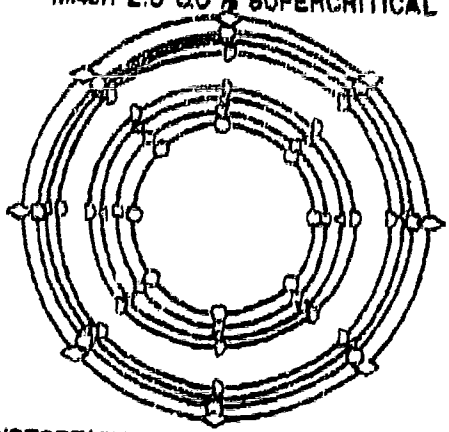


DISTORTION = 0.138 P_T LOCAL / P_T AVG

◇ 0.94 ◁ 1.04
○ 0.98 ● 1.06
□ 1.00
○ 1.02

B

MACH 2.5 0.0% SUPERCRITICAL



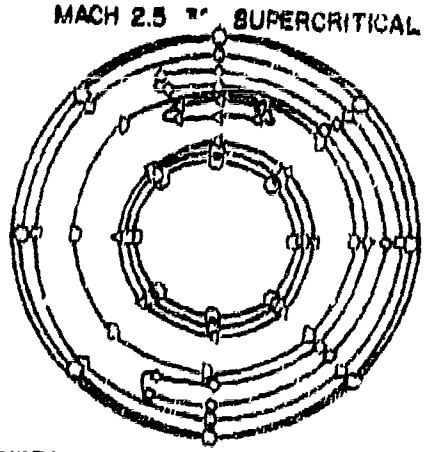
DISTORTION = 0.099
P R = 0.9140

P_T LOCAL / P_T AVG

◇ 0.94 ○ 1.02
○ 0.96 ◁ 1.04
□ 1.00 D 1.06

D

MACH 2.5 [illegible] SUPERCRITICAL



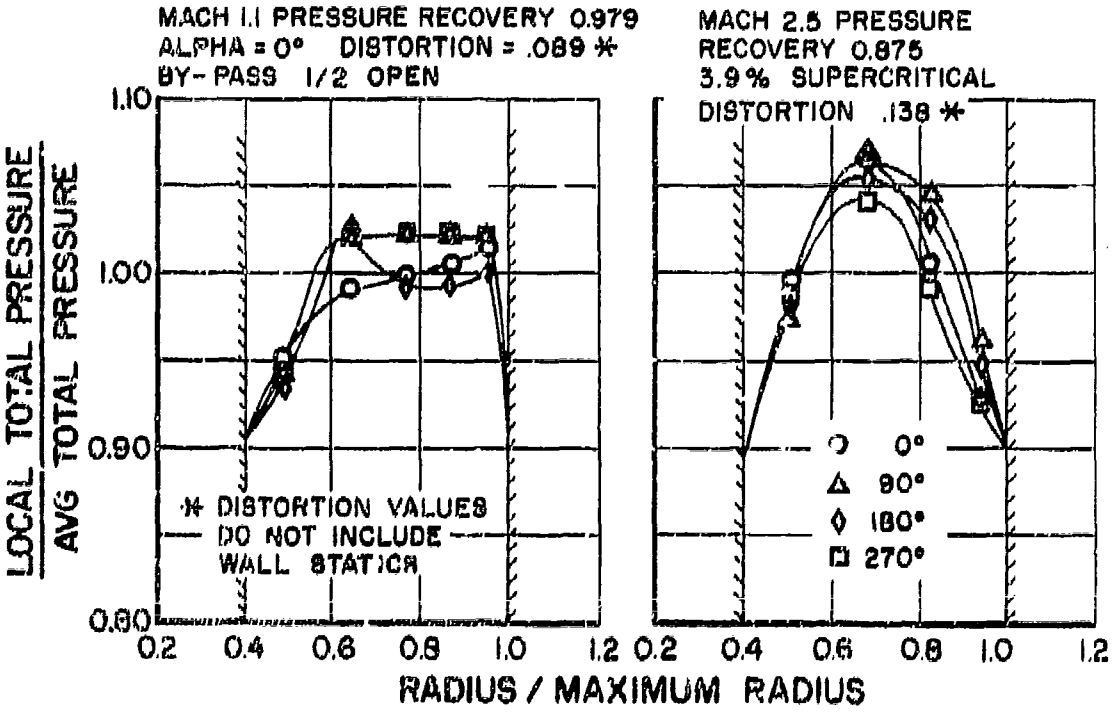
DISTORTION = 0.1237
P R = 0.8915

P_T LOCAL / P_T AVG

○ 0.94 ◁ 1.04
○ 0.98 D 1.06
□ 1.00 ◇ 1.08

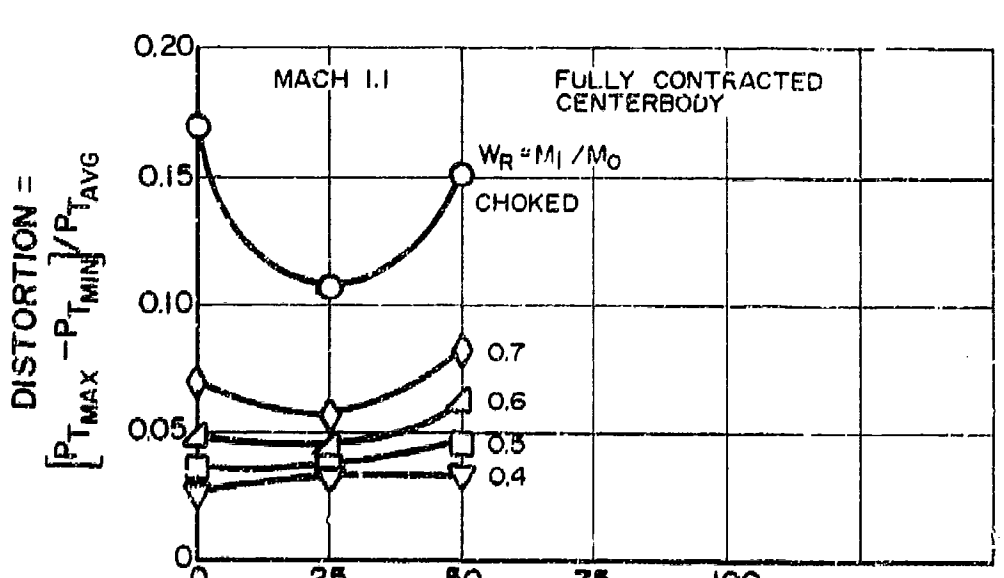
TYPICAL BOEING SST INLET MODEL DISTORTION PLOTS

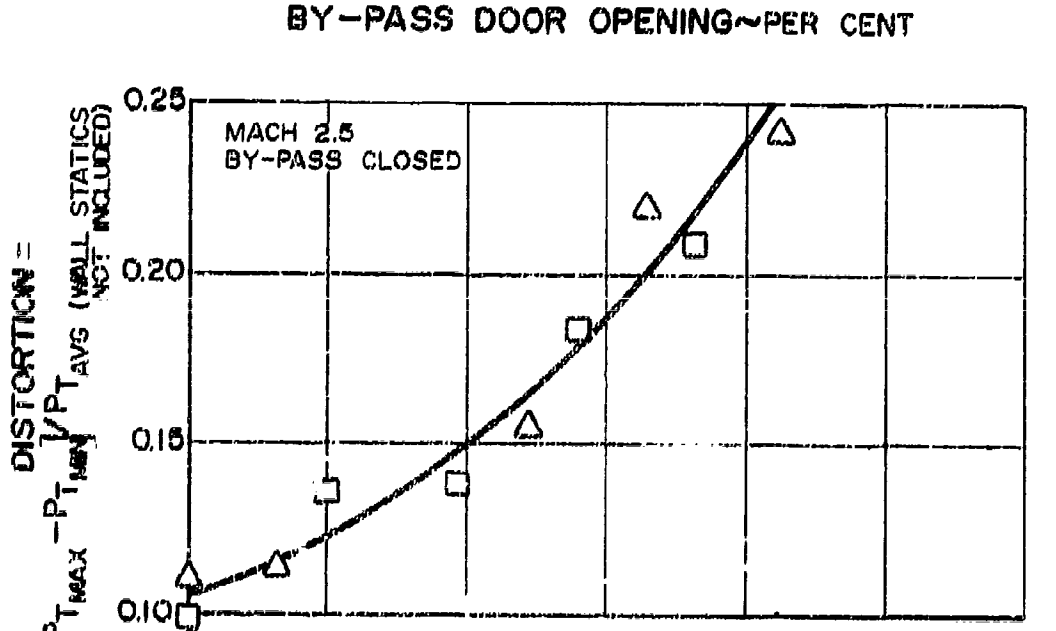
Figure 13-1



RADIAL TOTAL PRESSURE PROFILES FOR BOEING SST INLET

Figure 13-2





DISTORTION VERSUS PERCENT BYPASS DOOR OPENING AND PERCENT SUPERCRITICAL OPERATION FOR THE BOEING SST INLET

Figure 13-4

ITEM 14

MATERIALS AND MANUFACTURING TECHNIQUES



ITEM 14 - MATERIALS AND MANUFACTURING TECHNIQUES

OBJECTIVE

The goal of this program was to develop information concerning materials to aid the selection of optimum materials and manufacturing techniques suitable for the SST engine.

A. INTRODUCTION

Four development programs aimed at advancing the state of the art of compressor materials and manufacturing techniques were conducted during Phase IIB in support of the engine design effort. Because titanium will be used extensively in the rotating parts of the compressor, testing to determine the long term creep properties of titanium alloys were continued under this contract. The long time creep properties of IMI 679 titanium base alloy were determined at several stress and temperature levels for comparison with alloys evaluated in previous SST programs. In a second program, metallographic and physical properties tests were conducted on Waspaloy in order to obtain additional design information on this material. The blade containment program was continued from Phase IIA. Finally, diffusion bonding studies of titanium were undertaken with the object of determining ways of producing lightweight hollow titanium disks. These programs are discussed in the four sections which follow.

B. CREEP TESTING OF IMI 679 TITANIUM ALLOY

The creep properties of IMI 679 titanium base alloy were determined up to 0.1% creep for comparison with other compressor disk alloys tested in previous phases.

Twenty-two mechanical creep specimens were machined from IMI 679 disks forged by Wyman-Gordon and Ladish. Each test section was machined from rim sections of IMI 679 to dimensions of 0.250 inch diameter and two inch gage length. Each test specimen was allowed to creep 0.1% and was subsequently subjected to room temperature tensile stability test.

TMCA produced the master heat used by both Wyman-Gordon and Ladish to forge the typical IMI 679 titanium engine compressor disks. The percentage of chemical constituents of the titanium-based alloy was as follows:

Disk	C	Fe	Al	Mo	Sn	O	H	N	Zr	Si	Ti
W-G	0.01	0.10	2.40	0.93	10.81	0.098	0.005	0.015	5.60	0.23	balance
Ladish	0.02	0.10	2.30	0.91	10.60	0.097	0.005	0.015	5.60	0.20	balance

The Wyman-Gordon forging was air cooled from the solution anneal temperature of 1650°F; the Ladish disk forging was water quenched. Both disks were stabilized at 930°F and air cooled. The hardness of the water-quenched disk and the air-cooled disk was 35 and 38 Rockwell C respectively.

Photograph 14-1 exhibits the grain structures of both disks using Krolls etching reagent and 500 times magnification. Radial rim sections of the disk forgings were used for samples.

Eighteen mechanical creep specimen were fabricated from the Wyman-Gordon forgings and four similar specimens were made from the Ladish forgings. These test samples were tested at various load and temperature conditions to 0.10% creep. The test results are summarized on Figure 14-2.

Figure 14-2 also compares the creep properties of IMI 679 with PWA 1202 and PWA 1203. The creep properties of IMI 679 were superior to both PWA 1202 and PWA 1203 at 750°F and 850°F. All three materials were similar at 950°F. Limited testing at 1050°F indicated that PWA 1203 was superior to IMI 679 at this temperature. The creep data from the Ladish forgings were comparable to vendor supplied data, but a decrease in strength was noted in comparison with the Wyman-Gordon forgings.

Stability testing of IMI 679 indicated a slight increase in ultimate and yield strength with a corresponding decrease in percent elongation and area reduction. Since IMI 679 is aged at 930°F, the instability is attributed to aging during creep tests.

1. MECHANICAL PROPERTIES-IMI 679 TITANIUM ALLOY

Testing was conducted to evaluate the short time properties of IMI 679 titanium alloy and their effects on the component design. Test specimens were fabricated from IMI 679 titanium disk forgings, which were manufactured by both Wyman-Gordon and Ladish. The mechanical property tests included tensile tests at room and elevated temperatures, stress rupture, combined stress, stress corrosion, fracture toughness, and fatigue strength tests.

The following list of test specimens were fabricated from the same disk forgings used in the creep testing of Part A:

PROPERTY TESTS	WYMAN-GORDON SPECIMENS	LADISH SPECIMENS
Tensile	19	5
Stress Rupture	7	0
Combined Stress	6	0
Stress Corrosion	57	12
Fracture Toughness	16	0
Fatigue Strength	20	9

The tensile properties of both the Wyman-Gordon and Ladish forged IMI 679 disks are shown in Figure 14-3. A comparison is made between IMI 679 and PWA 1202 and 1203 data from the Phase IIA tests. Above room temperature, IMI 679 exhibited a higher ultimate and yield strength. The Ladish forgings had better tensile strength characteristics than the Wyman-Gordon forgings.

Stress-rupture specimens, tested at 950°F and 75,000 psi loading, ruptured in 321.6 hours. Testing at 750°F and 850°F at approximately 95 percent of the 0.2 percent yield strength was discontinued after 400 hours. The test indicated that IMI 679 is yield strength limited for stress to rupture in 100 hours.

Stress-corrosion tests indicated that IMI 679 is more resistant to NaCl salt corrosion than PWA 1202; both material specimens were tested for 100 hours of exposure. The "crack-no crack" line is indicated on Figure 14-4 for both materials. Stress-corrosion strength at 850°F improved when the specimen was glass bead blasted to an intensity of 6N2. An increase in stress of approximately 23,000 psi was required to produce stress-corrosion cracks in the treated specimen.

Similar stress-corrosion tests were conducted on IMI 679 for 300 hours of exposure with NaCl salt. The "crack-no crack" line shown on Figure 14-5 indicated that a substantial reduction in material strength results from prolonged salt exposure.

When preliminary stress-corrosion tests exposed IMI 679 to artificial sea salts, prepared in accordance with ASTM-D665, a marked decrease in stress-corrosion strength was noted. Additional tests will be conducted to establish the "crack-no crack" line for these salts.

Notched Westinghouse fatigue and combined stress fatigue test specimens were made from IMI 679 disk forgings. The results of a fatigue strength determination at room temperature is shown on Figure 14-6, a modified Goodman diagram. Additional testing at 800°F is currently in process.

Notched (K_t = 3.0) low cycle fatigue strength specimens were tested at room temperature (70°F) and 400°F. A tensile stress of 44,000 psi and an alternating stress of 44,000 psi were imposed on the test samples. The room temperature specimen endured 5,700 cycles; the 400°F specimen endured 4,100 cycles.

Charpy impact specimens were machined from the bore axial location of the disk with the V-notch (K_t = 3.8) on the bore face. Half of the specimens were precracked by reverse bending to produce a K_t of approximately 16.0. Two of the precracked specimens tested at 70°F were not fully cracked across the notch; therefore, the impact strength was high. Since the remaining six specimens were cracked across the entire notch width, legitimate fracture toughness test data was provided. Figure 14-7 shows the propagation energy (impact strength divided by the remaining area of the precracked specimen) and the initiation energy (V-notched impact strength minus precracked impact strength) versus temperature.

C. METALLOGRAPHIC STUDY OF PWA 1007 (WASPALOY)

A metallographic study was undertaken to determine the relationship between the microstructure and mechanical properties of PWA 1007.

Test specimens were machined from rings trepanned from rim sections of PWA 1007 disk forgings. Tensile and low cycle fatigue tests were conducted at room and elevated temperatures. Electron microscopy examinations were made to determine the grain boundary carbide precipitation as a function of grain size.

Seventeen tensile and twenty-two low cycle fatigue specimens were made from PWA 1007 disk forgings manufactured by Wyman-Gordon and Ladish. The two Wyman-Gordon disks had heat codes of XGCF-6 and XGPS-7; the two Ladish disks had heat codes of CGNK-119 and CJDA-38. Metallographic examinations were made of each material sample to determine the grain structure.

The tensile properties of PWA 1007 nickel-base alloy, determined at room and elevated temperatures, are summarized by Figure 14-8.

DOWNGRADED AT 3 YEAR INTERVALS
DECLASSIFIED AFTER 12 YEARS
DOD DIR 5200.10

The ultimate and yield strength were higher than the minimum strength design data. The low cycle fatigue specimens were tested; the results are currently being analyzed.

Metallographic examination of specimens exhibited in Figures 14-9 and 14-10 indicates a duplex-structured Wyman-Gordon material. While the predominant grain sizes were ASTM 4 to 10, some grains were as large as ASTM 2. The Ladish material was composed of an equiaxed structure with predominant grain sizes of ASTM 5 to 7, but some grains were as large as ASTM 4. Ladish disk CGNK-119 contained a few elongated grains; Wyman-Gordon disk XGCF-6 contained a majority of elongated larger grains. Both the Ladish CJDA-3 and Wyman-Gordon XGPS-7 disks were composed of equiaxed grains.

Electron metallographic examination of the four disk sections, exhibited in Figures 14-11 and -12, indicated a variable quantity of grain boundary precipitates. The Wyman-Gordon XGCF-6 disk had relatively clean boundaries, but XGPS-7 showed more grain boundary carbides. The Ladish CJDA-38 exhibited a low frequency of grain boundary carbide, while CGNK-119 showed a trend toward more continuous grain boundary carbide precipitation. The matrix duplex gamma prime precipitate showed a variation in size decreasing from CGNK-119, CJDA-38, XGCF-6, to XGPS-7.

D. CONTAINMENT TESTING

Containment testing was conducted to determine the optimum materials for blade containment applications.

Ballistic tests were conducted on 24 materials to evaluate their containment capability and to analyze the containment theory being used. Five materials were spin tested to establish the blade containment properties of the proposed materials under simulated engine conditions. An analytical investigation was conducted to obtain a better understanding of engine structural response to high energy impact loads.

A failed rotating fan blade will release energy upon impact with a structural member. It is necessary to provide a protective engine structure to absorb this energy, and thus prevent considerable aircraft damage. Since weight is always a primary consideration, an accurate design procedure was developed through three programs.

1. BALLISTIC TESTS

Ballistic tests were conducted on four-inch-square panels to evaluate the containment ability of different materials, which varied in thickness

DOWNGRADED AT 3 YEAR INTERVALS
DECLASSIFIED AFTER 12 YEARS
DOD DIR 5200.10

THIS DOCUMENT CONTAINS INFORMATION AFFECTING THE NATIONAL DEFENSE OF THE UNITED STATES WITHIN THE MEANING OF THE ESPIONAGE LAWS, TITLE 18, U.S.C., SECTIONS 793 AND 794. ITS TRANSMISSION OR THE REVELATION OF ITS CONTENTS IN ANY MANNER TO AN UNAUTHORIZED PERSON IS PROHIBITED BY LAW.

from 0.035 to 0.500 inch. These panels were rigidly mounted in a fixture designed for restraint at the side edges as shown by Figure 14-13. A back-up indicator panel was located four inches behind the test panel to assist in determining degree of containment. The panels were tested for impact through the use of a 30 caliber rifle mounted in a rack 20 feet from the panel. A 30-06 Springfield and a M-1 carbine rifle were used in the test program.

Three different projectiles were used during this test program: a 110 grain lead projectile used with the M-1, 110 grain steel and a 180 grain lead projectile used with the Springfield. The projectile velocity was varied by the use of different size powder charges. Velocity measurements were made by two chronographs spaced 10 ft. apart. The overall test set-up is exhibited in Figure 14-14.

2. SPIN CONTAINMENT TESTS

The spin containment tests were conducted in an evacuated spin pit, which utilized a typical fan compressor stage and a simulated containment ring sandwiched between two plates.

This arrangement simulated the vanes before and after the compressor rotor. Figure 14-15 shows a typical set-up with the containment ring sandwiched between the plates.

3. ANALYTICAL INVESTIGATION

An analytical procedure was devised to predict the response of structures to high impact loads. This procedure allowed a correlation to be made between the ballistic and the spin containment tests.

4. DISCUSSION OF RESULTS

The results of the ballistic tests are summarized in Figure 14-16, which lists the materials in descending order of Merit Factor. The Merit Factor is a means of defining the containment ability of a material; this factor is defined as the kinetic energy of the test panel divided by the weight of material per unit area of containment panel. These materials are taken at the blade tip speed range, which would be applicable to a SST engine.

Sintered ceramic test specimens, made from aluminum oxide and silicon carbide, were ordered from a vendor. They were not received in

sufficient time to test under this phase of the program. Preliminary testing indicated that the merit factor for ceramics would be considerably higher than that of the metals tested. Due to insufficient information, the relative magnitude of the merit factors for the ceramic specimens could not be determined.

Spin containments tests were conducted on five materials to establish a new baseline for the fan rotor. A summary of results are as follows:

Material	CWF
AMS 5524	1.0
AMS 4910	0.6
Hardened AMS 5508	0.7
AMS 5548	0.75
AMS 5525	1.0

Containment weight factor (CWF), or fraction of baseline AMS 5524 weight, is needed for the same containment capability. Sintered ceramics were ordered for testing in combination with the more promising metals, but the materials were not received during this period.

An analytical investigation was conducted to define the mechanical properties that influence containment. A theoretical method has been established to predict containment, but considerable refinement is necessary before it is usable.

E. DIFFUSION BONDING OF TITANIUM FAN DISK

Diffusion bonding studies of full-scale titanium fan disks were conducted to establish bonding parameters.

Twelve bonding trials were conducted on test samples simulating a section of a hollow disk. The bond strength of the test samples was up to 97% of the parent metal strength. The best parameters were selected to bond a full-scale fan disk. The fan disk is being finish machined for a final bonding evaluation.

A titanium alloy of AMS 4928 specification was selected for the fan disk bonding study. Figure 14-17 gives a comparison between the design and weight of the conventional solid disk and the diffusion-bonded disk.

Two methods of titanium diffusion bonding were evaluated, and the bonding parameters were determined for each. The first method, a vacuum hot press, satisfactorily bonded the test samples, but the equipment had insufficient capacity to bond the full-scale fan disk.

The second bonding method consisted of a vacuum retort placed within a furnace. The retort was designed and built to provide the proper environment and pressure for bonding. The top and bottom of the retort were dimensioned to provide the bonding pressure by utilizing the pressure differential between the vacuum and the atmosphere. The sides of the retort incorporated a bellows which did not restrain the atmospheric load; therefore, the load was exerted on the specimen or disk halves to be bonded.

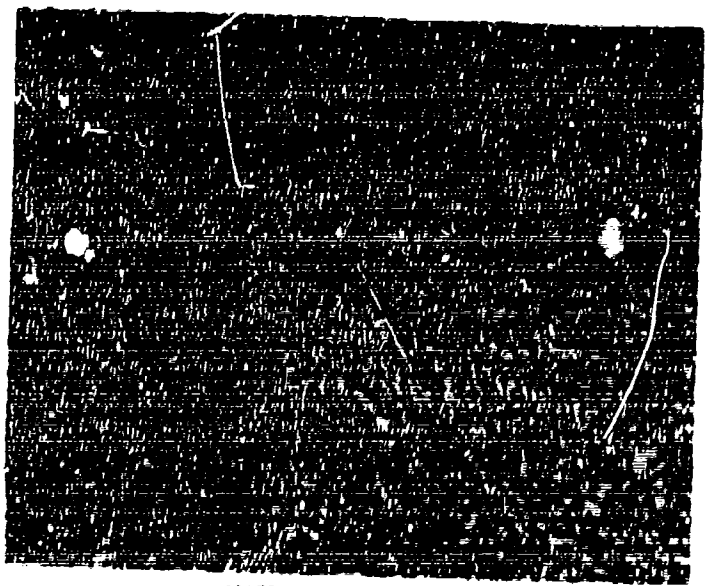
Figures 14-18 and -19 are photographs of the small vacuum retort used for the test specimens before and after the bonding cycle. Figures 14-20, -21 and -22 exhibit the furnace and retort used to bond the full-scale disk.

The bonding parameters selected for the full-scale disk were:

1. Environment-vacuum (5 microns or less),
2. Bonding temperature - 1650°F,
3. Bonding pressure - 425 psi,
4. Bonding time at temperature - 1 hour
5. Surface preparation-lapped surface cleaned with alcohol (4 - 6 micro-inches)

Figure 14-23 summarizes the bonding trials of both methods. A photograph of test specimens No. 3, 4, and 5, which failed in tension, is shown on Figure 14-24. Figure 14-25 is metallographic photograph of test specimen No. 12 showing grain growth across the bond joint.

The full-scale disk was visually inspected after bonding and machined to the final configuration shown in Figure 14-17(b).



WYMAN-GORDON



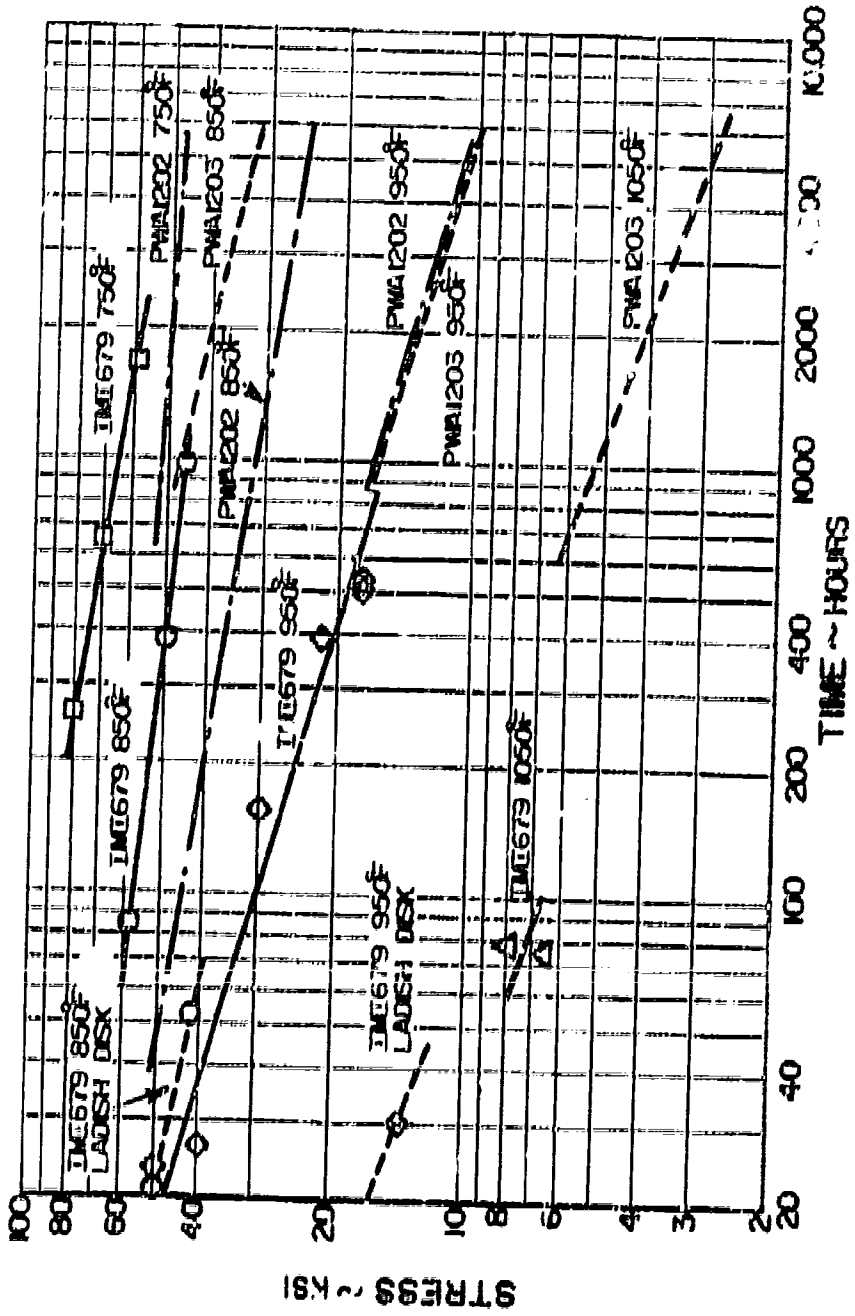
LADISH

Etchant: Kroll's

500 X Magnification

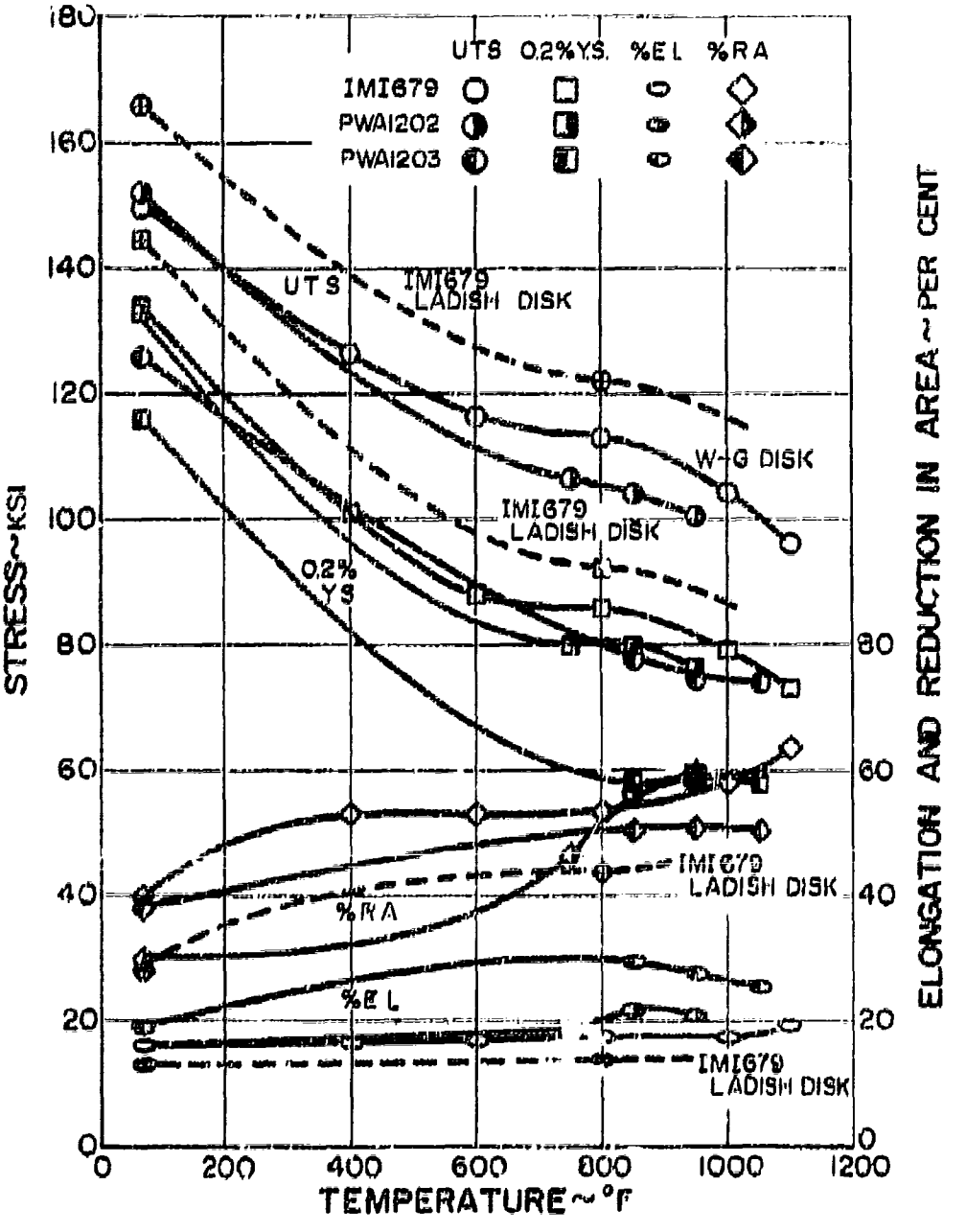
GRAIN STRUCTURE OF IMI 679 TITANIUM ALLOY, RADIAL RIM SECTIONS OF DISKS FORGED BY WYMAN-GORDON AND LADISH.

Figure 14-1



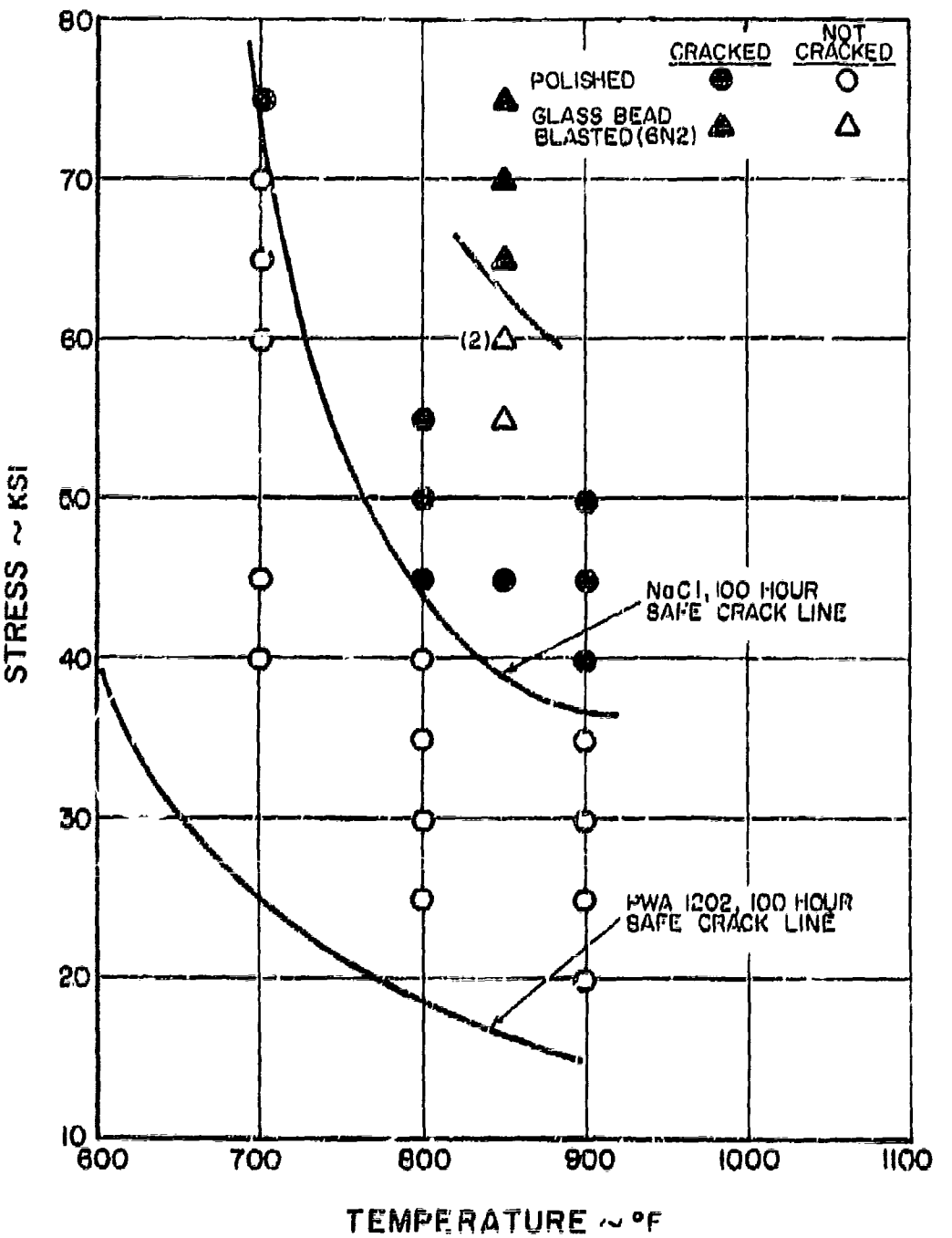
TIME TO CREEP 0.1% FOR IMI 679 TITANIUM BASE ALLOY COMPARED TO PWA 1202 AND PWA 1203.

Figure 14-2



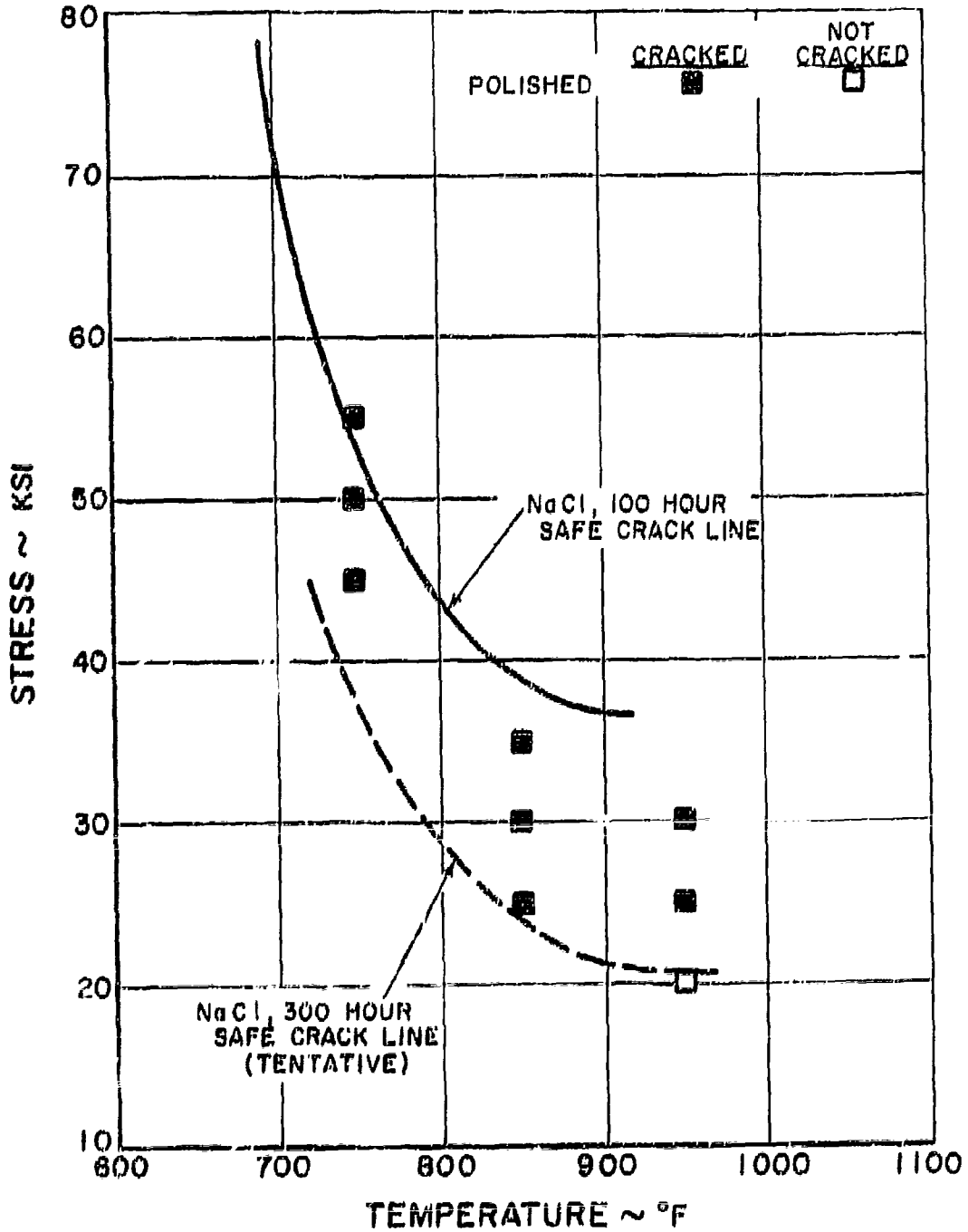
TENSILE PROPERTIES OF IMI 679 TITANIUM BASE ALLOY COMPARED TO PWA 1202 and PWA 1203.

Figure 14-3



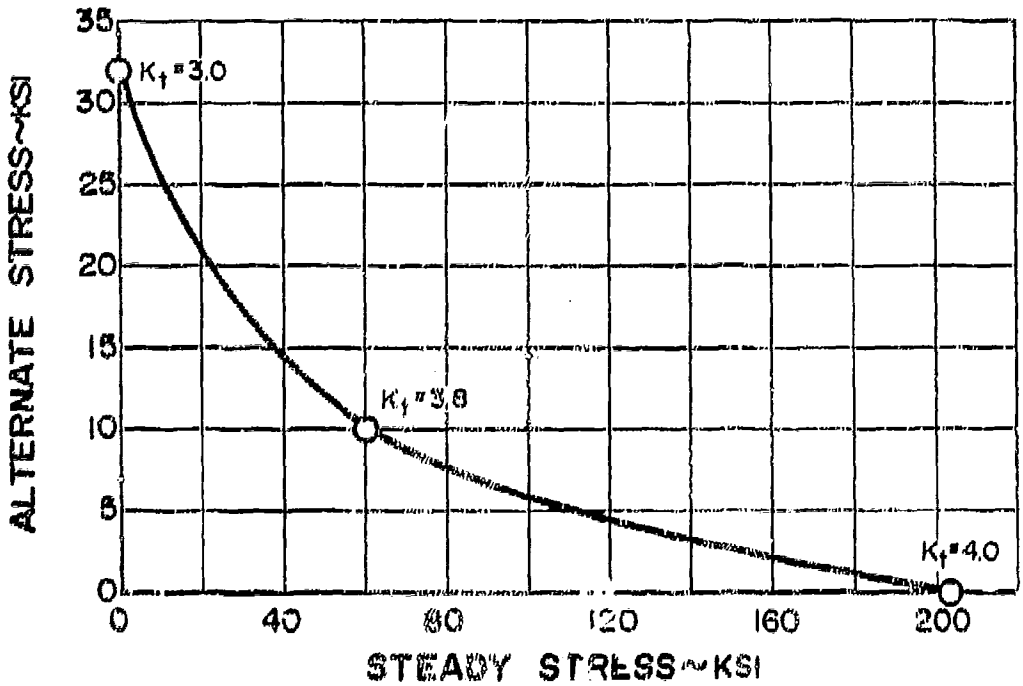
STRESS REQUIRED TO PRODUCE NaCL SALT, STRESS-CORROSION CRACKING IN 100 HOURS FOR IMI 679 TITANIUM BASE ALLOY.

Figure 19-4



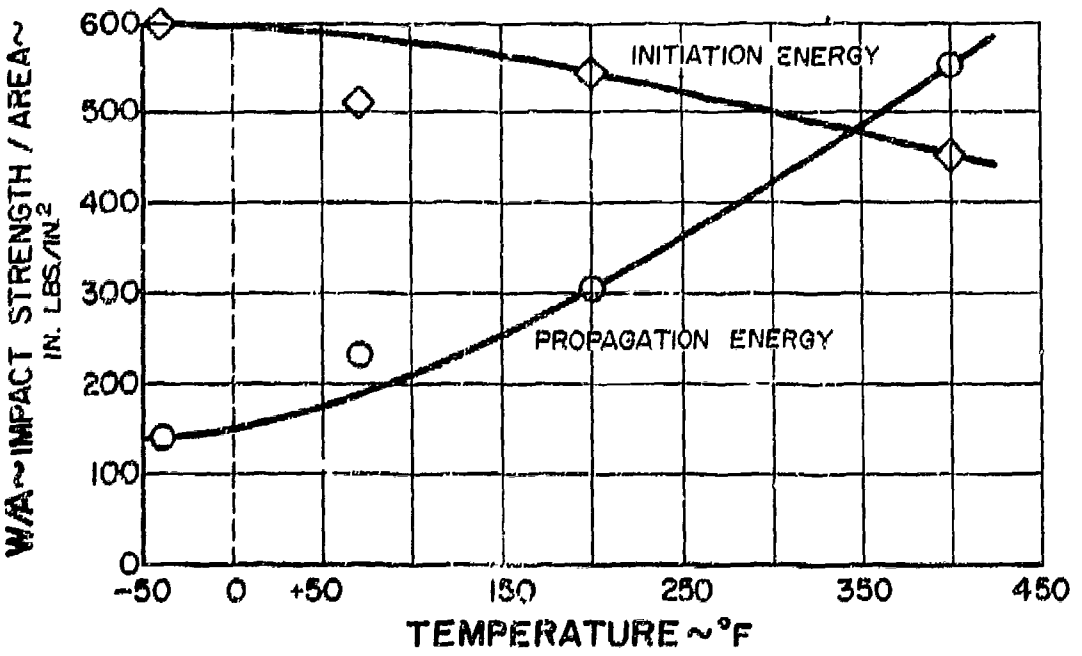
STRESS REQUIRED TO PRODUCE NaCL SALT, STRESS-CORROSION CRACKING IN 300 HOURS FOR IMI 679 TITANIUM BASE ALLOY.

Figure 14-5



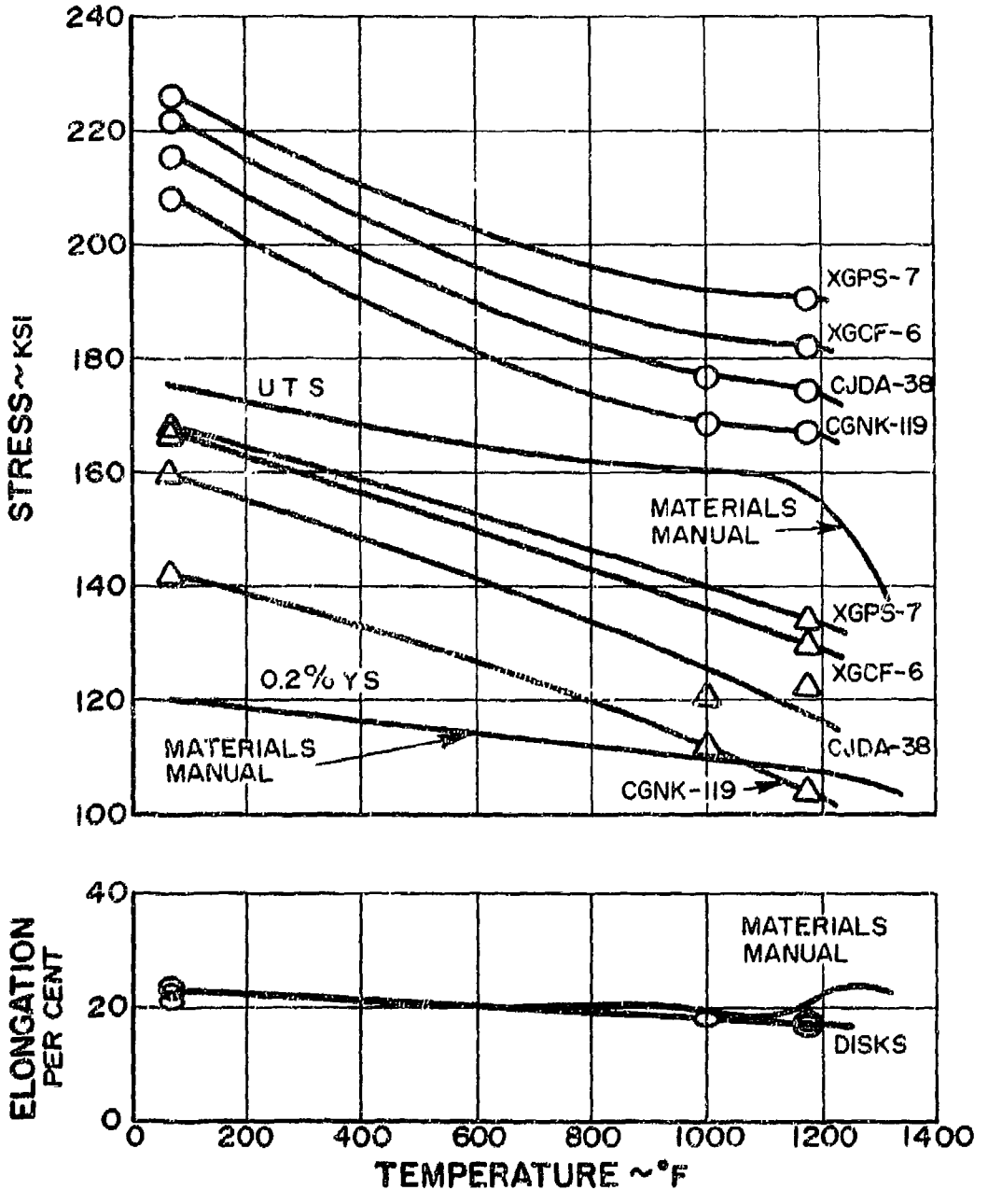
GOODMAN DIAGRAM OF FATIGUE LIFE FOR IMI 679 TITANIUM BASE ALLOY NOTCHED SPECIMENS. TEST TEMPERATURE = 70°F.

Figure 14-6



FRACTURE TOUGHNESS OF IMI 679 TITANIUM BASE ALLOY - PRECRACKED NOTCHED CHARPY IMPACT SPECIMENS.

Figure 14-7

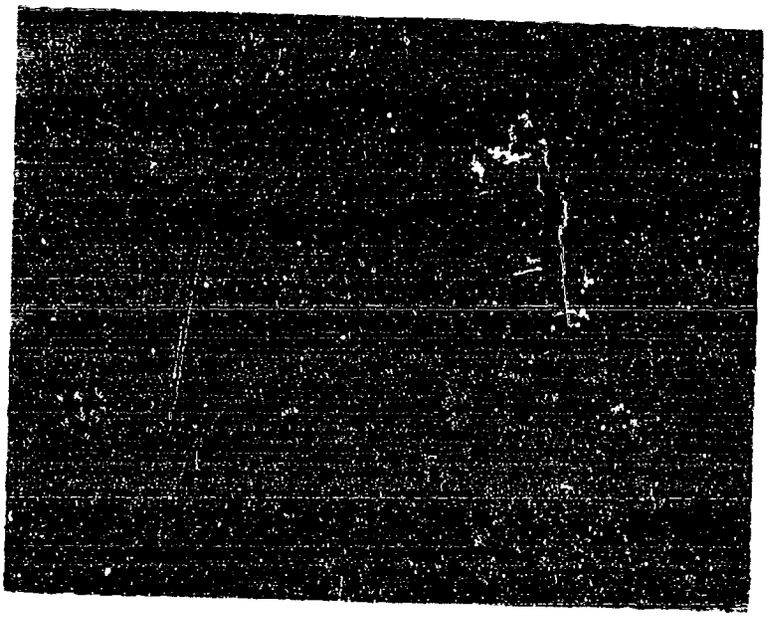


TENSILE PROPERTIES OF PWA 1007 NICKEL BASE ALLOY. DISK SPECIMENS MACHINED FROM TREPANNED RINGS.

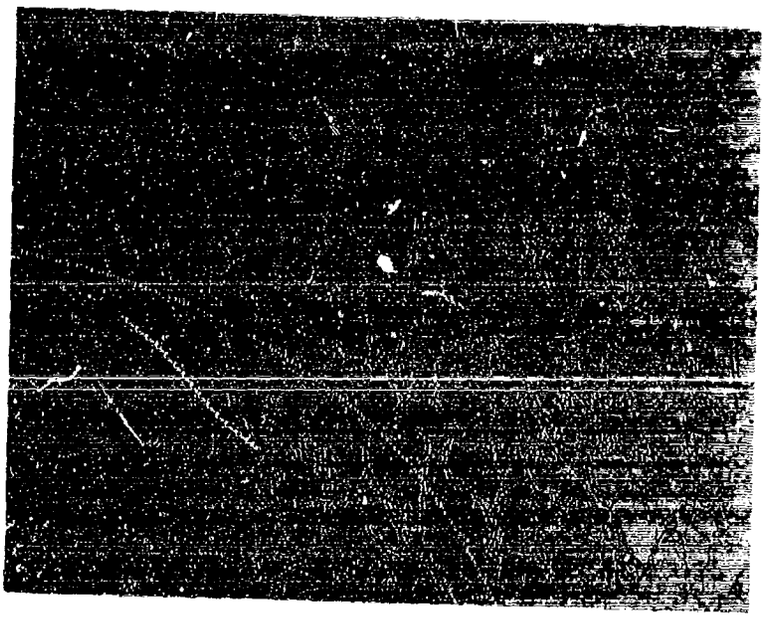
Figure 14-8

DOWNGRADED AT 3 YEAR INTERVALS
DECLASSIFIED AFTER 12 YEARS
DOD DIR 5200.10

THIS DOCUMENT CONTAINS INFORMATION AFFECTING THE NATIONAL DEFENSE OF THE UNITED STATES WITHIN THE MEANING OF THE ESPIONAGE LAWS, TITLE 18, U.S.C., SECTIONS 793 AND 794. ITS TRANSMISSION OR THE REVELATION OF ITS CONTENTS IN ANY MANNER TO AN UNAUTHORIZED PERSON IS PROHIBITED BY LAW.



XGCF-6



XGPS-7

Etchant: Kallings

Magnification: 100X

STRUCTURE OF XGCF-6 AND XGPS-7 WYMAN-GORDON TEST RINGS FROM PWA 1007 WASPALOY DISKS.

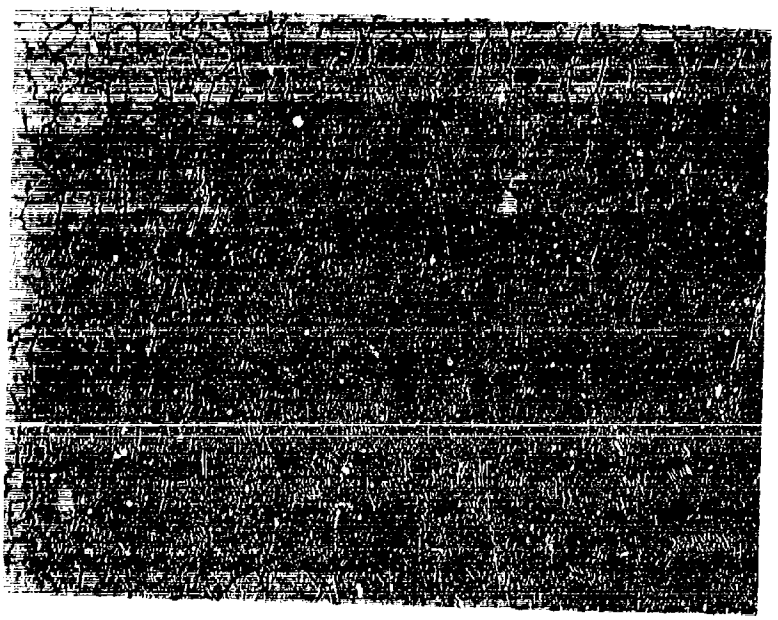
Figure 14-9

DOWNGRADED AT 3 YEAR INTERVALS
DECLASSIFIED AFTER 12 YEARS
DOD DIR 5200.10

THIS DOCUMENT CONTAINS INFORMATION AFFECTING THE NATIONAL DEFENSE OF THE UNITED STATES WITHIN THE MEANING OF THE ESPIONAGE LAWS, TITLE 18, U.S.C., SECTIONS 793 AND 794. THE TRANSMISSION OR THE REVELATION OF ITS CONTENTS IN ANY MANNER TO AN UNAUTHORIZED PERSON IS PROHIBITED BY LAW.



CGNK-119



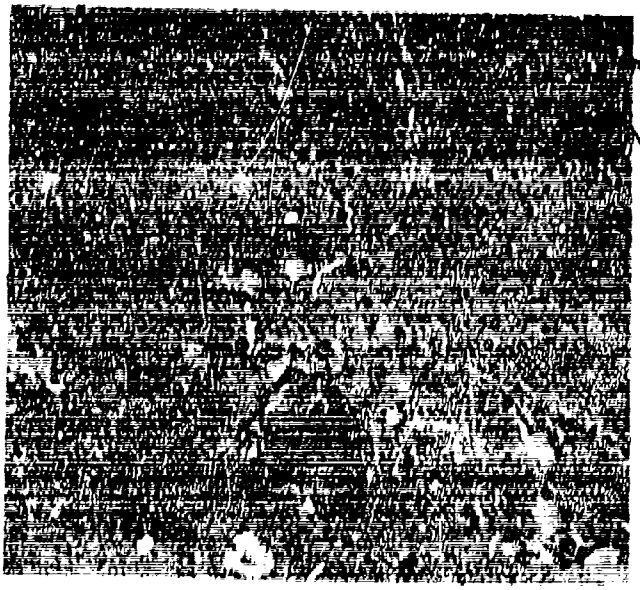
CJDA-38

Etchant: Kallings Magnification: 100X

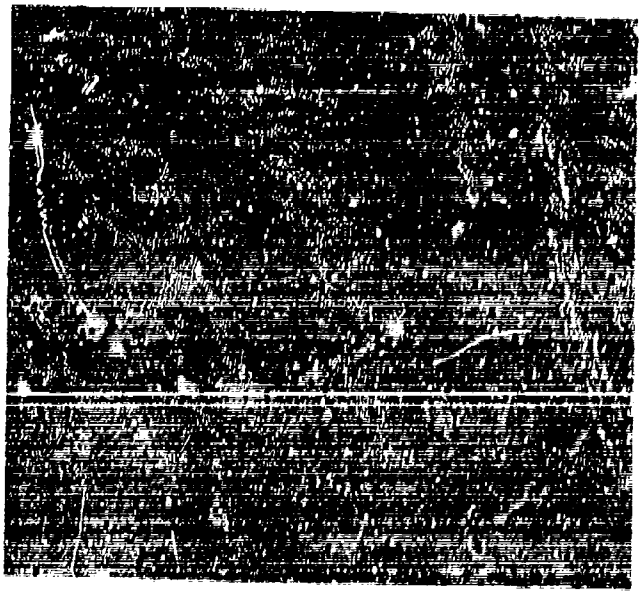
STRUCTURE OF CGNK-119 AND CJDA-38 LADISH TEST RINGS FROM PWA 1007 WASPALOY DISKS.

Figure 14-10

DOWNGRADED AT 3 YEAR INTERVALS
DECLASSIFIED AFTER 12 YEARS
DOD DIR 5200.10



Heat XGCF-6



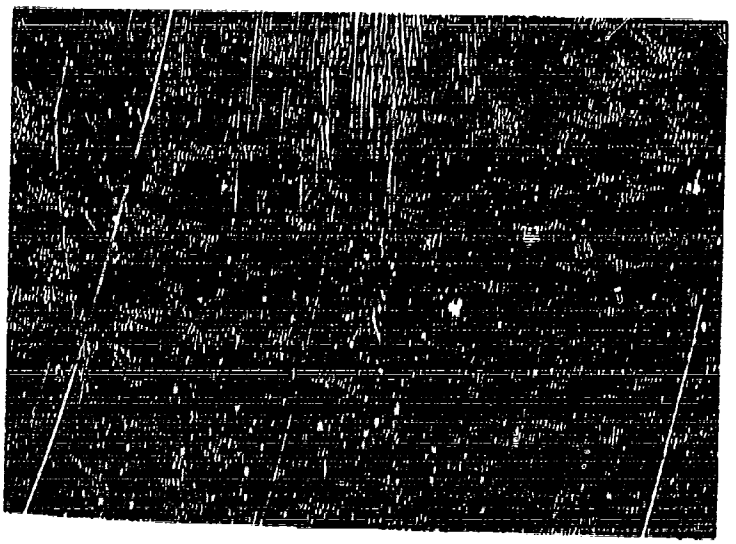
Heat XGPS-7

Etchant: Kallings

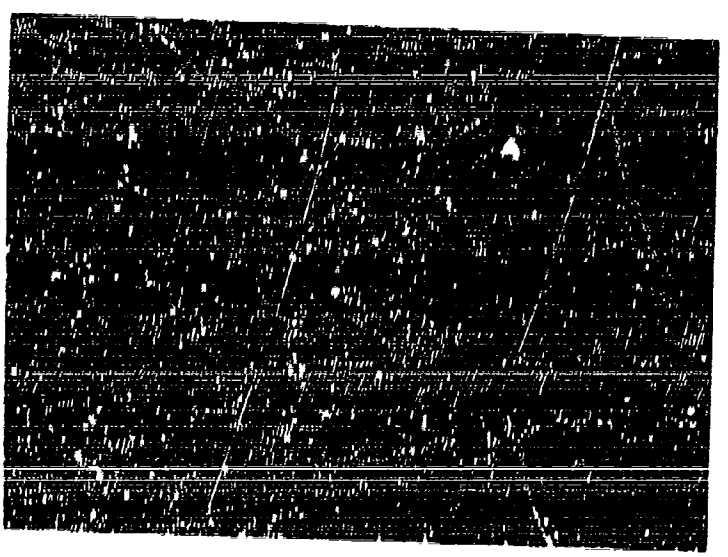
Magnification: 5,000X

STRUCTURE OF HEAT XGCF-6 AND HEAT XGPS-7
WYMAN-GORDON TEST RINGS FROM PWA 1007
WASPALOY DISKS.

Figure 14-11



Heat CGNK-119

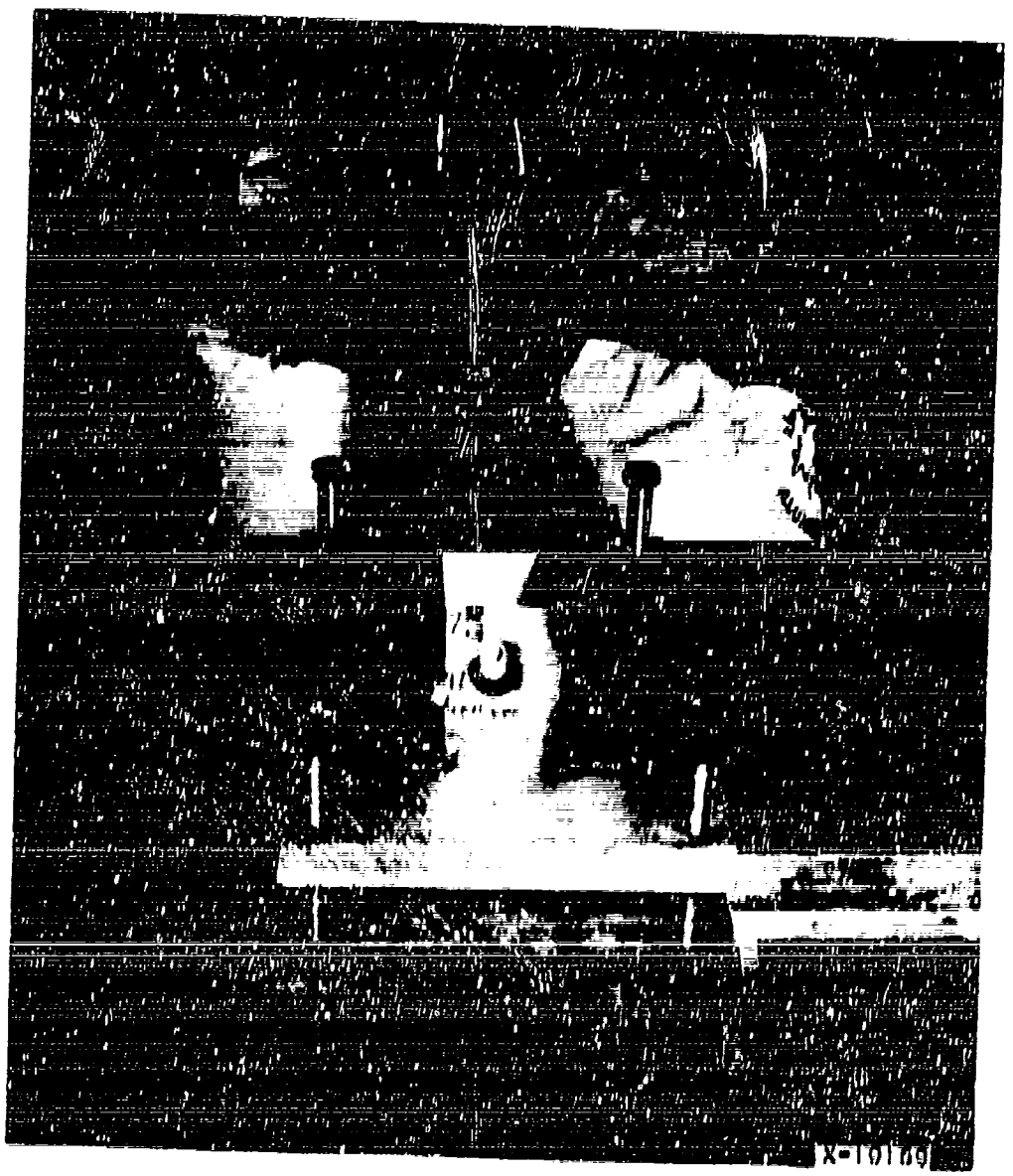


Heat CJDA-38

Etchant, Kallings Magnification: 5,000X

STRUCTURE OF HEAT CGNK-119 AND HEAT CJDA-38 LADISH TEST RINGS FROM PWA 1007 WASPALOY DISKS.

Figure 14-12



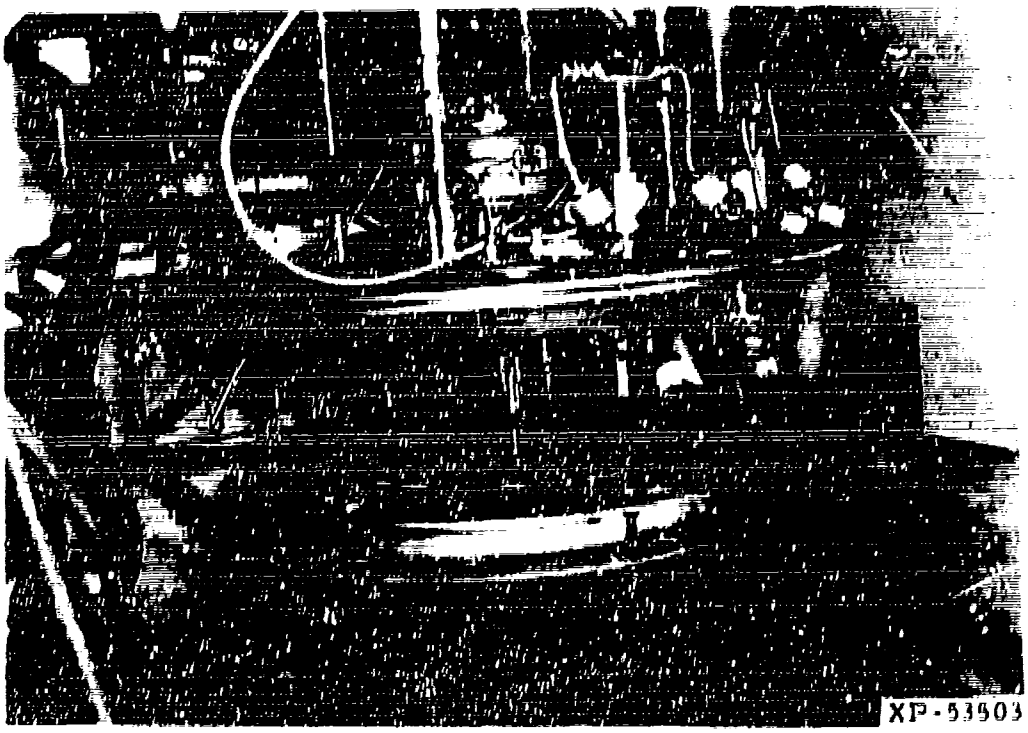
TEST SET-UP FOR SST BALLISTIC TESTS WITH PANELS RIGIDLY MOUNTED.

Figure 14-13



OVERALL TEST SET-UP FOR SST BALLISTIC TESTS.

Figure 14-14



TYPICAL TEST SET-UP WITH CONTAINMENT RING SANDWICHED BETWEEN THE PLATES.

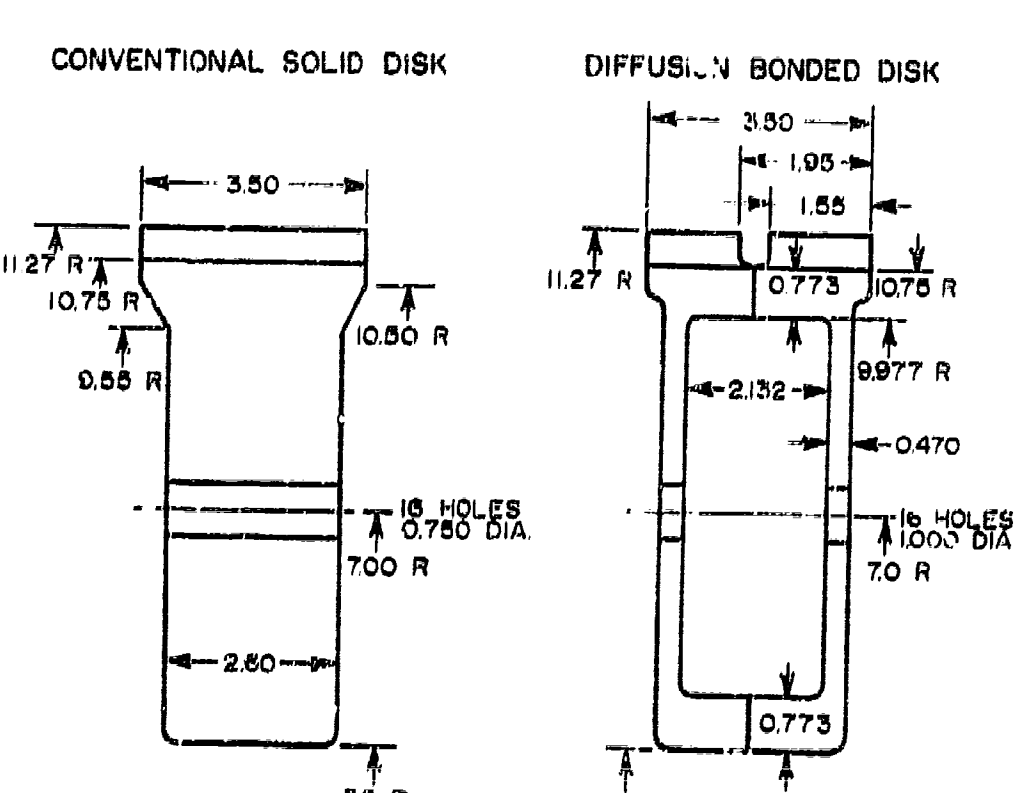
Figure II-15

BALLISTIC CONTAINMENT TEST RESULTS

Material		Merit Factor	Kinetic energy wt./unit area
AMS 4911		200	
PWA 1202		190	
PWA 738		165	
AMS 5504	Rc 44	160	
AMS 5508	Rc 48	155	
AMS 6355	Rc 50	154	
PWA 1030		154	
AMS 4910		140	
AMS 5508	Rc 28	140	
AMS 5510		135	
AMS 5517		135	
AMS 5540		132	
AMS 5512		130	
AMS 4901		130	
AMS 5524		130	
AMS 5542		127	
AMS 5536		121	
AMS 5525		120	
AMS 5515		120	
AMS 5504	Rb 90	110	
AMS 6355	Rb 80	108	
PWA 1033		100	
AMS 5040	Carburized	95	
AMS 5062		90	

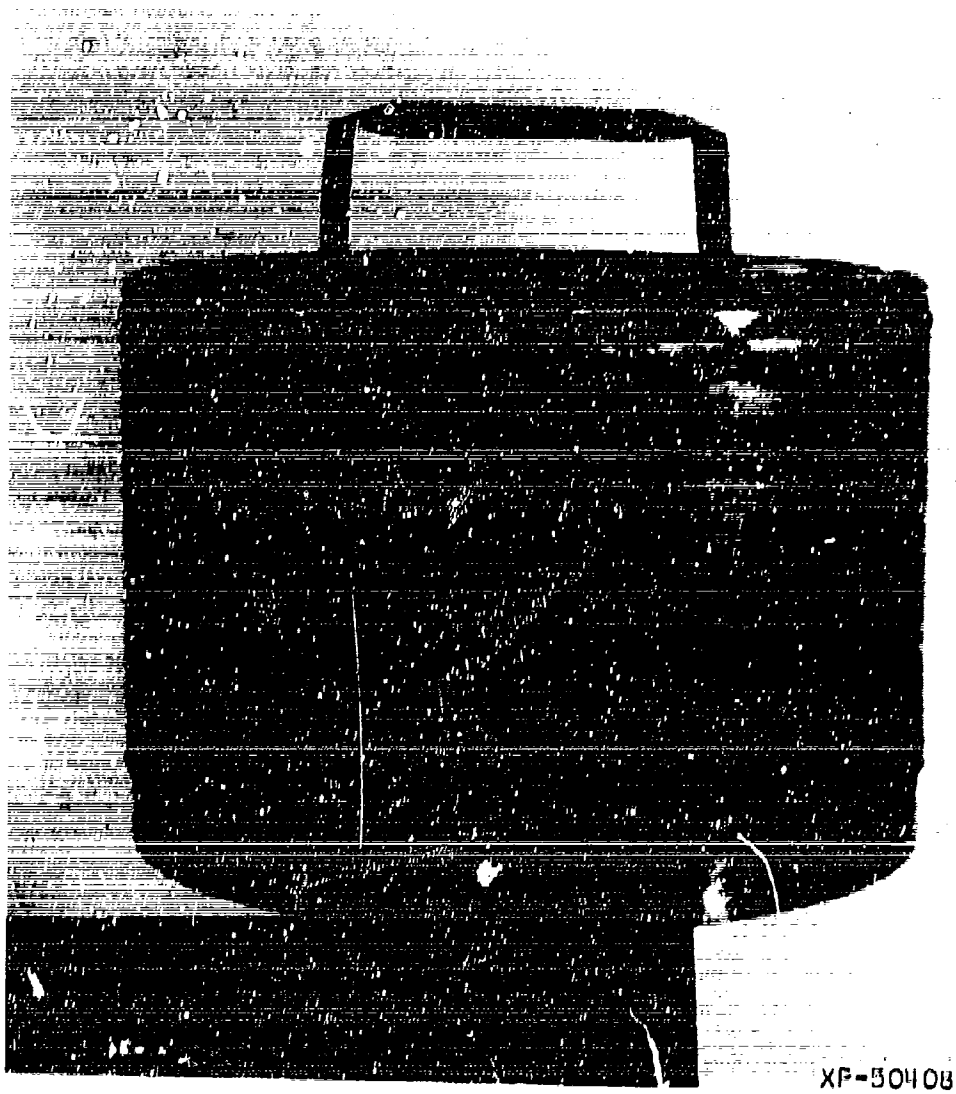
BALLISTIC CONTAINMENT TEST RESULTS

Figure 14-16



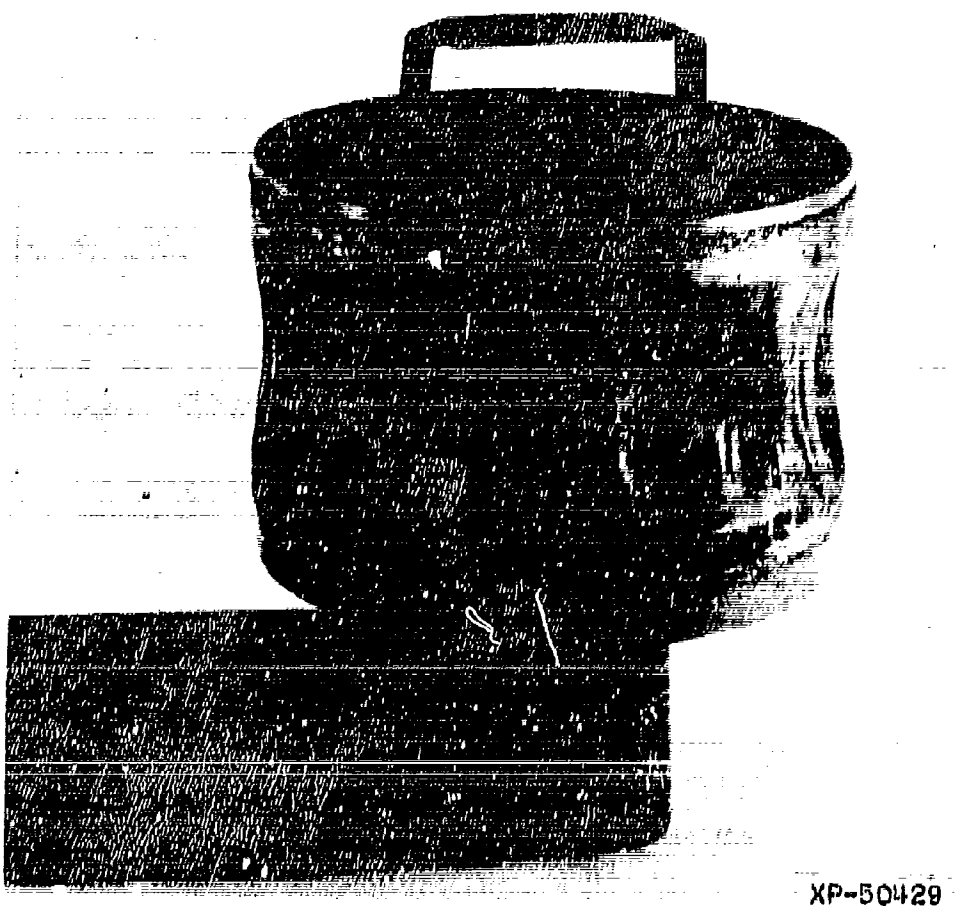
DESIGN AND WEIGHT COMPARISON BETWEEN THE CONVENTIONAL SOLID DISK AND THE DIFFUSION-BONDED DISK.

Figure 14-17



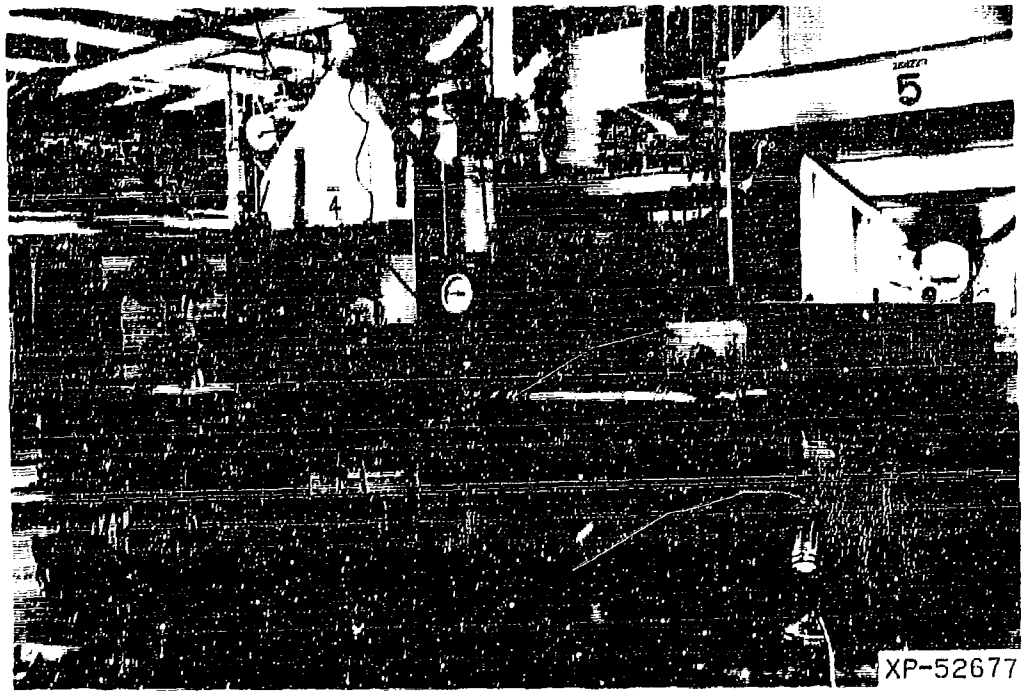
VACUUM RETORT BEFORE FURNANCE CYCLE.

Figure 14-18



VACUUM RETORT AFTER FURNANCE CYCLE.

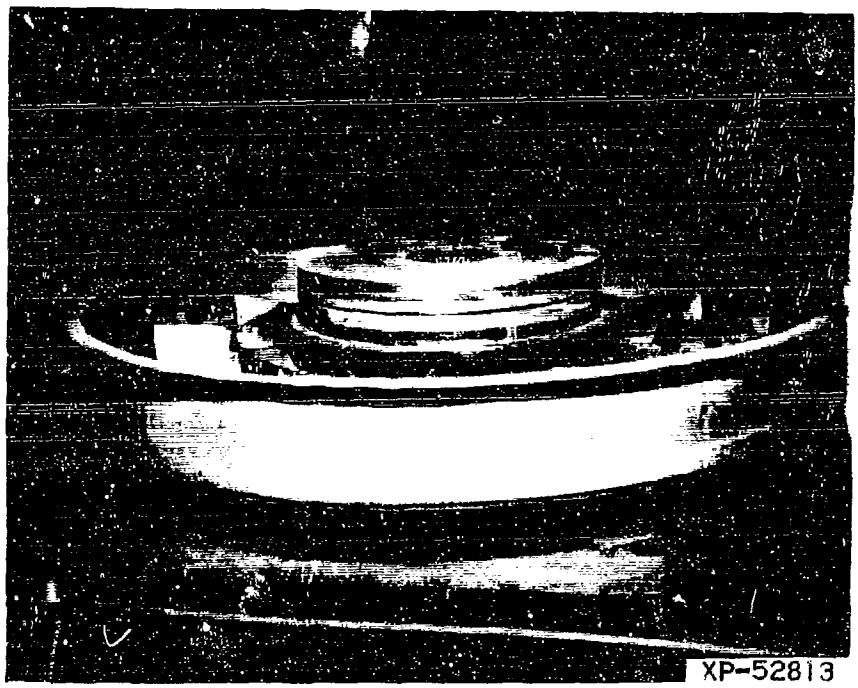
Figure 14-19



OVERALL VIEW OF VACUUM PUMP, RETORT, AND FURNACE.

Figure 14-20

DOWNGRADED AT 3 YEAR INTERVALS
DECLASSIFIED AFTER 12 YEARS
DOD DIR 5200.10

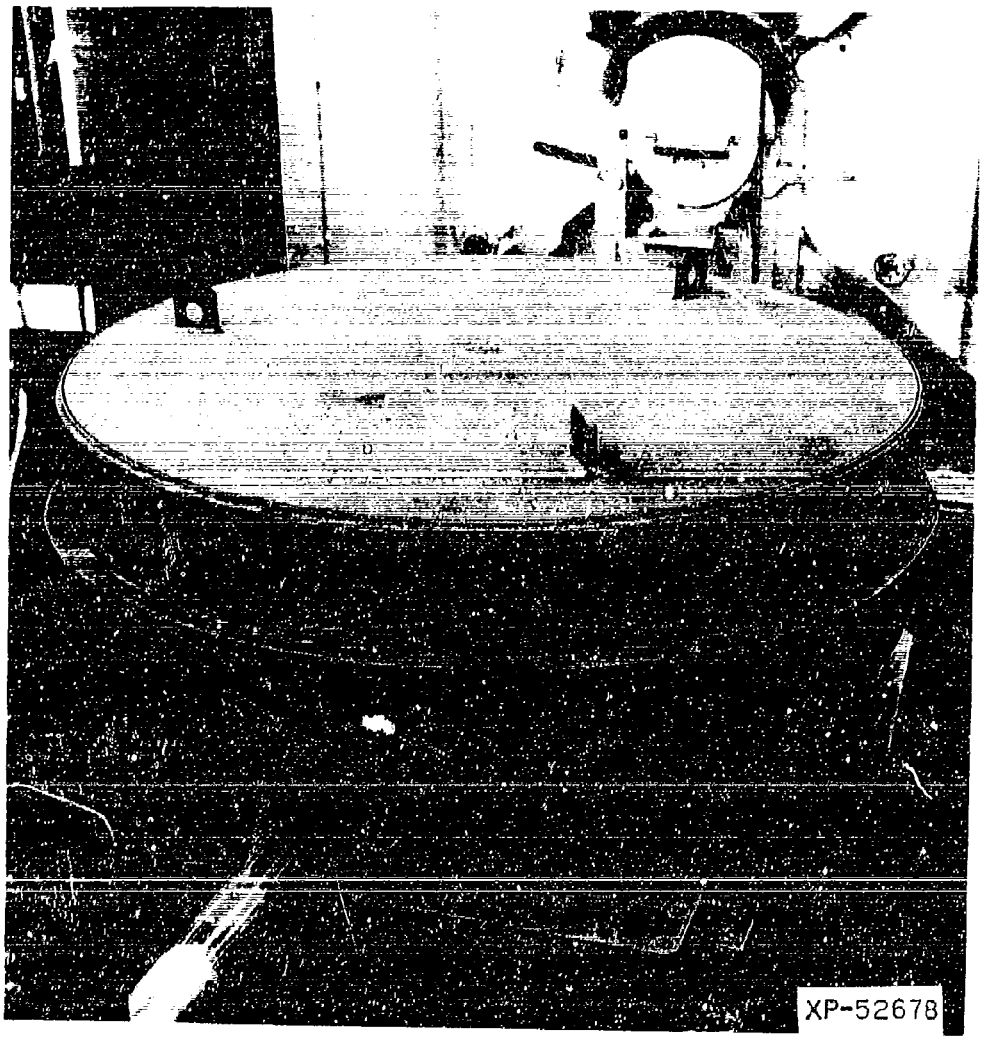


OPENED RETORT AFTER FURNACE CYCLE SHOWING BONDED DISK.

Figure 14-21

DOWNGRADED AT 3 YEAR INTERVALS
DECLASSIFIED AFTER 12 YEARS
DOD DIR 5200.10

THIS DOCUMENT CONTAINS INFORMATION AFFECTING THE NATIONAL DEFENSE OF THE UNITED STATES WITHIN THE MEANING OF THE ESPIONAGE LAWS, TITLE 18, U.S.C. SECTIONS 793 AND 794. THE TRANSMISSION OR THE REVELATION OF ITS CONTENTS IN ANY MANNER TO AN UNAUTHORIZED PERSON IS PROHIBITED BY LAW.



A 53-INCH DIAMETER RETORT AFTER FURNACE CYCLE.

Figure 14-22

DOWNGRADED AT 3 YEAR INTERVALS
DECLASSIFIED AFTER 12 YEARS
DOD DIR 5200.10

THIS DOCUMENT CONTAINS INFORMATION AFFECTING THE NATIONAL DEFENSE OF THE UNITED STATES WITHIN THE MEANING OF THE ESPIONAGE LAWS, TITLE 18 U.S.C. SECTIONS 793 AND 794. ITS TRANSMISSION OR THE REVELATION OF ITS CONTENTS IN ANY MANNER TO AN UNAUTHORIZED PERSON IS PROHIBITED BY LAW.

TEST SPECIMEN BONDING PARAMETERS

A. Vacuum Hot Press

Specimen Trial	Bonding Time-Hr.	Temp. °F	Press. Psi	Remarks
1.	1	1700	1000	Did not bond - excessive deformation
2.	1/2	1650	1000	147,000 psi U. T. S. - excessive deformation
3.	1/2	1650	650	140,000 psi U. T. S. - excessive deformation
4.	1/2	1650	425	145,000 psi U. T. S.
5.	1/2	1650	225	147,000 psi U. T. S. - brittle joint
6.	1/2	1600	425	Bond broke by bend test

B. Vacuum Retort

7.	1/2	1650	425	No bond - excessive heat up time
8.	1/2	1650	425	Satisfactory bond - broke by bend test
9.	1/2	1650	425	Outgassed for 8 hours - poor bond
10.	1/2	1625	425	Poor bond
11.	1/2	1650	425	Satisfactory bond - broke by bend test
12.	1/2	1650	425	Satisfactory bond

Figure 14-23

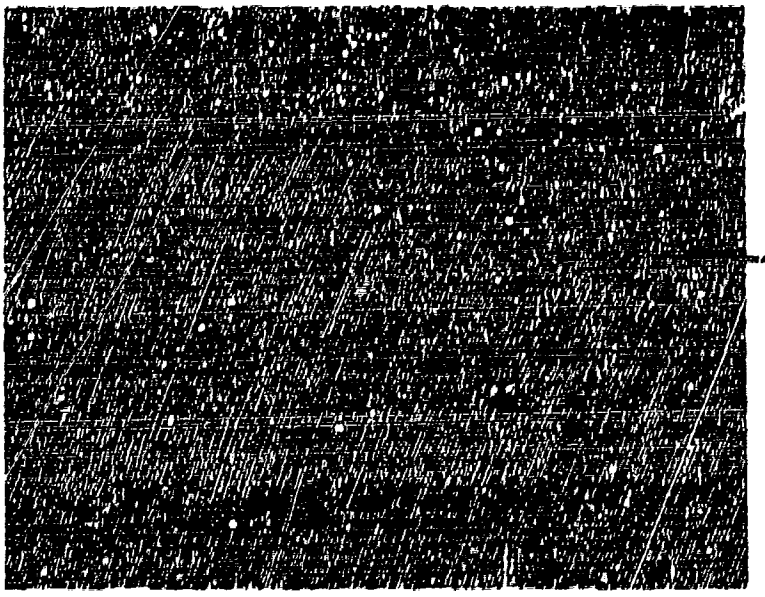
DOWNGRADED AT 3 YEAR INTERVALS
DECLASSIFIED AFTER 12 YEARS
DOD DIR 5200.10

THIS DOCUMENT CONTAINS INFORMATION AFFECTING THE NATIONAL DEFENSE OF THE UNITED STATES WITHIN THE MEANING OF THE ESPIONAGE LAWS, TITLE 18, U.S.C., SECTIONS 793 AND 794. THE TRANSMISSION OR THE REVELATION OF ITS CONTENTS IN ANY MANNER TO AN UNAUTHORIZED PERSON IS PROHIBITED BY LAW.



DIFFUSION-BONDED TITANIUM (AMS-4928) TENSILE TEST PIECES. BONDED AT 1650°F AND AT 235, 425, AND 650 PSI FOR 1/2 HOUR IN VACUUM FURNACE.

Figure 14-24



1650°F for 1/2 Hour. 500 X Magnification

METALLOGRAPHIC PHOTOGRAPH OF SPECIMEN NO. 12 SHOWING GRAIN GROWTH ACROSS BOND JOINT.

Figure 14-25

ITEM 15

SUPPORTING DESIGN CONSIDERATIONS

ITEM 15 - SUPPORTING DESIGN CONSIDERATIONS

OBJECTIVE

This item of the contract required Pratt & Whitney Aircraft to consider and report on the following factors in the work performed under this contract, and to recommend any improvements to be adopted in Phase III of the SST program for the following factors: reliability, configuration management, weight and center of gravity control, value engineering, maintainability, and safety.

A. RELIABILITY

1. INTRODUCTION

During the SST Phase II-B contract period, reliability continued to be one of the inputs into the overall design effort to assure optimization of the inherent reliability capability of the powerplant. Along with contributions in the field of reliability in support of the board design activity, the reliability predictions developed during Phase II-A were reviewed and updated. The following paragraphs summarize the reliability analyses completed during Phase II-B.

2. RELIABILITY SUPPORT OF THE DESIGN EFFORT

The detail designs generated as the result of the Phase II-B contract have been monitored and reviewed for the elements which affect operational reliability, aircraft availability, and component durability. Attention was focused on particular areas to assure that the reliability features which were established during Phase II-A have been maintained or improved upon. The need and feasibility for redundancy or fail-safe characteristics has been considered. The critical or marginal design areas were reviewed to assure that the mechanical configuration and the limiting stress margins are adequate to preclude failure modes. Feedback of service problems and their corrective solutions has been provided to design personnel to eliminate, where possible, these problems from the initial SST engine design. This feedback information was derived from military and commercial experience with engines having supersonic as well as subsonic capability.

DOWNGRADED AT 3 YEAR INTERVALS
DECLASSIFIED AFTER 12 YEARS
DOD DIR 5200.10

THIS DOCUMENT CONTAINS INFORMATION AFFECTING THE NATIONAL DEFENSE OF THE UNITED STATES WITHIN THE MEANING OF THE ESPIONAGE LAWS, TITLE 18, U.S.C. SECTIONS 793 AND 794. ITS TRANSMISSION OR THE REVELATION OF ITS CONTENTS IN ANY MANNER TO AN UNAUTHORIZED PERSON IS PROHIBITED BY LAW.

Design studies conducted during Phase II-B resulted in the incorporation of design features specifically intended to increase the inherent reliability capability of the basic STF219 engine configuration beyond that which was proposed for Phase II-A. The major improvements are listed below.

- Cover plates have been provided on the front and back sides of all high-pressure compressor disks outboard of the outer rotor spacers. These, together with submerged blade roots in the middle high-pressure compressor stages, reduce the disk thermal gradients during transient operating conditions, thus improving the fatigue life of these parts.

- The thrust balance scheme has been revised so that the magnitude of the thrust loads on the rotors is insensitive to the wear of the knife edge seals downstream of the last stage of the high-pressure compressor. Additionally, it assures that no thrust load reversal occurs for any operational condition of the engine.

- Improved high temperature materials (PWA 664 and B1900) have been used in the turbine section. The improved high temperature properties of these materials provide for increased reliability and part life.

- The Zone I spray bars of the duct heater have been moved upstream of the aerodynamic flameholder, out of the flame and into a cooler environment. This will reduce the possibility of clogging which could result in a faulty spray pattern. (The Zone II spray bars are already upstream of the flameholder.)

3. NUMERICAL RELIABILITY ANALYSIS

The numerical reliability analyses developed during Phase II-A have been updated and expanded to include the latest engine configuration. Additionally, these reliability prediction estimates reflect adjustments to the base failure rates as determined by more recent service data feedback plus any changes in the projected advances in the state-of-the-art at the time the SST engine is expected to enter commercial service operation.

The estimated mature-engine mean time between in-flight shutdown (MTBIFS) for the STF219 duct heating turbofan engine has been revised from the initial calculation of 10,000 hours to 13,000 hours. An in-flight shutdown is defined as any malfunction or discrepancy, chargeable to the engine, which causes or generates a decision to shut down the

DOWNGRADED AT 3 YEAR INTERVALS
DECLASSIFIED AFTER 12 YEARS
DOD DIR 5200.10

engine while in flight (i.e., from the moment a take-off roll begins until the landing roll begins). The increase in MTBIFS is attributed to an improvement in the projected reliability of the hot section parts over the initial estimates and the effectiveness of the fixes for service problems which have been incorporated in the engine design. These service fixes have had the effect of lowering the base failure rates for the STF219 engine.

Also, a study was conducted to estimate another index of reliability for the STF219 engine; namely, the mean time between premature engine removal (MTBPER). This index is an indication of aircraft availability. A premature engine removal is defined as an unscheduled removal of the engine from the aircraft, prior to the expiration of the assigned time between overhaul (TBO) interval, which is necessitated by the need for maintenance action in order to correct an engine-chargeable failure and restore the engine to an acceptable operating condition.

The estimated mature-engine MTBPER for the STF219 engine is 3700 hours. This reliability prediction is based on service data from commercial and military operations. As was done in estimating MTBIFS, each major engine section was analyzed using actual premature engine removal rates demonstrated in current operational service. These rates were adjusted by factors which take into account advanced design concepts, degree of complexity, and the operational environment of the SST engine. By this process an overall engine premature removal rate was obtained.

B. CONFIGURATION MANAGEMENT

1. OBJECTIVE

The objective of configuration management during the SST Phase II-B program was to manage the evolution of the engine designs to conform to the engine model and performance specifications, and to be compatible with the requirements of the airframe contractors. This necessitated close liaison with Boeing and Lockheed in order to coordinate and evaluate revisions affecting the installation and/or performance of the engine in the airframe.

2. DISCUSSION

Major areas requiring continuous coordination were interchange of

DOWNGRADED AT 3 YEAR INTERVALS
DECLASSIFIED AFTER 12 YEARS
DOD DIR 5200.10

THIS DOCUMENT CONTAINS INFORMATION AFFECTING THE NATIONAL DEFENSE OF THE UNITED STATES WITHIN THE MEANING OF THE ESPIONAGE LAWS, TITLE 18, U.S.C., SECTIONS 793 AND 794. THE TRANSMISSION OR THE REVELATION OF ITS CONTENTS IN ANY MANNER TO AN UNAUTHORIZED PERSON IS PROHIBITED BY LAW.

performance data engine mounting and mating to airframe inlet and wing, engine accessory locations, secondary cooling airflow control, ejector-reverser sizing, canting of the thrust line, and reverser targeting.

The Phase II-A system of SST coordination sheets established and monitored by the Pratt & Whitney Aircraft Installation Engineering Department to transmit data to and from the airframe contractors was continued. Telephone and telegraph communications were also used frequently to maintain liaison and transmit information. Pratt & Whitney Aircraft personnel and the airframe contractors' representatives held frequent meetings to exchange information and resolve problems. These meetings were held at Pratt & Whitney Aircraft facilities and at the two airframe contractors' facilities. In some instances, urgently needed performance data and drawings were carried by courier. Performance data, weights and installation dimensions were supplied for each different engine configuration for both turbofan and turbojet powerplants. The turbojet engine information included the effects of changes in the airflow schedule for supersonic operation. Dimensional and weight data were supplied for base, high, and low air flow schedules. Engine installation drawings of both a turbofan and a turbojet engine for each airframe contractor were prepared which represented the current configuration features.

At Boeing request, numerous installation studies were prepared to show various arrangements for mounting the engine to the Boeing inlet and wing in an effort to establish the optimum installation configuration. Objectives of the studies included minimizing the base drag of the wing-nacelle combination, canting the thrust line to get the best cruise performance and to avoid impingement on tail surfaces, and the achievement of reverse thrust targeting. Engine configuration revisions necessary to accomplish the improved installations were investigated. Mount locations, inlet duct extensions, and new ejector concepts were studied and changes were made where required.

Similar studies were conducted for Lockheed to meet their specific installation requirements. In addition, engine accessory relocation studies were made to obtain a more satisfactory accessory arrangement. The secondary cooling airflow system and its attendant pressure losses were also studied in detail, together with revisions to provide flame arrestors for this system.

For the turbojet powerplant, performance, weight, and external engine dimensions were made available to Boeing and Lockheed for each turbine inlet temperature and flow schedule. This information was supplied to permit each airframe contractor to select the one best configura-

DOWNGRADED AT 3 YEAR INTERVALS
DECLASSIFIED AFTER 12 YEARS
DOD DIR 5200.10

tion to fit within a single external envelope as had been done previously for the turbofan engine.

C. WEIGHT AND CENTER OF GRAVITY CONTROL

1. TURBOFAN ENGINES

The Phase II-A report presented the STF219, duct-burning turbofan engine, in sizes specified by Boeing and Lockheed. During Phase II-B, the STF219 was studied at an airflow of 650 pounds per second. The estimated weights for the Boeing and Lockheed engines are given in Figures 15-1 and 15-2, including a sectional weight breakdown.

During Phase II-B, two changes were incorporated that increased the engine weight. They are: (1) lower fan specific flow which increases the fan outer diameter and (2) redesign of the turbine section to provide for the required turbine efficiency level to be met at both the basic rating and the initial rating.

The engine center of gravity was estimated and supplied to the airframe companies and is shown on the installation drawing included in Item 1.

2. TURBOJET ENGINES

The Phase II-A report presented a 450 pound per second flow rate, full afterburning, turbojet engine weight of 8300 pounds. Subsequent studies have been concentrated on an engine with an airflow of 525 pounds per second. Three speed air flow schedules were studied: high, base, and low. These were considered at two turbine inlet temperatures, 2000 and 2300°F, resulting in a total of six configurations. The high flow, low temperature engine has a calculated weight of 10,800 pounds that allows a physical overspeed at the Mach 2.7 condition of 1.12 times the sea level take-off rpm. Figure 15-3 is the weight of this engine by section. Figure 15-4 shows the weight of the six configurations mentioned above for each airframe manufacturer's specific installation requirement.

The engine center of gravity was estimated and supplied to the airframe companies and is shown on the installation drawing included in Item 1.

D. VALUE ENGINEERING

During Phase II-B, three Value Engineers were assigned full time to the SST program. The various items of work accomplished by this group are discussed in the following paragraphs.

Target costs were set on the SST engine by major engine sections as

DOWNGRADED AT 3 YEAR INTERVALS
DECLASSIFIED AFTER 12 YEARS
DOD DIR 5200.10

goals for continued design and Value Engineering effort.

The basic Value Engineering program was reviewed and expanded to present a more detailed approach to Value Engineering consistent with the program requirements. This plan establishes the organization necessary, the means for implementing such a program, and the means for measuring and reporting on the effectiveness of the cost reduction efforts.

All layouts were reviewed as part of the general cost analysis approach of the Value Engineering program. Manufacturing cost estimates were made of all major design changes and published to the Program Manager and the Chief Design Engineer to keep them advised of the effect on manufacturing cost of the latest design revisions.

Meetings were held with design personnel to acquaint them with high-cost design features. Alternate design configurations were studied and cost data were published to the Program Manager and the Chief Design Engineer as an aid to incorporation decisions.

A cost versus function review was made to determine the cost consistency on parts in relation to current production engines. Items in question were reviewed with Production Engineering experts to assure that the designs were consistent with the latest manufacturing techniques. The designs were also scrutinized for congruity with such advanced manufacturing techniques as electron beam welding, flo turning, electric discharge machining, electrochemical machining and explosive forming.

Specialty vendors were contacted to discuss the use and economics of specialty products and processes such as advanced coring materials and configurations for cooled turbine blades and vanes, the state-of-the-art and potential of cast titanium, dual material extrusions, centrifugal castings, Feltmetal, etc.

All layouts were studied for potential cost reduction proposals. These proposals were reviewed with design personnel for feasibility and published to the Program Manager and the Chief Design Engineer for their consideration and incorporation into the SST engine Bill of Material.

A parametric study was conducted on price as a function of bypass ratio and the effects on airflow and thrust for direct operating cost studies on various supersonic engine cycles.

A complete review of the STF219 engine design has been made to keep

DOWNGRADED AT 3 YEAR INTERVALS
DECLASSIFIED AFTER 12 YEARS
DOD DIR 5200.10

THIS DOCUMENT CONTAINS INFORMATION AFFECTING THE NATIONAL DEFENSE OF THE UNITED STATES WITHIN THE MEANING OF THE ESPIONAGE LAWS, TITLE 18, U.S.C., SECTIONS 793 AND 794. THE TRANSMISSION OR THE REVELATION OF ITS CONTENTS IN ANY MANNER TO AN UNAUTHORIZED PERSON IS PROHIBITED BY LAW.

the Program Manager informed of the latest status of the estimated manufacturing cost for the engine. This manufacturing cost was compared to the target costs by major engine section to point out areas of Value Engineering concentration for future phases of the supersonic engine program.

E. MAINTAINABILITY

1. INTRODUCTION

During the SST Phase II-B contract period, the overall powerplant design effort was monitored from a maintainability viewpoint. In addition to supporting design board activity, a preliminary analysis of maintenance tasks was compiled. The following sections present the results of the maintainability effort.

2. MAINTAINABILITY REVIEW OF DESIGN LAYOUTS

Design layouts resulting from work completed during the Phase II-B contract were reviewed to ensure that maintainability aspects were considered. Maintenance features cited as desirable in the Phase II-A contract period were re-evaluated to check their validity in terms of present design concepts. Specific engine regions were selected for comment and a summary is contained in the following paragraphs.

a. Nos. 1 and 2 Bearing Region

This region is satisfactory from the maintainability standpoint. The bearings and seals can be readily replaced by either horizontal or vertical disassembly procedures without removal of either turbine unit.

b. No. 3 Bearing Region

This region is satisfactory from the maintainability standpoint. The bearing and compartment seals may be readily replaced after removal of both turbine units. This region is much more accessible than in current powerplants because of the unit component concept used for the turbines.

c. No. 4 Bearing Region

This region is satisfactory from a maintainability standpoint because the bearing and seals are replaceable without removing the turbine exhaust case.

DOWNGRADED AT 3 YEAR INTERVALS
DECLASSIFIED AFTER 12 YEARS
DOD DIR 5200.10

THIS DOCUMENT CONTAINS INFORMATION AFFECTING THE NATIONAL DEFENSE OF THE UNITED STATES WITHIN THE MEANING OF THE ESPIONAGE LAWS, TITLE 18, U.S.C. SECTIONS 793 AND 794. THE TRANSMISSION OR THE REVELATION OF ITS CONTENTS IN ANY MANNER TO AN UNAUTHORIZED PERSON IS PROHIBITED BY LAW.

d. Fan Region

The fan rotor unit may be replaced without removal of the low-pressure turbine. A study is in process which will permit replacement of damaged fan blades without the need for rebalancing the rotor. This concept will utilize moment-weight classified blades.

e. Intermediate Case Region

A questionable maintainability feature in this region is the access to the flange joining the intermediate case to the high-pressure compressor case. Various duct design configurations are being studied which will facilitate access to this flange. These design studies will permit removal of the intermediate case without disassembly of the engine from the rear. Any suggested design revisions in this region will be evaluated with regard to their effects on performance, cost and weight.

f. High-Pressure Compressor and Diffuser Region

The quantity of plumbing and associated items in this region presents a complex arrangement. However, design studies are in process which will keep the number of joints and connections to a minimum. Borescope inspection ports for the high-pressure compressor will be provided, and adequate access to these provisions will be considered in any design revisions in this region.

g. Combustion Section

A design permitting the telescoping of a one-piece burner case in a rearward direction to gain access to the combustion section is preferred to a design utilizing a longitudinally split burner case. The telescoping case design, by eliminating the longitudinal flanges and their associated hardware, lowers maintenance times needed for inspection and assembly and reduces engine weight.

Design studies are being conducted in an effort to provide individually replaceable nozzle guide vanes without the necessity of a sliding inner combustion liner to provide vane-removal space. A fixed liner design is preferred due to its greater durability in terms of even temperature distribution and improved wear resistance.

DOWNGRADED AT 3 YEAR INTERVALS
DECLASS. AFTER 12 YEARS

Another feature which will be studied is a provision to remove the combustion liners without removing the fuel nozzles. In addition to the time saved by eliminating the removal and replacement of the nozzles, the possibility of leaks, after reassembly, at the nozzle supply line connections will be avoided. One study involves designing the front section of the combustion liner as a separate part which is not removed with the aft portion of the liner.

h. Turbine Section

The turbine section is composed of two distinct units, the low- and high-pressure turbine units. The rotors, vanes and cases of each unit are assembled and the units are then installed in the remainder of the engine. The location of the flange joining these units permits replacement of individual second-stage nozzle vanes without stage-by-stage disassembly of the turbine rotors. This feature eliminates a potential source of assembly error associated with reassembly of the turbine rotor stages.

Other maintainability considerations in this region involve removal of the high-pressure turbine unit and replacement of high-pressure turbine blades. These procedures are discussed in paragraphs k and l, respectively.

i. Ducts and Exhaust System

The ducts will be designed to permit maximum accessibility to the fuel manifold, fuel nozzles, and borescope inspection ports and to facilitate the scheduled hot section inspection. Adequate access to these regions is vital so that necessary maintenance and inspection procedures may be accomplished. Several configurati are being studied to meet these requirements. In addition, as noted in paragraph e above, improved access to the flange joining the intermediate case to the high-pressure compressor case is being studied.

j. Main Fuel Manifold and Fuel Nozzles

The main fuel manifold will be mounted external to the engine diffuser case and will be removable through the ducts. The ability to replace individual fuel nozzles without opening the burner case is being studied.

k. Removal of the Hig. Pressure Turbine Unit

Th gn of the high-pressure turbine unit as presented in the Phase

DOWNGRADED AT 3 YEAR INTERVALS
DECLASSIFIED AFTER 12 YEARS
DOD DIR 5200.10

II-A report included two unsatisfactory features from a maintainability aspect. These features were the lack of accessibility of the high-pressure rotor coupling nut and the necessity for releasing the "trapped" No. 3 rear seal assembly when removing the turbine unit. In the Phase II-A design, release of the No. 3 rear seal required gaining access through the combustion chamber liners and inner nozzle case.

Figure 15-5 illustrates a configuration being studied to overcome both of these undesirable features. In this design, the high-pressure turbine coupling nut is readily accessible and the high-pressure turbine unit may be removed without releasing the No. 3 rear seal. This design does not compromise the cooling scheme for the first-stage rotor and provides the safety feature of double shafting under the bearing. Trade studies are being conducted which will evaluate the advantages of this design in relation to increases in cost, weight, and complexity of structural components.

Another design will be studied which will permit the high-pressure turbine case to slide aft without the necessity of removing the first-stage nozzle guide vanes. This design further facilitates removal of the high-pressure turbine unit.

1. Replacement of First-Stage Turbine Blades

The replacement of first-stage turbine blades is simplified by the unit component construction feature. The low- and high-pressure turbine units may be readily removed and any damaged blades replaced in moment-weight classified pairs.

3. MAINTENANCE ANALYSIS

The preliminary analysis of maintenance tasks compiled during the SST Phase II-B contract period is defined below. From this analysis, a maintainability index of 0.39 man-hour of maintenance time per hour of engine operating time has been estimated. This index is the sum of the indices for scheduled and unscheduled maintenance. The following criteria were used to determine these indices:

- Average mission length of two hours,
- Minor periodic inspection interval of 100 hours,
- Major periodic inspection interval of 1500 hours, and
- TBO of 3000 hours.

The analysis included only direct, active maintenance man-hours employed in the following preventive and corrective maintenance functions:

DOWNGRADED AT 3 YEAR INTERVALS
DECLASSIFIED AFTER 12 YEARS
DOD DIR 5200.10

- Scheduled preflight and postflight inspections,
- Scheduled minor periodic inspections,
- Scheduled major periodic inspections (including hot section inspection), and
- Unscheduled flight-line and field maintenance (including time for trouble-shooting, corrective action, and postmaintenance check-out).

The following maintenance functions have been excluded from this analysis:

- All assembly and disassembly functions associated with airframe-supplied equipment required to perform a quick engine change,
- Fuel servicing,
- Depot level activities,
- Engine removal from and replacement in the aircraft,
- All maintenance actions resulting from failures or discrepancies that are not chargeable to the engine,
- All maintenance actions to obtain access through airplane nacelles, position ground equipment, move the airplane, etc., in order to perform the required maintenance task,
- All maintenance actions involved in changes relating to up-grading engine performance or other revisions in specification requirements.

a. Scheduled Maintenance

The scheduled maintenance procedure, and man-hour requirements are outlined in the following tabulation:

Scheduled Inspection	Interval (hr)	No. per Overhaul	No. per Engine Operating Hour	Man-hours per Inspection	MHH/EOH*
Preflight	2.0	1500	0.5000	0.25	0.1250
Postflight	2.0	1470	0.4900	0.35	0.1715
Minor Periodic	100	28	0.0093	6.00	0.0558
Major Periodic	1500	1	0.0003	30.00	0.0090
			Scheduled Maintenance Index	=	0.3613

*Maintenance man-hours per engine operating hour.

DOWNGRADED AT 3 YEAR INTERVALS
INCREASED AFTER 12 YEARS
DOD DIR 5200.10

b. Unscheduled Maintenance

The frequency of the unscheduled maintenance was based on reliability estimates, reflecting adjustments to the base failure rates developed during Phase II-A. The man-hour estimates for the unscheduled maintenance were based on studies of the powerplant configuration with careful consideration for operational environment, task complexity, secondary damage, etc. The following unscheduled maintenance index has been determined from these estimates:

	MMH/EOH*
Unscheduled Maintenance on External Units	0.0055
Unscheduled Maintenance at Major Periodic Inspections	0.0049
Unscheduled Maintenance at Premature Engine Removals	0.0149
Unscheduled Maintenance Index =	0.0253

*Maintenance man-hours per engine operating hour.

F. SAFETY

1. SUPPORT OF DESIGN FOR FLIGHT SAFETY

As part of the reliability effort to monitor and review the detail designs generated during Phase II-B, operational reliability, insofar as it applies to flight safety, has been of prime consideration. Assurance was made that the safety features which were established during Phases I and II-A have been maintained. Studies were conducted to determine the need for expanding these fail-safe and redundant design features. The result of these studies indicated that the following fail-safe and redundant design features are to be incorporated in the engine in addition to those which were proposed during Phase II-A.

- Both inner and outer ends of all turbine vanes, instead of just first-stage turbine vanes, are retained so that in the event of a burn-through the vanes will be prevented from passing through the turbine causing further damage.
- Integral ferrules have been provided for all tubes carrying inflammable fluids. This will reduce the possibility of leakage that could occur

DOWNGRADED AT 3 YEAR INTERVALS
DECLASSIFIED AFTER 12 YEARS
DOD DIR 5200.10

THIS DOCUMENT CONTAINS INFORMATION AFFECTING THE NATIONAL DEFENSE OF THE UNITED STATES WITHIN THE MEANING OF THE ESPIONAGE LAWS, TITLE 18 U.S.C. SECTIONS 793 AND 794. ITS TRANSMISSION OR THE REVELATION OF ITS CONTENTS IN ANY MANNER TO AN UNAUTHORIZED PERSON IS PROHIBITED BY LAW.

in a brazed-on type ferrule connection.

- The sliding shroud ejector-reverser actuation system incorporates a synchronizing ring. Thus, failure of an actuator will not cause asymmetric operation of the system.

2. DESIGN SUPPORT FOR MAINTENANCE PERSONNEL SAFETY

During the maintainability design reviews, as discussed in the Maintainability section (reference Item 15E), the detail designs were analyzed for the required maintenance tasks involved to ensure that safe conditions and handling procedures have been provided for personnel engaged in maintenance or overhaul activities.

DOWNGRADED AT 3 YEAR INTERVALS
DECLASSIFIED AFTER 12 YEARS
DOD DIR 5200.10

BOEING INSTALLATION - WEIGHT SUMMARY

650 lb/sec airflow
Base Flow Schedule
Basic and Initial Ratings

Fan rotor, stator, case and front mount	795 lb
Intermediate case	655
High pressure compressor rotor, stator and case	615
Diffuser and burner	981
Turbine rotor, stator, and shaft	1377
Turbine exhaust	396
Ducts, liners, and variable area nozzle	1767
Ejector-reverser	1880
Accessories drive	184
Components and plumbing	910
Total estimated dry engine weight	9560
*Additional equipment and installation features	540
Total engine weight	10,100 lb

*Additional equipment and installation features are based on Phase II-A requirements. This weight does not include inlet extensions or ejector cant angles above 6°.

Figure 15-1

DOWNGRADED AT 3 YEAR INTERVALS
DECLASSIFIED AFTER 12 YEARS
DOD DIR 5200.10

LOCKHEED INSTALLATION - WEIGHT SUMMARY

650 lb/sec airflow
Base flow schedule
Basic and Initial Ratings

Fan rotor, stator, case and front mount	762 lb
Intermediate case	655
High pressure compressor rotor, stator and case	615
Diffuser and burner	981
Turbine rotor, stator, and shaft	1377
Turbine exhaust	396
Ducts, liners, and variable area nozzle	1730
Ejector-reverser	1880
Accessories drive	184
Components and plumbing	910
Total estimated dry engine weight	9490
*Additional equipment and installation features	180
Total engine weight	9670 lb

*Additional equipment and installation features are based on Phase II-A requirements except for addition of weight increase due to canting the ejector reverser four degrees from the engine centerline.

Figure 15-2

DOWNGRADED AT 3 YEAR INTERVALS
DECLASSIFIED AFTER 12 YEARS
DOD DIR 5200.10

THIS DOCUMENT CONTAINS INFORMATION AFFECTING THE NATIONAL DEFENSE OF THE UNITED STATES WITHIN THE MEANING OF THE ESPIONAGE LAWS, TITLE 18, U.S.C., SECTIONS 793 AND 794. THE TRANSMISSION OR THE REVELATION OF ITS CONTENTS IN ANY MANNER TO AN UNAUTHORIZED PERSON IS PROHIBITED BY LAW.

WEIGHT BREAKDOWN FOR STJ227 ENGINE

525 lb/sec airflow
High flow schedule
2000°F turbine inlet temperature

Compressor inlet	335 lb
Compressor rotor	1,010
Compressor stator	750
Diffuser	650
Burner	875
Turbine rotor and shafts	1,070
Turbine stator	810
Turbine exhaust	650
Afterburner	1,235
Ejector-reverser	2,000
Accessories drive	185
Components and plumbing	1,180
Total engine weight	10,800 lb

Figure 15-3

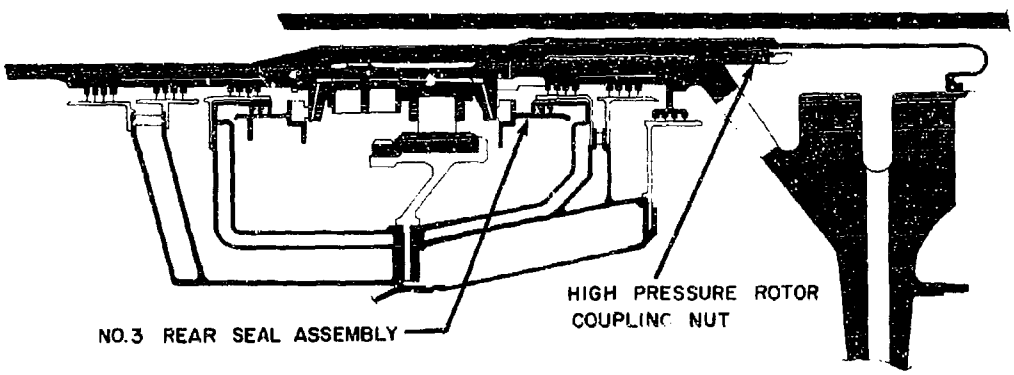
DOWNGRADED AT 3 YEAR INTERVALS
DECLASSIFIED AFTER 12 YEARS
DOD DIR 5200.10
THIS DOCUMENT CONTAINS INFORMATION AFFECTING THE NATIONAL DEFENSE OF THE UNITED STATES WITHIN THE MEANING OF THE ESPIONAGE LAWS, TITLE 18, U.S.C., SECTIONS 793 AND 794. THE TRANSMISSION OR REVELATION OF ITS CONTENTS IN ANY MANNER TO AN UNAUTHORIZED PERSON IS PROHIBITED BY LAW.

WEIGHT OF TURBOJET ENGINE CONFIGURATIONS

Wa, lb/sec	Turbine Inlet Temp., max, °F	Flow Schedule	Afterburner Aug	Afterburner Tailpipe Temp, °F	Ejector Diameter	Ejector L/D	Net Weight lb.	Cant	* Weight of Special Installation Features, lb	Gross Weight lb
Boeing										
525	2000	High	Full	3100	78	1.295	10,800	7° 55'	570	11,370
525	2000	Base	Full	3100	75	1.295	10,470	8° 35'	575	11,045
525	2000	Low	Full	3100	75	1.235	10,200	8° 50'	580	10,780
525	2300	High	Full	3100	78	1.265	10,760	8° 9'	570	11,330
525	2300	Base	Full	3100	75	1.285	10,455	8° 40'	575	11,030
525	2300	Low	Full	3100	75	1.28	10,215	9° 40'	585	10,800
Lockheed										
525	2000	High	Full	3100	78	1.295	10,800	4°	180	10,980
525	2000	Base	Full	3100	75	1.295	10,470	4°	180	10,650
525	2000	Low	Full	3100	75	1.235	10,200	4°	180	10,380
525	2300	High	Full	3100	78	1.265	10,760	4°	180	10,940
525	2300	Base	Full	3100	75	1.285	10,455	4°	180	10,635
525	2300	Low	Full	3100	75	1.28	10,215	4°	180	10,395

* This includes weight to cant ejector to the angles shown.

Figure 15-4



HIGH-PRESSURE TURBINE REGION

Figure 15-5

DOWNGRADED AT 3 YEAR INTERVALS
DECLASSIFIED AFTER 12 YEARS
DOD DIR 5200.10